



Zachodniopomorski
Uniwersytet Technologiczny
w Szczecinie

Joanna Klebeko, BEng, MSc

Amino acid ionic liquids as carrier systems for non-steroidal anti-inflammatory drugs

Aminokwasowe ciecze jonowe jako nośniki dla niesteroidowych leków przeciwzapalnych

Ph.D. thesis

Supervisor: Ewa Janus, PhD, DSc, Assoc. Prof.

Assistant supervisor: Paula Ossowicz-Rupniewska, PhD, DSc, Assoc. Prof.

Szczecin, 2024

Acknowledgement

I would like to extend my profound gratitude to my supervisor, Ewa Janus, PhD, DSc, Assoc. Prof. and assistant supervisor Paula Ossowicz-Rupniewska, PhD, DSc, Assoc. Prof. whose guidance and support have greatly contributed to the scope and quality of this thesis. The opportunities and resources provided by them have been instrumental throughout the course of this research.

I would like to express my sincere appreciation to Anna Nowak, BEng, PhD, DSc, and her research team, led by Professor Adam Klimowicz, PhD, DM, from the Department of Cosmetic and Pharmaceutical Chemistry at Pomeranian Medical University in Szczecin, for their outstanding work on the permeation and antioxidant study. Their expertise and dedicated efforts were essential to the successful execution and analysis of the performance component of this thesis.

I would like to extend my sincere gratitude to Edyta Kucharska, BEng, PhD, from the Department of Organic Chemical Technology and Polymer Materials at the West Pomeranian University of Technology in Szczecin, for her exemplary work on the biodegradation study. Her professionalism and dedication were essential in achieving the research objectives.

It is with great respect and gratitude that I acknowledge the role of Professor Oliver Krüger PhD, from the Berliner Hochschule für Technik in Berlin, for his invaluable contribution to this work. I profoundly appreciate the time and effort you dedicated to mentoring me and fostering an environment conducive to rigorous research and intellectual development throughout my internship.

CONTENTS

Abstract.....	6
Streszczenie	8
List of abbreviations, designations and acronyms	10
Introduction	15
1. Background and motivation	15
2. Objective and scope of the thesis	16
Chapter I: Theoretical framework	19
1. NSAIDs – Challenges in pain management.....	19
1.1. Problems with conventional solid-state NSAIDs	22
1.2. Avoiding the adverse effects of NSAIDs through structural modification.....	26
1.3. Topical and transdermal administration of NSAIDs	30
2. Ionic liquids – Redefining drug delivery strategies	34
2.1. API-ILs – better drug bioavailability	37
2.2. Adaptation of NSAIDs-based ionic liquids in pharmaceutical applications ...	41
Chapter II: Results and discussions	47
1. Synthesis and identification of NSAIDs salts with L-amino acids alkyl esters	47
2. Physicochemical properties of salts of L-amino acids alkyl esters and selected NSAIDs moieties	56
2.1. Solubility study.....	56
2.2. Lipophilicity study.....	63
2.3. Characteristics of the thermal properties	66
2.4. Specific rotation.....	78
3. Biological properties of salts of L-amino acids alkyl esters and selected NSAIDs moieties.....	81
3.1. Skin permeation studies.....	81
3.2. Skin accumulation studies	97
3.3. Antioxidant activity	98
3.4. Biodegradation study	100
3.5. Antimicrobial activity.....	105
Chapter III: Conclusions	111
Chapter IV: Experimental section	114
1. Synthesis of L-amino acids alkyl esters and their salts of selected acids from the group of non-steroidal anti-inflammatory drugs.....	114

1.1.	Synthesis of L-amino acid alkyl ester hydrochlorides.....	114
1.2.	Synthesis of alkyl esters of L-amino acids	114
1.3.	Synthesis of acid salts from the group of non-steroidal anti-inflammatory drugs.....	115
2.	Identification and determination of the purity of the obtained products and intermediate products.....	115
2.1.	Spectroscopic analysis	115
2.2.	Elemental analysis	115
3.	Characteristics of the physicochemical properties of the obtained products.....	116
3.1.	Determination of formation constant (pK _s).....	116
3.2.	X-ray diffraction (XRD)	116
3.3.	Thermogravimetric analysis	116
3.4.	Differential scanning calorimetry	116
3.5.	Stability testing under different storage conditions	117
3.6.	Specific rotation.....	117
3.7.	Solubility study.....	118
3.8.	Lipophilicity	119
4.	Characteristics of the biological properties of the obtained products	119
4.1.	Skin Permeation Studies.....	119
4.2.	Skin Accumulation Studies.....	120
4.3.	The antioxidant activity	121
4.4.	Biodegradation Studies.....	121
4.5.	Antimicrobial Activity Susceptibility Test	122
4.6.	Statistical Analysis.....	123
	References	124
	Appendix I	141
	L-amino acid alkyl ester salts of ibuprofen	141
	L-amino acid alkyl ester salts of ketoprofen.....	152
	L-amino acid ester salts of S-(+)-naproxen	161
	L-amino acid alkyl ester salts of salicylic acid	170
	Appendix II.....	179
	Reagents and Materials	179
	Formation constant, solubility and lipophilicity results.....	180

Thermal Properties results	191
Heat capacitvity experimental data	193
Stability test results	200
DSC curves for the stability study evaluation for NSAIDs and their L-amino acid isopropyl ester salts	204
Skin permeation results.....	224
Skin permeation profiles	224
Skin permeation parameters	228
Skin accumulation results.....	230
Antioxidant study results	231
Biodegradation study results	232
Antimicrobial activity results	234
Scientific achievements	236

Abstract

This thesis concerns the synthesis of salts of non-steroidal anti-inflammatory drugs (ibuprofen, ketoprofen, naproxen and salicylic acid) based on alkyl esters of L-amino acids. The main objective of this work was to obtain derivatives of the selected active substances, which belong to the group of ionic liquids, with an increased bioavailability and skin permeability compared with the parent drug.

The theoretical part focuses on the presentation of problems related to traditional forms of non-steroidal anti-inflammatory drugs (NSAIDs) and methods of counteracting them, with particular emphasis on transdermal and topical drug delivery and the transformation of the drug substance into an ionic liquid with pharmaceutical activity. The experimental part presents the synthesis and characterisation of the physico-chemical and biological properties of selected acids from the group of NSAIDs. The identification and the determination of the purity of the compounds obtained were mainly based on the analysis of the proton and carbon nuclear magnetic resonance spectra, the analysis of the FT-IR spectra and the elemental analysis.

Physical and chemical properties important for transdermal and systemic application were determined, such as: solubility in water, selected buffer solutions and organic solvents, lipophilicity, thermal stability, phase transition temperatures, and optical activity. The influence of the amino acid structure and the length of the alkyl chain in the ester part on the determined properties of the obtained derivatives and the possibility of their potential design depending on the selection of the starting cation were demonstrated.

In addition, the work focused on the determination of the biological properties, with particular emphasis on skin permeation tests and the ability to accumulate in the skin, which were carried out in collaboration with the Pomeranian Medical University in Szczecin. The biodegradability of the obtained derivatives, the antibacterial activity against selected strains of bacteria and the antioxidant activity have also been determined. A correlation between the biological properties and the drug counterion structure was also demonstrated.

It has been shown that modifying an acid from the NSAID group by combining it with an L-amino acid alkyl ester significantly increases the solubility of the drug substance in body fluids and its permeability through biological membranes. This can contribute to reducing the dose of the drug substance after its subsequent application and minimizing the occurrence of side effects. Furthermore, based on the research carried out, the structure

of the cation has also been selected to obtain salts with the most favourable parameters for further application and permeability through the skin.

Keywords: amino acid-based ionic liquids with pharmaceutical activity, non-steroidal anti-inflammatory drugs, transdermal and topical drug delivery

Streszczenie

Niniejsza praca dotyczy syntezy soli niesteroidowych leków przeciwzapalnych (ibuprofenu, ketoprofenu, naproksenu oraz kwasu salicylowego) na bazie estrów alkilowych L-aminokwasów. Głównym celem tej rozprawy było otrzymanie pochodnych wybranych substancji aktywnych, należących do grupy cieczy jonowych o zwiększonej biodostępności oraz przenikalności przez skórę w porównaniu do leku macierzystego.

Część literaturowa skupia się na przedstawieniu problemów związanych z tradycyjnymi postaciami niesteroidowych leków przeciwzapalnych (NLPZ) oraz metodami ich przeciwdziałania, ze szczególnym uwzględnieniem przezskórnego i naskórnego podawania leku oraz przekształcania substancji leczniczej w postać cieczy jonowej o aktywności farmaceutycznej.

W sekcji eksperymentalnej przedstawiono syntezę oraz charakterystykę właściwości fizykochemicznych i biologicznych pochodnych wybranych kwasów z grupy NLPZ. Identyfikację oraz określenie czystości otrzymywanych związków dokonano głównie w oparciu o analizę widm protonowego i węglowego magnetycznego rezonansu jądrowego, analizy widm FT-IR oraz analizy elementarnej.

Określone właściwości fizykochemiczne, istotne z punktu widzenia ich transdermalnej i ogólnoustrojowej aplikacji, obejmowały m.in. wyznaczenie rozpuszczalności w wodzie, wybranych roztworach buforowych oraz rozpuszczalnikach organicznych, lipofilowości, stabilności termicznej, temperatur przemian fazowych, aktywności optycznej. Wykazano wpływ budowy aminokwasu, długości łańcucha alkilowego w części estrowej na właściwości otrzymanych pochodnych oraz możliwość ich potencjalnego projektowania w zależności od doboru wyjściowego kationu.

Ponadto w pracy skupiono się na określeniu właściwości biologicznych, ze szczególnym uwzględnieniem badań przenikalności przez skórę oraz zdolności do akumulacji w skórze, przeprowadzonych przy współpracy z Pomorskim Uniwersytetem Medycznym w Szczecinie. Określono również zdolność biodegradacji otrzymanych pochodnych, aktywność przeciwbakteryjną wobec wybranych szczepów bakteryjnych oraz aktywność antyoksydacyjną. Wykazano również zależność między właściwościami biologicznymi a strukturą przeciwjonu dla substancji aktywnej.

Wykazano, iż modyfikacja kwasu z grupy NLPZ poprzez połączenie z estrem alkilowym L-aminokwasu znacząco wpływa na zwiększenie rozpuszczalności substancji leczniczej w płynach ustrojowych, przepuszczalności przez błony biologiczne,

co w następstwie późniejszej aplikacji może przyczynić się do obniżenia dawki leku i zmniejszenia skutków ubocznych. Dodatkowo, na podstawie przeprowadzonych badań wytypowano strukturę kationu, która zapewnia najkorzystniejsze parametry przenikalności przez skórę substancji aktywnej.

Słowa kluczowe: aminokwasowe ciecze jonowe o aktywności farmaceutycznej, niesteroidowe leki przeciwzapalne, transdermalne i naskórne podawanie leków

List of abbreviations, designations and acronyms

APIs	– Active pharmaceutical ingredients
API-ILs	– Active pharmaceutical ingredient-Ionic liquids
ATR-IR	– Attenuated Total Reflectance Infrared Spectroscopy
COX	– Cyclooxygenase
CUM	– Cumulative mass
D	– Diffusion coefficient
DMSO	– Dimethyl sulfoxide
DSC	– Differential Scanning Calorimetry
HPLC	– High-Performance Liquid Chromatography
(<i>R,S</i>)-IBU	– (<i>R,S</i>)-ibuprofen
S(+)-IBU	– S(+)-ibuprofen
ILs	– Ionic Liquids
J _{ss}	– Transdermal steady-state Flux
KETO	– (<i>R,S</i>)-ketoprofen
K _m	– Skin partition coefficient
K _p	– Permeability coefficient
logP	– Partition coefficient (<i>n</i> -octanol/ water)
L _T	– lag time
NAP	– S(+)-naproxen
NMR	– Nuclear Magnetic Resonance
NSAIDs	– Nonsteroidal anti-inflammatory drugs
PBS	– Phosphate-buffered saline
PGHS	– Prostaglandin endoperoxide H synthase
PGs	– Prostaglandin
SA	– salicylic acid
TG	– Thermogravimetric analysis
TMSCl	– Trimethylsilyl chloride
XRD	– X-Ray Diffraction Analysis

Abbreviations used for synthesized compounds:

[IleOMe]	L-isoleucine methyl ester
[IleOEt]	L-isoleucine ethyl ester
[IleOiPr]	L-isoleucine isopropyl ester
[IleOPr]	L-isoleucine propyl ester
[IleOBu]	L-isoleucine butyl ester
[IleOMe][HCl]	L-isoleucine methyl ester hydrochloride
[IleOEt][HCl]	L-isoleucine ethyl ester hydrochloride
[IleOiPr][HCl]	L-isoleucine isopropyl ester hydrochloride
[IleOPr][HCl]	L-isoleucine propyl ester hydrochloride
[IleOBu][HCl]	L-isoleucine butyl ester hydrochloride
[MetOMe]	L-methionine methyl ester
[MetOEt]	L-methionine ethyl ester
[MetOiPr]	L-methionine isopropyl ester
[MetOPr]	L-methionine propyl ester
[MetOBu]	L-methionine butyl ester
[MetOMe][HCl]	L-methionine methyl ester hydrochloride
[MetOEt][HCl]	L-methionine ethyl ester hydrochloride
[MetOiPr][HCl]	L-methionine isopropyl ester hydrochloride
[MetOPr][HCl]	L-methionine propyl ester hydrochloride
[MetOBu][HCl]	L-methionine butyl ester hydrochloride
[ThrOMe]	L-threonine methyl ester
[ThrOEt]	L-threonine ethyl ester
[ThrOiPr]	L-threonine isopropyl ester
[ThrOPr]	L-threonine propyl ester
[ThrOBu]	L-threonine butyl ester
[ThrOMe][HCl]	L-threonine methyl ester hydrochloride
[ThrOEt][HCl]	L-threonine ethyl ester hydrochloride
[ThrOiPr][HCl]	L-threonine isopropyl ester hydrochloride
[ThrOPr][HCl]	L-threonine propyl ester hydrochloride
[ThrOBu][HCl]	L-threonine butyl ester hydrochloride
[ValOMe]	L-valine methyl ester
[ValOEt]	L-valine ethyl ester
[ValOiPr]	L-valine isopropyl ester
[ValOPr]	L-valine propyl ester
[ValOBu]	L-valine butyl ester

[ValOAm]	L-valine pentyl ester
[ValOHex]	L-valine hexyl ester
[ValOHept]	L-valine heptyl ester
[ValOOct]	L-valine octyl ester
[ValOMe][HCl]	L-valine methyl ester hydrochloride
[ValOEt][HCl]	L-valine ethyl ester hydrochloride
[ValOiPr][HCl]	L-valine isopropyl ester hydrochloride
[ValOPr][HCl]	L-valine propyl ester hydrochloride
[ValOBu][HCl]	L-valine butyl ester hydrochloride
[ValOAm][HCl]	L-valine pentyl ester hydrochloride
[ValOHex][HCl]	L-valine hexyl ester hydrochloride
[ValOHept][HCl]	L-valine heptyl ester hydrochloride
[ValOOct][HCl]	L-valine octyl ester hydrochloride
[IleOMe][IBU]	L-isoleucinium methyl ester (<i>R,S</i>)-ibuprofenate
[IleOEt][IBU]	L-isoleucinium ethyl ester (<i>R,S</i>)-ibuprofenate
[IleOiPr][IBU]	L-isoleucinium isopropyl ester (<i>R,S</i>)-ibuprofenate
[IleOPr][IBU]	L-isoleucinium propyl ester (<i>R,S</i>)-ibuprofenate
[IleOBu][IBU]	L-isoleucinium butyl ester (<i>R,S</i>)-ibuprofenate
[MetOMe][IBU]	L-methioninium methyl ester (<i>R,S</i>)-ibuprofenate
[MetOEt][IBU]	L-methioninium ethyl ester (<i>R,S</i>)-ibuprofenate
[MetOiPr][IBU]	L-methioninium isopropyl ester (<i>R,S</i>)-ibuprofenate
[MetOPr][IBU]	L-methioninium propyl ester (<i>R,S</i>)-ibuprofenate
[MetOBu][IBU]	L-methioninium butyl ester (<i>R,S</i>)-ibuprofenate
[ThrOMe][IBU]	L-threoninium methyl ester (<i>R,S</i>)-ibuprofenate
[ThrOEt][IBU]	L-threoninium ethyl ester (<i>R,S</i>)-ibuprofenate
[ThrOiPr][IBU]	L-threoninium isopropyl (<i>R,S</i>)-ester ibuprofenate
[ThrOPr][IBU]	L-threoninium propyl ester (<i>R,S</i>)-ibuprofenate
[ThrOBu][IBU]	L-threoninium butyl ester (<i>R,S</i>)-ibuprofenate
[ValOMe][IBU]	L-valinium methyl ester (<i>R,S</i>)-ibuprofenate
[ValOMe][<i>S</i> (+)-IBU]	L-valinium methyl ester <i>S</i> -(+)-ibuprofenate
[ValOEt][IBU]	L-valinium ethyl ester (<i>R,S</i>)-ibuprofenate
[ValOEt][<i>S</i> (+)-IBU]	L-valinium ethyl ester <i>S</i> -(+)-ibuprofenate
[ValOiPr][IBU]	L-valinium isopropyl ester (<i>R,S</i>)-ibuprofenate
[ValOiPr][<i>S</i> (+)-IBU]	L-valinium isopropyl ester <i>S</i> -(+)-ibuprofenate
[ValOPr][IBU]	L-valinium propyl ester (<i>R,S</i>)-ibuprofenate
[ValOPr][<i>S</i> (+)-IBU]	L-valinium propyl ester <i>S</i> -(+)-ibuprofenate

[ValOBu][IBU]	L-valinium butyl ester (<i>R,S</i>)-ibuprofenate
[ValOBu][<i>S</i> (+)-IBU]	L-valinium butyl ester <i>S</i> -(+)-ibuprofenate
[ValOAm][IBU]	L-valinium pentyl ester (<i>R,S</i>)-ibuprofenate
[ValOAm][<i>S</i> (+)-IBU]	L-valinium pentyl ester <i>S</i> -(+)-ibuprofenate
[ValOHex][IBU]	L-valinium hexyl ester (<i>R,S</i>)-ibuprofenate
[ValOHex][<i>S</i> (+)-IBU]	L-valinium hexyl ester <i>S</i> -(+)-ibuprofenate
[ValOHept][IBU]	L-valinium heptyl ester (<i>R,S</i>)-ibuprofenate
[ValOHept][<i>S</i> (+)-IBU]	L-valinium heptyl ester <i>S</i> -(+)-ibuprofenate
[ValOOct][IBU]	L-valinium octyl ester (<i>R,S</i>)-ibuprofenate
[ValOOct][<i>S</i> (+)-IBU]	L-valinium octyl ester <i>S</i> -(+)-ibuprofenate
[IleOMe][KETO]	L-isoleucinium methyl ester (<i>R,S</i>)-ketoprofenate
[IleOEt][KETO]	L-isoleucinium ethyl ester (<i>R,S</i>)-ketoprofenate
[IleOiPr][KETO]	L-isoleucinium isopropyl ester (<i>R,S</i>)-ketoprofenate
[IleOPr][KETO]	L-isoleucinium propyl ester (<i>R,S</i>)-ketoprofenate
[IleOBu][KETO]	L-isoleucinium butyl ester (<i>R,S</i>)-ketoprofenate
[MetOMe][KETO]	L-methioninium methyl ester (<i>R,S</i>)-ketoprofenate
[MetOEt][KETO]	L-methioninium ethyl ester (<i>R,S</i>)-ketoprofenate
[MetOiPr][KETO]	L-methioninium isopropyl ester (<i>R,S</i>)-ketoprofenate
[MetOPr][KETO]	L-methioninium propyl ester (<i>R,S</i>)-ketoprofenate
[MetOBu][KETO]	L-methioninium butyl ester (<i>R,S</i>)-ketoprofenate
[ThrOMe][KETO]	L-threoninium methyl ester (<i>R,S</i>)-ketoprofenate
[ThrOEt][KETO]	L-threoninium ethyl ester (<i>R,S</i>)-ketoprofenate
[ThrOiPr][KETO]	L-threoninium isopropyl ester (<i>R,S</i>)-ketoprofenate
[ThrOPr][KETO]	L-threoninium propyl ester (<i>R,S</i>)-ketoprofenate
[ThrOBu][KETO]	L-threoninium butyl ester (<i>R,S</i>)-ketoprofenate
[ValOMe][KETO]	L-valinium methyl ester (<i>R,S</i>)-ketoprofenate
[ValOEt][KETO]	L-valinium ethyl ester (<i>R,S</i>)-ketoprofenate
[ValOiPr][KETO]	L-valinium isopropyl ester (<i>R,S</i>)-ketoprofenate
[ValOPr][KETO]	L-valinium propyl ester (<i>R,S</i>)-ketoprofenate
[ValOBu][KETO]	L-valinium butyl ester (<i>R,S</i>)-ketoprofenate
[IleOMe][NAP]	L-isoleucinium methyl ester <i>S</i> -(+)-naproxenate
[IleOEt][NAP]	L-isoleucinium ethyl ester <i>S</i> -(+)-naproxenate
[IleOiPr][NAP]	L-isoleucinium isopropyl ester <i>S</i> -(+)-naproxenate
[IleOPr][NAP]	L-isoleucinium propyl ester <i>S</i> -(+)-naproxenate
[IleOBu][NAP]	L-isoleucinium butyl ester <i>S</i> -(+)-naproxenate
[MetOMe][NAP]	L-methioninium methyl ester <i>S</i> -(+)-naproxenate

[MetOEt][NAP]	L-methioninium ethyl ester <i>S</i> -(+)-naproxenate
[MetOiPr][NAP]	L-methioninium isopropyl ester <i>S</i> -(+)-naproxenate
[MetOPr][NAP]	L-methioninium propyl ester <i>S</i> -(+)-naproxenate
[MetOBu][NAP]	L-methioninium butyl ester <i>S</i> -(+)-naproxenate
[ThrOMe][NAP]	L-threoninium methyl ester <i>S</i> -(+)-naproxenate
[ThrOEt][NAP]	L-threoninium ethyl ester <i>S</i> -(+)-naproxenate
[ThrOiPr][NAP]	L-threoninium isopropyl ester <i>S</i> -(+)-naproxenate
[ThrOPr][NAP]	L-threoninium propyl ester <i>S</i> -(+)-naproxenate
[ThrOBu][NAP]	L-threoninium butyl ester <i>S</i> -(+)-naproxenate
[ValOMe][NAP]	L-valinium methyl ester <i>S</i> -(+)-naproxenate
[ValOEt][NAP]	L-valinium ethyl ester <i>S</i> -(+)-naproxenate
[ValOiPr][NAP]	L-valinium isopropyl ester <i>S</i> -(+)-naproxenate
[ValOPr][NAP]	L-valinium propyl ester <i>S</i> -(+)-naproxenate
[ValOBu][NAP]	L-valinium butyl ester <i>S</i> -(+)-naproxenate
[IleOMe][SA]	L-isoleucinium methyl ester salicylate
[IleOEt][SA]	L-isoleucinium ethyl ester salicylate
[IleOiPr][SA]	L-isoleucinium isopropyl ester salicylate
[IleOPr][SA]	L-isoleucinium propyl ester salicylate
[IleOBu][SA]	L-isoleucinium butyl ester salicylate
[MetOMe][SA]	L-methioninium methyl ester salicylate
[MetOEt][SA]	L-methioninium ethyl ester salicylate
[MetOiPr][SA]	L-methioninium isopropyl ester salicylate
[MetOPr][SA]	L-methioninium propyl ester salicylate
[MetOBu][SA]	L-methioninium butyl ester salicylate
[ThrOMe][SA]	L-threoninium methyl ester salicylate
[ThrOEt][SA]	L-threoninium ethyl ester salicylate
[ThrOiPr][SA]	L-threoninium isopropyl ester salicylate
[ThrOPr][SA]	L-threoninium propyl ester salicylate
[ThrOBu][SA]	L-threoninium butyl ester salicylate
[ValOMe][SA]	L-valinium methyl ester salicylate
[ValOEt][SA]	L-valinium ethyl ester salicylate
[ValOiPr][SA]	L-valinium isopropyl ester salicylate
[ValOPr][SA]	L-valinium propyl ester salicylate
[ValOBu][SA]	L-valinium butyl ester salicylate

Introduction

1. Background and motivation

The group of non-steroidal anti-inflammatory drugs (NSAIDs), which have analgesic, anti-inflammatory, and antipyretic effects, is one of the most commonly used classes of drugs today. These drugs are attractive because of their broad spectrum of action and availability —most preparations containing active substances from this group are available without a prescription. Some of the most popular NSAIDs include ibuprofen, ketoprofen, naproxen, and salicylic acid.

Particularly in treating pain and fever, it is desirable to achieve rapid relief, which is directly related to the appropriate concentration of the drug in the blood. The rate of absorption into the blood, in turn, depends on the rate of dissolution of the active ingredient. However, the active ingredients of NSAIDs, which are carboxylic acids, have relatively high lipophilicity and poor solubility in aqueous media, especially in the acidic environment of the stomach. This necessitates the use of large doses, leading to a serious risk of side effects, such as damage to the mucous membrane of the stomach due to the acidic nature of the drugs.

Drug efficacy depends on bioavailability, influenced by solubility and permeability across biological membranes at the target site. The pharmaceutical market relies on crystalline forms of active pharmaceutical ingredients to meet the requirements of manufacturing methods, purity, thermal stability, and storage stability. However, in this form, drugs often have reduced solubility and undergo polymorphic transformations, resulting in compounds with different physical properties. An additional difficulty is posed by inactive and ballast substances present in medicines. All this can negatively affect their bioavailability and, consequently, the speed and effectiveness of the drug's action.

Effective drug formulation solutions must be sought due to the low solubility, bioavailability, stability and polymorphic transformation of solid drugs. Therefore, there is a growing interest in obtaining new NSAIDs that maintain or enhance the parent anti-inflammatory activity while avoiding the side effects associated with traditional drugs. The most promising trends concern the incorporation of pharmacological agents into ionic liquids (ILs) structures, so-called API-ILs (Active Pharmaceutical Ingredients-ILs). API-ILs can be used for topical and transdermal administration as an alternative to conventional crystalline salts. Another advantage of the salt form of NSAIDs is the avoidance of negative

side effects caused by the acidic nature of these drugs, mainly gastrointestinal damage. Overcoming some limitations in drug delivery is now an integral part of the strategy for advancing pharmaceutical molecules. One of the most promising solutions is the transdermal or topical administration of drugs. The main advantages are that they avoid the limitations associated with the gastrointestinal tract (effects of pH, gastrointestinal motility, intestinal transit time, and food intake) and first-pass metabolism. Topical administration also allows for the treatment of pain in patients suffering from gastrointestinal problems, dysphagia and vomiting. However, the low skin permeability of the active substance is another limitation. In this case, an important component of the pharmaceutical preparation to improve the therapeutic efficacy is the structural modification of the active ingredient or the use of appropriate percutaneous transport enhancers.

The challenge is to select a suitable counterion for the drug to improve bioavailability and permeability by achieving the desired physicochemical properties of the derivative. In this respect, the design of API-ILs based on amino acid alkyl ester moiety can stand as an improvement in the administration, not only for local but also for systemic administration of anti-inflammatory drugs. It is supposed to provide better bioavailability of pharmaceutical ingredients due to the presence of low toxic amino acid moiety as a counterion and contribute to significantly increased solubility in body fluids and permeability through biological membranes. In addition, the salts obtained can also be a potential source of essential exogenous amino acids.

2. Objective and scope of the thesis

The scope of the thesis was modification of acids from the group of non-steroidal anti-inflammatory drugs (ketoprofen, naproxen, salicylic acid and ibuprofen) with alkyl esters of selected L-amino acids (L-isoleucine, L-methionine, L-threonine and L-valine), to improve the solubility in body fluids and permeability across biological membranes, and thus bioavailability compared to the parent drug (Fig.1).

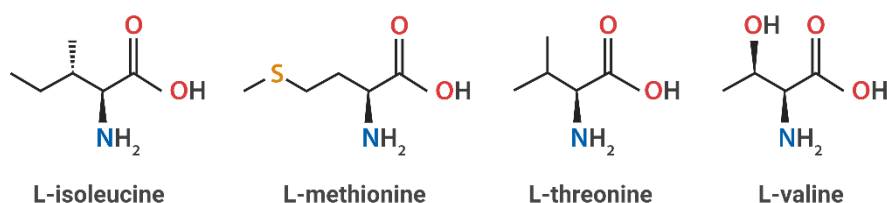


Fig. 1. The chemical structures of the L-amino acids selected to study in this work.

The selection of essential L-amino acids was based on their biological properties and chemical structure, which can potentially enhance the bioavailability of the compounds under investigation. L-valine, which has a bulky, highly hydrophobic side chain, is involved in various biological activities such as cell growth control and inhibition of fibroblast proliferation. L-isoleucine, another branched-chain aliphatic amino acid, is important for haemoglobin synthesis and regulation of blood sugar and energy levels. It is, therefore, important for maintaining physiological functions such as growth, immunity, protein metabolism, fatty acid metabolism and glucose transport. L-methionine, an aliphatic sulphur-containing amino acid, has been shown to regulate metabolic processes and the innate immune system and plays a crucial role in the activation of endogenous antioxidant enzymes. L-threonine, a polar amino acid containing a hydroxyl group in a side chain, making it polar, plays a role in the biosynthesis of proteins but also contributes to the maintenance of mucosal integrity, barrier structure and, ultimately, the control of immune function. The compounds obtained in the study are intended to be used as pharmacological agents in preparations applied to the skin with anti-inflammatory, analgesic and antipyretic effects while limiting the occurrence of negative side effects resulting from the acidic properties of NSAIDs in their traditional form.

The conversion of the drug molecule into the form of liquid organic salts, such as API-ILs, was particularly desirable. This approach should make it possible to neutralise the free carboxyl group, which is responsible for the adverse effects associated with orally administered drugs belonging to this group, and to avoid the polymorphism phenomenon that often occurs with solid-state drugs. In addition, the transformation of the active substance into the form of ionic liquids, with the cation obtained from natural and non-toxic raw materials such as amino acids, implies the possibility of increasing the permeability of the active substance through the skin.

In the present work, physicochemical properties, including solubility in water and some buffer solutions imitating body fluids, lipophilicity, thermal stability and phase transition temperatures were determined for salts of selected alkyl esters of L-amino acids with different alkyl chain lengths and acids from the NSAID group. Moreover, selected biological properties such as skin permeability and skin accumulation were determined. In addition, the increasing consumption of NSAIDs, inappropriate drug disposal practices and the lack of modern purification methods targeted at this group of pollutants influence the growing presence of NSAIDs in the environment. For this reason, the biodegradability of new NSAID derivatives was investigated in comparison with the parent acid. NSAIDs are

classified as non-antibiotics with broad antibacterial properties. This was also an incentive to investigate the effect of the applied NSAID modifications on selected strains of pathogenic bacteria.

The PhD thesis uses both the derivatives synthesized in this work for the first time and those obtained earlier and referred to in other studies.

The aim of the research was to look for correlations between the physicochemical and biological properties of the salts and the chemical structure of both the amino acid moiety and the length of the carbon chain in the ester group. On this basis, it was planned to select the optimal structures of counterion for each active substance molecule from among the examined alkyl esters of four amino acids, which allow the best results of drug bioavailability.

Chapter I: Theoretical framework

1. NSAIDs – Challenges in pain management

Non-steroidal anti-inflammatory drugs (NSAIDs) are among the most widely used pharmaceutical medicines because of their effectiveness in reducing pain and inflammation. In fact, ibuprofen is even included in the WHO's Model List of Essential Drugs [1]. These are a diverse group of compounds with similar biological abilities to reduce or eliminate erythema, swelling, fever and pain caused by various inflammatory stimuli. Currently, NSAIDs are among the world's most popular over-the-counter (OTC) medicines, representing also approximately 5-10% of all prescribed drugs [2–4].

NSAIDs are a large, structurally and functionally diverse drug class. Based on their chemical structure, they are mostly weak organic acids (consisting of an acidic moiety together with an aromatic functional group). They can be broadly classified into salicylates, aryl- and heteroaryl acetic acid derivatives, indole/indene acetic acid derivatives, anthranilates and oxicams (Fig. 2). In terms of functional diversity, the isoform-specific selectivity for the inhibition of prostaglandin endoperoxide H synthases (PGHS) was also used as a basis for the differentiation. Pharmacokinetic aspects of NSAID action in the systemic context, defined as serum half-life, were also considered for categorisation [4].

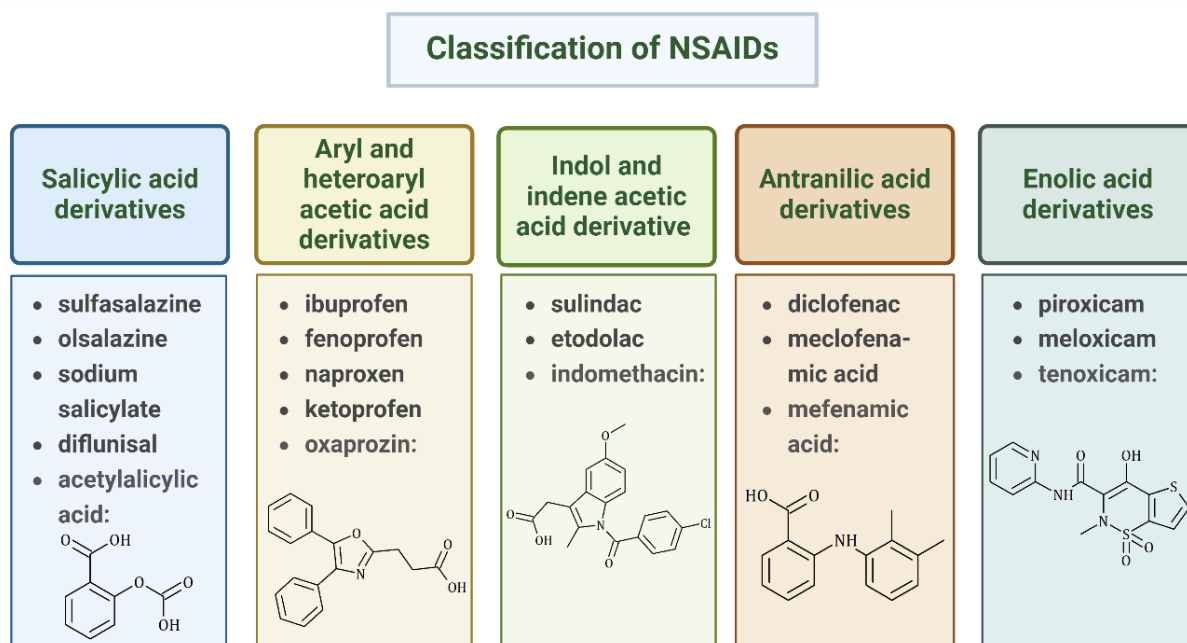


Fig. 2. Classification of NSAIDs according to chemical structure [4,5].

NSAIDs, like most formulated drugs, are administered orally, and by far, the most popular oral forms are tablets and other solid forms such as capsules. Some NSAIDs, such

as ketorolac, are also available parenterally. They are often stored as solids (mainly lyophilised products) and just before use. A range of pharmaceutical dosage forms, using different technologies to address a specific target profile or specific physicochemical properties of the active pharmaceutical ingredients (API), can be provided for each route of administration. The issue that needs to be addressed for any oral drug product is closely related to the properties of its solid state. The absorption profile of a drug from the gastrointestinal tract essentially depends on three factors: the dose, the solubility, and the permeability. The last two are the pillars of the Biopharmaceutical Classification System (BCS) proposed by Amidon et al. [6–10].

The majority of NSAIDs belong to Class II of the BCS due to their low solubility and high permeability profiles. With dissolution being the rate-limiting step, drugs in this group dissolve slowly and are absorbed rapidly. Thus, both oral and intravenous routes of administration are preferred. Regarding pharmacokinetics, most NSAIDs undergo no significant first-pass metabolism and enter the bloodstream almost exclusively via oral administration. However, this route of administration, while providing effective anti-inflammatory, analgesic and antipyretic properties, also has gastrointestinal side effects [9,11].

The main therapeutic action of non-steroidal anti-inflammatory drugs (Fig. 3) is based on their ability to inhibit the synthesis of certain prostaglandins (PGs) by blocking the activity of cyclooxygenase enzymes (COX-1 and COX-2). COX-1 is involved in the production of prostaglandins and thromboxane A₂, which are essential for the gastrointestinal (GI) mucosal barrier, renal homeostasis, platelet aggregation and other physiological functions. On the other hand, COX-2 is involved in the production of PGs associated with inflammation, pain and fever and is induced in inflammatory cells, unlike COX-1, which is expressed in normal cells. PGs are formed because of the conversion of polyunsaturated fatty acids, the most important of which is arachidonic acid (eicosatetraenoic acid). It is released from phospholipids under the influence of phospholipase A₂. Both COX enzymes convert arachidonic acid into prostaglandins (PGF_{2α}, PGD₂, PGE₂), thromboxanes (TXA₂) and prostacyclins (PGI₂). Prostaglandins are produced by almost all cell types, usually one or two major types, and act as autocrine and paracrine lipid mediators that help maintain local balance in the body. In situations of inflammation, there is a significant shift in both the amount and type of prostaglandins produced. Normally, prostaglandin levels are low in tissues without inflammation, but they

rise rapidly during episodes of acute inflammation, even before leukocytes arrive and immune cells begin to invade the affected areas [2,4,12–14].

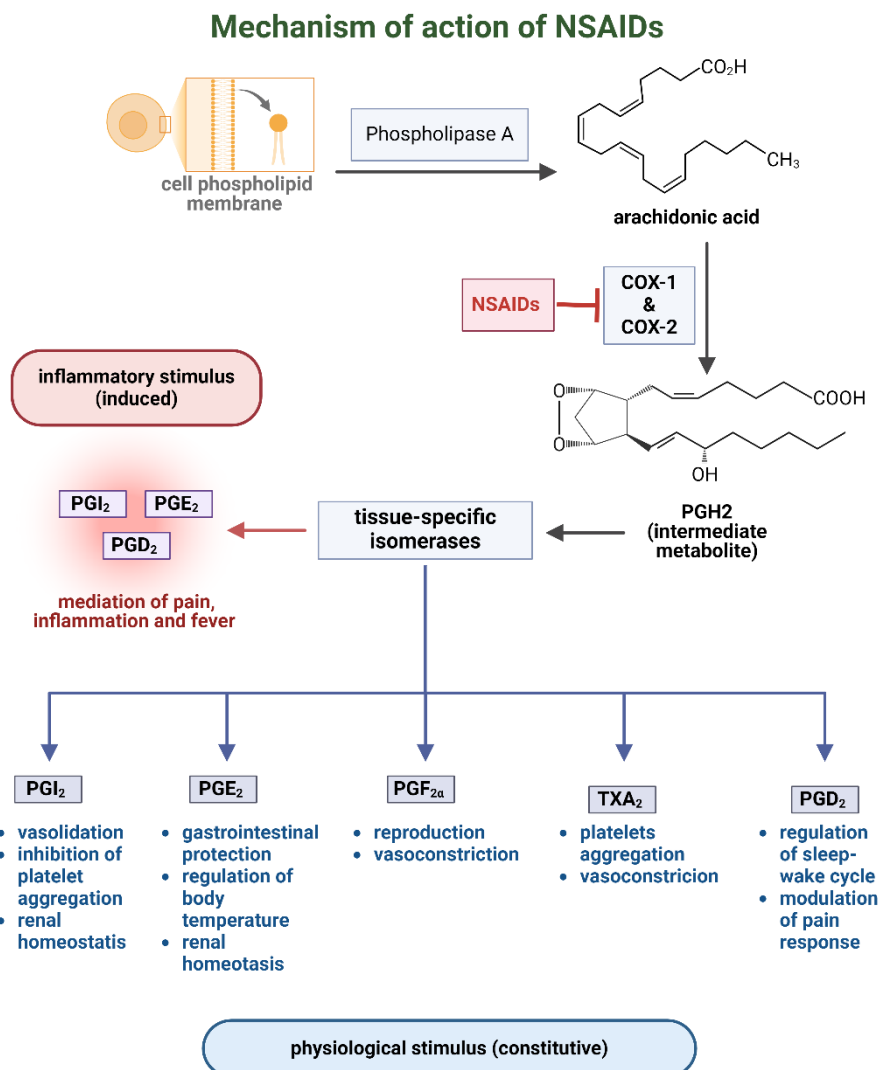


Fig. 3. Schematic of the mechanism of action of NSAIDs [4,15].

The different affinities of NSAIDs for these COX enzymes impact their therapeutic efficacy and potential for adverse effects. In particular, due to the role of COX-1 in maintaining the integrity of the gastroduodenal mucosa, preferential inhibition of COX-1 is associated with an increased risk of gastrointestinal complications. On the other hand, selective inhibition of COX-2 can lead to adverse cardiovascular and renal effects. This has been attributed to the expression of COX-2 in the vascular endothelium and its involvement in renal function. Inhibition of COX-2 can impair glomerular filtration rate and promote sodium retention, oedema and potentially heart and kidney failure. In addition, emerging evidence suggests that NSAIDs may also exert effects independent of PG endoperoxide-H synthase (PGHS)/COX inhibition, such as direct effects on mitochondria leading

to oxidative stress and apoptosis, thus highlighting alternative pathways of NSAID-induced cytopathology [2,3,16].

The discovery of two COX isoenzymes led to the development of COX-2-selected NSAIDs (e.g. celecoxib) designed to minimise gastrointestinal side effects by sparing COX-1, which maintains the integrity of the stomach lining. However, the benefits of COX-2 selectivity have been outweighed by concerns over cardiovascular and renal side effects, leading to the withdrawal of several COX-2 inhibitors by regulatory agencies. This situation highlights the complex balance between therapeutic efficacy and the risk of adverse effects associated with NSAID use. Furthermore, recent research suggests that NSAIDs can cause cytopathic effects through mechanisms not related to COX inhibition, including direct effects on mitochondria leading to oxidative stress and apoptosis. These findings suggest alternative pathways by which NSAIDs may cause harm and add complexity to the risk-benefit assessment of these drugs [17,18].

Despite advances in the understanding of NSAIDs and the development of selective inhibitors, optimising therapeutic outcomes while minimising adverse effects remains a major challenge, particularly in the management of chronic diseases such as rheumatoid arthritis and osteoarthritis. Given these complexities, there is an urgent need for careful management of NSAID use, particularly in vulnerable populations such as older people. This includes cautious drug selection, dosing, monitoring for adverse effects and consideration of drug-drug interactions. This underlines the need for continued research and development to improve the safety and efficacy of NSAID therapy. Continued advances in NSAID research are essential to develop safer therapeutic options that provide effective pain relief and inflammation control without compromising overall health.

1.1. Problems with conventional solid-state NSAIDs

When a drug substance is formulated as a solid, the form of the drug substance in the medicinal product can be selected from a wide variety of forms, including polymorphic, solvated, hydrated, salt, co-crystalline and amorphous. Each of these forms can have significantly different physicochemical properties. These, in turn, can affect solubility, dissolution rate, bioavailability, stability, processability or manufacturability [19,20].

The solid-state of drugs is generally considered to be safe and stable. However, there are a number of disadvantages associated with this form of the drug (Fig. 4). The main concern is poor solubility, which leads to reduced bioavailability, meaning less drug is absorbed into the bloodstream, reducing effectiveness. Crystalline drugs often have lower

solubility than their amorphous or liquid counterparts. In addition, the bioavailability and therapeutic efficacy of a solid drug can be affected by its dissolution rate - a slower dissolution rate can delay the onset of drug action, which can be a significant disadvantage in treatments where a rapid onset of action is desirable [21,22].

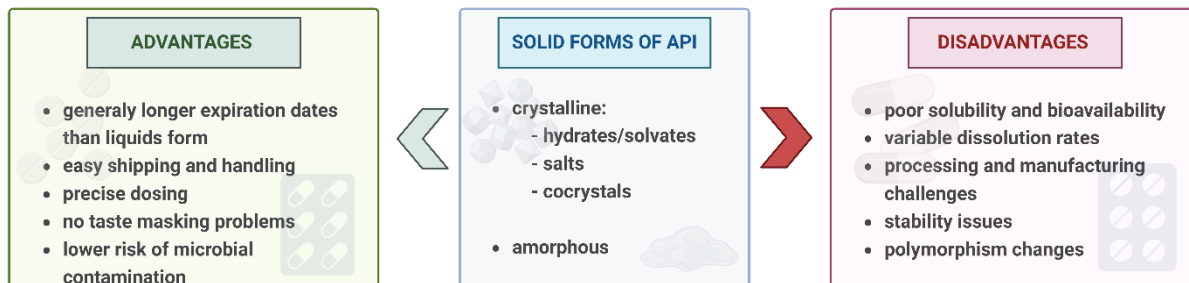


Fig. 4. Main advantages and disadvantages of the solid state of APIs [23,24].

The process of manufacturing solid dosage forms also presents its challenges. The behaviour of solid dosage forms can be significantly influenced by particle size, which in turn affects dissolution rate, absorption and bioavailability. Controlling particle size to the required specifications can be difficult and costly. Solid dosage forms can also be sensitive to changes in temperature, which can affect their stability. For example, exposure to high temperatures can cause melting, degradation or a change in crystalline structure. Solid drugs can also undergo different types of degradation, such as oxidation, hydrolysis and photodegradation. In addition, solid drugs can change their crystalline form alterations, known as polymorphism. They can also change from an amorphous state to a more stable crystalline form under certain conditions, which can alter their chemical stability and efficacy [20,25–29].

Furthermore, some solid drugs absorb moisture from the air, which can cause clumping, change the crystal structure or degrade the drug. Managing hygroscopicity requires careful packaging and storage, adding cost and complexity to the handling process. It can also be complex and costly to produce a consistent and stable solid form of a drug substance. Issues such as polymorphism, where the API may exist in multiple crystalline forms, each with different physical and chemical properties, further complicate the manufacturing process [30–34].

An important step in the integrated approach to solid-state problems is to identify and characterise all the relevant features of the solid form, as each has important implications for the future efficacy of the drug. To overcome the challenge of low aqueous solubility, these NSAIDs have been the subject of research to develop improved release systems, such as solid dispersions, microparticles, microcapsules, microemulsions and nanoparticles.

Modification of the solid state is another promising approach to increasing aqueous solubility. The active ingredient can exist as either a single or multiple components in the crystalline form of a drug molecule. Single-component drug molecules are limited to polymorphs and allow only subtle changes in the physicochemical properties of the API. Multi-component drug molecules, on the other hand, offer a wide range of altering the physicochemical properties. These solid-state modifications of a drug may include other polymorphic forms, solvates/hydrates, cocrystals or salts [8,20,35].

Polymorphism refers to the potential for a limited variety of solid-state manifestations inherent in each substance with a defined structural formula. A given compound can exist in multiple crystalline solid states. Polymorphs, therefore, contain molecules of a single chemical nature. In pharmaceutical development and manufacturing, the selection of a specific polymorph can be a strategy to optimise the performance of a drug. Most drugs exhibit polymorphism, but the most stable form is recommended to ensure reproducibility of the product formulation and stability throughout its lifetime. In the case of NSAIDs, the polymorph with the higher bioavailability is often the one with the higher dissolution rate, although this is not always directly proportional. Higher dissolution rates improve the amount of drug available for absorption in the gastrointestinal tract, potentially increasing bioavailability. However, these metastable forms (often with higher dissolution rates) also present challenges as they tend to transform into more stable forms under storage or physiological conditions, which can reduce their efficacy over time. The use of metastable polymorphs with higher bioavailability often requires careful formulation and stabilisation strategies to prevent them from converting to a more stable but less bioavailable form. Examples include form I of indomethacin and piroxicam, which are known to have a higher dissolution rate than the more stable form II [6,9,36–38].

Many drugs can form solvates or hydrates, specific types of crystal structures in which the drug incorporates molecules of a solvent or water into their crystal lattice. This incorporation can affect the stability, solubility, and bioavailability of the drug — generally, increased degrees of hydration result in lower dissolution rates. In the case of NSAIDs, substances that form hydrates and solvates under certain conditions are currently under investigation. These forms may exhibit different physical and chemical properties compared to the anhydrous form, which is marketed today as a single-component drug. Research is ongoing regarding the hydrates of NSAID salts. For example, sodium naproxenate exhibits improved compressibility when converted from its anhydrous to hydrate form. Sodium ibuprofenate, also marketed, exists in a stable dihydrate form. Understanding the hydration

and dehydration behaviour of drugs is fundamental for developing stable pharmaceutical formulations and predicting appropriate storage conditions for drugs and solid dosage forms. From a technological perspective, the processing and storage conditions of medicinal products can lead to the formation of undesirable solvates or hydrates, complicating the manufacturing processes. Non-stoichiometric hydrates can cause issues, as the drug substance may contain varying amounts of water, meaning the API content may not be proportional to the mass [20,39–44].

Cocrystals represent an innovative approach in pharmaceutical formulation, offering an alternative to salts when these do not possess the appropriate solid-state properties or cannot be formed due to the absence of ionisable sites in the API. This multi-component system improves previously poor physicochemical and mechanical properties through non-covalent interactions, thereby enhancing the dissolution behaviour and bioavailability of the drug. For pharmaceutical compounds like NSAIDs, which often exhibit poor solubility, co-crystallisation has the potential to improve their properties without modifying their therapeutic action. However, one of the primary challenges in cocrystal formation is the selection of appropriate co-formers. This task is critical as the difficulty in selecting co-formers can lead to unexpected results such as decreased solubility and dissolution rates, spring and parachute effects, microenvironment pH changes, instability, and polymorphisms during the cocrystal development process. These co-formers, often carboxylic acids and amides due to their pKa similarities with NSAIDs, must be pharmaceutically acceptable and capable of forming a stable, crystalline complex with the NSAID that exhibits desirable properties without adversely affecting the drug's efficacy. To date, the clinical success of the celecoxib-tramadol cocrystal, which has reached Phase III for the treatment of acute pain, marks the only cocrystal of an anti-inflammatory drug to have reached the pharmaceutical market [8,45,46].

Finding new solid dosage forms should utilise a systematic methodology that adapts to various product development and manufacturing stages. Each stage necessitates a distinct level of research into the solid state, tailored according to the development phase, the route of administration, and the dosage form. Ideally, the thermodynamically stable form should be ready for Phase I of clinical development under ambient conditions. However, a comprehensive understanding of the drug substance's behaviour is crucial for further pharmaceutical development and to ensure the successful delivery of the chosen form. The primary objective of solid dosage form screening and selection is to identify and select

the optimal forms, guided by biopharmaceutical and physicochemical considerations, ensuring the effective action of the drug in patients [6,20,47].

1.2. Avoiding the adverse effects of NSAIDs through structural modification

As mentioned before, the management of NSAID therapy is particularly complex in the elderly population, who are at high risk of polypharmacy and drug-drug interactions due to the multitude of medications typically required to manage their comorbidities. The potential for serious drug interactions and potentially fatal adverse effects if prescriptions are not carefully monitored is significant. NSAIDs are associated with numerous adverse effects that can affect several critical body systems. These include gastrointestinal complications such as ulcers and bleeding due to the impact on the gastric mucosa, renal damage caused by a decrease in prostaglandins, resulting in reduced renal plasma flow, increased risk of myocardial infarction, thromboembolic events and other cardiovascular problems due to effects on the cardiovascular system, hepatotoxicity usually associated with use of high doses or overdoses, and complications related to blood coagulation and other haematological functions due to impact on the haematological system [4,16–18,48–50].

While harnessing the therapeutic benefits of NSAIDs, some known preventive approaches that reduce the risk of complications by co-administering gastroprotective or cytoprotective agents, such as the PG E1 analogues Cytotec™ (misoprostol), which replace endogenous PGs and can significantly reduce both acute and chronic NSAID gastric and duodenal ulcers. Unfortunately, their use is often limited by high rates of GI side effects, including dyspepsia and diarrhoea, and poor compliance with multiple daily dosing [51,52].

However, the ultimate goal is to maintain the anti-inflammatory efficacy of NSAIDs with a reduction in their adverse effects. For this reason, there is an increasing focus on the development of therapeutic agents based on known NSAID molecules, known as pharmacophore modification. Pharmacophore modification is the alteration of the molecular structure of a drug to enhance its beneficial properties and minimise adverse effects. This can be achieved by changing certain chemical groups within the drug molecule. Alternatively, molecules can be designed to interact more selectively with biological targets. Prodrugs are a specific and increasingly popular approach within this strategy. A prodrug is a compound administered in an inactive or less active form. Once in the body, it is metabolised to its active form by chemical and/or enzymatic reactions. This process can help improve the tolerability, safety and efficacy of the drug. For NSAIDs, the use of prodrugs

can potentially reduce the exposure of the gastrointestinal tract to the active drug, thereby reducing the risk of side effects such as ulcers and bleeding [4,53,54].

Over the years, several non-acidic prodrug NSAIDs have been developed that require metabolic activation to form the active moiety, such as aspirin, nabumetone, loxoprofen, sulindac, fenbufen, salsalate, parecoxib, droxicam. Aspirin was originally thought to be a prodrug of salicylic acid. It was later found that aspirin also directly acetylates and irreversibly inhibits COX enzymes, resulting in anti-inflammatory and antithrombotic effects. The ongoing development of prodrug NSAIDs reflects the continuing evolution of drug safety profiles and the provision of more effective NSAID therapy for pain and inflammation [3,55–59].

Initially, most approaches to the synthesis of NSAID prodrugs were aimed at the masking of the acidic functional group or the carboxyl moiety. Of particular value is the development of NSAID prodrugs capable of releasing nitric oxide (NO) or hydrogen sulphide (H₂S), two important endogenous gaseous signalling molecules involved in various physiological functions. Their incorporation into NSAID structures is expected to improve the therapeutic profile of these drugs, as NO and H₂S provide additional benefits in gastric mucosal protection and modulation of various cardiovascular functions. By attaching their carboxylic acid to one or more dialkylphosphate moieties via a spacer, a novel group of modified NSAIDs, called phospho-NSAIDs, has been obtained. Preclinical studies have been conducted to evaluate the anti-inflammatory efficacy and GI safety of phospho-aspirin, phospho-ibuprofen and phospho-sulindac. They have been shown to be pharmacologically more potent and safer molecules than their parent NSAIDs. Despite these promising properties, these drugs have not yet been approved, as they are still in the clinical trial phase. A number of medicines in this class are currently in clinical trials, and a significant amount of clinical data will be required for their potential approval [3,55–59].

Over time, the concept of NSAIDs prodrugs evolved to the synthesis of derivatives with specific targets, including antioxidant properties, improved water solubility and dissolution rates, and achievement of targeted delivery to specific sites. Commonly used approaches for prodrug synthesis include amide, ester and mutual prodrugs (Fig. 5) [4,51,54,60,61].

Ester prodrugs are most commonly produced by combining drugs with carboxylic acid groups and drugs with alcoholic or phenolic groups under different esterification conditions. Esterification of NSAIDs masks the free carboxylic acid group, reducing gastrointestinal side effects until the ester linkage is cleaved enzymatically. This often occurs

in tissues with the appropriate enzymes or systemically in the liver. Common esterifying agents include alcohols such as ethanol, methanol or more complex alcohols that can impart additional desirable properties (e.g. increased lipophilicity). This modification can improve solubility, absorption and distribution, and often, the ester is hydrolysed to release the active NSAID once it reaches more favourable environments such as the bloodstream or specific target tissues [62–64].

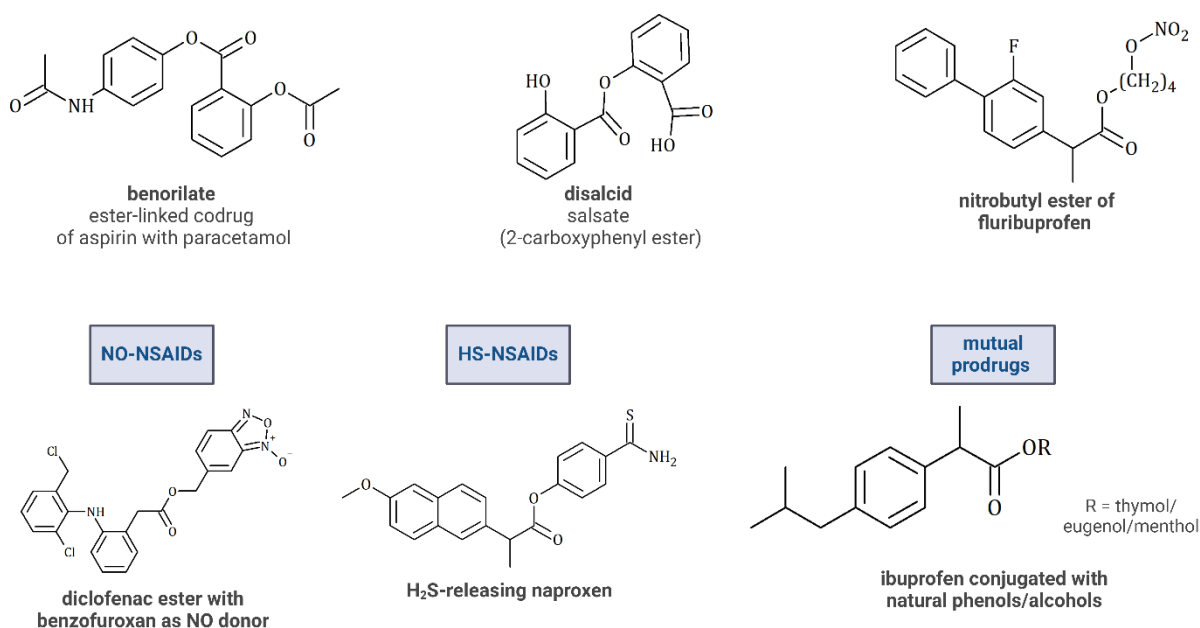


Fig. 5. Representation of the chemical structures of some NSAID prodrugs [4].

A hydrophobic ester of acetylsalicylic acid (aspirin) and *N*-acetyl-*p*-aminophenol (paracetamol) was the first NSAID mutual prodrug, often called a benorylate. In this formulation, the hydroxyl group of paracetamol has been ester-linked to the carboxylic acid group of aspirin. Paracetamol prevents the erosive effect of aspirin through the activation of gastric PG synthetase. As a result, the risk of irritation of the gastric mucosa was reduced. On the basis of this concept, various strategies have been used to combine two therapeutic agents by amide linkage, in which one component alleviates the gastrointestinal side effects of the other. There are known derivatives of NSAIDs obtained from gastroprotective agents, such as antioxidants, amino acids, flavonoids, glycerides, and polymers [65,66].

NSAIDs are good candidates for salt formation during the drug development process due to the presence of an acidic functional group. Neutralisation of the carboxyl group is the basis for the reduction of gastric irritation. However, this approach is known to impact some aspects of drug performance. Conversion of NSAIDs to salt forms affects other properties that are critical for further drug delivery.

It is well known that the formation of active ingredients in salt is an integral part of the formulation development process. The contribution of pharmaceutical salts to first-in-class drugs – that is, drugs with novel mechanisms of action that offer a new therapeutic approach to the treatment of a disease – is around 40%. Traditionally, improving solubility in aqueous solutions has been one of the main reasons for obtaining salts. Improved solubility often leads to better absorption in the gastrointestinal tract, which is particularly beneficial in oral formulations where rapid dissolution is required for fast absorption. This can further improve the bioavailability of the drug, which is the proportion of the drug that enters the bloodstream and can have an active effect when introduced into the body. As counter ions alter the pharmacokinetics and toxicokinetics, some salt forms are more rapidly absorbed than their parent drugs, which can be critical for therapeutic efficacy, particularly in the management of pain where a rapid onset of action is desired. Some salt forms can offer improved stability, reducing the degradation of the drug during storage and thereby extending the shelf life of the product. Finally, salt forms can provide versatility in drug formulation and extend the route of drug administration. For example, certain salts may be more suitable for injectable solutions, effervescent tablets or fast-acting formulations like aerosols, creams, ointments, and gels [53,67–69].

Various salts can be used to produce the ingredients of NSAIDs. For example, ibuprofen salts or complexes with sodium, magnesium, zinc and aluminium are known on the market. The choice of counterion for the active ingredient is critical to achieving the most effective therapeutic effect at a given drug dose. For example, the potassium salt of diclofenac has better solubility in water. It also dissolves and is absorbed more rapidly than sodium salt, resulting in more consistent absorption and a shorter onset of analgesia. Other counterions of choice are amino acids. These are used in several developed and marketed pharmaceutical salts due to their very low toxicity and ionisable properties, ease of implementation in the process, and low cost of production. The study showed that commercially available arginine and lysine-based ibuprofen salts provide a faster onset of action, giving patients greater pain relief than standard ibuprofen. Similarly, in addition to a better onset of action, the lysinium salt of ketoprofen shows better gastrointestinal and renal tolerability than standard ketoprofen [70–75].

While the conversion of NSAIDs to their salt forms offers several advantages leading to improved bioavailability, it also presents several disadvantages and potential challenges related to the formulation, stability, efficacy and regulatory aspects of drug development. Disadvantages include reduced drug content in the formulation, increased formation

of polymorphs and hydrates leading to greater variability in pharmaceutical properties, and additional synthesis steps leading to increased manufacturing time and cost. Therefore, the ongoing objective in the development of API salts is to improve therapeutic efficacy and patient compliance without compromising safety or significantly increasing the cost of the drug [76,77].

1.3. Topical and transdermal administration of NSAIDs

The increased attention on the consequences of oral NSAID use has led to increasing recommendations to use them via topical and transdermal routes. Topical and transdermal drug delivery systems represent advanced non-invasive methods for administering medications either locally or systemically (Fig. 6).

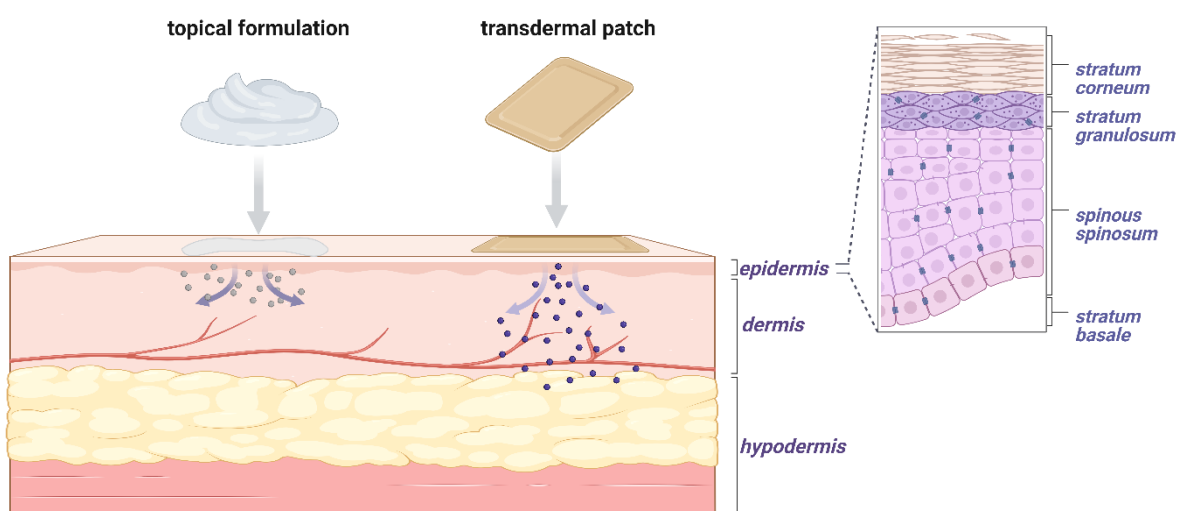


Fig. 6. Skin structure with applied topical formulation and transdermal patch (TDDS) [80,81].

These systems, which have evolved from simple concoctions to highly sophisticated delivery mechanisms, leverage a deep understanding of drug-product-skin interactions and percutaneous absorption. Topical delivery systems are primarily designed for local application, targeting skin disorders or localised pain directly beneath the skin. These systems utilise vehicles such as creams, gels, foams, sprays, and patches to facilitate passive drug transport across the skin layers — from the *stratum corneum* (SC) down to deeper tissues like the joint capsule and muscles. Transdermal delivery systems (TDDS), on the other hand, aim for systemic drug delivery by absorbing active substances through the skin into the bloodstream. This method employs technologies such as patches, often applied on areas like the chest, arm, or abdomen and can also involve active delivery mechanisms that disrupt the *stratum corneum* [78,79].

Topical and transdermal drug delivery systems are advantageous as they bypass the first-pass metabolism in the liver, enhancing the bioavailability of drugs. First-pass metabolism involves a decrease in the concentration of the active drug after it has been absorbed from the gastrointestinal tract and before it reaches the general circulation. This means that after being absorbed in the intestine, the drug enters the bloodstream almost exclusively through the portal circulation system, passing through the liver in the first place. Topical and transdermal drug delivery avoids the first-pass effect by allowing drugs to be absorbed directly into the systemic circulation. This also avoids potential degradation of the active ingredient in the gastrointestinal tract. Topical applications, such as gels, provide direct action at the application site. This method avoids gastrointestinal irritation and allows for the precise delivery of drugs to targeted areas. Moreover, the benefits of topical drug delivery systems are the convenience and ease of application, avoidance of the risks and inconveniences associated with intravenous therapy, and adaptability to pH changes and various gastric conditions. They allow for easy termination of drug administration when necessary. They can deliver drugs more selectively to specific sites, thereby enhancing patient compliance and potentially reducing the overall daily dose required for efficacy. These systems are particularly advantageous for active substances with short biological half-lives or a narrow therapeutic window as they maintain steady drug levels. On the other hand, TDDS also allows for controlled drug release (up to one week), which has become a crucial strategy in managing pain, hormonal therapies, and treating cardiovascular and central nervous system diseases. TDDS is well-known and beneficial for providing sustained drug delivery, achieving lower fluctuations in plasma drug levels, and avoiding metabolic interactions in the intestine and liver. This method is particularly favourable for drugs that induce nausea, interact with food or other drugs, or are inactivated in the gastrointestinal tract. Moreover, patient compliance is generally high due to the non-invasive nature of the delivery, the absence of needle phobia, and the ease of therapy termination [65,78,82–85].

Based on the pharmacokinetic evidence combined with the results of post-marketing surveillance, topical NSAIDs do not have the same risk of adverse events as oral NSAIDs. Transdermal drug delivery systems, particularly those involving NSAIDs, have shown great promise but have not yet been able to realise their potential in clinical practice fully. At the same time, topical formulations have been widely accepted and used, with various innovative strategies being employed to improve their efficacy and safety profiles. Topical NSAIDs have the same mechanism of action as systemic formulations and have also been shown to be more effective in mild to moderate acute pain conditions, with limited efficacy

in chronic musculoskeletal pain. Certain NSAIDs are widely used and have been tested on several different formulations and for many other conditions. High-quality evidence supports the analgesic role of several topical NSAIDs, including diclofenac (i.e. diclofenac sodium 1.5% topical solution, diclofenac hydroxyethylpyrrolidine 1.3% patch and diclofenac sodium 1% gel), ketoprofen (i.e. ketoprofen 2.5% gel), ibuprofen (ibuprofen 5% gel, ibuprofen 5% with levomenthol 3% gel). NSAIDs are also used for non-proprietary compound formulas of several active ingredients that can be custom-made by prescription. Salicylate-based topical products are also known but are more commonly used as rubefacients [18,86–90]. Transdermal patches containing diclofenac and flurbiprofen are available on the market for the treatment of short-term pain from minor strains, sprains and bruises. However, the potential of transdermal delivery systems is still being explored in the case of NSAIDs. For example, transdermal delivery of NSAIDs via nanocarriers has been studied as an interesting strategy and has been shown to offer both targeted therapy and a drug safety profile. Innovative materials such as chitosan and polyvinyl alcohol, when cross-linked with agents such as sodium tripolyphosphate, have also shown potential in improving transdermal permeation rates of drugs such as diclofenac sodium. These patches, tested in models like rabbit skin, have demonstrated increased drug delivery efficiency, suggesting their potential for wider applications [91–93].

Topical and transdermal delivery offers an attractive and non-invasive method of drug delivery. However, the human skin is remarkably efficient at preventing substance penetration. The skin is a complex, multi-layered structure that covers an area of 1.5 to 2 m² in adults. Its main function is a barrier between the body and the relatively hostile external environment. The *stratum corneum* is a highly structured, lipid-rich region that minimises the movement of water, oxygen and chemicals in and out of the skin. Topical products may act on sites in one or more of the different skin layers (i.e. epidermis, dermis and hypodermis), the skin appendages (i.e. hair follicles, with associated sebaceous glands, sweat glands and nails) and the underlying tissues. The viable epidermis is the primary target for most topical products. Targeted sites include nerves, keratinocytes, melanocytes, Langerhans cells and hair follicles. For transdermal delivery, a drug must cross the epidermis into the dermis (through the phospholipid membrane and the cytoplasm of the dead keratinocytes) to reach the cutaneous blood vessels and, subsequently, the systemic circulation. Therefore, having to overcome both lipophilic and hydrophilic barriers, drug molecules encounter resistance as they permeate [78,82,84,94].

Transdermal drug delivery is very simple in concept and very challenging to achieve. The effectiveness of topical and transdermal drug delivery systems is significantly influenced by the physicochemical properties of the compounds they carry, alongside several key factors related to the product and its interaction with the user. Many drugs, such as those from the NSAID class, often fail to meet the necessary criteria for effective skin penetration. These criteria include having a low molecular weight (typically molar mass under 500 g/mol), moderate lipophilicity (logP between 1 and 3), and a low melting point (below 250°C), which are essential for passive permeation through the skin in therapeutic quantities since it reflects the non-covalent interactions between drug molecules and relates to drug solubility in the SC. Furthermore, the overall success and safety of these products are affected by multiple factors: application conditions (these include how a product is applied, the area of application, and the duration of contact with the skin, all of which can alter drug delivery rates and effectiveness), skin physiology (individual differences in skin structure and function, such as skin hydration level, integrity of the *stratum corneum*, and the presence of skin disorders, can significantly influence drug absorption and action), product perception and consumer acceptance (the perceptions and experiences of users with a topical or transdermal product can affect its commercial success and therapeutic adherence) [78,80,84,94,95].

In general, the effectiveness of drug delivery to and through the skin is highly dependent on the formulation components. In addition, dermatological drugs often deliver only a portion of the total dose applied, resulting in low drug bioavailability in the skin. This limitation, compounded by the influence of the innate physicochemical properties of the active ingredient, limits the efficacy of purely topical formulations for the treatment and prevention of disease. In order to facilitate the delivery of therapeutic doses of drugs through the skin, various techniques have been developed to reduce skin barrier resistance temporarily. These methods can be broadly categorised into physical and chemical approaches, including chemical enhancers, vesicles and particles (e.g. high-velocity particles), microneedles, *stratum corneum* ablation (including lasers), iontophoresis, ultrasound and electroporation. For high molecular weight substances, mechanisms utilising both intracellular and intercellular pathways are employed due to the structural complexity of the skin, which contains lipid regions interspersed with cells and both hydrophilic and hydrophobic substances. However, the use of chemical and physical enhancers carries the risk of irritation, which can cause damage and compromise skin barrier function [82,94–99].

Developing a stable, effective topical or transdermal formulation to deliver NSAIDs is technically challenging. The formulation must maintain the stability and activity of the NSAID throughout the shelf life of the product, in addition to facilitating penetration of the skin. Drug delivery research continues to expand the therapeutic uses of NSAIDs delivered through the skin barrier by developing more sophisticated systems that could potentially overcome these challenges. In addition to the form of the NSAID (acid, anion, ion pair), the design of the formulation excipients, including penetration enhancers, plays a critical role in determining how to optimise topical and transdermal drug delivery.

2. Ionic liquids – Redefining drug delivery strategies

Ionic liquids (ILs), a class of substances that emerged in the early twentieth century, are versatile materials composed entirely of ions and primarily defined by their melting points below 100°C. Those that exist as liquids at or near room temperature due to their chemical structure, in which ion-ion interactions and symmetry are finely balanced, are known as room-temperature ionic liquids (RTILs). Typically, an IL consists of an organic cation, which may contain one or more substituted alkyl chains and an inorganic or organic anion. The wide variety of possible cation-anion combinations allows the properties of ILs to be tuned for specific applications. Interest in ILs surged in the mid to late 1990s, driven largely by the idea that they could contribute to green chemistry by eliminating volatile organic solvents in chemical synthesis. Due to their negligible vapour pressure caused by strong ionic bonds and high thermal stability, ILs lack the hazardous properties of VOCs. They are, therefore, almost ideal solvents with a low environmental impact. Furthermore, unlike some low-boiling solvents such as petroleum ether, dichloromethane, acetone, and many others, the non-volatile nature of most ILs also contributes to their non-flammability in ambient conditions. In addition to their low melting points and negligible volatility, ILs have other remarkable properties such as thermal and chemical stability, high ionic conductivity, compatibility with many compounds, non-flammability, moderate viscosity and high polarity [100–104].

Like other emerging materials, ionic liquids have gradually moved from basic research to industrial applications, entering a phase of iterative development that bridges fundamental science and practical applications. Given the variety of anions and cations, including the potential for binary and ternary mixtures, there is a wide range of possible IL structures. The physical and chemical properties of ionic liquids can be tailored by modifying the structure of both ions, including changes to functional groups and side

chains. This demonstrates the remarkable tunability of ionic liquids. As a result, researchers have made a number of intriguing discoveries using ILs. They continually expand their applications in materials science, chemistry, energy and environmental protection, revealing their innovative and substantial application potential [101,102].

Ionic liquids are classified into different generations based on their structural characteristics, applications, and environmental considerations (Fig. 7).

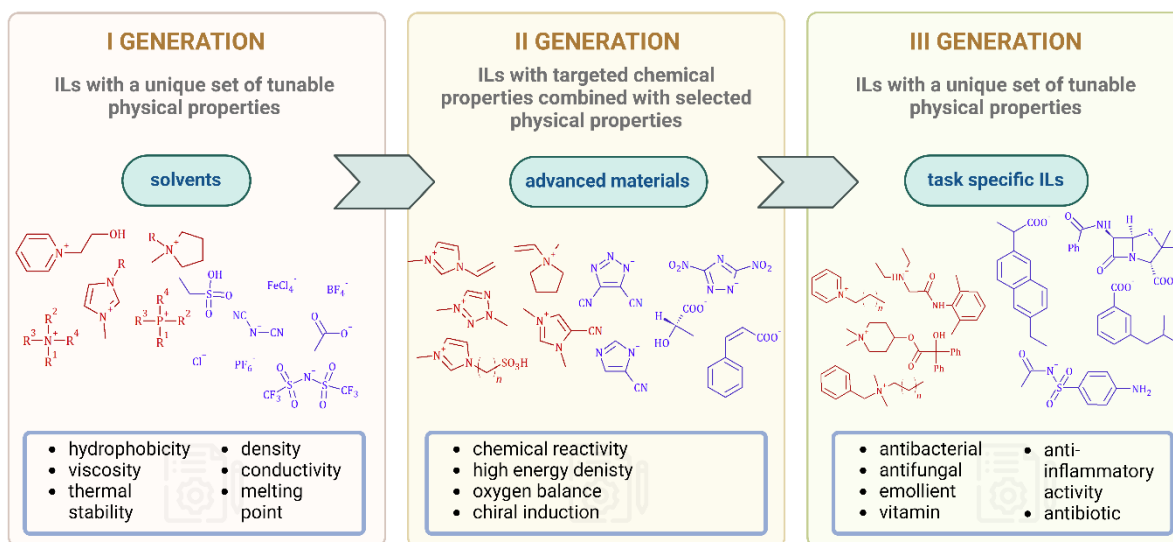


Fig. 7. The evolution of the ILs generations [105,106].

Due to their high hygroscopicity, first-generation ILs require careful handling in an inert atmosphere, and this limitation significantly limits their application. In addition, the environmental and health safety of some of these substances has not been adequately addressed, leading to concerns about their toxicity and biodegradability. Therefore, researchers have shifted their focus to the development of humidity-insensitive ILs to overcome these disadvantages [107,108].

The second generation of ionic liquids emerged after a decade due to the environmental concerns associated with first-generation ionic liquids. These compounds were developed with a focus on reducing toxicity and enhancing biodegradability and often feature modifications such as the introduction of ether, alcohol, or ester functional groups into the cation structure. Common cations included ammonium, alkylpyridinium, dialkylimidazolium and phosphonium, while hexafluorophosphate and tetrafluoroborate were the most commonly used anions. Due to their stability in air and water, they have found a wide range of applications in physical and chemical fields, serving as lubricants, reaction solvents and media in biocatalysis and pharmaceutical syntheses. These ILs have properties such as low viscosity and high solubility. However, like first-generation ILs, they are also

toxic and very expensive due to the high cost of starting materials and purification of the final product. As a result, researchers have focused on synthesising less toxic and less expensive ILs [107,108].

The transdermal drug delivery system is widely accepted due to its numerous advantages as it is a non-invasive drug administration process with prolonged therapeutic effect, reduced side effects, improved bioavailability, better patient compliance, and easy termination of drug therapy. Non-steroidal anti-inflammatory drugs such as Diclofenac sodium, Lornoxicam, Aceclofenac, Ibuprofen, antihypertensive drugs, for example, Repaglinide, Atenolol, and Antiviral agents such as Stavudine, zidovudine represents the most commonly used medications for the treatment of pain and inflammatory reaction but various side effects can limit their use. Therefore, transdermal delivery of these drugs has advantages of avoiding hepatic first-pass effect, gastric irritation and delivering the drug for an extended period of time at a sustained level. The present article mainly focuses on the work been done on these drugs by formulated and delivered as transdermal patches to decrease the side effects related to the oral delivery [104,108].

The third generation of ionic liquids represents a significant advance over their predecessors, focusing on addressing the environmental and health concerns associated with earlier generations. These newer ILs are specifically designed to be more environmentally friendly and less toxic. They incorporate biodegradable elements, such as cations derived from natural compounds such as choline, and anions less harmful to the environment, such as sugars, amino acids, alkyl phosphates or alkyl sulphates. One of the key features of third-generation ILs is their improved biodegradability and reduced toxicity, making them more suitable for use in biological systems and processes that require non-toxic conditions, such as pharmaceuticals, food processing and biorefining. In addition, these ILs are designed to be synthesised from cheaper and more readily available materials, helping to reduce overall production costs and improve the sustainability of the processes in which they are involved. In addition, third-generation ILs often have specific functional properties tailored for particular applications, such as task-specific ionic liquids (TSILs), which have functionalities that enable them to catalyse reactions, absorb gases or separate substances efficiently. This customisation further extends the range of applications for ILs into areas such as carbon capture, enzyme immobilisation and the extraction of valuable components from natural sources [108,109].

As this generation is new to the research field, they are at the forefront of the ongoing ionic liquids research. They emphasise sustainability, reduced environmental impact, and

improved economic viability, which aligns with the broader goals of green chemistry and sustainability.

2.1. API-ILs – better drug bioavailability

The pharmaceutical industry has recognised the utility of ionic liquids, particularly following studies that explored their use as solvents, reagents, and catalysts in the synthesis of APIs and the drug crystallisation process. These studies have shown that ILs can provide faster reaction rates, influence product regioselectivity, simplify pharmaceutical separations and offer significant synthetic advantages over traditional organic solvents used in pharmaceutical manufacturing. Their appropriate use can address several operational and functional challenges associated with conventional organic solvents, such as poor drug solubility, systemic toxicity and unacceptable stability. Furthermore, due to their unique properties, ILs have recently gained popularity in the pharmaceutical field, particularly for the development of efficient IL-based technologies. These include IL-in-oil microemulsions, IL-complexed drug nanoparticles, proteins/peptides in ILs and drugs in IL/IL-water binary mixtures used in synthetic and medicinal chemistry, pharmaceutical formulations, and drug delivery systems. Ionic liquids have been shown to enhance drug solubility, permeability, and stability, charge drug formulations, and facilitate site-specific or organ-targeted delivery. To date, ILs have been successfully developed to improve the dissolution of poorly soluble drugs and to cross physiological barriers such as the tight junction between the *stratum corneum* and the intestinal epithelium. In addition, the application of tailor-made ILs leads to the development of environmentally friendly and controllable drug nanocarriers. Research on ILs has advanced significantly, exploring their potential use as stabilisers, solubility enhancers and permeability enhancers [101,110–114].

Challenges such as poor solubility, thermal stability and bioavailability in traditional pharmaceuticals have been addressed by converting drug molecules into ionic liquids – known as Active Pharmaceutical Ingredient-Ionic Liquids (API-ILs). API-ILs are designed to maintain drug profiles while providing desirable counterion and solvent class properties. Research on the API-IL platform as a drug delivery vehicle has progressed significantly, demonstrating versatility in design and development. Initially, the production of API-ILs was largely focused on the synthesis of these new liquid salts to incorporate known pharmacophores. Subsequent research shifted to the evaluation of API-IL characterisation and began to assess formulation physicochemical properties, *in vitro* antibacterial, antitumor efficacy and potential for sustained drug release. As a result, API-ILs represent a promising

opportunity for pharmaceutical companies in a competitive market environment. The concept of using ILs in pharmaceutical applications emerged in 2007, almost a decade after their first use as green solvents. Since then, ILs composed of active pharmaceutical ingredients have become a new class of drugs, challenging the traditional preference for solid forms by demonstrating significant potential in industrial pharmacology as novel therapeutic agents. Rogers and coworkers introduced the idea of API-ILs as a method to overcome the problems of polymorphism and solubility associated with solid APIs (Fig.8) [92,101].

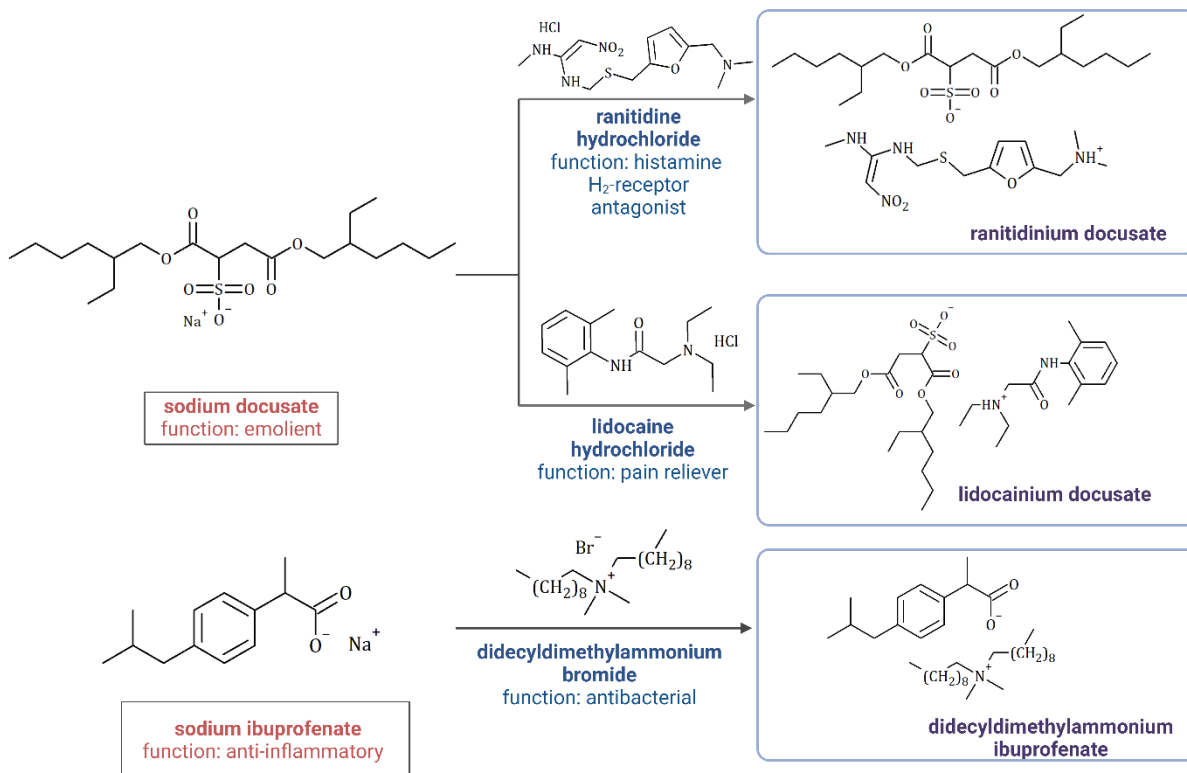


Fig. 8. The first examples of APIs converted into API-ILs [105].

They hypothesised that replacing a solid form with a pure liquid form would eliminate polymorphism and enhance the tuning of physical and biological properties, thereby introducing innovative drug delivery methods. The strategic selection of the counterion in API-ILs has the potential to add a secondary biological property and allow control over physical properties such as solubility, permeability, and stability. For example, the hydrophilic or lipophilic nature of the IL can be matched to the API to enhance the solubility of the drug as required, thereby facilitating its transport across cell membranes. In addition, counterions with high thermal stability can be transferred to the API, making it more resistant to temperature-induced degradation [101,115,116].

Despite the development of additional methods for the synthesis of ILs (e.g. sonication, microwave irradiation, electrochemical means), conventional approaches

remain the most common and widely used for API-ILs. These often involve a one-step synthesis process, known as direct synthesis or metathesis, where the target product is formed using cations, free acids or salts. For example, the acid-base neutralisation reaction between ibuprofen and the free base of lidocaine has been used to produce the API-IL lidocainium ibuprofenate. The simplicity of the preparation and the ease of purification make this a desirable method of obtaining API-IL, especially if the by-products of the salt/acid reaction can be easily removed. If the API-ILs cannot be obtained by the direct synthesis method, a two-step synthesis approach is required. This method is most commonly used to obtain API-ILs containing ions such as hexafluorophosphate and docusate. In the first step, alkanes and other compounds containing the desired cations are halogenated to form quaternised salts. This is followed by ion exchange with acids or salts containing the desired anions to produce the desired products. A comprehensive reaction must be carried out to ensure that no residual halogen anions remain in the target ILs. This is essential for their further use. In addition, taking into account the general methods for incorporating an API into an IL, they can be divided into three categories based on the mechanism of formation (Fig.9) [117–121].

The most common type involves readily ionisable APIs used directly as anions or cations to form the ionic bond (Type I API-ILs). The second category includes ionic prodrugs of neutral APIs that must first form a covalent bond before being introduced into an API-IL (Type II API-ILs). The third category involves the combination of both ionic and covalent binding methods to produce dual-active molecules in a single IL (Type III API-ILs). In this context, the API incorporated in the form of ILs can be an anionic component derived from weakly basic, a cationic component derived from weakly acidic, or can also be derived from both weakly acidic and weakly basic drugs, enabling the co-delivery of these two APIs on the same platform of ILs [117–121].

Selection of the counterion is critical to the successful design of API-ILs to overcome challenges such as low solubility, insufficient stability, polymorphism and poor oral drug bioavailability. By combining a biologically active ion with a counterion characterised by a high degree of asymmetry, dispersed charges or large ion size, the final salt can be liquefied, or a low-melting or non-melting product can be obtained. This approach, known as anti-crystal engineering, allows controlling the solid crystalline state and significantly influences the polymorph of the solid drug. For example, this method has been used by Dean et al. to synthesise salts that melt below room temperature, obtained from propantheline conjugated with tosylate and acesulfamate anions [115,121,124–126].

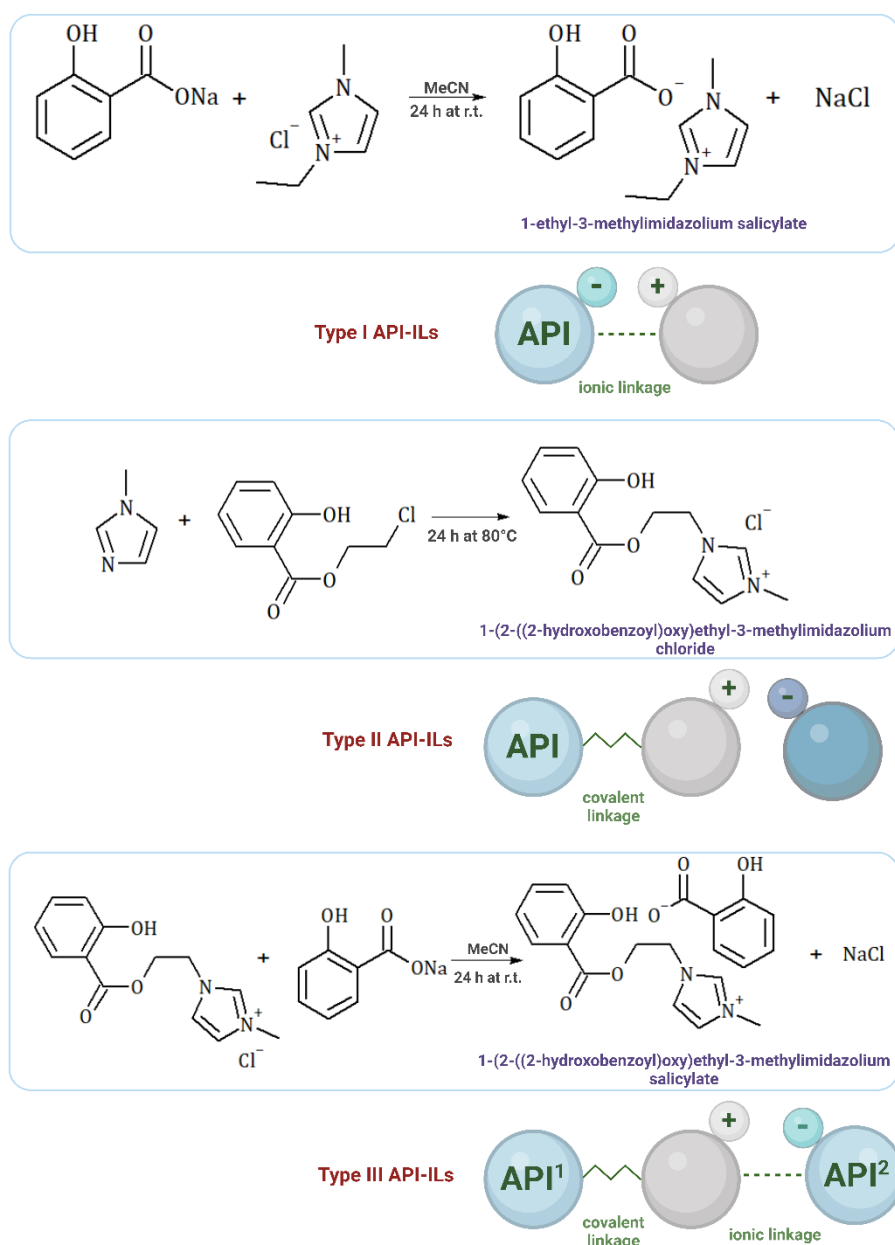


Fig. 9. Examples of a general synthesis pathway for obtaining Type I-III API-ILs [118,122,123].

Lowering the melting or glass transition point of solid salts can also be achieved by using an oligomer strategy, where the liquid range is increased by forming hydrogen bonds between larger oligomeric anions or cations. Crystal formation is prevented by delocalised proton sharing between hydrogen-bonded cations or anions and non-ionised drug moieties. This concept has been demonstrated by preparing tetrabutylphosphonium salicylates using excess salicylic acid to produce pure IL and lidocainium salicylate using excess salicylic acid or excess lidocaine. It was possible to add further salicylic acid while maintaining the liquid state until a level of saturation was reached at a given composition. As a result of oligomerisation, the addition of either excess acid or base to lidocainium salicylate resulted in an extension of the liquid range [115,121,124–126].

An interesting strategy for obtaining API-ILs involves the incorporation of more than two compounds, offering advantages such as therapeutic power, multiple biological activity and synergy. In addition to their effect on the crystalline form of the drug, it is necessary for the counterions to retain their therapeutic activity in order to achieve dual therapeutic performance. In general, any combination of two or more drugs is possible as long as both drugs form stable ions. There have been some reports of ionic liquids incorporating multiple APIs into their structure. For example, a salicylic acid-based dual-API IL approach has been used to improve the solubility of acetylsalicylate while reducing gastrointestinal irritation. Combinations of anionic acetylsalicylate with cationic tramadol, benzethonium, lidocainium and procainium have also been reported. Cations with antibacterial activity, such as benzalkonium and dodecyldimethylammonium, have been combined with saccharinate and acesulfame anions. This resulted in better antibacterial and insect-repellent efficacy than the drugs alone [115,118,127,128].

Ionic Liquids based on active pharmaceutical ingredients represent a novel approach to improving drug bioavailability, often limited by poor solubility, stability, and unfavourable pharmacokinetic profiles. As research continues, API-ILs are expected to provide more efficient, effective, and patient-friendly pharmaceutical solutions, potentially overcoming some of the most pressing limitations of modern medicine. This ongoing innovation represents a major shift in pharmaceutical development, aiming to meet the complex demands of modern healthcare with more sophisticated and refined drug delivery systems.

2.2. Adaptation of NSAIDs-based ionic liquids in pharmaceutical applications

The synthesis of NSAID-derived ionic liquids represents an innovative approach in medicinal chemistry, combining the design of novel compounds with specific properties and novel drug delivery systems. In order to optimise therapeutic effects, improve drug solubility, stability and bioavailability, and minimise side effects, much research has been devoted to exploring different combinations of ions. However, to achieve the desired therapeutic effect, it is not sufficient to design the appropriate structure of the cation and anion and the method of obtaining a given API-IL. In many cases, it is also necessary to design an appropriate vehicle or carrier to deliver the drug. For this reason, novel

formulations or drug delivery systems based on ILs have also been investigated to revolutionise pain and inflammation treatment (Fig. 10).

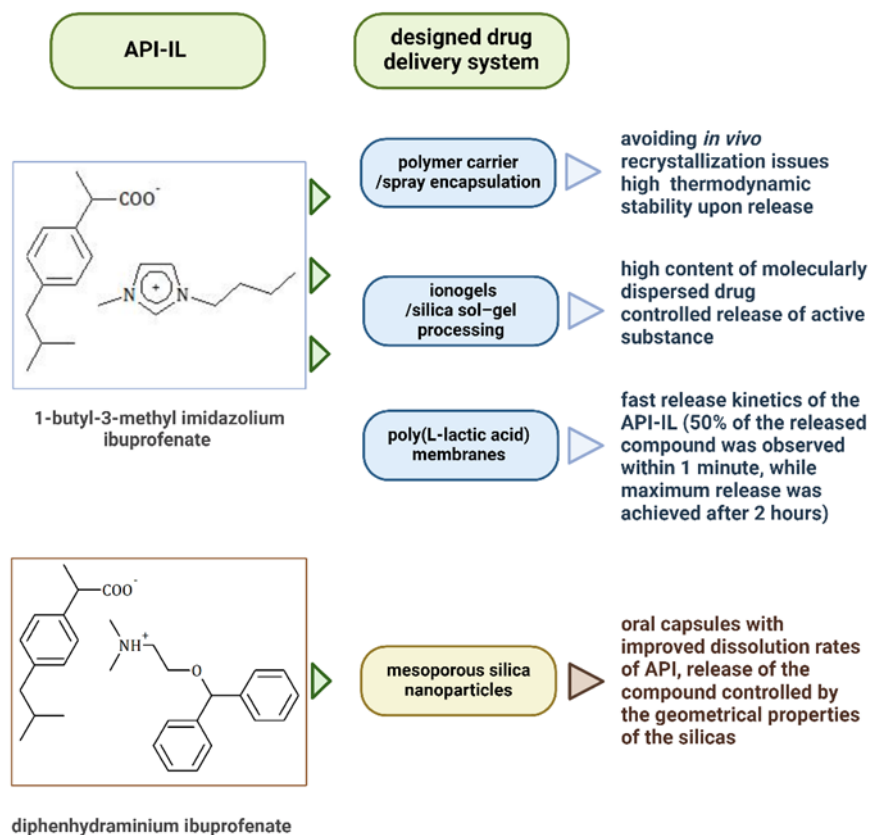


Fig. 10. Examples of drug delivery systems designed based on NSAIDs-ILs.

For instance, liquid 1-butyl-3-methylimidazolium ibuprofenate was successfully spray-dried into a polymer carrier to form a solid powder suitable for oral solid dosage formulation. Stocker and co-workers demonstrated that aqueous solutions of this API-IL can provide thermodynamic stability upon release, avoiding *in vivo* recrystallisation problems that limit the bioavailability of amorphous solid dispersions and some high-energy crystalline forms. The same ionic liquid has been used to prepare ionogels, which have been shown to be efficient drug-release systems with kinetics controlled by the nature of the silica wall. At the same time, membranes based on the biodegradable and biocompatible polymer poly(L-lactic acid) (PLLA) have been prepared. These membranes allowed the effective and rapid release of 1-butyl-3-methylimidazolium ibuprofenate. It was shown that 50% of the API-IL was released within 1 minute, while the maximum release was achieved after 2 hours [129–131]. Dual API-IL containing ibuprofen and diphenhydramine (an antihistamine drug) has been described as having low dissolution rates despite its high solubility and good wettability. However, dissolution rates were significantly improved when loaded into a mesoporous carrier. Furthermore, mesoporous silica-carrier composites were found to be

stable, easy-to-handle solids with rapid and complete release (controlled by the geometric properties of the silica) from the carrier when placed in an aqueous environment [132–135].

While searching for new drug delivery systems for NSAID-based ionic liquids is still ongoing, many efforts have been made in recent years to commercialise API-ILs. So far, most of these have involved transdermal or topical administration since this route has been recognised as a viable strategy to overcome a number of problems that often prevent compounds from ever being developed into marketed drugs. An example of a drug from the group of NSAIDs that has been transformed into API-ILs and has been subjected to a further stage of commercialisation is diclofenac (Fig. 11) [101,136].

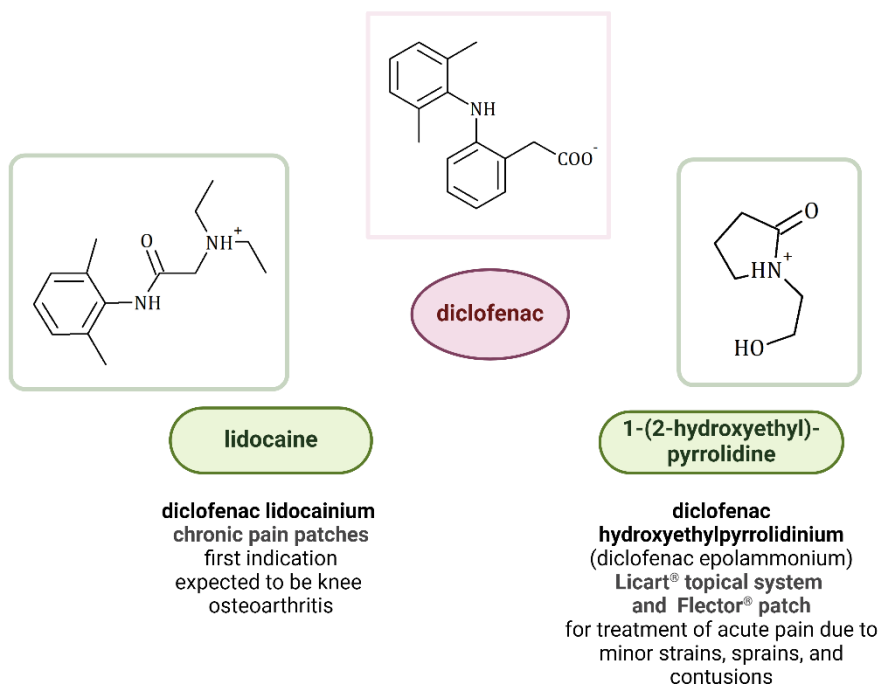


Fig. 11. Diclofenac-based ILs translated into pharmaceutical manufacturing.

The diclofenac moiety has been combined with lidocaine (study carried out by the company MEDRx, USA) and hydroxyethyl pyrrolidine, produced by IBSA (Institut Biochimique SA, Switzerland) under the trade names of Flector® (patch) and Licart® (topical system). The results obtained in clinical trials have shown excellent transdermal absorption, a low level of skin irritation and a high stability of the drug. The IL obtained from the drug etodolac in combination with lidocaine is also known, but the results obtained in the first phase of the clinical trials were not satisfactory enough for further phases of research to be continued. This demonstrates the importance of matching the appropriate chemical structure

of the counterion to the active ingredient in order to successfully bring the final form of the drug to market [101,136,137].

The search for a universal counterion structure is still ongoing, which would increase the bioavailability of a greater number of NSAIDs and make it possible to obtain an API-ILs form that could be applied to the skin or transdermally. API-ILs have been shown to be effective in controlling skin permeability, drug-polymer miscibility and release performance, and the pharmacokinetic behaviour of the drug. With continued advances in the field, this strategy holds great promise for the treatment of a variety of inflammatory and painful conditions by means of non-invasive and targeted drug delivery approaches. Although the use of ILs to enhance the transdermal delivery of drugs (dissolving active ingredients in ILs) to avoid the use of conventional chemical permeation enhancers in drug formulation is known, many studies have been carried out to obtain NSAID-derived ionic liquids which can be used transdermally or topically without the need to create complex drug delivery platforms [138,139].

In this context, choline-based ILs were obtained from ibuprofen, ketoprofen and (*S*)-naproxen and were incorporated into bacterial nanocellulose with a view to their use in topical drug delivery systems. A 2-fold increase in solubility in PBS aqueous solutions and a faster release of the obtained API-IL compared to the starting NSAIDs were demonstrated. In addition, the cytotoxicity and anti-inflammatory properties of the IL-incorporated membranes were similar to those of NSAIDs or ILs. This confirms their suitability as potential materials for topical drug release applications [140]. Moreover, the dual biofunctional ILs with analgesic and anti-inflammatory properties were prepared using lidocaine-derived cations and hydrophobic anions derived from NSAIDs (ibuprofen, diclofenac, naproxen). By converting the original drugs into dual-function API-ILs, their water solubility is increased up to 470-fold without significantly affecting their cytotoxic profile. The API-ILs were successfully incorporated into a hydrophobic polyvinylidene fluoride membrane with good wound-healing properties, allowing the release of API-ILs at higher doses than the parent drugs [141].

For the application of ILs in biomedicine, in addition to comprehensive research, including the determination of physicochemical properties, the toxicity and biocompatibility of the counterion should also be considered. As an environmental accumulation of drugs has attracted increasing attention, research should also focus on the search for natural ions of biological origin, taking into account biodegradation aspects. While API-IL formulations

may offer stability and improved drug delivery, there is a risk of environmental accumulation due to their persistence [142].

Amino acids, already known to be a natural and relatively cheap source of non-toxic and "green" ionic liquids, are one of the solutions in the search for substrates to obtain biodegradable and biocompatible counterions. Amino acids, used as cations or anions to provide stable chiral centres, have attracted considerable attention for the synthesis of amino acid ionic liquids (AAILs) with specific functions, which are designed and synthesised by modifying or changing the substituent groups of amino acid side chains using a simple method. In addition, AAILs are recognised as more environmentally friendly than conventional ionic liquids, being highly biodegradable and biocompatible. Furthermore, amino acids have been successfully used to obtain prodrugs of drugs with low solubility and permeability, representing a versatile strategy for optimising drug delivery and improving the therapeutic profile of existing pharmaceutical agents [143–145].

This concept was used by Furukawa et al. to prepare API-ILs containing proline ethyl ester as a counterion to the ibuprofen moiety, which enhanced transdermal drug penetration. When tested on porcine skin, the resulting salt showed a 10-fold increase in cumulative drug amount compared to free ibuprofen. In addition, the results of the cytotoxicity study clearly showed a reduced toxic effect on mouse fibroblast L929 cells [146]. This was an indication of the potential use of the L-amino acid ester cation for the further development of biocompatible API-IL formulations by Moshikur and co-workers for the pairing of alkyl esters of the L-amino acid series with salicylic acid. The method of obtaining API-IL is simple and based on an equimolar reaction without the need for harsh reaction conditions (Fig. 12).

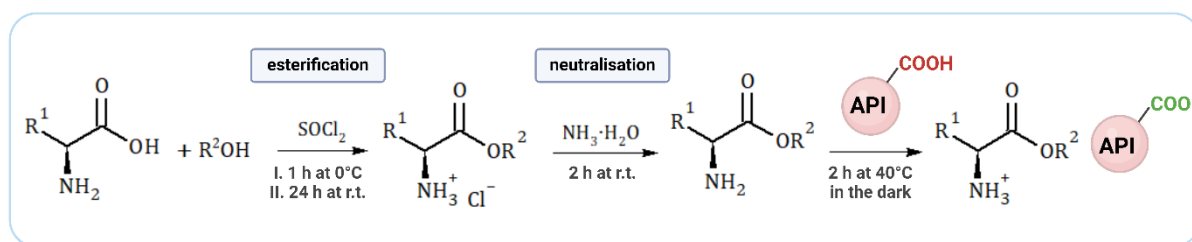


Fig. 12. General synthetic (path) of L-amino acid alkyl ester-based ionic liquids containing NSAID moieties [146,147].

The results showed that amino acid cations based on ethyl esters had lower toxicity than cations with other alkyl chain lengths. Further investigation also revealed that ILs derived from L-aspartic acid, L-alanine and L-proline ethyl esters were characterised by faster and improved skin permeation, 3–9 times higher compared to sodium salicylate.

As a result, this API-IL technique can effectively formulate drugs that are poorly soluble in water in the IL form and eliminate the use of traditional solvent vehicles for transdermal drug delivery [147]. Also, in this area, an interesting study was presented by Tanigawa et al. on the combination of acidic etodolac with L-proline ethyl ester (1:2) and tested for intranasal administration. The solubility of NSAIDs in the simulated nasal fluid was improved, and following the ionisation of the active ingredient, the retention of etodolac on the nasal mucosa and nose-to-brain delivery was enhanced [148].

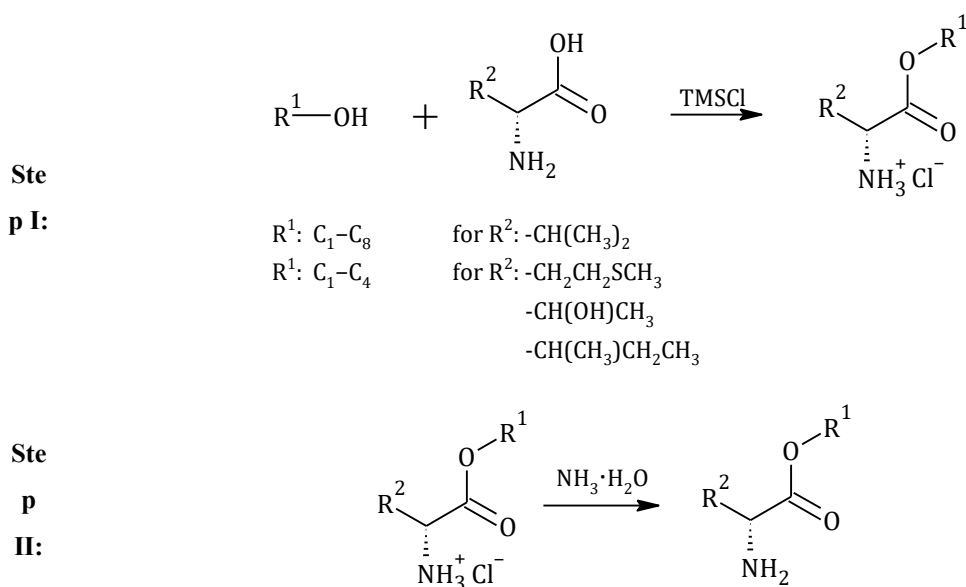
Pairing NSAIDs with amino acid esters represents a promising approach to developing API-ILs for transdermal or topical delivery. Amino acid esters can improve solubility, stability and bioavailability by acting as effective vehicles for acidic APIs. This strategy takes advantage of the unique properties of amino acids and ionic liquids to improve the delivery of drugs through the skin. However, further research is needed to take full advantage of this approach and understand the speciation of L-amino acid esters as counter ions to maximise their potential. It is essential to determine their speciation and physicochemical properties (such as water solubility, lipophilicity and thermal stability) to fully exploit the potential of NSAID salts derived from L-amino acid alkyl esters for transdermal or topical delivery, together with detailed permeation studies through the skin. Understanding how the amino acid ester interacts with the NSAID moiety and influences the final properties is critical for predicting the efficacy in transdermal or topical delivery systems and for the design of API-IL formulations for the effective and safe delivery of a wide range of therapeutic agents.

Chapter II: Results and discussions

1. Synthesis and identification of NSAIDs salts with L-amino acids alkyl esters

The synthesis of the compounds under investigation was based on the reaction of a selected pharmaceutically active acid with the corresponding alkyl ester of L-amino acid. The cation of the obtained salts was L-amino acid alkyl ester, while the anion was the selected drug. The three-step synthesis was carried out according to the reaction path shown in Figure 13. Derivatives of four NSAIDs: (*R,S*)-ibuprofen, *S*-(+)-naproxen, (*R,S*)-ketoprofen, salicylic acid and alkyl (Me, Et, Pr, *i*-Pr, Bu) esters of three amino acids – L-isoleucine, L-methionine, and L-threonine, were synthesized as part of this thesis and are new, excluding (*R,S*)-ibuprofenates of amino acids isopropyl esters.

In addition, *S*-(+)-ibuprofen derivatives with C₁-C₈ esters of L-valine were synthesized as new in this thesis in order to compare to the respective (*R,S*)-ibuprofen salts, previously referred to [149–151]. Synthesis of derivatives of *S*-(+)-naproxen, ketoprofen, salicylic acid and L-valine alkyl (C₁-C₄) esters were described in previous works and articles [149,152–154].



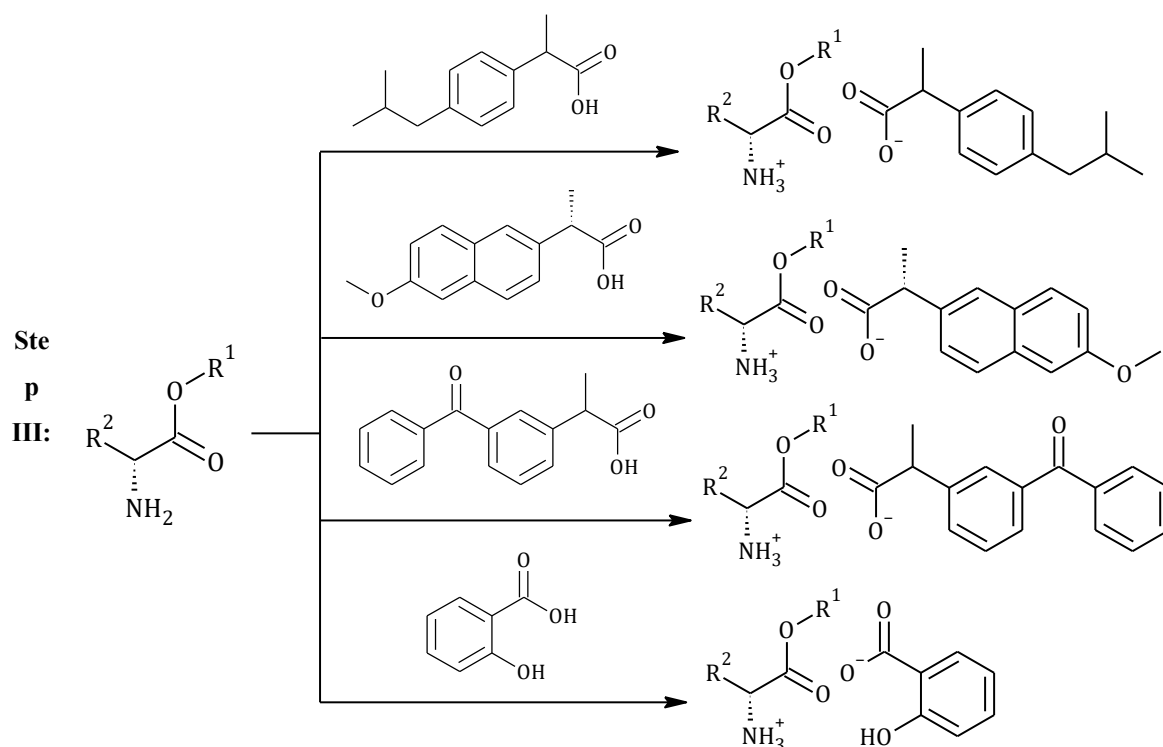


Fig. 13. The general synthesis pathway of NSAID salts with L-amino acid alkyl esters.

The process for the preparation of L-amino acid ester hydrochlorides by esterification of an amino acid moiety with a suitable alcohol in the presence of chlorotrimethylsilane (TMSCl) as a catalyst and a water-binding agent, as well as the process including the use of the ultrasound field, were described and included in the patent applications [155,156]. TMSCl is advantageous over other chlorinating agents, such as gaseous hydrogen chloride, aqueous hydrochloric acid (36%), thionyl chloride or phosgene [157]. Despite their widespread application in the esterification of amino acids, they still require time-consuming workup steps, safety and waste management challenges, and harsh reaction conditions (such as the use of a significant excess of any of the substrates, the use of corrosive, strong acids, e.g. HCl, or H₂SO₄) [158,159]. In addition, as described in the patent invention [155,156], ultrasonication greatly simplifies the process by eliminating the need for mechanical stirring due to the appropriate mass and heat exchange. Moreover, the use of ultrasound allows for a lower reaction temperature and a shorter reaction time compared to conventional heating. No destruction of the components of the reaction mixtures and no changes in the direction of the reaction were observed. The L-amino acid alkyl ester hydrochlorides with an alkyl chain length below C₆ were obtained in high yields (75-95%). In the case of L-valine alkyl ester hydrochlorides (from pentyl to octyl), the reaction yields by the non-ultrasound method were 46-65%, while the reaction yields performed in the ultrasound field were increased up to 70-80%.

For the purposes of this PhD thesis 24 L-amino acid alkyl ester hydrochlorides were obtained and identified according to the method described for the first time in patent applications by team of supervisor of my thesis with my participation [155,156]. The obtained L-valine alkyl ester hydrochlorides with short alkyl chain lengths (from methyl to pentyl), L-methionine alkyl (C₁-C₄) ester hydrochlorides, L-isoleucine methyl and ethyl ester hydrochlorides were white crystalline solids. The other L-valine alkyl (from hexyl to octyl) ester hydrochlorides, L-isoleucine and L-threonine isopropyl hydrochlorides synthesised were semi-solids. The obtained L-threonine alkyl (C₁-C₄) ester hydrochlorides and L-isoleucine propyl and butyl ester hydrochlorides were in the amorphous state.

The next steps involved the neutralisation of the resulting L-amino acid alkyl ester hydrochlorides, followed by an equimolar reaction with a drug from the NSAID group. As a result of the last step, the amino group of the amino acid was protonated with an appropriate acid and the final product was formed. The detailed description of the synthesis of L-amino acid alkyl ester salts of NSAIDs has been presented in some granted patents [160–163], not related to this PhD thesis or in granted patents resulting from, among others, my PhD studies [164,165]. In accordance with this procedure, the L-amino acid derivatives with different carbon chain lengths and selected drug moieties in the anionic part have been successfully obtained in equimolar reaction with high yields (95-99%) without the formation of by-products.

(*R,S*)-ibuprofenates, ketoprofenates, naproxenates, and salicylates based on alkyl esters (C₂-C₄, including C_{3-iso}) of L-valine were previously synthesised and partly characterized in my master's thesis [149] and articles not related to my PhD thesis [150–153]. Additionally, (*R,S*)-ibuprofenates of L-valine alkyl esters (C₅-C₈), L-methionine, and L-threonine isopropyl esters were also earlier synthesized and partly described [150,151,166]. These compounds and their properties are not within the scope of the scientific novelty of the presented PhD thesis. Their properties are mentioned here only for comparative purposes. The novelty in the presented work is permeability tests performed for some of them, antimicrobial activity tests biodegradability, antioxidant activity, stability under different storage conditions, lipophilicity study for L-valine alkyl esters (C₁, C₇, C₈) of (*R,S*)-ibuprofen and L-valine alkyl esters (C₁-C₄) of ketoprofen, naproxen, and salicylic acid and solubility study in water and selected buffer solutions for L-valine alkyl esters (C₁-C₄) of ketoprofen, naproxen and salicylic acid.

The study also included the modification of *S*-(+)-ibuprofen with alkyl esters (C₁-C₈) of L-valine. The modification of *R,S*-ibuprofen with the corresponding alkyl esters

of L-valine, including physicochemical properties and skin permeability, has been extensively described in other works [150,151]. Therefore, in this thesis, the properties of the *S*-(+)-ibuprofen modification products with L-valine alkyl esters (C₁-C₈) were evaluated solely in the context of the influence of the optical purity of the active ingredient on these properties, with reference to previous results on (*R,S*)-IBU derivatives.

All the obtained products and intermediates were identified by spectroscopic methods – NMR and IR analysis. In addition, the elemental analysis confirmed the high purity of the obtained compounds. Only samples of alkyl esters of L-amino acids, which are liquid at room temperature, were not subjected to elemental analysis. All of the individual results are given in the Appendix I.

The structure of the obtained derivatives were confirmed by XRD analysis. The characteristic reflections were shifted with respect to the diffractogram of the unmodified acid (ibuprofen (PDF 96-230-0213), naproxen (PDF 00-052-1902), ketoprofen (PDF 00-051-1988) and salicylic acid (PDF 00-014-0882).

The compounds were white crystalline, semi-solids or amorphous, depending on the starting active substance and the amino acid alkyl ester. All naproxen derivatives synthesised were in solid form (sharp peaks of high intensity in the XRD pattern of the sample). The salts of ibuprofen conjugated with L-valine (derivatives of both (*R,S*)- and *S*-(+)-ibuprofen), L-methionine and L-isoleucine alkyl esters were solids, whereas compounds based on the [ThrOR] cation were semi-solids (low intensity of XRD peaks and patterns suggesting the presence of systems with one phase being crystalline and the other amorphous). Almost all ketoprofen derivatives obtained were amorphous (no intensity or negligible low number of peaks, recorded XRD pattern) with no melting points determined (discussed in section 2.3 of this chapter). The exceptions were semi-solid salts based on [ValOMe], [ValOEt], [IleOMe] and [IleOBU] cations. The synthesised compounds were mostly in the solid state for salicylic acid salts. Semi-solid salicylates were obtained by conjugation with [ThrOEt], [IleOMe], [MetOMe], [MetOEt] and [ValOMe] cations. Only the salicylic acid derivative based on the [ThrOiPr] cation was the amorphous salt.

The presence of a characteristic signal visible as a broad singlet on the ¹H NMR spectra characterised the salt formation and obtaining the ionic structure. The chemical shifts for the proton signals of the ⁺NH₃ group in amino acid ester moiety were various for each group of NSAID acid derivatives. The positional variability of the mentioned shift was influenced by both starting L-amino acid and the parent drug forming the compound. In addition, in the case of corresponding hydrochlorides, the signal from the protonated

amino group occurred at 8.87 (for [MetOEt][HCl]) to 8.31 ppm (for [ValOOct][HCl]). These signals shifted upon salt formation: 6.68–4.67 ppm for ibuprofenates, 4.93–6.91 ppm for naproxenates, and 5.13–6.44 ppm for ketoprofenates. In general, for (*R,S*)-ibuprofenates, as well as for hydrochlorides, the characteristic signal shifts towards lower ppm shift values with the lengthening of the carbon chain in the ester part of the cation, and in the order of the L-amino acid moieties L-Met>L-Thr>L-Ile>L-Val. The signals for S(+)-ibuprofen-based salts occur at lower δ ppm values compared to corresponding (*R,S*)-ibuprofen salts. For salicylic acid derivatives, the signals assigned to the protonated amino group were broad and present in the range from 7.30 ppm (for [ThrOBU][SA]) to 9.96 ppm (for [IleOMe][SA]). The proton chemical shifts of the NH_3^+ group of alkyl ester salts of L-amino acids and their hydrochlorides are compared in Figure 14.

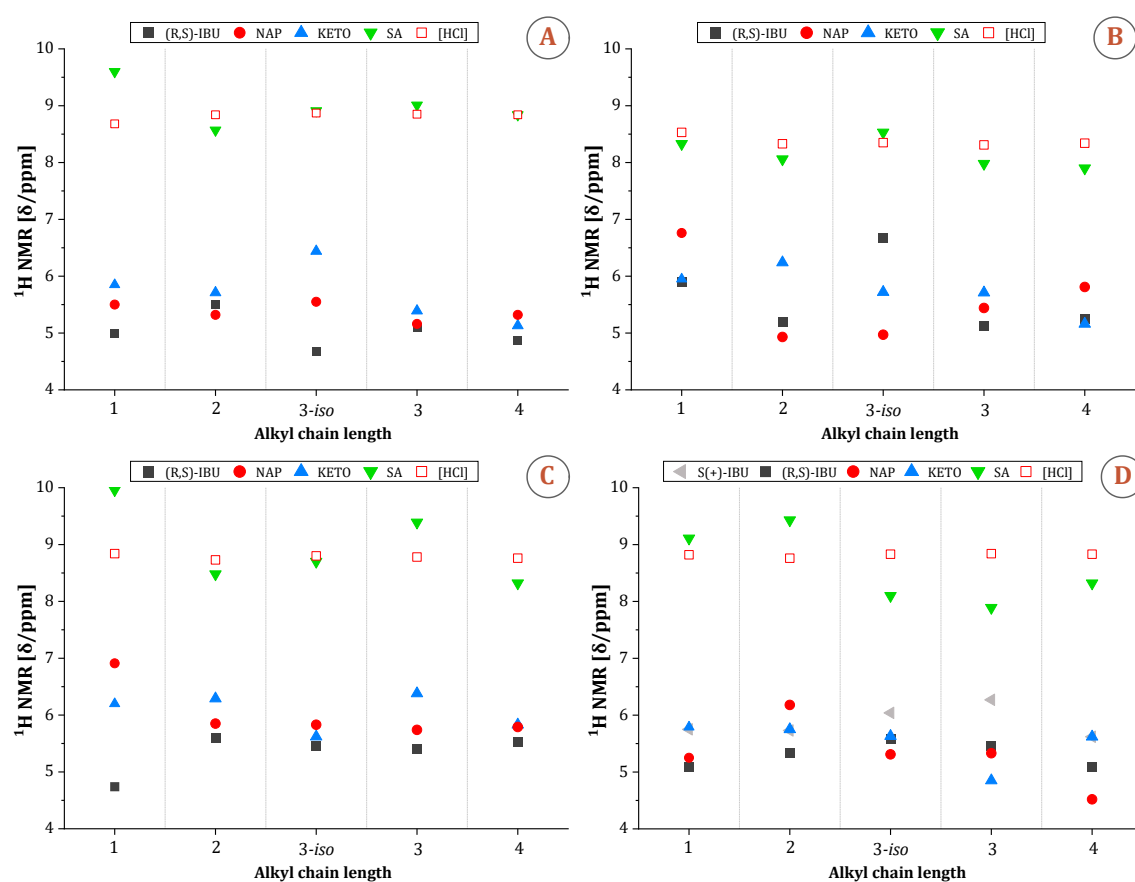


Fig. 14. The comparison of chemical shifts of the protons in the NH_3^+ group in ^1H NMR spectra of L-amino acids alkyl (C_1 – C_4) ester salts of: racemic ibuprofen (grey square), S-(+)-ibuprofen (light grey inverted triangle), naproxen (red circle), ketoprofen (blue triangle), and of salicylic acid (green inverted triangle); and hydrochlorides (red open square). A: L-methionine, B: L-threonine, C: L-isoleucine, and D: L-valine.

Furthermore, ionic structure formation was confirmed by the presence of carboxylate anion signals for L-amino acid alkyl salts. For the unmodified acid, the chemical shifts of the carbonyl carbon were recorded as follows: ibuprofen: 181.18 ppm, [(S+)-IBU]:

181.15 ppm, ketoprofen: 180.24 ppm, naproxen 181.00 ppm, and salicylic acid: 174.94 ppm. These signals shifted to lower values in the corresponding salts of ca. 2 ppm to about 179 ppm for salts of ibuprofen and naproxen and about 178 ppm for salts of ketoprofen. The exceptions were L-threoninium alkyl ester salts and all obtained salicylates, where this difference was about 1 ppm. In the case of corresponding hydrochlorides, the chemical shifts of the carbon in the carbonyl group were present in the range 168-170 ppm. The differences in chemical shifts of the carbonyl carbon in unmodified NSAID and its salts with amino acids alkyl esters are compared in Figure 15.

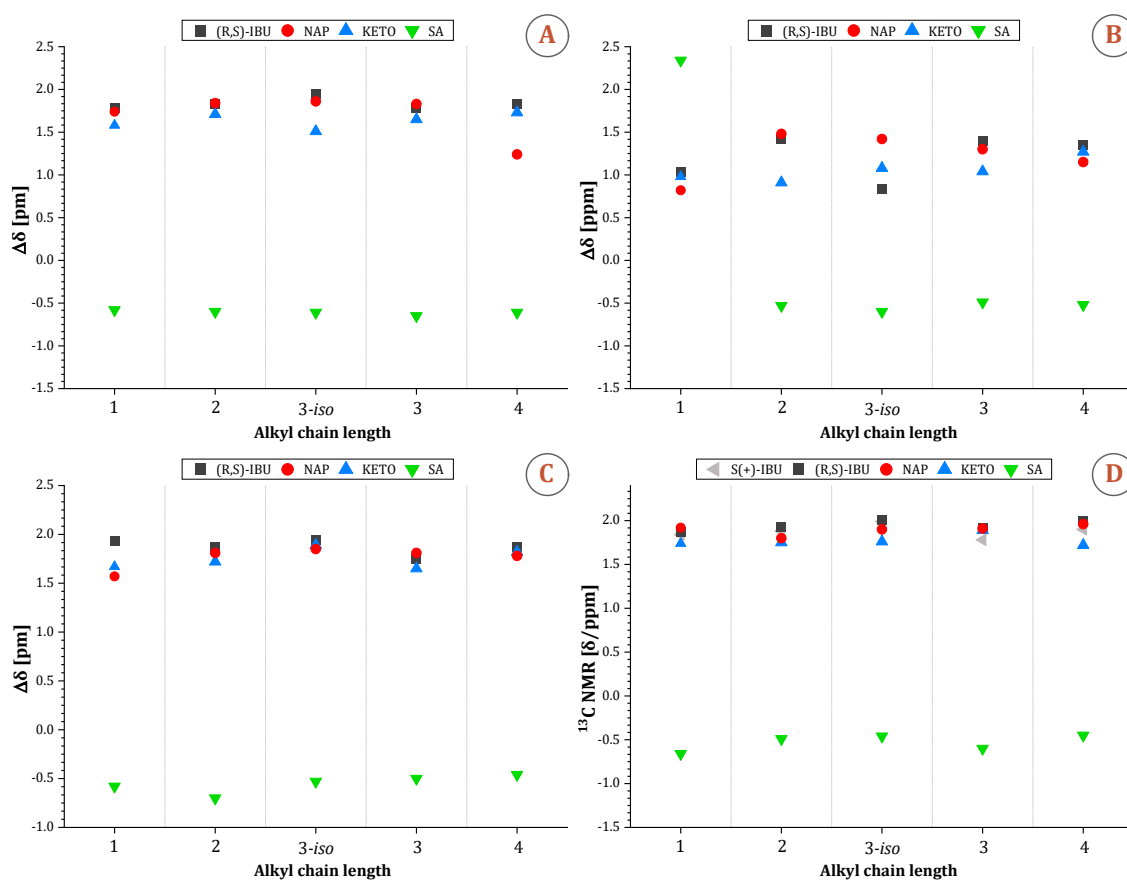


Fig. 15. The comparison of the difference in chemical shifts ($\Delta\delta$) of carbonyl carbon in ^{13}C NMR spectra between NSAIDs and their L-amino acids alkyl ($\text{C}_1\text{-C}_4$) salts of: racemic ibuprofen (grey square), *S*-(+)-ibuprofen (light grey inverted triangle), naproxen (red circle), ketoprofen (blue triangle), and of salicylic acid (green inverted triangle). A: L-methionine, B: L-threonine, C: L-isoleucine, and D: L-valine.

The ionic nature of the obtained salts was further supported by IR spectroscopy. The characteristic C=O and O-H stretching vibrations for unmodified acids with the carboxylic group were observed at 1709 cm^{-1} and 2954 cm^{-1} (ibuprofen), 1692 cm^{-1} and 2939 cm^{-1} (ketoprofen), and 1726 cm^{-1} and 3163 cm^{-1} (naproxen), 1653 cm^{-1} and 2853 cm^{-1} (salicylic acid) respectively. The sharp absorption band of the characteristic C=O stretching vibrations of the carboxylic acid group was observed in the range of $1733\text{-}1742\text{ cm}^{-1}$, while

the O-H stretching vibrations were missing after pairing with L-amino acid alkyl ester cations. Furthermore, the two visible characteristic absorption bands at about 1600 and 1390 cm^{-1} were assigned to asymmetric $\nu(\text{COO}^-)_{\text{asym}}$ and symmetric $\nu(\text{COO}^-)_{\text{sym}}$ vibrations. The difference between the two frequencies is equal to that above 200 cm^{-1} , which confirms the formation of the carboxylate anion [167–170].

The salt formation of NSAIDs, which are generally weak acids, can be problematic due to the possibility of disproportionation. This conversion of the salt form back to its free acid form shifts the ionisation state of the active ingredient and fundamentally alters its solubility, solid state properties, chemical stability and, consequently, the efficacy of the drug. To ensure effective salt formation, the pK_A value is one of the key components to consider, as it is used to determine the degree of ionisation. The pK_A rule states that the difference between a group's pK_A and its counterion's value should be $\Delta\text{pK}_\text{A} \geq 3$, especially when the drug is a particularly weak acid or base. Furthermore, ionised acid-base complexes are only observed for $\Delta\text{pK}_\text{A} \geq 4$, as shown by the detailed data provided by Cruz-Cazeba [171–173]. This ensures that both species are fully ionised and have a strong binding affinity. Otherwise, co-crystallisation may occur, resulting in mixed crystals in which the drug is crystallised with one or more co-formers (ΔpK_A below 0). Furthermore, knowledge of the $\log(\text{K}_\text{S})$ parameter can also be used to predict the degree of disproportionation expected if the salt were dissolved in pure water. Therefore, the strength of certain types of salt can be assessed, and the degree of salt formation can be predicted using the calculated $\log(\text{K}_\text{S})$ values [171–173].

In this context, formation constants, $\log(\text{K}_\text{S})$, were calculated based on their measurements for obtained NSAID derivatives based on the described acid-based complex dependencies [171]. The detailed $\log(\text{K}_\text{S})$ values, as well as pK_B values of corresponding L-amino acid alkyl esters, were summarised in Appendix II in Table A2. Figure 16. presents the dependence of the determined formation constants of L-amino acid alkyl ($\text{C}_1\text{--}\text{C}_4$) ester salts.

For the unmodified acid, the following pK_A values were obtained: 4.74 for *S*-(+)-ibuprofen, 4.65 for (*R,S*)-ibuprofen, 4.32 for naproxen, 4.11 for ketoprofen and 3.18 for salicylic acid. Based on the calculated pK_A values, the drugs tested belong to the group of weak acids, and L-amino acid alkyl esters belong to the group of strong bases. An increase in the basic character was observed as the carbon length in the ester moiety increased (i.e. the pK_B value ranged from 4.20 for [ValOMe] to 3.34 for [ValOOct]). The propyl ester derivatives showed a higher pK_B value than the corresponding esters

obtained from the branched-chain isopropyl alcohol. In general, the highest pK_B values were determined for L-methionine alkyl esters (3.88 for [MetOMe] and 3.65 for [MetOBu]), while the lowest values were determined for L-threonine alkyl esters (2.99 for [ThrOMe] and 2.52 for [ThrOBu]). The calculated ΔpK_A between ions for all the salts obtained is greater than 5, indicating the formation of ionised acid-base complexes and a strong affinity of the two species to bind, maintaining the principle of the ion-pair strategy.

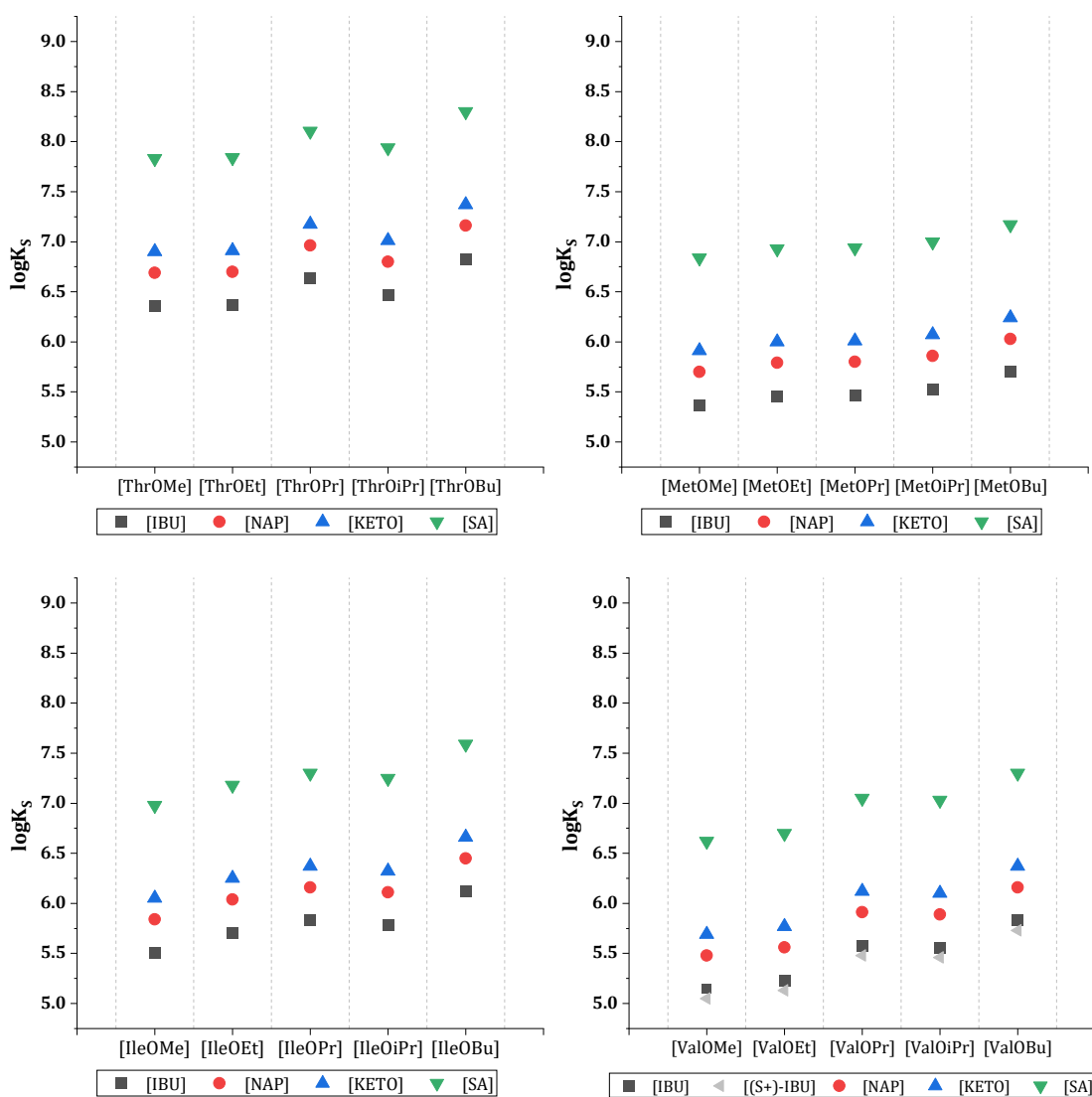


Fig. 16. The comparison of formation constants $\log(K_S)$ of L-amino acid alkyl (C_1 - C_4) esters salts of acids from NSAIDs group: salts of racemic ibuprofen (grey square), *S*-(+)-ibuprofen (light grey inverted triangle), naproxen (red circle), ketoprofen (blue square), and of salicylic acid (green inverted triangle).

The synthesised salts were characterised with $\log K_S$ in the range of 6.62-8.30 for salicylic acid derivatives, 5.69-7.37 for ketoprofen derivatives, 5.48-7.16 for naproxen derivatives and 5.15-6.83 for ibuprofen derivatives. In comparison with the corresponding (*R,S*)-ibuprofenate salts, the L-valine alkyl ester salts of *S*-(+)-ibuprofen were characterised

by lower values of $\log(K_s)$. They ranged from 5.06 for [ValOMe][S(+)-IBU] to 5.92 for [ValOOct][S(+)-IBU]. Furthermore, the calculated $\log(K_s)$ values ensure that the predicted degree of all salt formation obtained would be greater than 99%. Therefore, compounds would not disproportionately revert to the initial single species if not required. This is critical in the context of transdermal absorption, as the ionisation state of the compound also affects the rate at which it is able to diffuse across biological membranes. When exposed to extreme pH formulations, the skin is not only able to tolerate any pH change but also has the ability to bring the formulation into homeostasis with the pH of the skin (pH 5.4). Therefore, the amount of non-ionised drugs present in the skin pH is an important variable influencing absorption. At pH=4-5, substances characterised by lower pK_A will be more unionised, and this form will be more readily absorbed via non-polar transdermal routes through the skin. The ionised forms of the substance are largely absorbed through the skin via polar pathways, while the oppositely charged active substance can form neutral ion pairs, thus improving their absorption through the skin [174].

Summary:

- As precursors to the designed salts, 14 novel hydrochlorides of alkyl esters of L-amino acids were obtained with high yields (75-95%) and characterised.
- In the present work, salts of acids belonging to the group of non-steroidal anti-inflammatory drugs were obtained. Based on the ion-pairing strategy, the anion of the synthesised salts was derived from the active substance ((*R,S*)-ibuprofen, *S*-(+)-ibuprofen, *S*-(+)-naproxen, (*R,S*)-ketoprofen and salicylic acid), while the cation was derived from the alkyl ester of the L-amino acid (L-isoleucine, L-methionine, L-threonine, L-valine).
- High purity and high yields (95-99%) of L-amino alkyl ester derivatives and drugs were obtained.
- Identification and confirmation of high purity and ionic structure were based on ^1H and ^{13}C NMR, ATR-FTIR and elemental analysis. In addition, the complete ionisation of the formation of acid-base complexes was supported by the calculated values of $\log(K_s) > 5$.

2. Physicochemical properties of salts of L-amino acids alkyl esters and selected NSAIDs moieties

The characterisation of the physicochemical properties included the determination of solubility in organic solvents, detailed solubility tests in water and selected buffer solutions, and measurements of the lipophilicity of the salts obtained. Thermal stability, phase transition temperatures, and specific rotation studies were also part of the presented characterisation.

2.1. Solubility study

2.1.1. *Determining the solubility in organic solvents*

The solubility of drugs in organic solvents is an important consideration in the pharmaceutical development process, contributing to the successful formulation and delivery of safe and effective drug products. Organic solvents are often used in pharmaceutical research and manufacturing for various purposes, including synthesis, extraction, purification, and formulation of drug compounds [175]. Therefore, the solubility of the final salts and intermediates (L-amino acid alkyl esters and their corresponding hydrochlorides) was investigated. The conventional organic solvents chosen for this study were ethanol, DMSO, dichloromethane, chloroform, ethyl acetate, diethyl ether, toluene and *n*-hexane. The results are presented in Tables A7–A12 in the Appendix II. The values obtained for salts of L-valine alkyl esters in combination with ibuprofen, salicylic acid, naproxen and ketoprofen are presented in the author's Master's thesis [149]. The solvents were ranked in order of decreasing polarity based on the value of the empirical polarity parameter ($E_T(30)$) [176]. Depending on the amount of dissolved substance in 1 mL of solvent, the compounds under investigation and the parent acids were classified as soluble (>100 mg/mL), partially soluble (33–100 mg/mL) or insoluble (<33 mg/mL).

In general, all of the obtained L-amino acid alkyl ester hydrochlorides were soluble in ethanol, DMSO, dichloromethane, chloroform and ethyl acetate. A slight decrease in solubility in ethanol was observed for the [ThrOEt][HCl], [ThrOiPr][HCl], and L-valine alkyl ester hydrochlorides with longer carbon chain C_5 – C_8 . Only the L-amino acid methyl ester hydrochlorides were insoluble in chloroform and ethyl acetate. The synthesised L-amino alkyl esters were characterised by good solubility in all the solvents studied except *n*-hexane. Partial or good solubility in *n*-hexane was shown by L-methionine alkyl esters, L-threonine methyl ester and L-valine alkyl esters from pentyl to octyl, similar to the corresponding hydrochlorides.

Comparisons of the solubility of NSAIDs derivatives in these organic solvents depending on the L-amino acid alkyl ester cation structure are shown in Figures 17 and 18. Figure 17 shows the data obtained for L-valine alkyl esters paired with *S*-(+)-ibuprofen. The results of this solubility study evaluated for the corresponding (*R,S*)-ibuprofen derivatives are presented in previous work and publications [162, 175, 176].

All active substances were soluble in ethyl and diethyl ether and insoluble in *n*-hexane. Both ibuprofen and salicylic acid were soluble in toluene, while ketoprofen and naproxen insoluble. All of the synthesised NSAID salts were characterised as soluble or partially soluble in polar solvents such as ethanol, DMSO, dichloromethane, and chloroform, similar to parent drugs. Moreover, the improved solubility in chloroform was also observed when salicylic acid and naproxen were conjugated with L-amino acid alkyl esters. The exception was [ThrOMe][SA] salt, which was insoluble in chloroform and dichloromethane. The greatest differences between the solubility of unmodified acids and their derivatives were found for ethyl acetate, diethyl ether, toluene and *n*-hexane.

Both the starting L-amino acid and the length of the carbon chain in the ester moiety influenced the solubility in the organic solvents mentioned, which was most pronounced for ibuprofen salts paired with the L-valinium ester cation. Compounds based on [ValOR] with an alkyl length from methyl to propyl were insoluble, whereas [ValOBu][(S+)-IBU] was partially soluble and salts with a carbon chain from amyl to octyl were soluble in *n*-hexane. In addition, the derivatives with an intermediate alkyl chain length (*n*-propyl, *isopropyl* and *butyl*) of the L-valine alkyl ester showed a slightly worse solubility in ethyl acetate and diethyl ether. No differences were observed between the solubilities of L-valinium alkyl esters *S*-(+)-ibuprofenates and earlier described the respective (*R,S*)-IBU derivatives [149–151].

Similarly, the salts based on the L-threoninium alkyl ester cation showed a slightly worse solubility in ethyl acetate, diethyl ether and toluene in comparison to the parent drug. Only [MetOMe][IBU] was insoluble in ethyl acetate, diethyl ether and toluene, in contrast to the other ibuprofen salts obtained and the unmodified acid. The most pronounced influence of hydrophilic L-threonine on solubility derivatives was observed in the case of obtained salicylated. When [ThrOR] and [ValOMe] cations were conjugated with salicylic acid, the salts obtained were insoluble in ethyl acetate and toluene, in contrast to the free acid. Except for the compound based on [IleOiPr], the other L-isoleucinium alkyl ester

SOLUBLE	 $R^1 = C_2-C_4$	 $R^1 = C_2-C_4$	 $R^1 = C_2-C_4$	 $R^1 = C_5-C_8$	SOLUBLE	 $R^1 = C_1-C_4$	 $R^1 = C_2-C_4$	 $R^1 = C_1-C_4$	
	 $R^1 = C_1$	 $R^1 = C_1$	 $R^1 = C_1$			 $R^1 = C_2-C_4$	 $R^1 = C_3\text{-iso}$	 $R^1 = C_1-C_4$	
	 $R^1 = C_1, C_2, C_5-C_8$	 $R^1 = C_1, C_2, C_5-C_8$	 $R^1 = C_1-C_8$			 $R^1 = C_1-C_4$	 $R^1 = C_2, C_3, C_4$	 $R^1 = C_2-C_4$	
PARTIALLY SOLUBLE	 $R^1 = C_2-C_4$	 $R^1 = C_2-C_4$			PARTIALLY SOLUBLE		 $R^1 = C_1$		
	 $R^1 = C_1$	 $R^1 = C_1-C_4$	 $R^1 = C_2-C_4$	 $R^1 = C_4$		 $R^1 = C_3\text{-iso}$	 $R^1 = C_1-C_4$		
	 $R^1 = C_3-C_4$	 $R^1 = C_3-C_4$				 $R^1 = C_3\text{-iso}$			
INSOLUBLE	 $R^1 = C_1$	 $R^1 = C_1$	 $R^1 = C_1$	 $R^1 = C_1-C$	INSOLUBLE			 $R^1 = C_1-C$	
				 $R^1 = C_1-C_4$		 $R^1 = C_1$	 $R^1 = C_1-C_4$	 $R^1 = C_1-C_4$	
				 $R^1 = C_1-C_3$		 $R^1 = C_1$	 $R^1 = C_1$	 $R^1 = C_1-C$	 $R^1 = C_1-C_4$
	Ethyl acetate	Diethyl ether	Toluene	n-Hexane		Ethyl acetate	Diethyl ether	Toluene	n-Hexane

Fig. 17. Comparison of solubility in selected organic solvents for salts of (*R,S*)-ibuprofen and [ValOR][S(+)-IBU] (left) and salicylic acid (right) depending on the L-amino acid alkyl ester cation structure (L-Met: violet, L-Thr: orange, L-Ile: blue, L-Val: green).

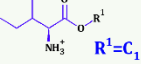
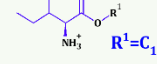
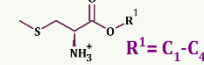
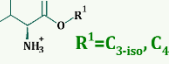
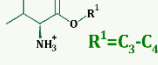
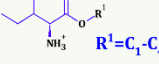
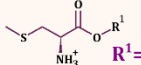
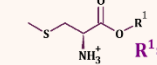
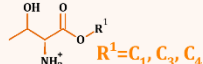
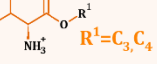
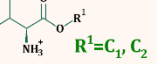
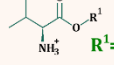
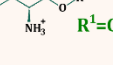
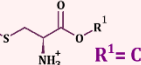
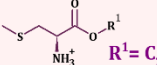
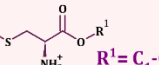
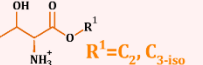
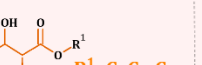
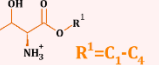
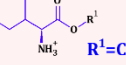
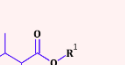
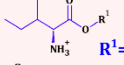
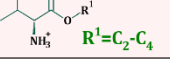
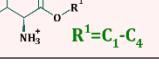
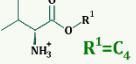
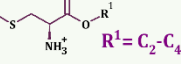
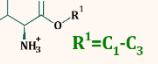
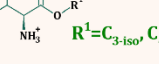
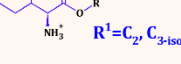
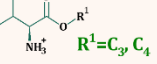
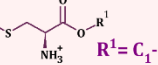
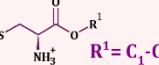
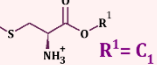
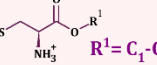
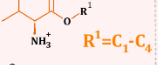
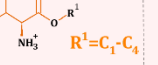
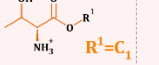
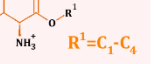
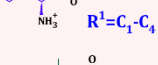
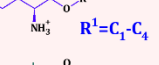
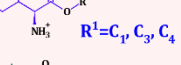
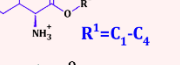
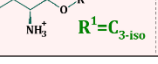
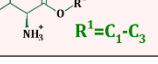
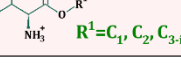
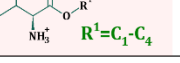
SOLUBLE	 $R^1 = C_1$	 $R^1 = C_1$	 $R^1 = C_1 - C_4$	
	 $R^1 = C_{3-iso}, C_4$	 $R^1 = C_3 - C_4$	 $R^1 = C_1 - C_4$	
PARTIALLY SOLUBLE	 $R^1 = C_1$	 $R^1 = C_1$		
	 $R^1 = C_1, C_3, C_4$	 $R^1 = C_3, C_4$	 $R^1 = C_1, C_2$	
	 $R^1 = C_1$	 $R^1 = C_1 - C_3$		
	 $R^1 = C_2 - C_4$	 $R^1 = C_2 - C_4$	 $R^1 = C_1 - C_4$	
INSOLUBLE	 $R^1 = C_2, C_{3-iso}$	 $R^1 = C_1, C_2, C_{3-iso}$	 $R^1 = C_1 - C_4$	
	 $R^1 = C_2 - C_4$	 $R^1 = C_2 - C_4$	 $R^1 = C_1 - C_4$	
	 $R^1 = C_2 - C_4$		 $R^1 = C_1 - C_4$	
	Ethyl acetate	Diethyl ether	Toluene	<i>n</i> -Hexane
SOLUBLE	 $R^1 = C_4$		 $R^1 = C_2 - C_4$	
PARTIALLY SOLUBLE	 $R^1 = C_1 - C_3$	 $R^1 = C_{3-iso}, C_4$	 $R^1 = C_2, C_{3-iso}$	
		 $R^1 = C_3, C_4$		
	 $R^1 = C_1 - C_4$	 $R^1 = C_1 - C_4$	 $R^1 = C_1$	 $R^1 = C_1 - C_4$
	 $R^1 = C_1 - C_4$	 $R^1 = C_1 - C_4$	 $R^1 = C_1$	 $R^1 = C_1 - C_4$
INSOLUBLE	 $R^1 = C_1 - C_4$	 $R^1 = C_1 - C_4$	 $R^1 = C_1, C_3, C_4$	 $R^1 = C_1 - C_4$
	 $R^1 = C_{3-iso}$	 $R^1 = C_1 - C_3$	 $R^1 = C_1, C_2, C_{3-iso}$	 $R^1 = C_1 - C_4$
	Ethyl acetate	Diethyl ether	Toluene	<i>n</i> -Hexane

Fig. 18. Comparison of solubility in selected organic solvents for salts of ketoprofen (left) and naproxen (right) depending on the L-amino acid alkyl ester cation structure (L-Met: violet, L-Thr: orange, L-Ile: blue, L-Val: green).

also showed a slightly worse solubility in diethyl ether. Most ketoprofenates and naproxenates were insoluble in ethyl acetate and diethyl ether. However, they showed good solubility in toluene, in contrast to the unmodified acids.

2.1.2. Determining the solubility in water and selected buffer solutions

The solubility of a drug significantly influences its concentration in the systemic circulation and thus determines its potential effect and pharmacological response in patients. Drugs with low aqueous solubility experience slower rates of absorption, resulting in inconsistent and inadequate bioavailability, which reduces their efficacy. Poor solubility can also lead to complications such as metabolic or permeability problems, drug-drug interactions or the need for prolonged drug release [177,178]. Therefore, improving the aqueous solubility of the active pharmaceutical ingredient is a primary goal in the development of API-based ionic liquids with the strategic design of counterions. These salts often exhibit favourable dissolution rates, largely due to the origin of the counterion from a strong base or acid. Upon contact with water, the counterion establishes a favourable pH within the aqueous interface, promoting the dissociation of the drug in water and facilitating its interaction with water molecules [179].

Besides the determination of solubility in water, it is essential to demonstrate solubility in aqueous solutions that closely mimic physiological conditions, as the salts obtained are intended for use in drug delivery systems. Therefore, the solubility of NSAIDs and their salts was evaluated in deionised water and two buffers with pH values of 5.4 and 7.4, reflecting the acidity of the skin surface and its deeper layers, respectively [180]. The saturation concentration results for the compounds under study were also expressed in terms of initial drug concentration and were presented in Appendix II (Tables A2–A6). A comparison of the saturation concentration values determined for L-amino acid alkyl (C₁-C₄) ester salts in selected media at various pH values is shown in Figure 19.

Among all selected acidic drugs, only salicylic acid showed good solubility in water (3.759 g/L). The saturation concentration [g/L] for the other unmodified acids in water were as follows: 0.076 for (*R,S*)-ibuprofen, 0.090 for *S*-(+)-ibuprofen, 0.013 for ketoprofen, and 0.147 for naproxen. All of the obtained salts were characterised with markedly higher solubility than the parent drug.

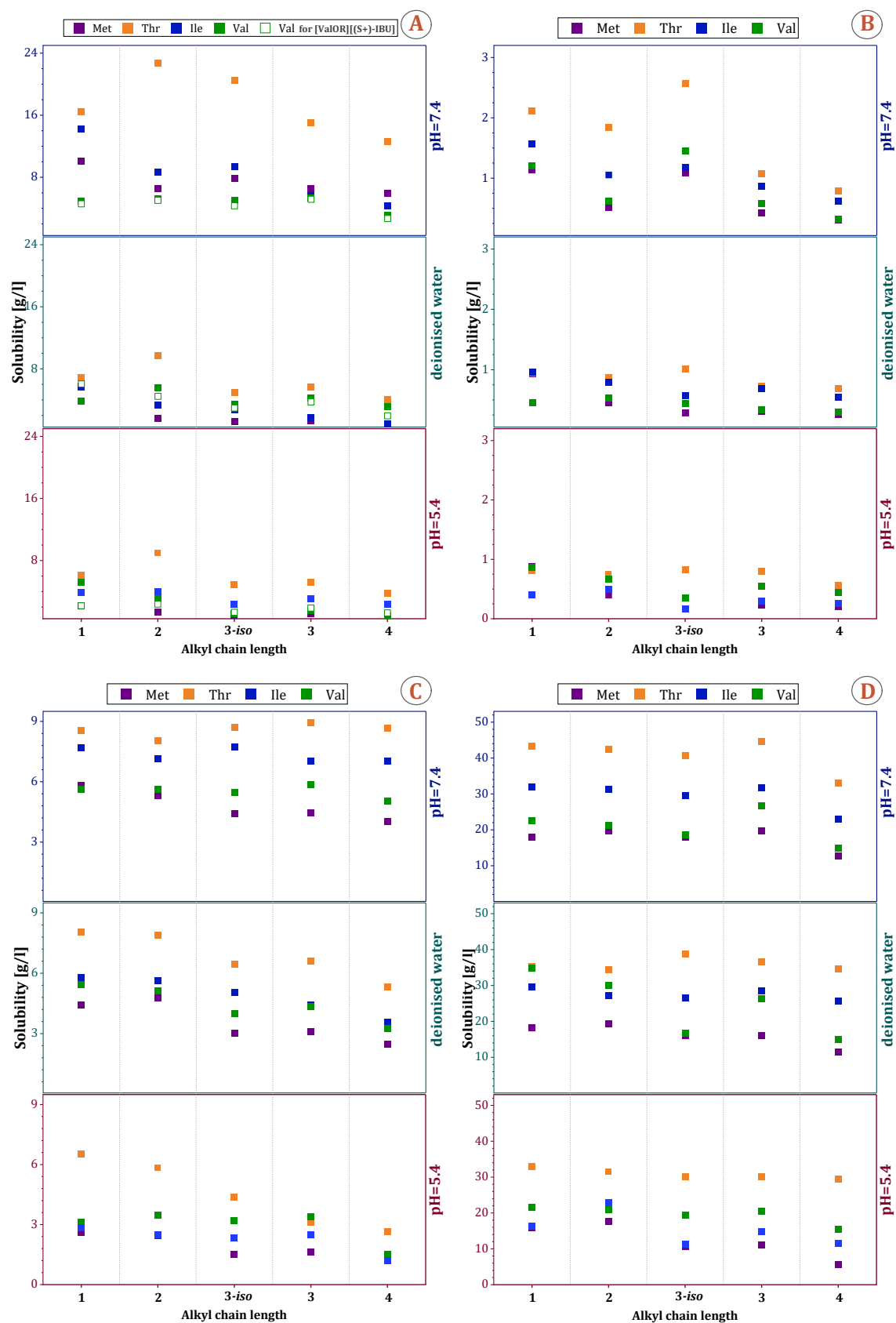


Fig. 19. The saturation concentration values determined for L-amino acid alkyl ester salts of A: (R,S)-ibuprofen and S-(+)-ibuprofen, B: ketoprofen, C: naproxen, and D: salicylic acid in selected aqueous media (phosphate buffer pH=5.4, deionised water pH=6.2, and phosphate buffer pH=7.4).

The highest values of saturation concentration in each group of NSAIDs derivatives were determined for the following compounds: [ThrOEt][IBU], [ThrOiPr][KETO], [ThrOMe][NAP], and [ThrOiPr][SA], for which the assessed solubility was 127, 78, 55, and 10 times higher, respectively, compared to the starting active acid. Furthermore, although the *S*-(+)-ibuprofen was better soluble in water than its racemic form, the L-valinium alkyl ester salts of (*R,S*)-ibuprofen described earlier were characterised by higher solubility than the respective *S*-(+)-IBU salts.

In general, the obtained L-amino acid alkyl ester salts demonstrated a decrease of solubility with the lengthening of the alkyl chain and in the order of the L-amino acid forming conjugates: L-Thr>L-Val>L-Ile>L-Met, which is consistent with previously described research [150,151,154,181,182]. In addition, in most cases, salts based on L-amino acid isopropyl esters were characterised by higher solubility compared to the corresponding salt consisting of a straight *n*-propyl chain.

It has been shown that the solubility of acids from the NSAID group depends on the pH of the medium and greatly increases in an alkaline environment due to ionisation, as the pH is above the pK_A [183–186]. These studies and complementary published research on solubility tests using selected buffer solutions representing the composition of body fluids demonstrated the dependence of the obtained derivatives solubility on the pH of the medium analysed [187].

Summary

- Except for the L-amino acid methyl ester hydrochlorides, which were insoluble in chloroform and ethyl acetate, the L-amino acid alkyl ester hydrochlorides were mostly soluble in ethanol, DMSO, dichloromethane, chloroform and ethyl acetate. A longer carbon chain (C₅-C₈) in L-valine alkyl ester hydrochlorides slightly reduced solubility in ethanol and improved solubility in *n*-hexane.
- Overall, the synthesised L-amino acid alkyl esters showed good solubility in most solvents studied. Partial or good solubility in *n*-hexane was observed only for L-methionine alkyl esters, L-threonine methyl ester and L-valine alkyl esters (from pentyl to octyl).
- The obtained salts of L-amino acid alkyl ester and selected NSAIDs were mostly soluble in polar solvents such as ethanol, DMSO, and nonpolar solvents such as dichloromethane and chloroform, similar to their parent drugs. Except for the [ThrOMe][SA] salt, which remained insoluble in both chloroform and

dichloromethane, the conjugation of salicylic acid and naproxen with L-amino acid alkyl esters improved their solubility in chloroform. In addition, most of the salts of ketoprofen and naproxen were insoluble in ethyl acetate and diethyl ether but had good solubility in toluene, in contrast to their unmodified forms.

- All the salts obtained showed a significantly higher solubility than the parent drug in deionised water and phosphate buffers with pH=5.4 and pH=7.4. Their solubility depends on the structure and hydrophobicity of the starting L-amino acid. The highest solubility in each aqueous medium studied was found for salts derived from polar L-threonine.
- Compared to the starting acid, the greatest increase in solubility (through conjugation with the [ThrOR] molecule) in water and the tested buffer at pH 5.4, after modification with amino acid esters, was obtained for (*R,S*)-ibuprofen, while in the buffer solution at pH 7.4 for ketoprofen. The highest solubility values in the tested media were obtained for salicylic acid derivatives and L-threonine alkyl esters.

2.2. Lipophilicity study

The lipophilicity measure of the affinity of the molecule to the oil phases is expressed by the *n*-octanol-water partition coefficient (logP). It is a key factor that describes and links the absorption and transport characteristics of the active pharmaceutical ingredient in the human body. Therefore, the role of lipophilicity is critical in the drug discovery and development process as it affects several pharmacokinetic factors. In general, increased lipophilicity results in increased permeability through the gastrointestinal tract, easier passage through barriers such as the blood-brain barrier and other tissue membranes, greater binding to proteins, and increased affinity to metabolising enzymes and efflux pumps. For a drug to be absorbed effectively, it must have adequate lipid solubility to cross membranes; otherwise, drugs not soluble enough to be transported into the bloodstream can reduce systemic bioavailability, resulting in suboptimal drug efficacy [188–190].

Regarding transdermal or topical delivery, logP is a useful tool for describing the partitioning of a drug between the hydrophilic living cells of the epidermis and the lipophilic *stratum corneum* (SC). Hydrophilic compounds with a log P value < -1 would have difficulty leaving the vehicle and entering the SC. At the same time, highly lipophilic compounds may accumulate in the SC, making it difficult to achieve stable plasma concentrations within a reasonable time. This suggests that compounds with log P values in the range of 1 to 3 should be considered as possible candidates for transdermal delivery,

having both aqueous and lipophilic properties, capable of crossing the lipophilic SC and the hydrophilic layers (epidermis) of the skin [191].

Considering that the salts obtained in this work are intended to be used in preparations applied dermally or transdermally, evaluating the lipophilicity properties is one of the most important parameters determining the behaviour of compounds in the skin structures. The obtained values of *n*-octanol-water are summarised in Appendix II in Tables A2–A6. At the same time, Figure 20 presents the dependence of logP on the solubility in water for NSAIDs and their L-amino acid alkyl (C₁–C₄) ester salts.

The solubility of a compound is strongly influenced by its lipophilicity. As shown in Figure 20, the poorly soluble unmodified acids were also characterised by high logP values: 3.208 for (*R,S*)-ibuprofen, 2.212 for *S*-(+)-IBU, 2.119 for naproxen and 1.577 for ketoprofen. It has been suggested that the presence of an additional oxygen atom, an acceptor for hydrogen bonds, is responsible for the decrease in logP values of ketoprofen and naproxen [192]. In the case of salicylic acid, which has good solubility in water, the logP obtained was equal to 1.321.

Conjugations with hydrophilic L-amino acid alkyl esters significantly reduced the lipophilic character of poorly soluble drugs. The exception was the salicylic acid derivatives, which showed a higher logP than the corresponding unmodified acid, indicating the formation of salts with higher lipophilicity.

The unmodified *S*-(+)-ibuprofen and its L-valinium alkyl esters salts exhibited lower logP than the corresponding compounds based on the racemic acid. The logP for L-valinium alkyl ester salts of *S*-(+)-IBU ranged from 0.833 (for [ValOMe][*S*(+)-IBU]) to 1.874 (for [ValOOct][*S*(+)-IBU]), while for the respective salts of (*R,S*)-IBU increased from 1.750 to 2.117 [150,187].

Furthermore, as described previously, in general, the determined values of solubility and logP of the L-amino acid ester isopropyl salts are in the range between those determined for the butyl and *n*-propyl derivatives since the value of the partition coefficient increases with the branched carbon chain in the ester moiety. Moreover, since the logP values determined correspond to the evaluated values of saturation concentration in deionised water, the increase in compound lipophilicity also follows the trend of order of L-amino acid modification: L-Thr<L-Ile<L-Val<L-Met [150,181,182].

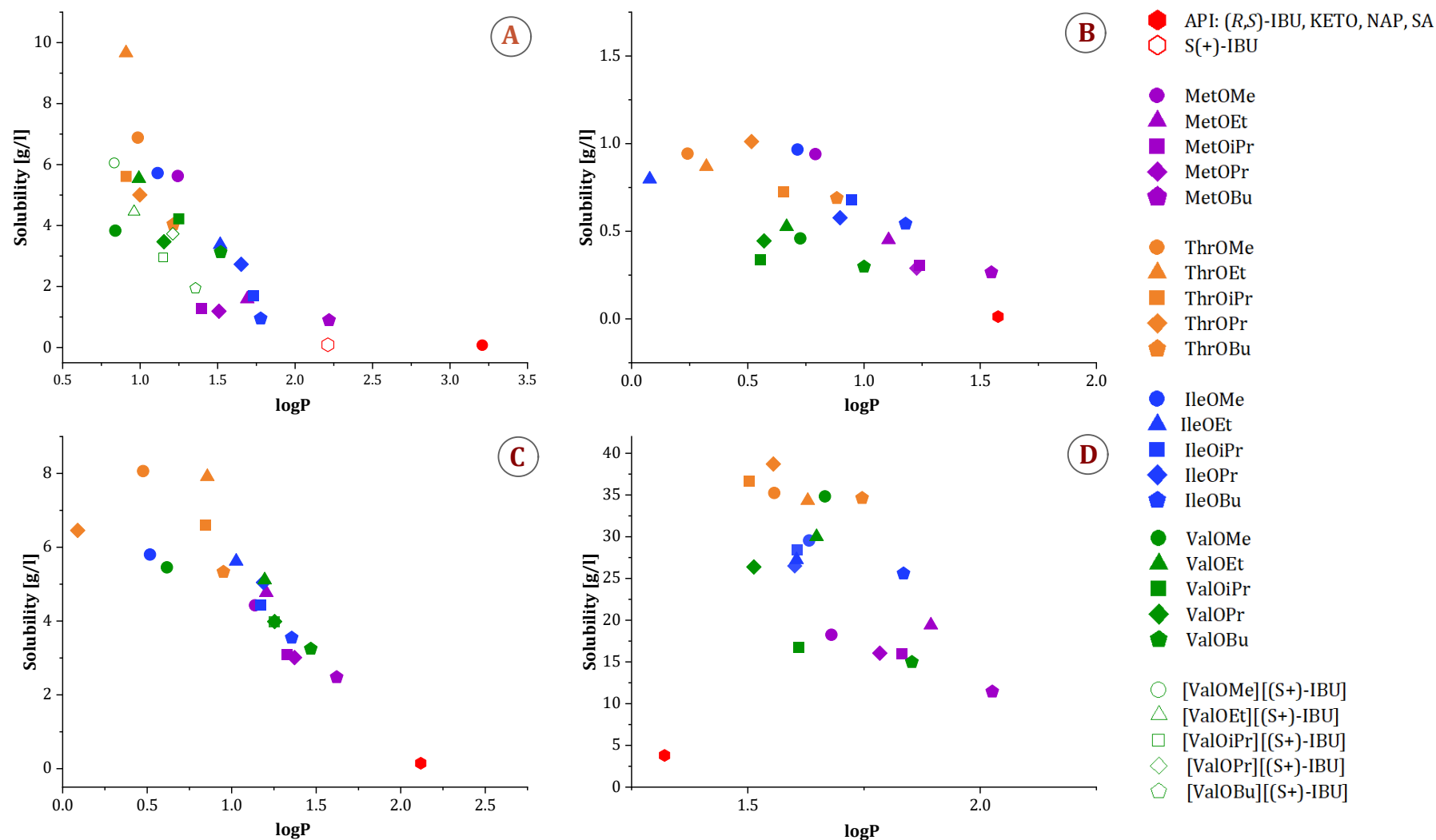


Fig. 20. The effect of the cation in salts of A: (R,S)-ibuprofen and S-(+)-ibuprofen, B: ketoprofen, C: naproxen, and D: salicylic acid and L-amino acid alkyl ester on the dependence of solubility in water on lipophilicity (logP). According to the starting amino acid marked as: L-Met (purple); L-Thr (orange), L-Ile (blue), L-Val (green). According to the alkyl ester, it is marked as: methyl (circle), ethyl (triangle), isopropyl (square), propyl (diamond), and butyl (pentagon).

Summary

- The combination of poorly soluble drugs with L-amino acids alkyl esters has achieved a reduction of lipophilicity. Solubility in aqueous media is strongly influenced by lipophilicity. Consequently, the logP value of the compound also increases with the length of the alkyl chain in the ester moiety, following the order of the L-amino acid: L-Thr<L-Ile<L-Val<L-Met.

2.3. Characteristics of the thermal properties

The pharmaceutical industry has a keen interest in the thermodynamic behaviour of drug molecules. These thermodynamic properties have a significant impact on the three pillars of drug development - stability, bioavailability and manufacturability. A lack of understanding of these properties can lead to unanticipated negative consequences throughout the entire product development process. Examples include unexpected polymorphism due to storage conditions, degradation leading to loss of stability and manufacturing process failures due to physical state change [193,194].

In this context, Thermal Gravimetric Analysis (TGA) was used to assess the thermal stability and thermal degradation of the synthesised compounds. In contrast, Differential Scanning Calorimetry (DSC) was used to investigate the heating/cooling behaviour and properties, including melting temperature, crystal identification and phase transition determination. In addition, the stability of selected compounds was evaluated to investigate the changes in properties with time under the influence of temperature. Tables A13-A17 in Appendix II summarise the stability temperatures and values and phase transition temperatures determined. The $T_{TGonset}$, T_{DTGmax} values determined for salts of L-valine alkyl esters in combination with ibuprofen, salicylic acid, naproxen and ketoprofen are presented in the author's master's thesis or previous publication [149,150,152–154,195].

The short-term thermal stability was evaluated based on the onset temperature of thermal degradation as the onset value of the TG curve ($T_{TGonset}$), which occurs in the first phase of the process. The values of the maximum mass loss ratio (T_{DTGmax}) were calculated from the maximum peak of the DTG curve. The melting point and crystallisation (the melting points being endothermic (positive peaks in the graphs) upon heating and crystallisation point being exothermic (negative peaks) upon cooling) data evaluated from the DSC analysis are based on both the measured $T_{DSConset}$ and T_{DSCmax} values and the T_{Conset} and T_{Cmax} values, as the registered peaks are mostly broad.

The $T_{TGonset}$ values determined for unmodified acids and their L-amino acid alkyl (from methyl to butyl) ester salts are presented in Figure 21, while the comparison of the TG and DTG curves for *S*-(+)-ibuprofen and their L-valinium alkyl ester salts are shown in Figure 22.

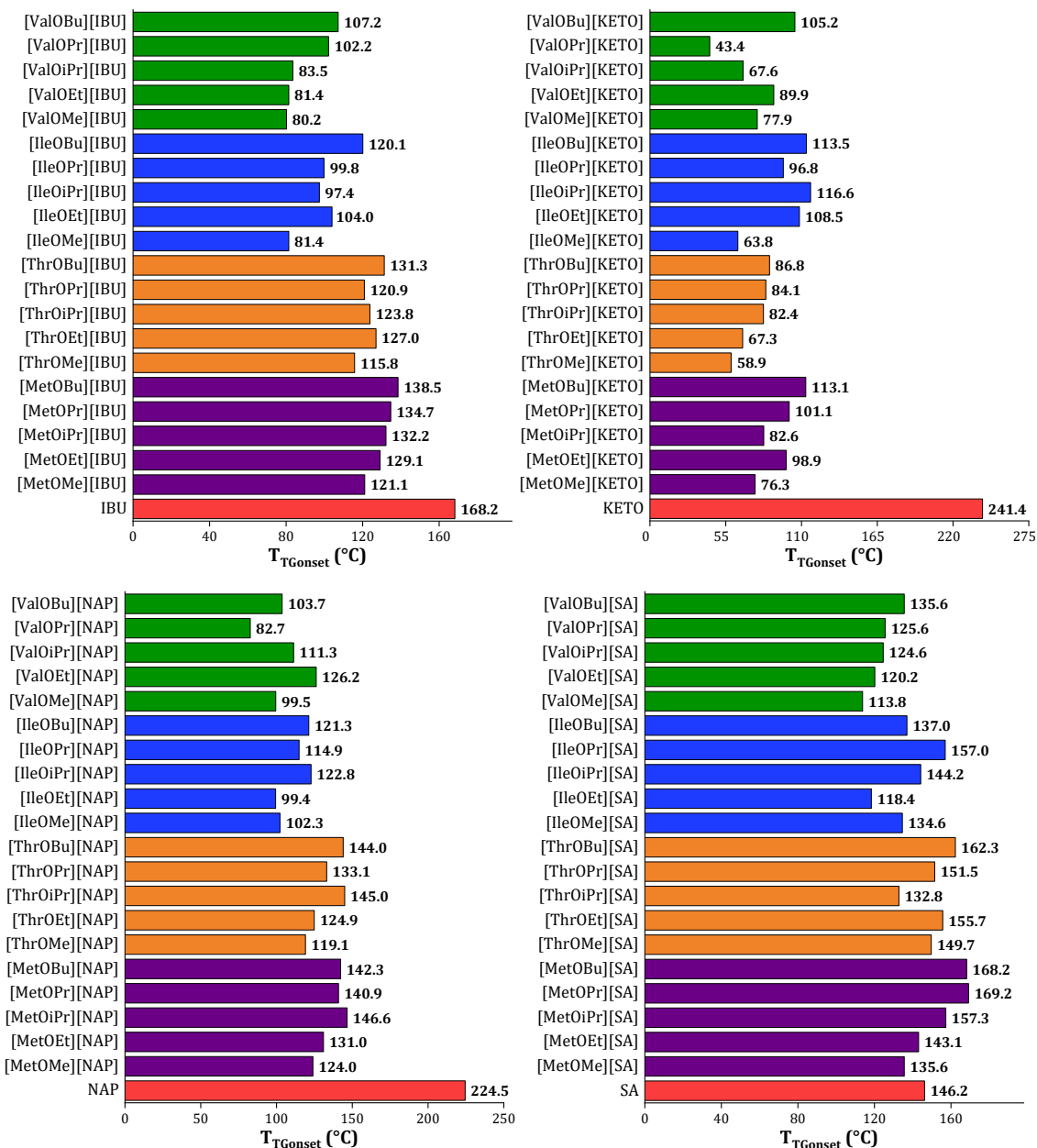


Fig. 21. Onset temperatures of thermal degradation of the NSAIDs and their salts with L-amino acid alkyl (C_1 – C_4) esters (data partly presented in: [149,150,152–154,195]).

Introducing the L-amino acid alkyl ester cation into the active acid moiety decreases the final thermal stability of the obtained compound compared to the unmodified drug, the salicylates being the only exception. They were characterised by $T_{TGonset}$ values comparable to or slightly lower than that of the unmodified drug. At the same time, the salts [IleOPr][SA], [ThrOBu][SA], [ThrOPr][SA], [ThrOMe][SA], [ThrOEt][SA],

[MetOBu][SA], [MetOPr][SA], and [MetOiPr][SA] showed higher thermal stability. The exceptions observed in this effect, where the obtained L-threonine alkyl ester salts of salicylic acid showed a higher thermal stability in comparison to the unmodified acid, can be explained by the presence of the hydroxyl group in the starting amino acid moiety. This group can participate in additional hydrogen bonding within the molecule (intramolecular hydrogen bonding between the hydroxyl group and the carboxyl group of salicylic acid) and between molecules, which can stabilise the molecular structure and thus block the thermal decomposition reaction to some extent [196,197]. In the case of choline-based amino acid ILs, it has been observed that longer alkyl chains on the cation create a strong hydrophobic interaction, which improves the overall thermal stability of the ILs [198]. For salicylates based on L-methionine cations with longer alkyl chain length in the ester part, similar phenomena can be observed.

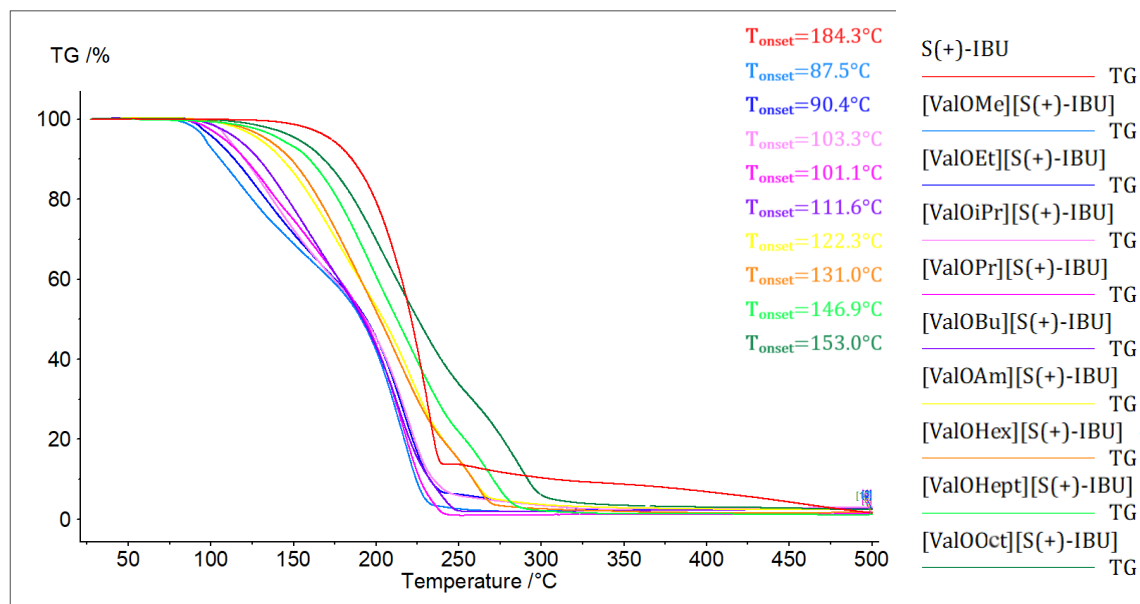


Fig. 22. Comparison of the thermal stability of the L-valinium alkyl ester salts of *S*-(+)-ibuprofen.

As described previously, the thermal stability of L-amino acid alkyl ester salts generally increases with the lengthening of the alkyl chain in the cationic moiety and in the following order of starting L-amino acids: L-Met>L-Thr>L-Ile>L-Val. In addition, the L-amino acid propyl ester salts of ibuprofen and naproxen were more stable than derivatives consisting of the corresponding L-amino acid isopropyl ester cation [150,151,181,182]. In a comparison of the stability of salts obtained from different enantiomers of ibuprofen, L-valinium alkyl ester *S*-(+)-ibuprofenates were slightly more stable than the corresponding salts obtained from (*R,S*)-ibuprofen [149–151,195].

The degradation onset temperature ranged 80.2–150.8°C for [ValOR][IBU] and 87.5–153.0°C for [ValOR][S(+)-IBU] salts.

As [ThrOPr][IBU], [ThrOBu][IBU], [ThrOiPr][SA], [IleOEt][SA], [IleOEt][KETO], [ValOPr][KETO] compounds and L-threoninium alkyl ester salts of ketoprofen are amorphous, no melting and crystallisation peaks were evaluated during the measurement. In addition, the salts of ketoprofen, as well as the unmodified acid, showed no crystallisation upon cooling. The crystallisation peaks were also not evaluated for any of the derivatives of the L-threonine alkyl esters synthesised, nor for the salts [MetOMe][SA], [MetOEt][SA], and [ValOEt][SA]. The decrease of the melting point has been described in the example of derivatives obtained from pure lidocaine or pure ibuprofen in different ratios, up to a certain composition where the sample does not crystallise at all, showing a slow crystallisation kinetics [199].

The relationship between the melting point (evaluated based on $T_{DSC\ max}$ in the first heating cycle) of the L-amino acid alkyl (C_1 - C_4) esters salts and their carbon chain length is presented in Figure 23.

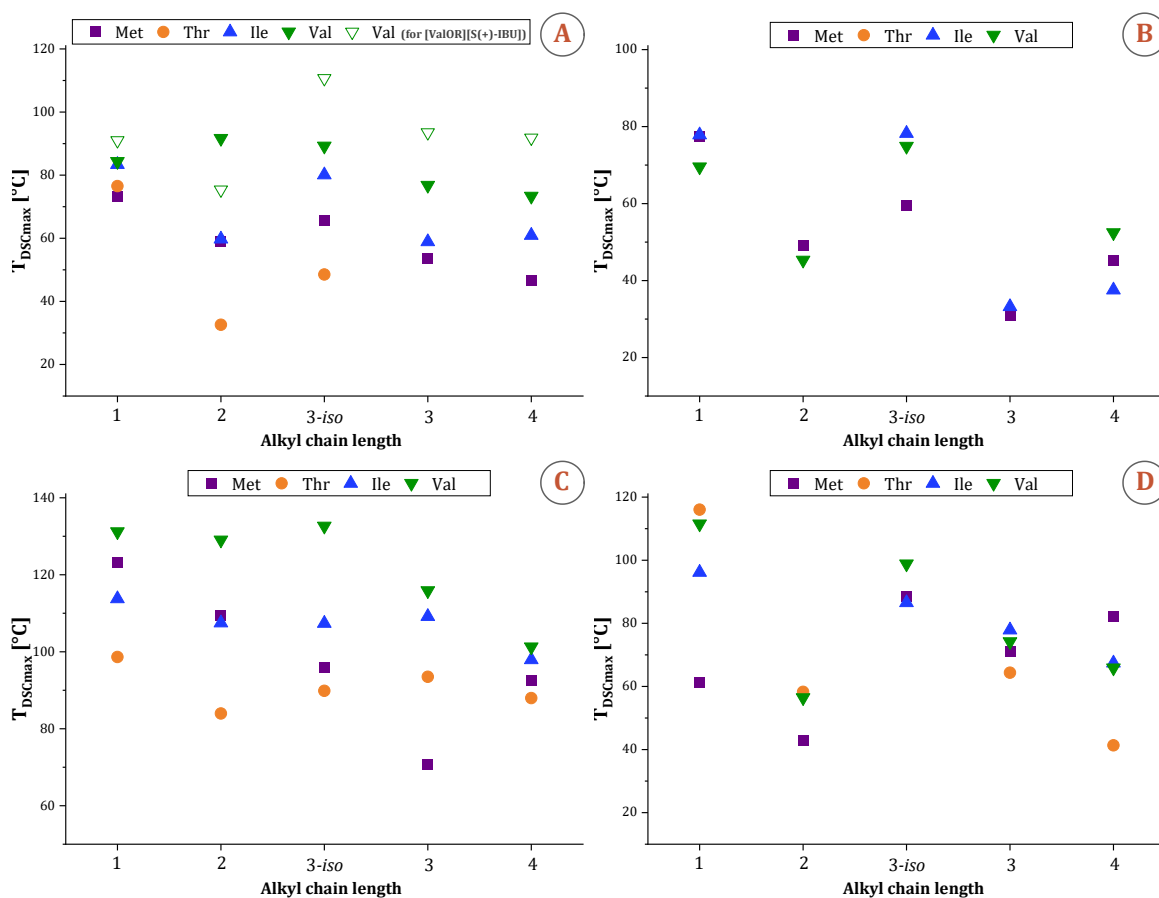


Fig. 23. The dependence of melting point ($T_{DSC\ max}$) on alkyl chain length in the ester moiety of L-amino acid ester salts of A: (R,S)-ibuprofen and S-(+)-ibuprofen, B: ketoprofen, C: naproxen and D: salicylic acid (data partly presented in: [150,152–154,181,182,195]).

Since the melting peaks recorded were broad, the T_{DSCmax} value determined was used to show the dependence on the chain length in the ester moiety as accurately as possible. For the unmodified acids, evaluated from the first heating cycle, the T_{DSCmax} values were as follows: 78.58°C for (*R,S*)-ibuprofen, 50.27°C for *S*-(+)-ibuprofen, 97.03°C for ketoprofen, 155.45°C for *S*-naproxen, and 160.04°C for salicylic acid. The salts obtained from L-valine alkyl esters and *S*-(+)-ibuprofen showed higher melting point values than the parent drug and also the corresponding salts derived from (*R,S*)-ibuprofen. In other cases, with the exception of [ValOMe][IBU], [ValOEt][IBU], and [IleOEt][IBU], the obtained derivatives show lower melting points than the parent drug. A lower melting point is advantageous for the extended use of the prodrugs in transdermal and topical applications. Creating a higher concentration gradient between the matrix and the skin facilitates skin penetration [200]. Except for most of the obtained salts of naproxen, [ValOMe][SA] and [ThrOMe][SA] compounds, the obtained derivatives showed melting points lower than 100°C. Together with the previously demonstrated ionic structure, these salts can be defined as belonging to the group of ionic liquids [201]. As shown in the graphs (Fig. 23), the increase in T_{DSCmax} follows, in general, the order of starting L-amino acids: L-Met<L-Thr<L-Ile<L-Val.

It was also observed that the melting point value decreases with the lengthening of the alkyl chain, which is most pronounced in the case of the L-valinium alkyl ester salts of (*R,S*)- and *S*-(+)-ibuprofen. The values of onset melting was equal 80.90°C and 83.13°C for [ValOMe][IBU] and [ValOMe][*S*(+)-IBU] respectively, while 43.28°C and 48.24°C for [ValOOct][IBU] and [ValOOct][*S*(+)-IBU] compounds [149–151]. A similar phenomenon was observed in tetraalkylphosphonium and 1-alkyl-3-methylimidazolium-based ionic liquids, where the melting point initially decreases with the increase in the number of carbon atoms in the straight aliphatic chain of the cations, up to a critical number, after which there is a change in tendency and the melting point starts to increase with the number of carbon atoms in the alkyl chain [202,203]. The role of the counterion in regulating salt properties has also been investigated using a homologous series of amines, finding that increasing chain length results in lower melting points of salts of carboxylic acid drugs [204]. Furthermore, the L-valinium alkyl ester salts obtained from (*R,S*)-ibuprofen were characterised by higher $T_{DSConset}$ and T_{DSCmax} values, although the melting point of the starting *S*-(+)-ibuprofen was lower than that of the racemic form.

Surprisingly, in the case of L-valinium alkyl ester salts of naproxen, two melting peaks were observed in both the first and subsequent heating cycles, and only one

crystallisation peak (in both cooling cycles) was observed. In the first cycle, this could indicate the presence of more than one initial crystalline form. During the subsequent heating cycles, the compound could retain these different forms, resulting in the reappearance of the double melting peaks. A similar phenomenon was observed for [IleOMe][KETO], [IleOBu][KETO], [IleOiPr][KETO] and [MetOEt][SA], which, however, do not show crystallisation peaks in the cooling cycle. The occurrence of double melting points in drug derivatives can often be attributed to the phenomenon of polymorphism or the existence of multiple crystalline forms of a substance. However, it is unusual for polymorphism to manifest itself in exactly the same way in successive cycles without different crystallisation events [205,206].

2.3.1. Stability testing

With the increasing demand for efficient drugs, stability testing is recognised as a fundamental part of the drug development process for performance evaluation and quality assurance of pharmaceutical products. The study was carried out to provide evidence of how the amino acid ester cation affects the quality of the obtained salts over time when exposed to varying temperatures.

The stability of L-amino acid isopropyl ester salts of NSAIDs was performed based on Stability Testing of New Drug Substances and Products [207]. These compounds, based on cations with an isopropyl carbon chain length in the ester part, have been selected for research as they show the most promising parameters in terms of skin permeability and biological activity [150–154,166]. The purpose of stability testing is to establish recommended storage conditions and to ensure the quality, safety and efficacy of the finished product by providing information on how the quality of a drug derivative changes over time under the influence of temperature.

The thermal stability changes were investigated for long-term conditions (storage for 12 months in refrigeration and room temperature) and accelerated conditions (storage for 6 months at 40°C). Table A38 in Appendix II summarises the comparison of the determined $T_{DSC\text{onset}}$ and $T_{DSC\text{max}}$ values obtained from the first heating cycle and T_{Conset} and the value obtained from the first cooling cycle. The individual DSC curves for studied compounds are presented in Figures A4-A23 in Appendix II. Figure 24 compares the evaluated melting point values ($T_{DSC\text{max}}$) for the tested compounds in each step of the performed stability test. No data were obtained for [ThrOiPr][KETO] samples, [ThrOiPrIBU] sample stored for 12 months at 25°C, the [ThrOiPr][SA] samples in the initial

state and after the stress test, and the [MetOiPr][KETO] sample after the stress test, which were in the amorphous state.

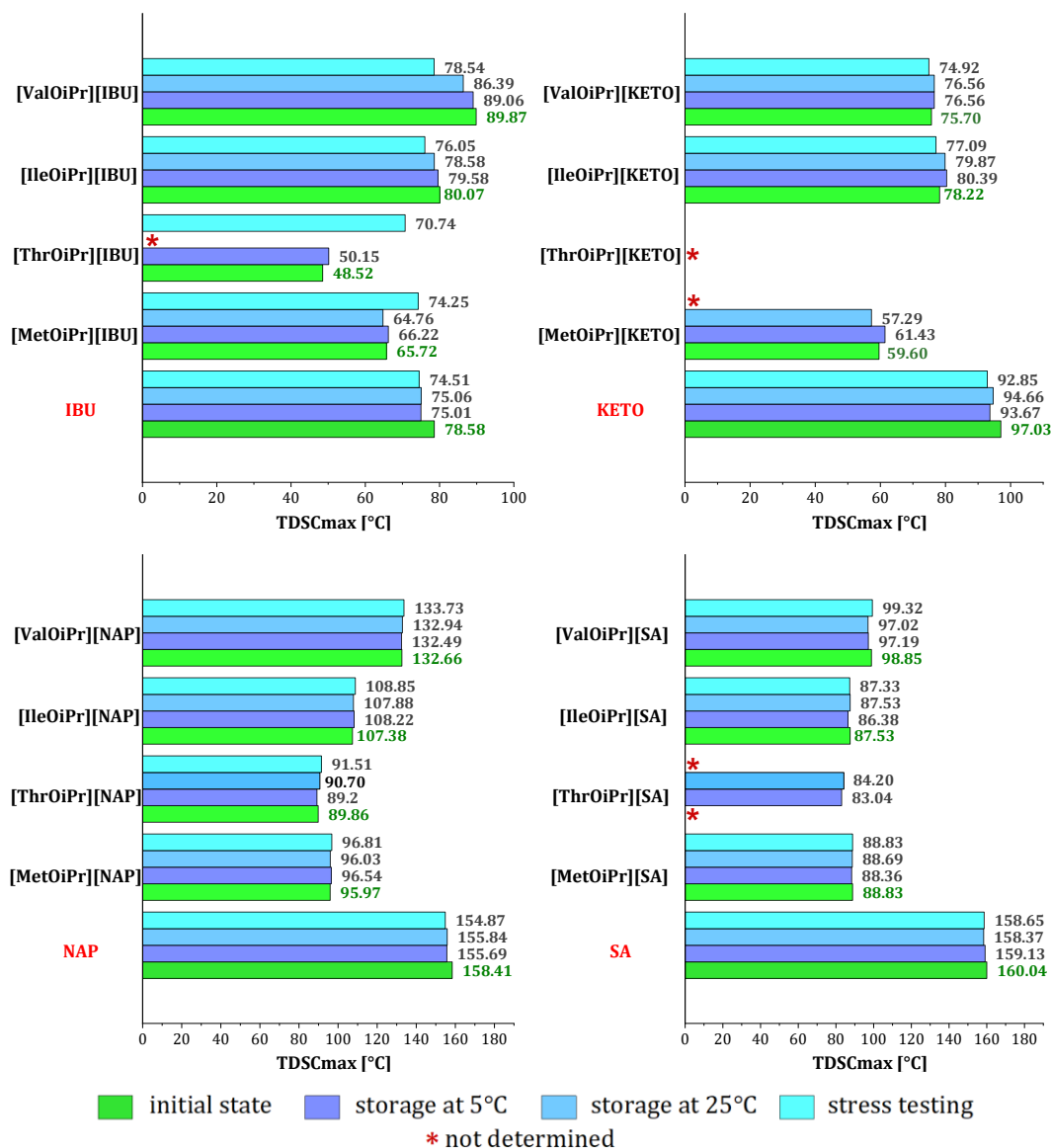


Fig. 24. Comparison of the melting point (T_{DSCmax}) for selected acids from NSAIDs group and their L-amino acid isopropyl ester salts after evaluation of stability testing.

In the case of the long-term stability test (storage for 12 months at 5 and 25°C), the studied conjugation of L-amino acid isopropyl esters with active ingredients has no effect on the deterioration of the stability of the obtained derivatives. The results obtained showed no differences in the measured phase transition temperature values of the stored compounds compared to the starting salts and unmodified acids. The irregular shapes of the overlapping melting peaks recorded during the first heating cycle are responsible for the changes in T_{DSCmax} values observed for compounds [ValOiPr][IBU] and [IleOiPr][IBU]. In other cases, the difference between the determined temperatures was within 1-3% error of the measurement. The exception was the [ThrOiPr][SA] salt, which was initially amorphous and

became semi-solid after 12 months of storage ($T_{DSC\text{onset}}=78.36^{\circ}\text{C}$ and $T_{DSC\text{max}}=83.04^{\circ}\text{C}$ for storage at 5°C , and $T_{DSC\text{onset}}=80.86^{\circ}\text{C}$ and $T_{DSC\text{max}}=90.70^{\circ}\text{C}$ for storage at 25°C , respectively). It was also observed that [ThrOiPr][IBU] became amorphous when stored at 25°C , whereas no noticeable difference in phase transition temperatures was noticed when stored at 5°C .

The pharmaceutical ingredients transformed into the amorphous state are considered to exhibit higher bioavailability, mainly due to the higher dissolving rate compared to the typical crystalline phase [208]. However, as this study has shown, the amorphous state can be lost during storage, as was the case with the crystallisation process of the [ThrOiPr][SA] compound after 12 months of storage at both temperatures tested. The crystalline form was thermodynamically stable, as proved by an additional stress testing study for this sample. The effective preparation of the amorphous salt was achieved in the case of [ThrOiPr][KETO], which maintains its state in each step of the performed long-term stability test.

Following the stress test study (stored for 6 months at 40°C), none of the starting active substances showed differences in phase transition temperatures. However, some of the L-amino acid isopropyl ester salts in the study showed noticeable changes.

The measured melting peaks of the compounds [ThrOiPr][NAP], [IleOiPr][KETO], [ValOiPr][KETO] were broader compared to the initial state of the samples, which explains the observed differences of the registered $T_{DSC\text{onset}}$ and $T_{DSC\text{max}}$ values in the heating cycles. Similarly, broad crystallisation peaks were registered in both cooling cycles performed for the conjugation of L-methioninium isopropyl ester with the salicylic acid moiety.

No differences were observed after the stress test for the other salicylates and naproxenates that were tested. In addition, the two overlapping melting peaks registered in the initial state in the heating cycles for [IleOiPr][NAP], [ValOiPr][NAP], and for [IleOiPr][IBU] were also observed after both the long-term stability tests and the stress tests performed. This suggests the thermodynamic stability of the observed state of these salts.

The compounds [MetOiPr][IBU], [ThrOiPr][IBU], [MetOiPr][KETO] and [ThrOiPr][KETO] were also observed to change colour to brown after the stress test. [MetOiPr][KETO], which was originally semi-solid, also became amorphous. Furthermore, the melting point temperatures evaluated for [ThrOiPr][IBU] in the first heating cycle were comparable to the $T_{DSC\text{onset}}$ and $T_{DSC\text{max}}$ determined for unmodified ibuprofen.

To account for the potential degradation of these compound, FTIR analysis was performed. For the salts [ValOiPr][KETO] and [IleOiPr][KETO], no changes were observed

compared to the initial state of the compound tested (data presented in Appendix II, Fig. A2-A3). Figures 25 and 26 show comparisons of ATR-FTIR spectra for L-methioninium and L-threoninium isopropyl salts of ibuprofen and ketoprofen before and after the stress testing step.

The ATR-IR analysis revealed the differences between the registered spectra for samples of the tested compounds after performing the stress test in comparison to the initial state of the compound in the fingerprint range of 400–1400 cm^{-1} (Fig. A1 in Appendix II). For example, for the tested sample of ibuprofenates, it was observed the disappearance of absorption bands initially assigned to the isopropyl L-amino acid ester (peaks at 520 and 1037 cm^{-1} and at 1056, 1100, 1220, 1284 cm^{-1} for [MetOiPr][IBU] and [ThrOiPr][IBU] respectively), while noticeable absorption bands assigned to the unmodified acid appeared (at 450, 635, 755, 782 cm^{-1} and at 521, 590, 637, 864, 932 cm^{-1} for [MetOiPr][IBU] and [ThrOiPr][IBU] respectively).

Similarly, for both samples [MetOiPr][KETO] and [ThrOiPr][KETO] after stress testing, bands assigned to the unmodified ketoprofen were visible at 610, 855, 787, and 930 cm^{-1} . It was also observed the disappearance of absorption bands at ca. 1606 and 1386 cm^{-1} for [MetOiPr][IBU] and [ThrOiPr][IBU], which were assigned to asymmetric $\nu(\text{COO}^-)_{\text{asym}}$ and symmetric $\nu(\text{COO}^-)_{\text{sym}}$ vibrations, initially confirming the formation of the carboxylate anion.

In the case of the ketoprofenates tested, those characteristic bands first observed at ca. 1595 and 1385 cm^{-1} were also missing. Furthermore, the sharp band initially observed at ca. 1735 cm^{-1} , which was attributed to C=O stretching vibrations characteristic of α -amino acids, was also obscured by absorption peaks at ca. 1700 cm^{-1} due to C=O stretching vibration in the dimeric carboxylic acid present in pure ketoprofen. For the [ThrOiPr][IBU] salt after the stress test, the characteristic band initially observed at about 1740 cm^{-1} was not recorded in the spectra. In addition, the visible absorption peak at ca. 1704 cm^{-1} was assigned to C=O stretching vibrations for ibuprofen with a free carboxyl group. This indicates the loss of ionic structure and the degradation of the pure salt form of the tested compounds after the stress test [209–211].

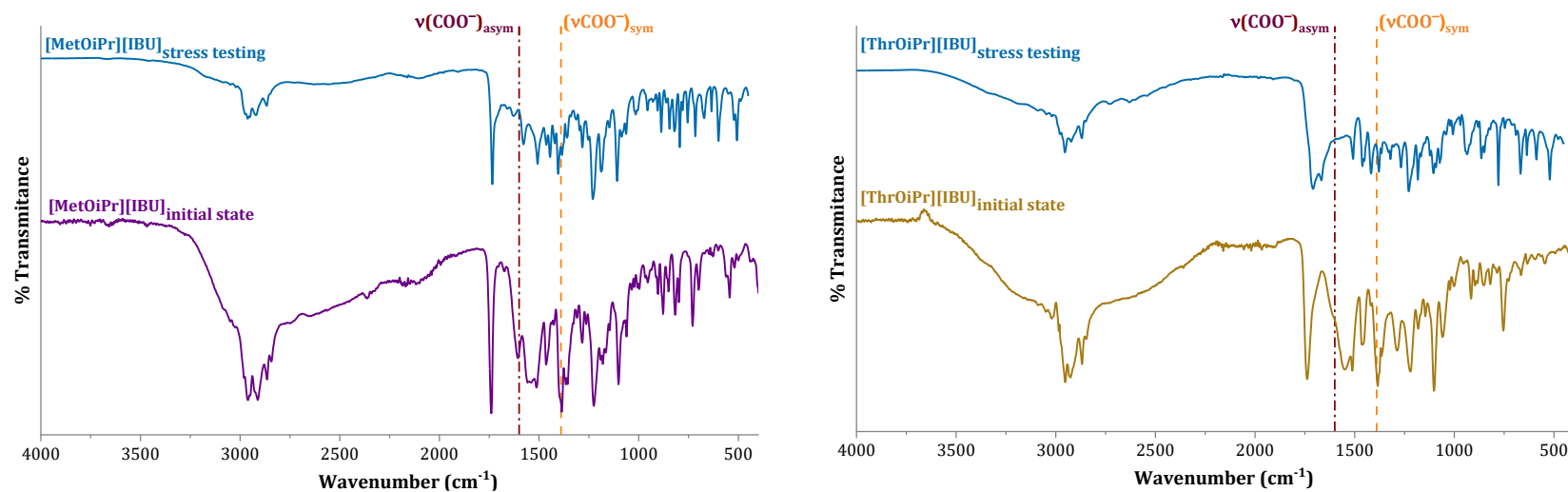


Fig. 25. Comparison of ATR-FTIR spectra for L-methioninium (left) and L-threoninium (right) isopropyl salts of ibuprofen before and after the stress testing step, asymmetric ($v_{\text{asym.}}$) (COO^-), and symmetric ($v_{\text{sym.}}$) (COO^-) stretching vibrations marked in brown and orange, respectively.

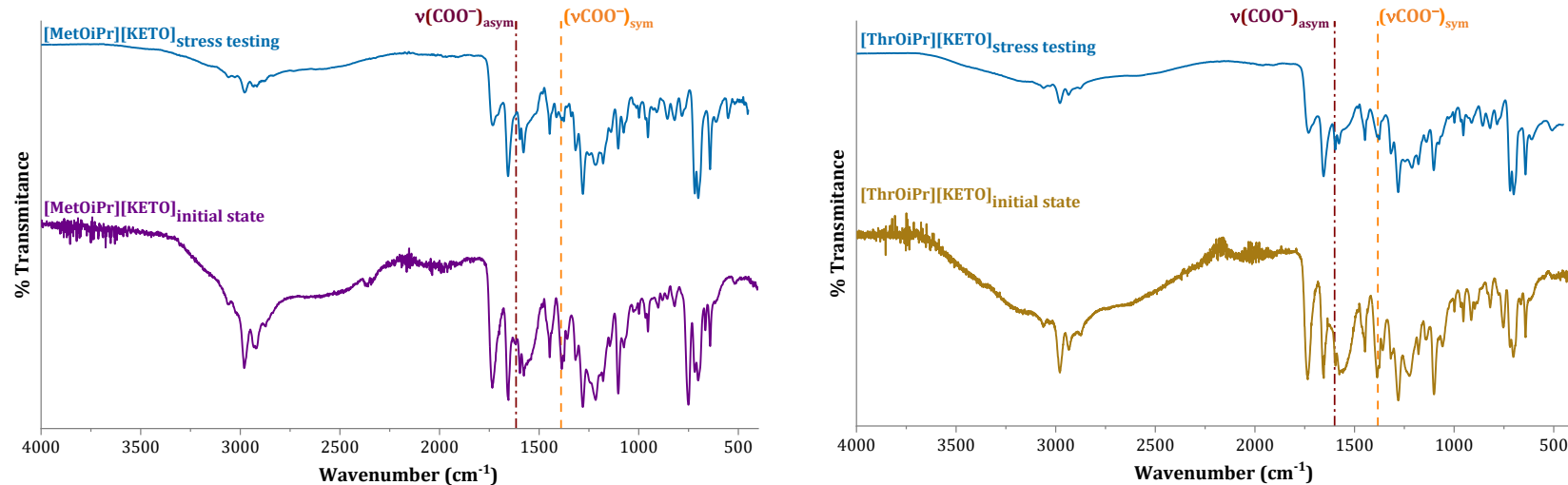


Fig. 26. Comparison of ATR-FTIR spectra for L-methioninium (left) and L-threoninium (right) isopropyl salts of ketoprofen before and after the stress testing step, asymmetric ($v_{\text{asym.}}$) (COO^-), and symmetric ($v_{\text{sym.}}$) (COO^-) stretching vibrations marked in brown and orange, respectively.

2.3.2. Evaluation of heat capacity

The heat capacity of drugs themselves is usually not a primary concern in pharmacology or drug formulation. However, the heat capacity of a substance can influence its behaviour during crystallisation and melting, which are crucial in the manufacture of drugs. Therefore, understanding the thermal behaviour of pharmaceutical substances, including their heat capacities, is essential for assessing the risks associated with thermal runaway reactions in industrial processes. It is part of the design of storage environments that maintain a stable temperature for substances sensitive to temperature changes. This ensures that the compounds do not undergo unwanted heat-induced decomposition over time. Heat capacity is also a physicochemical property that differs between crystalline and solvated forms of the same substance. It can also be used to identify polymorphs [212–215].

Moreover, the thermal properties of a substance (including its heat capacity) can influence the temperature of the skin surface and, therefore, the properties of the skin. However, the heat capacity itself may not directly affect skin permeability. For example, heating the skin can increase blood flow. This can temporarily increase skin permeability by making the skin more pliable and the pores more open. This principle is sometimes used in transdermal drug delivery systems, where heat is applied to the skin to increase the absorption of a drug through the skin [216].

The heat capacity measurements were carried out for selected acids from the NSAIDs group and their L-amino acid isopropyl ester salts using the three-curve method with sapphire disc as reference [217]. Data were recorded for solid samples up to the onset of melting, except for the salts [ThrOiPr][KETO] and [ThrOiPr][SA], which were in the amorphous state. The detailed experimental values of the molar heat capacities are summarised in the Appendix II (Tables A18-A37). A comparison of the evaluated data is shown in Figure 27.

The molar heat capacity value for the unmodified studied acid follows the order: KETO < IBU < NAP < SA. In the case of the studied L-amino isopropyl ester salts, except for [ValOiPr][NAP], the $C_{p,m}$ values were much higher compared with crystalline phases of unmodified acids. The obtained data showed increased C_p and m values along with temperature. For amino acid-based ionic liquids, this phenomenon was correlated with the influence of vibrational and rotational energy on the internal energy of the molecules [218]. The amorphous compounds [ThrOiPr][KETO], [ThrOiPr][SA] and semi-solid [ThrOiPr][IBU] showed the highest values of $C_{p,m}$, which is consistent with studies

describing that the lack of long-range order typical of crystalline solids can store thermal energy and compared to the crystalline form of a drug, the amorphous form is in a state of higher energy [219]. Similarly, the heat capacity value was influenced by both the parent anion and the state of the final compound. The semi-solid salts of ketoprofen showed the highest $C_{p,m}$ values, whereas the solid salts of salicylic acid and [ThrOiPr][NAP] had the lowest $C_{p,m}$ values.

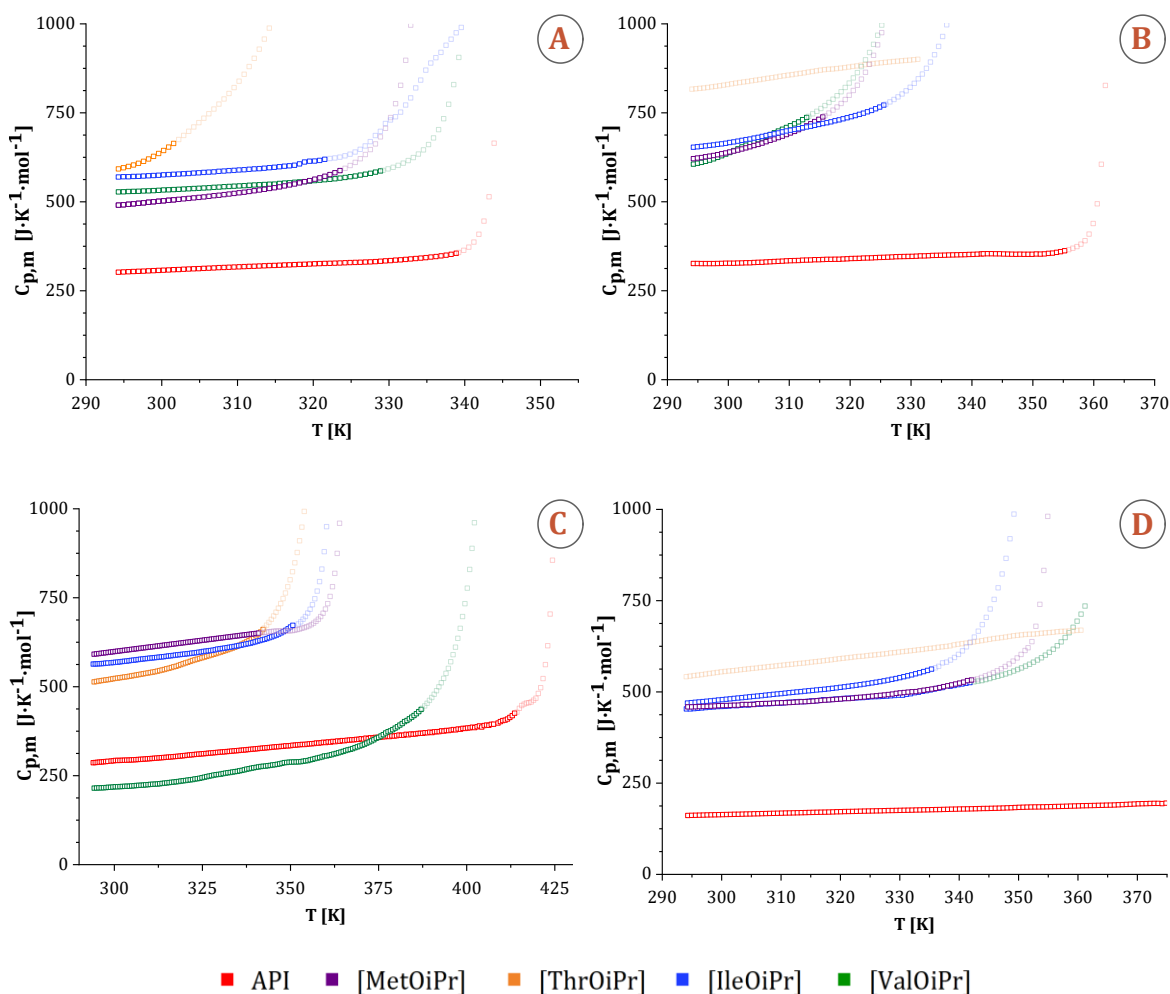


Fig. 27. Experimental molar heat capacity of NSAIDs (A: ibuprofen, B: ketoprofen, C: naproxen, and D: salicylic acid) and their L-amino acid isopropyl ester salts plotted against temperature.

Summary

- In general, pairing the active substance with the L-amino acid alkyl ester influenced the decrease in the thermal stability of the obtained compound. [IleOPr][SA], [ThrOBu][SA], [ThrOPr][SA], [ThrOMe][SA], [ThrOEt][SA], [MetOBu][SA], [MetOPr][SA], and [MetOiPr][SA] showed higher thermal stability compared to the parent acid.

- Increasing the alkyl chain length in the cationic moiety influences the higher thermal stability and lower melting points of the salts obtained. The increase in thermal stability follows the order of the starting L-amino acids: L-Met>L-Thr>L-Ile>L-Val, while in this order, a decrease in T_{DSCmax} values was observed.
- All obtained L-amino alkyl ester salts of ketoprofen, most ibuprofen derivatives (except [ValOiPr][S(+)-IBU] compound) and salicylic acid derivatives (except [ValOMe][SA] and [ThrOMe][SA] compounds) belong to the group of ionic liquids, based on the evaluated melting points and previously established ionic structure. Among the obtained salts of naproxen, only the derivatives based on [ThrOR], [MetOPr], [MetOiPr], [MetOBu] and [IleOBu] can be classified as ionic liquids.
- The studied L-amino acid isopropyl ester salts demonstrate high stability after long-term storage for 12 months at 5 and 25°C. Also, except conjugates of [MetOiPr] and [ThrOiPr] cations with ibuprofen and ketoprofen moieties, obtained salts showed no deterioration of the stability after storage for 6 months at 40°C. The results obtained showed no differences in the measured phase transition temperature values of the stored compounds compared to the starting salts and unmodified acids.
- The salts of the L-amino isopropyl ester generally showed higher heat capacity values than the parent drug. The parent anion and the state of the resulting compound influence the heat capacity. Among the compounds studied, the semi-solid salts of ketoprofen had the highest $C_{p,m}$ values, whereas the solid salts of salicylic acid and [ThrOiPr][NAP] had the lowest $C_{p,m}$ values.

2.4. Specific rotation

In recent years, a new subgroup of ionic liquids with at least a single point chiral centre, chiral ionic liquids, have attracted interest as solvents for use in asymmetric synthesis and as chiral agents with potential chiral discrimination capabilities and high specificity for target enantiomers. Currently, amino acids are also used as available precursors for the synthesis of CILs, in most cases as chiral anions. The majority of chiral CILs are based on chiral anions, and a limited number of CILs have both a chiral cation and a chiral anion. Some of the ways that amino acid-based CILs can be used are for capillary electrophoresis, high-performance liquid chromatography, chiral sensing, CO₂ capture, metal scavenging, and heterogeneous catalysis [220–222].

In the context of biological processes, the chirality of a molecule plays a crucial role in its properties, especially in the field of drugs or potential drug compounds. This is due

to the significant differences in the pharmacodynamic, pharmacokinetic and toxicological properties that are exhibited by the enantiomers (or diastereomers) of a molecule. Therefore, with particular emphasis on well-defined stereochemistry, there is a need to explore novel drugs that are more potent, efficient and safer [223]. The enantiomer responsible for the biological activity is called the *eutomer*, while the other, inactive or less active, is called the *distomer*. The drug industry is using chiral modification more and more to make the inactive enantiomer less harmful. They do this by either changing racemates that are already on the market or creating new drugs that only come in one enantiomeric form. This chiral switch approach has facilitated the introduction of a large number of drugs with a different stereochemical configuration to the market [223,224].

For example, the two enantiomers of ibuprofen and ketoprofen differ in their pharmacological activity. Only the *S*(+) enantiomer is capable of inhibiting both cyclooxygenases (COX-1 and COX-2) at clinically relevant concentrations. The drug moiety undergoes unidirectional enantiomerisation and is converted to the (*S*)-enantiomer *in vivo* when ibuprofen or ketoprofen is administered as a racemate. Both drugs are available on the market in single-enantiomer and racemic versions. Both of these drugs are available on the market in single-enantiomer versions. The metabolic chiral inversion of ibuprofen can be observed between 35% and 70%. For ketoprofen, metabolic enantiomerisation from (*R*) to (*S*) form *in vivo* was negligible in humans and limited to a maximum of about 10%. On the other hand, due to the well-documented hepatotoxicity and the effect of increasing the burden on the kidneys of (*R*)-naproxen, naproxen is administered exclusively as the stereochemically pure (*S*)-enantiomer [225,226].

In addition, preventing the racemisation of drugs and the production of unwanted enantiomeric forms is crucial to avoid the risk of side effects (as was the case with thalidomide). Some methods are used to secure enantiomerically pure substances, such as protection by chemical modification (use of protecting groups to shield functional groups that are prone to racemisation, especially in steps involving harsh conditions). However, additional expensive synthetic steps are required during the manufacturing process. Efforts are, therefore, made to design stereochemically stable compounds that are less likely to racemise. In order to obtain enantiopure drugs, the drug is either synthesised in an enantiopure manner or obtained from a racemic mixture by applying a post-synthetic physical chiral separation process. The most common synthetic approaches are the asymmetric approach (where the reaction preferentially leads to one enantiomer) or the chiral pool approach (where enantiopure starting materials are used) [227–231].

In this study, the selected L-amino acids were used as building blocks to synthesise the investigated salts as chiral cation sources. Among the active substances used, only S-(+)-ibuprofen and S-(+)-naproxen have optical activity. Ibuprofen, which was used to obtain most of the IBU derivatives, and ketoprofen are racemic mixtures. Salicylic acid has no chiral centre and is not an optically active compound.

The values obtained for the specific rotation of the starting L-amino acid were as follows: +34.00 (L-methionine), -25.18 (L-threonine), +37.90 (L-isoleucine), and +24.44 (L-valine), whereas the specific rotation values for S-(+)-ibuprofen and S-(+)-naproxen were +59.98 and +50.99, respectively. The evaluated specific and molar rotation values for the synthesised L-amino acid alkyl esters and their corresponding hydrochlorides and salts are compared in Figure 28.

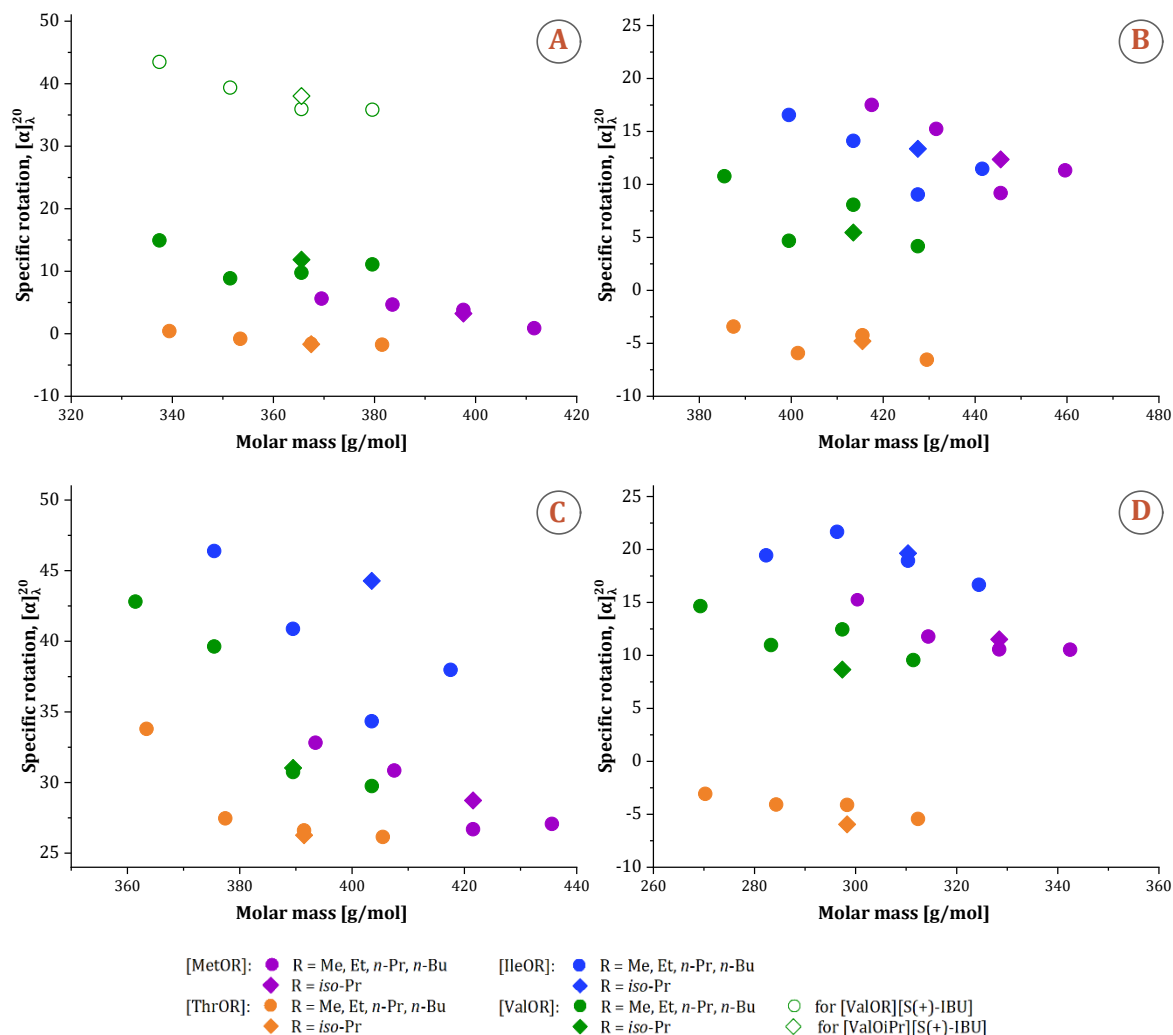


Fig. 28. The relationship between the specific rotation and molar mass of L-amino alkyl ester salts of A: (R,S)-ibuprofen and S-(+)-ibuprofen, B: ketoprofen, C: naproxen, and D: salicylic acid.

The obtained compounds, derived from the L-amino acids, exhibit optical activity and rotate the plane of polarised light in accordance with the rotation of the starting material.

Therefore, only L-threonine derivatives change the plane of polarisation to the left (–). The only exception in rotation direction was observed for [ThrOMe][IBU] salt and when L-threonine alkyl esters were conjugated with the naproxen moiety. In addition, compared with the corresponding drugs obtained from racemic ibuprofen, the L-valinium alkyl ester salts obtained from *S*-(+)-ibuprofen showed higher values of specific rotation. This suggests that the value of the optical rotation of the compound is influenced by the proportion of the individual ions in the molecule, both ester and active substance moieties. It was observed that among the derivatives of the active substance that showed no optical activity, the ketoprofen salts were mostly characterised by the lowest specific rotation values.

In general, the value of the specific rotation of the obtained compounds decreases with the lengthening of the alkyl chain in the cationic part, which results directly from the decreased share of the L-amino acid in the mass of the obtained derivatives and the order of the amino acid moieties: L-Ile>L-Val>L-Met>L-Thr [181,182].

Summary

- The compounds obtained have an optical activity, the value of which is mainly due to the proportion of the cation. Therefore, the rotation of the polarised light plane by salts coincides with the rotation of the starting L-amino acid. The determined specific and molar rotation values decrease in the following order of the used L-amino acid moieties: L-Ile>L-Val>L-Met>L-Thr.

3. Biological properties of salts of L-amino acids alkyl esters and selected NSAIDs moieties

Given the intended use of the obtained salts in preparations for dermal or transdermal application, selected biological properties of the obtained salts were determined, which are important from the point of view of their further use and provide the basis for determining the most favourable amino acid structure, in combination with which the best parameters of the increased bioavailability of the substance will be achieved. For this purpose, skin permeability, antioxidant activity, biodegradability and antimicrobial activity were investigated.

3.1. Skin permeation studies

Skin permeation studies play a critical role in evaluating the efficacy and quality of topical and transdermal formulations. The analysis of *ex vivo* permeation during pharmaceutical development aids in understanding the quality and performance

of a transdermal delivery system. The main objective of these evaluations is to identify factors that could potentially affect drug bioavailability in a living system. The primary method used to study drug release and skin permeation in these formulations is diffusion cells. In particular, the Franz diffusion cell is commonly used to determine drug permeation through the skin. While human skin explants remain the standard for drug delivery evaluation, inbred porcine skin has become a common substitute due to its availability, ability to be freshly excised for viability and enzymatic studies, and reduced variability, which may complicate the interpretation of the results [232,233].

This part of the research aimed to determine how selected variables influence the permeation of the active substance: lengthening of the carbon chain in the ester part of the amino acid and modification of the structure of the amino acid esters in the cation part used for the tested compounds.

In previous studies carried out in the Department of Chemical Organic Technology and Polymeric Materials of ZUT on the permeability of L-valinium alkyl esters (*R,S*)-ibuprofenates, the impact of various alcoholic carriers on skin permeability was analysed [150,151]. Alcoholic carriers, such as methanol, ethanol, and propan-2-ol, are often used in skin permeability studies due to their ability to enhance skin permeability, which is crucial for developing effective transdermal systems. In these studies, 70% (v/v) aqueous-alcoholic solutions were used as solvents of the test compounds. The compound was applied to the skin sample in the amount of 50 mg as the solution of the 0.1 g/mL concentration in the respective alcohol. The studies showed that the permeability of the compounds across the skin increased as the alcoholic carrier changed from methanol to ethanol to propan-2-ol. The studies also demonstrated that penetration parameters such as steady-state flux (J_{ss}), permeability coefficient (K_p) and lag time (L_T) were significantly higher for L-valinium alkyl esters (*R,S*)-ibuprofenates compared to the unmodified (*R,S*)-ibuprofen [150,151]. In a therapeutic context, the faster permeability may lead to faster achievement of the desired therapeutic effect. Further research conducted in the same department highlighted the importance of choosing the right carrier for improving drug delivery through the skin, making (*R,S*)-ibuprofen modified with amino acid alkyl esters could be more effective than existing commercial products [234,235]. These previous studies carried out on the example of derivatives of *RS*-ibuprofen and L-valine alkyl esters also revealed that propyl, isopropyl and butyl esters of valine lead to the most favourable permeation parameters of the API. Therefore, in the presented studies, it was also decided to use the salts of alkyl esters of three other amino acids besides L-valine with the same chain length in permeability tests

of various active substances ((*R,S*)-ibuprofen, *S*-(+)-ibuprofen, ketoprofen, *S*-(+)-naproxen and salicylic acid).

3.1.1. Comparison of permeation selected L-amino acid alkyl esters conjugated with NSAIDs

This part of the study, which is an extension of the previous research, includes an expanded group of compounds tested: derivatives of L-amino acid isopropyl, propyl, and butyl esters (derived from L-isoleucine, L-methionine, and L-threonine, L-valine) paired with selected drugs from the group of NSAIDs (ibuprofen, both racemic and *S*-(+)-enantiomer forms, ketoprofen, naproxen, and salicylic acid). The influence of cation structure on the skin permeability of the active substance has been the subject of detailed investigation.

In all experiments, the donor phase was 1 mL of a solution of the test compound in 70% ethanol, with a concentration of 0.01 g active substance/mL. In the Franz diffusion cell, abdominal porcine skin was used as the membrane, and PBS solution with pH=7.4 was used as the acceptor phase. The results obtained have been described in a publication related to the presented PhD thesis [182].

Figure 29 compares the determined cumulated mass after 24h in terms of each studied active substance paired with selected L-amino acid alkyl esters, while the relationship between the determined CUM values for selected NSAIDs and their L-amino acid alkyl ester salts and the evaluated lipophilicity and solubility in water is shown in Figures 30 and 31, respectively.

The cumulative mass measured after 24 h of permeation was influenced by both the parent drug and the structure of the conjugated cation. The determined CUM values of L-amino acid alkyl ester salts, as well as for the starting NSAIDs, were ranked in the following order: [SA], followed by [KETO], then [IBU] and finally [NAP] based derivatives. Among the studied cations, only [IleOBu] paired with ketoprofen and [IleOPr] and [IleOBu] paired with naproxen moiety showed lower permeation compared to the unmodified drug. In the case of other tested compounds, an increase in permeation of active substances through abdominal porcine skin has been observed.

The results indicate that salts containing highly hydrophilic propyl or isopropyl esters of L-threonine, which have the lowest lipophilicity and highest water solubility, generally exhibit the greatest skin permeation. In general, the highest CUM values were found for [ThrOiPr]-based salts of NSAIDs. These values were at least twice as high as the

cumulative mass of starting SA, NAP and IBU. Among the ketoprofenates studied, the highest permeation after 24 h was observed for the [ThrOPr][KETO] salt, with a 1.69-fold higher CUM value compared to the parent drug.

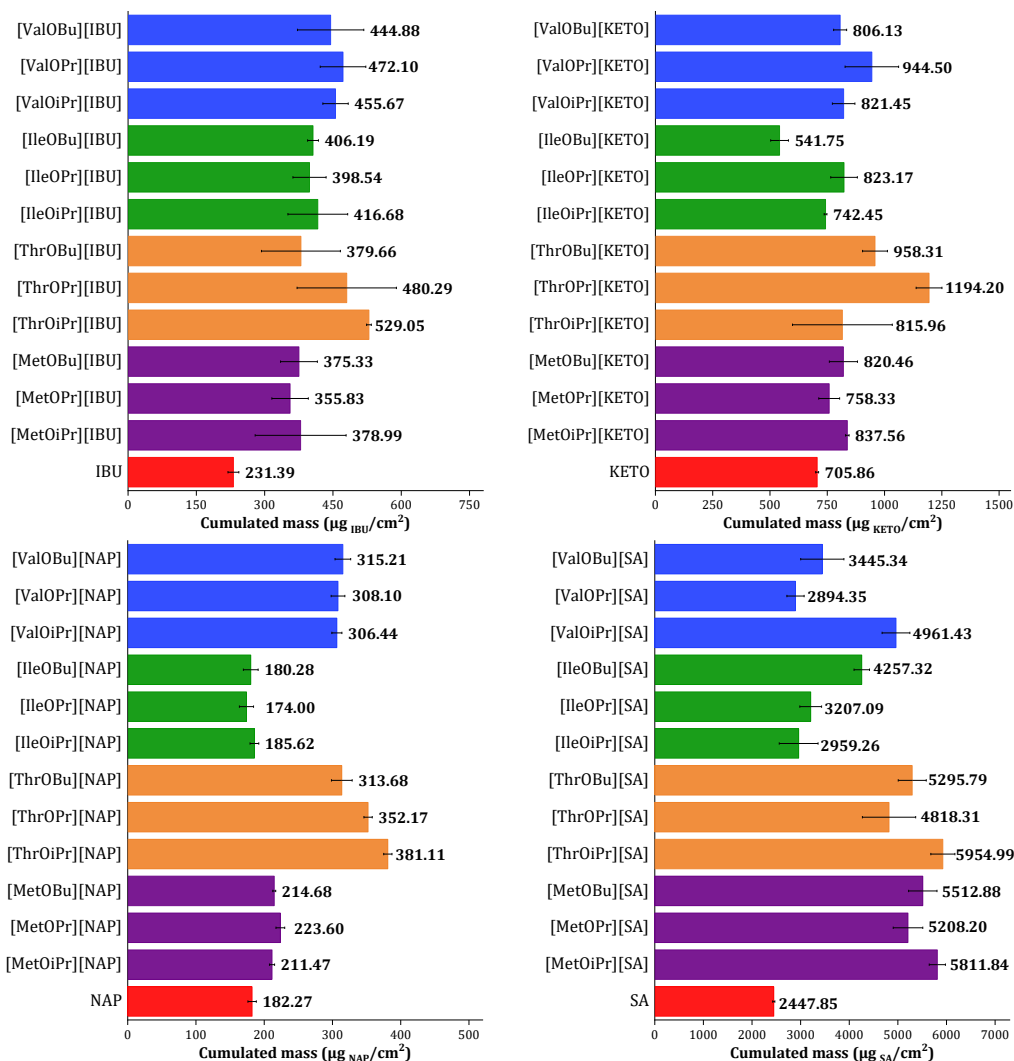


Fig. 29. Permeation as cumulative mass of selected drugs from NSAIDs group and their L-amino alkyl salts. Data presented in: [182].

This is consistent with previous research, which also demonstrated that modifying the structure of naproxen and ibuprofen by incorporating a highly hydrophilic L-amino acid ester moiety increased the ability of the drugs to penetrate the skin [166]. The study also showed that converting salicylic acid into L-amino acid ester ionic liquids significantly improves its permeation. The process was described as being facilitated by an increase in lipophilicity due to the amino acid esters' long alkyl chains, which help transport SA within the ionic liquids [236].

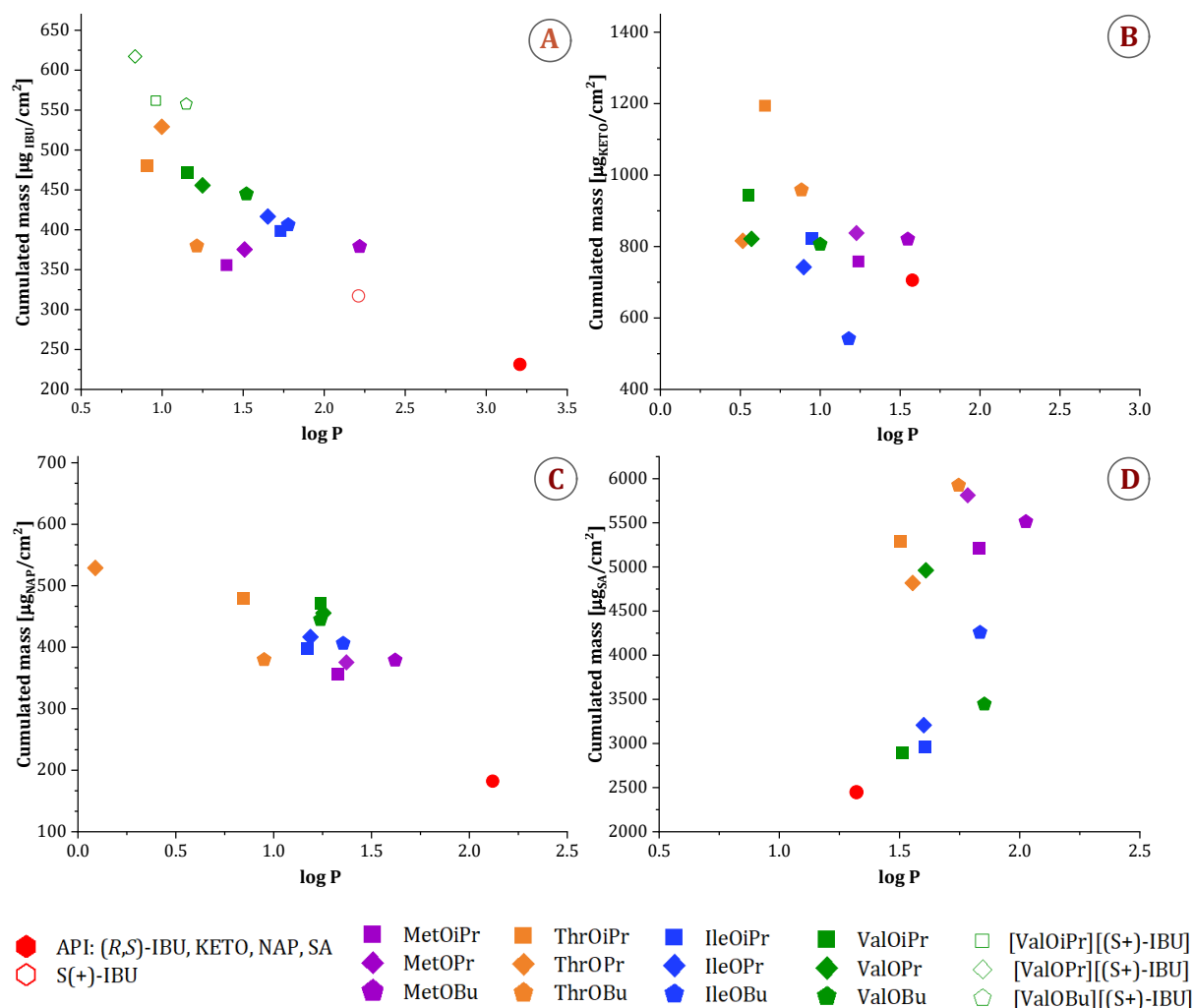


Fig. 30. The relationship between cumulated mass and logP values of L-amino acid alkyl ($\text{C}_1\text{-C}_4$) esters salts of acids from NSAIDs group (A: ibuprofen, B: ketoprofen, C: S(+)-naproxen, and D: salicylic acid).

As mentioned before, the higher solubility (with the exception of the [IleOBu][KETO] compound) resulted in a greater cumulative mass of the derivatives obtained compared to the unmodified acids, which is consistent with the statement that if more of the substance can be dissolved in the skin layers, then more of it will be available for diffusion. Conversely, poor penetration or diffusion through the skin tends to favour a lower cumulative mass due to the higher lipophilicity of the compounds [237]. The exception was the salicylic acid derivatives which, as described previously (in Chapter II 2.2.), were characterised by higher solubility despite higher lipophilicity. This may indicate a greater influence of water solubility than general lipophilic behaviour on the cumulative mass and ultimate availability to penetrate the skin. For the obtained salts of naproxen and ibuprofen, the relationship between lipophilicity (and water solubility) and cumulative skin permeation mass is linear, and for all salts obtained, the increase in CUM generally follows the order of L-amino acid: L-Met<L-Ile<L-Val<L-Thr.

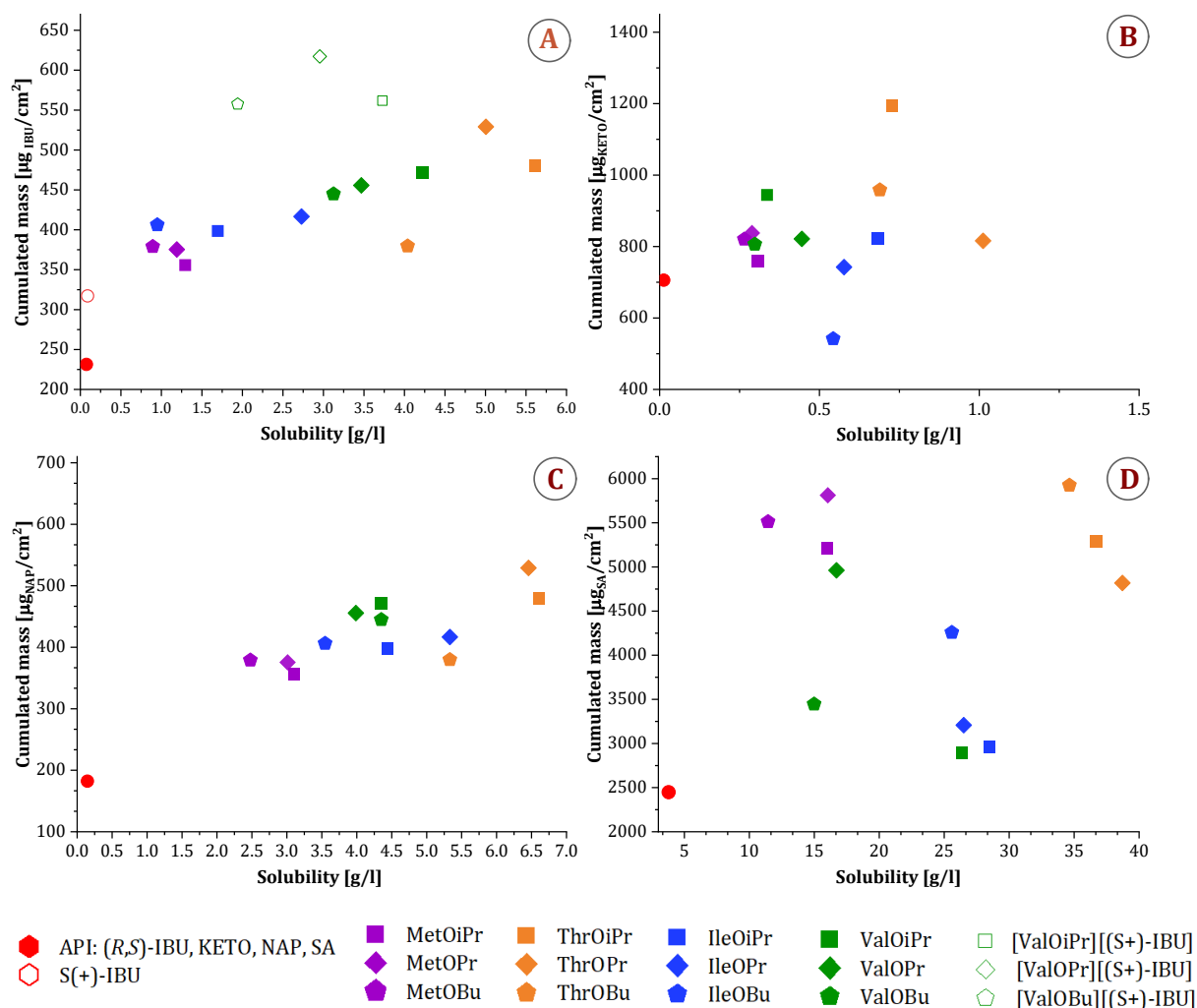


Fig. 31. The relationship between cumulated mass and solubility in water of L-amino acid alkyl (C1-C4) esters salts of acids from NSAIDs group (A: ibuprofen, B: ketoprofen, C: S(+)-naproxen, and D: salicylic acid).

The comparison of the permeation profiles for L-valine alkyl ester salts of S(+)-ibuprofen and (R,S)-ibuprofen is shown in Figure 32. The evaluated permeation profiles for the other investigated L-amino acid alkyl ester derivatives, unmodified parent acids, and the calculated parameters characterising skin permeation through abdominal porcine skin for ibuprofen moieties and their L-valinium alkyl ester salts are presented in Figure A24 and Table A39 in Appendix II.

Recent studies have shown that administration of the single S(+) enantiomer (also known as dexibuprofen) at a dose half that of the racemate can provide the clinical benefits of racemic ibuprofen. For example, 200 mg of S(+)-ibuprofen was found to be superior or equivalent to 400 mg of the racemate in relieving dental pain. Therefore, the direct use of S(+)-ibuprofen results in therapeutic effects with a lower total dose. As the adverse effects of NSAIDs such as ibuprofen can be dose-dependent, this may result in fewer side effects [225,238].

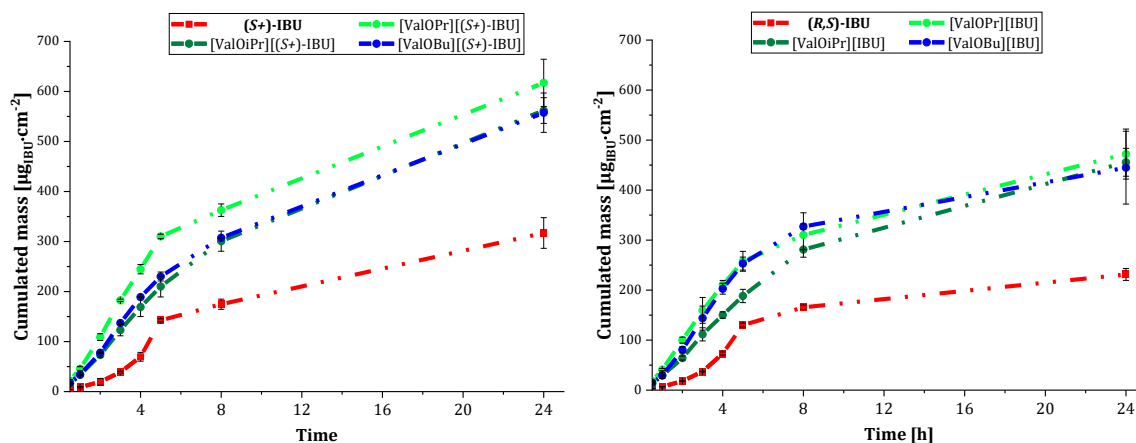


Fig. 32. The permeation profiles for *S*-(+)-ibuprofen (left) and (*R,S*)-ibuprofen (right) and their L-valinium alkyl ester salts through pig skin to acceptor phase with pH 7.40. Data is partly presented in: [182].

However, the use of racemic ibuprofen is well established, and extensive experience supports its efficacy and safety profile for a wide range of conditions. Furthermore, due to the presence of this isomer, most ibuprofen preparations available on the market are in the form of (*R,S*)-ibuprofen since the (*S*)-enantiomer is more difficult and expensive to produce and manufacture. This makes racemic ibuprofen more widely available and more accessible for routine use in the treatment of pain, fever and inflammation [225,238].

In this study, the cumulative mass determined after 24 h was 317.111 $\mu\text{gIBU}/\text{cm}^2$ for *S*-(+)-ibuprofen and 231.392 $\mu\text{gIBU}/\text{cm}^2$ for (*R,S*)-ibuprofen. Although higher CUM results were obtained for the tested L-valinium alkyl ester salts derived from (*S*)-enantiomer, also the conversion of racemic ibuprofen to a salt form allowed at least a twofold increase in the permeability of the active substance. On this basis, regardless of the enantiomeric form of ibuprofen, conjugation with an L-amino acid ester allows a significantly increased dose of the active ingredient to be delivered through the skin, which may subsequently enhance the therapeutic effect. The highest cumulative mass values in each group of obtained derivatives were found for salts, based on the [ValOPr] cation (CUM=617.240 $\mu\text{gIBU}/\text{cm}^2$ for [ValOPr][(*S*+)IBU] and CUM=472.102 $\mu\text{gIBU}/\text{cm}^2$ for [ValOiPr][IBU]).

The calculated parameters for abdominal porcine skin permeation for all studied NSAIDs and their L-amino acid alkyl ester salts are presented in Appendix (Tables A39–A42). The comparison of the determined parameters of each studied active substance paired with selected L-amino acid alkyl esters are presented in Figures: 33 (J_{ss} values), 34 (K_p values), 35 (L_T values), 36 (K_m values), and 35 ($Q_{24\%}$ values).

The transdermal flux values of the starting active substances were as follows: 25.00 and 46.407 $\mu\text{gIBU}/(\text{cm}^2\text{h})$ for *S*-(+)-ibuprofen and (*R,S*)-ibuprofen, 74.611 $\mu\text{g}_{\text{KETO}}/(\text{cm}^2\text{h})$

for ketoprofen, $29.813 \mu\text{g}_{\text{NAP}}/(\text{cm}^2\text{h})$ for naproxen, and $192.57 \mu\text{g}_{\text{SA}}/(\text{cm}^2\text{h})$ for salicylic acid, respectively.

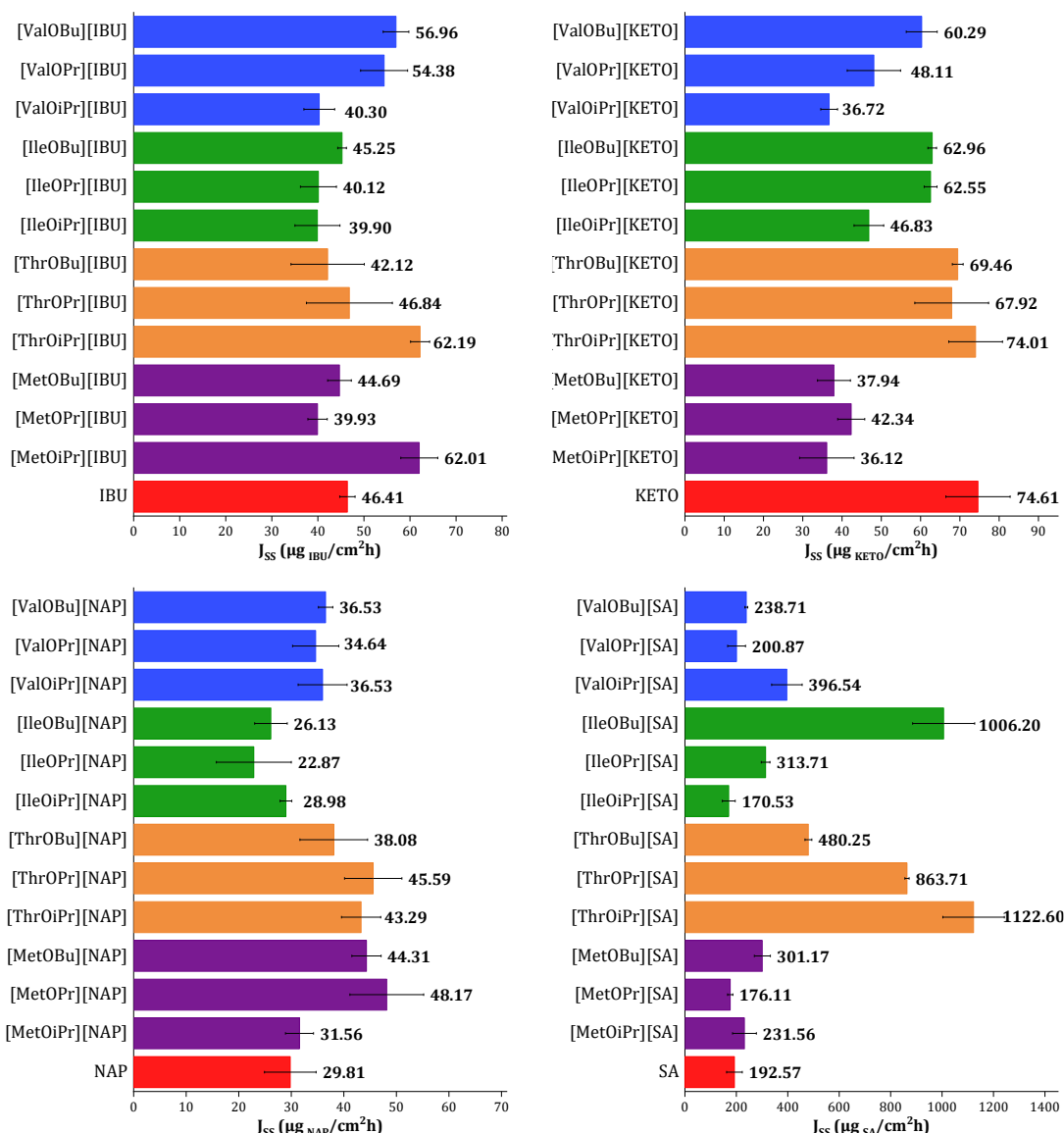


Fig. 33. The comparison of transdermal flux (J_{ss}) values of selected drugs from NSAIDs group and their L-amino alkyl ester salts. Data presented in: [182].

For the obtained (*R,S*)-ibuprofenates, the calculated J_{ss} values were higher only for compounds derived from [IleOPr], [ValOPr], [MetOiPr] and [MetOBu] cations. The other salts were described with comparable or lower flux values. In turn, the values of J_{ss} for synthesised *S*-(+)-ibuprofenates were about 2-fold higher compared to the parent drug. The flux values determined for ketoprofen salts were generally lower than those determined for the parent ketoprofen and ranged from $36.118 \mu\text{g}_{\text{KETO}}/(\text{cm}^2\text{h})$ (for [MetOiPr][KETO]) to $74.006 \mu\text{g}_{\text{KETO}}/(\text{cm}^2\text{h})$ (for [ThrOiPr][KETO]). With the exception of the salts obtained from L-isoleucine alkyl esters, the synthesised naproxen derivatives were characterised with comparable J_{ss} values to the unmodified acid,

the highest being calculated for the [ThrOPr][NAP] ($45.592 \mu\text{g}_{\text{NAP}}/(\text{cm}^2\text{h})$) and [MetOPr][NAP] ($48.174 \mu\text{g}_{\text{NAP}}/(\text{cm}^2\text{h})$) salts. The derivatives of salicylic acid were characterised by transdermal flux values ranging from $170.530 \mu\text{g}_{\text{SA}}/(\text{cm}^2\text{h})$ (for [IleOiPr][SA]) to $1122.600 \mu\text{g}_{\text{SA}}/(\text{cm}^2\text{h})$ (for [ThrOiPr][SA]). A significant increase in the J_{SS} was observed for the salicylates based on the [IleOBu] and L-threonine alkyl ester cations, which was 2–6 times higher in comparison to the parent drug.

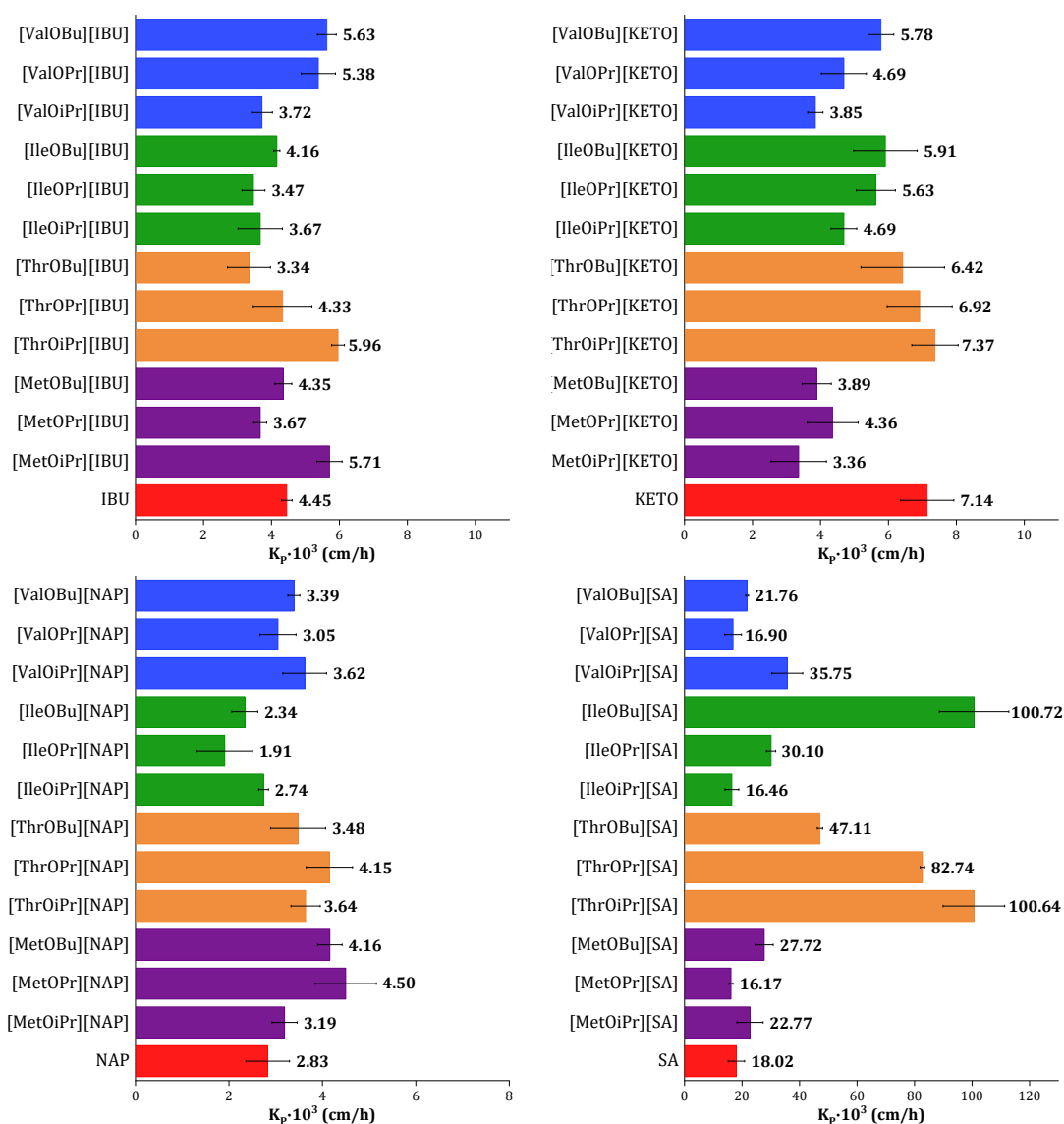


Fig. 34. The comparison of permeability coefficient (K_p) values of selected drugs from NSAIDs group and their L-amino alkyl ester salts. Data presented in: [182].

The determined permeability coefficient (K_p) values were generally comparable or lower for the obtained ibuprofenates compared to the unmodified acid ($4.453 \cdot 10^3 \text{ cm/h}$). The higher ability to penetrate the studied pig skin barrier was attributed to salts based on [ThrOiPr], [MetOiPr], [ValOBu], and [ValOPr] esters. *S*-(+)-ibuprofen was characterised by a lower K_p value ($2.394 \cdot 10^3 \text{ cm/h}$) than the racemic form, but its L-valinium alkyl esters

showed higher permeability coefficient values compared to the corresponding salts derived from (*R,S*)-ibuprofen. Among the ketoprofen salts studied, only K_P for [ThrOiPr][KETO] was comparable to the value of the starting active substance ($K_P=7.138 \cdot 10^3 \text{ cm/h}$). At the same time, the other compounds showed a reduced permeability coefficient. As with the J_{SS} values, naproxen derivatives obtained from L-isoleucine alkyl esters also had a lower skin barrier penetration ability than the unmodified acid ($K_P=2.832 \cdot 10^3 \text{ cm/h}$). Likewise, the highest K_P values were calculated similarly to the [MetOPr][NAP], [ThrOPr][NAP], [MetOBu][NAP] and [ThrOiPr][NAP] salts. The derivatives obtained from salicylic acid ($K_P=18.017 \cdot 10^3 \text{ cm/h}$) were characterised by the greatest increase in the permeability coefficient among all the compounds studied. The salts [IleOBu][SA], [ThrOiPr][SA] and [ThrOPr][SA], with calculated K_P values of 100.716, 100.640 and $82.740 \cdot 10^3 \text{ cm/h}$, respectively, were found to have the highest ability to penetrate the human skin barrier.

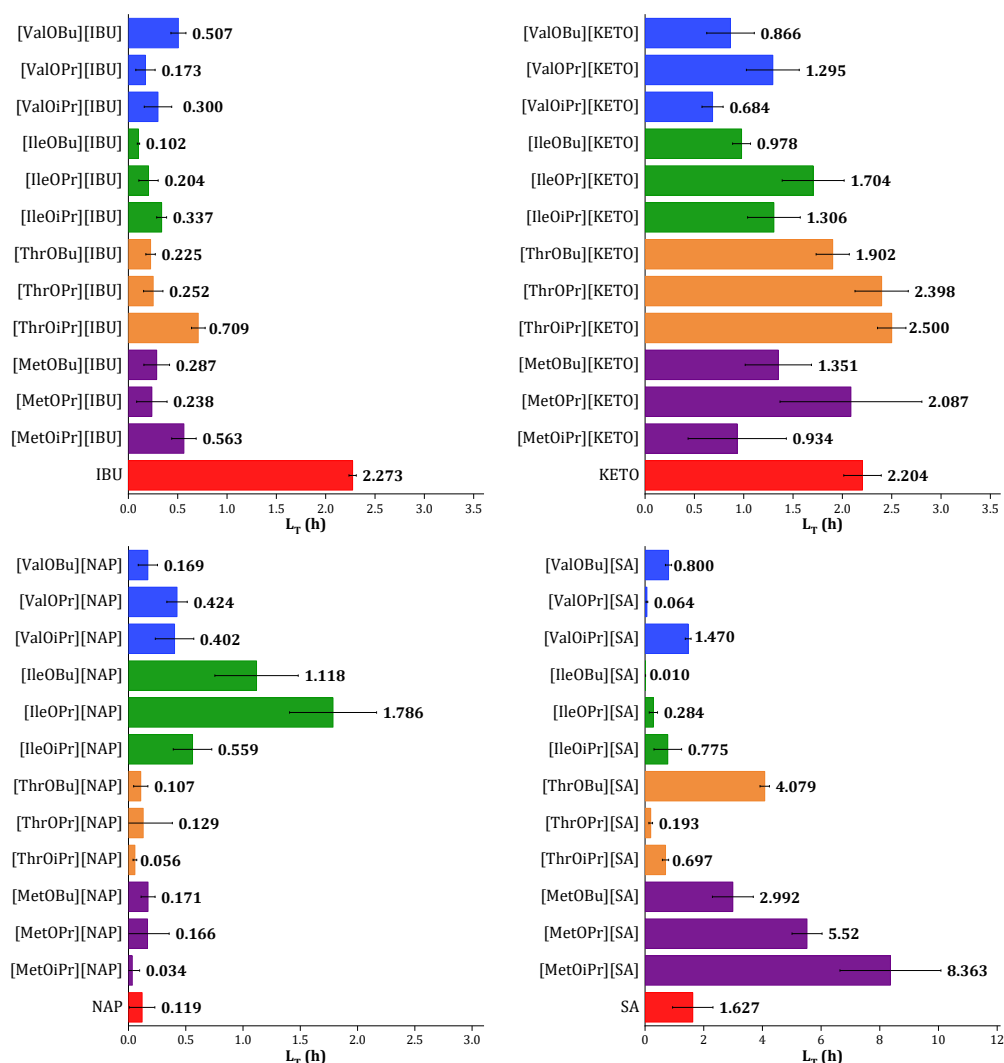


Fig. 35. The comparison of lag time (L_T) values of selected drugs from NSAIDs group and their L-amino alkyl ester salts. Data presented in: [182].

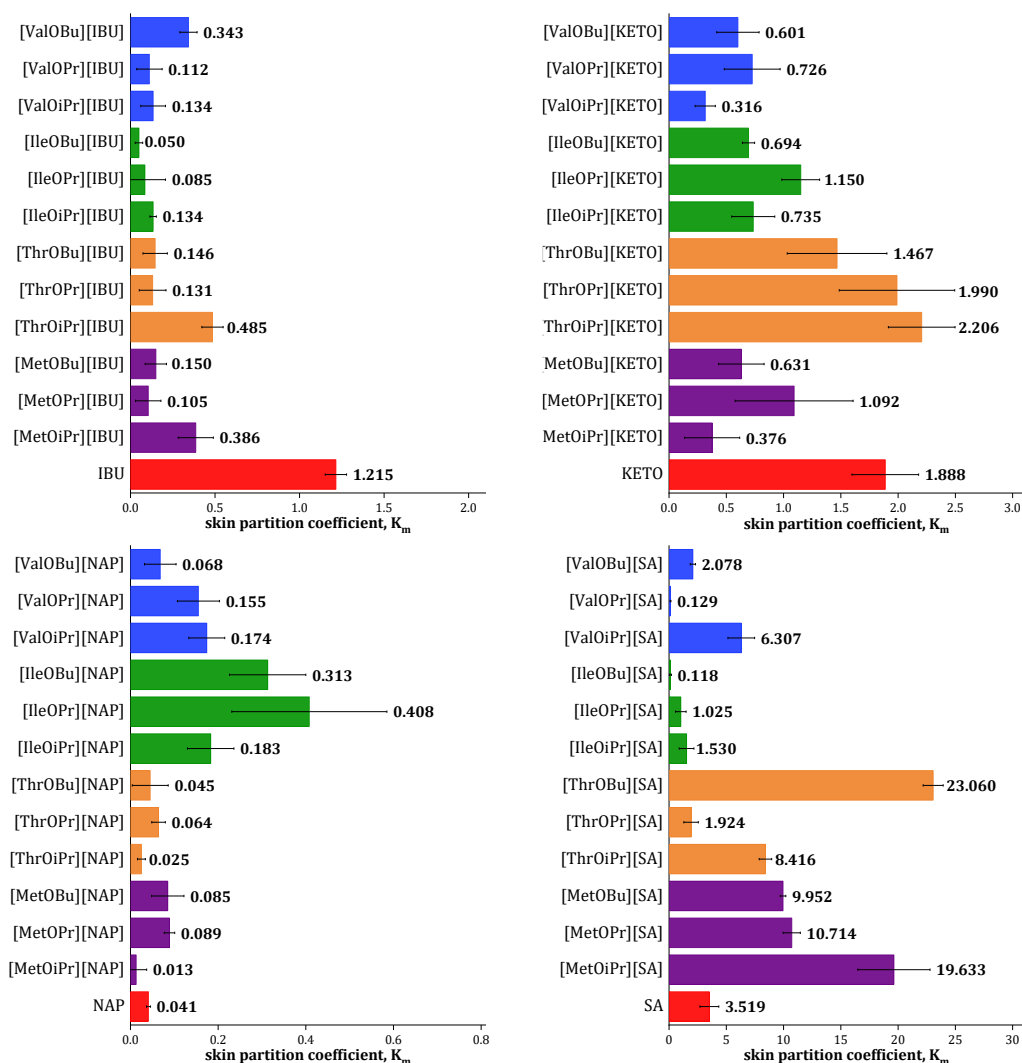


Fig. 36. The comparison of skin partition coefficient (K_m) values of selected drugs from NSAIDs group and their L-amino alkyl ester salts. Data presented in: [182].

The calculated lag time, L_T values, for ibuprofenates permeating through human skin were significantly reduced in comparison to both *S*-(+)-ibuprofen ($L_T=1.293$ h) and (*R,S*)-ibuprofen acids ($L_T=2.273$ h). This is beneficial in achieving a rapid onset of action and is particularly relevant for drugs used in the treatment of acute conditions or for pain relief where rapid relief of symptoms is a primary goal. The L_T for ibuprofen derivatives ranged from 0.102 h for [IleOBu][IBU] to 0.709 h for [IleOBu][IBU], which were 22- and 3-fold lower compared to unmodified acid, respectively. [ThrOPr][KETO] and [ThrOiPr][KETO] salts, which were characterised by the highest permeability coefficient, however, as the only ketoprofenates obtained, showed higher lag time values compared to the parent drug. A distinct correlation was observed in the case of naproxen conjugations, where the predominant feature was an extended lag time when naproxen was paired with L-amino acid

alkyl ester cations. The reduced L_T values were calculated only for [ThrOiPr][NAP], [ThrOBu][NAP] and [MetOiPr][NAP].

A different relationship occurred for the salts of salicylic acid, which, in general, were characterised by a faster ability to reach the steady flux, in particular, the [IleOBu][SA], designed with a negligible low value of lag time ($L_T=0.6$ min). The conjugates based on L-methionine alkyl ester and L-threonine butyl ester showed a prolongation of the lag times in comparison to the unmodified acid. However, [MetOiPr][SA], [MetOPr][SA], [MetOBu][SA], and [ThrOiPr][SA] were also characterised by the highest values of cumulative mass. Therefore, these compounds can be successfully used in formulations where a prolonged drug release is intended to be more beneficial than a rapid onset, e.g. for the treatment of chronic atopic conditions [239].

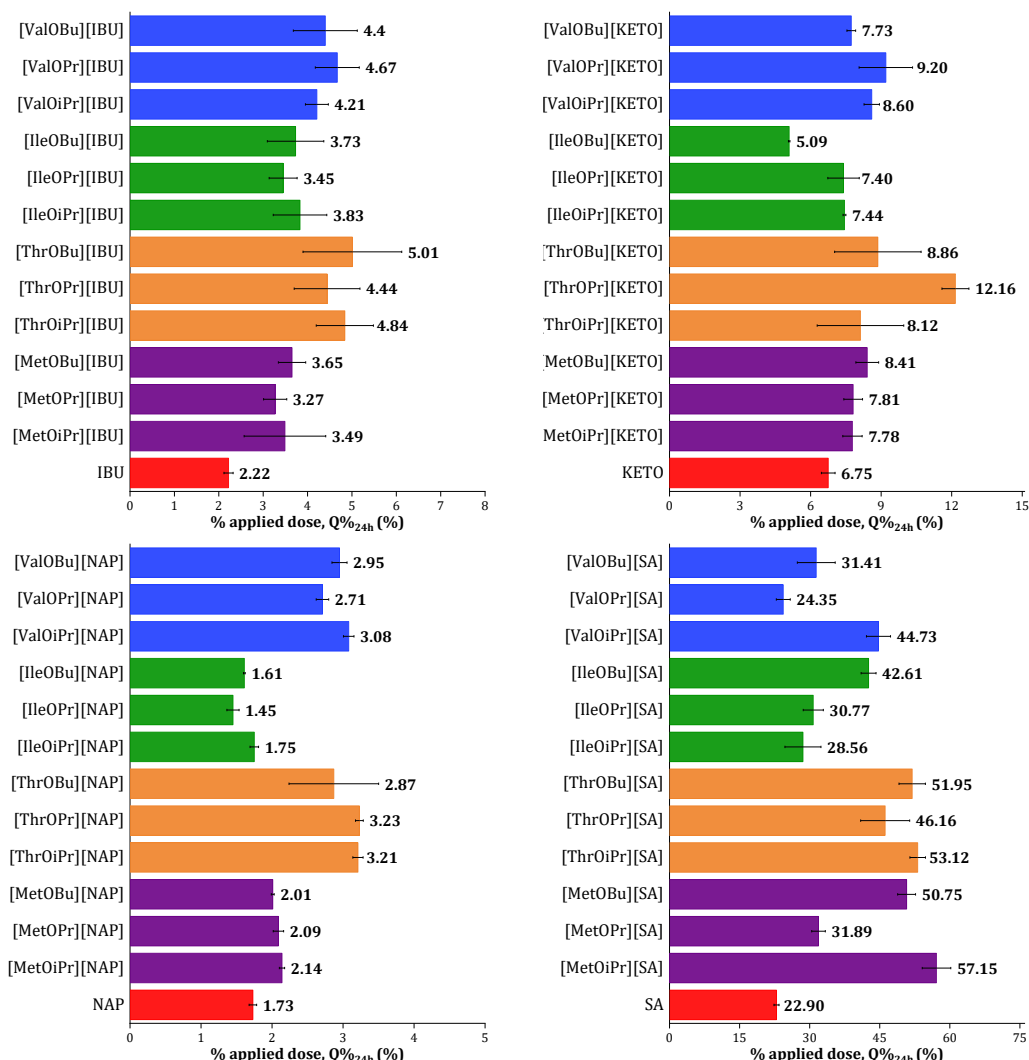


Fig. 37. The comparison of percentage of the applied dose after 24 h (Q_{24h}) of selected drugs from NSAIDs group and their L-amino alkyl ester salts. Data presented in: [182].

Since the diffusion coefficient (D) is inversely related to the value of L_T . As a result, the determined D values for the obtained ibuprofenates, most of the ketoprofenates and salicylates, were significantly higher compared to the parent drug. This suggests that these compounds are able to move through the skin layers more efficiently.

The values of the skin partition coefficient (K_m) were determined in this study for unmodified acids in the following order: $[SA] > [KETO] > [IBU] > [(S+)-IBU] > [NAP]$. Although the K_m parameter for $(S+)$ -IBU was three times lower than for the racemic form ($K_m=1.215$), the obtained L-valinium alkyl salts showed a comparable ability to transport from the studied vehicle to the outermost layers of the *stratum corneum*. The assigned K_m values showed a significant decrease compared to the parent drugs for the L-amino acid alkyl ester salts of ibuprofen and ketoprofen. Naproxen showed a negligible low ability to promote partitioning in the skin ($K_m=0.041$), but in the case of most of its salts, these values were higher. Of all the NSAIDs tested, salicylic acid had the highest tendency to partition into the skin ($K_m=3.519$). However, the calculated K_m values for its salts varied widely and ranged from 0.129 (for $[ValOPr][SA]$) to 23.060 (for $[ThrOBu][SA]$). For salts based on $[ThrOiPr]$, $[ThrOBu]$, $[ValOiPr]$ and L-methioninium alkyl esters, higher values of this parameter were calculated compared to unmodified acid.

With regard to the active substance, the percentage of the applied dose after 24 h was higher for all the derivatives obtained, except for $[IleOBu][KETO]$, $[IleOPr][NAP]$ and $[IleOBu][NAP]$ salts, in comparison with the parent drug. In a comparison of salts derived from different enantiomeric forms of the ibuprofen moiety, the higher $Q_{24\%}$ values were determined for the L-valinium alkyl ester salts based on $S-(+)$ -ibuprofen. Within each group of NSAIDs salts examined, the compounds that yielded the highest values of $Q_{24\%h}$ were those based on the following cations: $[ThrOBu]$ when conjugated with ibuprofen moiety, $[ThrOPr]$ when conjugated with ketoprofen, both $[ThrOiPr]$ and $[ThrOPr]$ when conjugated with naproxen, and $[MetOiPr]$ and $[ThrOiPr]$ when conjugated with salicylic acid moiety.

Figure 38 compares the permeation rate profiles evaluated for L-valinium alkyl ester salts of $S-(+)$ -ibuprofen and (R,S) -ibuprofen. The comparison of the permeation rate profiles of selected NSAIDs and their L-amino acid alkyl ester salts is shown in Figure 39.

Both unmodified $S-(+)$ -ibuprofen and (R,S) -ibuprofen moieties achieved the highest permeation rate in the 4–5 h interval, while for most ibuprofenates, the higher permeation rates were observed from 2 to 4 h. However, the highest flux of active substance was determined for $[ThrOiPr][IBU]$ ($79.452 \mu g_{IBU}/(cm^2h)$) in the 3–4 h intervals. Throughout the experiment, except for a period of 4 to 5 hours when the unmodified ibuprofen had the

highest permeation rate, the flux values of all ibuprofen salts were consistently higher than the parent drug.

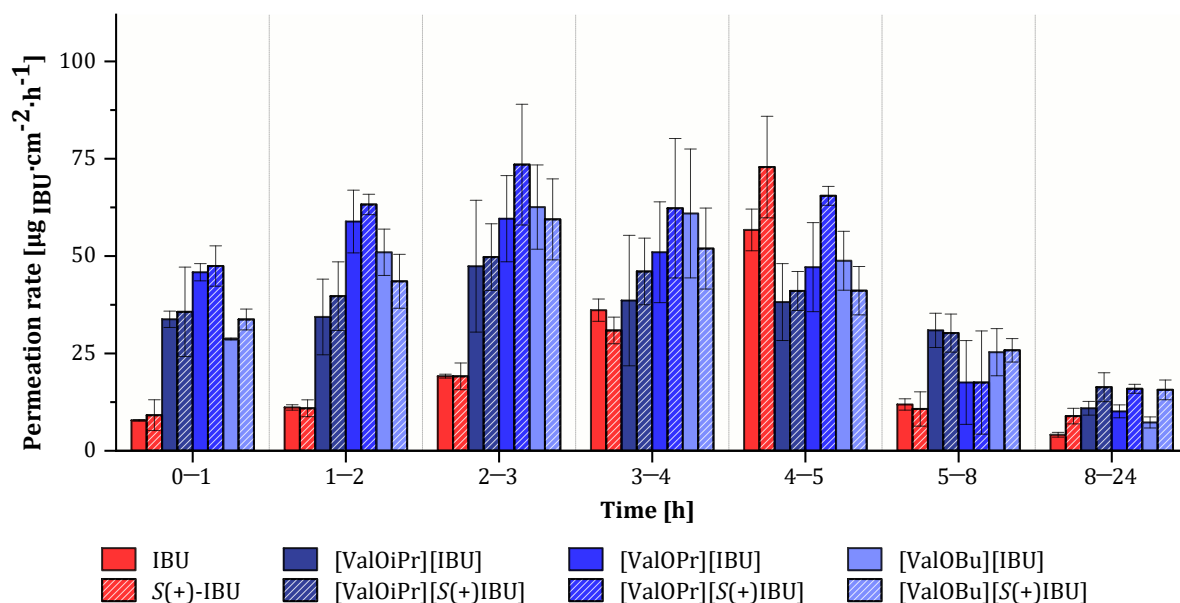


Fig. 38. Comparison of the permeation rates *S*-(+)-ibuprofen and (*R,S*)-ibuprofen and their L-valinium alkyl ester salts through porcine skin to acceptor phase with pH 7.40. Values are the means with standard deviation; *n*=3. Data are partly presented in: [182].

The permeation rates for L-valine alkyl ester salts paired with *S*-(+)-ibuprofen were slightly higher in comparison to the corresponding salts obtained from (*R,S*)-ibuprofen. The highest flux values were observed at 2 to 3 h intervals, especially for [ValOBu][IBU] ($73.486 \mu\text{g}_{\text{IBU}}/(\text{cm}^2\text{h})$) and [ValOPr][(*S*)-IBU] ($62.581 \mu\text{g}_{\text{IBU}}/(\text{cm}^2\text{h})$).

The highest permeation rates were observed at 4–5 h intervals in the case of ketoprofen and most of its salts. After this time, however, the flux values of the unmodified acid rapidly decreased, while the ketoprofen derivatives salts maintained a relatively high and sustained permeation rate by the end of the experiment. The highest permeation rates were observed for [ThrOBu][KETO] ($85.670 \mu\text{g}_{\text{KETO}}/(\text{cm}^2\text{h})$) – at intervals of 3–4 h, for [ThrOiPr][KETO] ($86.832 \mu\text{g}_{\text{KETO}}/(\text{cm}^2\text{h})$) – at intervals of 4–5 h and for [ThrOPr][KETO] ($75.078 \mu\text{g}_{\text{KETO}}/(\text{cm}^2\text{h})$) – at intervals of 5–6 h.

The highest efficiency of skin permeation for most naproxen salts was observed between 1 and 3 h, similar to the parent drug. For example, the [ThrOiPr] cation-based derivative achieved the highest permeation rate already in the first hour of the study ($51.400 \mu\text{g}_{\text{NAP}}/(\text{cm}^2\text{h})$) and the [ThrOPr] compound in the 2–3 h period ($50.552 \mu\text{g}_{\text{NAP}}/(\text{cm}^2\text{h})$). Surprisingly, of all the naproxenates studied, [MetOPr] and [MetOiPr] proved the most efficient at penetrating this barrier. These salts achieved the highest permeation at 1–2 h ($52.298 \mu\text{g}_{\text{NAP}}/(\text{cm}^2\text{h})$) and 2–3 h intervals ($52.941 \mu\text{g}_{\text{NAP}}/(\text{cm}^2\text{h})$), respectively.

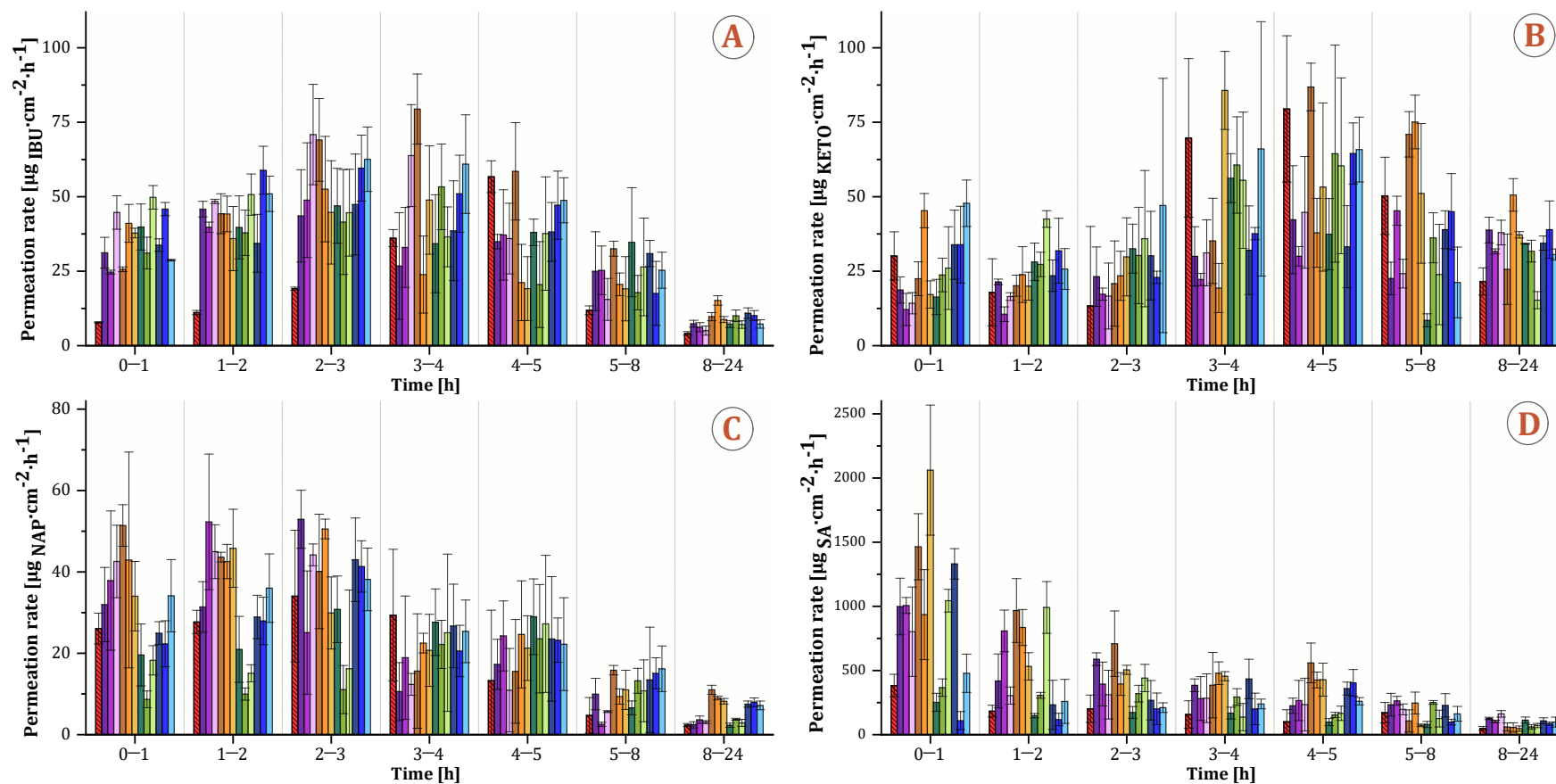


Fig. 39. The permeation rate profiles for selected NSAIDs (A: ibuprofen, B: ketoprofen, C: naproxen, and D: salicylic acid) and their L-amino acid alkyl ester salts through porcine skin to acceptor phase with pH 7.40 from ethanolic solution (data presented in: [182]).

The most remarkable permeation rates were observed for the first hour for salicylic acid and its L-amino alkyl ester salts and were in the range of $109.577 \mu\text{g}_{\text{SA}}/(\text{cm}^2\text{h})$ for [ValOPr][SA] and $2061.380 \mu\text{g}_{\text{SA}}/(\text{cm}^2\text{h})$ for [ThrOBu][SA], which was a 5-fold higher value of permeation compared to the unmodified drug ($382.720 \mu\text{g}_{\text{SA}}/(\text{cm}^2\text{h})$). In addition, L-threoninium alkyl ester salts showed relatively high prolonged permeation of the active substance up to the 4–5 h interval, especially [ThrOiPr][SA] with flux equal to $559.040 \mu\text{g}_{\text{SA}}/(\text{cm}^2\text{h})$. Therefore, they can be used to maintain therapeutic levels of the drug in the bloodstream for longer periods of time, potentially reducing the need for frequent dosing.

Summary

- The structure of both anions and cations influenced the efficacy of skin permeation of the tested compounds. In terms of the average cumulative mass of active substance, the highest values were obtained for ibuprofen, naproxen and salicylic acid when paired with [ThrOiPr] cation, while for ketoprofen when paired with [ThrOPr].
- The conjugation of acids from the NSAIDs group with L-amino acid alkyl esters allows a higher permeation rate of the drug through the abdominal porcine skin, which can result in more effective treatment as the drug reaches the target site faster and in higher concentrations.
- Comparing the permeability through abdominal porcine skin of *S*-(+)-ibuprofen and (*R,S*)-ibuprofen converted into the L-valinium alkyl ester salts form, the greater effectiveness of permeation was achieved for derivatives obtained from *S*-enantiomer. Therefore, when *S*-(+)-ibuprofen is used as the active ingredient, it can also be absorbed into the bloodstream in greater amounts. As a result, it may be possible to reduce the dose and cost of manufacturing formulations based on the more expensive *S*-(+)-enantiomer form.
- Based on the results obtained, the best parameters in terms of drug permeation were shown by the synthesised salts based on L-threonine alkyl esters ([ThrOPr], [ThrOiPr], [ThrOBu]). Therefore, as the best substitutes for pharmaceutical NSAIDs, these compounds have the greatest potential to be further explored as novel components in topical formulations and to optimise therapeutic outcomes.

3.2. Skin accumulation studies

Substances delivered transdermally and topically can penetrate through the skin and have the potential to accumulate in the skin. It is essential to understand and control the accumulation of applied substances to develop and safely use dermatological products with a minimised risk of adverse reactions in drug delivery systems. Depending on the chosen route of administration and intended purpose of the drug - treatment or control of skin disorders, deep penetration beyond the site of application or access to the general circulation - the ability to accumulate in the skin is desired to varying extents. Low permeation combined with high accumulation is desirable for the topical delivery system. The reverse relationship is preferred for the transdermal delivery system, where the more rapid and greater permeation and the lower accumulation in the skin are more favourable [79,89,240,241].

The accumulation was determined for all tested substances after performing the skin permeability study after 24 h of penetration. The obtained results were described in published research [150,151,182,234,235].

The accumulation in the skin of other active substances from the NSAIDs group: (*R,S*)-ibuprofen, ketoprofen, naproxen, and salicylic acid, as well as their L-amino alkyl ester salts, were determined and compared in Figure 40, while detailed results are presented in Appendix II in Table A43.

The determined accumulation masses of unmodified acids were as follows: 896.652 $\mu\text{g}_{\text{IBU}}/\text{g}$ for (*R,S*)-ibuprofen, 1799.932 $\mu\text{g}_{\text{KETO}}/\text{g}$ for ketoprofen, 1108.243 $\mu\text{g}_{\text{NAP}}/\text{g}$ for naproxen, and 1145.136 $\mu\text{g}_{\text{SA}}/\text{g}$ for salicylic acid. The studied L-amino acid alkyl ester salts generally accumulate less than the parent drug. The exception was [IleO_iPr][KETO], and most of the naproxenate salts were obtained. It was also observed that the highest values of accumulated mass in the skin were generally found for compounds with the lowest permeation mass. However, *S*-(+)-ibuprofen (with accumulated mass equal to 972.568 $\mu\text{g}_{\text{IBU}}/\text{g}$) and its L-valinium alkyl ester salts showed both higher accumulation and permeation ability than corresponding derivatives based on the racemic form of the active substance.

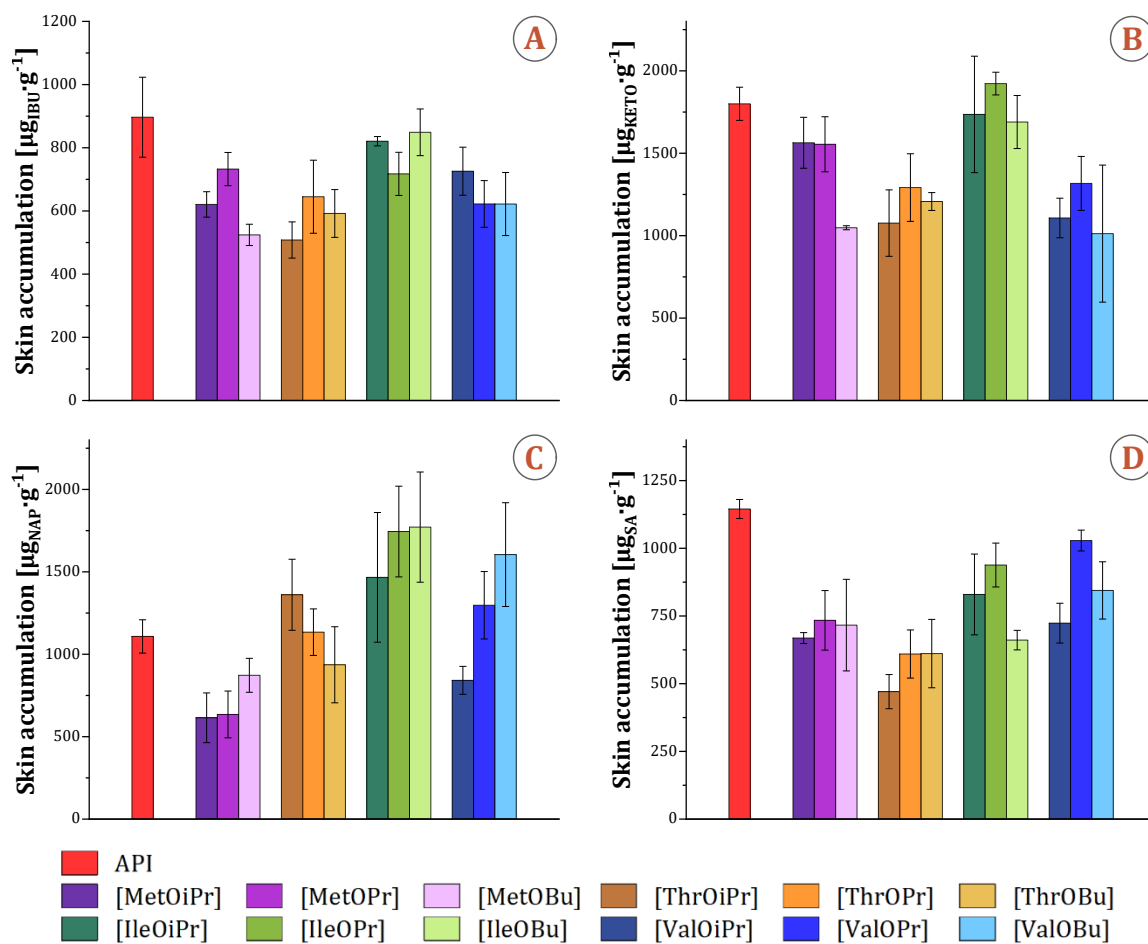


Fig. 40. The comparison of accumulation in the abdominal porcine skin of different NSAIDs (A: (*R,S*)-ibuprofen, B: ketoprofen, C: naproxen, and D: salicylic acid) and its derivatives during the 24 h penetration (data presented in: [182]).

Summary

- In general, the L-amino alkyl ester salts accumulated to a lesser extent than the parent drugs. Furthermore, those compounds which tended to accumulate more in the membrane tested also tended to show lower permeability. They, therefore, showed potential for development not only in topical but also in transdermal formulations.

3.3. Antioxidant activity

Antioxidants inhibit oxidation, a chemical reaction that can produce free radicals and lead to chain reactions that may damage an organism's cells. Regarding skin health, antioxidants are essential to protect the skin from the damaging effects of oxidative stress caused by environmental factors such as UV exposure, pollution, and other toxins. Transdermal and topical products deliver active ingredients through the skin to achieve systemic effects, but they can also provide local benefits, including antioxidant activity, if these substances have such properties. The antioxidant activity of substances in topically

applied products plays an important role in skincare and dermatology. In the transdermal delivery system, products can assist in the elimination of oxidative stress at a systemic level or the deeper layers of the skin [242–245].

Oxidative stress occurs when there is an imbalance between the production of reactive oxygen species (ROS) and the body's ability to detoxify these reactive intermediates or repair the damage they cause. This further stimulates the production of ROS, which are generally oxygen radical species such as hydroxyl radicals, superoxide anion radicals, hydrogen peroxide, and singlet oxygen. Some experimental studies have shown that NSAIDs have antioxidant activity via antiradical activity mediated by free radical scavenging and antioxidant enzyme activation. This results in the inhibition of lipid peroxidation, which is a major cause of skin ageing. In addition, the antioxidant activity of NSAIDs may contribute to their anti-inflammatory effects and potential to protect against diseases associated with oxidative stress [246–251].

The antioxidant activity of studied active substances from the NSAIDs group and their L-amino alkyl ester salts (derived from propyl, *isopropyl*, and butyl alcohols) were evaluated by using the α,α -diphenyl- β -picrylhydrazyl (DPPH) free radical scavenging method. The test is based on determining the ability of compounds to act as donors of hydrogen atoms or electrons in the conversion of DPPH• to its reduced form, DPPH-H [252]. The results of these studies have been discussed in published research [182].

Figure 41 shows the antioxidant activity of the compounds tested, expressed as DPPH radical scavenging activity (%). The detailed results, including the values evaluated for *S*-(+)-ibuprofen and its L-valinium alkyl ester salts are given in Table A44 in Appendix II.

All acids of NSAIDs and their L-amino alkyl ester salts tested showed the ability to reduce DPPH to the DPPH form. Among the non-modified acids tested, salicylic acid showed the highest DPPH inhibition percentage (14.22%) and (*R,S*)-ibuprofen the lowest (9.61%). *S*-(+)-ibuprofen was characterised by a slightly lower antioxidant activity compared to the racemic form of ibuprofen. However, its L-valinium alkyl ester showed stronger DPPH-scavenging activity than both parent drugs and corresponding derivatives obtained from (*R,S*)-ibuprofen.

The obtained L-amino alkyl ester salts generally showed comparable %DPPH inhibition as the parent drugs. When ibuprofen and naproxen moieties were paired with [IleOiPr] and [IleOPr] cations, whereas ketoprofen was paired with [MetOiPr], [ThrOiPr] and [ThrOBu] cations, a significant increase in antioxidant activity was observed. Among all the derivatives obtained, the strongest DPPH-scavenging activity was observed

for [IleOiPr][IBU] and [IleOPr][IBU] compounds, for which the %inhibition DPPH was 2.0-fold and 1.9-fold higher, respectively, compared to the unmodified acid.

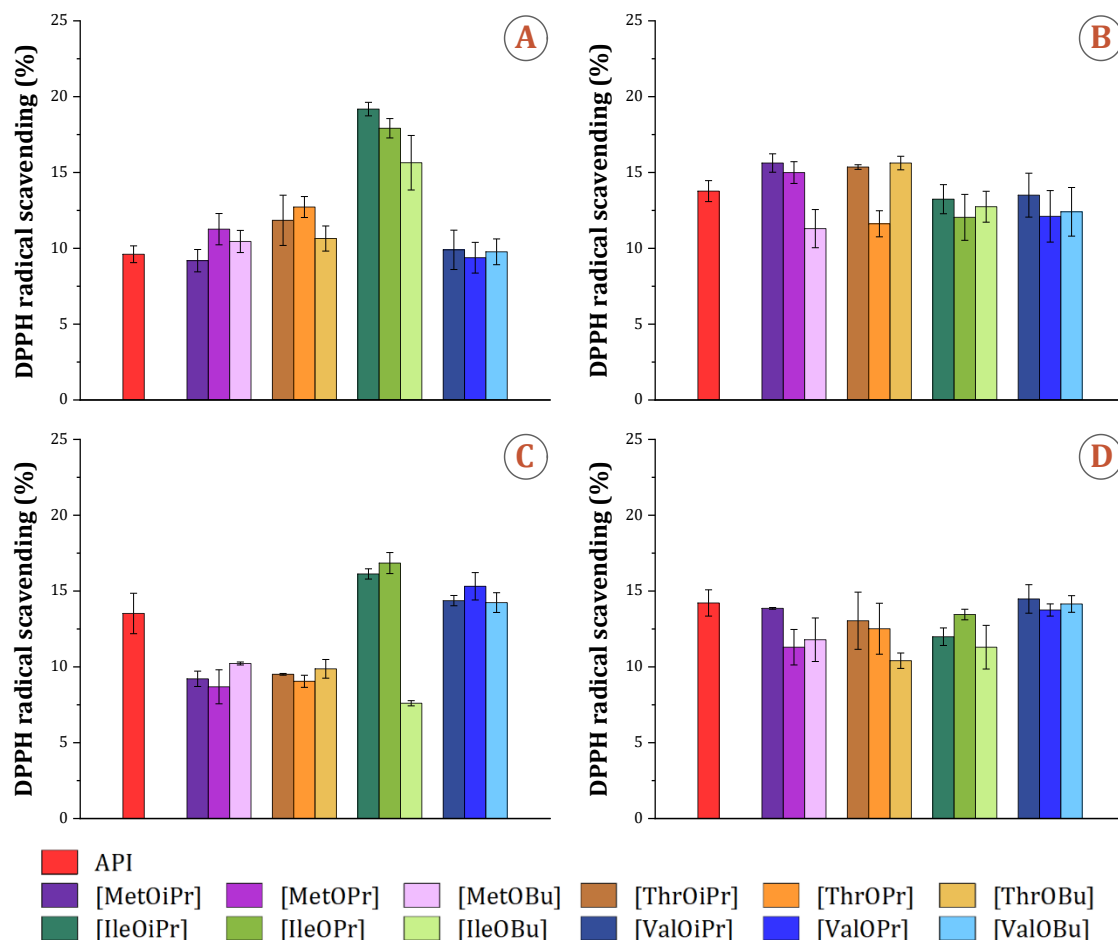


Fig. 41. The antioxidant activity of NSAIDs (A: ibuprofen, B: ketoprofen, C: naproxen, and D: salicylic acid) and their L-amino alkyl ester salts (data presented in: [182]).

Summary

- All compounds tested in this study were able to reduce the stable radical form of DPPH. The DPPH scavenging activity evaluated for the synthesised salts and the parent drugs were generally comparable. The highest antioxidant activity was shown by conjugated L-isoleucine alkyl esters with the ibuprofen moiety – [IleOiPr][IBU] and [IleOPr][IBU] salts. These findings suggest that L-amino acid alkyl ester salts of NSAIDs may be used to develop formulations further to protect the skin from oxidative stress, thereby preventing skin ageing.

3.4. Biodegradation study

The increasing environmental pollution caused by pharmaceuticals has received particular attention recently. Non-steroidal anti-inflammatory drugs (NSAIDs) are one of the

most frequently detected pollutants of this type. Their widespread use and inappropriate disposal result in significant environmental exposure, especially as many NSAIDs are not 100% metabolised, and a high percentage are excreted in humans, resulting in their discharge into wastewater. Toxic effects on aquatic organisms are higher due to their greater capacity for bioaccumulation as a result of their high lipophilicity. In addition, topical products have been shown to contribute significantly to environmental contamination compared to the amount released using oral products [253–256].

Biological treatment is a well-established water treatment process currently used in wastewater treatment plants. It involves the use of microorganisms, such as bacteria, fungi or algae, that are able to degrade or transform pharmaceutical compounds into less harmful substances. Pharmaceuticals can be removed by autotrophic biodegradation during the activated sludge process. However, the effectiveness of this method in removing pharmaceuticals can vary considerably depending on the specific compounds and their concentrations. Some studies have even shown that some pharmaceuticals resist conventional biological treatment processes [257,258].

Therefore, the development of drugs that retain their therapeutic efficacy while being more susceptible to degradation once they enter the environment is linked to the principles of green chemistry and sustainable pharmacy, which aim to minimise the environmental footprint of pharmaceutical compounds [259]. In this context, the biodegradability of the obtained conjugates of selected NSAID acids with L-amino acid alkyl esters was investigated using activated sludge as a source of microorganisms. The influence of both alkyl chain length and cation structure on the biodegradation of active substances has been investigated and reported in published studies [182,260].

Figure 42 presents the comparison of biodegradation, determined for L-valinium alkyl ester (*R,S*)-ibuprofenates after 28 days of study and the calculated half-life values. Biodegradation profiles were evaluated for the compounds studied, and the detailed results of the degradation phases are presented in the Appendix II, Figure A28 and Table A45, respectively.

The unmodified (*R,S*)-ibuprofen achieved 65.42% biodegradation after 28 days of study. A clear relationship between carbon alkyl chain length and biodegradation susceptibility was observed in the case of its L-valinium alkyl ester derivatives. In addition, the influence of solubility and lipophilicity on the biodegradation rate was also a consideration [260]. The maximum level of biodegradation was in the range of 94.67% for [ValOMe][IBU] to 39.17% for [ValOOct][IBU] salt, but an increase in biodegradability was

observed for the conjugation of ibuprofen with the propyl and isopropyl esters of L-valine. According to OECD standards, compounds were considered "readily biodegradable" if they had a biodegradability of 60% or more" [261]. Therefore, salts based on cations with extended alkyl carbon chains (C₆-C₈) were characterised as poorly biodegradable.

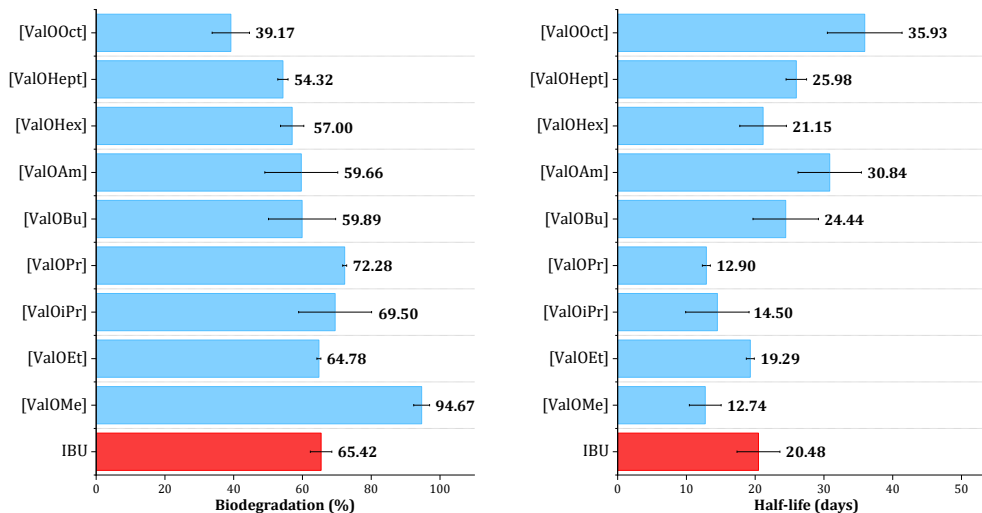


Fig. 42. Assessment of biodegradation after 28 days (left) and the half-life time (right) for ibuprofen and its L-valinium alkyl ester salts (data presented in: [260]).

In this study, the lag phase is understood to be a period of adaptation during which the bacteria adapt to the new conditions before the main degradation process begins, and 10% of the tested compound is also biodegraded. The half-life was defined as 50% of the degradation of a given compound achieved during this period (ending with a plateau phase). The conjugations with L-valinium alkyl esters with carbon chain length C₁-C₃ showed a lower half-life compared to the unmodified acid. The salt based on [ValOiPr], with the branched alkyl chain in the ester moiety, was more resistant to the degradation in activated sludge than the corresponding straight-chain derivative. Furthermore, the complete degradation of the ibuprofen and its L-valinium alkyl ester salts was observed after 68 days of conducting the process [260].

The comparison of the biodegradation profiles evaluated for (*R,S*)-ibuprofen and *S*-(+)-ibuprofen conjugated with selected L-valine alkyl esters is shown in Figure 43. The detailed characteristic values are summarised in Appendix II, Table A45.

Some studies have investigated the enantioselective biodegradation of ibuprofen and found that (*S*)-ibuprofen dominates incoming wastewater due to chiral inversion during human metabolism and is preferentially degraded during wastewater treatment. This indirectly indicates an easier biodegradation pathway for bacteria of this compound. In addition, despite better solubility in water, racemic ibuprofen salts were shown to be much

more resistant to bacterial degradation than *S*-(+)-ibuprofenates. The structure of racemic ibuprofenate salts was characterised as more toxic to bacteria, which means that their adaptation, or rather the adaptation process, requires long periods, slowing down the bioremediation of the contaminated ecosystem [262–265].

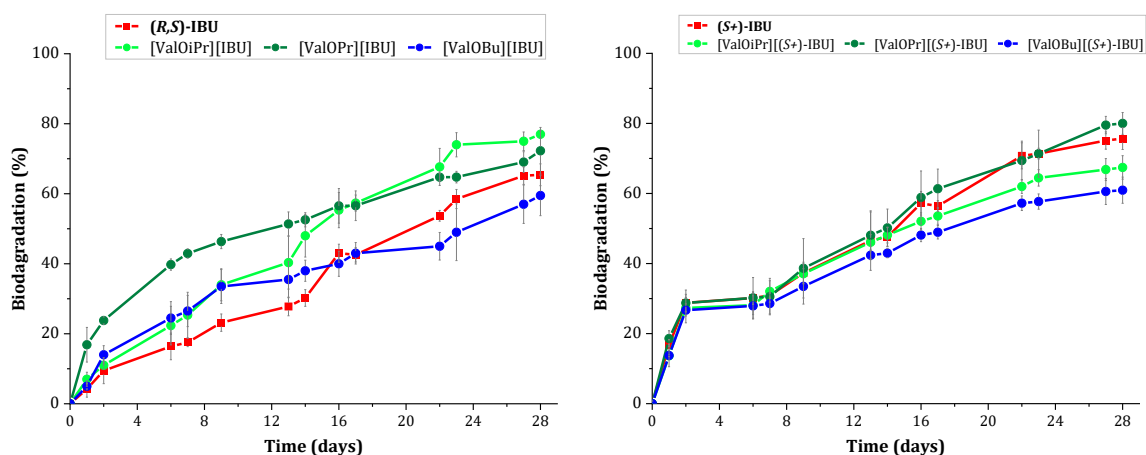


Fig. 43. Biodegradation curves for (*R,S*)-ibuprofen (right) and *S*-(+)-ibuprofen (left) and their L-valinium alkyl ester salts (data partly presented in: [182]).

These findings confirm that shorter lag phases were evaluated in the case of *S*-(+)-ibuprofenates under study. Moreover, the biodegradability after 28 days of the *S*-(+)-enantiomer was higher (75.68%) as well as for its L-valinium alkyl ester salts derivatives (67.43%, 80.00%, and 60.95% for [ValOiPr][(S+)-IBU], [ValOPr][(S+)-IBU], and [ValOBu][(S+)-IBU], respectively) compared to the corresponding conjugates of (*R,S*)-ibuprofen.

Based on the result obtained, the propyl esters of amino acids were selected for further biodegradability study to determine the influence of the structure of the starting active substance and the amino acid on the biodegradability of the obtained salts.

The comparison of the determined biodegradation after 28 days for selected L-amino acid propyl ester salts of acids from the NSAID group is presented in Figure 44, while the biodegradation profiles and detailed results are summarised in Appendix II (Figure A29 and Tables A46–A48).

It is well known that cyclic compounds are less susceptible to biodegradation than aliphatic compounds, similar to the fact that monocyclic compounds are more readily biodegradable than polycyclic compounds, which is mainly determined by the size of the molecules. Small molecules have simpler carbon chains and a spatial organisation that facilitates enzymatic access [266].

Salicylic acid is the only compound considered biodegradable among the drugs studied. SA contains a hydroxyl group directly attached to an aromatic ring, which can make it more susceptible to attack by microbes through enzymatic reactions such as hydroxylation. This process can make the compound more susceptible to further degradation by initiating the breakdown of the aromatic ring. At the same time, ibuprofen, ketoprofen and naproxen are more resistant to microbes due to their structural complexity, and their residues can still be detected in surface water because they are not completely removed by conventional treatment technologies [267–271].

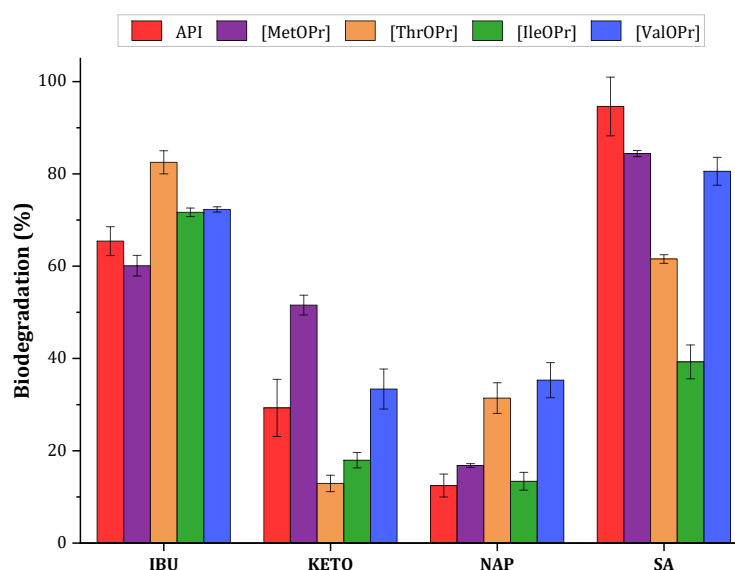


Fig. 44. Comparison of the biodegradation after 28 days for acids from the NSAIDs group and their L-amino acid propyl ester salts (data presented in [182]).

The biodegradation evaluated for other active substances of NSAIDs were as follows: 29.28% for ketoprofen, 12.45% for naproxen and 94.61% for salicylic acid. The results obtained confirm that a more complex structure, such as the methoxy-naphthalene ring or the presence of the ketone group, influences the susceptibility to be degraded by the activated sludge. In the case of drugs considered poorly biodegradable, conjugation with the L-amino acid propyl ester moiety significantly improved the biodegradation of the drug. However, the increase was variable and depended on the structure of both paired ions. In the case of (*R,S*)-ibuprofen, the highest percentage of biodegradation was obtained when conjugated with [ThrOPr] ester (82.50%), ketoprofen when conjugated with [MetOPr] ester (51.56%) and naproxen when conjugated with [ValOPr] ester (35.29%).

All salicylates obtained showed reduced biodegradability compared to the starting acid. The decrease in the efficiency of the biodegradation process may be the introduction

of additional functional groups that increase the complexity of the final molecular structure, as well as the increase in the lipophilic character of the synthesised derivatives. Nevertheless, the obtained L-amino acid propyl salts, with the exception of the [IleOPr][SA] compound (39.24%), were characterised as readily biodegradable and were in the range 61.54%, for [ThrOPr][SA] to 84.40% for [ValOPr][SA].

The relationship between the lipophilic character (and water solubility) and susceptibility to biodegradation was observed. The ibuprofen salts obtained showed an increase in biodegradability, followed by an increase in water solubility. However, the opposite relationship was observed for ketoprofen, naproxen and salicylic acid derivatives. In general, as the lipophilic character increases and the water solubility decreases, the level of biodegradation tends to be higher.

Summary

- As a result of the biodegradability study using activated sludge (under aerobic conditions), the following compounds were classified as readily biodegradable: salicylates based on [MetOPr], [ThrOPr], and [ValOPr] cations, all L-amino acid propyl salt of ibuprofen under study, and ibuprofen conjugates of L-valine alkyl esters with carbon chain length C₁-C₅.
- The [MetOPr][SA] (84.40%), [ValOPr][SA] (80.55%), and [ThrOPr][IBU] (82.50%) salts showed the highest level of biodegradability among all the compounds studied.
- The relationship between lipophilicity and biodegradability was observed. An increase in biodegradability was followed by a decrease in lipophilicity for the ibuprofen salts. Furthermore, compounds with a short alkyl chain in the cationic form showed the highest biodegradation. In the case of ketoprofen, naproxen, and salicylic acid salts, biodegradability was improved by compounds with a higher lipophilicity.

3.5. Antimicrobial activity

Ionic liquids offer an alternative with a wide range of applications for the elimination of antibiotic-resistant bacteria, such as disinfectant detergents, antiseptics, or additives to dressing materials. ILs can disrupt the bacterial membrane of both gram-negative and gram-positive bacteria by interacting with and forming pores in the cell membrane, altering the orientation of the phospholipids, the membrane potential, and ultimately, the overall fluidity and viscoelasticity of the membrane [272–275]. In the context of API-ILs, the design of such ionic liquids with antimicrobial activity represents an innovative approach to drug

formulation and delivery. It combines the properties of ionic liquids with a drug moiety to not only deliver the active substance but also to enhance the delivery of antimicrobial agents to specific sites in the body. In particular, the strategy of increased focus involves the selection of adjuvants that can improve the action of already approved drugs against multidrug-resistant bacteria, either reducing the impact and emergence of resistance or enhancing the antimicrobial activity [272,276,277].

Numerous studies suggest that non-steroidal anti-inflammatory drugs appear to have some antimicrobial and anti-biofilm activity against clinically relevant bacteria. This may stimulate interest in repurposing these well-tolerated drugs as adjunctive therapies for the treatment of biofilm-associated infections. A number of mechanisms have been proposed for the antibacterial and anti-biofilm effects of NSAIDs, and these differ from one species to another. The antibacterial mode of action of NSAIDs may be related to their ability to affect the integrity of the bacterial cytoplasmic membrane and to alter the physicochemical properties of the bacterial surface. Other aspects of their mode of action may be related to inhibition of DNA synthesis, prevention of DNA replication, and inhibition of bacterial membrane repair. However, the inhibition of microbial growth is observed at the above concentrations, which can be achieved in blood plasma after oral administration of NSAIDs. Therefore, topical or transdermal administration of active substances may overcome this disadvantage as a localised treatment method in the area of skin inflammation [278–281].

L-amino acids have also been studied for their antimicrobial activity and potential use as antimicrobial agents. However, more research is being done on certain peptides, particularly the D-amino acids. These have broad-spectrum antimicrobial activity and, therefore, offer an advantageous alternative to traditional antimicrobial drugs as they are less likely to be resisted by microbes. Some amino acid-based surfactants have been reported to interact with the lipid bilayer of cell membranes. For example, known amino acid-based substances derived from arginine and lysine show good antimicrobial activity, high biodegradability, and a low toxicity profile [282–285].

The evaluation of the antibacterial activity of selected drugs from the group of NSAIDs and their L-amino acid isopropyl ester salts was carried out using the disc diffusion method. The gram-negative bacteria *Escherichia coli* and the gram-positive bacteria *Staphylococcus epidermidis* and *Micrococcus luteus* were selected for this study. The detailed results obtained, expressed in terms of the diameter of the inhibition zone, are summarised in Tables A49-A51 in Appendix II. At the same time, the comparison of the antimicrobial activity of the tested compounds used at the highest concentrations

(1000 mg/mL) is shown in Figures 45–47. The results of this study have been the subject of published research [181].

E. coli, classified as gram-negative bacteria, have been documented to be resistant to several drugs, including extensive and pan-drug resistance. *S. epidermidis*, a member of the skin flora and commonly found on mucous membranes in animals, has the potential to breach human epithelial barriers, leading to nosocomial infections and acting as a significant source of contamination in blood cultures. Another bacteria, *M. Luteus*, is typically found as a commensal organism on human skin and in the upper respiratory tract. Despite its generally benign nature, it can facilitate the colonisation of more dangerous microorganisms on the skin [53,286–288].

In general, resistance to the salts tested was lower in gram-positive bacteria, which have a thick outer layer of peptidoglycan and readily absorb substances from the environment. In contrast to gram-negative *E. coli*, the cells are surrounded by a complex outer membrane that contains lipopolysaccharides and plays several functional roles in detoxification and drug resistance. This may influence the observed differences in susceptibility of each bacterium to the L-amino acid isopropyl ester derivatives studied [289].

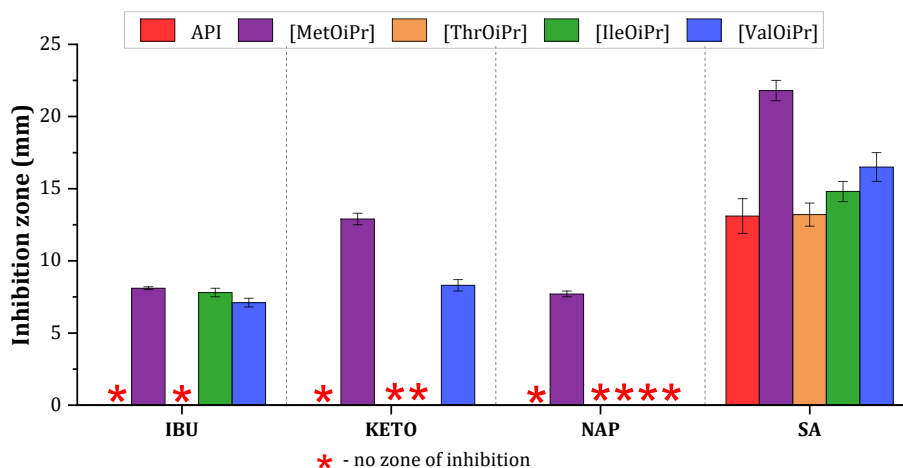


Fig. 45. Antimicrobial activity (Inhibition diameter zone) against *Escherichia coli* of acids from NSAIDs group and their L-amino acid isopropyl ester salts at a concentration of 1000 mg/mL.

The results showed that both ions influenced the inhibition of the bacteria tested and were not solely the result of the concentration of the NSAID moiety or its molar fraction in the compound. A similar effect was observed in the study of ibuprofen lysine, which showed higher antimicrobial activity than pure ibuprofen [281]. This effect is most pronounced in the case of gram-negative bacteria. Among the parent acids, only salicylic acid showed an inhibitory effect. The presence of the L-amino acid isopropyl ester follows

the antimicrobial activity for the other conjugations of the NSAID salts tested and the significant growth inhibition effect against gram-negative bacteria compared with the parent drug for the SA-based salts. In addition, lipophilicity may affect penetration through the bacterial cell wall, which is composed of hydrophobic lipid layers. The salicylic acid derivatives were characterised by the highest values of logP (1.610–1.1784) among all the salts synthesised, which facilitates the uptake of these compounds.

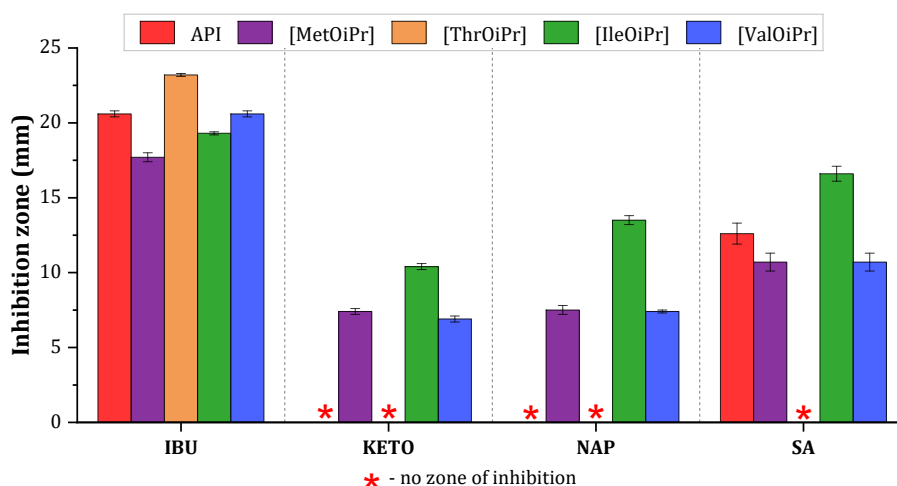


Fig. 46. Antimicrobial activity (Inhibition diameter zone) against *Staphylococcus epidermidis* of acids from NSAIDs group and their L-amino acid isopropyl ester salts at a concentration of 1000 mg/mL.

The antimicrobial activity against *E. coli* was observed for concentrations from 100 mg/mL (for [MetOiPr][IBU] and [ValOiPr][IBU] salts), but the increase of the inhibitory effect was observed for used concentrations from 400 mg/mL. The highest antimicrobial activity was exhibited by the [MetOiPr] based derivatives, which is most prominent for the studied naproxen and its salts, where the inhibitory effect was observed only for the [MetOiPr][NAP] compound. On the other hand, the [ThrOiPr] conjugations did not show any antimicrobial effect for any of the salts tested, and this evaluation for [ThrOiPr][SA] is most likely due to the presence of the salicylic acid moiety. Taking into account the molar fraction of both ions, the inhibition zone values obtained for [ThrOiPr][SA] are comparable to those obtained for the parent drug. Moreover, the salicylate salts are characterised by the highest inhibitory activity, resulting in a synergistic antibacterial activity of both ions.

E. coli bacteria have been described to export L-threonine via efflux pumps encoded by the *rhtC* gene. Overexpression of *rhtC* has been shown to increase resistance to externally supplied L-threonine and further reduce the accumulation of threonine-derived metabolites. This effect results in a threefold increase in L-threonine export in the modified production strain [290,291]. The lack of susceptibility effect of salts derived from L-threonine against the bacteria studied may be explained by this mechanism.

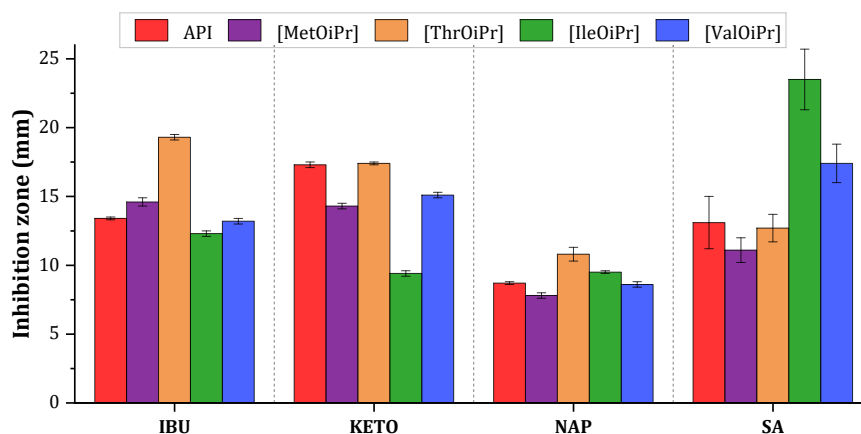


Fig. 47. Antimicrobial activity (Inhibition diameter zone) against *Micrococcus Luteus* of acids from NSAIDs group and their L-amino acid isopropyl ester salts at a concentration of 1000 mg/mL.

Among the NSAIDs studied, the inhibitory activity against *S. epidermidis* was evaluated for ibuprofen (at all concentrations tested) and salicylic acid (at concentrations ranging from 400 mg/mL). Similarly, no antimicrobial activity was evaluated for the [ThrOiPr] based derivatives, but the pairing of the ibuprofen moiety with the L-threonine isopropyl ester caused a slight increase in the inhibitory effect (for tested concentrations from 100 mg/mL).

The Msr enzymes protect *Staphylococcus* bacteria against some types of oxidative stress induced by sulphur-containing amino acids such as cysteine or methionine, as described by Beavers et al. The resistance of *S. epidermidis* to L-methionine derivatives may be controlled by a specialised defence mechanism based on these enzymes [292]. This can be an explanation for the lower antimicrobial activity of conjugations with the MetOiPr moiety.

Furthermore, the inhibitory effect was observed for ibuprofen and its salts at all concentrations tested. For derivatives of other drugs studied, antimicrobial activity was observed at concentrations ranging from 200 mg/mL (for [MetOiPr][SA] compound) to 400 mg/mL (for [IleOiPr][KETO], [ValOiPr][KETO] and [ValOiPr][SA] compounds). The highest values of inhibition zones were obtained for [IleOiPr] based salts obtained from ketoprofen, naproxen and salicylic acid.

In the case of another gram-positive bacteria, *M. luteus*, the highest susceptibility to both unmodified acids from the NSAID group and their L-amino acid isopropyl ester salts was observed in almost all concentration ranges tested. The increase in antimicrobial activity caused by conjugation with the L-amino acid ester moiety differed for each parent drug. Compared to the parent acid, at the highest concentrations tested (600–1000 mg/mL), higher values of inhibition zones were observed for ibuprofen salts of [ThrOiPr] and [MetOiPr],

for ketoprofen conjugated with [ThrOiPr] and for naproxen salts of [ThrOiPr] and [IleOiPr]. Most changes were observed in the study evaluated for salicylic acid and its derivatives. The antimicrobial effect for unmodified drugs was observed for concentrations ranging from 400 mg/mL while for [MetOiPr][SA] from 100 mg/mL and for [ThrOiPr][SA] from 250 mg/mL. In the case of [ValOiPr][SA] and [IleOiPr][SA], the increase in inhibitory activity was the highest among all the compounds studied, but the antimicrobial activity was only evaluated for concentrations from 600 mg/mL.

In the context of bacterial growth, excessive supplementation of a single amino acid can cause a temporary auxotrophy for other amino acids, resulting in reduced growth rate and synthesis capacity. For example, conjugation reactions with the leucine production pathway are involved in the valine biosynthesis pathway of *M. luteus*. It has been suggested that by inhibiting leucine biosynthesis and simultaneously reducing transcription of the comEA/EC gene, which is responsible for receptor processes but also plays a fundamental role in intracellular transport, additional supplementation with branched-chain amino acids such as valine or isoleucine affects transcriptional and post-transcriptional transformability [293–295]. This mechanism may explain the low level of antimicrobial activity of the isopropyl esters of branched-chain amino acids in the present study.

Summary

- The antimicrobial activity of selected NSAIDs was improved by conjugation with the L-amino acid isopropyl ester cation. The inhibition of bacterial growth was influenced by both starting ions, with possible synergistic antibacterial activity.
- The tested compounds generally showed higher antimicrobial activity against gram-positive (*Staphylococcus epidermidis* and *Micrococcus luteus*) than gram-negative (*Escherichia coli*) bacteria. In addition, the highest susceptibility to both unmodified acids from the NSAID group and their L-amino acid isopropyl ester salts was evaluated for *M. luteus* bacteria.
- The susceptibility of each bacterium to the salts of the active compounds is different. In most cases, the highest antimicrobial activity was shown by [MetOiPr] based derivatives against *E. coli*, [IleOiPr] based derivatives against *S. epidermidis* and [ThrOiPr] based derivatives against *M. luteus*.

Chapter III: Conclusions

The presented concept of structural modification of non-steroidal anti-inflammatory drugs based on L-amino acid alkyl esters demonstrates the possibility of improving the bioavailability of the drug, thereby reducing the effective dose of the drug and the risk of adverse effects of NSAIDs. This is achieved by converting the active ingredients into salts and reducing their acidic character. As an interdisciplinary work with an emphasis on possible applications, the results of the dissertation have a number of profound implications for the field of chemical and pharmaceutical engineering. The main implications can be outlined as follows:

1. The research involved the reaction of the organic acid with an organic base, resulting in the formation of a salt, to obtain new non-steroidal anti-inflammatory drug derivatives. Ibuprofen, ketoprofen, naproxen and salicylic acid were used as anions. The cation consisted of alkyl esters of L-isoleucine, L-methionine, L-threonine and L-valine with different alkyl chain lengths and different branching (*n*-propyl and *iso*-propyl chains). The cation was also used to provide an additional function and biological activity, resulting in bifunctional compounds. In addition, based on melting points lower than 100°C, according to an arbitrary definition, the following derivatives obtained can be classified as ionic liquids: all (*R,S*)-ibuprofenates and (*R,S*)-ketoprofenates based on L-isoleucine, L-methionine, L-threonine and L-valine alkyl esters cations, L-valinium alkyl ester salts of *S*-(+)-ibuprofen (excluding [ValOiPr][S(+)-IBU] salt), *S*-(+)-naproxenates based on [IleOBu], [MetOPr], [MetOiPr], [MetOBu], and L-threonine alkyl esters, salicylates based on L-isoleucine, L-methionine, L-threonine and L-valine alkyl esters cations (excluding [ValOMe][SA] and [ThrOMe][SA] derivatives).
2. The presented concept of structural modification of non-steroidal anti-inflammatory drugs based on L-amino acids demonstrates the possibility of improving the desired physicochemical properties and their design, depending on the choice of the starting amino acid and the length of the alkyl chain in the ester moiety:
 - a. Conjugation of the drug with L-amino alkyl esters mostly reduced the lipophilicity of poorly soluble drugs (with the exception of salicylic acid derivatives). All the salts obtained showed significantly higher solubility than the parent drug in all the media studied (deionised water and phosphate buffers

at pH 5.4 and 7.4). The solubility in aqueous media decreases with the length of the alkyl chain in the ester moiety, according to the order of modification: L-Thr>L-Ile>L-Val> L-Met.

- b. The compounds obtained are optically active, and the rotation of the plane of polarization by the salts corresponds to the rotation of the starting L-amino acid. The specific and molar rotation values determined decreasing in the following order of the L-amino acid residues used L-Ile>L-Val>L-Met>L-Thr.
 - c. Research has shown that modification of NSAIDs with L-amino acid alkyl esters, in general, reduces their thermal stability. However, the stability test showed that the L-amino acid isopropyl ester salts studied retained a high degree of stability after long-term storage for 12 months at 5 and 25°C. Increasing the length of the alkyl chain in the cationic moiety influences the higher thermal stability and lower melting points of the salts obtained. The increase in thermal stability and the decrease in melting point values follow the order of the starting L-amino acids: L-Met>L-Thr>L-Ile>L-Val.
3. The main outcome of this work was to develop modifications to active ingredients to increase the transport of the active ingredient through the skin, with increased safety compared to other routes of administration, including the most commonly used oral route. In the studies conducted, the following were found:
- a. Derivatives with the best skin penetration parameters were found to have a 3-carbon substituent in the alkyl chain in the cationic moiety, while the derivatives based on 3- (*n*-propyl and *iso*-propyl) and 4-carbon chain length showed the highest tendency to accumulate. The best parameters in terms of drug permeation were shown by the conjugations of NSAID moieties with L-threonine alkyl esters ([ThrOPr], [ThrOiPr], [ThrOBu]).
 - b. It has been shown that the increase in solubility resulting from changing the starting L-amino acid increases the value of the cumulative mass penetrating the skin. The increase in cumulative mass generally follows the order of the L-amino acid: L-Met<L-Ile<L-Val<L-Thr.
 - c. The combination of the hydrophobic moiety of the NSAID with the hydrophilic particle of the L-amino acid ester creates a compound with favourable properties that could allow the derivatives obtained to penetrate the stratum corneum lipid

barrier and reach the epidermal layer. This makes it possible to use the resulting salts in topical formulations without the need to add excipients.

4. In addition, the obtained L-amino acid alkyl ester salts of NSAIDs showed the greatest potential for further application as novel components in topical and transdermal formulations, as they showed a favourable biological activity:
 - a. Since the obtained derivatives reduced the stable radical form of DPPH, they can be used to develop further formulations that protect the skin from oxidative stress and thus prevent skin ageing.
 - b. The antimicrobial activity of selected NSAIDs against *Escherichia coli*, *Staphylococcus epidermidis* and *Micrococcus luteus* was improved by conjugation with the L-amino acid isopropyl esters due to a possible synergistic effect of both ions. The salts obtained could, therefore, potentially be used in topical or transdermal systems for the treatment of delayed healing wounds.

Chapter IV: Experimental section

1. Synthesis of L-amino acids alkyl esters and their salts of selected acids from the group of non-steroidal anti-inflammatory drugs

1.1. Synthesis of L-amino acid alkyl ester hydrochlorides

The esterification reactions of selected L-amino acids: 2-amino-3-methylbutanoic acid (L-valine, Val), 2-amino-3-methylpentanoic acid (L-isoleucine, Ile), 2-amino-3-hydroxybutanoic acid (L-threonine, Thr), and 2-amino-4-(methylthio)butanoic acid (L-methionine, Met) were carried out in the presence of the chlorinating agent chlorotri(methyl)silane (TMSCl), which also acted as a catalyst and a water-binding agent. L-valine alkyl ester hydrochlorides were obtained by esterification of L-amino acid with C₁-C₈ alcohols. In the case of other L-amino acids, the process was carried out in the presence of C₁-C₄ alcohols, including isopropyl alcohol. Esterification was conducted at a temperature of 60-75°C for 12-24 h using TMSCl in a molar ratio to the amino acid of 2.5:1, and the alcohol was used in an amount of at least 5 moles per 1 mole of L-amino acid. In the case of obtaining L-valine alkyl ester hydrochlorides (C₁-C₈), the process was additionally carried out in the ultrasound field (35kHz and power 180W). After the esterification was completed, the volatile components, i.e. the excess of the alcohol used, unreacted TMSCl, unreacted TMSOH, hydroxytrimethylsilane (TMSOH), hexamethyldisiloxane ((TMS)₂O) and alkyl trimethylsilyl ether (TMSOR) formed as by-products, were distilled off at a temperature of 60°C to 90°C under reduced pressure. The resulting crude product was washed with diethyl ether to remove unreacted TMSCl and hydroxytrimethylsilane by-products. The obtained crude product was then dissolved in chloroform, and the resulting solution was filtered under reduced pressure to separate the undissolved residue, which was unreacted amino acid and/or non-esterified amino acid hydrochloride. Pure L-amino acid alkyl ester hydrochloride was thus obtained by distilling off the solvent from the filtrate at 60°C under reduced pressure.

1.2. Synthesis of alkyl esters of L-amino acids

The L-amino acid alkyl ester was obtained by neutralizing the corresponding L-amino acid alkyl ester hydrochloride with aqueous ammonia in a molar ratio of 3:1 to the hydrochloride. Extractions with diethyl ether, ethyl acetate or methylene chloride were performed to isolate the obtained ester from the obtained mixture. The separated organic

layer was dried over anhydrous sodium sulfate. Then, the organic solvent was distilled under reduced pressure to obtain pure L-amino acid alkyl ester as a pale yellow liquid.

1.3. Synthesis of acid salts from the group of non-steroidal anti-inflammatory drugs

Derivatives of selected acids from the group of non-steroidal anti-inflammatory drugs were obtained in an equimolar reaction with the appropriate L-amino acid alkyl ester. As active substances, (*R,S*)-2-(4-(2-methylpropyl)phenyl)propanoic acid, (2*S*)-2-(4-(2-methylpropyl)phenyl)propanoic acid, (*R,S*)-2-(3-benzoylphenyl)propanoic acid, (2*S*)-2-(6-methoxy-2-naphthyl)propanoic acid, and 2-hydroxybenzoic acid were chosen for the study. Reactions were carried out at room temperature for 5-15 minutes in a chloroform as a solvent. Subsequently, the solvent was distilled off under reduced pressure at 60°C. The obtained product was dried in an oven for 24 h under reduced pressure at 60°C.

2. Identification and determination of the purity of the obtained products and intermediate products

2.1. Spectroscopic analysis

One-dimensional NMR spectra were recorded using a BRUKER DPX-400 spectrometer (Billerica, MA, USA) with a spectral generation frequency of 400.13 MHz for proton spectra and 100.62 MHz for carbon spectra. Tetramethylsilane (TMS) was used as an external standard. The compounds were analysed as solutions in deuterated chloroform (CDCl₃) and dimethyl sulfoxide (DMSO-*d*₆). Data processing was performed using MestreNova Software (v, 12.0.0-2008), Mestrelab Research S.L.

IR absorption was measured using the transmission method using a Nicolet 380 Thermo Scientific™ spectrometer (Waltham, MA, USA) equipped with an ATR attachment with a diamond crystal. Spectra were recorded in the 4000–400 cm⁻¹ range with resolution 4 cm⁻¹. Data acquisition and processing were performed using OMNIC 9.2.86 software by Thermo Fisher Scientific Inc.

2.2. Elemental analysis

The percentage content of carbon, nitrogen, hydrogen, sulfur and oxygen was determined using the Thermo Scientific™ FLASH 2000 CHNS/O Analyzer (Waltham, MA, USA), using the full combustion method at 900°C in an oxidation-reduction furnace equipped with a thermal conductivity detector (TCD).

3. Characteristics of the physicochemical properties of the obtained products

3.1. Determination of formation constant (pK_s)

The salt formation constant was calculated according to the equation (1):

$$pK_S = pK_A(\text{for acid}) + pK_B(\text{for base}) - pK_W \quad (1)$$

where: pK_A – dissociation constant of the unmodified active substance; pK_B – dissociation constant of an L-amino acid alkyl ester

The pK_A and pK_B values were determined by the potentiometric method using a pH meter (CP-505, Elmetron, Zabrze, Poland) equipped with an EPS-1 electrode (Elmetron, Zabrze, Poland). In the case of measurements of the dissociation constant of unmodified acid, 0.1 M NaOH was used for the titration. To determine the pK_A constant of the base, the study used a 0.60 mM aqueous solution of the appropriate L-amino acid alkyl ester hydrochloride (acidified to pH=3.5) and 5 mM NaOH for titration. The pK_B value of the L-amino acid alkyl ester was calculated from the difference between the pK_W product of water and the determined pK_A value of the base.

3.2. X-ray diffraction (XRD)

The crystallinity of the obtained compounds was examined by XRD diffraction using an Aeris X-Rays ON X-ray diffractometer, Malvern Panalytical Ltd. (Malvern, UK). The tests were carried out in the range of diffraction angles of 7–90° 2θ, using Cu-Kα radiation (λ=1.54056 Å).

3.3. Thermogravimetric analysis

The thermal stability of the obtained compounds was tested using the thermogravimetric method (TG) using the Netzsch Proteus Thermal Analysis TG 209 F1 Libra apparatus by Netzsch (Selb, Germany). The measurements were carried out in the 25–1000°C temperature range with a heating rate of 10°C/min in an atmosphere of air (flow 25 mL/min) and nitrogen (flow 10 mL/min). Samples of weigh 5–7 mg were used for the tests.

3.4. Differential scanning calorimetry

Phase change temperatures were measured using a PerkinElmer DSC-7 (Rotgau, Germany). Samples weighing 2–3 mg were loaded on the aluminium pan with a crimped lid. The nitrogen atmosphere used for the measurements was 20 mL/min. Unless otherwise

stated, two complete heating and cooling cycles were performed at a rate of 10°C/min. The sample was heated from 0°C to a temperature 10°C lower than the sample decomposition onset temperature (determined individually for each compound, determined based on TG analysis). The temperatures obtained from the DSC data are shown as peaks of the curve. Indium and tin were used as standards for temperature calibration. Calibration of the enthalpy measurement was performed using indium. The experimental apparent heat capacity was obtained with a heating rate of 20°C /min. An indium sample was used to calibrate the temperature.

The three-step method was used for the heat capacity evaluation. The first thermal scan was performed on an empty pan. The reference material (sapphire) was measured in the second thermal scan. The third run was carried out with a sample of the tested compound. Measurements were made between 10°C and the maximum temperature specified for each compound tested. For crystalline compounds, it was at least 5°C lower than the determined melting point (T_{onset}). For the amorphous compounds, the maximum temperature was 100°C. The research was carried out at the Berliner Hochschule für Technik in Berlin under the supervision of Prof. Oliver Krüger, PhD.

3.5. Stability testing under different storage conditions

The stability of the selected compounds under three different storage conditions: refrigeration (5°C±2°C for 12 months), room temperature (25°C±2°C for 12 months) and stress test (40°C±2°C for 6 months) was evaluated. Samples weighing 50 mg were stored in darkened and sealed PP vials. Differential scanning calorimetry and FT-IR analysis (performed on Spectrum Two FT-IR Spectrometer equipped with LiTaO₃ Detector) were used to monitor stability and determine possible changes in thermochemical properties. The research was carried out at the Berliner Hochschule für Technik under the supervision of Prof. Oliver Krüger, PhD.

3.6. Specific rotation

Optical rotation was measured using an AUTOPOL IV Polarimeter from Rudolph Research Analytical (Hackettstown, NJ, USA) at a λ wavelength of 589 nm at 20.0±0.1°C. The angle of rotation of the plane of polarized light was determined with an accuracy of 0.001° in a measuring cell 100 mm long. Solutions with a concentration of 0.5–1% prepared in anhydrous ethanol were used for the study.

The specific and specific molar rotation values were calculated according to the following equations (2 and 3):

$$[\alpha]_{\lambda}^T = \frac{\alpha_{\lambda}^T}{c \cdot l} \quad (2)$$

$$[M]_{\lambda}^T = \frac{M \cdot [\alpha]_{\lambda}^T}{100} \quad (3)$$

Where: $[\alpha]_{\lambda}^T$ – specific rotation at temperature T (°C) and wavelength λ [°Arc]; $[M]_{\lambda}^T$ – specific molar rotation; α_{λ}^T – optical rotation; c – concentration [g/mL]; l – cell length [dm]; M – molar mass of compound under study [g/mol].

3.7. Solubility study

The solubility experiments using selected organic polar and non-polar solvents were carried out using a modified Vogel method [296]. Samples of the tested compounds weighing 100 mg were placed in screw cap vials equipped with a magnetic stirring bar. Then, 1 mL of the appropriate solvent was added and stirred for 10 minutes at 25°C. For heterogeneous solutions, another 1 mL of solvent was added and stirred. Based on the amount of compound dissolved in 1 mL of proper solvent, compounds were classified as: a) soluble (100 mg of the compound is dissolved in 1 mL), b) partly soluble (33-100 mg of the compound is dissolved in 1 mL), or c) insoluble (less than 33 mg of the compound is dissolved in 1 mL).

Solubility in water and selected buffer solutions (phosphate buffers with pH=5.40 and pH=7.40) was carried out for unmodified active acids and their salts of alkyl esters of L-amino acids. For this purpose, the excess of the test compound was mixed with 2 mL of the given solvent and stirred intensively at 25°C for 24 h in a screw cap vial. The resulting mixture was centrifuged, and the supernatant was decanted, diluted and subjected to HPLC analysis to determine the quantitative concentration of the analyte.

The SHIMADZU Nexera-i LC-2040C 3D High Plus Liquid Chromatograph HPLC (Kyoto, Japan), outfitted with a DAD/FLD detector, was used to perform the chromatographic measurements. The analysis was carried out using Kinetex® F5 100 Å column from Phenomenex (Torrance, CA, USA) with a 2.6 µm particle size and dimensions of 150×4.6 mm, and the mobile phase constituted of water and acetonitrile (50:50, v/v) with a flow rate of 1 mL/min. The column temperature was set at 30°C, and the injection volume was 50 µL. Data acquisition and processing were performed using a LabSolutions/LC Solution System (software). The concentration of NSAIDs and their salts were calculated using peak area measurements using a calibration curve method.

3.8. Lipophilicity

The lipophilicity of the obtained salts was determined by measurement of the partition coefficient in the *n*-octanol/water system. For this purpose, 10 mg of the analysed substance was dissolved in 5 mL of *n*-octanol saturated with water and 5 mL of water saturated with *n*-octanol and then stirred intensively at 25°C for 3 h. The layers were separated, and the aqueous layer was analysed using high-performance liquid chromatography (HPLC) to quantify the concentration of the salt being tested, analogous to the solubility experiments. The value of the partition coefficient was calculated according to the following equation (4):

$$\log P = \log \left(\frac{C_o}{C_w} \right) = \log \left(\frac{C_o - C_w}{C_w} \right) \quad (4)$$

where: C_o – is the concentration of the substance in the octanol layer; C_w – is the concentration of the substance dissolved in the aqueous layer; $C_o - C_w$ – is the total concentration of the substance used in the experiment [mg/mL].

4. Characteristics of the biological properties of the obtained products

4.1. Skin Permeation Studies

In vitro, skin permeation studies were performed using a Franz diffusion chamber (Phoenix DB-6, ABL&E-JASCO, Vienna, Austria) containing donor and acceptor chambers of 2 and 8 mL volume, respectively. The diffusion surface through which the active ingredients permeated was 1 cm². Phosphate-buffered saline (PBS) with pH=7.40 was used as the acceptor fluid. The temperature was maintained constant at 37.0±0.5°C. The research used pig skin as a membrane. The natural tissue samples of 0.5 mm in thickness were cut into appropriate pieces 2 cm×2 cm. The donor chamber was filled with 1 mL of a solution with a concentration of 0.01 g_{active substance}/mL of the test compound, dissolved in 70% ethanol. The experiment was carried out for 24 h, taking 0.5 mL of the solution from the acceptor chamber at set intervals: 0.5 h, 1 h, 2 h, 3 h, 4 h, 5 h, 8 h and 24 h from the start of mixing. Each time, the acceptor chamber was filled with a fresh portion of the buffer used. The concentration of the compound in the collected solution sample was determined by HPLC.

Based on the conducted tests, the following permeation parameters of the tested compounds were determined in terms of the active substance (API): the determined concentration was used to calculate the cumulative mass (μg_{API}·cm⁻²). The cumulative mass

in the acceptor fluid versus time was plotted, and the time needed to reach the steady-state permeation (L_T) was chosen as the point of intersection of the function plot with the X-axis. This resulted in the steady-state period flux (in $\mu\text{g}_{\text{API}}\cdot\text{cm}^{-2}\cdot\text{h}^{-1}$) through the skin into the acceptor phase. Based on Fick's law of diffusion and the following equation, the permeability coefficients (K_p) were assessed:

$$K_p = \frac{J_{ss}}{C_D} \quad (5)$$

where: J_{ss} is the steady-state period flux, and C_D is the compound concentration in the donor phase.

The skin partition coefficient (K_m) and diffusion coefficient (D) were calculated based on the following equations:

$$K_m = K_p \times \frac{h}{D} \quad (6)$$

$$D = \frac{h^2}{6L_T} \quad (7)$$

Where: h is the skin thickness, mm.

In this study, chromatographic measurements were performed on a Knauer (Berlin, Germany) HPLC system equipped with unit a model 2600 UV detector, a Smartline model 1050 pump, and a Smartline model 3950 autosampler with ClarityChrom 2009 software. The Hypersil ODS (C18) column, 125×4 mm, particle size 5 μm was used for analysis. As the mobile phase, 0.02 M potassium dihydrogen phosphate-acetonitrile (60/40 v/v) (for analysis of ibuprofen, ketoprofen, and naproxen) and 1% acetic acid, acetonitrile, and MeOH (64/30/6 v/v/v) (for analysis of salicylic acid) were used. The flow rate was 1 mL/min, the column temperature was 25°C, the injection volume was 20 μL , and signals were detected at 210 nm.

The research was carried out at the Department of Cosmetic and Pharmaceutical Chemistry, Pomeranian Medical University in Szczecin, in the research group of Anna Nowak, BEng, PhD, DSc.

4.2. Skin Accumulation Studies

The accumulation studies were performed 24 hours after the skin permeability study. For this purpose, the donor chamber was disconnected from the Franz diffusion cell. Each skin sample was taken out and carefully rinsed in PBS solution (pH=7.4). Then, skin samples were dried at room temperature and weighed. The diffusion area was cut out, and minced samples were placed in 2 mL of methanol and incubated for 24 hours at 4°C. The skin samples were then homogenised using an IKA®T18 computerised ULTRA TURRAX

homogenizer (Staufen im Breisgau, Germany) and centrifuged. The concentration of an active substance in the obtained supernatant was determined using the HPLC method, analogous to the skin permeability experiments. Accumulation of API in the skin was measured in the mass of studied active substance per mass of skin ($\mu\text{g}_{\text{API}} \cdot \text{g}^{-1}$) and was determined by dividing the amount of the substance still present in the skin by a mass of skin sample.

The research was carried out at the Department of Cosmetic and Pharmaceutical Chemistry, Pomeranian Medical University in Szczecin, in the research group of Anna Nowak, BEng, PhD, DSc.

4.3. The antioxidant activity

The DPPH (2,2-diphenyl-1-picrylhydrazyl) radical scavenging inhibition technique was chosen for evaluating the antioxidant activity of the selected L-amino acid alkyl ester salts. As a radical solution, 0.3 mM DPPH produced in 96% ethanol was employed. Prior to the investigation, the absorbance of the DPPH solution was measured at 517 nm and corrected using 96% ethanol to a value equal to 1.00 ± 0.02 . For the primary test, 2.5 mL of the radical solution was combined with 0.1 mL of the 70% ethanol solution that had been tested and contained 1.0% active ingredient. The ethanolic solution was used as a negative control, while the solution containing the tested compound was used as a positive control. The mixture was incubated for 10 minutes at room temperature in the dark. Three independent tests were conducted, and the obtained results were given as mean values. The following formula (eq. 8) was used to calculate the percentage inhibition, expressing the scavenging of the DPPH radical:

$$\%DPPH_{scavenging\ effect} = 1 - \frac{A_s}{A_c} \cdot 100\% \quad (8)$$

where: A_s and A_c are the absorbance of the tested and control samples, respectively.

The research was carried out at the Department of Cosmetic and Pharmaceutical Chemistry, Pomeranian Medical University in Szczecin, in the research group of Anna Nowak, BEng, PhD, DSc.

4.4. Biodegradation Studies

The experiment's active sludge originates from the "Pomorzany" sewage treatment facility in Szczecin, Poland. A microbiological test (Schulke Mikrocount Duo, Norderstedt, Germany) was used to identify the total number of bacteria in order to determine the concentration of active sludge suspension. The amount of organic carbon that made up

the examined compound's concentration was 40 mg/L. The reference substance, sodium dodecyl sulphate (SDS), had a starting concentration of SDS=84.12 mg/L. The 28-day experiment was conducted. Total organic carbon analysis (TOC-LCSH/CSN, Shimadzu Corporation) was used to calculate the volume of carbon dioxide that was created.

The research was carried out at the Department of Organic Chemical Technology and Polymer Materials, West Pomeranian University of Technology in Szczecin by Edyta Kucharska, BEng, PhD.

4.5. Antimicrobial Activity Susceptibility Test

Antibacterial activity was evaluated using the EUCAST diffusion disc method. The zone of inhibition was measured against *Escherichia coli* (ACCT 29425), *Micrococcus luteus* (ATCC 7468) and *Staphylococcus epidermidis* (ACCT 12228). Liquid nutrients and agar medium for bacterial growth were prepared according to the manufacturer's recommendations. Sterilisation was performed at 120 °C for 15 min. Enriched broth was used to grow *E. coli*, lysogenic broth was used to grow *M. luteus* and brain heart broth was used to grow *S. epidermidis* bacteria. The agar medium used was Nutrient LAB-AGAR™ for the isolation of *M. luteus* and Brain Heart Infusion LAB-AGAR™ for the isolation of *S. epidermidis*. The TTC lactose agar medium with Tergitol®7 was used to determine the number of *E. coli* bacterial cells, as a selective factor in the form of Tergitol-7 medium inhibits the growth of gram-positive bacteria and limits the growth of *Proteus spp.* In addition, the so-called indicator system in the form of bromothymol blue and TTC allows easier differentiation of *E. coli*.

The prepared agar medium was poured into sterile plastic Petri plates and allowed to be set. The agar was then allowed to solidify and transferred to an incubator set at 37°C for 48 hours to allow the water to evaporate from the surface of the agar. Filter paper discs with a diameter of 5 mm were used to test antibacterial resistance. They were saturated with the appropriate solution of each compound and allowed to dry for 10 minutes in a laminar airflow cabinet. The discs were then placed manually with sterile forceps on the indicated agar plates, previously inoculated evenly throughout the Petri plate with a specific bacterial culture ($1.5 \cdot 10^6$ CFU/mL, CFU colony forming units). Compound concentrations studied were 1000, 800, 600, 400, 200, 100, 50, and 25 mg/mL in absolute ethanol. The plates were incubated for 24 hours at a temperature of 37°C. The inhibition zone, defined as the circular area around the disc in which bacterial colonies do not grow, was evaluated by measuring the diameter of the clear zone (in mm) to an accuracy of 0.1 mm. Each prepared sample was

measured in triplicate. The results obtained were expressed as the mean of the inhibition zones with standard deviation.

4.6. Statistical Analysis

The Statistica 13 PL programme (StatSoft, Kraków, Poland) was used to do the statistical calculations. When completing a one-way analysis of variance (ANOVA), the standard deviation (SD) was employed to represent the final data as the mean. Tuckey's test ($\alpha < 0.05$) was used to determine the significance of differences between individual groups in the cases of the results from the skin permeation, accumulation, and antioxidant activity investigations.

References

- [1] Web Annex A WHO Model List of Essential Medicines - 23rd list, 2023, in: The Selection and Use of Essential Medicines 2023: Executive Summary of the Report of the 24th WHO Expert Committee on the Selection and Use of Essential Medicines, 24 – 28 April 2023. Geneva: World Health Organization; 2023 (WHO/MHP/HPS/EML/2023.02)., 2023.
- [2] K. Jahnavi, P. Pavani Reddy, B. Vasudha, B. Narender, Non-steroidal anti-inflammatory drugs: an overview, *J. Drug Delivery Ther.* 9 (2019) 442–448.
- [3] R. Sohail, M. Mathew, K.K. Patel, S.A. Reddy, Z. Haider, M. Naria, A. Habib, Z.U. Abdin, W. Razzaq Chaudhry, A. Akbar, Effects of Non-steroidal Anti-inflammatory Drugs (NSAIDs) and Gastroprotective NSAIDs on the Gastrointestinal Tract: A Narrative Review, *Cureus* (2023).
- [4] S. Bindu, S. Mazumder, U. Bandyopadhyay, Non-steroidal anti-inflammatory drugs (NSAIDs) and organ damage: A current perspective, *Biochemical Pharmacology* 180 (2020) 114147.
- [5] A. Ozleyen, Y.B. Yilmaz, S. Donmez, H.N. Atalay, G. Antika, T.B. Tumer, Looking at NSAIDs from a historical perspective and their current status in drug repurposing for cancer treatment and prevention, *J Cancer Res Clin Oncol* 149 (2023) 2095–2113.
- [6] M. Von Raumer, R. Hilfiker, Solid State and Polymorphism of the Drug Substance in the Context of Quality by Design and ICH Guidelines Q8–Q12, in: R. Hilfiker, M.V. Raumer (Eds.), *Polymorphism in the Pharmaceutical Industry*, 1st ed., Wiley, 2018: pp. 1–30.
- [7] P.H. Stahl, B. Sutter, A. Grandeur, M. Mutz, Alternative Solid Forms: Salts, in: R. Hilfiker, M.V. Raumer (Eds.), *Polymorphism in the Pharmaceutical Industry*, 1st ed., Wiley, 2018: pp. 31–59.
- [8] A.L.C.S. Nascimento, R.P. Fernandes, M.D. Charpentier, J.H. Ter Horst, F.J. Caires, M. Chorilli, Co-crystals of non-steroidal anti-inflammatory drugs (NSAIDs): Insight toward formation, methods, and drug enhancement, *Particuology* 58 (2021) 227–241.
- [9] B.M. Couillaud, P. Espeau, N. Mignet, Y. Corvis, State of the Art of Pharmaceutical Solid Forms: from Crystal Property Issues to Nanocrystals Formulation, *ChemMedChem* 14 (2019) 8–23.
- [10] G.L. Amidon, H. Lennernäs, V.P. Shah, J.R. Crison, A theoretical basis for a biopharmaceutic drug classification: the correlation of in vitro drug product dissolution and in vivo bioavailability, *Pharmaceutical Research* 12 (1995) 413–420.
- [11] W. Badri, K. Miladi, Q.A. Nazari, H. Greige-Gerges, H. Fessi, A. Elaissari, Encapsulation of NSAIDs for inflammation management: Overview, progress, challenges and prospects, *International Journal of Pharmaceutics* 515 (2016) 757–773.
- [12] Y. Zhou, J. Lin, Y. Bian, C. Ren, N. Xiao-li, C. Yang, X. Xiao-xue, X. Feng, Non-steroidal anti-inflammatory drugs (NSAIDs) in the environment: Updates on pretreatment and determination methods, *Ecotoxicology and Environmental Safety* 267 (2023) 115624.
- [13] S. Wongrakpanich, A. Wongrakpanich, K. Melhado, J. Rangaswami, A Comprehensive Review of Non-Steroidal Anti-Inflammatory Drug Use in The Elderly, *A&D* 9 (2018) 143.
- [14] E. Ricciotti, G.A. FitzGerald, Prostaglandins and Inflammation, *ATVB* 31 (2011) 986–1000.
- [15] M. Burian, NSAIDs, Mode of Action, in: R.F. Schmidt, W.D. Willis (Eds.), *Encyclopedia of Pain*, Springer Berlin Heidelberg, Berlin, Heidelberg, 2007: pp. 1473–1476.
- [16] H. Ribeiro, I. Rodrigues, L. Napoleão, L. Lira, D. Marques, M. Veríssimo, J.P. Andrade, M. Dourado, Non-steroidal anti-inflammatory drugs (NSAIDs), pain and aging: Adjusting prescription to patient features, *Biomedicine & Pharmacotherapy* 150 (2022) 112958.

- [17] M.F. Singgih, Huldani, H. Achmad, B.I. Sukmana, A.B. Carmelita, A.P. Putra, S. Ramadhany, A.P. Putri, A Review of Nonsteroidal Anti-Inflammatory Drugs (NSAIDs) Medications in Dentistry: Uses and Side Effects, *Systematic Reviews in Pharmacy* 11 (2020) 293–298.
- [18] T.J. Atkinson, J. Fudin, Nonsteroidal Antiinflammatory Drugs for Acute and Chronic Pain, *Physical Medicine and Rehabilitation Clinics of North America* 31 (2020) 219–231.
- [19] U. Garg, Y. Azim, Challenges and opportunities of pharmaceutical cocrystals: a focused review on non-steroidal anti-inflammatory drugs, *RSC Med. Chem.* 12 (2021) 705–721.
- [20] R. Hilfiker, F. Blatter, M. Szelagiewicz, M. Von Raumer, Approaches to Solid-Form Screening, in: R. Hilfiker, M.V. Raumer (Eds.), *Polymorphism in the Pharmaceutical Industry*, 1st ed., Wiley, 2018: pp. 241–259.
- [21] M. Stielow, A. Witczyńska, N. Kubryń, Ł. Fijałkowski, J. Nowaczyk, A. Nowaczyk, The Bioavailability of Drugs—The Current State of Knowledge, *Molecules* 28 (2023) 8038.
- [22] A. Schittny, J. Huwyler, M. Puchkov, Mechanisms of increased bioavailability through amorphous solid dispersions: a review, *Drug Delivery* 27 (2020) 110–127.
- [23] S.N. Somnache, A.M. Godbole, P.S. Gajare, S. Kashyap, Significance of Pharmaceutical Excipients on Solid Dosage form Development: A Brief Review, *Asian Jour. Pharmac. Res.* 6
- [24] S.M. Carl, D.J. Lindley, G.T. Knipp, K.R. Morris, E. Oliver, G.W. Becker, R.D. Arnold, Biotechnology-Derived Drug Product Development, in: S.C. Gad (Ed.), *Pharmaceutical Manufacturing Handbook*, 1st ed., Wiley, 2008: pp. 1–32.
- [25] K.R. Chu, E. Lee, S.H. Jeong, E.-S. Park, Effect of particle size on the dissolution behaviors of poorly water-soluble drugs, *Arch. Pharm. Res.* 35 (2012) 1187–1195.
- [26] Z. Vinarov, B. Abrahamsson, P. Artursson, H. Batchelor, P. Berben, A. Bernkop-Schnürch, J. Butler, J. Ceulemans, N. Davies, D. Dupont, G.E. Flaten, N. Fotaki, B.T. Griffin, V. Jannin, J. Keemink, F. Kesisoglou, M. Koziol, M. Kuentz, A. Mackie, A.J. Meléndez-Martínez, M. McAllister, A. Müllertz, C.M. O’Driscoll, N. Parrott, J. Paszkowska, P. Pavek, C.J.H. Porter, C. Reppas, C. Stillhart, K. Sugano, E. Toader, K. Valentová, M. Vertzoni, S.N. De Wildt, C.G. Wilson, P. Augustijns, Current challenges and future perspectives in oral absorption research: An opinion of the UNGAP network, *Advanced Drug Delivery Reviews* 171 (2021) 289–331.
- [27] T. Zelesky, S.W. Baertschi, C. Foti, L.R. Allain, S. Hostyn, J.R. Franca, Y. Li, S. Marden, S. Mohan, M. Ultramari, Z. Huang, N. Adams, J.M. Campbell, P.J. Jansen, D. Kotoni, C. Laue, Pharmaceutical Forced Degradation (Stress Testing) Endpoints: A Scientific Rationale and Industry Perspective, *Journal of Pharmaceutical Sciences* 112 (2023) 2948–2964.
- [28] A. Gabrič, Ž. Hodnik, S. Pajk, Oxidation of Drugs during Drug Product Development: Problems and Solutions, *Pharmaceutics* 14 (2022) 325.
- [29] P. Pandi, R. Bulusu, N. Kommineni, W. Khan, M. Singh, Amorphous solid dispersions: An update for preparation, characterization, mechanism on bioavailability, stability, regulatory considerations and marketed products, *International Journal of Pharmaceutics* 586 (2020) 119560.
- [30] L.H. Ng, J.K.U. Ling, K. Hadinoto, Formulation Strategies to Improve the Stability and Handling of Oral Solid Dosage Forms of Highly Hygroscopic Pharmaceuticals and Nutraceuticals, *Pharmaceutics* 14 (2022) 2015.
- [31] N. Jawahar, A. Arigò, Effect of Hygroscopicity on pharmaceutical ingredients, methods to determine and overcome: An Overview, in: 2019.
- [32] A. Newman, R. Wenslow, Solid form changes during drug development: good, bad, and ugly case studies, *AAPS Open* 2 (2016) 2.
- [33] A. Domokos, B. Nagy, B. Szilágyi, G. Marosi, Z.K. Nagy, Integrated Continuous Pharmaceutical Technologies—A Review, *Org. Process Res. Dev.* 25 (2021) 721–739.

- [34] J. Wahlich, Review: Continuous Manufacturing of Small Molecule Solid Oral Dosage Forms, *Pharmaceutics* 13 (2021) 1311.
- [35] R. Diodone, P.C. Hidber, M. Kammerer, R. Meier, U. Schwitter, J. Thun, Industry Case Studies, in: R. Hilfiker, M.V. Raumer (Eds.), *Polymorphism in the Pharmaceutical Industry*, 1st ed., Wiley, 2018: pp. 447–468.
- [36] F.M. Cañellas, V. Verma, J. Kujawski, R. Geertman, L. Tajber, L. Padrela, Controlling the Polymorphism of Indomethacin with Poloxamer 407 in a Gas Antisolvent Crystallization Process, *ACS Omega* 7 (2022) 43945–43957.
- [37] A.R. Sheth, S. Bates, F.X. Muller, D.J.W. Grant, Polymorphism in Piroxicam, *Crystal Growth & Design* 4 (2004) 1091–1098.
- [38] V. Tantishaiyakul, P. Permkam, K. Suknuntha, Use of Drifts and PLS for the Determination of Polymorphs of Piroxicam Alone and in Combination with Pharmaceutical Excipients: A Technical Note, *AAPS PharmSciTech* 9 (2008) 95–99.
- [39] R. Censi, V. Martena, E. Hoti, L. Malaj, P. Di Martino, Sodium ibuprofen dihydrate and anhydrous: Study of the dehydration and hydration mechanisms, *J Therm Anal Calorim* 111 (2013) 2009–2018.
- [40] L. Malaj, R. Censi, Z. Gashi, P. Di Martino, Compression behaviour of anhydrous and hydrate forms of sodium naproxen, *International Journal of Pharmaceutics* 390 (2010) 142–149.
- [41] F. Tian, H. Qu, A. Zimmermann, T. Munk, A.C. Jørgensen, J. Rantanen, Factors affecting crystallization of hydrates, *Journal of Pharmacy and Pharmacology* 62 (2010) 1534–1546.
- [42] M. Zhang, Y. Huang, D. Hao, Y. Ji, D. Ouyang, Solvation structure and molecular interactions of ibuprofen with ethanol and water: A theoretical study, *Fluid Phase Equilibria* 510 (2020) 112454.
- [43] G. Perlovich, A. Bauer-Brandl, Solvation of Drugs as a Key for Understanding Partitioning and Passive Transport Exemplified by NSAIDs, *CDD* 1 (2004) 213–226.
- [44] A.M. Healy, Z.A. Worku, D. Kumar, A.M. Madi, Pharmaceutical solvates, hydrates and amorphous forms: A special emphasis on cocrystals, *Advanced Drug Delivery Reviews* 117 (2017) 25–46.
- [45] S.S. Buddhadev, K.C. Garala, Pharmaceutical Cocrystals—A Review, in: *The 2nd International Online Conference on Crystals*, MDPI, 2021: p. 14.
- [46] I. Nugrahani, R.D. Parwati, Challenges and Progress in Nonsteroidal Anti-Inflammatory Drugs Co-Crystal Development, *Molecules* 26 (2021) 4185.
- [47] R. Hilfiker, M. von Raumer, *Polymorphism in the pharmaceutical industry: solid form and drug development*, 2nd ed, Wiley-VCH Verlag, Weinheim, 2019.
- [48] N. Abdu, A. Mosazghi, S. Teweldemedhin, L. Asfaha, M. Teshale, M. Kibreab, I.S. Anand, E.H. Tesfamariam, M. Russom, Non-Steroidal Anti-Inflammatory Drugs (NSAIDs): Usage and co-prescription with other potentially interacting drugs in elderly: A cross-sectional study, *PLoS ONE* 15 (2020) e0238868.
- [49] S. Drożdżal, K. Lechowicz, B. Szostak, J. Rosik, K. Kotfis, A. Machoy-Mokrzyńska, M. Białecka, K. Ciechanowski, B. Gawrońska-Szkłarz, Kidney damage from nonsteroidal anti-inflammatory drugs—Myth or truth? Review of selected literature, *Pharmacology Res & Perspec* 9 (2021) e00817.
- [50] N.K. Panchal, E. Prince Sabina, Non-steroidal anti-inflammatory drugs (NSAIDs): A current insight into its molecular mechanism eliciting organ toxicities, *Food and Chemical Toxicology* 172 (2023) 113598.
- [51] N.M. Davies, J.K. Reynolds, M.R. Undeberg, B.J. Gates, Y. Ohgami, K.R. Vega-Villa, Minimizing risks of NSAIDs: cardiovascular, gastrointestinal and renal, *Expert Review of Neurotherapeutics* 6 (2006) 1643–1655.
- [52] C.-G. Guo, W.K. Leung, Potential Strategies in the Prevention of Nonsteroidal Anti-inflammatory Drugs-Associated Adverse Effects in the Lower Gastrointestinal Tract, *Gut and Liver* 14 (2020) 179–189.

- [53] D. Gupta, D. Bhatia, V. Dave, V. Sutariya, S. Varghese Gupta, Salts of Therapeutic Agents: Chemical, Physicochemical, and Biological Considerations, *Molecules* 23 (2018) 1719.
- [54] K. Shah, J.K. Gupta, N.S. Chauhan, N. Upmanyu, S.K. Shrivastava, P. Mishra, Prodrugs of NSAIDs: A Review, *TOMCJ* 11 (2017) 146–195.
- [55] C. Pereira-Leite, C. Nunes, S.K. Jamal, I.M. Cuccovia, S. Reis, Nonsteroidal Anti-Inflammatory Therapy: A Journey Toward Safety, *Medicinal Research Reviews* 37 (2017) 802–859.
- [56] Y.J. Lim, J.S. Lee, Y.S. Ku, K. Hahm, Rescue strategies against non-steroidal anti-inflammatory drug-induced gastroduodenal damage, *J of Gastro and Hepatol* 24 (2009) 1169–1178.
- [57] J.L. Wallace, D. Vaughan, M. Dicay, W.K. MacNaughton, G. De Nucci, Hydrogen Sulfide-Releasing Therapeutics: Translation to the Clinic, *Antioxidants & Redox Signaling* 28 (2018) 1533–1540.
- [58] B. Gemici, W. Elsheikh, K.B. Feitosa, S.K.P. Costa, M.N. Muscara, J.L. Wallace, H₂S-releasing drugs: Anti-inflammatory, cytoprotective and chemopreventative potential, *Nitric Oxide* 46 (2015) 25–31.
- [59] S. Ramos-Inza, A.C. Ruberte, C. Sanmartín, A.K. Sharma, D. Plano, NSAIDs: Old Acquaintance in the Pipeline for Cancer Treatment and Prevention—Structural Modulation, Mechanisms of Action, and Bright Future, *J. Med. Chem.* 64 (2021) 16380–16421.
- [60] T. Jóhannesson, [Aspirin. Acetylsalicylic acid and aspirinlike drugs. A review.], *Laeknabladid* 86 (2000) 755–768.
- [61] P. Halen, P. Murumkar, R. Giridhar, M. Yadav, Prodrug Designing of NSAIDs, *MRMC* 9 (2009) 124–139.
- [62] M. Sahoo, N. Agrawal, M. Jaiswal, S.K. Lanjhiyana, Exploring the Potential of Ester Prodrugs of NSAIDs: A Comprehensive Overview, in: Prof.R.S.G. Mahmoud (Ed.), *Advanced Concepts in Pharmaceutical Research Vol. 3*, B P International, 2023: pp. 151–159.
- [63] S.K. Mandal, K. Pati, A. Bose, S. Dey, A. De, S. Bose, A. De, Various Ester Prodrugs of NSAIDs with Low Ulcerogenic Activity, *Int. J. Pharm. Sci. Rev. Res* 54 (2019) 45–49.
- [64] J.P. Peesa, P.R. Yalavarthi, A. Rasheed, V.B.R. Mandava, A perspective review on role of novel NSAID prodrugs in the management of acute inflammation, *Journal of Acute Disease* 5 (2016) 364–381.
- [65] J. Patil, Enhancing Gastrointestinal Tolerance -The Promise of Mutual Prodrugs in NSAID Therapy: A Review., *International Journal of All Research Education & Scientific Methods* 12 (2024) 1227–1241.
- [66] S. Hammoodi, S. Ismael, Y. Mustafa, Mutual prodrugs for colon targeting: A review, *Eurasian Chem. Commun.* (2022).
- [67] S.S. Bharate, Recent developments in pharmaceutical salts: FDA approvals from 2015 to 2019, *Drug Discovery Today* 26 (2021) 384–398.
- [68] C. Saal, A. Becker, Pharmaceutical salts: A summary on doses of salt formers from the Orange Book, *European Journal of Pharmaceutical Sciences* 49 (2013) 614–623.
- [69] S.S. Bharate, Carboxylic Acid Counterions in FDA-Approved Pharmaceutical Salts, *Pharm Res* 38 (2021) 1307–1326.
- [70] S. Bashyal, IBUPROFEN AND ITS DIFFERENT ANALYTICAL AND MANUFACTURING METHODS: A REVIEW, *Asian J Pharm Clin Res* 11 (2018) 25.
- [71] R. Altman, B. Bosch, K. Brune, P. Patrignani, C. Young, Advances in NSAID Development: Evolution of Diclofenac Products Using Pharmaceutical Technology, *Drugs* 75 (2015) 859–877.
- [72] A. Tilborg, B. Norberg, J. Wouters, Pharmaceutical salts and cocrystals involving amino acids: A brief structural overview of the state-of-art, *European Journal of Medicinal Chemistry* 74 (2014) 411–426.

- [73] A.R. Moore, S. Derry, S. Straube, J. Ireson-Paine, P.J. Wiffen, Faster, higher, stronger? Evidence for formulation and efficacy for ibuprofen in acute pain, *Pain* 155 (2014) 14–21.
- [74] J.M. Ferrero-Cafiero, I. Gich, M. Puntos, J. Martínez, M.R. Ballester, J. Coimbra, Y. Mathison, M. Tarré, X. Font, R.M. Antonijoan, Ibuprofen lysinate, quicker and less variable: relative bioavailability compared to ibuprofen base in a pediatric suspension dosage form, *CP* 53 (2015) 972–979.
- [75] A. Cimini, L. Brandolini, R. Gentile, L. Cristiano, P. Menghini, A. Fidoamore, A. Antonosante, E. Benedetti, A. Giordano, M. Allegratti, Gastroprotective Effects of L-Lysine Salification of Ketoprofen in Ethanol-Injured Gastric Mucosa, *Journal Cellular Physiology* 230 (2015) 813–820.
- [76] P. Cerreia Vioglio, M.R. Chierotti, R. Gobetto, Pharmaceutical aspects of salt and cocrystal forms of APIs and characterization challenges, *Advanced Drug Delivery Reviews* 117 (2017) 86–110.
- [77] M.S. Hossain Mithu, S. Economidou, V. Trivedi, S. Bhatt, D. Douroumis, *Advanced Methodologies for Pharmaceutical Salt Synthesis, Crystal Growth & Design* 21 (2021) 1358–1374.
- [78] M.S. Roberts, H.S. Cheruvu, S.E. Mangion, A. Alinaghi, H.A.E. Benson, Y. Mohammed, A. Holmes, J. van der Hoek, M. Pastore, J.E. Grice, Topical drug delivery: History, percutaneous absorption, and product development, *Advanced Drug Delivery Reviews* 177 (2021) 113929.
- [79] H.A.E. Benson, J.E. Grice, Y. Mohammed, S. Namjoshi, M.S. Roberts, Topical and Transdermal Drug Delivery: From Simple Potions to Smart Technologies, *CDD* 16 (2019) 444–460.
- [80] H.A.E. Benson, Skin Structure, Function, and Permeation, in: H.A.E. Benson, A.C. Watkinson (Eds.), *Topical and Transdermal Drug Delivery*, John Wiley & Sons, Inc., Hoboken, NJ, USA, 2012: pp. 1–22.
- [81] N.S. Serkhacheva, A.A. Gainanova, G.M. Kuz'micheva, V.V. Podbelskiy, N.V. Sadovskaya, A.M. Zybinskiy, E.N. Domoroshchina, A.V. Dorokhov, V.V. Chernyshev, N.I. Prokopov, A.Yu. Gerval'd, Composites Based on Polystyrene Microspheres with Nano-Scaled Titanium Dioxide, *International Journal of Polymer Analysis and Characterization* 20 (2015) 743–753.
- [82] W.Y. Jeong, M. Kwon, H.E. Choi, K.S. Kim, Recent advances in transdermal drug delivery systems: a review, *Biomater Res* 25 (2021) 24.
- [83] D. Bird, N.M. Ravindra, Transdermal drug delivery and patches—An overview, *Med Devices & Sens* 3 (2020) e10069.
- [84] A. Kováčik, M. Kopečná, K. Vávrová, Permeation enhancers in transdermal drug delivery: benefits and limitations, *Expert Opinion on Drug Delivery* 17 (2020) 145–155.
- [85] M.R. Prausnitz, R. Langer, Transdermal drug delivery, *Nat Biotechnol* 26 (2008) 1261–1268.
- [86] R. Van Rensburg, H. Reuter, An overview of analgesics: NSAIDs, paracetamol, and topical analgesics Part 1, *South African Family Practice* 61 (2019) S4–S10.
- [87] C. Bhat, H. Rosenberg, D. James, Topical nonsteroidal anti-inflammatory drugs, *CMAJ* 195 (2023) E1231–E1231.
- [88] S. Stanos, Topical Analgesics, *Physical Medicine and Rehabilitation Clinics of North America* 31 (2020) 233–244.
- [89] R.L. Barkin, Topical Nonsteroidal Anti-Inflammatory Drugs: The Importance of Drug, Delivery, and Therapeutic Outcome, *American Journal of Therapeutics* 22 (2015) 388–407.
- [90] S. Derry, P.R.L. Matthews, P.J. Wiffen, R.A. Moore, Salicylate-containing rubefacients for acute and chronic musculoskeletal pain in adults, *Cochrane Database of Systematic Reviews* 2019 (2014).

- [91] A. Vitória Pupo Silvestrini, J.S.R. Viegas, M.T. Luiz, L.D.Q.C. Silva, F.G. Praça, M.V.L.B. Bentley, Advanced Topical and Transdermal Drug Delivery (TTDS) Used in Skin Diseases and Lesions of the Aging, in: Topical and Transdermal Drug Delivery Systems, 1st ed., Apple Academic Press, New York, 2022: pp. 79–127.
- [92] D. Choudhury, K.N. Dutta, R. Kalita, A Review on Transdermal Patches Used as an Anti-Inflammatory Agent, *Asian J Pharm Clin Res* (2021) 21–26.
- [93] D.G. Wolff, C. Christophersen, S.M. Brown, M.K. Mulcahey, Topical nonsteroidal anti-inflammatory drugs in the treatment of knee osteoarthritis: a systematic review and meta-analysis, *The Physician and Sportsmedicine* 49 (2021) 381–391.
- [94] T. Benbow, J. Campbell, Microemulsions as transdermal drug delivery systems for nonsteroidal anti-inflammatory drugs (NSAIDs): a literature review, *Drug Development and Industrial Pharmacy* 45 (2019) 1849–1855.
- [95] R.M. Haley, H.A. von Recum, Localized and targeted delivery of NSAIDs for treatment of inflammation: A review, *Exp Biol Med* (Maywood) 244 (2019) 433–444.
- [96] F. Iliopoulos, B.C. Sil, C.L. Evans, The role of excipients in promoting topical and transdermal delivery: Current limitations and future perspectives, *Front. Drug. Deliv.* 2 (2022) 1049848.
- [97] J. Maloney, S. Pew, C. Wie, R. Gupta, J. Freeman, N. Strand, Comprehensive Review of Topical Analgesics for Chronic Pain, *Curr Pain Headache Rep* 25 (2021) 7.
- [98] G. Pennick, A. Robinson-Miller, I. Cush, Topical NSAIDs for acute local pain relief: *in vitro* characterization of drug delivery profiles into and through human skin, *Drug Development and Industrial Pharmacy* 47 (2021) 908–918.
- [99] J. Pradal, C. Vallet, G. Frappin, F. Bariguan, M.S. Lombardi, Importance of the formulation in the skin delivery of topical diclofenac: not all topical diclofenac formulations are the same, *JPR Volume* 12 (2019) 1149–1154.
- [100] J.S. Wilkes, A short history of ionic liquids—from molten salts to neoteric solvents, *Green Chem.* 4 (2002) 73–80.
- [101] J.L. Shamshina, R.D. Rogers, Ionic Liquids: New Forms of Active Pharmaceutical Ingredients with Unique, Tunable Properties, *Chem. Rev.* 123 (2023) 11894–11953.
- [102] S. Magina, A. Barros-Timmons, S.P.M. Ventura, D.V. Evtuguin, Evaluating the hazardous impact of ionic liquids – Challenges and opportunities, *Journal of Hazardous Materials* 412 (2021) 125215.
- [103] S. Zhang, ed., *Encyclopedia of Ionic Liquids*, Springer Nature Singapore, Singapore, 2022.
- [104] S.K. Singh, A.W. Savoy, Ionic liquids synthesis and applications: An overview, *Journal of Molecular Liquids* 297 (2020) 112038.
- [105] W.L. Hough, M. Smiglak, H. Rodríguez, R.P. Swatloski, S.K. Spear, D.T. Daly, J. Pernak, J.E. Grisel, R.D. Carliss, M.D. Soutullo, J.H. Davis, Jr., R.D. Rogers, The third evolution of ionic liquids: active pharmaceutical ingredients, *New J. Chem.* 31 (2007) 1429.
- [106] T.S. De Almeida, R. Caparica, A. Júlio, C.P. Reis, An Overview on Ionic Liquids: A New Frontier for Nanopharmaceuticals, in: V.K. Yata, S. Ranjan, N. Dasgupta, E. Lichtfouse (Eds.), *Nanopharmaceuticals: Principles and Applications Vol. 1*, Springer International Publishing, Cham, 2021: pp. 181–204.
- [107] D.R. MacFarlane, A.L. Chong, M. Forsyth, M. Kar, R. Vijayaraghavan, A. Somers, J.M. Pringle, New dimensions in salt–solvent mixtures: a 4th evolution of ionic liquids, *Faraday Discuss.* 206 (2018) 9–28.
- [108] S. Brahma, R.L. Gardas, History and Development of Ionic Liquids, in: P. Singh, S. Rajkhowa, A. Sen, J. Sarma (Eds.), *Handbook of Ionic Liquids*, 1st ed., Wiley, 2024: pp. 1–28.
- [109] A.A.M. Elgharbawy, M. Moniruzzaman, M. Goto, Recent advances of enzymatic reactions in ionic liquids: Part II, *Biochemical Engineering Journal* 154 (2020) 107426.

- [110] C. Liu, B. Chen, W. Shi, W. Huang, H. Qian, Ionic Liquids for Enhanced Drug Delivery: Recent Progress and Prevailing Challenges, *Mol. Pharmaceutics* 19 (2022) 1033–1046.
- [111] N.R. Jadhav, S.P. Bhosale, S.S. Bhosale, S.D. Mali, P.B. Toraskar, T.S. Kadam, Ionic liquids: Formulation avenues, drug delivery and therapeutic updates, *Journal of Drug Delivery Science and Technology* 65 (2021) 102694.
- [112] S.N. Pedro, C.S. R. Freire, A.J.D. Silvestre, M.G. Freire, The Role of Ionic Liquids in the Pharmaceutical Field: An Overview of Relevant Applications, *IJMS* 21 (2020) 8298.
- [113] M.N. Uddin, D. Basak, R. Hopefl, B. Minofar, Potential Application of Ionic Liquids in Pharmaceutical Dosage Forms for Small Molecule Drug and Vaccine Delivery System, *J Pharm Pharm Sci* 23 (2020) 158–176.
- [114] R. Md Moshikur, Md.R. Chowdhury, M. Moniruzzaman, M. Goto, Biocompatible ionic liquids and their applications in pharmaceutics, *Green Chem.* 22 (2020) 8116–8139.
- [115] H. Choudhary, K. Li, R.D. Rogers, Active Pharmaceutical Ingredient Ionic Liquid: A New Platform for the Pharmaceutical Industry, in: S. Zhang (Ed.), *Encyclopedia of Ionic Liquids*, Springer Singapore, Singapore, 2019: pp. 1–14.
- [116] A.M. Curreri, S. Mitragotri, E.E.L. Tanner, Recent Advances in Ionic Liquids in Biomedicine, *Advanced Science* 8 (2021) 2004819.
- [117] K.S. Egorova, V.P. Ananikov, Biological Activity of Ionic Liquids Involving Ionic and Covalent Binding: Tunable Drug Development Platform, in: S. Zhang (Ed.), *Encyclopedia of Ionic Liquids*, Springer Singapore, Singapore, 2019: pp. 1–8.
- [118] M. Handa, W.H. Almalki, R. Shukla, O. Afzal, A.S.A. Altamimi, S. Beg, M. Rahman, Active pharmaceutical ingredients (APIs) in ionic liquids: An effective approach for API physiochemical parameter optimization, *Drug Discovery Today* (2022) S135964462200263X.
- [119] Y. Miwa, H. Hamamoto, T. Ishida, Lidocaine self-sacrificially improves the skin permeation of the acidic and poorly water-soluble drug etodolac via its transformation into an ionic liquid, *European Journal of Pharmaceutics and Biopharmaceutics* 102 (2016) 92–100.
- [120] O.A. Cojocaru, K. Bica, G. Gurau, A. Narita, P.D. McCrary, J.L. Shamshina, P.S. Barber, R.D. Rogers, Prodrug ionic liquids: functionalizing neutral active pharmaceutical ingredients to take advantage of the ionic liquid form, *Med. Chem. Commun.* 4 (2013) 559.
- [121] L. Jiang, Y. Sun, A. Lu, X. Wang, Y. Shi, Ionic Liquids: Promising Approach for Oral Drug Delivery, *Pharm Res* 39 (2022) 2353–2365.
- [122] P.C.A.G. Pinto, D.M.G.P. Ribeiro, A.M.O. Azevedo, V. Dela Justina, E. Cunha, K. Bica, M. Vasiliou, S. Reis, M.L.M.F.S. Saraiva, Active pharmaceutical ingredients based on salicylate ionic liquids: insights into the evaluation of pharmaceutical profiles, *New J. Chem.* 37 (2013) 4095.
- [123] K.S. Egorova, M.M. Seitkalieva, A.V. Posvyatenko, V.N. Khrustalev, V.P. Ananikov, Cytotoxic Activity of Salicylic Acid-Containing Drug Models with Ionic and Covalent Binding, *ACS Med. Chem. Lett.* 6 (2015) 1099–1104.
- [124] P.M. Dean, J. Turanjanin, M. Yoshizawa-Fujita, D.R. MacFarlane, J.L. Scott, Exploring an Anti-Crystal Engineering Approach to the Preparation of Pharmaceutically Active Ionic Liquids, *Crystal Growth & Design* 9 (2009) 1137–1145.
- [125] K. Bica, R.D. Rogers, Confused ionic liquid ions—a “liquification” and dosage strategy for pharmaceutically active salts, *Chem. Commun.* 46 (2010) 1215.
- [126] T.J. Kemp, Ionic Liquids – Pharmaceutical Potential, *Science Progress* 95 (2012) 224–230.
- [127] W.L. Hough-Troutman, M. Smiglak, S. Griffin, W. Matthew Reichert, I. Mirska, J. Jodynys-Liebert, T. Adamska, J. Nawrot, M. Stasiewicz, R.D. Rogers, J. Pernak, Ionic liquids with dual biological function: sweet and anti-microbial, hydrophobic quaternary ammonium-based salts, *New J. Chem.* 33 (2009) 26–33.

- [128] G. Chatel, J.F.B. Pereira, V. Debbeti, H. Wang, R.D. Rogers, Mixing ionic liquids – “simple mixtures” or “double salts”?, *Green Chem.* 16 (2014) 2051.
- [129] M.W. Stocker, A.M. Healy, S. Ferguson, Spray Encapsulation as a Formulation Strategy for Drug-Based Room Temperature Ionic Liquids: Exploiting Drug–Polymer Immiscibility to Enable Processing for Solid Dosage Forms, *Mol. Pharmaceutics* 17 (2020) 3412–3424.
- [130] L. Viau, C. Tourné-Péteilh, J.-M. Devoisselle, A. Vioux, Ionogels as drug delivery system: one-step sol–gel synthesis using imidazolium ibuprofenate ionic liquid, *Chem. Commun.* 46 (2010) 228–230.
- [131] C. Jouannin, C. Tourné-Péteilh, V. Darcos, T. Sharkawi, J.-M. Devoisselle, P. Gaveau, P. Dieudonné, A. Vioux, L. Viau, Drug delivery systems based on pharmaceutically active ionic liquids and biocompatible poly(lactic acid), *J. Mater. Chem. B* 2 (2014) 3133–3141.
- [132] C. Wang, S.A. Chopade, Y. Guo, J.T. Early, B. Tang, E. Wang, M.A. Hillmyer, T.P. Lodge, C.C. Sun, Preparation, Characterization, and Formulation Development of Drug–Drug Protic Ionic Liquids of Diphenhydramine with Ibuprofen and Naproxen, *Mol. Pharmaceutics* 15 (2018) 4190–4201.
- [133] K.M. Wust, T.S. Beck, R.A. Burrow, S.M. Oliveira, E.S. Brum, I. Brusco, G. Machado, O. Bianchi, M.A. Villetti, C.P. Frizzo, Physicochemical characterization, released profile, and antinociceptive activity of diphenhydraminium ibuprofenate supported on mesoporous silica, *Materials Science and Engineering: C* 108 (2020) 110194.
- [134] K. Bica, H. Rodríguez, G. Gurau, O. Andreea Cojocaru, A. Riisager, R. Fehrmann, R.D. Rogers, Pharmaceutically active ionic liquids with solids handling, enhanced thermal stability, and fast release, *Chem. Commun.* 48 (2012) 5422.
- [135] J.C.B. Vieira, V.E. Priebe, K.M. Wust, E.V. Benvenuti, M.A. Villetti, C.R. Bender, C.P. Frizzo, Adsorption and release of diphenhydraminium ibuprofenate from SBA-15 and MCM-41 explained by intermolecular interactions, *J Mater Sci* 58 (2023) 6998–7010.
- [136] Y. Lu, J. Qi, W. Wu, Ionic Liquids-Based Drug Delivery: a Perspective, *Pharm Res* 39 (2022) 2329–2334.
- [137] Y. Sahbaz, T.-H. Nguyen, L. Ford, C.L. McEvoy, H.D. Williams, P.J. Scammells, C.J.H. Porter, Ionic Liquid Forms of Weakly Acidic Drugs in Oral Lipid Formulations: Preparation, Characterization, in Vitro Digestion, and in Vivo Absorption Studies, *Mol. Pharmaceutics* 14 (2017) 3669–3683.
- [138] H. Wu, Z. Deng, B. Zhou, M. Qi, M. Hong, G. Ren, Improved transdermal permeability of ibuprofen by ionic liquid technology: Correlation between counterion structure and the physicochemical and biological properties, *Journal of Molecular Liquids* 283 (2019) 399–409.
- [139] X. Chen, Z. Li, C. Yang, D. Yang, Ionic liquids as the effective technology for enhancing transdermal drug delivery: Design principles, roles, mechanisms, and future challenges, *Asian Journal of Pharmaceutical Sciences* 19 (2024) 100900.
- [140] G. Chantereau, M. Sharma, A. Abednejad, B.M. Neves, G. Sèbe, V. Coma, M.G. Freire, C.S.R. Freire, A.J.D. Silvestre, Design of Nonsteroidal Anti-Inflammatory Drug-Based Ionic Liquids with Improved Water Solubility and Drug Delivery, *ACS Sustainable Chem. Eng.* 7 (2019) 14126–14134.
- [141] A. Abednejad, A. Ghatee, E.S. Morais, M. Sharma, B.M. Neves, M.G. Freire, J. Nourmohammadi, A.A. Mehrizi, Polyvinylidene fluoride–Hyaluronic acid wound dressing comprised of ionic liquids for controlled drug delivery and dual therapeutic behavior, *Acta Biomaterialia* 100 (2019) 142–157.
- [142] B. Gworek, M. Kijeńska, J. Wrzosek, M. Graniewska, Pharmaceuticals in the Soil and Plant Environment: a Review, *Water Air Soil Pollut* 232 (2021) 145.
- [143] M. Ye, Y. Gu, Amino Acids Ionic Liquids, in: S. Zhang (Ed.), *Encyclopedia of Ionic Liquids*, Springer Singapore, Singapore, 2021: pp. 1–8.

- [144] Y. Singh, S. Saklani, T. Tantra, S. Thareja, Amino Acid Derived Prodrugs: An Approach to Improve the Bioavailability of Clinically Approved Drugs, *CTMC* 21 (2021) 2170–2183.
- [145] S. Dhaneshwar, P.P. Joshi, S. Pawar, Codrugs: Optimum Use through Prodrugs, in: K. Shah, D.N. Chauhan, N.S. Chauhan, P. Mishra (Eds.), *Recent Advancement in Prodrugs*, 1st ed., CRC Press, 2020; pp. 21–65.
- [146] S. Furukawa, G. Hattori, S. Sakai, N. Kamiya, Highly efficient and low toxic skin penetrants composed of amino acid ionic liquids, *RSC Adv.* 6 (2016) 87753–87755.
- [147] R.Md. Moshikur, Md.R. Chowdhury, R. Wakabayashi, Y. Tahara, M. Moniruzzaman, M. Goto, Characterization and cytotoxicity evaluation of biocompatible amino acid esters used to convert salicylic acid into ionic liquids, *International Journal of Pharmaceutics* 546 (2018) 31–38.
- [148] H. Tanigawa, N. Suzuki, T. Suzuki, Application of ionic liquid to enhance the nose-to-brain delivery of etodolac, *European Journal of Pharmaceutical Sciences* 178 (2022) 106290.
- [149] J. Klebko, The new amino acid and non-steroidal anti-inflammatory drugs derivatives as potential pharmacological agents, Master Thesis supervised by Paula Ossowicz, The West Pomeranian University of Technology in Szczecin, 2018.
- [150] E. Janus, P. Ossowicz, J. Klebko, A. Nowak, W. Duchnik, Ł. Kucharski, A. Klimowicz, Enhancement of ibuprofen solubility and skin permeation by conjugation with L-valine alkyl esters, *RSC Adv.* 10 (2020) 7570–7584.
- [151] P. Ossowicz, J. Klebko, E. Janus, A. Nowak, W. Duchnik, Ł. Kucharski, A. Klimowicz, The effect of alcohols as vehicles on the percutaneous absorption and skin retention of ibuprofen modified with L -valine alkyl esters, *RSC Adv.* 10 (2020) 41727–41740.
- [152] P. Ossowicz, P. Kardaleva, M. Guncheva, J. Klebko, E. Świątek, E. Janus, D. Yancheva, I. Angelov, Ketoprofen-Based Ionic Liquids: Synthesis and Interactions with Bovine Serum Albumin, *Molecules* 25 (2020) 90.
- [153] P. Ossowicz, E. Janus, J. Klebko, E. Świątek, P. Kardaleva, S. Taneva, E. Krachmarova, M. Rangelov, N. Todorova, M. Guncheva, Modulation of the binding affinity of naproxen to bovine serum albumin by conversion of the drug into amino acid ester salts, *Journal of Molecular Liquids* 319 (2020) 114283.
- [154] J. Klebko, P. Ossowicz-Rupniewska, E. Świątek, J. Szachnowska, E. Janus, S.G. Taneva, E. Krachmarova, M. Guncheva, Salicylic Acid as Ionic Liquid Formulation May Have Enhanced Potency to Treat Some Chronic Skin Diseases, *Molecules* 27 (2021) 216.
- [155] P. Ossowicz-Rupniewska, E. Janus, J. Klebko, Sposób wytwarzania chlorowodorku estru alkilowego L-waliny, Patent No. PL239320, 06.09.2021.
- [156] P. Ossowicz-Rupniewska, E. Janus, J. Klebko, Sposób otrzymywania chlorowodorków estrów alkilowych aminokwasów, Patent no. PL238790, 14.07.2021.
- [157] J. Li, Y. Sha, A Convenient Synthesis of Amino Acid Methyl Esters, *Molecules* 13 (2008) 1111–1119.
- [158] C. Salvitti, G. De Petris, A. Troiani, M. Managò, A. Di Noi, A. Ricci, F. Pepi, Sulfuric Acid Catalyzed Esterification of Amino Acids in Thin Film, *J. Am. Soc. Mass Spectrom.* (2023) jasms.3c00284.
- [159] M. Sathe, M.P. Kaushik, An efficient method for the esterification of amino acids using silica chloride, *Catalysis Communications* 7 (2006) 644–646.
- [160] P. Ossowicz-Rupniewska, J. Klebko, E. Janus, Organiczna pochodna ketoprofenu i sposób wytwarzania organicznej pochodnej ketoprofenu, Patent no. PL237698, 14.12.2020
- [161] P. Ossowicz-Rupniewska, J. Klebko, E. Janus, Pochodna naproksenu i sposób wytwarzania pochodnej naproksenu, Patent no. PL237318, 18.12.2020.

- [162] P. Ossowicz-Rupniewska, J. Kleboko, E. Janus, Aminokwasowa pochodna ibuprofenu i sposób wytwarzania aminokwasowej pochodnej ibuprofenu, Patent no. PL237699, 14.12.2020.
- [163] P. Ossowicz-Rupniewska, J. Kleboko, E. Świątek, E. Janus, Aminokwasowa pochodna ibuprofenu i sposób wytwarzania aminokwasowej pochodnej ibuprofenu, Application no. PL.438193, 18.06.2021.
- [164] P. Ossowicz-Rupniewska, J. Kleboko, E. Janus, Organiczna sól kwasu salicylowego i sposób wytwarzania organicznej soli kwasu salicylowego, Patent no. PL236161, 25.08.2020.
- [165] E. Janus, P. Ossowicz-Rupniewska, J. Kleboko, E. Świątek, Naproksenian estru alkilowego aminokwasu i sposób wytwarzania naproksenianu estru alkilowego aminokwasu, Application no. P.446045, 28.09.2021.
- [166] P. Ossowicz-Rupniewska, J. Kleboko, E. Świątek, K. Bilska, A. Nowak, W. Duchnik, Ł. Kucharski, Ł. Struk, K. Wenelska, A. Klimowicz, E. Janus, Influence of the Type of Amino Acid on the Permeability and Properties of Ibuprofenates of Isopropyl Amino Acid Esters, *IJMS* 23 (2022) 4158.
- [167] A.R. Katritzky, A Guide to the Complete Interpretation of Infrared Spectra of Organic Structures By Noel P. G. Roeges (Katholieke Industriële Hogeschool O-VI). Wiley: New York. 1994. x + 340 pp. \$69.95. ISBN 0-471-93998-6., *J. Am. Chem. Soc.* 118 (1996) 3543–3543.
- [168] S. Vairam, T. Premkumar, S. Govindarajan, Trimellitate complexes of divalent transition metals with hydrazinium cation: Thermal and spectroscopic studies, *J Therm Anal Calorim* 100 (2010) 955–960.
- [169] T. Kolev, M. Spittler, B. Koleva, Spectroscopic and structural elucidation of amino acid derivatives and small peptides: experimental and theoretical tools, *Amino Acids* 38 (2010) 45–50.
- [170] A. Balk, J. Wiest, T. Widmer, B. Galli, U. Holzgrabe, L. Meinel, Transformation of acidic poorly water soluble drugs into ionic liquids, *European Journal of Pharmaceutics and Biopharmaceutics* 94 (2015) 73–82.
- [171] A.J. Cruz-Cabeza, Acid–base crystalline complexes and the pKa rule, *CrystEngComm* 14 (2012) 6362.
- [172] H.G. Brittain, Strategy for the Prediction and Selection of Drug Substance Salt Forms, *Pharm. Tech.* 31 (2007) 78–88.
- [173] S.L. Childs, G.P. Stahly, A. Park, The Salt–Cocrystal Continuum: The Influence of Crystal Structure on Ionization State, *Mol. Pharmaceutics* 4 (2007) 323–338.
- [174] Committee on the Assessment of the Available Scientific Data Regarding the Safety and Effectiveness of Ingredients Used in Compounded Topical Pain Creams, Board on Health Sciences Policy, Health and Medicine Division, National Academies of Sciences, Engineering, and Medicine, Compounded Topical Pain Creams: Review of Select Ingredients for Safety, Effectiveness, and Use, National Academies Press, Washington, D.C., 2020.
- [175] K. Grodowska, A. Parczewski, Organic solvents in the pharmaceutical industry., *Acta Pol Pharm* 67 (2010) 3–12.
- [176] C. Reichardt, T. Welton, Solvents and solvent effects in organic chemistry, 4th, updated and enl. ed ed., Wiley-VCH, Weinheim, Germany, 2011.
- [177] S.S. Jambhekar, P.J. Breen, Drug dissolution: significance of physicochemical properties and physiological conditions, *Drug Discovery Today* 18 (2013) 1173–1184.
- [178] K.T. Savjani, A.K. Gajjar, J.K. Savjani, Drug Solubility: Importance and Enhancement Techniques, *ISRN Pharmaceutics* 2012 (2012) 1–10.
- [179] M. Saedtler, L. Meinel, Amorphous Ionic Liquid Strategies for Pharmaceutical Application, in: S. Zhang (Ed.), *Encyclopedia of Ionic Liquids*, Springer Singapore, Singapore, 2019: pp. 1–11.

- [180] E. Proksch, pH in nature, humans and skin, *The Journal of Dermatology* 45 (2018) 1044–1052.
- [181] J. Klebeko, O. Krüger, M. Dubicki, P. Ossowicz-Rupniewska, E. Janus, Isopropyl Amino Acid Esters Ionic Liquids as Vehicles for Non-Steroidal Anti-Inflammatory Drugs in Potential Topical Drug Delivery Systems with Antimicrobial Activity, *IJMS* 23 (2022) 13863.
- [182] J. Klebeko, P. Ossowicz-Rupniewska, A. Nowak, E. Kucharska, Ł. Kucharski, W. Duchnik, Ł. Struk, A. Klimowicz, E. Janus, Cations of amino acid alkyl esters conjugated with an anion from the group of NSAIDs - as tunable pharmaceutical active ionic liquids, *Journal of Molecular Liquids* (2023) 122200.
- [183] A. Elezović, A. Marić, A. Bišćević, J. Hadžiabdić, S. Škrbo, S. Špirtović-Halilović, O. Rahić, E. Vranić, A. Elezović, In vitro pH dependent passive transport of ketoprofen and metformin, *ADMET DMPK* 9 (2020) 57–68.
- [184] A.T.M. Serajuddin, C.I. Jarowski, Effect of Diffusion Layer pH and Solubility on the Dissolution Rate of Pharmaceutical Acids and Their Sodium Salts II: Salicylic Acid, Theophylline, and Benzoic Acid, *Journal of Pharmaceutical Sciences* 74 (1985) 148–154.
- [185] J. Hadgraft, C. Valenta, pH, pKa and dermal delivery, *International Journal of Pharmaceutics* 200 (2000) 243–247.
- [186] L. Kumar, B. Suhas, G.K. Pai, R. Verma, Determination of Saturated Solubility of Naproxen using UV Visible Spectrophotometer, *Rese. Jour. of Pharm. and Technol.* 8 (2015) 825.
- [187] J. Klebeko, P. Ossowicz, Modyfikacje strukturalne ibuprofenu, jako metoda zwiększania przenikalności przez skórę, in: *Postępy w technologii i inżynierii chemicznej 2021*, Wydawnictwo Uczelniane Zachodniopomorskiego Uniwersytetu Technologicznego w Szczecinie, 2021: pp. 26–34.
- [188] J.A. Arnott, S.L. Planey, The influence of lipophilicity in drug discovery and design, *Expert Opinion on Drug Discovery* 7 (2012) 863–875.
- [189] T.W. Johnson, R.A. Gallego, M.P. Edwards, Lipophilic Efficiency as an Important Metric in Drug Design, *J. Med. Chem.* 61 (2018) 6401–6420.
- [190] F. Tsopeles, C. Giaginis, A. Tsantili-Kakoulidou, Lipophilicity and biomimetic properties to support drug discovery, *Expert Opinion on Drug Discovery* 12 (2017) 885–896.
- [191] H.A.E. Benson, J.E. Grice, Y. Mohammed, S. Namjoshi, M.S. Roberts, Topical and Transdermal Drug Delivery: From Simple Potions to Smart Technologies, *CDD* 16 (2019) 444–460.
- [192] A. Czyrski, Determination of the Lipophilicity of Ibuprofen, Naproxen, Ketoprofen, and Flurbiprofen with Thin-Layer Chromatography, *Journal of Chemistry* 2019 (2019) 1–6.
- [193] R. O'Brien, N. Markova, G.A. Holdgate, Thermodynamics in Drug Discovery, in: D. Huddler, E.R. Zartler (Eds.), *Applied Biophysics for Drug Discovery*, 1st ed., Wiley, 2017: pp. 7–28.
- [194] N.C. Garbett, J.B. Chaires, Thermodynamic studies for drug design and screening, *Expert Opinion on Drug Discovery* 7 (2012) 299–314.
- [195] P. Ossowicz-Rupniewska, J. Klebeko, E. Świątek, J. Szachnowska, E. Janus, M. Rangelov, N. Todorova, S.G. Taneva, E. Krachmarova, M. Guncheva, Binding behavior of ibuprofen-based ionic liquids with bovine serum albumin: Thermodynamic and molecular modeling studies, *Journal of Molecular Liquids* 360 (2022) 119367.
- [196] W. Chen, Z. Xue, J. Wang, J. Jiang, X. Zhao, T. Mu, Investigation on the Thermal Stability of Deep Eutectic Solvents, *Acta Physico-Chimica Sinica* 34 (2018) 904–911. <https://doi.org/10.3866/PKU.WHXB201712281>.
- [197] C. Xu, Z. Cheng, Thermal Stability of Ionic Liquids: Current Status and Prospects for Future Development, *Processes* 9 (2021) 337.
- [198] S. Bhattacharyya, F.U. Shah, Thermal stability of choline based amino acid ionic liquids, *Journal of Molecular Liquids* 266 (2018) 597–602.

- [199] H. Wang, G. Gurau, J. Shamshina, O.A. Cojocaru, J. Janikowski, D.R. MacFarlane, J.H. Davis, R.D. Rogers, Simultaneous membrane transport of two active pharmaceutical ingredients by charge assisted hydrogen bond complex formation, *Chem. Sci.* 5 (2014) 3449.
- [200] Y. Zhang, C. Liu, J. Wang, S. Ren, Y. Song, P. Quan, L. Fang, Ionic liquids in transdermal drug delivery system: Current applications and future perspectives, *Chinese Chemical Letters* (2022) S1001841722006301.
- [201] T. Welton, Ionic liquids: a brief history, *Biophys Rev* 10 (2018) 691–706.
- [202] Y. Zhang, E.J. Maginn, Molecular dynamics study of the effect of alkyl chain length on melting points of $[C_n \text{MIM}][PF_6]$ ionic liquids, *Phys. Chem. Chem. Phys.* 16 (2014) 13489–13499.
- [203] P.B.P. Serra, F.M.S. Ribeiro, M.A.A. Rocha, M. Fulem, K. Růžicka, J.A.P. Coutinho, L.M.N.B.F. Santos, Solid-liquid equilibrium and heat capacity trend in the alkylimidazolium PF6 series, *Journal of Molecular Liquids* 248 (2017) 678–687.
- [204] S.E. David, P. Timmins, B.R. Conway, Impact of the counterion on the solubility and physicochemical properties of salts of carboxylic acid drugs, *Drug Development and Industrial Pharmacy* 38 (2012) 93–103.
- [205] E. Gunn, I.A. Guzei, T. Cai, L. Yu, Polymorphism of Nifedipine: Crystal Structure and Reversible Transition of the Metastable β Polymorph, *Crystal Growth & Design* 12 (2012) 2037–2043.
- [206] C. Yao, I.A. Guzei, Y. Jin, S. Ruan, G. Sun, Y. Gui, L. Wang, L. Yu, Polymorphism of Piroxicam: New Polymorphs by Melt Crystallization and Crystal Structure Prediction, *Crystal Growth & Design* 20 (2020) 7874–7881.
- [207] Q 1 A (R2) Stability Testing of new Drug Substances and Products, (2006).
- [208] Y. Wang, Y. Wang, J. Cheng, H. Chen, J. Xu, Z. Liu, Q. Shi, C. Zhang, Recent Advances in the Application of Characterization Techniques for Studying Physical Stability of Amorphous Pharmaceutical Solids, *Crystals* 11 (2021) 1440.
- [209] S.A. Pullano, G. Marcianò, M.G. Bianco, G. Oliva, V. Rania, C. Vocca, E. Cione, G. De Sarro, L. Gallelli, P. Romeo, A. La Gatta, A.S. Fiorillo, FT-IR Analysis of Structural Changes in Ketoprofen Lysine Salt and KiOil Caused by a Pulsed Magnetic Field, *Bioengineering* 9 (2022) 503.
- [210] E. Dinte, E. Bodoki, S. Leucuta, C.A. Iuga, Compatibility studies between drugs and excipients in the preformulation phase of buccal mucoadhesive systems, *Farmacia* 61 (2013) 703–712.
- [211] M. Hesse, H. Meier, B. Zeeh, *Spektroskopische Methoden in der organischen Chemie*, 8., überarb. und erw. Aufl, Thieme, Stuttgart, 2012.
- [212] M. Tawalbeh, H.A. Khan, A. Al-Othman, F. Almomani, S. Ajith, A comprehensive review on the recent advances in materials for thermal energy storage applications, *International Journal of Thermofluids* 18 (2023) 100326.
- [213] J. Bernstein, Crystal Polymorphism, in: J.J. Novoa, D. Braga, L. Addadi (Eds.), *Engineering of Crystalline Materials Properties*, Springer Netherlands, Dordrecht, 2008: pp. 87–109.
- [214] E.V. Boldyreva, V.A. Drebuschak, I.E. Paukov, Y.A. Kovalevskaya, T.N. Drebuschak, DSC and adiabatic calorimetry study of the polymorphs of paracetamol, *Journal of Thermal Analysis and Calorimetry* 77 (2004) 607–623.
- [215] W. Guo, C. Li, P. Du, Y. Wang, S. Zhao, J. Wang, C. Yang, Thermal properties of drug polymorphs: A case study with felodipine form I and form IV, *Journal of Saudi Chemical Society* 24 (2020) 474–483.
- [216] J. Hao, P. Ghosh, S.K. Li, B. Newman, G.B. Kasting, S.G. Raney, Heat effects on drug delivery across human skin, *Expert Opinion on Drug Delivery* 13 (2016) 755–768.
- [217] G.W.H. Höhne, W. Hemminger, H.-J. Flammersheim, *Differential Scanning Calorimetry*, Springer Berlin Heidelberg, Berlin, Heidelberg, 1996.

- [218] T.S. Beck, M. De Mattos, C.R.T. Jortieke, J.C.B. Vieira, C.M. Verdi, R.C.V. Santos, M.R. Sagrillo, A. Rossato, L. Da Silva Silveira, C.P. Frizzo, Structural effects of amino acid-based ionic liquids on thermophysical properties, and antibacterial and cytotoxic activity, *Journal of Molecular Liquids* 364 (2022) 120054.
- [219] K.A. Graeser, J.E. Patterson, J.A. Zeitler, T. Rades, The Role of Configurational Entropy in Amorphous Systems, *Pharmaceutics* 2 (2010) 224–244.
- [220] J. Flieger, J. Feder-Kubis, M. Tatarczak-Michalewska, Chiral Ionic Liquids: Structural Diversity, Properties and Applications in Selected Separation Techniques, *IJMS* 21 (2020) 4253.
- [221] A.R.F. Carreira, S.N. Rocha, F.A. E Silva, T.E. Sintra, H. Passos, S.P.M. Ventura, J.A.P. Coutinho, Amino-acid-based chiral ionic liquids characterization and application in aqueous biphasic systems, *Fluid Phase Equilibria* 542–543 (2021) 113091.
- [222] S.S. Aloni, M. Perovic, M. Weitman, R. Cohen, M. Oschatz, Y. Mastai, Amino acid-based ionic liquids as precursors for the synthesis of chiral nanoporous carbons, *Nanoscale Adv.* 1 (2019) 4981–4988.
- [223] M. Abram, M. Jakubiec, K. Kamiński, Chirality as an Important Factor for the Development of New Antiepileptic Drugs, *ChemMedChem* 14 (2019) 1744–1761.
- [224] J. Ceramella, D. Iacopetta, A. Franchini, M. De Luca, C. Saturnino, I. Andreu, M.S. Sinicropi, A. Catalano, A Look at the Importance of Chirality in Drug Activity: Some Significant Examples, *Applied Sciences* 12 (2022) 10909.
- [225] A.M. Evans, Comparative Pharmacology of S(+)-Ibuprofen and (RS)-Ibuprofen, *Clin Rheumatol* 20 (2001) 9–14.
- [226] J. Siódmiak, T. Siódmiak, A. Tarczykowska, K. Czirson, J. Dulęba, M.P. Marszałł, Metabolic chiral inversion of 2-arylpropionic acid derivatives (profens), *Medical Research Journal* 2 (2017) 1–5.
- [227] J. Gawroński, Asymmetric syntheses and transformations--tools for chirality multiplication in drug synthesis, *Acta Pol Pharm* 63 (2006) 333–351.
- [228] J. Sui, N. Wang, J. Wang, X. Huang, T. Wang, L. Zhou, H. Hao, Strategies for chiral separation: from racemate to enantiomer, *Chem. Sci.* 14 (2023) 11955–12003.
- [229] E. Tokunaga, T. Yamamoto, E. Ito, N. Shibata, Understanding the Thalidomide Chirality in Biological Processes by the Self-disproportionation of Enantiomers, *Sci Rep* 8 (2018) 17131.
- [230] A. Ballard, S. Narduolo, H.O. Ahmad, D.A. Cosgrove, A.G. Leach, N.J. Buurma, The problem of racemization in drug discovery and tools to predict it, *Expert Opinion on Drug Discovery* 14 (2019) 527–539.
- [231] L.A. Nguyen, H. He, C. Pham-Huy, Chiral drugs: an overview, *Int J Biomed Sci* 2 (2006) 85–100.
- [232] S. Supe, P. Takudage, Methods for evaluating penetration of drug into the skin: A review, *Skin Research and Technology* 27 (2021) 299–308.
- [233] R. Neupane, S.H.S. Boddu, J. Renukuntla, R.J. Babu, A.K. Tiwari, Alternatives to Biological Skin in Permeation Studies: Current Trends and Possibilities, *Pharmaceutics* 12 (2020) 152. <https://doi.org/10.3390/pharmaceutics12020152>.
- [234] J. Klebeko, P. Ossowicz-Rupniewska, A. Nowak, E. Janus, W. Duchnik, U. Adamiak-Giera, Ł. Kucharski, P. Prowans, J. Petriczko, N. Czapla, P. Bargiel, M. Markowska, A. Klimowicz, Permeability of Ibuprofen in the Form of Free Acid and Salts of L-Valine Alkyl Esters from a Hydrogel Formulation through Strat-M™ Membrane and Human Skin, *Materials* 14 (2021) 6678.
- [235] P. Ossowicz-Rupniewska, A. Nowak, J. Klebeko, E. Janus, W. Duchnik, U. Adamiak-Giera, Ł. Kucharski, P. Prowans, J. Petriczko, N. Czapla, P. Bargiel, M. Markowska, A. Klimowicz, Assessment of the Effect of Structural Modification of Ibuprofen on the Penetration of Ibuprofen from Pentravan® (Semisolid) Formulation Using Human Skin and a Transdermal Diffusion Test Model, *Materials* 14 (2021) 6808.

- [236] R.Md. Moshikur, Md.R. Chowdhury, R. Wakabayashi, Y. Tahara, M. Moniruzzaman, M. Goto, Characterization and cytotoxicity evaluation of biocompatible amino acid esters used to convert salicylic acid into ionic liquids, *International Journal of Pharmaceutics* 546 (2018) 31–38.
- [237] X. Liu, B. Testa, A. Fahr, Lipophilicity and Its Relationship with Passive Drug Permeation, *Pharm Res* 28 (2011) 962–977.
- [238] N. Moore, Ibuprofen: A Journey from Prescription to Over-the-Counter Use, *J R Soc Med* 100 (2007) 2–6.
- [239] O.A. Al Hanbali, H.M.S. Khan, M. Sarfraz, M. Arafat, S. Ijaz, A. Hameed, Transdermal patches: Design and current approaches to painless drug delivery, *Acta Pharmaceutica* 69 (2019) 197–215.
- [240] M. Elmowafy, Skin penetration/permeation success determinants of nanocarriers: Pursuit of a perfect formulation, *Colloids and Surfaces B: Biointerfaces* 203 (2021) 111748.
- [241] E. Tuitou, V.M. Meidan, E. Horwitz, Methods for quantitative determination of drug localized in the skin, *Journal of Controlled Release* 56 (1998) 7–21.
- [242] İ. Gulcin, Antioxidants and antioxidant methods: an updated overview, *Arch Toxicol* 94 (2020) 651–715.
- [243] M. Darvin, L. Zastrow, W. Sterry, J. Lademann, Effect of Supplemented and Topically Applied Antioxidant Substances on Human Tissue, *Skin Pharmacol Physiol* 19 (2006) 238–247.
- [244] A. Ascenso, H. Margarida Ribeiro, H. Cabral Marques, S. Simoes, Topical Delivery of Antioxidants, *CDD* 8 (2011) 640–660.
- [245] J. Chen, Y. Liu, Z. Zhao, J. Qiu, Oxidative stress in the skin: Impact and related protection, *Intern J of Cosmetic Sci* 43 (2021) 495–509.
- [246] S. Sehajpal, D.N. Prasad, R.K. Singh, Novel ketoprofen–antioxidants mutual codrugs as safer nonsteroidal anti-inflammatory drugs: Synthesis, kinetic and pharmacological evaluation, *Arch. Pharm. Chem. Life Sci* 352 (2019) 1800339.
- [247] M. Rinnerthaler, J. Bischof, M. Streubel, A. Trost, K. Richter, Oxidative Stress in Aging Human Skin, *Biomolecules* 5 (2015) 545–589.
- [248] K.J. Trouba, H.K. Hamadeh, R.P. Amin, D.R. Germolec, Oxidative Stress and Its Role in Skin Disease, *Antioxidants & Redox Signaling* 4 (2002) 665–673.
- [249] K.-A. S. Mahmood, J. H. Ahmed, A. M. Jawad, Non steroidal Anti-inflammanatory drugs (NSAIDs) Free radicals and reactive species (ROS): A Review of literature, *MJBU* 27 (2009) 46–53.
- [250] D. Costa, L. Moutinho, J.L.F.C. Lima, E. Fernandes, Antioxidant Activity and Inhibition of Human Neutrophil Oxidative Burst Mediated by Arylpropionic Acid Non-steroidal Anti-inflammatory Drugs, *Biological & Pharmaceutical Bulletin* 29 (2006) 1659–1670.
- [251] R. Ghosh, A. Alajbegovic, A.V. Gomes, NSAIDs and Cardiovascular Diseases: Role of Reactive Oxygen Species, *Oxidative Medicine and Cellular Longevity* 2015 (2015) 1–25.
- [252] S.B. Kedare, R.P. Singh, Genesis and development of DPPH method of antioxidant assay, *J Food Sci Technol* 48 (2011) 412–422.
- [253] R. Cruz-Ornelas, J.E. Sánchez-Vázquez, L. Amaya-Delgado, K. Guillén-Navarro, A. Calixto-Romo, Biodegradation of NSAIDs and their effect on the activity of ligninolytic enzymes from *Pleurotus djamor*, *3 Biotech* 9 (2019) 373.
- [254] T.J. Austin, S. Comber, E. Forrester, M. Gardner, O.R. Price, R. Oldenkamp, A.M.J. Ragas, A.J. Hendriks, The importance of over-the-counter-sales and product format in the environmental exposure assessment of active pharmaceutical ingredients, *Science of The Total Environment* 752 (2021) 141624.
- [255] A. Rastogi, M.K. Tiwari, M.M. Ghangrekar, A review on environmental occurrence, toxicity and microbial degradation of Non-Steroidal Anti-Inflammatory Drugs (NSAIDs), *Journal of Environmental Management* 300 (2021) 113694.

- [256] A. Khalidi-Idrissi, A. Madinzi, A. Anouzla, A. Pala, L. Mouhir, Y. Kadmi, S. Souabi, Recent advances in the biological treatment of wastewater rich in emerging pollutants produced by pharmaceutical industrial discharges, *Int. J. Environ. Sci. Technol.* 20 (2023) 11719–11740.
- [257] P. Alfonso-Muniozguren, E.A. Serna-Galvis, M. Bussemaker, R.A. Torres-Palma, J. Lee, A review on pharmaceuticals removal from waters by single and combined biological, membrane filtration and ultrasound systems, *Ultrasonics Sonochemistry* 76 (2021) 105656.
- [258] M. Zupanc, T. Kosjek, M. Petkovšek, M. Dular, B. Kompare, B. Širok, Ž. Blažeka, E. Heath, Removal of pharmaceuticals from wastewater by biological processes, hydrodynamic cavitation and UV treatment, *Ultrasonics Sonochemistry* 20 (2013) 1104–1112..
- [259] M.A. El-Gammal, A.S. Elsaedy, H. Ashry, A.W.M. Jobran, Biodegradation Method of Pharmaceuticals and Personal Care Products, in: G.A.M. Ali, A.S.H. Makhoulf (Eds.), *Handbook of Biodegradable Materials*, Springer International Publishing, Cham, 2023: pp. 1093–1131.
- [260] E. Makuch, P. Ossowicz-Rupniewska, J. Klebko, E. Janus, Biodegradation of L-Valine Alkyl Ester Ibuprofenates by Bacterial Cultures, *Materials* 14 (2021) 3180.
- [261] J. Ahtiainen, M. Aalto, P. Pessala, Biodegradation of chemicals in a standardized test and in environmental conditions, *Chemosphere* 51 (2003) 529–537.
- [262] S.J. Khan, L. Wang, N.H. Hashim, J.A. McDonald, Distinct Enantiomeric Signals of Ibuprofen and Naproxen in Treated Wastewater and Sewer Overflow, *Chirality* 26 (2014) 739–746.
- [263] C. Caballo, M.D. Sicilia, S. Rubio, Enantioselective determination of representative profens in wastewater by a single-step sample treatment and chiral liquid chromatography–tandem mass spectrometry, *Talanta* 134 (2015) 325–332.
- [264] A. Marchlewicz, U. Guzik, K. Hupert-Kocurek, A. Nowak, S. Wilczyńska, D. Wojcieszynska, Toxicity and biodegradation of ibuprofen by *Bacillus thuringiensis* B1(2015b), *Environ Sci Pollut Res* 24 (2017) 7572–7584.
- [265] J. Jan-Roblero, J.A. Cruz-Maya, Ibuprofen: Toxicology and Biodegradation of an Emerging Contaminant, *Molecules* 28 (2023) 2097.
- [266] S.E. Musson, P. Campo, T. Tolaymat, M. Suidan, T.G. Townsend, Assessment of the anaerobic degradation of six active pharmaceutical ingredients, *Science of The Total Environment* 408 (2010) 2068–2074.
- [267] Z.H. Mussa, F.F. Al-Qaim, A.H. Jawad, M. Scholz, Z.M. Yaseen, A Comprehensive Review for Removal of Non-Steroidal Anti-Inflammatory Drugs Attained from Wastewater Observations Using Carbon-Based Anodic Oxidation Process, *Toxics* 10 (2022) 598.
- [268] U. Guzik, D. Wojcieszynska, Biodegradation of Non-steroidal Anti-inflammatory Drugs and Their Influence on Soil Microorganisms, in: A. Kumar, S. Sharma (Eds.), *Microbes and Enzymes in Soil Health and Bioremediation*, Springer Singapore, Singapore, 2019: pp. 379–401.
- [269] J. Lin, Y. Zhang, Y. Bian, Y. Zhang, R. Du, M. Li, Y. Tan, X. Feng, Non-steroidal anti-inflammatory drugs (NSAIDs) in the environment: Recent updates on the occurrence, fate, hazards and removal technologies, *Science of The Total Environment* 904 (2023) 166897.
- [270] M. Hasan, K. Alfredo, S. Murthy, R. Riffat, Biodegradation of salicylic acid, acetaminophen and ibuprofen by bacteria collected from a full-scale drinking water biofilter, *Journal of Environmental Management* 295 (2021) 113071.
- [271] T.L. da Silva, C.S.D. Costa, M.G.C. da Silva, M.G.A. Vieira, Overview of non-steroidal anti-inflammatory drugs degradation by advanced oxidation processes, *Journal of Cleaner Production* 346 (2022) 131226.

- [272] F.M.S. Costa, M.L.M.F.S. Saraiva, M.L.C. Passos, Ionic liquids and organic salts with antimicrobial activity as a strategy against resistant microorganisms, *Journal of Molecular Liquids* 368 (2022) 120750.
- [273] N. Nikfarjam, M. Ghomi, T. Agarwal, M. Hassanpour, E. Sharifi, D. Khorsandi, M. Ali Khan, F. Rossi, A. Rossetti, E. Nazarzadeh Zare, N. Rabiee, D. Afshar, M. Vosough, T. Kumar Maiti, V. Mattoli, E. Lichtfouse, F.R. Tay, P. Makvandi, Antimicrobial Ionic Liquid-Based Materials for Biomedical Applications, *Adv Funct Materials* 31 (2021) 2104148.
- [274] Z. Fang, X. Zheng, L. Li, J. Qi, W. Wu, Y. Lu, Ionic Liquids: Emerging Antimicrobial Agents, *Pharm Res* 39 (2022) 2391–2404.
- [275] J. Michalski, C. Odrzygóźdź, P. Mester, D. Narożna, T. Cłapa, Defeat undefeatable: Ionic liquids as novel antimicrobial agents, *Journal of Molecular Liquids* 369 (2023) 120782.
- [276] J.L. Shamshina, P. Berton, H. Wang, X. Zhou, G. Gurau, R.D. Rogers, Ionic Liquids in Pharmaceutical Industry, in: W. Zhang, B.W. Cue (Eds.), *Green Techniques for Organic Synthesis and Medicinal Chemistry*, 1st ed., Wiley, 2018: pp. 539–577.
- [277] T. Gundolf, R. Kalb, P. Rossmanith, P. Mester, Bacterial Resistance Toward Antimicrobial Ionic Liquids Mediated by Multidrug Efflux Pumps, *Front. Microbiol.* 13 (2022) 883931.
- [278] R.C. Paes Leme, R.B. da Silva, Antimicrobial Activity of Non-steroidal Anti-inflammatory Drugs on Biofilm: Current Evidence and Potential for Drug Repurposing, *Front. Microbiol.* 12 (2021) 707629.
- [279] C. Leão, A. Borges, M. Simões, NSAIDs as a Drug Repurposing Strategy for Biofilm Control, *Antibiotics* 9 (2020) 591.
- [280] R.C. Paes Leme, R.B. da Silva, Antimicrobial Activity of Non-steroidal Anti-inflammatory Drugs on Biofilm: Current Evidence and Potential for Drug Repurposing, *Front. Microbiol.* 12 (2021) 707629.
- [281] J. Obad, J. Šušković, B. Kos, Antimicrobial activity of ibuprofen: New perspectives on an “Old” non-antibiotic drug, *European Journal of Pharmaceutical Sciences* 71 (2015) 93–98.
- [282] T.D. Karaca, H. Balci, A. Aysan, Evaluation and comparison of the antimicrobial and cytotoxic activities of some amino acid methyl esters, *Hacettepe Journal of Biology and Chemistry* 51 (2023) 133–140.
- [283] M. Idrees, A.R. Mohammad, N. Karodia, A. Rahman, Multimodal Role of Amino Acids in Microbial Control and Drug Development, *Antibiotics* 9 (2020) 330.
- [284] M.G. Nowak, A.S. Skwarecki, M.J. Milewska, Amino Acid Based Antimicrobial Agents – Synthesis and Properties, *ChemMedChem* 16 (2021) 3513–3544.
- [285] S. Kapil, V. Sharma, D -Amino acids in antimicrobial peptides: a potential approach to treat and combat antimicrobial resistance, *Can. J. Microbiol.* 67 (2021) 119–137.
- [286] F.E.-Z. Amrati, M. Bourhia, H. Saghrouchni, M. Slighoua, A. Grafov, R. Ullah, E. Ezzeldin, G.A. Mostafa, A. Bari, S. Ibenmoussa, D. Bousta, *Caralluma europaea* (Guss.) N.E.Br.: Anti-Inflammatory, Antifungal, and Antibacterial Activities against Nosocomial Antibiotic-Resistant Microbes of Chemically Characterized Fractions, *Molecules* 26 (2021) 636.
- [287] K.Y. Le, M.D. Park, M. Otto, Immune Evasion Mechanisms of *Staphylococcus epidermidis* Biofilm Infection, *Front. Microbiol.* 9 (2018) 359.
- [288] A.V. Gannesen, M.I. Schelkunov, O.V. Geras’kina, N.E. Makarova, M.V. Sukhacheva, N.D. Danilova, M.A. Ovcharova, S.V. Mart’yanov, T.A. Pankratov, D.S. Muzychenko, M.V. Zhurina, A.V. Feofanov, E.A. Botchkova, V.K. Plakunov, Epinephrine affects gene expression levels and has a complex effect on biofilm formation in *Micrococcus luteus* strain C01 isolated from human skin, *Biofilm* 3 (2021) 100058.
- [289] D.S. Goodsell, *Escherichia coli*, *Biochem. Mol. Biol. Educ.* 37 (2009) 325–332.
- [290] C.M. Jones, N.J. Hernández Lozada, B.F. Pfleger, Efflux systems in bacteria and their metabolic engineering applications, *Appl Microbiol Biotechnol* 99 (2015) 9381–9393.

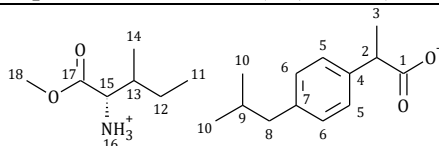
- [291] T.K. Van Dyk, Bacterial Efflux Transport in Biotechnology, in: *Advances in Applied Microbiology*, Elsevier, 2008: pp. 231–247.
- [292] W.N. Beavers, A.L. DuMont, A.J. Monteith, K.N. Maloney, K.A. Tallman, A. Weiss, A.H. Christian, F.D. Toste, C.J. Chang, N.A. Porter, V.J. Torres, E.P. Skaar, *Staphylococcus aureus* Peptide Methionine Sulfoxide Reductases Protect from Human Whole-Blood Killing, *Infect Immun* 89 (2021) e00146-21.
- [293] A. Lichev, A. Angelov, I. Cucurull, W. Liebl, Amino acids as nutritional factors and (p)ppGpp as an alarmone of the stringent response regulate natural transformation in *Micrococcus luteus*, *Sci Rep* 9 (2019) 11030.
- [294] I. Draskovic, D. Dubnau, Biogenesis of a putative channel protein, ComEC, required for DNA uptake: membrane topology, oligomerization and formation of disulphide bonds: Channel protein ComEC, *Molecular Microbiology* 55 (2004) 881–896.
- [295] E.J. Torasso Kasem, A. Angelov, E. Werner, A. Lichev, S. Vanderhaeghen, W. Liebl, Identification of New Chromosomal Loci Involved in com Genes Expression and Natural Transformation in the Actinobacterial Model Organism *Micrococcus luteus*, *Genes* 12 (2021) 1307.
- [296] B.S. Furniss, A.I. Vogel, eds., *Vogel's textbook of practical organic chemistry*, New. ed., 5. ed., rev. [Nachdr.], Pearson/Prentice Hall, Harlow, 2009.

Appendix I

L-AMINO ACID ALKYL ESTER SALTS OF IBUPROFEN

L-isoleucinium methyl ester (*R,S*)-ibuprofenate - [IleOMe][IBU]

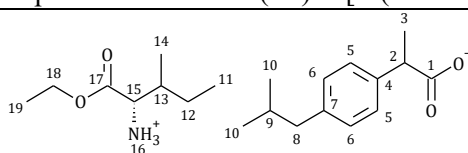
(2*S*)-1-methoxy-3-methyl-1-oxopentane-2-aminium (2*R*)-2-[4-(2-methylpropyl)phenyl]propanoate



¹H NMR (400 MHz, CDCl₃) δ [ppm]: 7.21 (d, *J*_{5,6}=8.4 Hz, 2H, H5), 7.09 (d, *J*_{6,5}=7.9 Hz, 2H, H6), 4.74 (s, 3H, H16), 3.71 (s, 3H, H18), 3.71–3.61 (m, 1H, H2), 3.45 (d, *J*_{15,13}=4.6 Hz, 1H, H14), 2.44 (d, *J*_{9,8}=7.2 Hz, 2H, H8), 1.91–1.70 (m, 2H, H13, H9), 1.47 (d, *J*_{2,3}=7.1 Hz, 3H, H3), 1.47–1.33 (m, 1H, H12'), 1.26–1.11 (m, 1H, H12''), 0.94–0.85 (m, 12H, H10, H14, H11). **¹³C NMR** (100 MHz, CDCl₃) δ [ppm]: 179.25 (C1), 175.14 (C17), 140.51 (C7), 137.90 (C4), 129.31 (C6), 127.26 (C5), 58.40 (C15), 51.91 (C2), 45.30 (C8), 45.06 (C18), 38.77, 30.21 (C9), 24.77 (C12), 22.42 (C10), 18.37 (C3), 15.50 (C14), 11.68 (C11). **FT-IR**: ν (ATR): 2954.30, 2932.41, 2867.79, 2847.20, 2726.27, 2645.81, 2180.08, 2161.80, 1738.79, 1702.41, 1677.76, 1610.24, 1509.04, 1473.29, 1454.62, 1438.43, 1423.18, 1380.90, 1356.87, 1319.80, 1283.13, 1256.12, 1231.86, 1201.22, 1163.72, 1105.46, 1085.85, 1061.31, 1024.10, 991.05, 965.42, 912.55, 882.82, 845.40, 817.61, 791.52, 768.47, 754.69, 725.76, 717.48, 689.13, 676.21, 634.74, 595.92, 540.83, 513.13, 479.29, 443.91 cm⁻¹. **[α]_D²⁰** = +20.234 (c=0.598% (m/v) in EtOH). **UV-Vis** (EtOH): λ_{max}=229.0 nm. **Elemental analysis**: C₂₀H₃₃NO₄ (351.480 g/mol), calculated (%): C (68.34), H (9.46), N (3.98), O (18.21), found: C (68.22), H (9.50), N (4.00), O (18.28).

L-isoleucinium ethyl ester (*R,S*)-ibuprofenate - [IleOEt][IBU]

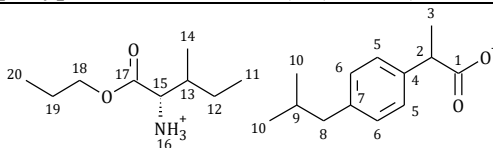
(2*S*)-1-ethoxy-3-methyl-1-oxopentane-2-aminium (2*R*)-2-[4-(2-methylpropyl)phenyl]propanoate



¹H NMR (400 MHz, CDCl₃) δ [ppm]: 7.21 (d, *J*_{5,6}= 8.2 Hz, 2H, H5), 7.07 (d, *J*_{6,5}= 8.3 Hz, 2H, H6), 5.59 (s, 3H, H16), 4.25–4.08 (m, 2H, H18), 3.69–3.59 (q, 1H, H2), 3.45 (d, *J*_{15,13}=4.5 Hz, 1H, H15), 2.43 (d, *J*_{9,8}=7.1 Hz, 2H, H8), 1.94–1.66 (m, 2H, H9, H13), 1.49–1.33 (m, 4H, H12', H3), 1.30–1.11 (m, 4H, H19, H12''), 0.93–0.84 (m, 12H, H13, H11, H10). **¹³C NMR** (100 MHz, CDCl₃) δ [ppm]: 179.31 (C1), 174.14 (C17), 140.34 (C7), 138.21 (C4), 129.25 (C6), 127.26 (C5), 60.99 (C18), 58.17 (C15), 45.53 (C2), 45.07 (C8), 38.59 (C13), 30.20 (C9), 24.87 (C12), 22.42 (C10), 18.46 (C3), 15.38 (C19), 14.24 (C11), 11.70 (C14). **FT-IR**: ν (ATR): 2357.22, 2929.92, 2867.96, 2173.45, 1740.82, 1673.53, 1612.58, 1512.59, 1464.90, 1358.01, 1364.90, 1356.92, 1304.14, 1283.32, 1255.10, 1220.69, 1167.47, 1102.58, 1091.84, 1060.53, 1027.20, 997.52, 968.46, 920.39, 881.24, 853.91, 881.24, 853.91, 800.62, 759.57, 727.00, 685.58, 635.11, 593.34, 543.05, 495.59, 459.21, 432.37 cm⁻¹.

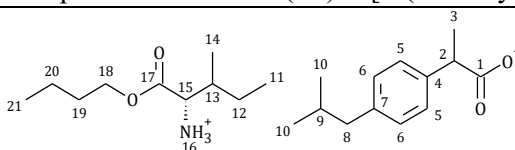
¹. $[\alpha]_D^{20} = +12.971$ (c=0.478% (m/v) in EtOH). **UV-Vis** (EtOH): $\lambda_{\max}=229.0$ nm. **Elemental analysis:** C₂₁H₃₅NO₄ (365.507 g/mol), calculated (%): C (69.01), H (9.65), N (3.83), O (17.51), found: C (69.19), H (9.61), N (3.80), O (17.33).

L-isoleucinium propyl ester (*R,S*)-ibuprofenate - [IleOPr][IBU]
 (2*S*)-3-methyl-1-oxo-1-propoxypentan-2-aminium (2*R*)-2-[4-(2-methylpropyl)phenyl]propanoate



¹H NMR (400 MHz, CDCl₃) δ [ppm]: 7.22 (d, $J_{5,6}=8.3$ Hz, 2H, H5), 7.08 (d, $J_{6,5}=8.3$ Hz, 2H, H6), 5.41 (s, 3H, H16), 4.15–3.99 (m, 2H, H18), 3.70–3.60 (m, 1H, H2), 3.46 (d, $J_{15,14}=4.5$ Hz, 1H, H15), 2.43 (d, $J_{9,8}=7.1$ Hz, 2H, H8), 1.91–1.73 (m, 2H, H13, H9), 1.71–1.58 (m, 2H, H19), 1.50–1.33 (m, 4H, H3, H12'), 1.25–1.15 (m, 1H, H12''), 0.97–0.85 (m, 15H, H21, H13, H11, H10). **¹³C NMR** (100 MHz, CDCl₃) δ [ppm]: 174.43 (C17), 140.37 (C7), 138.16 (C4), 129.26 (C6), 127.26 (C5), 66.63 (C18), 58.25 (C15), 45.48 (C2), 45.07 (C8), 38.65 (C14), 30.20 (C9), 24.84 (C12), 22.42 (C10), 21.96 (C19), 18.44 (C3), 15.44 (C20), 11.72 (C11), 10.45 (C13). **FT-IR:** ν (ATR): 2959.91, 2932.05, 2876.93, 2867.87, 2727.31, 2161.92, 1736.43, 1676.31, 1613.91, 1512.06, 1456.37, 1512.06, 1456.37, 1391.87, 1379.67, 1364.58, 1357.66, 1309.87, 1262.12, 1212.62, 1167.15, 1104.68, 1085.06, 1060.50, 1037.03, 1024.49, 1000.93, 960.49, 916.65, 883.60, 850.45, 813.57, 801.46, 790.64, 739.90, 729.61, 718.18, 688.17, 656.35, 634.61, 599.44, 571.22, 527.02, 501.37, 463.50, 432.30 cm⁻¹. $[\alpha]_D^{20} = +14.822$ (c=0.506% (m/v) in EtOH). **UV-Vis** (EtOH): $\lambda_{\max}=228.0$ nm. **Elemental analysis:** C₂₂H₃₇NO₄ (379.533 g/mol), calculated (%): C (69.62), H (9.83), N (3.69), O (16.86); found: C (69.55), H (9.80), N (3.61), O (16.79).

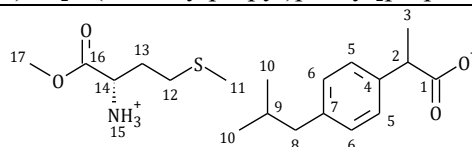
L-isoleucinium butyl ester (*R,S*)-ibuprofenate - [IleOBu][IBU]
 (2*S*)-1-butoxy-3-methyl-1-oxopentan-2-aminium (2*R*)-2-[4-(2-methylpropyl)phenyl]propanoate



¹H NMR (400 MHz, CDCl₃) δ [ppm]: 7.21 (d, $J_{5,6}=8.1$ Hz, 2H, H5), 7.07 (d, $J_{6,5}=8.0$ Hz, 2H, H6), 5.53 (s, 3H, H16), 4.19–4.03 (m, 2H, H18), 3.69–3.60 (m, 1H, H2), 3.47 (d, $J_{15,14}=4.5$ Hz, 1H, H15), 2.43 (d, $J_{9,8}=7.1$ Hz, 2H, H8), 1.91–1.73 (m, 2H, H13, H9), 1.67–1.55 (m, 2H, H19), 1.46 (d, $J_{13,12}=7.1$ Hz, 3H, H3), 1.43–1.31 (m, 3H, H20, H12'), 1.26–1.13 (m, 1H, H12''), 0.97–0.84 (m, 15H, H21, H13, H11, H10). **¹³C NMR** (100 MHz, CDCl₃) δ [ppm]: 179.31 (C1), 174.22 (C17), 140.36 (C7), 138.18 (C4), 129.26 (C6), 127.26 (C5), 64.92 (C18), 58.19 (C15), 45.50 (C2), 45.07 (C8), 38.55 (C14), 30.60 (C9), 30.20 (C12), 24.86 (C19), 22.42 (C10), 19.14 (20), 18.45 (C3), 15.41 (C21), 13.67 (C11), 11.71 (C13). **FT-IR:** ν (ATR): 2957.84, 2929.54, 2868.66, 2845.39, 2618.44, 2182.62, 1738.84, 1672.76, 1612.14, 1543.28, 1512.57, 1454.44, 1393.21, 1366.34, 1356.92, 1318.08,

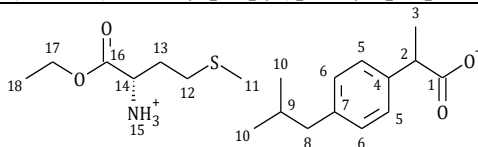
1288.48, 1244.32, 1207.81, 1168.24, 1115.37, 1104.70, 1087.62, 1027.33, 999.66, 950.08, 950.08, 896.99, 880.72, 848.94, 821.13, 801.94, 792.94, 765.79, 786.52, 729.18, 988.45, 634.15, 599.45, 575.00, 554.89, 526.89, 501.96, 462.60, 424.31 cm⁻¹. [α]_D²⁰ = +13.393 (c=0.576% (m/v) in EtOH). **UV–Vis** (EtOH): λ_{max} =229.0 nm. **Elemental analysis:** C₂₃H₃₉NO₄ (393.560 g/mol), calculated (%): C (70.19), H (9.99), N (3.56), O (16.26); found: C (70.05), H (9.91), N (3.52), O (16.13).

L-methioninium methyl ester (*R,S*)-ibuprofenate - [MetOMe][IBU]
 (2*S*)-1-methoxy-4-(methylsulfanyl)-1-oxobutan-2-aminium
 (2*R*)-2-[4-(2-methylpropyl)phenyl]propanoate



¹H NMR (400 MHz, CDCl₃) δ [ppm]: 7.22 (d, $J_{5,6}$ =7.9 Hz, 2H, H5), 7.09 (d, $J_{6,5}$ =8.6 Hz, 2H, H6), 5.00 (s, 3H, H15), 3.73 (s, 3H, H17), 3.71–3.62 (m, 2H, H14, H2), 2.53 (t, $J_{12,13}$ =8.0 Hz, 2H, H12), 2.44 (d, $J_{8,9}$ =7.2 Hz, 2H, H8), 2.08 (s, 3H, H11), 2.11–1.98 (m, 1H, H13'), 1.91–1.76 (m, 2H, H13''), H9), 1.48 (d, $J_{2,3}$ =7.2 Hz, 3H, H3), 0.92–0.86 (2d, 6H, H10). **¹³C NMR** (100 MHz, CDCl₃) δ [ppm]: 179.40 (C1), 175.45 (C16), 140.58 (C7), 137.75 (C4), 129.34 (C6), 127.26 (C5), 52.85 (C17), 52.31 (C14), 45.24 (C2), 45.06 (C8), 33.22 (C9), 30.25 (C12), 30.20 (C13), 22.42 (C1), 18.33 (C3), 15.33 (C11). **FT–IR:** ν (ATR): 3026.01, 2953.08, 2916.97, 2867.42, 2846.14, 2177.48, 2162.16, 1746.68, 1675.89, 1614.29, 1545.20, 1510.45, 1462.89, 1450.70, 1437.93, 1389.68, 1359.53, 1310.32, 1288.39, 1225.37, 1184.86, 1165.12, 1121.64, 1062.28, 1020.49, 1002.79, 974.94, 950.66, 880.82, 854.41, 835.88, 817.94, 799.42, 754.44, 728.77, 692.46, 634.91, 586.30, 547.32, 509.73, 486.40, 433.59, 409.85 cm⁻¹. [α]_D²⁰ = +5.421 (c=0.535% (m/v) in EtOH). **UV–Vis** (EtOH): λ_{max} =228.6 nm. **Elemental analysis:** C₁₉H₃₁NO₄S (369.519 g/mol), calculated (%): C (61.76), H (8.46), N (3.79), O (17.32), S (8.68) found: C (61.70), H (8.37), N (3.61), O (17.29), S (8.55).

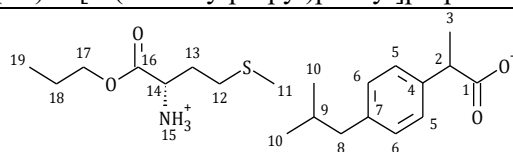
L-methioninium ethyl ester (*R,S*)-ibuprofenate - [MetOEt][IBU]
 (2*S*)-1-ethoxy-4-(methylsulfanyl)-1-oxobutan-2-aminium
 (2*R*)-2-[4-(2-methylpropyl)phenyl]propanoate



¹H NMR (400 MHz, CDCl₃) δ [ppm]: 7.21 (d, $J_{5,6}$ =8.6 Hz, 2H, H5), 7.08 (d, $J_{6,5}$ =7.6 Hz, 2H, H6), 5.50 (s, 3H, H15), 4.23–4.12 (m, 2H, H17), 3.70–3.60 (m, 2H, H14, H2), 2.57 (t, $J_{12,13}$ =8.0 Hz, 2H), 2.44 (d, $J_{8,9}$ =7.2 Hz, 2H, H8), 2.07 (s, 3H, H11), 2.05–1.99 (m, 1H, H13'), 1.92–1.76 (m, 2H, H13''), H9), 1.46 (d, $J_{2,3}$ =7.2 Hz, 3H, H3), 1.27 (t, $J_{17,18}$ =7.1 Hz, 3H, H18), 0.86–0.90 (2d, 6H, H10). **¹³C NMR** (100 MHz, CDCl₃) δ [ppm]: 179.35 (C1), 174.70 (C16), 140.47 (C7), 137.92 (C4), 129.30 (C6), 127.26 (C5), 61.36 (C17), 52.89 (C14), 45.35 (C2), 45.06 (C8), 33.15 (C9), 30.23 (C12), 30.19 (C13), 22.42 (C1), 18.37 (C3), 15.30 (C11), 14.20 (C18). **FT–IR:** ν (ATR): 2953.87, 2920.58,

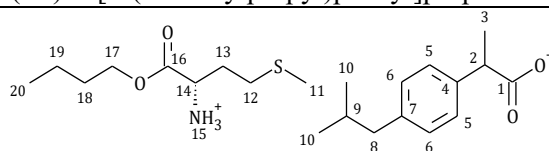
2867.13, 2630.70, 1742.46, 1677.76, 1615.21, 1552.77, 1511.36, 1463.11, 1451.01, 1388.15, 1357.25, 1287.85, 1263.27, 1216.61, 1164.31, 1121.66, 1094.92, 1062.19, 1031.87, 1019.71, 1006.97, 956.63, 920.67, 881.30, 854.38, 816.87, 798.57, 754.17, 728.79, 694.29, 650.34, 635.49, 546.99, 484.41, 442.90, 413.08 cm⁻¹. $[\alpha]_D^{20} = +4.669$ (c=0.514% (m/v) in EtOH). **UV-Vis** (EtOH): λ_{\max} =228.6 nm. **Elemental analysis:** C₂₀H₃₃NO₄S (383.545 g/mol), calculated (%): C (62.63), H (8.67), N (3.65), O (16.69), S (8.36) found: C (62.79), H (8.61), N (3.57), O (16.53), S (7.76).

L-methioninium propyl ester (*R,S*)-ibuprofenate - [MetOPr][IBU]
 (2*S*)-4-(methylsulfanyl)-1-oxo-1-propoxybutan-2-aminium
 (2*R*)-2-[4-(2-methylpropyl)phenyl]propanoate



¹H NMR (400 MHz, CDCl₃) δ [ppm]: 7.22 (d, $J_{5,6}$ =8.1 Hz, 2H, H5), 7.09 (d, $J_{6,5}$ =8.1 Hz, 2H, H6), 5.09 (s, 3H, H15), 4.14–4.02 (m, 2H, H17), 3.71–3.61 (m, 2H, H2, H14), 2.58 (t, $J_{12,13}$ =7.4 Hz, 2H, H12), 2.44 (d, $J_{8,9}$ =7.1 Hz, 2H, H8), 2.07 (s, 3H, H11), 2.05–1.98 (m, 1H, H13'), 1.92–1.76 (m, 2H, H13'', H9), 1.73–1.59 (m, 2H, H18), 1.47 (d, $J_{3,2}$ =7.2 Hz, 3H, H3), 0.94 (t, J =7.4 Hz, 3H, H19), 0.89–0.96 (2d, 6H, H10). **¹³C NMR** (100 MHz, CDCl₃) δ [ppm]: 179.40 (C1), 174.93 (C16), 140.54 (C7), 137.80 (C4), 129.32 (C6), 127.26 (C5), 66.91 (C17), 52.93 (C14), 45.27 (C2), 45.06 (C8), 33.25 (C9), 30.25 (C12), 30.19 (C13), 22.42 (C10), 21.95 (C3), 18.34 (C18), 15.30 (C11), 10.39 (C19). **FT-IR:** ν (ATR): 3048.40, 2963.39, 2921.81, 2864.81, 1740.72, 1677.99, 1606.37, 1548.36, 1512.08, 1459.39, 1420.61, 1390.22, 1366.12, 1354.33, 1312.62, 1284.67, 1216.77, 1196.11, 1165.40, 1119.213, 1007.64, 993.09, 977.16, 956.76, 938.92, 919.33, 908.22, 880.86, 844.50, 808.74, 781.38, 755.70, 728.31, 709.21, 692.60, 645.95, 636.43, 624.89, 606.04, 567.16, 548.06, 529.80, 506.09, 477.71, 429.96 cm⁻¹. $[\alpha]_D^{20} = +3.808$ (c=0.499% (m/v) in EtOH). **UV-Vis** (EtOH): λ_{\max} =228.8 nm. **Elemental analysis:** C₂₁H₃₅NO₄S (397.572 g/mol), calculated (%): C (63.44), H (8.87), N (3.52), O (16.10), S (8.07) found: C (63.27), H (8.85), N (3.49), O (16.09), S (7.98).

L-methioninium butyl ester (*R,S*)-ibuprofenate - [MetOBu][IBU]
 (2*S*)-1-butoxy-4-(methylsulfanyl)-1-oxobutan-2-aminium
 (2*R*)-2-[4-(2-methylpropyl)phenyl]propanoate

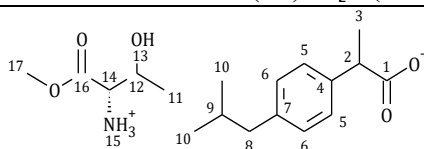


¹H NMR (400 MHz, CDCl₃) δ [ppm]: 7.22 (d, $J_{5,6}$ =8.6 Hz, 2H, H5), 7.09 (d, $J_{6,5}$ =8.1 Hz, 2H, H6), 4.87 (s, 3H, H15), 4.18–4.08 (m, 2H, H17), 3.72–3.61 (m, 2H, H2, H14), 2.58 (t, $J_{12,13}$ =8.1, 2H, H12), 2.44 (d, $J_{8,9}$ =7.2 Hz, 2H, H8), 2.08 (s, 3H, H11), 2.06–1.98 (m, 1H, H13'), 1.91–1.76 (m, 2H, H13'', H9), 1.70–1.57 (m, 2H, H18), 1.47 (d, $J_{2,3}$ =7.2 Hz, 3H, H3), 1.45–1.31 (m, 2H, H19), 0.94 (t, $J_{19,20}$ =7.4 Hz, 3H, H20), 0.89 (2d, 6H, H10). **¹³C NMR** (100 MHz, CDCl₃) δ [ppm]: 179.35 (C1),

175.07 (C16), 140.57 (C7), 137.74 (C4), 129.33 (C6), 127.26 (C5), 65.18 (C17), 52.98 (C14), 45.23 (C2), 45.06 (C8), 33.33 (C9), 30.60 (C18), 30.28 (C12), 30.19 (C13), 22.42 (C10), 19.12 (C3), 18.33 (C19), 15.32 (C11), 13.70 (C20). **FT-IR:** ν (ATR): 2962.13, 2928.67, 2865.39, 2843.66, 1741.17, 1677.30, 1607.88, 1548.17, 1511.63, 1460.50, 1420.04, 1365.6, 1354.24, 1310.25, 1284.12, 1265.21, 1239.88, 1214.29, 1194.17, 1166.42, 1119.80, 1082.55, 1064.05, 1037.08, 1019.88, 1006.58, 993.08, 961.69, 949.27, 880.12, 845.09, 813.60, 781.15, 753.84, 729.14, 629.87, 645.28, 636.51, 567.12, 549.44, 529.74, 505.84, 483.94, 430.42 cm^{-1} . $[\alpha]_D^{20} = +3.231$ ($c=0.588\%$ (m/v) in EtOH). **UV-Vis** (EtOH): $\lambda_{\text{max}}=228.6$ nm. **Elemental analysis:** $\text{C}_{21}\text{H}_{35}\text{NO}_4\text{S}$ (411.598 g/mol), calculated (%): C (64.20), H (9.06), N (3.40), O (15.55), S (7.79) found: C (64.18), H (9.00), N (3.40), O (15.49), S (7.70).

L-threoninium methyl ester (*R,S*)-ibuprofenate - [ThrOMe][IBU]

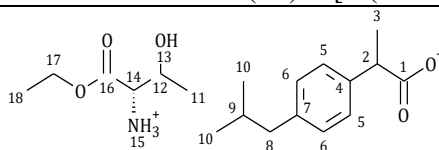
(2*S*)-3-hydroxy-1-methoxy-1-oxobutan-2-aminium (2*R*)-2-[4-(2-methylpropyl)phenyl]propanoate



^1H NMR (400 MHz, CDCl_3) δ [ppm]: 7.20 (d, $J_{5,6}=8.2$ Hz, 2H, H5), 7.06 (d, $J_{6,5}=7.9$ Hz, 2H, H6), 5.90 (s, 3H, H15), 4.03–3.92 (m, 1H, H13), 3.70 (s, 3H, H17), 3.71–3.58 (m, 1H, H12), 3.36 (d, $J_{14,12}=5.0$ Hz, 1H, H14), 2.43 (d, $J_{8,9}=7.2$ Hz, 2H, H8), 1.90–1.76 (m, 1H, H9), 1.44 (d, $J_{11,12}=7.2$ Hz, 3H, H11), 1.19 (d, $J_{2,3}=6.4$ Hz, 3H, H3), 0.95–0.81 (2d, 6H, H10). **^{13}C NMR** (100 MHz, CDCl_3) δ [ppm]: 180.14 (C1), 172.54 (C16), 140.36 (C7), 138.33 (C4), 129.25 (C6), 127.30 (C5), 67.44 (C17), 59.32 (C12), 52.59 (C14), 45.81 (C2), 45.05 (C8), 30.21 (C9), 22.42 (C10), 19.87 (C3), 18.49 (C11). **FT-IR:** ν (ATR): 3049.51, 3022.10, 2952.35, 2927.74, 2867.88, 2846.66, 2647.60, 2359.46, 2054.69, 2042.40, 1747.15, 1704.49, 1666.07, 1511.82, 1460.06, 1436.40, 1422.24, 1391.60, 1359.15, 1327.29, 1305.55, 1279.73, 1259.10, 1224.13, 1183.38, 1166.75, 1118.59, 1068.56, 1021.75, 1006.57, 986.79, 965.42, 920.65, 883.60, 859.79, 845.79, 799.76, 792.84, 747.50, 731.76, 679.44, 634.63, 623.58, 609.28, 564.69, 547.81, 489.70, 447.13, 430.62 cm^{-1} . $[\alpha]_D^{20} = +0.430$ ($c=0.465\%$ (m/v) in EtOH). **UV-Vis** (EtOH): $\lambda_{\text{max}}=228.8$ nm. **Elemental analysis:** $\text{C}_{18}\text{H}_{29}\text{NO}_5$ (339.427 g/mol), calculated (%): C (63.69), H (8.61), N (4.13), O (23.57), found: C (63.60), H (8.57), N (4.20), O (23.41).

L-threoninium ethyl ester (*R,S*)-ibuprofenate - [ThrOEt][IBU]

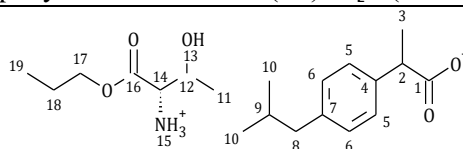
(2*S*)-1-ethoxy-3-hydroxy-1-oxobutan-2-aminium (2*R*)-2-[4-(2-methylpropyl)phenyl]propanoate



^1H NMR (400 MHz, CDCl_3) δ [ppm]: 7.24 (d, $J_{5,6}=7.8$ Hz, 2H, H5), 7.07 (d, $J_{6,5}=7.9$ Hz, 2H, H6), 5.20 (s, 3H, H15), 4.26–4.14 (m, 2H, H17), 4.01–3.91 (m, 1H, H12), 3.70–3.60 (m, 1H, H13), 3.33

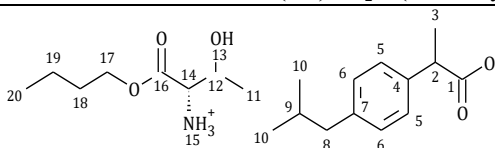
(d, 1H, $J_{14,12}=5.2$ Hz, 1H, H14), 2.43 (d, $J_{7,8}=7.2$ Hz, 2H, H8), 1.89–1.76 (m, 1H, H9), 1.46 (d, $J_{11,12}=7.2$ Hz, 3H, H11), 1.27 (t, $J_{18,17}=7.1$ Hz, 3H, H18), 1.23 (d, $J_{3,2}=6.4$ Hz, 3H, H3), 0.96–0.89 (2d, 6H, H10). ^{13}C NMR (100 MHz, CDCl_3) δ [ppm]: 179.76 (C1), 172.95 (C16), 140.45 (C7), 137.93 (C4), 129.26 (C6), 127.25 (C5), 67.84 (C17), 61.53 (C13), 59.52 (C14), 45.44 (C2), 45.03 (C8), 30.16 (C9), 22.38 (C10), 19.85 (C3), 18.36 (C12), 14.11 (C11). **FT-IR**: ν (ATR): 2953.43, 2927.49, 2867.94, 2080.10, 1743.26, 1511.58, 1460.17, 1382.89, 1364.60, 1286.60, 1218.50, 1184.90, 1546.45, 1115.11, 1058.09, 1021.39, 911.21, 882.47, 854.60, 786.48, 754.13, 725.51, 667.02, 634.41, 548.55, 484.36, 413.36 cm^{-1} . $[\alpha]_D^{20} = -0.795$ ($c=0.503\%$ (m/v) w EtOH). **UV-Vis** (EtOH): $\lambda_{\text{max}}=228.8$ nm. **Elemental analysis**: $\text{C}_{19}\text{H}_{31}\text{NO}_5$ (353.453 g/mol). calculated (%): C (64.56), H (8.84), N (3.96), O (22.63), found: C (64.49), H (8.71), N (3.80), O (22.52).

L-threoninium propyl ester (*R,S*)-ibuprofenate - [ThrOPr][IBU]
 (2*S*)-3-hydroxy-1-oxo-1-propoxybutan-2-aminium (2*R*)-2-[4-(2-methylpropyl)phenyl]propanoate



^1H NMR (400 MHz, CDCl_3) δ [ppm]: 7.20 (d, $J_{5,6}=8.9$ Hz, 2H, H5), 7.07 (d, $J_{6,5}=6.3$ Hz, 2H, H6), 5.12 (s, 3H, H15), 4.14–4.05 (m, 2H, H17), 3.99–3.91 (m, 1H, H12), 3.68–3.57 (m, 1H, H11), 3.33 (d, $J_{14,15}=5.2$ Hz, 1H, H14), 2.43 (d, $J_{8,7}=7.1$ Hz, 2H, H8), 1.91–1.76 (m, 1H, H9), 1.73–1.60 (m, 2H, H18), 1.45 (d, $J_{11,12}=7.1$ Hz, 3H, H11), 1.22 (d, $J_{3,2}=6.4$ Hz, 3H, H3), 0.94 (d, $J_{19,18}=7.5$ Hz, 3H, H19), 0.91–0.84 (2d, 6H, H10). ^{13}C NMR (100 MHz, CDCl_3) δ [ppm]: 179.78 (C1), 172.98 (C16), 140.38 (C7), 138.22 (C4), 129.26 (C6), 127.28 (C5), 67.86 (C17), 67.15 (C12), 59.58 (C14), 45.65 (C2), 45.06 (C8), 30.19 (C9), 22.42 (C18), 21.89 (C10), 19.91 (C3), 18.47 (C11), 10.36 (C10). **FT-IR**: ν (ATR): 3013.75, 2978.83, 2954.61, 2925.50, 2868.51, 2086.04, 1743.13, 1548.20, 1511.69, 1460.11, 1383.37, 1364.43, 1286.47, 1217.62, 1185.28, 1117.18, 1059.25, 1021.60, 1001.42, 920.64, 883.41, 851.78, 786.33, 754.30, 727.09, 666.19, 634.03, 596.46, 547.87, 424.33 cm^{-1} . $[\alpha]_D^{20} = -1.679$ ($c=0.536\%$ (m/v) in EtOH). **UV-Vis** (EtOH): $\lambda_{\text{max}}=228.3$ nm. **Elemental analysis**: $\text{C}_{20}\text{H}_{33}\text{NO}_5$ (367.480 g/mol), calculated (%): C (65.37), H (9.05), N (3.81), O (21.77); found: C (64.36); H (9.01); N (3.79); O (21.79).

L-threoninium butyl ester (*R,S*)-ibuprofenate - [ThrOBu][IBU]
 (2*S*)-1-butoxy-3-hydroxy-1-oxobutan-2-aminium (2*R*)-2-[4-(2-methylpropyl)phenyl]propanoate

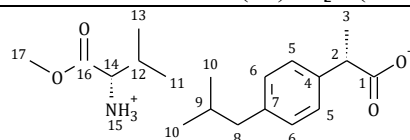


^1H NMR (400 MHz, CDCl_3) δ [ppm]: 7.21 (d, $J_{5,6}=8.1$ Hz, 2H, H5), 7.08 (d, $J_{6,5}=8.1$ Hz, 2H, H6), 5.24 (s, 4H, H15, H13), 4.20–4.09 (m, 2H, H17), 4.00–3.90 (m, 1H, H12), 3.70–3.60 (m, 1H, H11), 3.33 (d, $J_{14,15}=5.2$ Hz, 1H, H14), 2.43 (d, $J_{8,7}=7.2$ Hz, 2H, H8), 1.89–1.76 (m, 1H, H9), 1.69–1.57

(m, 2H, H18), 1.46 (d, $J_{11,12}=7.1$ Hz, 3H, H11), 1.44–1.31 (m, 2H, H19), 1.23 (d, $J_{3,2}=6.4$ Hz, 3H, H3), 0.98–0.86 (m, 9H, H20, H10). **^{13}C NMR** (100 MHz, CDCl_3) δ [ppm]: 179.83 (C1), 173.12 (C16), 140.50 (C7), 137.94 (C4), 129.30 (C6), 127.28 (C5), 67.90 (C17), 65.44 (C12), 59.58 (C14), 45.46 (C2), 45.06 (C8), 30.54 (C9), 30.19 (C18), 22.42 (C19), 19.91 (C10), 19.10 (C3), 18.39 (C11), 13.68 (C20). **FT-IR**: ν (ATR): 2955.34, 2930.45, 2930.45, 2072.04, 1742.03, 1550.59, 1511.43, 1459.70, 1383.22, 1364.73, 1285.74, 1216.36, 1117.40, 1060.97, 1021.30, 919.47, 883.51, 846.11, 785.85, 754.67, 727.18, 665.67, 633.50, 596.62, 548.13, 465.86, 431.14, 412.85 cm^{-1} . $[\alpha]_D^{20} = -1.737$ ($c=0.518\%$ (m/v) in EtOH). **UV-Vis** (EtOH): $\lambda_{\text{max}}=228.7$ nm. **Elemental analysis**: $\text{C}_{21}\text{H}_{35}\text{NO}_5$ (381.506 g/mol). calculated (%): C (66.11), H (9.25), N (3.67), O (20.97), found: C (66.15), H (9.13), N (3.65), O (20.67).

L-valinium methyl ester *S*-(+)-ibuprofenate - [ValOMe][*S*(+)-IBU]

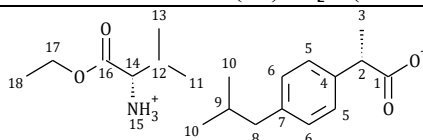
(2*S*)-1-methoxy-3-methyl-1-oxobutan-2-aminium (2*S*)-2-[4-(2-methylpropyl)phenyl]propanoate



^1H NMR (400 MHz, CDCl_3) δ [ppm]: 7.21 (d, $J_{5,6}=8.1$ Hz, 2H, H5), 7.06 (d, $J_{6,5}=8.1$ Hz, 2H, H6), 5.75 (s, 3H, H15), 3.69 (s, 3H, H17), 3.67–3.58 (q, 1H, H2), 3.40 (d, $J_{14,15}=4.6$ Hz, 1H, H14), 2.42 (d, $J_{8,9}=7.1$ Hz, 2H, H8), 2.11–1.98 (m, 1H, H12), 1.90–1.76 (m, 1H, H9), 1.43 (d, $J_{3,2}=7.1$ Hz, 3H, H3), 0.97–0.81 (m, 12H, H13, H11, H10). **^{13}C NMR** (100 MHz, CDCl_3) δ [ppm]: 179.31 (C1), 174.21 (C16), 140.19 (C7), 138.54 (C4), 129.19 (C5), 127.28 (C6), 59.01 (C17), 52.02 (C14), 45.76 (C8), 45.06 (C2), 31.45 (C12), 30.20 (C9), 22.41 (C10), 18.74 (C13), 18.55 (C3), 17.37 (C11). **FT-IR**: ν (ATR): 2965.41, 2954.34, 2929.03, 2867.37, 2844.34, 2726.65, 2614.94, 2187.96, 1740.44, 1704.20, 1621.22, 1578.28, 1510.06, 1461.34, 1433.53, 1421.55, 1394.31, 1379.14, 1363.87, 1326.02, 1284.60, 1263.55, 1227.18, 1202.92, 1171.20, 1107.39, 1080.04, 1063.01, 1050.82, 1021.96, 992.56, 927.27, 882.38, 850.15, 812.88, 800.44, 793.20, 767.82, 754.18, 740.16, 726.94, 679.36, 595.13, 539.62, 487.65, 469.95, 427.66 cm^{-1} . $[\alpha]_D^{20} = +43.487$ ($c=0.522\%$ (m/v) in EtOH). **UV-Vis** (EtOH): $\lambda_{\text{max}}=223.0$ nm. **Elemental analysis**: $\text{C}_{20}\text{H}_{33}\text{NO}_4$ (337.458 g/mol), calculated (%): C (67.63), H (9.26), N (4.15), O (18.96), found: C (69.28), H (9.46), N (4.18), O (18.95).

L-valinium ethyl ester *S*-(+)-ibuprofenate - [ValOEt][*S*(+)-IBU]

(2*S*)-1-ethoxy-3-methyl-1-oxobutan-2-aminium (2*S*)-2-[4-(2-methylpropyl)phenyl]propanoate

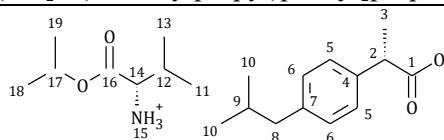


^1H NMR (400 MHz, CDCl_3) δ [ppm]: 7.20 (d, $J_{5,6}=8.1$ Hz, 2H, H5), 7.05 (d, $J_{6,5}=7.7$ Hz, H6), 5.73 (s, 3H, H15), 4.25–4.08 (m, 2H, H17), 3.68–3.58 (q, 1H, H2), 3.39 (d, $J_{14,12}=4.6$ Hz, 1H, H14), 2.42 (d, $J_{8,7}=7.1$ Hz, 2H, H8), 2.12–1.99 (m, 1H, H12), 1.90–1.76 (m, 1H, H9), 1.44 (d, $J_{3,2}=7.2$ Hz, 3H, H3),

H3), 1.25 (t, $J_{18,19}=7.1$ Hz, H18), 0.92 (d, $J_{13,12}=6.9$ Hz, 3H, H13); 0.92–0.85 (m, 9H, H11, H10). **^{13}C NMR** (100 MHz, CDCl_3) δ [ppm]: 179.27 (C1), 173.82 (C16), 140.23 (C7), 138.46 (C4), 129.21 (C5), 127.27 (C6), 61.07 (C17), 58.99 (C14), 45.70 (C8), 45.07 (C2), 31.47 (C12), 30.20 (C9), 22.42 (C10), 18.76 (C13), 18.52 (C3), 17.30 (C11), 14.22 (C18). **FT-IR**: ν (ATR): 2965.60, 2952.69, 2927.46, 2867.68, 2846.77, 2659.37, 2192.95, 1740.86, 1703.12, 1619.86, 1581.74, 1509.28, 1460.28, 1420.84, 1381.04, 1362.56, 1328.32, 1287.83, 1254.14, 1224.98, 1205.67, 1153.85, 1115.43, 1088.03, 1057.88, 1020.54, 1004.10, 881.81, 855.64, 814.20, 800.25, 755.52, 727.32, 717.46, 688.27, 636.22, 595.22, 546.63, 522.03, 465.34, 429.55, 401.14 cm^{-1} . $[\alpha]_D^{20} = +38.021$ (c=0.576% (m/v) w EtOH). **UV-Vis** (EtOH): $\lambda_{\text{max}}=223.0$ nm. **Elemental analysis**: $\text{C}_{20}\text{H}_{33}\text{NO}_4$ (351.485 g/mol). calculated (%): C (68.34), H (9.46), N (3.99), O (18.21), found: C (68.72), H (9.31), N (4.07), O (18.10).

L-valinium isopropyl ester *S*-(+)-ibuprofenate - [ValOiPr][*S*(+)-IBU]

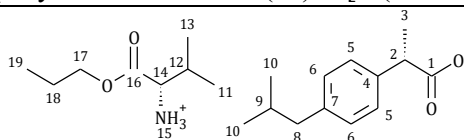
(2*S*)-3-methyl-1-oxo-1-[(propan-2-yl)oxy]butan-2-aminium
(2*S*)-2-[4-(2-methylpropyl)phenyl]propanoate



^1H NMR (400 MHz, CDCl_3) δ [ppm]: 7.20 (d, $J_{5,6}=8.5$ Hz, 2H, H5), 7.06 (d, $J_{6,5}=7.8$ Hz, H6), 6.04 (s, 3H, H15), 5.10–4.96 (m, 1H, H17), 3.67–3.57 (q, 1H, H2), 3.36 (d, $J_{14,12}=4.4$ Hz, 1H, H14), 2.42 (d, $J_{8,9}=7.1$ Hz, 2H, H8), 2.11–1.98 (m, 1H, H12), 1.89–1.76 (m, 1H, H9), 1.43 (d, $J_{3,2}=7.3$ Hz, 3H, H3), 1.23 (2d, dd, $J_{19,17}=6.1$ Hz, $J_{18,17}=6.0$ Hz, 6H, H19, H18), 0.95–0.84 (m, 12H, H13, H11, H10). **^{13}C NMR** (100 MHz, CDCl_3) δ [ppm]: 179.16 (C1), 173.16 (C16), 140.06 (C4), 138.66 (C7), 129.13 (C5), 127.25 (C6), 68.71 (C17), 58.91 (C14), 45.79 (C8), 45.04 (C2), 31.37 (C12), 30.15 (C9), 22.38 (C10), 21.74 (C18), 21.74 (C19), 18.65 (C13), 18.56 (C3), 17.25 (C11). **FT-IR**: ν (ATR): 3024.48, 2967.27, 2952.54, 2934.35, 2901.79, 2868.71, 2839.07, 2603.72, 2195.02, 1740.10, 1619.66, 1578.47, 1503.45, 1462.87, 1416.87, 1383.27, 1367.70, 1330.49, 1288.25, 1228.16, 1189.25, 1178.05, 1145.17, 1104.26, 1068.30, 1051.98, 1019.06, 1008.03, 962.10, 915.96, 893.27, 877.70, 846.31, 825.62, 806.77, 784.70, 773.62, 755.81, 699.57, 669.94, 638.98, 588.32, 522.03, 486.67, 433.42, 417.79, 401.14 cm^{-1} . $[\alpha]_D^{20} = +35.945$ (c=0.587% (m/v) in EtOH). **UV-Vis** (EtOH): $\lambda_{\text{max}}=225.0$ nm. **Elemental analysis**: $\text{C}_{21}\text{H}_{35}\text{NO}_4$ (365.512 g/mol), calculated (%): C (69.01), H (9.65), N (3.85), O (17.51), found: C (69.48), H (9.66), N (4.02), O (17.47).

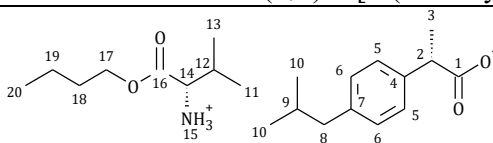
L-valinium propyl ester *S*-(+)-ibuprofenate - [ValOPr][*S*(+)-IBU]

(2*S*)-3-methyl-1-oxo-1-propoxybutan-2-aminium (2*S*)-2-[4-(2-methylpropyl)phenyl]propanoate



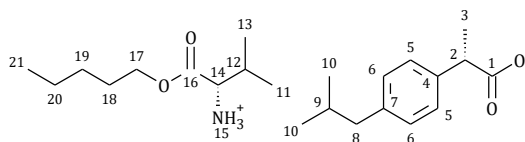
¹H NMR (400 MHz, CDCl₃) δ [ppm]: 7.20 (d, *J*_{5,6}=8.0 Hz, 2H, H5), 7.06 (d, *J*_{6,5}=8.0 Hz, 2H, H6), 6.27 (s, 3H, H15), 4.14–3.98 (m, 2H, H17), 3.65–3.58 (m, 1H, H2), 3.41 (d, *J*_{14,12}=4.6 Hz, 1H, H14), 2.43 (d, *J*_{8,9}=7.2 Hz, 2H, H8), 2.12–1.99 (m, 1H, H12), 1.89–1.76 (m, 1H, H9), 1.72–1.56 (m, 2H, H18), 1.44 (d, *J*_{3,2}=7.1 Hz, 3H, H3), 1.04–0.75 (m, 15H, H13, H11, H10, H9). **¹³C NMR** (100 MHz, CDCl₃) δ [ppm]: 179.37 (C1), 173.62 (C16), 140.15 (C7), 138.58 (C4), 129.18 (C5), 127.28 (C6), 66.78 (C17), 58.91 (C14), 45.79 (C8), 45.08 (C2), 31.36 (C12), 30.20 (C9), 22.42 (C10), 21.93 (C18), 18.62 (C13), 17.36 (C11), 10.41 (C19). **FT-IR**: ν (ATR): 2966.30, 2930.74, 2908.92, 2868.54, 2842.33, 2684.98, 2200.92, 1741.30, 1704.54, 1619.00, 1581.58, 1495.72, 1459.48, 1417.83, 1386.64, 1359.76, 1328.87, 1318.16, 1289.01, 1247.72, 1227.03, 1213.11, 1150.40, 1116.97, 1087.07, 1061.52, 1023.57, 1002.35, 969.24, 928.96, 903.78, 881.15, 848.43, 825.12, 812.03, 786.85, 777.16, 756.01, 694.21, 635.91, 596.22, 523.26, 466.57, 417.32 cm⁻¹. $[\alpha]_D^{20} = +39.576$ (c=0.513% (m/v) in EtOH). **UV-Vis** (EtOH): λ_{max}=229.0 nm. **Elemental analysis**: C₂₁H₃₅NO₄ (365.512 g/mol), calculated (%): C (69.01), H (9.65), N (3.85), O (17.51), found: C (70.24), H (9.72), N (3.68), O (17.27).

L-valinium butyl ester *S*-(+)-ibuprofenate - [ValOBu][*S*-(+)-IBU]
 (2*S*)-1-butoxy-3-methyl-1-oxobutan-2-aminium (*R,S*)-2-[4-(2-methylpropyl)phenyl]propanoate



¹H NMR (400 MHz, CDCl₃) δ [ppm]: 7.21 (d, *J*_{5,6}=8.1 Hz, 2H, H5), 7.05 (d, *J*_{6,5}=8.0 Hz, 2H, H6), 5.62 (s, 3H, H15), 4.19–4.01 (m, 2H, H17), 3.68–3.58 (q, 1H, H2), 3.39 (d, *J*_{14,12}=4.6 Hz, 1H, H14), 2.42 (d, *J*_{8,9}=7.2 Hz, 2H, H8), 2.12–1.98 (m, 1H, H12), 1.91–1.76 (m, 1H, H9), 1.67–1.55 (m, 2H, H18), 1.44 (d, *J*_{3,2}=7.1 Hz, 3H, H3), 1.43–1.30 (m, 2H, H19), 0.97–0.85 (m, 15H, H20, H13, H11, H10). **¹³C NMR** (100 MHz, CDCl₃) δ [ppm]: 179.25 (C1), 174.05 (C6), 140.22 (C7), 138.44 (C4), 129.21 (C5), 127.27 (C6), 64.98 (C7), 59.02 (C14), 45.70 (C8), 45.07 (C2), 31.51 (C12), 30.60 (C18), 30.20 (C9), 22.42 (C10), 19.12 (C19), 18.80 (C13), 18.53 (C3), 17.30 (C11), 13.67 (C20). **FT-IR**: ν (ATR): 3020.37, 2954.35, 2931.50, 2911.14, 2868.39, 2685.85, 2196.85, 1741.24, 1703.91, 1618.50, 1581.80, 1508.55, 1464.15, 1417.04, 1386.12, 1362.21, 1317.01, 1308.69, 1286.87, 1253.09, 1226.11, 1210.06, 1149.20, 1118.06, 1089.06, 1061.42, 1019.09, 1002.71, 961.06, 934.23, 908.37, 879.09, 854.34, 841.37, 827.00, 812.68, 786.66, 774.05, 757.77, 734.99, 709.10, 691.98, 636.12, 598.80, 524.28, 504.11, 468.37, 419.04, 404.37 cm⁻¹. $[\alpha]_D^{20} = +35.846$ (c=0.544% (m/v) in EtOH). **UV-Vis** (EtOH): λ_{max}=223.0 nm. **Elemental analysis**: C₂₂H₃₇NO₄ (379.539 g/mol), calculated (%): C (69.62), H (9.83), N (3.69), O (16.86), found: C (70.14), H (9.80), N (3.80), O (16.80).

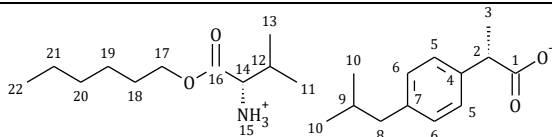
L-valinium pentyl ester *S*-(+)-ibuprofenate - [ValOAm][*S*-(+)-IBU]
 (2*S*)-3-methyl-1-oxo-1-(pentylloxy)butan-2-aminium (2*S*)-2-[4-(2-methylpropyl)phenyl]propanoate



¹H NMR (400 MHz, CDCl₃) δ [ppm]: 7.21 (d, $J_{5,6}$ =7.9 Hz, 2H, H5), 7.07 (d, $J_{6,5}$ =7.8 Hz, 2H, H6), 5.49 (s, 3H, H15), 4.19–4.02 (m, 2H, H17), 3.72–3.54 (q, 1H, H2), 3.39 (d, $J_{14,13}$ =4.5 Hz, 1H, H14), 2.43 (d, $J_{8,9}$ =7.2 Hz, 2H, H8), 2.15–1.98 (m, 1H, H12), 1.91–1.73 (m, 1H, H9), 1.93–1.53 (m, 2H, H18), 1.44 (d, $J_{3,2}$ =7.3 Hz, 3H, H3), 1.40–1.26 (m, 4H, H20, H19), 1.06–0.76 (m, 15H, H21, H13, H11, H10). **¹³C NMR** (100 MHz, CDCl₃) δ [ppm]: 179.22 (C1), 174.26 (C16), 140.28 (C7), 138.32 (C4), 129.23 (C5), 127.26 (C6), 65.22 (C17), 59.09 (C14), 45.57 (C8), 45.07 (C2), 31.58 (C12), 30.20 (C9), 28.27 (C18), 28.03 (C19), 22.42 (C10), 22.27 (C20), 18.86 (C13), 18.50 (C3), 17.27 (C11), 13.96 (C21). **FT-IR**: ν (ATR): 2955.77, 2931.51, 2870.07, 2843.45, 2648.06, 2198.10, 1740.24, 1619.95, 1582.39, 1506.54, 1460.65, 1419.67, 1386.74, 1362.73, 1328.99, 1317.27, 1288.41, 1208.13, 1167.09, 1150.46, 1115.98, 1056.55, 1020.01, 1004.77, 968.76, 879.31, 856.04, 812.39, 786.90, 726.64, 691.11, 596.26, 543.31, 520.43, 467.96, 416.89 cm⁻¹. $[\alpha]_D^{20}$ = +33.915 (c=0.516% (m/v) in EtOH). **UV-Vis** (EtOH): λ_{max}=224.0 nm. **Elemental analysis**: C₂₃H₃₉NO₄ (393.565 g/mol), calculated (%): C (70.08), H (9.99), N (3.56), O (16.26), found: C (70.90), H (10.03), N (3.77), O (16.10).

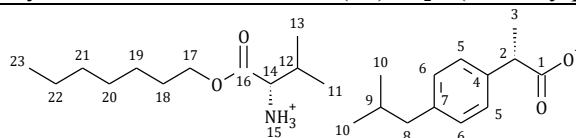
L-valinium hexyl ester S-(+)-ibuprofenate - [ValOHex][S(+)-IBU]

(2S)-1-(hexyloxy)-3-methyl-1-oxobutan-2-aminium (2S)-2-[4-(2-methylpropyl)phenyl]propanoate



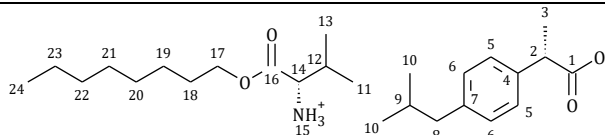
¹H NMR (400 MHz, CDCl₃) δ [ppm]: 7.21 (d, $J_{5,6}$ =7.8 Hz, 2H, H5), 7.06 (d, $J_{6,5}$ =8.1 Hz, H6), 5.74 (s, 3H, H15), 4.18–4.02 (m, 2H, H17), 3.68–3.58 (q, 1H, H2), 3.40 (d, $J_{14,12}$ =4.6 Hz, 1H, H14), 2.43 (d, $J_{8,9}$ =7.2 Hz, H2, H8), 2.12–1.99 (m, 1H, H12), 1.91–1.76 (m, 1H, H9), 1.68–1.56 (m, 2H, H18), 1.45 (d, $J_{3,2}$ =7.3 Hz, 3H, H3), 1.40–1.23 (m, 6H, H21, H20, H19), 0.94–0.87 (m, 15H, H22, H13, H11, H10). **¹³C NMR** (100 MHz, CDCl₃) δ [ppm]: 179.21 (C1), 173.94 (C16), 140.18 (C7), 138.43 (C4), 129.17 (C5), 127.24 (C6), 65.23 (C17), 58.99 (C14), 45.65 (C8), 45.04 (C2), 31.46 (C12), 31.34 (C18), 30.16 (C9), 28.50 (C19), 25.52 (C20), 22.49 (C21), 22.38 (C10), 18.75 (C13), 18.49 (C3), 17.27 (C11), 13.96 (C22). **FT-IR**: ν (ATR): 2955.25, 2927.86, 2868.63, 2664.90, 2194.08, 1741.30, 1704.08, 1619.98, 1582.23, 1508.70, 1461.69, 1419.80, 1387.39, 1363.19, 1328.99, 1318.47, 1288.93, 1255.81, 1224.34, 1210.10, 1167.27, 1116.72, 1059.22, 1021.33, 1004.17, 983.77, 918.08, 903.71, 880.70, 856.42, 813.06, 800.05, 786.91, 774.87, 756.32, 726.51, 692.97, 636.44, 597.20, 544.64, 521.00, 470.31, 429.43, 417.31 cm⁻¹. $[\alpha]_D^{20}$ = +33.650 (c=0.526% (m/v) in EtOH). **UV-Vis** (EtOH): λ_{max}=224.3 nm. **Elemental analysis**: C₂₄H₄₁NO₄ (405.576 g/mol), calculated (%): C (70.72), H (10.14), N (3.44), O (15.70), found: C (71.18), H (10.15), N (3.57), O (15.58).

L-valinium heptyl ester *S*-(+)-ibuprofenate - [ValOHept][*S*(+)-IBU]
(2*S*)-1-(heptyloxy)-3-methyl-1-oxobutan-2-aminium (2*S*)-2-[4-(2-methylpropyl)phenyl]propanoate



¹H NMR (400 MHz, CDCl₃) δ [ppm]: 7.21 (d, *J*_{5,6}=8.0 Hz, 2H, H5), 7.08 (d, *J*_{6,5}=8.1 Hz, 2H, H6), 5.46 (s, 3H, H15), 4.17–4.03 (m, 2H, H17), 3.70–3.58 (q, 1H, H2), 3.39 (d, *J*_{14,12}=4,5 Hz, 1H, H14), 2.43 (d, *J*_{8,9}=7,2 Hz, 2H, H9), 2.12–2.00 (m, 1H, H12), 1.89–1.76 (m, 1H, H8, H22, H21, H20, H18), 1.68–1.50 (m, 2H, H18), 1.46 (d, *J*_{3,2}=7,1 Hz, 3H, H3), 1.37–1.22 (m, 8H), 0.72–1.02 (m, 15H). **¹³C NMR** (100 MHz, CDCl₃) δ [ppm]: 179.23 (C1), 173.86 (C16), 140.13 (C7), 138.60 (C4), 129.17 (C5), 127.28 (C6), 65.28 (C17), 58.99 (C14), 45.77 (C8), 45.08 (C2), 31.70 (C12), 31.44 (C18), 30.19 (C9), 28.87 (C19), 28.57 (C20), 25.85 (C21), 22.58 (C22), 22.41 (C10), 18.74 (C13), 18.57 (C4), 17.33 (C11), 14.06 (C23). **FT-IR**: ν (ATR): 2959.24, 2923.48, 2859.48, 2686.08, 2090.11, 1737.37, 1701.24, 1619.06, 1582.57, 1509.77, 1464.06, 1419.14, 1387.19, 1358.24, 1316.82, 1288.78, 1254.31, 1210.38, 1165.63, 1148.23, 1116.70, 1087.08, 1059.97, 1021.84, 1003.03, 967.45, 929.90, 882.28, 854.43, 824.86, 813.27, 785.80, 773.57, 755.90, 726.58, 694.03, 636.46, 597.22, 525.26, 470.91, 429.31, 417.15 cm⁻¹. **[α]_D²⁰** = +31.250 (c=0.560% (m/v) in EtOH). **UV-Vis** (EtOH): λ_{max}=223.9 nm. **Elemental analysis**: C₂₅H₄₃NO₄ (421.619 g/mol), calculated (%): C (71.72), H (10.23), N (3.32), O (15.18), found: C (71.15), H (10.38), N (3.49), O (15.10).

L-valinium octyl ester *S*-(+)-ibuprofenate - [ValOOct][*S*(+)-IBU]
(2*S*)-3-methyl-1-(octyloxy)-1-oxobutan-2-aminium (2*S*)-2-[4-(2-methylpropyl)phenyl]propanoate

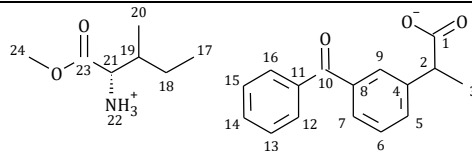


¹H NMR (400 MHz, CDCl₃) δ [ppm]: 7.21 (d, *J*_{5,6}=8.1 Hz, 2H, H5), 7.05 (d, *J*_{6,5}=8.1 Hz, 2H, H6), 6.12 (s, 3H, H15), 4.17–4.01 (m, 2H, H17), 3.66–3.55 (q, 1H, H2), 3.41 (d, *J*_{3,2}=4,5 Hz, 1H, H14), 2.43 (d, *J*_{8,9}=7.2 Hz, 2H, H8), 2.13–1.97 (m, 1H, H12), 1.92–1.74 (m, 1H, H9), 1.66–1.53 (m, 2H, H18), 1.43 (d, *J*_{3,2}=7.1 Hz, 3H, H3), 1.37–1.25 (m, 10H, H23, H22, H21, H20, H19), 0.94–0.87 (m, 15H, H24, H13, H11, H10). **¹³C NMR** (100 MHz, CDCl₃) δ [ppm]: 179.38 (C1), 173.40 (C16), 140.11 (C7), 138.72 (C4), 129.16 (C5), 127.29 (C6), 65.36 (C17), 58.86 (C14), 45.89 (C8), 45.08 (C2), 31.79 (C12), 31.30 (C18), 30.21 (C9), 29.17 (C20), 28.55 (C21), 25.88 (C22), 22.65 (C23), 22.42 (C10), 18.78 (C13), 18.64 (C3), 17.38 (C11), 14.11 (C24). **FT-IR**: ν (ATR): 2955.66, 2921.70, 2854.68, 2654.85, 2195.52, 1739.88, 1702.41, 1619.35, 1583.35, 1508.89, 1462.00, 1419.73, 1388.92, 1364.18, 1317.65, 1288.12, 1253.31, 1223.92, 1209.62, 1116.57, 1086.95, 1059.48, 1021.34, 1003.64, 965.64, 940.78, 881.63, 855.72, 813.51, 800.23, 786.14, 774.76, 755.95, 726.58, 693.15, 636.43, 596.87, 543.06, 523.64, 470.20, 415.78 cm⁻¹. **[α]_D²⁰** = +30.841 (c=0.535% (m/v) in EtOH). **UV-Vis** (EtOH): λ_{max}=223.3 nm. **Elemental analysis**: C₂₆H₄₅NO₄ (435.645 g/mol),

calculated (%): C (71.68), H (10.41), N (3.21), O (14.69), found: C (72.24), H (10.70), N (3.10), O (14.69).

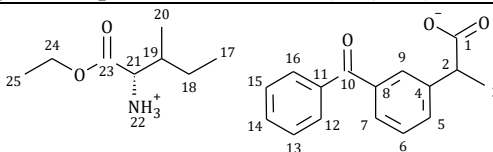
L-AMINO ACID ALKYL ESTER SALTS OF KETOPROFEN

L-isoleucinium methyl ester (*R,S*)-ketoprofenate - [IleOMe][KETO] (2*S*)-1-methoxy-3-methyl-1-oxopentan-2-aminium (*R,S*)-2-(3-benzoylphenyl)propanoate



¹H NMR (400 MHz, CDCl₃) δ [ppm]: 7.80–7.77 (m, 3H, H16, H12, H7), 7.64 (d, *J*_{9,8}=7.7 Hz, 1H, H9), 7.60–7.53 (m, 2H, H14, H13), 7.47 (d, *J*_{5,6}=7.3 Hz, 2H, H5, H15), 7.40 (t, *J*_{6,5}=7.7 Hz, 1H, H6), 6.20 (s, 3H, H22), 3.78–3.72 (m, 1H, H2), 3.70 (s, 3H, H24), 3.51 (d, *J*_{19,21}=4.5 Hz, 1H, H21), 1.89–1.66 (m, 1H, H19), 1.49 (d, *J*_{3,2}=7.1 Hz, 3H, H3), 1.43–1.32 (m, 1H, H18'), 1.25–1.13 (m, 1H, H18''), 0.92–0.83 (m, 6H, H17, H20). **¹³C NMR** (100 MHz, CDCl₃) δ [ppm]: 196.68 (C10), 178.57 (C1), 174.17 (C23), 141.61 (C8), 137.72 (C11), 137.53 (C4), 132.48 (C5), 131.77 (C14), 130.11 (C12/C16), 129.32 (C9), 128.83 (C6), 128.39 (C7), 128.30 (C13/C15), 58.05 (C24), 52.06 (C21), 45.99 (C2), 38.39 (C19), 24.86 (C18), 18.53 (C3), 15.32 (C20), 11.66 (C17). **FT-IR**: ν (ATR): 3057.34, 2966.65, 2934.32, 2876.84, 2592.70, 2102.63, 1957.56, 1957.56, 1742.21, 1655.66, 1596.42, 1577.29, 1481.78, 1447.04, 1388.37, 1358.52, 1316.96, 1279.94, 1217.10, 1178.00, 1137.83, 1074.53, 1015.65, 998.57, 964.30, 908.69, 857.32, 818.53, 750.05, 717.96, 701.52, 665.78, 641.47, 517.30, 408.14 cm⁻¹. **[α]_D²⁰** = +16.562 (c=0.634% (m/v) in EtOH). **UV-Vis** (EtOH): λ_{max}=203.1 nm. **Elemental analysis**: C₂₃H₂₉NO₅ (399.480 g/mol), calculated (%): C (69.15), H (7.32), N (3.51), O (20.03), found: C (68.97), H (7.25), N (3.45), O (19.87).

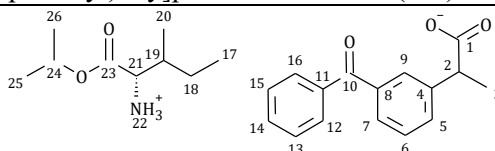
L-isoleucinium ethyl ester (*R,S*)-ketoprofenate - [IleOEt][KETO] (2*S*)-1-ethoxy-3-methyl-1-oxopentan-2-aminium (*R,S*)-2-(3-benzoylphenyl)propanoate



¹H NMR (400 MHz, CDCl₃) δ [ppm]: 7.84–7.73 (m, 3H, H16, H12, H7), 7.64 (d, *J*_{9,8}=7.7 Hz, 1H, H9), 7.62–7.50 (m, 2H, H14, H13), 7.46 (t, *J*_{5,6}=7.6 Hz, 2H, H15, H5), 7.39 (t, *J*_{6,5}=7.7 Hz, 1H, H6), 6.29 (s, 3H, H22), 4.27–4.03 (m, 2H, H24), 3.80–3.66 (m, 1H, H2), 3.50 (d, *J*_{19,21}=4.4 Hz, 1H, H21), 1.91–1.68 (m, 1H, H19), 1.49 (d, *J*_{3,2}=7.2 Hz, 3H, H3), 1.47–1.33 (m, 1H, H18'), 1.25 (t, *J*_{20,19}=7.2 Hz, 3H, H20), 1.21–1.18 (m, 1H, H18''), 0.94–0.82 (m, 6H, H25, H17). **¹³C NMR** (100 MHz, CDCl₃) δ [ppm]: 196.66 (C10), 178.52 (C1), 173.58 (C23), 141.79 (C8), 137.69 (C11), 137.55 (C4), 132.45 (C5), 131.77 (C14), 130.11 (C12/C16), 129.33 (C9), 128.76 (C6), 128.36 (C7), 128.28 (C7/C15), 61.14 (C24), 57.99 (C21), 46.11 (C2), 38.36 (C19), 24.91 (C18), 18.57 (C3), 15.30 (C20), 14.22 (C17), 11.70 (C25). **FT-IR**: ν (ATR): 3180.05, 3056.96, 2964.45, 2932.56, 2875.81, 1982.72,

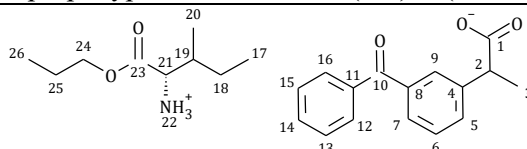
1738.23, 1656.90, 1596.07, 1575.44, 1446.94, 1384.83, 1356.82, 1316.95, 1279.35, 1217.78, 1178.32, 1138.56, 1095.82, 1074.49, 1059.50, 1024.86, 998.78, 965.22, 953.49, 908.26, 877.83, 859.24, 833.84, 777.13, 719.49, 702.78, 641.59, 524.54, 488.12, 439.05, 429.14, 418.41, 401.96 cm⁻¹. $[\alpha]_D^{20} = +14.108$ (c=0.482% (m/v) in EtOH). **UV-Vis** (EtOH): $\lambda_{\max}=202.5$ nm. **Elemental analysis:** C₂₄H₃₁NO₅ (413.507 g/mol), calculated (%): C (69.71), H (7.56), N (3.93), O (19.35), found: C (69.51), H (7.40), N (3.87), O (19.23).

L-isoleucinium isopropyl ester (*R,S*)-ketoprofenate - [IleOiPr][KETO]
 (2*S*)-3-methyl-1-oxo-1-[(propan-2-yl)oxy]pentan-2-aminium (*R,S*)-2-(3-benzoylphenyl)propanoate



¹H NMR (400 MHz, CDCl₃) δ [ppm]: 7.83–7.77 (m, 3H, H16, H12, H7), 7.65 (d, $J_{9,8}=7.7$ Hz, 1H, H9), 7.62–7.52 (m, 2H, H14, H13), 7.47 (t, $J_{6,5}=7.7$ Hz, 2H, H15, H5), 7.41 (t, $J_{6,5}=7.7$ Hz, 1H, H6), 5.62 (s, 3H, H22), 5.09–4.99 (m, 1H, H24), 3.79–3.69 (m, 1H, H21), 3.44 (d, $J_{19,21}=4.4$ Hz, 1H, H21), 1.84–1.71 (m, 1H, H19), 1.50 (d, $J_{3,2}=7.2$ Hz, 3H, H3), 1.47–1.32 (m, 1H, H18'), 1.28–1.25 (2d, 6H, H26, H25), 1.21–1.13 (m, 1H, H18''), 0.94–0.80 (m, 6H, H20, H17). **¹³C NMR** (100 MHz, CDCl₃) δ [ppm]: 196.64 (C10), 178.35 (C1), 173.48 (C23), 141.60 (C8), 137.74 (C11), 137.56 (C4), 132.45 (C5), 131.74 (C14), 130.11 (C12/C16), 129.34 (C9), 128.82 (C6), 128.40 (C7), 128.29 (C13/C15), 68.73 (C24), 58.16 (C21), 45.95 (C2), 38.54 (C19), 24.88 (C18), 21.81 (C25), 18.52 (C26), 15.36 (C20), 11.74 (C17). **FT-IR:** ν (ATR): 2970.17, 2934.55, 2877.08, 2641.28, 2178.17, 2167.80, 1735.50, 1653.79, 1608.38, 1577.04, 1528.28, 1464.46, 1446.23, 1424.47, 1410.58, 1382.88, 1359.72, 1316.74, 1306.66, 1289.00, 1277.93, 1224.39, 1174.00, 1146.91, 1105.20, 1073.82, 1061.16, 1025.74, 999.50, 970.71, 950.16, 905.41, 877.43, 842.26, 825.05, 812.94, 796.79, 784.09, 717.51, 707.84, 690.71, 657.92, 641.23, 610.79, 591.42, 560.08, 520.08, 484.23, 429.76 cm⁻¹. $[\alpha]_D^{20} = +9.053$ (c=0.486% (m/v) in EtOH). **UV-Vis** (EtOH): $\lambda_{\max}=205.0$ nm. **Elemental analysis:** C₂₅H₃₃NO₅ (427.533 g/mol), calculated (%): C (70.23), H (7.78), N (3.28), O (18.71), found: C (70.19), H (7.61), N (3.15), O (18.64).

L-isoleucinium propyl ester (*R,S*)-ketoprofenate - [IleOPr][KETO]
 (2*S*)-3-methyl-1-oxo-1-propoxypentan-2-aminium (*R,S*)-2-(3-benzoylphenyl)propanoate

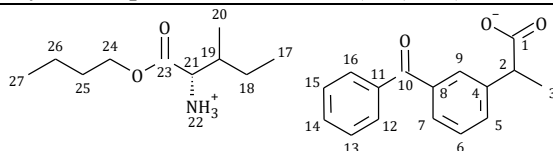


¹H NMR (400 MHz, CDCl₃) δ [ppm]: 7.80–7.76 (m, 3H, H16, H12, H7), 7.63 (d, $J_{9,8}=7.7$, 1H, H9), 7.59–7.53 (m, 2H, H14, H13), 7.46 (t, $J_{5,6}=7.3$ Hz, 2H, H5, H15), 7.38 (t, $J_{6,5}=7.7$ Hz, 1H, H6), 6.38 (s, 3H, H22), 4.11–4.00 (m, 2H, H24), 3.73–3.68 (m, 1H, H2), 3.53 (d, $J_{19,21}=4.3$ Hz, 1H, H21), 1.84–1.75 (m, 1H, H19), 1.68–1.61 (m, 2H, H25), 1.46 (d, $J_{3,2}=7.2$ Hz, 3H, H3), 1.43–1.34 (m, 1H, H18'),

1.26–1.14 (m, 1H, H18”), 0.94–0.84 (m, 9H, H17, H20, H26). ^{13}C NMR (100 MHz, CDCl_3) δ in ppm: 196.68 (C10), 178.59 (C1), 173.33 (C23), 142.10 (C8), 137.64 (C11), 137.57 (C4), 132.43 (C5), 131.80 (C14), 130.10 (C12/C16), 129.33 (C9), 128.65 (C6), 128.29 (C7), 128.27 (C13/C15), 66.84 (C24), 57.90 (C21), 46.33 (C2), 38.22 (C19), 24.97 (C18), 21.91 (C25), 18.65 (C3), 15.22 (C20), 11.69 (C17), 10.41 (C26).

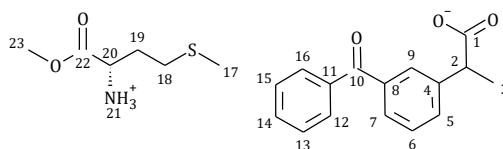
FT-IR: ν (ATR): 2966.98, 2925.49, 2877.40, 2366.06, 2028.40, 2004.01, 1740.25, 1651.37, 1609.62, 1595.99, 1573.66, 1540.28, 1479.80, 1456.48, 1445.88, 1391.55, 1359.25, 1318.05, 1280.35, 1250.36, 1217.32, 1172.88, 1157.12, 1102.59, 1059.64, 996.94, 967.10, 923.41, 879.81, 822.08, 788.47, 779.63, 727.00, 716.50, 705.71, 643.39, 606.13, 532.34, 501.74, 458.27, 443.56, 433.54, 418.98, 414.97, 411.37, 406.46 cm^{-1} . $[\alpha]_D^{20} = +13.360$ ($c=0.509\%$ (m/v) in EtOH). **UV-Vis** (EtOH): $\lambda_{\text{max}}=203.8$ nm. **Elemental analysis:** $\text{C}_{25}\text{H}_{33}\text{NO}_5$ (427.533 g/mol), calculated (%): C (70.23), H (7.78), N (3.28), O (18.71), found: C (70.34), H (7.92), N (3.30), O (18.83).

L-isoleucinium butyl ester (*R,S*)-ketoprofenate - [IleOBu][KETO]
 (2*S*)-1-butoxy-3-methyl-1-oxopentan-2-aminium (*R,S*)-2-(3-benzoylphenyl)propanoate



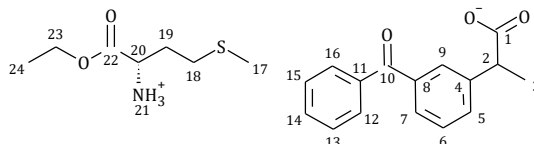
^1H NMR (400 MHz, CDCl_3) δ [ppm]: 7.81–7.77 (m, 3H, H16, H12, H7), 7.63 (d, $J_{9,8}=7.7$, 1H, H9), 7.60–7.54 (m, 2H, H14, H13), 7.45 (t, $J_{5,6}=7.3$ Hz, 2H, H15, H5), 7.41 (t, $J_{6,5}=7.7$ Hz, 1H, H6), 5.83 (s, 3H, H22), 4.17–4.05 (m, 2H, H24), 3.77–3.71 (m, 1H, H2), 3.49 (d, $J_{19,21}=4.4$ Hz, 1H, H21), 1.83–1.75 (m, 1H, H19), 1.65–1.57 (m, 2H, H25), 1.49 (d, $J_{3,2}=7.2$ Hz, 3H, H3), 1.45–1.40 (m, 1H, H18”), 1.38–1.32 (m, 2H, H26), 1.28–1.14 (m, 1H, H18”), 0.94–0.86 (m, 9H, H17, H20, H27). ^{13}C NMR (100 MHz, CDCl_3) δ in ppm: 196.63 (C10), 178.42 (C1), 174.05 (C23), 141.53 (C8), 137.75 (C11), 137.55 (C4), 132.46 (C5), 131.74 (C14), 130.11 (C12/16), 129.34 (C9), 128.84 (C6), 128.40 (C7), 128.29 (C13/C15), 64.98 (C24), 58.14 (C21), 45.91 (C2), 38.50 (C19), 30.59 (C26), 24.85 (C18), 19.13 (C25), 18.50 (C3), 15.40 (C20), 13.65 (C17), 11.70 (C27). **FT-IR:** ν (ATR): 3051.93, 2961.58, 2933.43, 2874.57, 2190.95, 2180.37, 1738.18, 1701.00, 1684.65, 1655.24, 1595.21, 1540.23, 1480.20, 1457.55, 1447.60, 1391.23, 1358.13, 1317.75, 1277.85, 1242.59, 1214.13, 1185.08, 1117.03, 1106.55, 1074.31, 1058.50, 1027.61, 999.98, 952.30, 923.06, 916.83, 898.97, 876.51, 832.40, 820.18, 806.26, 788.34, 775.95, 754.67, 719.89, 714.93, 704.63, 666.58, 642.95, 611.11, 549.49, 505.37, 467.92, 421.31, 417.26 cm^{-1} . $[\alpha]_D^{20} = +11.469$ ($c=0.497\%$ (m/v) in EtOH). **UV-Vis** (EtOH): $\lambda_{\text{max}}=201.9$ nm. **Elemental analysis:** $\text{C}_{26}\text{H}_{35}\text{NO}_5$ (441.560 g/mol), calculated (%): C (70.72), H (7.99), N (3.17), O (18.12), found: C (70.50), H (7.87), N (3.11), O (18.09).

L-methioninium methyl ester (*R,S*)-ketoprofenate - [MetOMe][KETO]
 (2*S*)-1-methoxy-4-(methylsulfanyl)-1-oxobutan-2-aminium (*R,S*)-2-(3-benzoylphenyl)propanoate



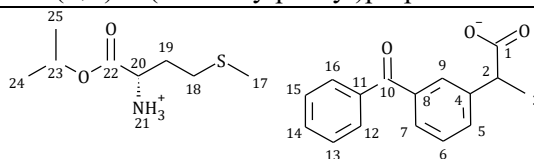
¹H NMR (400 MHz, CDCl₃) δ [ppm]: 7.85–7.75 (m, 3H, H16, H12, H7), 7.63 (d, $J_{9,8}$ =7.6 Hz, 1H, H9), 7.60–7.54 (m, 2H, H14, H13), 7.48 (t, $J_{6,5}$ =7.8 Hz, 2H, H15, H5), 7.40 (t, $J_{5,6}$ =7.7 Hz, 1H, H6), 5.85 (s, 3H, H21), 3.79–3.68 (m, 4H, H23, H20), 2.67–2.44 (m, 2H, H18), 2.13–1.96 (m, 4H, H17, H19'), 1.94–1.79 (m, 1H, H19''), 1.50 (d, $J_{3,2}$ =7.1 Hz, 3H, H3). **¹³C NMR** (100 MHz, CDCl₃) δ [ppm]: 196.72 (C10), 178.66 (C1), 174.74 (C22), 141.51 (C8), 137.75 (C11), 137.47 (C4), 132.53 (C5), 131.79 (C14), 130.13 (C12/C16), 129.26 (C9), 128.91 (C6), 128.42 (C7), 128.31 (C13/C15), 52.67 (C23), 52.41 (C20), 45.91 (C2), 32.72 (C19), 30.12 (C18), 18.48 (C3), 15.26 (C17). **FT-IR**: ν (ATR): 3344.7, 3152.08, 3060.02, 2973.07, 2918.04, 2136.48, 1746.83, 1696.03, 1654.63, 1595.58, 1575.77, 1446.25, 1385.65, 1357.08, 1316.99, 1280.55, 1243.36, 1217.21, 1178.18, 1137.80, 1074.64, 998.04, 965.68, 953.94, 907.75, 878.81, 858.56, 831.59, 751.16, 719.04, 702.36, 665.30, 641.39, 512.77, 455.46 cm⁻¹. $[\alpha]_D^{20}$ = +17.514 (c=0.531% (m/v) in EtOH). **UV-Vis** (EtOH): λ_{max}=205.1 nm. **Elemental analysis**: C₂₂H₂₇NO₅S (417.518 g/mol), calculated (%): C (63.29), H (6.52), N (3.35), O (19.16), S (7.68), found: C (63.18), H (6.48), N (3.26), O (19.01), S (7.43).

L-methioninium ethyl ester (*R,S*)-ketoprofenate - [MetOEt][KETO]
 (2*S*)-1-ethoxy-4-(methylsulfanyl)-1-oxobutan-2-aminium (*R,S*)-2-(3-benzoylphenyl)propanoate



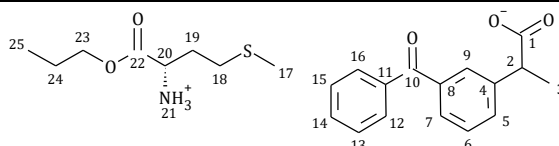
¹H NMR (400 MHz, CDCl₃) δ [ppm]: 7.87–7.72 (m, 3H, H16, H12, H7), 7.65 (d, $J_{9,8}$ =7.6 Hz, 1H, H9), 7.63–7.52 (m, 2H, H14, H13), 7.52–7.36 (m, 3H, H15, H6, H5), 5.71 (s, 3H, H21), 4.23–4.13 (m, 2H, H23), 3.81–3.71 (m, 1H, H20), 3.71–3.65 (m, 1H, H 20), 2.65–2.50 (m, 2H, H18), 2.13–1.98 (m, 4H, H17, H19'), 1.94–1.79 (m, 1H, H19''), 1.51 (d, $J_{3,2}$ =7.2 Hz, 3H, H3), 1.26 (t, $J_{24,23}$ =7.1 Hz, 3H, H24). **¹³C NMR** (100 MHz, CDCl₃) δ [ppm]: 196.61 (C10), 178.53 (C1), 174.35 (C22), 141.25 (C8), 137.79 (C11), 137.50 (C4), 132.50 (C5), 131.73 (C14), 130.11 (C12/C16), 129.31 (C9), 128.95 (C6), 128.45 (C7), 128.31 (C13/C15), 61.44 (C3), 52.80 (C20), 45.74 (C2), 32.88 (C23), 30.16 (C18), 18.42 (C3), 15.28 (C17), 14.19 (C24). **FT-IR**: ν (ATR): 3057.00, 2978.22, 2917.14, 2872.46, 2368.29, 2343.17, 1740.43, 1701.02, 1684.46, 1654.17, 1617.29, 1595.58, 1576.42, 1479.91, 1446.19, 1385.03, 1357.22, 1316.88, 1279.73, 1243.00, 1214.03, 1178.49, 1138.21, 1074.34, 1017.45, 998.97, 965.21, 953.43, 909.11, 877.26, 858.12, 831.21, 816.19, 778.16, 754.26, 719.53, 702.81, 641.49, 510.80, 477.74, 462.91, 448.27, 443.19, 434.82, 425.22, 418.75, 415.05, 406.97 cm⁻¹. $[\alpha]_D^{20}$ = +15.242 (c=0.501% (m/v) in EtOH). **UV-Vis** (EtOH): λ_{max}=205.1 nm. **Elemental analysis**: C₂₃H₂₉NO₅S (431.545 g/mol), calculated (%): C (64.01), H (6.77), N (3.25), O (18.54), S (7.43), found: C (63.97), H (6.62), N (3.17), O (18.41), S (7.29).

L-methioninium isopropyl ester (*R,S*)-ketoprofenate - [MetOiPr][KETO]
 (2*S*)-4-(methylsulfanyl)-1-oxo-1-[(propan-2-yl)oxy]butan-2-aminium
 (*R,S*)-2-(3-benzoylphenyl)propanoate



¹H NMR (400 MHz, CDCl₃) δ [ppm]: 7.81–7.76 (m, 3H, H16, H12, H7), 7.65 (d, *J*_{9,8}=7.4 Hz, 1H, H9), 7.60–7.53 (m, 2H, H14, H13), 7.49–7.40 (m, 3H, H15, H6), 6.44 (s, 3H, H21), 5.09–4.98 (m, 1H, H23), 3.81–3.71 (m, 1H, H20), 3.71–3.63 (m, 1H, H9), 2.62–2.49 (m, 2H, H18), 2.11–1.98 (m, 4H, H17, H19'), 1.95–1.81 (m, 1H, H19''), 1.51 (d, *J*_{3,2}=7.2 Hz, 3H, H3), 1.29–1.15 (2d, 6H, H25, H24). **¹³C NMR** (100 MHz, CDCl₃) δ [ppm]: 196.62 (C10), 178.73 (C1), 173.54 (C22), 141.22 (C8), 137.78 (C11), 137.49 (C4), 132.51 (C5), 131.74 (C14), 130.12 (C12/C16), 129.32 (C9), 128.96 (C6), 128.46 (C7), 128.31 (C13/C15), 69.21 (C23), 52.83 (C20), 45.76 (C2), 32.68 (C19), 30.08 (C18), 21.76 (C24), 21.74 (C24), 18.43 (C3), 15.27 (C25). **FT-IR**: ν (ATR): 3059.35, 2980.15, 2921.29, 2872.26, 2373.56, 1734.71, 1701.07, 1654.09, 1617.23, 1596.14, 1576.65, 1481.27, 1446.89, 1386.33, 1375.26, 1358.77, 1317.32, 1280.83, 1216.37, 1178.86, 1145.02, 1102.92, 1074.33, 1026.09, 998.81, 965.38, 953.64, 902.29, 881.16, 856.35, 819.01, 750.46, 718.86, 701.43, 665.67, 641.56, 519.45, 483.01, 454.02, 439.86, 425.23, 415.09, 405.06 cm⁻¹. **[α]_D²⁰** = +9.182 (c=0.503% (m/v) in EtOH). **UV-Vis** (EtOH): λ_{max}=204.9 nm. **Elemental analysis**: C₂₄H₃₁NO₅S (445.572 g/mol), calculated (%): C (64.69), H (7.01), N (3.14), O (17.95), S (7.20), found: C (64.53), H (7.12), N (3.05), O (17.84), S (7.11).

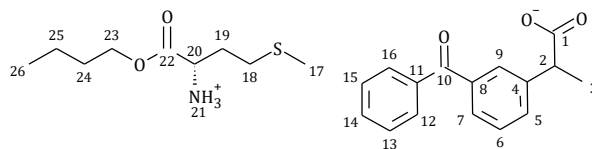
L-methioninium propyl ester (*R,S*)-ketoprofenate - [MetOPr][KETO]
 (2*S*)-4-(methylsulfanyl)-1-oxo-1-propoxybutan-2-aminium (*R,S*)-2-(3-benzoylphenyl)propanoate



¹H NMR (400 MHz, CDCl₃) δ [ppm]: 7.81–7.77 (m, 3H, H16, H12, H7), 7.66 (d, *J*_{9,8}=7.2 Hz, 1H, H9), 7.61–7.55 (m, 2H, H14, H13), 7.50–7.40 (m, 3H, H15, H6), 5.39 (s, 3H, H21), 4.12–4.07 (m, 2H, H23), 3.81–3.76 (m, 1H, H20), 3.69–3.67 (m, 1H, H9), 2.61–2.57 (m, 2H, H18), 2.07 (s, 3H, H17), 2.06–2.02 (m, 1H, H19'), 1.91–1.82 (m, 1H, H19''), 1.71–1.61 (m, 2H, H24), 1.52 (d, *J*_{3,2}=7.2 Hz, 3H, H3), 0.91 (t, *J*_{25,24}=7.1 Hz, H25). **¹³C NMR** (100 MHz, CDCl₃) δ in ppm: 196.57 (C10), 178.59 (C1), 174.86 (C22), 140.88 (C8), 137.85 (C11), 137.49 (C4), 132.52 (C5), 131.70 (C14), 130.12 (C12/C16), 129.33 (C9), 129.08 (C6), 128.52 (C7), 128.32 (C13/C15), 66.94 (C23), 52.92 (C20), 45.50 (C2), 33.18 (C19), 30.25 (C18), 21.95 (C24), 18.34 (C3), 15.31 (C17), 10.39 (C25). **FT-IR**: ν (ATR): 3059.65, 2967.67, 2918.79, 2877.92, 2373.91, 1740.53, 1701.01, 1654.06, 1595.82, 1576.57, 1446.76, 1385.72, 1356.14, 1316.77, 1280.16, 1243.57, 1213.09, 1178.54,

1137.96, 1074.32, 1057.98, 997.75, 964.98, 953.57, 929.91, 906.68, 877.55, 831.36, 753.29, 719.59, 703.33, 703.33, 641.46, 616.42, 511.80, 472.46, 460.79, 426.55, 418.63, 406.66 cm⁻¹. [α]_D²⁰ = +11.332 (c=0.482% (m/v) in EtOH). **UV-Vis** (EtOH): λ_{max} =204.0 nm. **Elemental analysis:** C₂₄H₃₁NO₅S (445.572 g/mol), calculated (%): C (64.69), H (7.01), N (3.14), O (17.95), S (7.20), found: C (64.60), H (7.05), N (3.10), O (17.76), S (7.13).

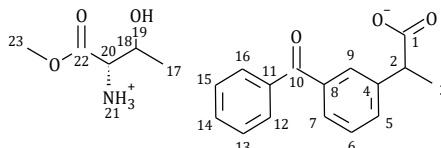
L-methioninium butyl ester (*R,S*)-ketoprofenate - [MetOBu][KETO]
 (2*S*)-1-butoxy-4-(methylsulfanyl)-1-oxobutan-2-aminium (*R,S*)-2-(3-benzoylphenyl)propanoate



¹H NMR (400 MHz, CDCl₃) δ [ppm]: 7.81–7.78 (m, 3H, H16, H12, H7), 7.66 (d, $J_{9,8}$ =7.4 Hz, 1H, H9), 7.63–7.55 (m, 2H, H14, H13), 7.50–7.41 (m, 3H, H15, H6), 5.13 (s, 3H, H21), 4.19–4.07 (m, 2H, H23), 3.82–3.76 (m, 1H, H20), 3.67–3.64 (m, 1H, H9), 2.66–2.53 (m, 2H, H18), 2.08 (s, 3H, H17), 2.05–2.02 (m, 1H, H19'), 1.90–1.81 (m, 1H, H19''), 1.66–1.59 (m, 2H, H24), 1.53 (d, $J_{3,2}$ =7.2 Hz, 3H, H3), 1.43–1.32 (m, 2H, H25), 0.94 (t, $J_{26,25}$ =7.4 Hz, 3H, H26). **¹³C NMR** (100 MHz, CDCl₃) δ in ppm: 196.55 (C10), 178.51 (C1), 175.04 (C22), 140.80 (C8), 137.87 (C11), 137.49 (C4), 132.52 (C5), 131.69 (C14), 130.12 (C12/C16), 129.33 (C9), 129.10 (C6), 128.54 (C7), 128.32 (C13/C15), 65.20 (C23), 52.99 (C20), 45.43 (C2), 33.30 (C19), 30.60 (C24), 30.29 (C18), 19.12 (C25), 18.33 (C3), 15.33 (C17), 13.70 (C26).

FT-IR: ν (ATR): 3056.02, 3024.63, 2959.82, 2929.60, 2872.11, 2362.72, 2343.23, 2056.14, 1740.30, 1701.02, 1684.64, 1654.19, 1617.23, 1595.87, 1576.43, 1560.30, 1480.65, 1446.72, 1386.16, 1356.34, 1316.93, 1279.50, 1241.86, 1210.65, 1178.25, 1073.81, 1061.23, 1016.72, 998.39, 964.49, 953.18, 907.63, 877.84, 831.95, 778.04, 719.20, 702.86, 641.51, 616.91, 513.92, 498.70, 442.66, 429.73, 425.08, 419.32, 415.83, 406.98 cm⁻¹. [α]_D²⁰ = +12.364 (c=0.531% (m/v) in EtOH). **UV-Vis** (EtOH): λ_{max} =203.9 nm. **Elemental analysis:** C₂₅H₃₃NO₅S (459.598 g/mol), calculated (%): C (65.33), H (7.24), N (3.05), O (17.41), S (6.98), found: C (65.29), H (7.17), N (3.00), O (17.16), S (6.21).

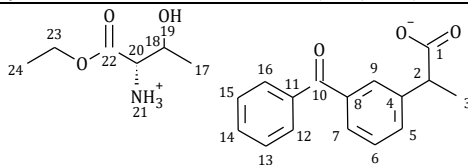
L-threoninium methyl ester (*R,S*)-ketoprofenate - [ThrOMe][KETO]
 (2*S*)-3-hydroxy-1-methoxy-1-oxobutan-2-aminium (*R,S*)-2-(3-benzoylphenyl)propanoate



¹H NMR (400 MHz, CDCl₃) δ [ppm]: 7.82–7.73 (m, 3H, H16, H12, H7), 7.66–7.49 (m, 3H, H14, H13, H9), 7.52–7.41 (m, 2H, H15, H5), 7.37 (t, $J_{5,6}$ =7.7 Hz, 1H, H6), 5.95 (s, 4H, H21, H19), 4.06–3.95 (m, 1H, H18), 3.77–3.62 (m, 1H, H2), 3.70 (s, 3H, H21), 3.43 (d, $J_{20,21}$ =5.1 Hz, 1H, H20), 1.47 (d, $J_{3,2}$ =7.2 Hz, 3H, H3), 1.20 (d, $J_{18,17}$ =6.5 Hz, 3H, H18). **¹³C NMR** (100 MHz, CDCl₃) δ [ppm]:

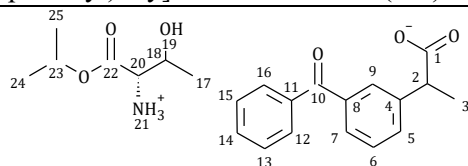
196.86 (C10), 179.26 (C1), 172.31 (C22), 142.07 (C8), 137.67 (C11), 137.45 (C4), 132.55 (C5), 131.87 (C14), 130.15 (C12/C15), 129.21 (C9), 128.75 (C9), 128.32 (C6), 67.36 (C20), 59.32 (C18), 52.62 (C18), 46.40 (C2), 19.90 (C3), 18.64 (C17). **FT-IR**: ν (ATR): 3059.25, 2977.01, 2934.37, 1746.32, 1711.21, 1654.85, 1595.60, 1576.06, 1446.56, 1389.84, 1360.80, 1316.93, 1280.27, 1218.36, 1178.22, 1135.80, 1058.66, 998.42, 966.18, 953.81, 922.79, 885.89, 856.88, 829.36, 752.46, 718.27, 700.72, 666.26, 641.10 cm^{-1} . $[\alpha]_D^{20} = -3.422$ ($c=0.526$ % (m/v) in EtOH). **UV-Vis** (EtOH): $\lambda_{\text{max}}=204.6$ nm. **Elemental analysis**: $\text{C}_{21}\text{H}_{25}\text{NO}_6$ (387.426 g/mol), calculated (%): C (65.10), H (6.50), N (3.62), O (24.78), found: C (65.00), H (6.42), N (3.56), O (24.68).

L-threoninium ethyl ester (*R,S*)-ketoprofenate - [ThrOEt][KETO]
 (2*S*)-1-ethoxy-3-hydroxy-1-oxobutan-2-aminium (*R,S*)-2-(3-benzoylphenyl)propanoate



^1H NMR (400 MHz, CDCl_3) δ [ppm]: 7.80–7.75 (m, 3H, H16, H12, H7), 7.65–7.50 (m, 3H, H14, H13, H9), 7.45 (t, $J_{5,6}=7.6$ Hz, 2H, H15, H5), 7.37 (t, $J_{6,5}=7.7$ Hz, 1H, H6), 6.24 (s, 4H, H21, H19), 4.20–4.13 (m, 2H, H23), 4.05–3.96 (m, 1H, H18), 3.73–3.67 (m, 1H, H2), 3.42 (d, $J_{20,21}=5.1$ Hz, 1H, H20), 1.46 (d, $J_{3,2}=7.2$ Hz, 3H, H3), 1.25–1.18 (2d, 6H, H24, H17). **^{13}C NMR** (100 MHz, CDCl_3) δ [ppm]: 196.85 (C10), 179.33 (C1), 171.50 (C22), 142.13 (C8), 137.65 (C11), 137.46 (C4), 132.53 (C5), 131.87 (C14), 130.15 (C12/C15), 129.24 (C9), 128.72 (C6), 128.31 (C7), 67.25 (C23), 61.89 (C20), 59.31 (C18), 46.46 (C2), 19.96 (C3), 18.67 (C17), 14.06 (C24). **FT-IR**: ν (ATR): 3064.08, 2977.50, 2977.50, 1740.66, 1695.72, 1653.92, 1651.23, 1595.51, 1576.26, 1555.83, 1537.41, 1506.14, 1480.26, 1456.51, 1447.17, 1387.72, 1360.61, 1317.25, 1280.72, 1218.47, 1178.60, 1133.28, 1116.62, 1116.62, 1023.71, 998.53, 965.87, 953.33, 908.86, 882.88, 858.79, 832.20, 751.42, 719.62, 701.70, 665.46, 641.30 cm^{-1} . $[\alpha]_D^{20} = -5.919$ ($c=0.495$ % (m/v) in EtOH). **UV-Vis** (EtOH): $\lambda_{\text{max}}=203.1$ nm. **Elemental analysis**: $\text{C}_{22}\text{H}_{27}\text{NO}_6$ (401.453 g/mol), calculated (%): C (65.82), H (6.78), N (3.49), O (23.91), found: C (65.74), H (6.65), N (3.42), O (23.87).

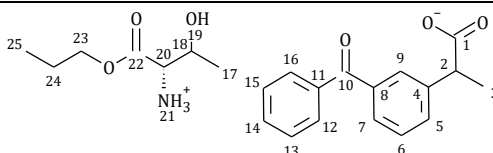
L-threoninium isopropyl ester (*R,S*)-ketoprofenate - [ThrOiPr][KETO]
 (2*S*)-3-hydroxy-1-oxo-1-[(propan-2-yl)oxy]butan-2-aminium (*R,S*)-2-(3-benzoylphenyl)propanoate



^1H NMR (400 MHz, CDCl_3) δ [ppm]: 7.86–7.70 (m, 3H, H16, H12, H7), 7.66–7.51 (m, 3H, H14, H13), 7.47 (t, $J_{5,6}=7.2$ Hz, 2H, H15, H5), 7.38 (t, $J_{6,5}=7.7$ Hz, 1H, H6), 5.72 (s, 4H, H21, H19), 5.09–4.98 (m, 1H, H23), 4.04–3.92 (m, 1H, H20), 3.77–3.65 (m, 1H, H2), 3.36 (d, $J_{20,18}=5.3$ Hz, 1H, H20), 1.48 (d, $J_{3,2}=7.2$ Hz, 3H, H3), 1.27–1.18 (3d, 9H, H25, H24, H17). **^{13}C NMR** (100 MHz, CDCl_3) δ

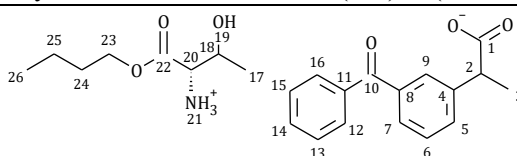
[ppm]: 196.80 (C10), 179.16 (C1), 171.53 (C22), 141.85 (C8), 137.70 (C11), 137.47 (C4), 132.52 (C5), 131.83 (C14), 130.15 (C12/C15), 129.28 (C9), 129.26 (C6), 128.78 (C7), 128.36 (C7), 128.31 (C13), 69.63 (C23), 67.52 (C20), 59.51 (C18), 46.26 (C2), 21.70 (C24), 21.66 (C25), 19.96 (C3), 18.61 (C17). **FT-IR**: ν (ATR): 3062.06, 3033.13, 2978.79, 2933.96, 2874.98, 2367.73, 1734.81, 1698.84, 1654.38, 1651.30, 1595.60, 1576.18, 1558.61, 1504.89, 1447.21, 1435.65, 1385.84, 1358.39, 1318.07, 1280.71, 1224.71, 1179.25, 1143.13, 1100.95, 1058.11, 998.78, 964.98, 953.60, 913.36, 897.11, 819.02, 752.64, 719.34, 702.10, 664.32, 640.93, 547.33, 508.29, 502.10, 497.82, 492.70, 484.11, 471.60, 466.24, 461.16, 457.65, 446.93, 443.90, 435.36, 430.16, 419.87, 407.61, 404.26, 402.16 cm^{-1} . $[\alpha]_D^{20} = -4.242$ ($c=0.698$ % (m/v) in EtOH). **UV-Vis** (EtOH): $\lambda_{\text{max}}=204.8$ nm. **Elemental analysis**: $\text{C}_{23}\text{H}_{29}\text{NO}_6$ (415.479 g/mol), calculated (%): C (66.49), H (7.04), N (3.37), O (23.11), found: C (66.40), H (7.00), N (3.31), O (23.09).

L-threoninium propyl ester (R,S)-ketoprofenate - [ThrOPr][KETO]
 (2S)-3-hydroxy-1-oxo-1-propoxybutan-2-aminium (R,S)-2-(3-benzoylphenyl)propanoate



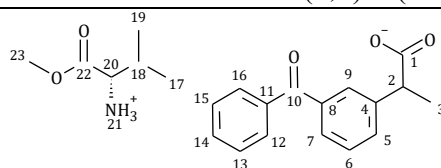
^1H NMR (400 MHz, CDCl_3) δ [ppm]: 7.79–7.76 (m, 3H, H16, H12, H7), 7.63–7.51 (m, 3H, H9, H14, H13), 7.44 (t, $J_{5,6}=7.3$ Hz, 2H, H5, H15), 7.38 (t, $J_{6,5}=7.7$ Hz, 1H, H6), 5.71 (s, 4H, H21, H19), 4.13–4.05 (m, 2H, H23), 4.03–3.97 (m, 1H, H18), 3.74–3.69 (m, 1H, H2), 3.41 (d, $J_{20,21}=5.2$ Hz, 1H, H20), 1.69–1.61 (m, 2H, H24), 1.46 (d, $J_{3,2}=7.2$ Hz, 3H, H3), 1.22 (d, $J_{17,18}=6.5$ Hz, 3H, H17), 0.92 (t, $J_{25,24}=7.5$ Hz, 3H, H25). **^{13}C NMR** (100 MHz, CDCl_3) δ in ppm: 196.82 (C10), 179.20 (C1), 172.04 (C22), 141.90 (C8), 137.69 (C11), 137.46 (C4), 132.54 (C5), 131.84 (C14), 130.15 (C12/C15), 129.26 (C9), 129.24 (C6), 128.78 (C7), 128.35 (C13), 128.31 (C15), 67.47 (C23), 67.36 (C20), 59.42 (C18), 46.29 (C2), 21.84 (C24), 19.97 (C3), 18.61 (C17), 10.33 (C25). **FT-IR**: ν (ATR): 3551.98, 2969.57, 2933.19, 2269.51, 2251.15, 1740.49, 1698.21, 1654.30, 1595.44, 1576.77, 1447.21, 1388.56, 1357.40, 1317.64, 1279.81, 1217.51, 1178.39, 1117.41, 1058.31, 998.88, 953.94, 910.61, 752.25, 719.62, 702.34, 641.37, 457.91, 429.18, 418.58, 407.16, 403.12 cm^{-1} . $[\alpha]_D^{20} = -4.802$ ($c=0.479$ % (m/v) in EtOH). **UV-Vis** (EtOH): $\lambda_{\text{max}}=204.6$ nm. **Elemental analysis**: $\text{C}_{23}\text{H}_{29}\text{NO}_6$ (415.479 g/mol), calculated (%): C (66.49), H (7.04), N (3.37), O (23.11), found: C (66.33), H (7.06), N (3.35), O (23.15).

L-threoninium butyl ester (R,S)-ketoprofenate - [ThrOBu][KETO]
 (2S)-1-butoxy-3-hydroxy-1-oxobutan-2-aminium (R,S)-2-(3-benzoylphenyl)propanoate



¹H NMR (400 MHz, CDCl₃) δ [ppm]: 7.81–7.77 (m, 3H, H16, H12, H7), 7.65–7.51 (m, 3H, H14, H13, H9), 7.47 (t, $J_{5,6}$ =7.3 Hz, 2H, H15, H5), 7.40 (t, $J_{5,6}$ =7.7 Hz, 1H, H6), 5.16 (s, 4H, H21, H19), 4.17–4.11 (m, 2H, H23), 4.01–3.95 (m, 1H, H18), 3.77–3.72 (m, 1H, H2), 3.38 (d, $J_{20,21}$ =5.2 Hz, 1H, H20), 1.65–1.57 (m, 2H, H24), 1.49 (d, $J_{3,2}$ =7.2 Hz, 3H, H3), 1.41–1.34 (m, 2H, H25), 1.23 (d, $J_{17,18}$ =6.4 Hz, 3H, H17), 0.92 (t, $J_{26,25}$ =7.4 Hz, 3H, H26). **¹³C NMR** (100 MHz, CDCl₃) δ in ppm: 196.72 (C10), 178.97 (C1), 172.69 (C22), 141.41 (C8), 137.77 (C11), 137.46 (C4), 132.54 (C5), 131.77 (C14), 130.14 (C12/15), 129.28 (C9), 128.93 (C6), 128.43 (C7), 128.32 (C13), 67.73 (C23), 65.55 (C20), 59.52 (C18), 45.91 (C2), 30.51 (C25), 19.95 (C24), 19.07 (C3), 18.49 (C17), 13.68 (C26). **FT-IR**: ν (ATR): 3057.86, 3045.87, 2962.31, 2933.06, 2872.71, 2362.71, 1740.14, 1698.53, 1694.35, 1654.42, 1651.18, 1595.96, 1576.18, 1559.57, 1556.77, 1537.83, 1505.10, 1456.47, 1447.23, 1434.37, 1389.55, 1357.77, 1318.10, 1280.61, 1241.12, 1216.44, 1177.50, 1134.64, 1117.22, 1059.91, 1028.55, 998.80, 965.32, 953.24, 916.12, 882.29, 832.77, 752.11, 719.10, 703.46, 665.45, 641.70, 556.37, 523.15, 516.97, 512.08, 509.15, 484.51, 473.04, 467.59, 452.10, 443.26, 436.78, 429.47, 426.12, 415.92, 407.05, 403.17 cm⁻¹. $[\alpha]_D^{20} = -6.545$ (c=0.479 % (m/v) in EtOH). **UV-Vis** (EtOH): λ_{max}=205.8 nm. **Elemental analysis**: C₂₄H₃₁NO₆ (429.506 g/mol), calculated (%): C (67.11), H (7.27), N (3.26), O (22.35), found: C (67.08), H (7.19), N (3.21), O (22.04).

L-valinium methyl ester (*R,S*)-ketoprofenate - [ValOMe][KETO]
 (2*S*)-1-methoxy-3-methyl-1-oxobutan-2-aminium (*R,S*)-2-(3-benzoylphenyl)propanoate

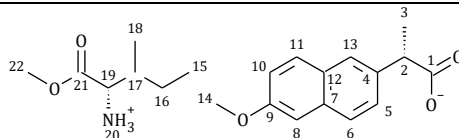


¹H NMR (400 MHz, CDCl₃) δ [ppm]: 7.83–7.74 (m, 3H, H16, H12, H7), 7.64 (d, $J_{9,8}$ =7.7 Hz, 1H, H9), 7.61–7.51 (m, 2H, H14, H13), 7.47 (t, $J_{5,6}$ =8.3 Hz, 2H, H5, H15), 7.40 (t, $J_{6,5}$ =7.7 Hz, 1H, H6), 5.79 (s, 3H, H21), 3.78–3.71 (m, 1H, H2), 3.70 (s, 3H, H23), 3.46 (d, $J_{20,18}$ =4.6 Hz, 1H, H20), 2.14–2.01 (m, 1H, H18), 1.49 (d, $J_{3,2}$ =7.2 Hz, 3H, H3), 0.93 (d, $J_{18,19}$ =6.9 Hz, 3H, H19), 0.89 (d, $J_{17,18}$ =6.9 Hz, 3H, H17). **¹³C NMR** (100 MHz, CDCl₃) δ [ppm]: 196.66 (C10), 178.50 (C1), 174.07 (C22), 141.57 (C8), 137.73 (C11), 137.52 (C4), 132.48 (C5), 131.77 (C14), 130.11 (C12/C16), 129.30 (C9), 128.83 (C6), 128.39 (C7), 128.30 (C13), 59.00 (C23), 52.11 (C20), 45.96 (C2), 31.41 (C19), 18.73 (C18), 18.51 (C17), 17.35 (C19). **FT-IR**: ν (ATR): 3056.22, 2979.80, 2934.05, 2883.44, 2608.28, 2202.95, 2161.62, 1743.11, 1649.67, 1596.72, 1577.30, 1519.31, 1456.98, 1443.10, 1383.40, 1354.31, 1317.07, 1287.86, 1226.59, 1177.65, 1108.14, 1075.51, 1051.48, 1023.83, 982.91, 934.97, 878.25, 782.21, 720.83, 700.79, 666.33, 642.37, 591.22 cm⁻¹. $[\alpha]_D^{20} = +10.769$ (c=0.650 % (m/v) in EtOH). **UV-Vis** (EtOH): λ_{max}=203.0 nm. **Elemental analysis**: C₂₂H₂₇NO₅ (385.453 g/mol), calculated (%): C (68.55), H (7.06), N (3.63), O (20.75), found: C (68.46), H (6.95), N (3.45), O (20.60).

L-AMINO ACID ESTER SALTS OF S-(+)-NAPROXEN

L-isoleucinium methyl ester S-(+)-naproxenate - [IleOMe][NAP]

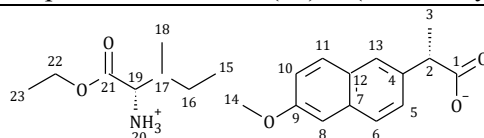
(2S)-1-methoxy-3-methyl-1-oxopentane-2-aminium (2S)-2-(6-methoxynaphthalen-2-yl)propanoate



¹H NMR (400 MHz, CDCl₃) δ [ppm]: 7.64–7.59 (s+d, 3H, H11, H8, H8), 7.40 (d, $J_{11,10}$ =7.6 Hz, 1H, H10), 7.10–7.04 (s+d, 2H, H13, H5), 6.91 (s, 3H, H20), 3.88 (s, 3H, H22), 3.79–3.72 (m, 1H, H2), 3.61 (s, 3H, H14), 3.45 (d, $J_{19,17}$ =4.4 Hz, 1H, H19), 1.74–1.64 (m, 1H, H19), 1.51 (d, $J_{3,2}$ =7.1 Hz, 3H, H3), 1.35–1.23 (m, 1H, H16'), 1.17–1.01 (m, 1H, H16''), 0.83–0.75 (m, 6H, H18, H15). **¹³C NMR** (100 MHz, CDCl₃) δ [ppm]: 179.43 (C1), 173.48 (C21), 157.43 (C9), 136.83 (C4), 133.54 (C7), 129.29 (C11), 128.96 (C12), 126.92 (C5), 126.60 (C13), 125.93 (C6), 118.73 (C10), 105.54 (C8), 57.78 (C22), 55.29 (C19), 52.04 (C14), 46.33 (C2), 38.07 (C17), 24.94 (C16), 18.68 (C3), 15.08 (C18), 11.60 (C15). **FT-IR** ν (ATR): 2959.75, 2932.96, 2875.30, 2726.51, 2179.15, 1740.95, 1678.40, 1604.69, 1581.34, 1522.21, 1504.47, 1486.37, 1460.14, 1439.12, 1419.20, 1379.00, 1356.41, 1297.15, 1257.11, 1202.50, 1193.85, 1174.91, 1158.3, 1125.90, 1102.79, 1088.72, 1065.15, 1029.49, 1002.94, 986.99, 966.15, 925.58, 897.94, 881.11, 857.47, 819.42, 787.78, 764.71, 749.53, 710.45, 683.16, 656.40, 622.84, 522.93, 531.53, 544.93, 476.39, 447.40, 445.00 cm⁻¹. $[\alpha]_D^{20}$ = +46.393 (c=0.570 % (m/v) in EtOH). **UV-Vis** (EtOH): λ_{\max} =229.0 nm. **Elemental analysis**: C₂₂H₂₉NO₅ (375.457 g/mol), calculated (%): C (67.18), H (7.79), N (3.73), O (21.31), found: C (67.20), H (7.62), N (3.74), O (20.84).

L-isoleucinium ethyl ester S-(+)-naproxenate - [IleOEt][NAP]

(2S)-1-ethoxy-3-methyl-1-oxopentane-2-aminium (2S)-2-(6-methoxynaphthalen-2-yl)propanoate



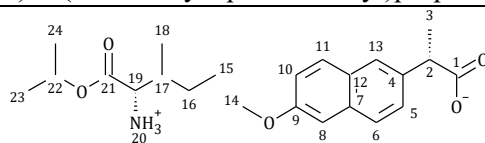
¹H NMR (400 MHz, CDCl₃) δ [ppm]: 7.68–7.63 (s+d, 3H, H11, H8, H6), 7.41 (d, $J_{11,10}$ =6.8 Hz, 1H, H10), 7.13–7.06 (s+d, 2H, H13, H5), 5.85 (s, 3H, H20), 4.22–4.05 (m, 2H, H22), 3.90 (s, 3H, H14), 3.84–3.74 (m, 1H, H2), 3.43 (d, $J_{19,17}$ =4.5 Hz, 1H, H19), 1.81–1.69 (m, 1H, H17), 1.53 (d, $J_{3,2}$ =7.1 Hz, 3H, H3), 1.42–1.32 (m, 1H, H16'), 1.22 (t, $J_{22,23}$ =7.1 Hz, 3H, H23), 1.19–1.07 (m, 1H, H16''), 0.93–0.78 (m, 6H, H18, H15). **¹³C NMR** (100 MHz, CDCl₃) δ [ppm]: 179.19 (C1), 173.95 (C21), 157.52 (C9), 136.26 (C4), 133.63 (C7), 129.29 (C11), 128.96 (C12), 127.02 (C5), 126.46 (C13), 125.98 (C6), 118.82 (C10), 105.58 (C8), 61.01 (C22), 58.12 (C19), 55.30 (C14), 45.91 (C2), 38.53 (C17), 24.87 (C16), 18.50 (C3), 15.34 (C18), 14.21 (C23), 11.67 (C15). **FT-IR** ν (ATR): 2961.54, 2929.96, 2602.24, 2195.91, 1738.56, 1629.28, 1603.69, 1583.20, 1522.79, 1504.47, 1481.12, 1463.26, 1415.41, 1386.88, 1377.36, 1363.91, 1346.21, 1308.36, 1272.15, 1266.49, 1251.77, 1211.02, 1195.29, 1159.71, 1116.78, 1092.45, 1063.59, 1030.26, 969.36, 956.48, 924.55, 893.85,

881.19, 855.75, 840.35, 819.29, 808.91, 788.41, 761.40, 747.17, 696.53, 659.35, 606.57, 553.34, 531.24, 522.42, 497.00, 473.07, 436.84 cm⁻¹. $[\alpha]_D^{20} = +40.877$ (c=0.570 % (m/v) in EtOH). **UV-Vis** (EtOH): λ_{\max} =229.1 nm. **Elemental analysis:** C₂₂H₃₁NO₅ (389.485 g/mol), calculated (%): C (67.84), H (8.02), N (3.60), O (20.54), found: C (66.98), H (8.03), N (3.60), O (20.01).

L-isoleucinium isopropyl ester *S*-(+)-naproxenate - [IleOiPr][NAP]

(2*S*)-3-methyl-1-oxo-1-[(propan-2-yl)oxy]pentan-2-aminium

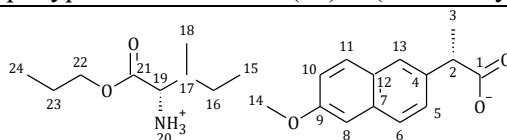
(2*S*)-2-(6-methoxynaphthalen-2-yl)propanoate



¹H NMR (400 MHz, CDCl₃) δ [ppm]: 7.69–7.61 (s+d, 3H, H11, H8, H6), 7.41 (d, $J_{10,11}$ =8.5 Hz, 1H, H10), 7.14–7.05 (s+d, 2H, H13, H5), 5.83 (s, 3H, H20), 5.09–4.95 (m, 1H, H22), 3.89 (s, 3H, H14), 3.83–3.73 (m, 1H, H2), 3.40 (d, $J_{19,17}$ =4.4 Hz, 1H, H19), 1.80–1.69 (m, 1H, H17), 1.53 (d, $J_{3,2}$ =7.2 Hz, 3H, H3), 1.42–1.31 (m, 1H, H16'), 1.28–1.16 (m, 6H, H24, H23), 1.18–1.07 (m, 1H, H16''), 0.90–0.79 (m, 6H, H18, H15). **¹³C NMR** (100 MHz, CDCl₃) δ [ppm]: 179.15 (C1), 173.42 (C21), 157.49 (C9), 136.40 (C4), 133.61 (C7), 129.29 (C11), 128.97 (C12), 126.99 (C5), 126.50 (C13), 125.96 (C6), 118.78 (C10), 105.57 (C8), 68.71 (C22), 58.12 (C19), 55.29 (C14), 45.99 (C2), 38.51 (C17), 24.89 (C16), 21.79 (C23/C24), 18.55 (C3), 15.30 (C18), 11.72 (C15). **FT-IR** ν (ATR): 3061.20, 2973.03, 2933.17, 2879.12, 2837.57, 2658.48, 2189.29, 1741.10, 1628.09, 1603.92, 1505.48, 1480.84, 1468.52, 1455.31, 1417.39, 1382.83, 1355.74, 1314.18, 1271.71, 1262.78, 1226.16, 1211.36, 1193.93, 1175.06, 1158.17, 1116.68, 1105.37, 1060.29, 1030.99, 998.39, 964.97, 941.73, 924.63, 907.40, 896.69, 880.20, 855.03, 817.50, 808.16, 793.97, 771.20, 761.78, 749.98, 711.32, 683.25, 652.41, 620.70, 572.02, 531.83, 522.90, 507.47, 477.14, 419.94 cm⁻¹. $[\alpha]_D^{20} = +34.343$ (c=0.524 % (m/v) in EtOH). **UV-Vis** (EtOH): λ_{\max} =229.6 nm. **Elemental analysis:** C₂₃H₃₃NO₅ (403.512 g/mol), calculated (%): C (68.46), H (8.24), N (3.47), O (19.83), found: C (67.94), H (8.18), N (3.51), O (19.76).

L-isoleucinium propyl ester *S*-(+)-naproxenate - [IleOPr][NAP]

(2*S*)-3-methyl-1-oxo-1-propoxypentan-2-aminium (2*S*)-2-(6-methoxynaphthalen-2-yl)propanoate

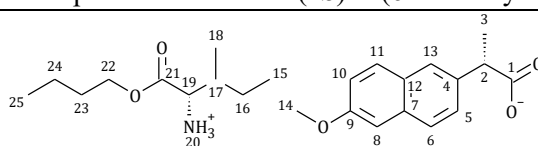


¹H NMR (400 MHz, CDCl₃) δ in ppm: 7.67–7.65 (s+d, 3H, H8, H6, H11), 7.40 (d, $J_{10,11}$ =7.2 Hz, 1H, H10), 7.12–7.08 (s+d, 2H, H13, H5), 5.74 (s, 3H, H20), 4.10–3.98 (m, 2H, H22), 3.90 (s, 3H, H14), 3.83–3.77 (m, 1H, H2), 3.45 (d, $J_{19,17}$ =4.4 Hz, 1H, H19), 1.81–1.72 (m, 1H, H17), 1.67–1.60 (m, 2H, H23), 1.53 (d, $J_{3,2}$ =7.2 Hz, 3H, H3), 1.43–1.32 (m, 1H, H16'), 1.25–1.10 (m, 1H, H16''), 0.93–0.84 (m, 9H, H24, H18, H15). **¹³C NMR** (100 MHz, CDCl₃) δ in ppm: 179.19 (C1), 174.23 (C21), 157.54 (C9), 136.11 (C4), 133.65 (C7), 129.30 (C11), 128.95 (C12), 127.04 (C5), 126.43 (C13), 125.99

(C6), 118.84 (C10), 105.58 (C8), 66.66 (C22), 58.19 (C19), 55.30 (C14), 45.82 (C2), 38.58 (C17), 24.85 (C16), 21.94 (C23), 18.47 (C3), 15.40 (C18), 11.69 (C24), 10.42 (C15). **FT-IR** ν (ATR): 2958.75, 2927.66, 2874.27, 2595.81, 2184.68, 2177.10, 2167.13, 1736.71, 1629.68, 1603.68, 1502.83, 1484.67, 1463.52, 1454.01, 1437.88, 1414.49, 1383.97, 1367.44, 1344.54, 1308.96, 1283.62, 1262.70, 1249.28, 1210.37, 1159.26, 1116.26, 1105.82, 1060.78, 1035.28, 959.15, 944.33, 924.98, 892.25, 877.35, 860.80, 839.48, 812.29, 792.01, 763.80, 746.25, 691.78, 658.34, 568.90, 529.08, 522.18, 472.09, 432.85 cm^{-1} . $[\alpha]_D^{20} = +44.275$ ($c=0.594$ % (m/v) in EtOH). **UV-Vis** (EtOH): $\lambda_{\text{max}}=229.0$ nm. **Elemental analysis:** $\text{C}_{23}\text{H}_{33}\text{NO}_5$ (403.512 g/mol), calculated (%): C (68.46), H (8.24), N (3.47), O (19.83), found: C (67.95), H (8.19), N (3.47), O (19.77).

L-isoleucinium butyl ester *S*-(+)-naproxenate - [IleOBu][NAP]

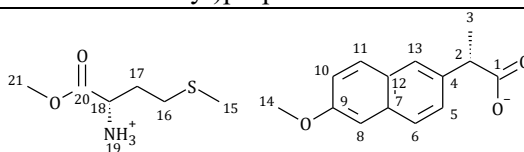
(2*S*)-1-butoxy-3-methyl-1-oxopentan-2-aminium (2*S*)-2-(6-methoxynaphthalen-2-yl)propanoate



^1H NMR (400 MHz, CDCl_3) δ in ppm: 7.68–7.65 (s+d, 3H, H11, H8, H6), 7.41 (d, $J_{10,11} = 6.9$ Hz, 1H, H10), 7.12–7.08 (s+d, 2H, H13, H5), 5.79 (s, 3H, H20), 4.14 – 4.02 (m, 2H, H22), 3.90 (s, 3H, H14), 3.83 – 3.77 (m, 1H,), 3.44 (d, $J=4.4$ Hz, 1H), 1.79–1.72 (m, 1H), 1.62–1.56 (m, 2H), 1.53 (d, $J=7.1$ Hz, 3H), 1.42–1.30 (m, 3H), 1.21–1.10 (m, 1H), 0.93–0.82 (m, 9H, H25, H18, H15). **^{13}C NMR** (100 MHz, CDCl_3) δ in ppm: 179.22 (C1), 174.26 (C21), 157.55 (C9), 136.06 (C4), 133.66 (C7), 129.30 (C11), 128.95 (C12), 127.05 (C5), 126.42 (C13), 126.00 (C6), 118.85 (C10), 105.58 (C8), 64.91 (C22), 58.20 (C19), 55.30 (C14), 45.79 (C2), 38.57 (C17), 30.59 (C23), 24.83 (C16), 19.12 (C24), 18.46 (C3), 15.41 (C25), 13.66 (C18), 11.69 (C15). **FT-IR** ν (ATR): 3056.85, 3008.75, 2968.80, 2935.10, 2872.63, 2596.88, 2190.60, 1740.83, 1630.41, 1603.75, 1582.73, 1503.75, 1486.00, 1462.83, 1384.38, 1365.32, 1347.54, 1308.75, 1271.52, 1252.93, 1212.53, 1159.79, 1117.08, 1061.56, 1038.27, 1028.56, 959.33, 936.98, 924.73, 894.16, 878.75, 860.02, 840.25, 819.72, 811.83, 793.27, 770.25, 747.38, 695.26, 658.70, 603.90, 568.92, 528.49, 522.07, 506.25, 484.08, 472.38, 432.32, 402.20 cm^{-1} . $[\alpha]_D^{20} = +37.977$ ($c=0.570$ % (m/v) in EtOH). **UV-Vis** (EtOH): $\lambda_{\text{max}}=228.9$ nm. **Elemental analysis:** $\text{C}_{24}\text{H}_{35}\text{NO}_5$ (417.538 g/mol), calculated (%): C (69.04), H (8.45), N (3.36), O (19.16), found: C (68.98), H (8.39), N (3.29), O (18.89).

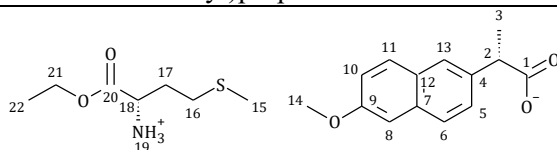
L-methioninium methyl ester *S*-(+)-naproxenate -[MetOMe][NAP]

(2*S*)-1-methoxy-4-(methylsulfanyl)-1-oxobutan-2-aminium (2*S*)-2-(6-methoxynaphthalen-2-yl)propanoate



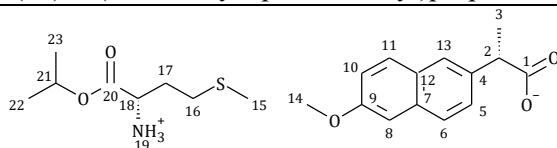
¹H NMR (400 MHz, CDCl₃) δ [ppm]: 7.71–7.64 (s+d, 3H, H16, H12, H7), 7.41 (d, *J*_{9,8}=7.8 Hz, 1H, H10), 7.15–7.06 (s+d, 2H, H14, H13), 5.50 (s, 3H, H21), 3.90 (s, 3H, H14), 3.86–3.76 (m, 1H, H2), 3.70 (s, 3H, H21), 3.69–3.62 (m, 1H, H18), 2.61–2.48 (m, 2H, H16), 2.09–1.96 (m, 4H, H17', H15), 1.90–1.76 (m, 1H), 1.55 (d, *J*_{3,2}=7.2 Hz, 3H, H3). **¹³C NMR** (100 MHz, CDCl₃) δ [ppm]: 179.26 (C1). 175.24 (C20). 157.58 (C9). 135.83 (C4), 133.69 (C7). 129.30 (C11). 128.93 (C12). 127.12 (C5). 126.36 (C13). 126.03 (C6). 118.93 (C10). 105.56 (C8). 55.32 (C21). 52.79 (C14). 52.32 (C18). 45.66 (C2), 33.08 (C17), 30.21 (C16), 18.38 (C3), 15.29 (C5). **FT-IR** ν (ATR): 3150.85, 3034.80, 3000.26, 2962.20, 2934.66, 2838.88, 2615.89, 2215.88, 2165.91, 2165.91, 20459.87, 2023.72, 1927.07, 1745.83, 1729.29, 1673.81, 1629.79, 1603.97, 1524.90, 1503.99, 1486.48, 1449.43, 1418.99, 1385.14, 1356.25, 1266.44, 1228.76, 1193.39, 1175.49, 1157.86, 1123.91, 1069.03, 1028.40, 957.90, 925.80, 855.77, 810.66, 761.52, 749.17, 713.74, 683.68, 583.79, 522.91, 531.47, 473.63, 421.79 cm⁻¹. $[\alpha]_D^{20} = +32.815$ (c=0.576% (m/v) in EtOH). **UV-Vis** (EtOH): λ_{max}=228.9 nm. **Elemental analysis**: C₂₀H₂₇NO₅S (393.498 g/mol), calculated (%): C (61.05), H (6.92), N (3.56), O (20.33). S (8.15), found: C (61.15), H (6.85), N (3.44), O (20.20). S (8.05).

L-methioninium ethyl ester *S*-(+)-naproxenate - [MetOEt][NAP]
 (2*S*)-1-ethoxy-4-(methylsulfanyl)-1-oxobutan-2-aminium (2*S*)-2-(6-methoxynaphthalen-2-yl)propanoate



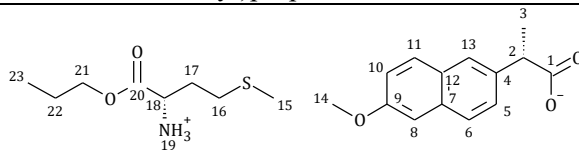
¹H NMR (400 MHz, CDCl₃) δ [ppm]: 7.73–7.62 (s+d, 3H, H11, H8, H6), 7.41 (d, *J*_{10,11}=7.0 Hz, 1H, H10), 7.15–7.06 (s+d, 2H, H13, H5), 5.32 (s, 3H, H19), 4.22–4.10 (m, 2H, H21), 3.90 (s, 3H, H14), 3.87–3.76 (m, 1H, H2), 3.67–3.59 (m, 1H, H18), 2.56 (t, *J*_{16,17}=8.1 Hz, 2H, H16), 2.05 (s, 3H, H15), 2.09–1.96 (m, 1H, H17'), 1.90–1.77 (m, 1H, H17''), 1.55 (d, *J*_{3,2}=7.2 Hz, 3H, H3), 1.25 (t, *J*_{22,21}=7.1 Hz, 3H, H22). **¹³C NMR** (100 MHz, CDCl₃) δ [ppm]: 179.16 (C1), 174.71 (C20), 157.58 (C9), 135.88 (C4), 133.69 (C7), 129.30 (C11), 128.94 (C12), 127.10 (C5), 126.37 (C13), 126.02 (C6), 118.90 (C21), 105.58 (C14), 61.32 (C21), 55.31 (C14), 52.90 (C18), 45.67 (C2), 33.15 (C17), 30.23 (C16), 18.39 (C22), 15.29 (C3), 14.19 (C22). **FT-IR** ν (ATR): 3061.45, 2968.21, 2914.40, 2869.15, 2192.99, 1741.66, 1683.65, 1604.24, 1524.75, 1504.37, 1486.04, 1451.54, 1419.57, 1386.74, 1353.16, 1302.09, 1265.08, 1230.15, 1194.67, 1176.73, 1158.90, 1117.31, 1096.48, 1068.58, 1029.88, 1010.85, 989.25, 956.54, 926.70, 892.86, 854.07, 810.49, 762.01, 715.13, 684.05, 655.26, 626.65, 573.90, 532.22, 523.26, 475.05, 441.63, 419.65, 405.87 cm⁻¹. $[\alpha]_D^{20} = +30.847$ (c=0.496% (m/v) in EtOH). **UV-Vis** (EtOH): λ_{max}=228.9 nm. **Elemental analysis**: C₂₁H₂₉NO₅S (407.524 g/mol), calculated (%): C (61.89), H (7.17), N (3.44), O (19.63), S (7.87), found: C (60.95), H (7.19), N (3.60), O (19.55), S (7.86).

L-methioninium isopropyl ester *S*-(+)-naproxenate - [MetOiPr][NAP]
 (2*S*)-4-(methylsulfanyl)-1-oxo-1-[(propan-2-yl)oxy]butan-2-aminium
 (2*S*)-2-(6-methoxynaphthalen-2-yl)propanoate



¹H NMR (400 MHz, CDCl₃) δ [ppm]: 7.73–7.61 (s+d, 3H, H11, H8, H6), 7.42 (d, $J_{10,11}$ =6.8 Hz, 1H, H10), 7.15–7.06 (s+d, 2H, H13, H5), 5.55 (s, 3H, H19), 5.09–4.95 (m, 1H, H21), 3.90 (s, 3H, H14), 3.85–3.75 (m, 1H, H2), 3.63–3.56 (m, 1H, H18), 2.53 (d, $J_{16,17}$ =8.0 Hz, 2H, H16), 2.03 (s, 3H, H15), 2.06–1.94 (m, 1H, H17'), 1.89–1.76 (m, 1H, H17''), 1.54 (d, $J_{3,2}$ =7.2 Hz, 3H, H3), 1.29–1.17 (2d, 6H, H23, H22). **¹³C NMR** (100 MHz, CDCl₃) δ [ppm]: 179.14 (C1), 174.06 (C20), 157.56 (C9), 136.00 (C4), 133.67 (C7), 129.30 (C11), 128.95 (C12), 127.08 (C5), 126.40 (C13), 126.00 (C6), 118.88 (C10), 105.58 (C8), 68.99 (C21), 55.30 (C14), 52.99 (C18), 45.75 (C2), 33.09 (C17), 30.19 (C3), 21.77 (C23), 21.74 (C22), 18.42 (C3), 15.28 (C15). **FT-IR** ν (ATR): 3056.84, 3031.03, 2981.32, 2911.67, 2865.90, 2176.98, 2021.03, 1739.84, 1681.78, 1604.32, 1548.45, 1505.37, 1482.29, 1464.14, 1450.41, 1421.01, 1380.80, 1352.99, 1343.89, 1261.75, 1227.69, 1194.17, 1178.86, 1160.04, 1118.23, 1100.09, 1070.10, 1028.28, 990.17, 955.39, 926.85, 896.39, 884.68, 855.44, 823.54, 811.48, 761.27, 750.31, 718.51, 684.18, 667.45, 654.20, 628.61, 574.42, 531.11, 522.56, 501.87, 476.80, 469.36, 442.56, 435.88, 425.77 cm⁻¹. **¹. $[\alpha]_D^{20}$** = +26.693 (c=0.520% (m/v) in EtOH). **UV-Vis** (EtOH): λ_{\max} =229.0 nm. **Elemental analysis:** C₂₂H₃₁NO₅S (421.550 g/mol), calculated (%): C (62.68), H (7.41), N (3.32), O (18.98). S (7.61), found: C (61.95), H (7.36), N (3.30), O (18.61). S (7.51).

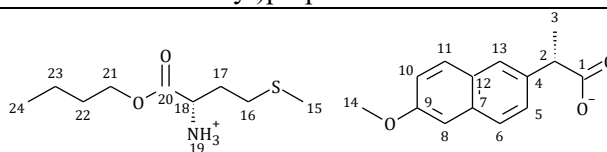
L-methioninium propyl ester *S*-(+)-naproxenate - [MetOPr][NAP]
 (2*S*)-4-(methylsulfanyl)-1-oxo-1-propoxybutan-2-aminium (2*S*)-2-(6-methoxynaphthalen-2-yl)propanoate



¹H NMR (400 MHz, CDCl₃) δ in ppm: 7.71–7.65 (s+d, 3H, H11, H8, H6), 7.41 (d, $J_{10,11}$ =6.8 Hz, 1H, H10), 7.15–7.07 (s+d, 2H, H13, H5), 5.16 (s, 3H, H19), 4.14–4.00 (m, 2H, H21), 3.90 (s, 3H, H14), 3.87–3.77 (m, 1H, H2), 3.68–3.61 (m, 1H, H18), 2.57 (t, $J_{16,17}$ =8.1 Hz, 2H, H16), 2.05 (s, 3H, H15), 2.10–1.97 (m, 1H, H17'), 1.91–1.77 (m, 1H, H17''), 1.71–1.60 (m, 2H, H22), 1.56 (d, $J_{3,2}$ =7.2 Hz, 3H, H3), 0.93 (t, J =7.4 Hz, 3H, H23). **¹³C NMR** (100 MHz, CDCl₃) δ in ppm: 179.17 (C1), 174.96 (C20), 157.60 (C9), 135.73 (C4), 133.71 (C7), 129.30 (C11), 128.94 (C12), 127.13 (C5), 126.34 (C13), 126.04 (C6), 118.93 (C10), 105.59 (C8), 66.89 (C21), 55.31 (C14), 52.97 (C18), 45.57 (C2), 33.29 (C17), 30.27 (C16), 21.94 (C22), 18.36 (C3), 15.29 (C15), 10.37 (C10). **FT-IR** ν (ATR):

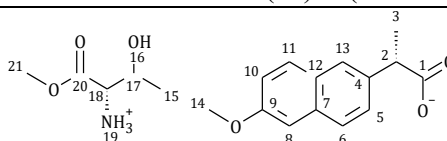
3062.39, 3023.41, 2965.48, 2926.59, 2880.48, 2173.65, 2162.12, 1741.62, 1683.51, 1604.97, 1549.30, 1505.04, 1486.78, 1449.87, 1419.95, 1386.46, 1353.02, 1344.22, 1311.55, 1287.98, 1265.95, 1217.06, 1193.17, 1177.99, 1159.47, 1120.92, 1085.56, 1071.34, 1029.95, 990.40, 979.19, 960.78, 927.30, 889.73, 854.02, 822.90, 810.56, 755.42, 718.88, 683.94, 668.45, 653.37, 629.06, 531.49, 522.55, 474.60, 468.78, 425.48 cm⁻¹. $[\alpha]_D^{20} = +27.072$ (c=0.543% (m/v) in EtOH). **UV-Vis** (EtOH): λ_{\max} =228.9 nm. **Elemental analysis:** C₂₂H₃₁NO₅S (421.550 g/mol), calculated (%): C (62.68), H (7.41), N (3.32), O (18.98). S (7.61), found: C (61.97), H (7.39), N (3.26), O (18.90). S (7.58).

L-methioninium butyl ester *S*-(+)-naproxenate - [MetOBu][NAP]
(2*S*)-1-butoxy-4-(methylsulfanyl)-1-oxobutan-2-aminium (2*S*)-2-(6-methoxynaphthalen-2-yl)propanoate



¹H NMR (400 MHz, CDCl₃) δ in ppm: 7.71–7.64 (s+d, 3H, H11, H8, H6), 7.41 (d, $J_{10,11} = 7.0$ Hz, 1H, H10), 7.15 – 7.06 (s+d, 2H, H13, 5), 5.32 (s, 3H, H19), 4.17–4.04 (m, 2H, H21), 3.90 (s, 3H, H14), 3.87–3.77 (m, 1H, H2), 3.68–3.60 (m, 1H, H18), 2.56 (t, $J_{16,17}=7.4$ Hz, 2H, H16), 2.05 (s, 3H, H15), 2.06–1.96 (m, 1H, H17'), 1.90–1.77 (m, 1H, H17''), 1.67–1.55 (m, 2H, H22), 1.55 (d, $J_{3,2}=7.1$ Hz, 3H, H3), 1.46–1.29 (m, 2H, H23), 0.92 (t, $J_{23,24}=7.4$ Hz, 3H, H24). **¹³C NMR** (100 MHz, CDCl₃) δ in ppm: 174.76 (C1), 157.57 (C20), 135.92 (C4), 133.68 (C7), 129.30 (C11), 128.94 (C12), 127.10 (C5), 126.38 (C13), 126.02 (C6), 118.90 (C10), 105.56 (C8), 65.23 (C21), 55.31 (C14), 52.88 (C18), 45.72 (C2), 33.10 (C17), 30.57 (C16), 30.22 (C22), 19.10 (C23), 18.42 (C3), 15.27 (C15), 13.69 (C24). **FT-IR** ν (ATR): 2960.66, 2931.60, 2870.49, 2189.26, 2184.48, 1740.79, 1684.01, 1604.90, 1556.55, 1504.72, 1486.60, 1454.64, 1444.32, 1420.03, 1401.37, 1386.54, 1377.56, 1353.18, 1342.06, 1315.73, 1289.49, 1265.23, 1259.30, 1236.82, 1215.22, 1193.68, 1179.38, 1159.14, 1118.74, 1086.10, 1072.53, 1030.75, 989.27, 969.45, 961.18, 951.46, 927.79, 889.92, 854.35, 822.86, 807.21, 759.99, 750.64, 719.78, 685.16, 654.00, 629.55, 576.57, 530.38, 522.22, 469.00, 431.43 cm⁻¹. $[\alpha]_D^{20} = +28.733$ (c=0.529% (m/v) in EtOH). **UV-Vis** (EtOH): λ_{\max} =229.9 nm. **Elemental analysis:** C₂₂H₃₁NO₅S (435.587 g/mol), calculated (%): C (63.42), H (7.64), N (3.22), O (18.3). S (7.36), found: C (62.52), H (8.00), N (3.30), O (18.16). S (7.47).

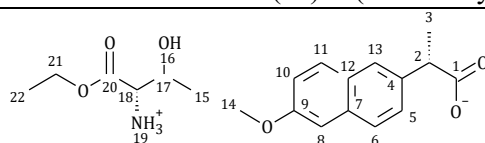
L-threoninium methyl ester *S*-(+)-naproxenate - [ThrOMe][NAP]
(2*S*)-3-hydroxy-1-methoxy-1-oxobutan-2-aminium (2*S*)-2-(6-methoxynaphthalen-2-yl)propanoate



¹H NMR (400 MHz, CDCl₃) δ [ppm]: 7.64–7.56 (s+d, 3H, H11, H8, H6), 7.37 (d, $J_{11,10}=7.5$ Hz, 1H, H10), 7.12–7.02 (s+d, 2H, H13, H5), 6.76 (s, 4H, H19, H16), 3.95–3.86 (m, 1H, H17), 3.88 (s, 3H, H14), 3.78–3.68 (m, 1H, H2), 3.59 (s, 3H, H14), 3.26 (d, $J_{18,17}=5.0$ Hz, 1H, H18), 1.48 (d, $J_{3,2}=7.1$ Hz, 3H, H3), 1.09 (d, $J_{15,17}=6.5$ Hz, 3H, H15). **¹³C NMR** (100 MHz, CDCl₃) δ [ppm]: 180.18 (C1), 171.68 (C21), 157.47 (C9), 136.77 (C4), 133.52 (C7), 129.26 (C11), 128.92 (C12), 126.95 (C5), 126.56 (C13), 125.94 (C6), 118.82 (C10), 105.54 (C8), 67.05 (C17), 59.12 (C21), 55.30 (C18), 52.61 (C14), 46.48 (C2), 19.84 (C15), 18.63 (C3). **FT-IR** ν (ATR): 3061.39, 2975.41, 2938.02, 2894.01, 2162.52, 2124.68, 1746.01, 1726.89, 1680.75, 1630.80, 1604.28, 1530.56, 1505.28, 1486.07, 1460.39, 1433.76, 1389.66, 1357.77, 1292.56, 1260.43, 1227.76, 1215.40, 1194.92, 1175.72, 1158.00, 1072.86, 1091.20, 1050.35, 1040.92, 1028.47, 1005.65, 966.30, 924.89, 889.17, 856.12, 794.35, 751.92, 742.92, 707.61, 685.82, 673.78, 642.76, 600.18, 530.70, 483.59, 471.61, 404.07 cm⁻¹. **$[\alpha]_D^{20}$** = +33.797 (c=0.497 % (m/v) in EtOH). **UV-Vis** (EtOH): λ_{\max} =230.2 nm. **Elemental analysis**: C₁₉H₂₅NO₆ (363.405 g/mol), calculated (%): C (62.80), H (6.93), N (3.85), O (26.42), found: C (62.71), H (6.89), N (3.77), O (26.30).

L-threoninium ethyl ester *S*-(+)-naproxenate - [ThrOEt][NAP]

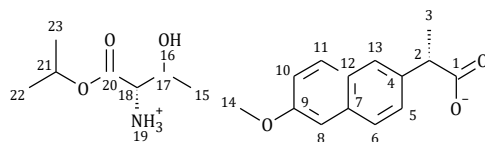
(2*S*)-1-ethoxy-3-hydroxy-1-oxobutan-2-aminium (2*S*)-2-(6-methoxynaphthalen-2-yl)propanoate



¹H NMR (400 MHz, CDCl₃) δ [ppm]: 7.70–7.63 (s+d, 3H, H11, H8, H6), 7.40 (d, $J_{10,11}=6.9$ Hz, 1H, H10), 7.14–7.06 (s+d, 2H, H13, H5), 4.93 (s, 4H, H19, H16), 4.23–4.12 (m, 2H, H21), 3.96–3.91 (m, 1H, H17), 3.90 (s, 3H, H14), 3.84–3.77 (m, 1H, H2), 3.28 (d, $J_{18,17}=5.2$ Hz, 1H, H18), 1.55 (d, $J_{3,2}=7.1$ Hz, 3H, H3), 1.27–1.21 (m, 6H, H22, H15). **¹³C NMR** (100 MHz, CDCl₃) δ [ppm]: 179.52 (C1), 173.13 (C21), 157.59 (C9), 135.85 (C4), 133.68 (C7), 129.29 (C11), 128.92 (C12), 127.11 (C5), 126.37 (C13), 126.03 (C6), 118.93 (C10), 105.57 (C8), 67.92 (C17), 61.52 (C21), 59.57 (C18), 55.32 (C14), 45.72 (C2), 19.88 (C15), 18.40 (C3), 14.14 (C22). **FT-IR** ν (ATR): 3135.68, 2979.96, 2936.13, 2098.98, 2036.60, 1749.17, 1627.80, 1605.19, 1505.13, 1483.96, 1463.17, 1443.68, 1421.67, 1375.73, 1357.33, 1342.72, 1285.22, 1270.35, 1256.58, 1217.58, 1194.60, 1180.34, 1159.70, 1128.93, 1065.28, 1022.49, 999.41, 956.96, 929.53, 897.84, 864.90, 854.11, 825.04, 811.96, 759.30, 684.14, 533.22, 523.52, 499.00, 477.02, 469.93, 402.66 cm⁻¹. **$[\alpha]_D^{20}$** = +27.455 (c=0.440% (m/v) in EtOH). **UV-Vis** (EtOH): λ_{\max} =229.8nm. **Elemental analysis**: C₂₀H₂₇NO₆ (377.431 g/mol), calculated (%): C (63.64), H (7.21), N (3.71), O (25.43), found: C (63.53), H (7.20), N (3.67), O (25.43).

L-threoninium isopropyl ester *S*-(+)-naproxenate - [ThrOiPr][NAP]

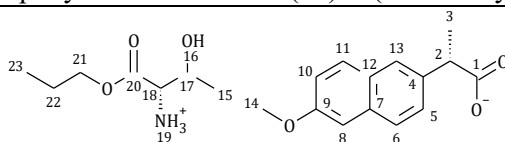
(2*S*)-3-hydroxy-1-oxo-1-[(propan-2-yl)oxy]butan-2-aminium
(2*S*)-2-(6-methoxynaphthalen-2-yl)propanoate



¹H NMR (400 MHz, CDCl₃) δ [ppm]: 7.70–7.63 (s+d, 3H, H11, H8, H6), 7.40 (d, $J_{11,10}$ =6.9 Hz, 1H, H10), 7.14–7.06 (s+d, 2H, H13, H5), 5.06–5.01 (m, 1H, H21), 4.97 (s, 4H, H19, H16), 3.94–3.85 (m, 4HH17, H14), 3.83–3.75 (m, 1H, H2), 3.25 (d, $J_{18,17}$ =5.4 Hz, 1H, H18), 1.54 (d, $J_{3,2}$ =7.2 Hz, 3H, H3), 1.26–1.20 (m, 9H, H23, H22, H14). **¹³C NMR** (100 MHz, CDCl₃) δ [ppm]: 179.58 (C1), 172.49 (C21), 157.56 (C9), 136.03 (C4), 133.65 (C7), 129.29 (C11), 128.93 (C12), 127.08 (C5), 126.41 (C13), 126.01 (C6), 118.90 (C10), 105.56 (C8), 69.31 (C17), 67.90 (C21), 59.66 (C18), 55.31 (C14), 45.86 (C2), 21.73 (C23), 21.70 (C22), 19.88 (C15), 18.45 (C3). **FT-IR** ν (ATR): 3062.56, 2977.06, 2936.31, 2905.00, 2080.00, 1742.10, 1652.14, 1629.99, 1605.23, 1563.90, 1541.37, 1532.62, 1520.59, 1516.17, 1506.41, 1504.91, 1486.69, 1457.65, 1456.11, 1445.11, 1436.24, 1423.04, 1384.83, 1356.47, 1341.84, 1290.04, 1257.60, 1228.28, 1213.00, 1197.75, 1180.67, 1160.67, 1142.56, 1121.43, 1103.63, 1072.39, 1051.13, 1031.83, 1005.59, 985.28, 957.14, 925.84, 913.22, 891.65, 857.74, 853.45, 818.93, 808.05, 783.87, 757.78, 712.32, 684.98, 670.97, 530.78, 522.29, 474.25 cm⁻¹. $[\alpha]_D^{20}$ = +26.608 (c=0.451% (m/v) in EtOH). **UV-Vis** (EtOH): λ_{\max} =229.6nm. **Elemental analysis:** C₂₁H₂₉NO₆ (391.458 g/mol), calculated (%): C (64.43), H (7.47), N (3.58), O (24.52), found: C (64.39), H (7.39), N (3.43), O (24.18).

L-threoninium propyl ester S-(+)-naproxenate - [ThrOPr][NAP]

(2S)-3-hydroxy-1-oxo-1-propoxybutan-2-aminium (2S)-2-(6-methoxynaphthalen-2-yl)propanoate

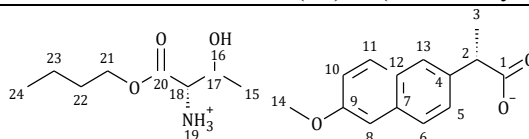


¹H NMR (400 MHz, CDCl₃) δ in ppm: 7.67–7.64 (s+d, 3H, H11, H8, H6), 7.38 (d, $J_{10,11}$ =6.9 Hz, 1H, H10), 7.12–7.08 (s+d, 2H, H13, H5), 5.44 (s, 4H, H19, H16), 4.11–4.02 (m, 2H, H21), 3.96–3.92 (m, 1H, H17), 3.90 (s, 3H, H14), 3.82–3.77 (m, 1H, H2), 3.29 (d, $J_{18,17}$ =5.2 Hz, 1H, H18), 1.68–1.61 (m, 2H, H22), 1.52 (d, $J_{3,2}$ =7.2 Hz, 3H, H3), 1.19 (d, $J_{15,17}$ =6.4 Hz, 3H, H15), 0.92 (t, $J_{23,22}$ =7.4 Hz, 3H, H23). **¹³C NMR** (100 MHz, CDCl₃) δ in ppm: 179.70 (C1), 172.92 (C21), 157.56 (C9), 136.05 (C4), 133.65 (C7), 129.29 (C11), 128.92 (C12), 127.07 (C5), 126.41 (C13), 126.01 (C6), 118.90 (C10), 105.56 (C8), 67.81 (C17), 67.15 (C21), 59.53 (C18), 55.31 (C14), 45.89 (C2), 21.87 (C22), 19.91 (C15), 18.44 (C3), 10.34 (C23). **FT-IR** ν (ATR): 3056.35, 2968.95, 2935.60, 2899.28, 2878.28, 878.78, 2839.45, 2060.63, 1739.77, 1670.26, 1631.75, 1604.55, 1552.54, 1504.58, 1483.56, 1456.51, 1389.03, 1359.78, 1290.10, 1264.54, 1226.27, 1211.49, 1174.08, 1158.93, 1119.84, 1059.06, 1031.13, 959.92, 925.24, 889.98, 852.34, 810.28, 747.96, 682.02, 665.48, 521.87, 554.76, 474.35 400.24 cm⁻¹. $[\alpha]_D^{20}$ = +26.269 (c=0.453% (m/v) in EtOH). **UV-Vis** (EtOH):

$\lambda_{\text{max}}=229.9\text{nm}$. **Elemental analysis:** $\text{C}_{21}\text{H}_{29}\text{NO}_6$ (391.458 g/mol), calculated (%): C (64.43), H (7.47), N (3.58), O (24.52), found: C (64.33), H (7.51), N (3.61), O (23.89).

L-threoninium butyl ester *S*-(+)-naproxenate - [ThrOBu][NAP]

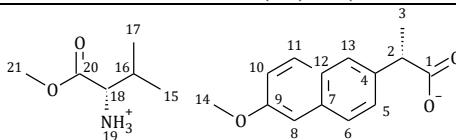
(2*S*)-1-butoxy-3-hydroxy-1-oxobutan-2-aminium (2*S*)-2-(6-methoxynaphthalen-2-yl)propanoate



^1H NMR (400 MHz, CDCl_3) δ in ppm: 7.66–7.62 (s+d, 3H, H11, H8, H6), 7.38 (d, $J_{10,11}=6.7$ Hz, 1H, H10), 7.11–7.07 (s+d, 2H, H13, H5), 5.81 (s, 4H, H19, H16), 4.13–4.03 (m, 2H, H21), 3.96–3.86 (m, 4H, H17, H14), 3.81–3.73 (m, 1H, H2), 3.28 (d, $J_{18,19}=5.1$ Hz, 1H, H18), 1.62–1.53 (m, 2H, H22), 1.51 (d, $J_{3,2}=7.1$ Hz, 3H, H3), 1.40–1.27 (m, 2H, H23), 1.17 (d, $J_{15,17}=6.4$ Hz, 3H, H15), 0.91 (t, $J_{23,24}=7.4$ Hz, 3H, H24). **^{13}C NMR** (100 MHz, CDCl_3) δ in ppm: 179.85 (C1), 172.39 (C21), 157.52 (C9), 136.39 (C4), 133.59 (C7), 129.28 (C11), 128.93 (C12), 127.01 (C5), 126.48 (C13), 125.97 (C6), 118.85 (C10), 105.55 (C8), 67.58 (C17), 65.55 (C21), 59.42 (C18), 55.30 (C14), 46.15 (C2), 30.47 (C23), 19.91 (C22), 19.05 (C15), 18.54 (C3), 13.67 (C24). **FT-IR** ν (ATR): 3129.76, 2973.87, 2954.03, 2932.75, 2872.39, 2738.79, 2082.47, 1750.49, 1732.63, 1636.77, 1627.13, 1616.03, 1605.19, 1561.40, 1559.50, 1557.00, 1553.77, 1544.60, 1541.44, 1539.84, 1524.82, 1522.18, 1519.66, 1516.45, 1508.02, 1506.45, 1505.04, 1495.66, 1485.07, 1472.99, 1462.36, 1456.24, 1444.77, 1436.12, 1431.44, 1421.97, 1385.58, 1358.08, 1344.37, 1327.31, 1311.95, 1286.67, 1270.65, 1257.65, 1214.64, 1194.84, 1180.63, 1159.90, 1136.69, 1073.23, 1023.32, 1005.25, 929.20, 898.05, 854.46, 824.85, 811.87, 685.00, 477.60, 470.90 cm^{-1} . $[\alpha]_D^{20} = +26.154$ ($c=0.455\%$ (m/v) in EtOH). **UV-Vis** (EtOH): $\lambda_{\text{max}}=229.4\text{nm}$. **Elemental analysis:** $\text{C}_{22}\text{H}_{31}\text{NO}_6$ (405.485 g/mol), calculated (%): C (65.17), H (7.71), N (3.45), O (23.67), found: C (64.98), H (7.66), N (3.44), O (23.01).

L-valinium methyl ester *S*-(+)-naproxenate - [ValOMe][NAP]

(2*S*)-1-methoxy-3-methyl-1-oxobutan-2-aminium (2*S*)-2-(6-methoxynaphthalen-2-yl)propanoate

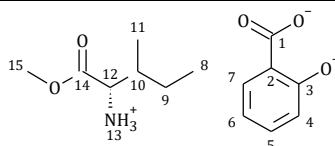


^1H NMR (400 MHz, CDCl_3) δ [ppm]: 7.70–7.61 (s+d, 3H, H11, H8, H6), 7.41 (d, $J_{10,11}=7.8$ Hz, 1H, H10), 7.14–7.05 (s+d, 2H, H13, H5), 5.25 (s, 3H, H19), 3.90 (s, 3H, H21), 3.76–3.82 (m, 1H, H2), 3.67 (s, 3H, H14), 3.38 (d, $J_{18,16}=4.8$ Hz, 1H, H18), 2.08–1.96 (m, 1H, H16), 1.53 (d, $J_{3,2}=7.1$ Hz, 3H, H3), 0.92 (d, $J_{16,15}=6.9$ Hz, 3H, H15), 0.86 (d, $J_{16,17}=7.4$ Hz, 3H, H17). **^{13}C NMR** (100 MHz, CDCl_3) δ [ppm]: 179.08 (C1), 174.63 (C20), 157.52 (C9), 136.25 (C4), 133.63 (C7), 129.29 (C11), 128.95 (C12), 127.02 (C6), 126.45 (C13), 125.97 (C5), 118.82 (C10), 105.58 (C8), 59.15 (C21), 55.30 (C18), 51.97 (C14), 45.88 (C2), 31.61 (C16), 29.71 (C17), 18.84 (C15), 18.49 (C3), 17.30

(C14). **FT-IR** ν (ATR): 2980.30, 2889.50, 2489.50, 2497.69, 2048.99, 1744.70, 1628.80, 1602.89, 1504.45, 1484.02, 1462.59, 1387.95, 1361.41, 1292.96, 1253.93, 1226.85, 1208.46, 1175.61, 1159.45, 1117.27, 1058.44, 1027.86, 958.59, 925.11, 892.20, 855.60, 812.47, 795.79, 745.03, 704.19, 681.28, 616.33, 574.96 cm^{-1} . $[\alpha]_D^{20} = +42.805$ ($c=0.549\%$ (m/v) in EtOH). **UV-Vis** (EtOH): $\lambda_{\text{max}}=228.1$ nm. **Elemental analysis**: $\text{C}_{20}\text{H}_{27}\text{NO}_5$ (361.432 g/mol), calculated (%): C (66.46), H (7.53), N (3.88), O (22.13), found: C (65.95), H (7.48), N (3.81), O (22.20).

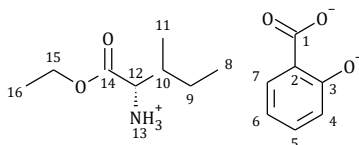
L-AMINO ACID ALKYL ESTER SALTS OF SALICYLIC ACID

L-isoleucinium methyl ester salicylate - [IleOMe][SA] (2S)-1-methoxy-3-methyl-1-oxopentan-2-aminium 2-hydroxybenzoate



^1H NMR (400 MHz, CDCl_3) δ [ppm]: 7.79 (d, $J_{7,8}=7.8$ Hz, 1H, H7), 7.33 (t, $J_{5,4}=6.6$ Hz, 1H, H5), 6.89 (d, $J_{4,5}=7.4$ Hz, 1H, H4), 6.76 (t, $J_{6,7}=6.5$ Hz, 1H, H6), 3.92 (d, $J_{12,10}=4.2$ Hz, 1H, H12), 3.60 (s, 3H, H15), 2.04–1.92 (m, 1H, H10), 1.53–1.37 (m, 1H, H9'), 1.36–1.22 (m, 1H, H9''), 0.95 (d, $J_{11,10}=6.9$ Hz, 3H, H11), 0.82 (t, $J_{8,9}=7.4$ Hz, 3H, H8). **^{13}C NMR** (100 MHz, CDCl_3) δ [ppm]: 175.52 (C1), 169.51 (C14), 161.62 (C3), 134.05 (C5), 130.63 (C7), 118.34 (C2), 116.90 (C6), 116.89 (C4), 57.41 (C15), 52.75 (C12), 36.76 (C1), 25.65 (C9), 14.59 (C11), 11.45 (C8). **FT-IR**: ν (ATR): 2972.05, 2937.76, 2861.71, 2861.71, 2547.46, 2124.85, 2015.77, 1925.92, 1733.93, 1697.73, 1593.98, 1554.70, 1536.94, 1481.91, 1451.29, 1441.26, 1407.26, 1379.72, 1352.24, 1338.62, 1309.50, 1279.46, 1252.64, 1226.58, 1199.59, 1169.11, 1155.56, 1144.37, 1133.87, 1099.80, 1083.48, 1054.34, 1032.89, 996.52, 975.82, 961.38, 910.44, 872.63, 860.61, 829.98, 807.04, 786.61, 754.94, 705.32, 664.85, 566.34, 536.11, 492.91, 454.65, 421.11 cm^{-1} . $[\alpha]_D^{20} = +19.452$ ($c=0.730\%$ (m/v) in EtOH). **UV-Vis** (EtOH): $\lambda_{\text{max}}=229.1$ nm. **Elemental analysis**: $\text{C}_{14}\text{H}_{20}\text{NO}_5$ (282.313 g/mol), calculated (%): C (59.56), H (7.14), N (4.96), O (28.34), found: C (59.78), H (7.23), N (4.98), O (27.99).

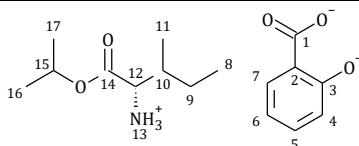
L-isoleucinium ethyl ester salicylate - [IleOEt][SA] (2S)-1-ethoxy-3-methyl-1-oxopentan-2-aminium 2-hydroxybenzoate



^1H NMR (400 MHz, CDCl_3) δ [ppm]: 7.79 (d, $J_{7,6}=7.8$ Hz, 1H, H7), 7.31 (t, $J_{5,4}=6.5$ Hz, 1H, H5), 6.88 (d, $J=7.3$ Hz, 1H, H4), 6.75 (t, $J_{6,7}=7.4$ Hz, 1H, H6), 4.16–3.96 (m, 2H, H15), 3.85 (d, $J_{12,10}=4.1$ Hz, 1H, H12), 2.03–1.90 (m, 1H, H4), 1.53–1.39 (m, 1H, H9'), 1.37–1.22 (m, 1H, H9''), 1.15 (t, $J_{16,15}=7.2$ Hz, 3H, H16), 0.95 (d, $J_{11,10}=7.0$ Hz, 3H, H11), 0.82 (t, $J_{9,8}=7.4$ Hz, 3H, H8). **^{13}C NMR** (100 MHz, CDCl_3) δ [ppm]: 175.64 (C1), 169.40 (C14), 161.65 (C3), 133.65 (C5), 130.63 (C7),

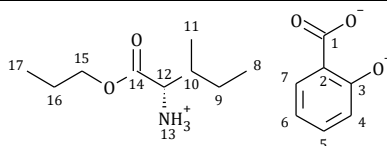
118.10 (C2), 117.63 (C6), 116.78 (C4), 62.19 (C15), 57.39 (C12), 36.91 (C10), 25.70 (C9), 14.60 (C11), 13.92 (C16), 11.50 (C8). **FT-IR:** ν (ATR): 2963.82, 2936.43, 2878.60, 2593.31, 2161.09, 1730.07, 1614.53, 1594.39, 1557.04, 1505.04, 1481.66, 1452.14, 1380.86, 1351.37, 1307.80, 1286.10, 1254.20, 1225.29, 1198.07, 1157.14, 1139.28, 1098.99, 1055.46, 1029.43, 1011.48, 993.39, 973.49, 949.32, 930.82, 860.40, 823.30, 806.53, 786.54, 751.49, 702.57, 665.75, 568.02, 532.19, 458.09, 420.36 cm^{-1} . $[\alpha]_D^{20} = +21.673$ ($c=0.521\%$ (m/v) in EtOH). **UV-Vis** (EtOH): $\lambda_{\text{max}}=228.7$ nm. **Elemental analysis:** $\text{C}_{15}\text{H}_{22}\text{NO}_5$ (296.339 g/mol), calculated (%): C (60.80), H (7.48), N (7.48), O (27.00), found: C (60.98), H (7.51), N (4.60), O (26.90).

L-isoleucinium isopropyl ester salicylate - [IleOiPr][SA]
(2S)-3-methyl-1-oxo-1-[(propan-2-yl)oxy]pentan-2-aminium 2-hydroxybenzoate



^1H NMR (400 MHz, CDCl_3) δ [ppm]: 7.80 (d, $J_{7,6}=7.8$ Hz, 1H, H7), 7.30 (t, $J_{7,6}=6.6$ Hz, 1H, H5), 6.87 (d, $J_{4,5}=7.2$ Hz, 1H, H4), 6.74 (t, $J_{6,7}=7.6$ Hz, 1H, H6), 5.02–4.88 (m, 1H, H15), 3.86 (d, $J_{12,10}=3.9$ Hz, 1H, H12), 2.04–1.93 (m, 1H, H10), 1.54–1.39 (m, 1H, H9'), 1.38–1.23 (m, 1H, H9''), 1.19 (d, $J_{11,10}=6.2$ Hz, 3H, H11), 1.14 (d, $J_{17,15}=6.3$ Hz, 3H, H17), 0.97 (d, $J_{16,15}=6.8$ Hz, 3H, H16), 0.83 (t, $J_{8,9}=7.4$ Hz, 3H, H8). **^{13}C NMR** (100 MHz, CDCl_3) δ [ppm]: 175.47 (C1), 169.03 (C14), 161.66 (C3), 133.68 (C5), 130.69 (C7), 118.14 (C2), 117.43 (C6), 116.76 (C4), 70.52 (C15), 57.29 (C12), 36.93 (C10), 25.75 (C9), 21.60 (C16), 21.46 (C17), 14.57 (C11), 11.57 (C8). **FT-IR:** ν (ATR): 2966.13, 2934.94, 2878.33, 2637.64, 2160.77, 2147.55, 1733.13, 1591.53, 1561.80, 1540.80, 1480.75, 1465.50, 1449.72, 1410.96, 1378.04, 1358.38, 1308.42, 1283.76, 1251.31, 1230.10, 1192.73, 1159.51, 1141.36, 1100.39, 1054.29, 1029.32, 998.19, 956.01, 936.73, 903.24, 860.13, 846.60, 826.62, 806.93, 755.75, 705.08, 665.21, 614.62, 569.61, 536.00, 452.94, 452.94 cm^{-1} . $[\alpha]_D^{20} = +18.939$ ($c=0.528\%$ (m/v) in EtOH). **UV-Vis** (EtOH): $\lambda_{\text{max}}=228.5$ nm. **Elemental analysis:** $\text{C}_{16}\text{H}_{24}\text{NO}_4$ (310.366 g/mol), calculated (%): C (61.92), H (7.79), N (4.51), O (25.78), found: C (62.13), H (7.85), N (4.48), O (25.52).

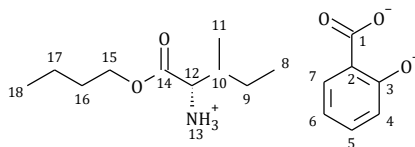
L-isoleucinium propyl ester salicylate - [IleOPr][SA]
(2S)-3-methyl-1-oxo-1-propoxypentan-2-aminium 2-hydroxybenzoate



^1H NMR (400 MHz, CDCl_3) δ in ppm: 7.80 (d, $J_{7,6}=7.8$ Hz, 1H, H7), 7.32 (t, $J_{5,4}=6.3$ Hz, 1H, H5), 6.88 (d, $J_{4,5}=7.3$ Hz, 1H, H4), 6.75 (t, $J_{6,7}=7.6$ Hz, 1H, H6), 4.06–3.96 (m, 1H, H12), 3.97–3.87 (m, 2H, H15), 2.08–1.93 (m, 1H, H10), 1.60–1.49 (m, 2H, H16), 1.50–1.38 (m, 1H, H9'), 1.37–1.25 (m, 1H, H9''), 0.97 (d, $J_{11,10}=6.9$ Hz, 3H, H11), 0.90–0.77 (2t, 6H, H17, H8). **^{13}C NMR** (100 MHz,

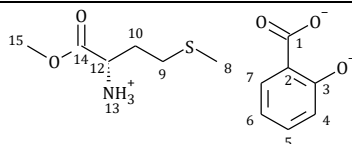
CDCl₃) δ in ppm: 175.44 (C1), 169.40 (C14), 161.65 (C3), 133.89 (C5), 130.68 (C7), 118.25 (C2), 117.04 (C6), 116.83 (C4), 67.87 (C15), 57.32 (C12), 36.81 (C10), 25.71 (C9), 21.66 (C16), 14.61 (C11), 11.52 (C17), 10.25 (C8). **FT-IR:** ν (ATR): 2967.58, 2933.30, 2877.54, 2724.67, 2630.32, 2173.42, 2115.87, 1738.36, 1702.10, 1596.50, 1564.18, 1515.88, 1480.30, 1455.15, 1424.12, 1384.14, 1351.10, 1339.29, 1320.37, 1305.72, 1291.93, 1249.56, 1219.08, 1187.85, 1155.31, 1142.38, 1115.98, 1091.37, 1058.31, 1028.98, 1015.89, 964.84, 943.09, 923.26, 898.79, 860.80, 845.52, 807.54, 794.61, 753.26, 704.04, 664.50, 566.23, 534.03, 520.75, 486.33, 450.57, 428.99 cm⁻¹. $[\alpha]_D^{20} = +19.639$ (c=0.479% (m/v) in EtOH). **UV-Vis** (EtOH): λ_{\max} =228.6 nm. **Elemental analysis:** C₁₆H₂₄NO₄ (310.366 g/mol), calculated (%): C (61.92), H (7.79), N (4.51), O (25.78), found: C (61.87), H (7.84), N (4.59), O (25.69).

L-isoleucinium butyl ester salicylate -[IleOBu][SA]
(2*S*)-1-butoxy-3-methyl-1-oxopentan-2-aminium 2-hydroxybenzoate



¹H NMR (400 MHz, CDCl₃) δ in ppm: 7.79 (d, $J_{7,6}$ =7.8 Hz, 1H, H7), 7.32 (t, $J_{5,4}$ =6.4 Hz, 1H, H5), 6.88 (d, $J_{4,5}$ =7.2 Hz, 1H, H4), 6.75 (t, $J_{6,7}$ =7.7 Hz, 1H, H6), 4.12–3.94 (m, 2H, H15), 3.88 (d, $J_{12,14}$ =4.0 Hz, 1H, H12), 2.04–1.93 (m, 1H, H4), 1.56–1.42 (m, 3H, H16, H9'), 1.33–1.22 (m, 3H, H17, H9''), 0.97 (d, $J_{11,10}$ =6.9 Hz, 3H, H11), 0.90–0.81 (2t, 6H, H18, H8). **¹³C NMR** (100 MHz, CDCl₃) δ in ppm: 175.40 (C1), 169.81 (C14), 161.67 (C3), 133.84 (C5), 130.68 (C7), 118.21 (C2), 117.11 (C6), 116.82 (C4), 66.08 (C15), 57.38 (C12), 36.97 (C10), 30.29 (C16), 25.61 (C9), 18.99 (C17), 14.71 (C11), 13.56 (C18), 11.53 (C8). **FT-IR:** ν (ATR): 2959.85, 2933.17, 2873.12, 2165.04, 2120.51, 1731.20, 1731.20, 1593.22, 1560.28, 1480.57, 1463.17, 1450.73, 1416.76, 1381.81, 1353.13, 1336.61, 1309.50, 1252.76, 1219.46, 1167.19, 1157.23, 1139.59, 1061.68, 1029.10, 955.23, 937.17, 885.33, 861.33, 826.61, 806.34, 793.48, 750.90, 703.80, 664.24, 566.97, 534.67, 518.97, 508.62, 472.09, 456.19 cm⁻¹. $[\alpha]_D^{20} = +16.667$ (c=0.558% (m/v) in EtOH). **UV-Vis** (EtOH): λ_{\max} =229.2 nm. **Elemental analysis:** C₁₇H₂₆NO₄ (324.393 g/mol), calculated (%): C (62.94), H (8.08), N (4.32), O (24.66), found: C (63.16), H (8.21), N (4.46), O (24.15).

L-methioninium methyl ester salicylate - [MetOMe][SA]
(2*S*)-1-methoxy-4-(methylsulfanyl)-1-oxobutan-2-aminium 2-hydroxybenzoate

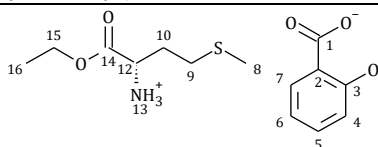


¹H NMR (400 MHz, CDCl₃) δ [ppm]: 7.78 (d, $J_{7,6}$ =7.8 Hz, 1H, H7), 7.33 (t, $J_{5,4}$ =6.6 Hz, 1H, H5), 6.89 (d, $J_{4,5}$ =7.1 Hz, 1H, H4), 6.77 (t, $J_{6,7}$ =7.1 Hz, 1H, H6), 4.18–4.09 (m, 1H, H12), 3.60 (s, 3H, H15), 2.70–2.48 (m, 2H, H10), 2.26–2.07 (m, 2H, H9), 1.96 (s, 3H, H8). **¹³C NMR** (100 MHz,

CDCl₃) δ [ppm]: 175.52 (C1), 170.36 (C14), 161.54 (C3), 134.15 (C5), 130.54 (C7), 118.51 (C2), 117.00 (C6), 116.92 (C4), 53.18 (C15), 51.93 (C12), 29.91 (C10), 29.42 (C9), 14.93 (C8). **FT-IR:** ν (ATR): 2952.79, 2918.04, 2112.46, 1740.84, 1694.88, 1591.84, 1563.75, 1481.27, 1451.68, 1379.56, 1348.15, 1307.50, 1284.14, 1250.16, 1222.98, 1154.27, 1139.71, 1079.18, 1029.85, 961.80, 939.32, 882.11, 859.87, 827.08, 805.56, 703.78, 664.37, 566.37, 534.21, 451.49, 408.63 cm⁻¹. $[\alpha]_D^{20} = +15.245$ (c=0.551% (m/v) in EtOH). **UV-Vis** (EtOH): $\lambda_{\max}=228.9$ nm. **Elemental analysis:** C₁₃H₁₈NO₅S (300.351 g/mol), calculated (%): C (51.99), H (6.04), N (4.66), O (26.63), S (10.68), found: C (51.75), H (5.95), N (4.60), O (26.58), S (10.54).

L-methioninium ethyl ester salicylate - [MetOEt][SA]

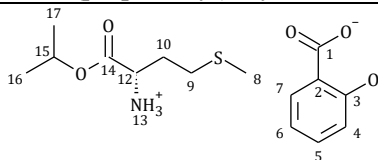
(2S)-1-ethoxy-4-(methylsulfanyl)-1-oxobutan-2-aminium 2-hydroxybenzoate



¹H NMR (400 MHz, CDCl₃) δ [ppm]: 7.79 (d, $J_{7,8}=7.8$ Hz, 1H, H7), 7.32 (t, $J_{5,4}=6.6$ Hz, 1H, H5), 6.89 (d, $J_{4,5}=7.3$ Hz, 1H, H4), 6.77 (t, $J_{6,5}=7.5$ Hz, 1H, H6), 4.14–4.07 (m, 2H, H12), 4.05–3.98 (m, 1H, H16), 2.70–2.53 (m, 2H, H10), 2.25–2.07 (m, 2H, H9), 1.97 (s, 3H, H8), 1.15 (t, $J_{16,15}=7.2$ Hz, H16). **¹³C NMR** (100 MHz, CDCl₃) δ [ppm]: 175.54 (C1), 170.15 (C14), 161.61 (C3), 134.03 (C5), 130.55 (C7), 118.39 (C2), 117.06 (C6), 116.97 (C4), 62.65 (C15), 52.07 (C12), 30.18 (C16), 29.49 (C10), 14.97 (C9), 13.86 (C8). **FT-IR:** ν (ATR): 2980.66, 2917.54, 2112.53, 1739.86, 1622.62, 1590.72, 1559.25, 1481.39, 1452.49, 1378.50, 1347.23, 1304.73, 1249.05, 1218.09, 1154.81, 1140.55, 1091.98, 1078.14, 1028.56, 1014.56, 955.79, 858.57, 806.18, 753.27, 704.16, 664.76, 566.55, 535.42, 456.54, 427.83 cm⁻¹. $[\alpha]_D^{20} = +11.776$ (c=0.518 % (m/v) in EtOH). **UV-Vis** (EtOH): $\lambda_{\max}=229.1$ nm. **Elemental analysis:** C₁₄H₂₀NO₅S (314.379 g/mol), calculated (%): C (53.49), H (6.41), N (4.46), O (25.45), S (10.20), found: C (53.38), H (6.38), N (4.57), O (25.34), S (10.13).

L-methioninium isopropyl ester salicylate - [MetOiPr][SA]

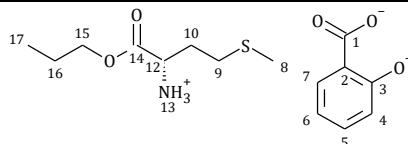
(2S)-4-(methylsulfanyl)-1-oxo-1-[(propan-2-yl)oxy]butan-2-aminium 2-hydroxybenzoate



¹H NMR (400 MHz, CDCl₃) δ [ppm]: 7.79 (d, $J_{7,8}=7.8$ Hz, 1H), 7.32 (t, $J_{5,4}=6.7$ Hz, 1H, H5), 6.88 (d, $J_{4,5}=7.4$ Hz, 1H, H4), 6.76 (t, $J_{6,5}=7.4$ Hz, 1H, H6), 5.01–4.87 (m, 1H, H15), 4.09–4.02 (m, 1H, H12), 2.70–2.52 (m, 2H, H10), 2.24–2.06 (m, 2H, H9), 1.97 (s, 3H, H8), 1.17 (d, $J_{17,15}=6.3$ Hz, 3H, H17), 1.12 (d, $J_{16,15}=6.3$ Hz, 3H, H16). **¹³C NMR** (100 MHz, CDCl₃) δ [ppm]: 175.55 (C1), 169.59 (C14), 161.65 (C3), 133.97 (C5), 130.57 (C7), 118.34 (C2), 117.14 (C6), 116.96 (C4), 70.84 (C15), 52.14 (C12), 30.23 (C16), 29.47 (C10), 21.51 (C17), 21.39 (C16), 14.98 (C8). **FT-IR:** ν (ATR): 2981.24, 2918.03, 2834.66, 2755.53, 2630.57, 2116.31, 1732.50, 1683.52, 1625.38, 1592.59,

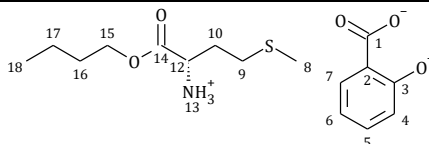
1556.98, 1480.52, 1447.94, 1383.82, 1375.92, 1348.86, 1308.73, 1285.15, 1248.46, 1232.05, 1202.08, 1182.41, 1159.81, 1143.19, 1103.03, 1029.02, 1007.16, 965.14, 955.45, 944.17, 915.75, 901.82, 883.92, 860.86, 821.31, 807.59, 797.46, 753.26, 703.63, 665.26, 567.44, 533.62, 495.61, 476.16, 455.41, 431.33 cm⁻¹. $[\alpha]_D^{20} = +10.575$ (c=0.539 % (m/v) in EtOH). **UV-Vis** (EtOH): λ_{\max} =229.3 nm. **Elemental analysis:** C₁₅H₂₂NO₅S (328.404 g/mol), calculated (%): C (54.86), H (6.75), N (4.26), O (24.36), S (9.76), found: C (54.96), H (6.79), N (4.24), O (24.10), S (9.59).

L-methioninium propyl ester salicylate - [MetOPr][SA]
 (2*S*)-4-(methylsulfanyl)-1-oxo-1-propoxybutan-2-aminium 2-hydroxybenzoate



¹H NMR (400 MHz, CDCl₃) δ in ppm: 7.78 (d, $J_{7,6}$ =7.8 Hz, 1H, H7), 7.32 (t, $J_{5,4}$ =6.4 Hz, 1H, H5), 6.88 (d, $J_{4,5}$ =7.2 Hz, 1H, H4), 6.76 (d, $J_{6,5}$ =7.5 Hz, 1H, H6), 4.16–4.08 (m, 1H, H12), 4.04–3.87 (m, 2H, H15), 2.70–2.53 (m, 2H, H10), 2.26–2.07 (m, 2H, H9), 1.96 (s, 3H, H8), 1.58–1.48 (m, 2H, H16), 0.83 (t, $J_{17,16}$ =7.4 Hz, 3H, H17). **¹³C NMR** (100 MHz, CDCl₃) δ in ppm: 175.59 (C1), 161.62 (C14), 133.95 (C5), 130.55 (C7), 118.34 (C2), 117.22 (C6), 116.94 (C4), 68.10 (C15), 52.04 (C12), 30.19 (C10), 29.48 (C9), 21.63 (C16), 14.94 (C8), 10.16 (C17). **FT-IR:** ν (ATR): 2963.18, 2934.86, 2916.38, 2877.28, 2752.43, 2623.53, 2147.33, 1738.68, 1683.85, 1621.53, 1591.69, 1556.63, 1480.33, 1444.73, 1411.74, 1380.14, 1351.70, 1308.57, 1245.54, 1224.67, 1187.68, 1157.36, 1142.70, 1079.19, 1031.67, 996.15, 976.21, 962.10, 940.36, 923.39, 884.51, 873.29, 860.58, 823.29, 807.21, 784.24, 754.78, 706.60, 663.83, 568.00, 537.32, 476.43, 454.88 cm⁻¹. $[\alpha]_D^{20} = +11.515$ (c=0.495% (m/v) in EtOH). **UV-Vis** (EtOH): λ_{\max} =229.1 nm. **Elemental analysis:** C₁₅H₂₂NO₅S (328.404 g/mol), calculated (%): C (54.86), H (6.75), N (4.26), O (24.36), S (9.76), found: C (54.74), H (6.68), N (4.16), O (23.85), S (9.57).

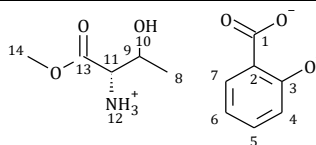
L-methioninium butyl ester salicylate - [MetOBu][SA]
 (2*S*)-1-butoxy-4-(methylsulfanyl)-1-oxobutan-2-aminium 2-hydroxybenzoate



¹H NMR (400 MHz, CDCl₃) δ in ppm: 7.78 (d, $J_{7,6}$ =7.8 Hz, 1H, H7), 7.32 (t, $J_{5,4}$ =6.4 Hz, 1H, H5), 6.88 (d, $J_{4,5}$ =7.3 Hz, 1H, H4), 6.77 (t, $J_{6,5}$ =7.5 Hz, 1H, H6), 4.14–4.07 (m, 1H, H12), 4.09–3.93 (m, 2H, H15), 2.70–2.53 (m, 2H, H10), 2.25–2.07 (m, 2H, H9), 1.97 (s, 3H, H8), 1.57–1.42 (m, 2H, H16), 1.37–1.14 (m, 2H, H17), 0.85 (t, $J_{18,17}$ =7.4 Hz, 3H, H18). **¹³C NMR** (100 MHz, CDCl₃) δ in ppm: 175.55 (C1), 170.22 (C14), 161.63 (C3), 134.00 (C5), 130.56 (C7), 118.36 (C2), 117.07 (C6), 116.96 (C4), 66.45 (C15), 52.04 (C12), 30.23 (C16), 30.18 (C10), 29.49 (C9), 18.94 (C16), 14.95 (C8), 13.61 (C18). **FT-IR:** ν (ATR): 2957.97, 2929.41, 2873.16, 2845.19, 2755.41, 2630.42,

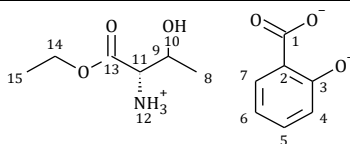
2118.76, 1736.31, 1703.00, 1683.67, 1669.56, 1594.44, 1556.45, 1480.97, 1450.00, 1381.55, 1354.93, 1331.21, 1307.45, 1283.53, 1253.76, 1221.73, 1171.66, 1153.87, 1139.33, 1082.93, 1057.85, 1031.04, 1018.32, 993.60, 964.97, 932.02, 860.50, 829.09, 805.74, 750.76, 725.97, 702.75, 664.96, 566.59, 533.77, 506.24, 452.36, 427.92 cm⁻¹. $[\alpha]_D^{20} = +10.537$ (c=0.503 % (m/v) in EtOH). **UV-Vis** (EtOH): λ_{\max} =229.5 nm. **Elemental analysis:** C₁₆H₂₄NO₅S (342.431 g/mol), calculated (%): C (56.12), H (7.06), N (4.09), O (23.36), S (9.36), found: C (56.24), H (7.10), N (4.02), O (23.48), S (9.24).

L-threoninium methyl ester salicylate - [ThrOMe][SA]
(2S)-3-hydroxy-1-methoxy-1-oxobutan-2-aminium 2-hydroxybenzoate



¹H NMR (400 MHz, DMSO-*d*₆) δ [ppm]: 7.72 (d, $J_{7,6}$ =7.7 Hz, 1H, H7), 7.26 (t, $J_{5,6}$ =7.5 Hz, 1H, H5), 6.74 (d, $J_{4,5}$ =7.2 Hz, 1H, H4), 6.71 (t, $J_{6,5}$ =7.7 Hz, 1H, H6), 4.20–4.10 (m, 1H, H9), 3.98 (d, $J_{11,9}$ =3.9 Hz, 1H, H11), 3.74 (s, 3H, H14), 2.56–2.45 (m, 1H, H10), 1.22 (d, $J_{8,9}$ =6.6 Hz, 3H, H8). **¹³C NMR** (100 MHz, DMSO-*d*₆) δ [ppm]: 172.60 (C1), 169.36 (C13), 162.48 (C3), 133.27 (C5), 130.60 (C7), 118.44 (C2), 117.65 (C6), 116.65 (C4), 65.55 (C9), 58.41 (C14), 53.15 (C11), 20.42 (C8). **FT-IR:** ν (ATR): 3016.23, 2988.66, 2953.96, 2953.96, 2865.69, 2733.49, 2689.98, 2551.76, 2078.74, 1864.17, 1833.98, 1742.08, 1701.15, 1655.55, 1603.00, 1587.91, 1574.30, 1525.02, 1482.43, 1465.82, 1444.60, 1385.75, 1363.21, 1328.66, 1297.53, 1244.77, 1211.09, 1154.54, 1144.81, 1122.78, 1059.85, 1043.23, 1030.63, 994.94, 967.10, 921.45, 891.95, 860.76, 841.73, 804.63, 786.02, 767.42, 737.08, 705.94, 663.26, 568.89, 533.78, 487.83, 455.56, 432.45, 422.25 cm⁻¹. $[\alpha]_D^{20} = -3.069$ (c=0.619% (m/v) in EtOH). **UV-Vis** (EtOH): λ_{\max} =229.1 nm. **Elemental analysis:** C₁₂H₁₆NO₆ (270.259 g/mol), calculated (%): C (53.33), H (5.97), N (5.18), O (35.52), found: C (53.10), H (5.91), N (5.04), O (36.64).

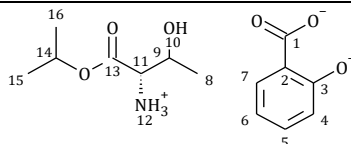
L-threoninium ethyl ester salicylate - [ThrOEt][SA]
(2S)-1-ethoxy-3-hydroxy-1-oxobutan-2-aminium 2-hydroxybenzoate



¹H NMR (400 MHz, CDCl₃) δ [ppm]: 7.76 (d, $J_{7,6}$ =7.7 Hz, 1H, H7), 7.29 (t, $J_{5,6}$ =7.5 Hz, 1H, H5), 6.85 (d, $J_{4,5}$ =7.3 Hz, 1H, H4), 6.74 (t, $J_{6,5}$ =7.7 Hz, 1H, H6), 4.27–4.17 (m, 1H, H9), 4.16–3.98 (m, 2H, H14), 3.80 (d, $J_{11,9}$ =5.3 Hz, 1H, H11), 1.33 (d, $J_{8,9}$ =6.4 Hz, 3H, H8), 1.13 (t, $J_{15,14}$ =7.1 Hz, 3H, H15). **¹³C NMR** (100 MHz, CDCl₃) δ [ppm]: 175.47 (C1), 169.15 (C13), 161.32 (C3), 134.02 (C5), 130.57 (C7), 118.56 (C2), 116.94 (C6), 116.86 (C4), 66.31 (C9), 62.98 (C14), 59.20 (C11), 20.33 (C8), 13.75 (C15). **FT-IR:** ν (ATR): 2981.33, 2938.04, 2905.68, 2724.44, 2118.63, 2104.07,

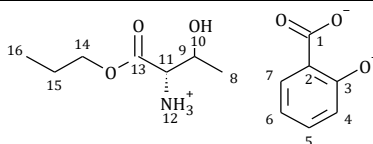
1735.39, 1591.97, 1560.55, 1482.09, 1454.04, 1380.20, 1351.70, 1300.67, 1250.00, 1216.82, 1155.45, 1141.12, 1048.68, 1029.92, 934.37, 914.01, 859.05, 831.25, 805.90, 749.61, 704.36, 664.62, 565.86, 533.67, 449.71 cm⁻¹. $[\alpha]_D^{20} = -4.068$ (c=0.590 % (m/v) in EtOH). **UV-Vis** (EtOH): λ_{\max} =229.3 nm. **Elemental analysis:** C₁₃H₁₈NO₆ (284.286 g/mol), calculated (%): C (54.92), H (6.38), N (4.93), O (33.77), found: C (54.98), H (6.42), N (4.90), O (33.68).

L-threoninium isopropyl ester salicylate - [ThrOiPr][SA]
(2*S*)-3-hydroxy-1-oxo-1-[(propan-2-yl)oxy]butan-2-aminium 2-hydroxybenzoate



¹H NMR (400 MHz, CDCl₃) δ [ppm]: 7.76 (d, $J_{7,6}$ =7.8 Hz, 1H, H7), 7.27 (t, $J_{5,6}$ =7.3 Hz, 1H, H5), 6.84 (d, $J_{4,5}$ =8.2 Hz, 1H, H4), 6.72 (t, $J_{6,5}$ =7.7 Hz, 1H, H6), 5.02–4.88 (m, 1H, H14), 4.26–4.15 (m, 1H, H9), 3.79 (d, $J_{11,9}$ =5.3 Hz, 1H, H11), 1.34 (d, $J_{9,8}$ =6.5 Hz, 3H, H8), 1.18–1.08 (2t, 6H, H16, H15). **¹³C NMR** (100 MHz, CDCl₃) δ [ppm]: 175.54 (C1), 168.48 (C13), 161.30 (C3), 133.86 (C5), 130.59 (C7), 118.50 (C2), 117.22 (C4), 116.81 (C6), 71.32 (C9), 66.32 (C14), 59.28 (C11), 21.41 (C16), 21.38 (C15), 20.42 (C8). **FT-IR:** ν (ATR): 3048.29, 2981.18, 2935.69, 2070.02, 1735.37, 1683.53, 1590.93, 1560.08, 1482.48, 1454.56, 1377.14, 1351.25, 1293.63, 1249.50, 1223.99, 1182.55, 1141.42, 1097.72, 1050.19, 1029.84, 952.85, 913.19, 895.62, 859.58, 807.58, 754.74, 703.77, 664.82, 566.35, 534.71, 493.78, 457.51, 418.13 cm⁻¹. $[\alpha]_D^{20} = -4.105$ (c=0.609 % (m/v) in EtOH). **UV-Vis** (EtOH): λ_{\max} =229.2 nm. **Elemental analysis:** C₁₄H₂₀NO₆ (298.312 g/mol), calculated (%): C (56.37), H (6.76), N (4.70), O (32.18), found: C (56.24), H (6.67), N (4.65), O (32.02).

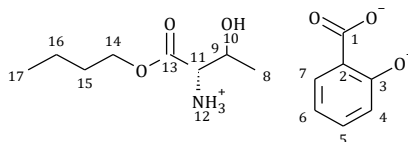
L-threoninium propyl ester salicylate - [ThrOPr][SA]
(2*S*)-3-hydroxy-1-oxo-1-propoxybutan-2-aminium 2-hydroxybenzoate



¹H NMR (400 MHz, CDCl₃) δ in ppm: 7.77 (d, $J_{7,8}$ =7.6 Hz, 1H), 7.30 (t, $J_{5,4}$ =7.4 Hz, 1H, H5), 6.86 (d, $J_{4,5}$ =8.3 Hz, 1H, H4), 6.74 (t, $J_{6,5}$ =7.5 Hz, 1H, H6), 4.27–4.17 (m, 1H, H9), 4.07–3.91 (m, 2H, H14), 3.80 (d, $J_{11,12}$ =5.3 Hz, 1H, H11), 1.59–1.49 (m, 2H, H15), 1.35 (d, $J_{8,9}$ =6.5 Hz, 3H, H8), 0.83 (t, $J_{16,15}$ =7.4 Hz, 3H, H16). **¹³C NMR** (100 MHz, CDCl₃) δ in ppm: 175.43 (C1), 169.44 (C13), 161.37 (C3), 134.08 (C5), 130.58 (C7), 118.56 (C2), 116.89 (C6), 116.79 (C4), 68.39 (C9), 66.44 (C14), 59.23 (C11), 21.58 (C15), 20.36 (C8), 10.14 (C16). **FT-IR:** ν (ATR): 3018.35, 2974.54, 2945.24, 2887.22, 2718.09, 2635.27, 2084.75, 1726.59, 1687.49, 1630.14, 1612.14, 1596.54, 1566.65, 1527.34, 1481.18, 1449.59, 1437.46, 1402.34, 1385.78, 1351.74, 1324.46, 1307.36, 1287.79, 1252.14, 1222.50, 1155.34, 1143.15, 1128.37, 1112.34, 1059.76, 1047.29, 1031.72, 943.23,

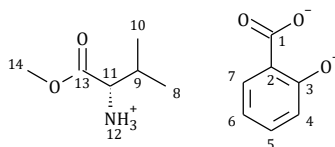
921.31, 899.45, 860.27, 830.08, 803.27, 754.56, 704.08, 664.78, 566.13, 542.05, 534.49, 495.70, 450.03 cm⁻¹. $[\alpha]_D^{20} = -5.952$ (c=0.605% (m/v) in EtOH). **UV-Vis** (EtOH): $\lambda_{\max}=229.4$ nm. **Elemental analysis:** C₁₄H₂₀NO₆ (298.312 g/mol), calculated (%): C (56.37), H (6.76), N (4.70), O (32.18), found: C (56.32), H (6.71), N (4.63), O (32.10).

L-threoninium butyl ester salicylate - [ThrOBu][SA]
(2*S*)-1-butoxy-3-hydroxy-1-oxobutan-2-aminium 2-hydroxybenzoate



¹H NMR (400 MHz, CDCl₃) δ in ppm: 7.76 (d, $J_{7,6}=7.8$ Hz, 1H, H7), 7.29 (t, $J_{5,6}=7.5$ Hz, 1H, H5), 6.86 (d, $J_{4,5}=7.3$ Hz, 1H, H4), 6.75 (t, $J_{6,5}=7.5$ Hz, 1H, H6), 4.26–4.16 (m, 1H, H9), 4.11–3.94 (m, 2H, H14), 3.79 (d, $J_{11,9}=5.5$ Hz, 1H, H11), 1.54–1.41 (m, 2H, H15), 1.34 (d, $J_{8,9}=6.4$ Hz, 3H, H8), 1.31–1.17 (m, 2H, H16), 0.83 (t, $J_{17,16}=7.3$ Hz, 3H, H17). **¹³C NMR** (100 MHz, CDCl₃) δ in ppm: 175.46 (C1), 169.39 (C13), 161.37 (C3), 134.03 (C5), 130.58 (C7), 118.54 (C2), 116.88 (C4), 66.76 (C9), 66.41 (C14), 59.23 (C11), 30.17 (C16), 20.35 (C8), 18.90 (C15), 13.58 (C16). **FT-IR:** ν (ATR): 2963.43, 2934.54, 2875.90, 2797.88, 2741.13, 2649.14, 2598.03, 2484.59, 2316.45, 2185.48, 2124.82, 2018.02, 2008.59, 1965.34, 1945.93, 1918.39, 1808.21, 1734.34, 1697.10, 1639.04, 1629.30, 1618.34, 1594.48, 1555.39, 1532.80, 1482.62, 1451.67, 1388.92, 1359.24, 1349.53, 1324.75, 1311.11, 1292.61, 1251.93, 1222.10, 1156.30, 1145.63, 1102.64, 1056.28, 1044.14, 1029.90, 959.81, 942.65, 927.46, 911.63, 862.18, 829.93, 820.90, 796.05, 769.26, 750.10, 704.84, 664.50, 566.35, 549.00, 532.35, 511.37, 476.32, 450.66, 402.38 cm⁻¹. $[\alpha]_D^{20} = -5.442$ (c=0.588 % (m/v) in EtOH). **UV-Vis** (EtOH): $\lambda_{\max}=229.1$ nm. **Elemental analysis:** C₁₅H₂₂NO₆ (312.339 g/mol), calculated (%): C (57.68), H (7.10), N (4.48), O (30.74), found: C (57.51), H (7.13), N (4.37), O (30.65).

L-valinium methyl ester salicylate - [ValOMe][SA]
(2*S*)-1-methoxy-3-methyl-1-oxobutan-2-aminium 2-hydroxybenzoate



¹H NMR (400 MHz, CDCl₃) δ [ppm]: 7.78 (d, $J_{7,6}=7.6$ Hz, 1H, H7), 7.32 (t, $J_{5,4}=6.3$ Hz, 1H, H5), 6.89 (d, $J_{4,3}=7.2$ Hz, 1H, H4), 6.76 (t, $J_{6,5}=8.2$ Hz, 1H, H6), 3.79 (d, $J_{11,9}=4.8$ Hz, 1H, H11), 3.59 (s, 3H, H14), 2.33–2.17 (m, 1H, H9), 1.04–0.97 (2t, 6H, H10, H8). **¹³C NMR** (100 MHz, CDCl₃) δ [ppm]: 175.60 (C1), 169.87 (C13), 161.60 (C3), 133.86 (C5), 130.60 (C7), 118.25 (C2), 117.29 (C6), 116.85 (C4), 58.65 (C14), 52.76 (C11), 30.17 (C9), 18.21 (C10), 18.06 (C8). **FT-IR:** ν (ATR): 2986.80, 2936.24, 2726.31, 2581.01, 2145.81, 1735.97, 1605.29, 1555.14, 1482.53, 1451.32, 1410.35, 1375.75, 1344.03, 1308.84, 1255.25, 1225.82, 1200.70, 1175.34, 1141.82, 1107.69,

1072.90, 1051.03, 1030.76, 981.06, 934.19, 871.35, 859.93, 845.53, 805.32, 769.37, 755.17, 705.17, 664.68, 537.61, 453.82, 416.25 cm⁻¹. $[\alpha]_D^{20} = +14.679$ (c=0.545% (m/v) in EtOH). **UV-Vis** (EtOH): $\lambda_{\text{max}}=230.1$ nm. **Elemental analysis:** C₁₃H₁₉NO₅ (269.297 g/mol), calculated (%): C (57.98), H (7.11), N (5.20), O (29.71), found: C (57.98), H (7.12), N (5.12), O (29.76).

Appendix II

REAGENTS AND MATERIALS

Table A1. List of materials and reagents.

Name	Supplier	Purity	Numer CAS
Active substances from the group of non-steroidal anti-inflammatory drugs			
<i>S</i> -(+)-ibuprofen	Ark Pharm, Inc. (Arlington Hts, Illinois, USA)	≥98%	51146-56-6
(<i>R,S</i>)-ibuprofen	AmBeed (Arlington Hts, USA).	≥98%	15687-27-1
(<i>R,S</i>)-ketoprofen	Biosynth Carbosynth (Staad, Switzerland)	≥98%	22071-15-4
salicylic acid	Sigma-Aldrich (Steinheim am Albuch, Germany)	≥99%	69-72-7
<i>S</i> -(+)-naproxen	AmBeed (Arlington Hts, USA)	≥98%	22204-53-1
L-amino acids			
L-isoleucine	FluoroChem (Derbyshire, UK)	≥98%	73-32-5
L-methionine	FluoroChem (Derbyshire, UK)	≥98%	63-68-3
L-valine	FluoroChem (Derbyshire, UK)	≥98%	72-18-4
L-threonine	FluoroChem (Derbyshire, UK)	≥98%	72-19-5
Organic solvents for HPLC analysis			
acetonitrile (HPLC GR)	POCH (Gliwice, Poland)	≥99.9%	75-05-8
methanol (HPLC GR)	Sigma-Aldrich (Steinheim am Albuch, Germany)	≥99.9%	67-56-1
2-propanol (HPLC GR)	Chempur (Piekary Śląskie, Poland)	≥99.9%	67-63-0
Alcohols and organic solvents			
methanol	Chempur (Piekary Śląskie, Poland)	p.a.	67-56-1
ethanol anhydrous	POCH (Gliwice, Poland)	p.a.	64-17-5
propanol	POCH (Gliwice, Poland)	p.a.	71-23-8
2-propanol	Chempur (Piekary Śląskie, Poland)	p.a.	71-23-8
<i>n</i> -butanol	Eurochem BGD. (Tarnów, Poland)	p.a.	71-36-3
<i>n</i> -pentanol	Acros Organic	99%	71-41-0
<i>n</i> -hexanol	Alfa Aesar (Kandel, Germany)	99%	111-27-3
<i>n</i> -heptanol	Alfa Aesar (Kandel, Germany)	99%	
<i>n</i> -octanol	Alfa Aesar (Kandel, Germany)	99%	111-87-5
acetone	PH Karpinex (Warszwa, Poland)	p.a.	67-64-1
dimethyl sulfoxide	Chempur (Piekary Śląskie, Poland)	p.a.	67-68-5
methylene chloride	Chempur (Piekary Śląskie, Poland)	p.a.	75-09-2
chloroform	P.P.H. StanLab (Lublin, Poland)	p.a.	67-66-3
<i>n</i> -hexan	Chempur (Piekary Śląskie, Poland)	p.a.	110-777-6
ethyl acetate	POCH (Gliwice, Poland)	99.8%	141-78-6
toluene	P.P.H. StanLab (Lublin, Poland)	p.a.	108-88-3
diethyl ether	POCH (Gliwice, Poland)	p.a.	60-29-7
chloroform-d (+0.03% TMSCl)	Deutero GmbH (Kastellaun, Germany)	99.8%	865-49-6
(methyl sulfoxide)-d ₆ (+0.03% TMSCl)	Deutero GmbH (Kastellaun, Germany)	99.8%	2206-27-1
Other analytical reagents			

Name	Supplier	Purity	Numer CAS
Phosphate Buffered Saline (PBS), tablets for solution preparation	EMD Millipore Corp.; Merck. (Darmstadt, Germany)	p.a.	-
sodium chloride	Eurochem BGD. (Tarnów, Poland)	p.a.	7647-14-5
potassium chloride	Eurochem BGD. (Tarnów, Poland)	p.a.	7447-40-7
chlorotrimethylsilane	Sigma-Aldrich (Steinheim am Albuch, Germany)	≥98%	75-77-4
sodium sulfate anhydrous	Chempur (Piekary Śląskie, Poland)	p.a.	7757-82-8
magnesium sulfate	Eurochem BGD. (Tarnów, Poland)	p.a.	10034-99-8
ammonia solution 25%	P.P.H. StanLab (Lublin, Poland)	p.a.	1336-21-6
potassium dihydrogen phosphate	Fisher Scientific, (Loughborough, UK)	≥99.5%	7778-77-0
dipotassium hydrogen phosphate anhydrous	Fisher Scientific, (Loughborough, UK)	≥99%	7758-11-4
disodium hydrogen phosphate	Eurochem BGD. (Tarnów, Poland)	p.a.	10039-32-4
Celugel (hydroxyethylcellulose mucilago)	Actifarm, Caesar&Loretz GmbH (Hilden, Germany)	p.a.	-

FORMATION CONSTANT, SOLUBILITY AND LIPOPHILICITY RESULTS

Table A2. The formation constants log(K_s) of L-amino acid alkyl esters salts.

Compound	pK _B of base	Log(K _s)				
		[(S+)-IBU]	[IBU]	[NAP]	[KETO]	[SA]
[MetOMe]	3.98±0.01	—	5.37±0.10	5.70±0.04	5.91±0.05	6.84±0.05
[MetOEt]	3.87±0.02	—	5.46±0.02	5.79±0.06	6.00±0.11	6.93±0.04
[MetOiPr]	3.82±0.02	—	5.53±0.09 ^[181]	5.86±0.04 ^[181]	6.07±0.07 ^[181]	7.00±0.08 ^[181]
[MetOPr]	3.88±0.01	—	5.47±0.05 ^[182]	5.80±0.06 ^[182]	6.01±0.06 ^[182]	6.94±0.07 ^[182]
[MetOBu]	3.65±0.02	—	5.70±0.06 ^[182]	6.03±0.06 ^[182]	6.24±0.06 ^[182]	7.17±0.07 ^[182]
[ThrOMe]	2.99±0.05	—	6.36±0.04	6.69±0.22	6.90±0.04	7.83±0.04
[ThrOEt]	2.98±0.03	—	6.37±0.05	6.70±0.06	6.91±0.21	7.84±0.11
[ThrOiPr]	2.88±0.02	—	6.47±0.08 ^[181]	6.80±0.09 ^[181]	7.01±0.05 ^[181]	7.94±0.21 ^[181]
[ThrOPr]	2.72±0.01	—	6.63±0.07 ^[182]	6.96±0.07 ^[182]	7.17±0.07 ^[182]	8.10±0.08 ^[182]
[ThrOBu]	2.52±0.01	—	6.83±0.07 ^[182]	7.16±0.06 ^[182]	7.37±0.07 ^[182]	8.30±0.08 ^[182]
[IleOMe]	3.84±0.02	—	5.51±0.06	5.84±0.24	5.84±0.09	6.98±0.06
[IleOEt]	3.64±0.01	—	5.71±0.21	6.04±0.13	6.04±0.10	7.18±0.08
[IleOiPr]	3.57±0.03	—	5.78±0.11 ^[181]	6.11±0.08 ^[181]	6.11±0.04 ^[181]	7.25±0.06 ^[181]
[IleOPr]	3.52±0.02	—	5.83±0.06 ^[182]	6.16±0.06 ^[182]	6.37±0.06 ^[182]	7.30±0.07 ^[182]
[IleOBu]	3.23±0.02	—	6.12±0.06 ^[182]	6.45±0.06 ^[182]	6.66±0.06 ^[182]	7.59±0.07 ^[182]
[ValOMe]	4.20±0.01	5.06±0.07	5.15±0.07	5.48±0.04	5.69±0.03	6.62±0.05
[ValOEt]	4.12±0.05	5.14±0.05	5.23±0.05	5.56±0.09	5.77±0.09	6.70±0.11
[ValOiPr]	3.79±0.03	5.47±0.01	5.56±0.04 ^[181]	5.89±0.07 ^[181]	6.10±0.07 ^[181]	7.03±0.13 ^[181]
[ValOPr]	3.77±0.01	5.49±0.04	5.58±0.06 ^[182]	5.91±0.06 ^[182]	6.12±0.06 ^[182]	7.05±0.07 ^[182]
[ValOBu]	3.52±0.02	5.74±0.03	5.83±0.06 ^[182]	6.16±0.06 ^[182]	6.37±0.06 ^[182]	7.30±0.07 ^[182]

Compound	pK _B of base	Log(K _s)				
		[(S+)-IBU]	[IBU]	[NAP]	[KETO]	[SA]
[ValOAm]	3.47±0.04	5.79±0.02	5.88±0.08	–	–	–
[ValOHex]	3.44±0.03	5.82±0.02	5.91±0.07	–	–	–
[ValOHept]	3.39±0.05	5.87±0.10	5.96±0.07	–	–	–
[ValOOct]	3.34±0.03	5.92±0.04	6.01±0.08	–	–	–

– not synthesised

Table A3. The summary of values of the partition coefficient (logP) and solubility in water and phosphate buffer with pH=5.40 and pH=7.40 [g/L] for ibuprofen and its alkyl esters of L-amino acids at 25°C.

Compound	logP	Solubility					
		water		phosphate buffer			
				pH= 5.40		pH= 7.40	
		g/L	g _{IBU} /L	g/L	g _{IBU} /L	g/L	g _{IBU} /L
(R,S)-IBU	3.208 ±0.002	0.076 ±0.001	0.076 ±0.001	0.082 ±0.001	0.082 ±0.001	0.432 ±0.001	0.432 ±0.001
[MetOMe][IBU]	1.243 ±0.004	5.624 ±0.023	3.140 ±0.023	2.169 ±0.081	1.211 ±0.081	4.370 ±0.017	2.440 ±0.017
[MetOEt][IBU]	1.692 ±0.001	1.590 ±0.015	0.855 ±0.015	1.367 ±0.005	0.735 ±0.005	2.829 ±0.033	1.521 ±0.033
[MetOiPr][IBU]	1.509 ±0.001 ^[166]	1.191 ±0.056 ^[166]	0.618 ±0.029 ^[166]	0.932 ±0.011 ^[181]	0.483 ±0.011 ^[181]	3.376 ±0.001 ^[181]	1.752 ±0.001 ^[181]
[MetOPr][IBU]	1.397 ±0.006	1.294 ±0.005	0.671 ±0.005	1.161 ±0.017	0.603 ±0.017	2.829 ±0.076	1.468 ±0.076
[MetOBu][IBU]	2.219 ±0.013	0.894 ±0.019	0.448 ±0.019	0.716 ±0.023	0.359 ±0.023	2.558 ±0.051	1.282 ±0.051
[ThrOMe][IBU]	0.985 ±0.027	6.883 ±0.021	4.208 ±0.021	6.127 ±0.041	3.745 ±0.041	7.107 ±0.102	4.345 ±0.102
[ThrOEt][IBU]	0.909 ±0.018	9.663 ±0.017	5.640 ±0.017	9.023 ±0.025	5.266 ±0.025	9.821 ±0.037	5.732 ±0.037
[ThrOiPr][IBU]	0.998 ±0.001 ^[166]	5.005 ±0.007 ^[166]	2.809 ±0.004 ^[166]	4.931 ±0.013 ^[181]	2.768 ±0.013 ^[181]	8.839 ±0.005 ^[181]	4.962 ±0.005 ^[181]
[ThrOPr][IBU]	0.909 ±0.015	5.614 ±0.012	3.151 ±0.012	5.221 ±0.065	2.931 ±0.065	6.513 ±0.141	3.656 ±0.141
[ThrOBu][IBU]	1.214 ±0.003	4.039 ±0.035	2.184 ±0.035	3.774 ±0.014	2.041 ±0.014	5.457 ±0.098	2.951 ±0.098
[IleOMe][IBU]	1.113 ±0.015	5.722 ±0.001	3.358 ±0.001	5.218 ±0.022	3.063 ±0.022	6.147 ±0.113	3.608 ±0.113
[IleOEt][IBU]	1.517 ±0.011	3.374 ±0.005	1.904 ±0.005	3.096 ±0.018	1.747 ±0.018	3.748 ±0.015	2.115 ±0.015
[IleOiPr][IBU]	1.652 ±0.008 ^[166]	2.729 ±0.180 ^[166]	1.483 ±0.098 ^[166]	1.161 ±0.002 ^[181]	0.631 ±0.002 ^[181]	4.038 ±0.021 ^[181]	2.195 ±0.021 ^[181]
[IleOPr][IBU]	1.730 ±0.007	1.695 ±0.021	0.921 ±0.007	1.557 ±0.118	0.846 ±0.118	2.447 ±0.025	1.330 ±0.025
[IleOBu][IBU]	1.778 ±0.011	0.950 ±0.015	0.498 ±0.015	0.865 ±0.251	0.453 ±0.251	1.874 ±0.066	0.982 ±0.066
S(+)-IBU	2.212 ±0.001 ^[187]	0.090 ±0.001	0.090 ±0.001	0.137 ±0.001	0.137 ±0.001	0.514 ±0.021	0.514 ±0.021
[ValOMe][S(+)-IBU]	0.833 ±0.002 ^[187]	6.053 ±0.008	3.700 ±0.008	2.176 ±0.033	3.876 ±0.033	4.581 ±0.003	2.801 ±0.003

Compound	logP	Solubility					
		water		phosphate buffer			
				pH= 5.40		pH= 7.40	
		g/L	g _{IBU} /L	g/L	g _{IBU} /L	g/L	g _{IBU} /L
[ValOEt][S(+)-IBU]	0.961 ±0.013 ^[187]	4.454 ±0.004	2.614 ±0.004	2.380 ±0.007	3.380 ±0.007	5.027 ±0.004	2.950 ±0.004
[ValOiPr][S(+)-IBU]	1.149 ±0.001 ^[187]	2.955 ±0.013	1.668 ±0.013	1.332 ±0.005	2.232 ±0.005	4.326 ±0.012	2.441 ±0.012
[ValOPr][S(+)-IBU]	1.211 ±0.001 ^[187]	3.728 ±0.012	2.104 ±0.012	1.885 ±0.009	2.885 ±0.009	5.165 ±0.010	2.915 ±0.010
[ValOBu][S(+)-IBU]	1.357 ±0.001 ^[187]	1.942 ±0.002	1.055 ±0.002	1.249 ±0.006	2.049 ±0.006	2.683 ±0.007	1.458 ±0.007
[ValOAm][S(+)-IBU]	1.606 ±0.001 ^[187]	1.247 ±0.020	0.653 ±0.020	0.583 ±0.008	1.183 ±0.008	1.472 ±0.034	0.772 ±0.034
[ValOHex][S(+)-IBU]	1.739 ±0.001 ^[187]	0.814 ±0.001	0.414 ±0.001	0.366 ±0.004	0.683 ±0.004	1.068 ±0.017	0.543 ±0.017
[ValOHept][S(+)-IBU]	1.796 ±0.001 ^[187]	0.376 ±0.001	0.184 ±0.001	0.251 ±0.001	0.351 ±0.001	0.811 ±0.021	0.397 ±0.021
[ValOOct][S(+)-IBU]	1.874 ±0.001 ^[187]	0.234 ±0.002	0.111 ±0.002	0.154 ±0.001	0.254 ±0.001	0.432 ±0.014	0.205 ±0.014

Table A4. The summary of values of the partition coefficient (logP) and solubility in water and phosphate buffer with pH=5.40 and pH=7.40 [g/L] for ketoprofen and its alkyl esters of L-amino acids at 25°C.

Compound	logP	Solubility					
		water		phosphate buffer			
				pH=5.40		pH= 7.40	
		g/L	g _{KETO} /L	g/L	g _{KETO} /L	g/L	g _{KETO} /L
KETO	1.577 ±0.010 ^[181]	0.013 ±0.001 ^[181]	0.013 ±0.001 ^[181]	0.024 ±0.001 ^[181]	0.024 ±0.001 ^[181]	0.079 ±0.003 ^[181]	0.079 ±0.003 ^[181]
[MetOMe][KETO]	0.791 ±0.008	0.94 ±0.007	0.617 ±0.007	0.876 ±0.045	0.575 ±0.045	1.143 ±0.030	0.750 ±0.030
[MetOEt][KETO]	1.106 ±0.007	0.451 ±0.015	0.266 ±0.015	0.398 ±0.028	0.235 ±0.028	0.516 ±0.021	0.304 ±0.021
[MetOiPr][KETO]	1.227 ±0.015 ^[181]	0.289 ±0.004 ^[181]	0.165 ±0.004 ^[181]	0.171 ±0.058 ^[181]	0.098 ±0.058 ^[181]	1.086 ±0.007 ^[181]	0.622 ±0.007 ^[181]
[MetOPr][KETO]	1.239 ±0.015 ^[182]	0.307 ±0.012 ^[182]	0.175 ±0.012 ^[182]	0.233 ±0.074	0.133 ±0.074	0.425 ±0.50	0.243 ±0.050
[MetOBu][KETO]	1.548 ±0.015 ^[182]	0.265 ±0.041 ^[182]	0.147 ±0.041 ^[182]	0.201 ±0.028	0.111 ±0.028	0.307 ±0.044	0.170 ±0.044
[ThrOMe][KETO]	0.241 ±0.031	0.943 ±0.105	0.619 ±0.105	0.815 ±0.100	0.535 ±0.100	2.120 ±0.112	1.391 ±0.112
[ThrOEt][KETO]	0.322 ±0.015	0.869 ±0.023	0.550 ±0.023	0.751 ±0.014	0.476 ±0.014	1.846 ±0.072	1.169 ±0.072
[ThrOiPr][KETO]	0.516 ±0.001 ^[181]	1.012 ±0.001 ^[181]	0.619 ±0.001 ^[181]	0.823 ±0.027 ^[181]	0.504 ±0.027 ^[181]	2.566 ±0.036 ^[181]	1.570 ±0.036 ^[181]
[ThrOPr][KETO]	0.654 ±0.032 ^[182]	0.727 ±0.011 ^[182]	0.449 ±0.011 ^[182]	0.804 ±0.094	0.492 ±0.094	1.078 ±0.102	0.660 ±0.102
[ThrOBu][KETO]	0.883 ±0.021 ^[182]	0.689 ±0.009 ^[182]	0.408 ±0.009 ^[182]	0.566 ±0.007	0.335 ±0.007	0.784 ±0.014	0.464 ±0.014

Compound	logP	Solubility					
		water		phosphate buffer			
				pH=5.40		pH= 7.40	
		g/L	g _{KETO} /L	g/L	g _{KETO} /L	g/L	g _{KETO} /L
[IleOMe][KETO]	0.714 ±0.001	0.966 ±0.058	0.615 ±0.058	0.869 ±0.019	0.553 ±0.019	1.570 ±0.041	0.999 ±0.041
[IleOEt][KETO]	0.781 ±0.005	0.797 ±0.018	0.490 ±0.018	0.664 ±0.004	0.408 ±0.004	1.054 ±0.084	0.648 ±0.084
[IleOiPr][KETO]	0.897 ±0.004 ^[181]	0.577 ±0.006 ^[181]	0.343 ±0.006 ^[181]	0.344 ±0.032 ^[181]	0.205 ±0.032 ^[181]	1.173 ±0.024 ^[181]	0.698 ±0.024 ^[181]
[IleOPr][KETO]	0.946 ±0.011 ^[182]	0.682 ±0.004 ^[182]	0.406 ±0.004 ^[182]	0.545 ±0.087 ^[182]	0.324 ±0.087	0.864 ±0.052	0.514 ±0.052
[IleOBu][KETO]	1.179 ±0.006 ^[182]	0.543 ±0.002 ^[182]	0.313 ±0.002 ^[182]	0.443 ±0.005 ^[182]	0.255 ±0.005	0.613 ±0.078	0.353 ±0.078
[ValOMe][KETO]	0.726 ±0.005	0.459 ±0.050	0.303 ±0.050	0.401 ±0.027	0.265 ±0.027	1.206 ±0.019	0.796 ±0.019
[ValOEt][KETO]	0.667 ±0.001	0.526 ±0.033	0.335 ±0.033	0.499 ±0.025	0.318 ±0.025	0.620 ±0.110	0.395 ±0.110
[ValOiPr][KETO]	0.570 ±0.006 ^[181]	0.445 ±0.014 ^[181]	0.274 ±0.014 ^[181]	0.162 ±0.054 ^[181]	0.100 ±0.054 ^[181]	1.447 ±0.011 ^[181]	0.890 ±0.011 ^[181]
[ValOPr][KETO]	0.553 ±0.016 ^[182]	0.336 ±0.011 ^[182]	0.207 ±0.011 ^[182]	0.300 ±0.010	0.184 ±0.010	0.578 ±0.021	0.355 ±0.021
[ValOBu][KETO]	1.000 ±0.025 ^[182]	0.298 ±0.002 ^[182]	0.177 ±0.002 ^[182]	0.256 ±0.008	0.152 ±0.008	0.315 ±0.025	0.187 ±0.025

Table A5. The summary of values of the partition coefficient (logP) and solubility in water and phosphate buffer with pH=5.40 and pH=7.40 [g/L] for naproxen and its alkyl esters of L-amino acids at 25°C.

Compound	logP	Solubility					
		water		phosphate buffer			
				pH= 5.40		pH= 7.40	
		g/L	g _{NAP} /L	g/L	g _{NAP} /L	g/L	g _{NAP} /L
NAP	2.119 ±0.021 ^[181]	0.147 ±0.001 ^[181]	0.147 ±0.001 ^[181]	0.221 ±0.015 ^[181]	0.221 ±0.015 ^[181]	1.379 ±0.021 ^[181]	1.379 ±0.021 ^[181]
[MetOMe][NAP]	1.138 ±0.013	4.427 ±0.010	2.805 ±0.010	2.607 ±0.045	1.652 ±0.045	5.820 ±0.018	3.688 ±0.018
[MetOEt][NAP]	1.205 ±0.048	4.770 ±0.025	2.695 ±0.025	2.451 ±0.069	1.385 ±0.069	5.319 ±0.024	3.005 ±0.024
[MetOiPr][NAP]	1.372 ±0.005 ^[181]	3.011 ±0.038 ^[181]	1.645 ±0.038 ^[181]	1.509 ±0.015 ^[181]	0.824 ±0.015 ^[181]	4.404 ±0.033 ^[181]	2.405 ±0.033 ^[181]
[MetOPr][NAP]	1.329 ±0.006 ^[182]	3.100 ±0.015 ^[182]	1.693 ±0.015 ^[182]	1.645 ±0.043	0.899 ±0.043	4.455 ±0.26	2.433 ±0.026
[MetOBu][NAP]	1.621 ±0.009 ^[182]	2.478 ±0.011 ^[182]	1.310 ±0.011 ^[182]	1.236 ±0.016	0.653 ±0.016	4.024 ±0.031	2.127 ±0.031
[ThrOMe][NAP]	0.476 ±0.072	8.064 ±0.064	5.110 ±0.064	6.517 ±0.025	4.129 ±0.025	8.547 ±0.117	5.416 ±0.117
[ThrOEt][NAP]	0.856 ±0.021	7.913 ±0.044	4.828 ±0.044	5.862 ±0.019	3.576 ±0.019	8.051 ±0.109	4.912 ±0.109
[ThrOiPr][NAP]	0.089 ±0.005 ^[181]	6.457 ±0.019 ^[181]	3.798 ±0.019 ^[181]	4.381 ±0.008 ^[181]	2.585 ±0.008 ^[181]	8.711 ±0.029 ^[181]	5.137 ±0.029 ^[181]
[ThrOPr][NAP]	0.844 ±0.004 ^[182]	6.603 ±0.015 ^[182]	3.884 ±0.015 ^[182]	3.124 ±0.019	1.838 ±0.019	8.939 ±0.036	5.258 ±0.036

Compound	logP	Solubility					
		water		phosphate buffer			
				pH= 5.40		pH= 7.40	
		g/L	g _{NAP} /L	g/L	g _{NAP} /L	g/L	g _{NAP} /L
[ThrOBu][NAP]	0.951 ±0.003 ^[182]	5.332 ±0.027 ^[182]	3.028 ±0.027 ^[182]	2.663 ±0.450	1.512 ±0.450	8.669 ±0.087	4.923 ±0.087
[IleOMe][NAP]	0.517 ±0.001	5.803 ±0.024	3.559 ±0.024	3.113 ±0.103	1.909 ±0.103	7.690 ±0.122	4.716 ±0.122
[IleOEt][NAP]	1.027 ±0.020	5.620 ±0.090	3.323 ±0.090	3.480 ±0.300	2.057 ±0.300	7.140 ±0.018	4.221 ±0.018
[IleOiPr][NAP]	1.188 ±0.033 ^[181]	5.048 ±0.027 ^[181]	2.881 ±0.027 ^[181]	3.206 ±0.017 ^[181]	1.829 ±0.017 ^[181]	7.736 ±0.030 ^[181]	4.415 ±0.030 ^[181]
[IleOPr][NAP]	1.170 ±0.010 ^[182]	4.436 ±0.010 ^[182]	2.531 ±0.010 ^[182]	3.398 ±0.022	1.939 ±0.022	7.038 ±0.064	4.016 ±0.064
[IleOBu][NAP]	1.355 ±0.017 ^[182]	3.547 ±0.009 ^[182]	1.956 ±0.009 ^[182]	1.527 ±0.104	0.842 ±0.104	7.020 ±0.090	3.871 ±0.090
[ValOMe][NAP]	0.617 ±0.035	5.456 ±0.091	3.476 ±0.091	2.841 ±0.079	1.810 ±0.079	5.615 ±0.035	3.577 ±0.035
[ValOEt][NAP]	1.195 ±0.017	5.113 ±0.172	3.136 ±0.172	2.502 ±0.118	1.534 ±0.118	5.611 ±0.141	3.441 ±0.141
[ValOiPr][NAP]	1.254 ±0.016 ^[181]	3.988 ±0.020 ^[181]	2.358 ±0.020 ^[181]	2.323 ±0.033 ^[181]	1.320 ±0.033 ^[181]	5.484 ±0.012 ^[181]	3.241 ±0.012 ^[181]
[ValOPr][NAP]	1.239 ±0.018 ^[182]	4.350 ±0.013 ^[182]	2.572 ±0.013 ^[182]	2.486 ±0.068	1.470 ±0.068	5.860 ±0.055	3.464 ±0.055
[ValOBu][NAP]	1.468 ±0.021 ^[182]	3.247 ±0.005 ^[182]	1.853 ±0.005 ^[182]	1.211 ±0.014	0.691 ±0.014	5.036 ±0.104	2.874 ±0.104

Table A6. The summary of values of the partition coefficient (logP) and solubility in water and phosphate buffer with pH=5.40 and pH=7.40 [g/L] for salicylic acid and its alkyl esters of L-amino acids at 25°C.

Compound	logP	Solubility					
		water		phosphate buffer			
				pH= 5.40		pH= 7.40	
		g/L	g _{SA} /L	g/L	g _{SA} /L	g/L	g _{SA} /L
SA	1.321 ±0.018 ^[181]	3.795 ±0.004 ^[181]	3.795 ±0.004 ^[181]	3.862 ±0.005 ^[181]	3.862 ±0.005 ^[181]	5.757 ±0.024 ^[181]	5.757 ±0.024 ^[181]
[MetOMe][SA]	1.680 ±0.023	18.253 ±0.017	8.394 ±0.017	15.868 ±0.317	7.297 ±0.317	17.868 ±0.913	8.217 ±0.913
[MetOEt][SA]	1.894 ±0.058	19.407 ±0.044	8.526 ±0.044	17.714 ±0.712	7.783 ±0.712	19.693 ±0.307	8.652 ±0.307
[MetOiPr][SA]	1.784 ±0.035 ^[181]	16.046 ±0.053 ^[181]	6.749 ±0.053 ^[181]	10.550 ±0.007 ^[181]	4.437 ±0.007 ^[181]	18.036 ±0.046 ^[181]	7.586 ±0.046 ^[181]
[MetOPr][SA]	1.832 ±0.018 ^[182]	15.985 ±0.015 ^[182]	6.712 ±0.015 ^[182]	11.163 ±0.457	4.695 ±0.457	19.795 ±0.082	8.325 ±0.082
[MetOBu][SA]	2.026 ±0.020 ^[182]	11.445 ±0.014 ^[182]	4.616 ±0.014 ^[182]	5.676 ±0.447	2.289 ±0.447	12.769 ±0.322	5.150 ±0.322
[ThrOMe][SA]	1.557 ±0.083	35.241 ±0.022	18.011 ±0.022	32.880 ±0.159	16.804 ±0.159	43.361 ±0.593	22.160 ±0.593
[ThrOEt][SA]	1.629 ±0.039	34.333 ±0.089	16.681 ±0.089	31.571 ±1.108	15.339 ±1.108	42.333 ±0.188	20.568 ±0.188
[ThrOiPr][SA]	1.555 ±0.021 ^[181]	38.714 ±0.241 ^[181]	17.925 ±0.241 ^[181]	30.189 ±0.018 ^[181]	13.978 ±0.018 ^[181]	40.757 ±0.125 ^[181]	18.777 ±0.125 ^[181]
[ThrOPr][SA]	1.503 ±0.042 ^[182]	36.691 ±0.012 ^[182]	16.988 ±0.012 ^[182]	30.143 ±0.055	13.956 ±0.055	44.584 ±0.773	20.643 ±0.773

Compound	logP	Solubility					
		water		phosphate buffer			
				pH= 5.40		pH= 7.40	
		g/L	g _{SA} /L	g/L	g _{SA} /L	g/L	g _{SA} /L
[ThrOBu][SA]	1.746 ±0.030 ^[182]	34.636 ±0.018 ^[182]	15.317 ±0.018 ^[182]	29.485 ±0.116	13.039 ±0.116	33.151 ±0.339	14.660 ±0.339
[IleOMe][SA]	1.632 ±0.036	29.55 ±0.019	14.457 ±0.019	21.571 ±1.121	10.554 ±1.121	31.979 ±0.317	15.646 ±0.317
[IleOEt][SA]	1.605 ±0.033	27.249 ±0.047	12.701 ±0.047	20.872 ±1.177	9.728 ±1.177	31.377 ±1.114	14.625 ±1.114
[IleOiPr][SA]	1.601 ±0.034 ^[181]	26.500 ±0.422 ^[181]	11.793 ±0.422 ^[181]	19.281 ±0.015 ^[181]	8.581 ±0.015 ^[181]	29.548 ±0.041 ^[181]	13.149 ±0.041 ^[181]
[IleOPr][SA]	1.606 ±0.014 ^[182]	28.445 ±0.021 ^[182]	12.659 ±0.021 ^[182]	20.445 ±0.977	9.099 ±0.977	31.800 ±1.226	14.152 ±1.226
[IleOBu][SA]	1.835 ±0.016 ^[182]	25.588 ±0.022 ^[182]	10.895 ±0.022 ^[182]	15.533 ±0.522	6.614 ±0.522	23.055 ±1.701	9.816 ±1.701
[ValOMe][SA]	1.666 ±0.014	34.834 ±0.178	17.933 ±0.178	16.287 ±1.030	8.385 ±1.030	22.547 ±0.901	11.608 ±0.901
[ValOEt][SA]	1.648 ±0.078	29.998 ±1.010	14.676 ±1.010	22.813 ±1.701	11.161 ±1.701	21.185 ±0.614	10.365 ±0.614
[ValOiPr][SA]	1.610 ±0.057 ^[181]	16.708 ±2.044 ^[181]	7.761 ±2.044 ^[181]	11.322 ±0.014 ^[181]	5.259 ±0.014 ^[181]	18.733 ±0.027 ^[181]	8.702 ±0.027 ^[181]
[ValOPr][SA]	1.513 ±0.032 ^[182]	26.383 ±0.031 ^[182]	12.255 ±0.031 ^[182]	14.738 ±0.670	6.869 ±0.670	26.645 ±0.901	12.419 ±0.901
[ValOBu][SA]	1.853 ±0.020 ^[182]	14.987 ±0.019 ^[182]	6.670 ±0.019 ^[182]	11.574 ±0.712	5.151 ±0.712	14.987 ±1.055	6.670 ±1.055

Table A7. Solubility of L-amino acid alkyl ester hydrochlorides in selected organic solvents at 25°C.

Compound	Ethanol	DMSO	Dichloromethane	Chloroform	Ethyl acetate	Diethyl ether	Toluene	<i>n</i> -Hexane
[MetOMe][HCl]	○	○	●	●	●	●	●	●
[MetOEt][HCl]	○	○	○	○	○	○	●	○
[MetOiPr][HCl]	○	○	○	○	○	○	●	○
[MetOPr][HCl]	○	○	○	○	○	○	●	○
[MetOBu][HCl]	○	○	○	○	○	○	●	○
[ThrOMe][HCl]	○	○	●	●	●	●	●	●
[ThrOEt][HCl]	●	○	○	○	○	●	●	●
[ThrOiPr][HCl]	●	○	●	○	○	●	●	●
[ThrOPr][HCl]	○	○	○	○	○	●	●	●
[ThrOBu][HCl]	○	○	○	○	○	●	●	●
[IleOMe][HCl]	○	○	●	●	●	●	●	●
[IleOEt][HCl]	○	○	○	○	○	●	○	●
[IleOiPr][HCl]	○	○	●	○	○	●	○	●
[IleOPr][HCl]	○	○	○	○	○	●	○	●
[IleOBu][HCl]	○	○	○	○	○	●	○	●
[ValOMe][HCl]	○	○	●	●	●	●	●	●
[ValOEt][HCl] ^[149]	○	○	○	○	○	○	●	●
[ValOiPr][HCl] ^[149]	○	○	○	○	○	●	●	●
[ValOPr][HCl] ^[149]	○	○	○	○	○	○	●	○
[ValOBu][HCl] ^[149]	○	○	○	○	○	○	●	○
[ValOAm][HCl]	●	○	○	○	○	○	○	○
[ValOHex][HCl]	●	○	●	○	○	○	○	○
[ValOHept][HCl]	●	○	●	○	○	○	○	○
[ValOOct][HCl]	●	○	●	○	○	○	○	○

Categories: “○”: soluble >100 mg/mL; “●”: partially soluble 33–100 mg/mL; “●”: insoluble <33 mg/mL

Table A8. Solubility of L-amino acid alkyl esters in selected organic solvents at 25°C.

Compound	Ethanol	DMSO	Dichloromethane	Chloroform	Ethyl acetate	Diethyl ether	Toluene	<i>n</i> -Hexane
[MetOMe]	○	○	○	○	○	●	●	○
[MetOEt]	○	○	○	○	○	○	○	○
[MetOiPr]	○	○	○	○	○	○	○	○
[MetOPr]	○	○	○	○	○	○	○	○
[MetOBu]	○	○	○	○	○	○	○	○
[ThrOMe]	○	○	○	○	○	○	○	○

Compound	Ethanol	DMSO	Dichloromethane	Chloroform	Ethyl acetate	Diethyl ether	Toluene	<i>n</i> -Hexane
[ThrOEt]	●	○	○	○	●	○	●	●
[ThrOiPr]	●	○	●	○	●	○	●	●
[ThrOPr]	●	○	○	○	○	○	●	●
[ThrOBu]	●	○	○	○	○	○	●	●
[IleOMe]	○	○	○	○	○	○	○	●
[IleOEt]	○	○	○	○	○	○	●	●
[IleOiPr]	○	○	●	○	○	○	●	●
[IleOPr]	○	○	○	○	○	○	●	●
[IleOBu]	○	○	○	○	○	○	●	●
[ValOMe]	○	○	○	○	○	○	○	●
[ValOEt] ^[149]	○	○	○	○	○	○	○	●
[ValOiPr] ^[149]	○	○	○	○	○	○	○	●
[ValOPr] ^[149]	○	○	○	○	○	○	○	●
[ValOBu] ^[149]	○	○	○	○	○	○	○	●
[ValOAm]	○	○	○	○	○	○	○	○
[ValOHex]	○	○	○	○	○	○	○	○
[ValOHept]	○	○	○	○	○	○	○	○
[ValOOct]	○	○	○	○	○	○	○	○

Categories: “○”: soluble >100 mg/mL; “●”: partially soluble 33–100 mg/mL; “●”: insoluble <33 mg/mL

Table A9. Solubility of (R,S)- and S-(+)-ibuprofen and their L-amino acid alkyl ester salts in selected organic solvents at 25°C.

Compound	Ethanol	DMSO	Dichloromethane	Chloroform	Ethyl acetate	Diethyl ether	Toluene	<i>n</i> -Hexane
(R,S)-IBU ^[149]	○	○	○	○	○	○	○	●
S-(+)-IBU	○	○	○	○	○	○	○	●
[MetOMe][IBU]	●	○	○	○	●	●	●	●
[MetOEt][IBU]	○	○	○	○	○	○	○	●
[MetOiPr][IBU] ^[166]	○	○	○	○	○	○	○	●
[MetOPr][IBU] ^[182]	○	○	○	○	○	○	○	●
[MetOBu][IBU] ^[182]	○	○	○	○	○	○	○	●
[ThrOMe][IBU]	○	○	○	○	○	○	○	●
[ThrOEt][IBU]	○	○	○	○	●	●	●	●
[ThrOiPr][IBU] ^[166]	○	○	○	○	●	●	●	●
[ThrOPr][IBU] ^[182]	○	○	○	○	●	●	●	●
[ThrOBu][IBU] ^[182]	○	○	○	○	●	●	●	●
[IleOMe][IBU]	○	○	○	○	○	○	○	●

Compound	Ethanol	DMSO	Dichloromethane	Chloroform	Ethyl acetate	Diethyl ether	Toluene	<i>n</i> -Hexane
[IleOEt][IBU]	○	○	○	○	○	●	○	●
[IleOiPr][IBU] ^[166]	○	○	○	○	○	●	○	●
[IleOPr][IBU] ^[182]	○	○	○	○	○	●	○	●
[IleOBu][IBU] ^[182]	○	○	○	○	○	●	○	●
[ValOMe][<i>S</i> (+)-IBU]	○	○	○	○	○	○	○	●
[ValOEt][<i>S</i> (+)-IBU]	○	○	○	○	○	○	○	●
[ValOiPr][<i>S</i> (+)-IBU]	○	○	○	○	●	●	○	●
[ValOPr][<i>S</i> (+)-IBU]	○	○	○	○	●	●	○	●
[ValOBu][<i>S</i> (+)-IBU]	○	○	○	○	●	●	○	●
[ValOAm][<i>S</i> (+)-IBU]	○	○	○	○	○	○	○	○
[ValOHex][<i>S</i> (+)-IBU]	○	○	○	○	○	○	○	○
[ValOHept][<i>S</i> (+)-IBU]	○	○	○	○	○	○	○	○
[ValOOct][<i>S</i> (+)-IBU]	○	○	○	○	○	○	○	○

Categories: “○”: soluble >100 mg/mL; “●”: partially soluble 33–100 mg/mL; “●”: insoluble <33 mg/mL

Table A10. Solubility of (*R,S*)-ketoprofen and its L-amino acid alkyl ester salts in selected organic solvents at 25°C.

Compound	Ethanol	DMSO	Dichloromethane	Chloroform	Ethyl acetate	Diethyl ether	Toluene	<i>n</i> -Hexane
KETO ^[149]	○	○	○	○	●	●	●	●
[MetOMe][KETO]	●	●	●	●	○	○	○	●
[MetOEt][KETO]	○	○	○	○	●	●	○	●
[MetOiPr][KETO] ^[181]	●	○	○	○	●	●	○	●
[MetOPr][KETO] ^[182]	●	●	○	○	●	●	○	●
[MetOBu][KETO] ^[182]	●	●	○	○	●	●	○	●
[ThrOMe][KETO]	●	●	○	○	○	●	○	●
[ThrOEt][KETO]	○	●	○	○	●	●	○	●
[ThrOiPr][KETO] ^[181]	○	○	●	○	●	●	○	●
[ThrOPr][KETO] ^[182]	○	○	○	○	○	○	○	●
[ThrOBu][KETO] ^[182]	○	○	○	○	○	○	○	●
[IleOMe][KETO]	○	○	○	○	○	○	○	●
[IleOEt][KETO]	○	○	○	○	●	●	○	●
[IleOiPr][KETO] ^[181]	○	○	○	○	●	●	○	●
[IleOPr][KETO] ^[182]	○	○	○	○	●	●	○	●
[IleOBu][KETO] ^[182]	○	○	○	○	●	●	○	●

Compound	Ethanol	DMSO	Dichloromethane	Chloroform	Ethyl acetate	Diethyl ether	Toluene	<i>n</i> -Hexane
[ValOMe][KETO]	○	○	○	○	●	●	●	●
[ValOEt][KETO] ^[149]	○	○	○	○	●	●	●	●
[ValOiPr][KETO] ^[149]	○	○	○	●	●	○	○	●
[ValOPr][KETO] ^[149]	○	○	○	○	●	●	○	●
[ValOBu][KETO] ^[149]	○	○	○	○	●	○	○	●

Categories: “○”: soluble >100 mg/mL; “●”: partially soluble 33–100 mg/mL; “●”: insoluble <33 mg/mL

Table A11. Solubility of naproxen and its L-amino acid alkyl ester salts in selected organic solvents at 25°C.

Compound	Ethanol	DMSO	Dichloromethane	Chloroform	Ethyl acetate	Diethyl ether	Toluene	<i>n</i> -Hexane
NAP ^[149]	○	○	○	●	●	●	●	●
[MetOMe][NAP]	●	○	●	●	●	●	●	●
[MetOEt][NAP]	○	○	○	○	●	●	○	●
[MetOiPr][NAP] ^[181]	○	○	○	○	●	●	○	●
[MetOPr][NAP] ^[182]	○	○	○	○	●	●	○	●
[MetOBu][NAP] ^[182]	○	○	○	○	●	●	○	●
[ThrOMe][NAP]	○	○	○	○	●	●	●	●
[ThrOEt][NAP]	○	○	○	○	●	●	●	●
[ThrOiPr][NAP] ^[181]	○	○	○	○	●	●	●	●
[ThrOPr][NAP] ^[182]	○	○	○	○	●	●	●	●
[ThrOBu][NAP] ^[182]	○	○	○	○	●	●	●	●
[IleOMe][NAP]	○	○	○	○	●	●	○	●
[IleOEt][NAP]	○	○	○	○	●	●	●	●
[IleOiPr][NAP] ^[181]	○	○	○	○	●	●	●	●
[IleOPr][NAP] ^[182]	○	○	○	○	●	●	○	●
[IleOBu][NAP] ^[182]	○	○	○	○	●	●	○	●
[ValOMe][NAP]	○	○	●	●	○	●	●	●
[ValOEt][NAP] ^[149]	○	○	●	●	○	●	●	●
[ValOiPr][NAP] ^[149]	●	○	○	○	●	○	●	●
[ValOPr][NAP] ^[149]	○	○	○	○	○	●	○	●
[ValOBu][NAP] ^[149]	○	○	○	○	○	○	○	●

Categories: “○”: soluble >100 mg/mL; “●”: partially soluble 33–100 mg/mL; “●”: insoluble <33 mg/mL

Table A12. Solubility of salicylic acid and it L-amino acid alkyl ester salts in selected organic solvents at 25°C.

Compound	Ethanol	DMSO	Dichloromethane	Chloroform	Ethyl acetate	Diethyl ether	Toluene	<i>n</i> -Hexane
SA ^[149]	○	○	○	●	○	○	●	●
[MetOMe][SA]	○	●	●	●	○	●	○	●
[MetOEt][SA]	○	○	○	○	○	○	○	●
[MetOiPr][SA] ^[181]	○	○	○	○	○	○	○	●
[MetOPr][SA] ^[182]	○	○	○	○	○	○	○	●
[MetOBu][SA] ^[182]	○	○	○	○	○	○	○	●
[ThrOMe][SA]	○	○	●	●	●	●	●	●
[ThrOEt][SA]	○	○	○	○	○	●	●	●
[ThrOiPr][SA] ^[181]	○	○	○	○	○	●	●	●
[ThrOPr][SA] ^[182]	○	○	○	○	○	●	●	●
[ThrOBu][SA] ^[182]	○	○	○	○	○	●	●	●
[IleOMe][SA]	○	○	○	○	○	●	○	●
[IleOEt][SA]	○	○	○	○	○	●	○	●
[IleOiPr][SA] ^[181]	○	○	○	○	○	○	○	●
[IleOPr][SA] ^[182]	○	○	○	○	○	●	○	●
[IleOBu][SA] ^[182]	○	○	○	○	○	●	○	●
[ValOMe][SA]	○	○	○	○	○	●	●	●
[ValOEt][SA] ^[149]	○	○	○	○	○	○	○	●
[ValOiPr][SA] ^[149]	○	○	○	○	●	●	○	●
[ValOPr][SA] ^[149]	○	○	○	○	○	○	○	●
[ValOBu][SA] ^[149]	●	○	○	○	○	○	○	●

Categories: “○”: soluble >100 mg/mL; “●”: partially soluble 33–100 mg/mL; “●”: insoluble <33 mg/m

THERMAL PROPERTIES RESULTS

Table A13. Phase transition temperatures and thermal stabilities of L-amino acid alkyl ester hydrochlorides.

Compound	T _{TGonset} (°C)	T _{DTGmax} (°C)	T _{DSConset} (°C)	T _{DSCmax} (°C)	T _{Conset} (°C)	T _{Cmax} (°C)
[MetOMe][HCl]	164.7	193.8	119.11	129.08	—	—
[MetOEt][HCl]	183.6	218.3	84.72	87.00	—	—
[MetOiPr][HCl]	188.1	227.8	113.19	117.53	54.888	52.70
[MetOPr][HCl]	192.0	224.2	73.42	76.89	—	—
[MetOBu][HCl]	198.5	227.7	79.66	84.51	55.52	48.26
[ThrOMe][HCl]	75.2	198.7	—	—	—	—
[ThrOEt][HCl]	177.5	214.0	—	—	—	—
[ThrOiPr][HCl]	189.1	221.9	—	—	—	—
[ThrOPr][HCl]	182.1	218.0	—	—	—	—
[ThrOBu][HCl]	195.0	220.8	—	—	—	—
[IleOMe][HCl]	132.2	237.9	74.38	63.96	—	—
[IleOEt][HCl]	184.6	257.9	85.88	88.16	—	—
[IleOiPr][HCl]	176.4	216.9	—	—	—	—
[IleOPr][HCl]	185.3	223.5	—	—	—	—
[IleOBu][HCl]	196.6	222.6	—	—	—	—
[ValOMe][HCl]	161.7	249.6	158.54	163.38	—	—
[ValOEt][HCl]	171.6 ^[149]	211.5 ^[149]	81.54	89.00	—	—
[ValOiPr][HCl]	174.6 ^[149]	224.0 ^[149]	113.13	116.71	58.50	52.22
[ValOPr][HCl]	183.1 ^[149]	214.7 ^[149]	56.40	64.88	—	—
[ValOBu][HCl]	181.2 ^[149]	215.8 ^[149]	69.10	73.69	—	—
[ValOAm][HCl]	177.1	220.4	39.65	55.46	—	—
[ValOHex][HCl]	185.1	229.9	19.89	38.53	—	—
[ValOHept][HCl]	179.1	222.7	12.84	29.94	—	—
[ValOOct][HCl]	187.9	225.9	—	—	—	—

T_{TGonset}: the onset of the thermal degradation, T_{DTGmax}: maximum decomposition temperature, T_{DSConset}: the peak onset temperature in DSC, T_{DSCmax}: the peak maximum temperature in DSC, T_{Conset}: the peak onset crystallisation temperature, T_{Cmax}: crystallisation maximum peak temperature

Table A14. Phase transition temperatures and thermal stability of (*R,S*)- and *S*-(+)-ibuprofen and their L-amino acid alkyl ester salts.

Compound	T _{TGonset} (°C)	T _{DTGmax} (°C)	T _{DSConset} (°C)	T _{DSCmax} (°C)	T _{Conset} (°C)	T _{Cmax} (°C)
(<i>R,S</i>)-IBU	168.2 ^[149]	218.8 ^[149]	76.23	78.58	—	—
<i>S</i> -(+)-IBU	177.9	232.9	48.73	50.27	—	—
[MetOMe][IBU]	121.1	223.8	70.76	73.33	49.26	47.47
[MetOEt][IBU]	129.1	222.8	54.84	59.09	45.61	43.84
[MetOiPr][IBU]	132.2 ^[166]	211.5 ^[166]	63.80	65.72	52.16	49.80
[MetOPr][IBU]	134.7	222.9	50.78	53.62	40.77	38.13
[MetOBu][IBU]	138.5	302.8	40.63	46.50	18.89	15.81
[ThrOMe][IBU]	115.8	241.2	72.59	76.53	—	—
[ThrOEt][IBU]	127.0	211.4	24.60	32.60	—	—
[ThrOiPr][IBU]	122.8 ^[166]	209.6 ^[166]	40.70	48.52	—	—
[ThrOPr][IBU]	120.9	206.4	—	—	—	—
[ThrOBu][IBU]	131.3	211.3	—	—	—	—
[IleOMe][IBU]	81.4	218.6	77.25/83.03	81.37/83.37	66.34	64.81
[IleOEt][IBU]	104.0	228.2	56.17	59.74	45.25	42.54
[IleOiPr][IBU]	97.4 ^[166]	222.6 ^[166]	72.74/78.74	76.07/80.07	52.10	50.31
[IleOPr][IBU]	99.8	219.8	56.46	58.90	35.23	32.62
[IleOBu][IBU]	120.1	227.2	58.03	60.90	31.07	27.44
[ValOMe][<i>S</i> -(+)-IBU]	87.5	215.0	83.02/88.83	87.50/90.99	80.44	79.75
[ValOEt][<i>S</i> -(+)-IBU]	90.4	215.7	72.57	75.36	53.42	51.59
[ValOiPr][<i>S</i> -(+)-IBU]	103.3	219.0	108.06	110.68	80.44	79.82
[ValOPr][<i>S</i> -(+)-IBU]	101.1	215.5	91.58	93.50	70.47/71.41	70.16/70.63
[ValOBu][<i>S</i> -(+)-IBU]	111.6	213.7	89.70	91.82	66.83	66.05

Compound	T _{TGonset} (°C)	T _{DTGmax} (°C)	T _{DSConset} (°C)	T _{DSCmax} (°C)	T _{Conset} (°C)	T _{Cmax} (°C)
[ValOAm][S(+)-IBU]	122.3	219.5	83.08	84.66	61.17/62.86	60.84/62.00
[ValOHex][S(+)-IBU]	131.0	210.8	70.90	73.38	58.74	57.22
[ValOHept][S(+)-IBU]	146.9	197.5	67.56	72.69	62.01	60.31
[ValOOct][S(+)-IBU]	153.0	210.7	43.58	51.65	36.59	34.02

T_{TGonset}: the onset of the thermal degradation, T_{DTGmax}: maximum decomposition temperature, T_{DSConset}: the peak onset temperature in DSC, T_{DSCmax}: the peak maximum temperature in DSC, T_{Conset}: the peak onset crystallisation temperature, T_{Cmax}: crystallisation maximum peak temperature

Table A15. Phase transition temperatures and thermal stability of ketoprofen and its L-amino acid alkyl ester salts.

Compound	T _{TGonset} (°C)	T _{DTGmax} (°C)	T _{DSConset} (°C)	T _{DSCmax} (°C)	T _{Conset} (°C)	T _{Cmax} (°C)
KETO	241.4 ^[149]	304.9 ^[149]	95.14	97.03	—	—
[MetOMe][KETO]	76.3	308.9	69.84	77.52	—	—
[MetOEt][KETO]	98.9	300.5	33.77	49.11	—	—
[MetOiPr][KETO]	82.6	308.5	50.02	59.60	—	—
[MetOPr][KETO]	101.1	304.3	20.03	31.05	—	—
[MetOBu][KETO]	113.1	303.4	29.10	45.12	—	—
[ThrOMe][KETO]	58.9	299.5	—	—	—	—
[ThrOEt][KETO]	67.3	286.1	—	—	—	—
[ThrOiPr][KETO]	82.4	295.1	—	—	—	—
[ThrOPr][KETO]	84.1	296.9	—	—	—	—
[ThrOBu][KETO]	86.8	301.5	—	—	—	—
[IleOMe][KETO]	63.8	232.7	53.46/75.09	63.05/77.84	—	—
[IleOEt][KETO]	108.5	314.3	—	—	—	—
[IleOiPr][KETO]	116.6	319.8	62.27/71.74	67.58/78.22	—	—
[IleOPr][KETO]	96.8	290.8	23.26	33.21	—	—
[IleOBu][KETO]	113.5	302.3	20.01/30.57	26.81/37.54	—	—
[ValOMe][KETO]	77.9	307.2	62.98	69.55	—	—
[ValOEt][KETO]	89.9 ^[149]	311.2 ^[149]	33.21	45.32	—	—
[ValOiPr][KETO]	67.6 ^[149]	309.6 ^[149]	44.88/68.65	52.31/74.90	—	—
[ValOPr][KETO]	43.4 ^[149]	298.5 ^[149]	—	—	—	—
[ValOBu][KETO]	105.2 ^[149]	311.6 ^[149]	45.87	52.44	—	—

T_{TGonset}: the onset of the thermal degradation, T_{DTGmax}: maximum decomposition temperature, T_{DSConset}: the peak onset temperature in DSC, T_{DSCmax}: the peak maximum temperature in DSC, T_{Conset}: the peak onset crystallisation temperature, T_{Cmax}: crystallisation maximum peak temperature

Table A16. Phase transition temperatures and thermal stability of naproxen and its L-amino acid alkyl ester salts.

Compound	T _{TGonset} (°C)	T _{DTGmax} (°C)	T _{DSConset} (°C)	T _{DSCmax} (°C)	T _{Conset} (°C)	T _{Cmax} (°C)
NAP	224.5 ^[149]	284.0 ^[149]	153.76	155.45	80.12	78.88
[MetOMe][NAP]	124.0	306.9	121.62	123.17	71.95	69.87
[MetOEt][NAP]	131.0	285.3	107.88	109.31	72.24	70.05
[MetOiPr][NAP]	146.6	293.2	94.51	95.97	71.44	69.67
[MetOPr][NAP]	140.9	283.3	68.65	70.69	38.85	33.79
[MetOBu][NAP]	142.3	299.2	90.93	92.47	52.44	48.91
[ThrOMe][NAP]	119.1	283.4	96.23	98.64	—	—
[ThrOEt][NAP]	124.9	276.8	81.07	83.97	—	—
[ThrOiPr][NAP]	145.0	295.3	86.06	89.86	—	—
[ThrOPr][NAP]	133.1	272.2	90.81	93.49	—	—
[ThrOBu][NAP]	144.0	276.6	85.36	87.97	—	—
[IleOMe][NAP]	102.3	278.0	112.14	113.77	80.77	79.68
[IleOEt][NAP]	99.4	277.4	105.22	107.49	61.28	57.70
[IleOiPr][NAP]	122.8	287.4	89.82/103.19	93.53/107.38	64.84	63.54
[IleOPr][NAP]	114.9	297.9	107.66	109.16	66.61	65.11
[IleOBu][NAP]	121.3	280.3	95.54	97.93	65.35	63.91
[ValOMe][NAP]	99.5	273.5	112.50/126.17	116.99/131.20	90.26	88.78

Compound	T _{TGonset} (°C)	T _{DTGmax} (°C)	T _{DSConset} (°C)	T _{DSCmax} (°C)	T _{Conset} (°C)	T _{Cmax} (°C)
[ValOEt][NAP]	126.2 ^[149]	282.1 ^[149]	90.23/124.56	99.14/129.05	82.52	81.33
[ValOiPr][NAP]	111.3 ^[149]	275.8 ^[149]	124.04/130.48	127.13/132.66	86.69	85.01
[ValOPr][NAP]	82.7 ^[149]	267.6 ^[149]	92.57/109.97	97.86/115.88	61.41	57.47
[ValOBu][NAP]	103.7 ^[149]	270.9 ^[149]	91.21/98.07	93.60/101.28	65.85	64.07

T_{TGonset}: the onset of the thermal degradation, T_{DTGmax}: maximum decomposition temperature, T_{DSConset}: the peak onset temperature in DSC, T_{DSCmax}: the peak maximum temperature in DSC, T_{Conset}: the peak onset crystallisation temperature, T_{Cmax}: crystallisation maximum peak temperature

Table A17. Phase transition temperatures and thermal stabilities of salicylic acid and its L-amino acid alkyl ester salts.

Compound	T _{TGonset} (°C)	T _{DTGmax} (°C)	T _{DSConset} (°C)	T _{DSCmax} (°C)	T _{Conset} (°C)	T _{Cmax} (°C)
SA	146.2 ^[149]	198.8 ^[149]	158.05	160.04	107.64	107.83
[MetOMe][SA]	135.6	201.2	47.06/58.64	51.26/61.38	–	–
[MetOEt][SA]	143.1	211.5	27.68	42.83	–	–
[MetOiPr][SA]	157.3	205.0	85.17	88.36	65.47	63.19
[MetOPr][SA]	169.2	211.2	67.07	71.05	34.50	26.39
[MetOBu][SA]	168.2	206.5	80.16	82.15	50.14/55.33	45.73/52.45
[ThrOMe][SA]	149.7	190.4	113.51	116.02	–	–
[ThrOEt][SA]	155.7	190.6	48.39	58.28	–	–
[ThrOiPr][SA]	132.8	191.4	–	–	–	–
[ThrOPr][SA]	151.5	188.4	60.15	64.36	–	–
[ThrOBu][SA]	162.3	194.5	25.31	41.34	–	–
[IleOMe][SA]	134.6	195.0	94.02	96.16	54.11	48.01
[IleOEt][SA]	118.4	198.1	–	–	–	–
[IleOiPr][SA]	144.2	202.4	84.18	86.53	67.25	64.66
[IleOPr][SA]	157.0	208.0	74.86	77.88	51.82	49.98
[IleOBu][SA]	137.0	201.8	64.64	67.40	42.68	36.98
[ValOMe][SA]	113.8	192.5	107.34	111.51	65.06	61.98
[ValOEt][SA]	120.2 ^[149]	185.6 ^[149]	52.31	56.43	–	–
[ValOiPr][SA]	124.6 ^[149]	197.5 ^[149]	96.90	98.85	84.46	81.73
[ValOPr][SA]	125.6 ^[149]	193.6 ^[149]	71.97	74.20	52.39	47.75
[ValOBu][SA]	135.6 ^[149]	206.4 ^[149]	60.46	65.89	46.84	42.85

T_{TGonset}: the onset of the thermal degradation, T_{DTGmax}: maximum decomposition temperature, T_{DSConset}: the peak onset temperature in DSC, T_{DSCmax}: the peak maximum temperature in DSC, T_{Conset}: the peak onset crystallisation temperature, T_{Cmax}: crystallisation maximum peak temperature

Heat capacity experimental data

Table A18. The experimental values of the heat capacity of the solid phase of (*R,S*)-ibuprofen averaged over 3 runs.

T, K	C _{p,m} , J·K ⁻¹ ·mol ⁻¹	T, K	C _{p,m} , J·K ⁻¹ ·mol ⁻¹	T, K	C _{p,m} , J·K ⁻¹ ·mol ⁻¹
294.24	302.92	308.03	314.47	323.32	332.37
295.21	303.41	309.02	315.33	324.32	333.78
296.18	303.99	310.02	316.37	325.00	334.6
297.16	304.48	311.01	317.36	326.00	335.92
298.14	305.10	312.01	318.68	327.00	337.37
299.12	305.89	313.01	319.75	328.00	338.85
300.10	306.59	314.00	320.82	329.00	340.25
301.09	307.45	315.00	322.06	330.00	341.57
302.07	308.36	316.00	323.01	331.00	343.06
303.06	309.27	317.00	324.08	332.00	344.50
304.06	310.22	318.33	325.73	333.00	346.11
305.05	311.21	319.33	327.01	334.00	347.47
306.04	312.16	320.33	328.33	335.00	349.21
307.03	313.23	322.32	331.01	336.00	351.35

Table A19. The experimental values of the heat capacity of the solid phase of [MetOiPr][IBU] averaged over 3 runs.

T, K	$C_{p,m}$, $J \cdot K^{-1} \cdot mol^{-1}$	T, K	$C_{p,m}$, $J \cdot K^{-1} \cdot mol^{-1}$	T, K	$C_{p,m}$, $J \cdot K^{-1} \cdot mol^{-1}$
294.13	477.02	305.27	489.93	318.21	529.65
295.10	477.36	306.26	491.96	319.21	535.42
296.07	478.04	307.25	494.00	320.21	542.21
297.05	478.72	308.24	496.38	321.21	549.34
298.02	479.40	309.24	498.75	322.21	557.83
299.01	480.08	310.24	501.47	323.21	567.34
300.32	481.44	311.23	503.85	324.20	579.90
301.31	483.14	312.23	506.90	324.88	588.05
302.29	484.49	313.22	509.62	325.21	590.76
302.95	485.85	314.22	513.01	325.55	594.16
303.28	486.19	314.55	514.37	325.88	598.23
303.61	486.87	314.88	515.39	326.22	603.33
303.95	487.55	315.22	516.41	326.55	608.76
304.27	488.23	316.21	520.48		
304.60	488.57	317.21	524.90		

Table A20. The experimental values of the heat capacity of the solid phase of [ThrOiPr][IBU] averaged over 3 runs.

T, K	$C_{p,m}$, $J \cdot K^{-1} \cdot mol^{-1}$	T, K	$C_{p,m}$, $J \cdot K^{-1} \cdot mol^{-1}$	T, K	$C_{p,m}$, $J \cdot K^{-1} \cdot mol^{-1}$
294.03	665.51	300.22	729.69	306.16	868.60
295.00	672.49	301.21	746.47	307.15	904.61
296.30	682.66	302.20	765.46	308.15	946.14
297.28	691.84	303.19	786.77	309.14	993.91
298.26	702.74	304.18	810.29	310.13	1049.30
299.24	715.36	305.17	837.24	311.13	1113.00

Table A21. The experimental values of the heat capacity of the solid phase of [IleOiPr][IBU] averaged over 3 runs.

T, K	$C_{p,m}$, $J \cdot K^{-1} \cdot mol^{-1}$	T, K	$C_{p,m}$, $J \cdot K^{-1} \cdot mol^{-1}$	T, K	$C_{p,m}$, $J \cdot K^{-1} \cdot mol^{-1}$
294.13	619.27	309.25	646.85	324.21	695.18
295.11	620.54	310.25	649.00	325.56	700.74
296.08	622.18	311.24	651.28	326.56	706.31
297.05	624.08	312.24	653.68	327.56	712.89
298.03	625.60	313.23	656.09	328.23	717.70
299.02	627.37	314.23	658.36	328.56	720.48
300.00	629.14	315.23	661.02	329.22	725.54
301.31	631.54	316.22	664.06	330.22	733.26
302.30	633.31	317.22	666.97	331.23	741.48
303.29	635.21	318.22	670.38	332.23	751.85
304.28	636.98	319.22	673.67	333.23	764.25
305.28	639.13	320.22	677.34	334.23	781.46
306.27	641.03	321.22	680.88	335.23	801.45
307.26	643.06	322.22	684.68	336.23	830.54
308.25	645.21	323.21	690.12		

Table A22. The experimental values of the heat capacity of the solid phase of [ValOiPr][IBU] averaged over 3 runs.

T, K	$C_{p,m}$, $J \cdot K^{-1} \cdot mol^{-1}$	T, K	$C_{p,m}$, $J \cdot K^{-1} \cdot mol^{-1}$	T, K	$C_{p,m}$, $J \cdot K^{-1} \cdot mol^{-1}$
294.00	542.86	307.12	560.48	320.08	590.81
295.30	543.52	308.12	562.30	321.08	594.03
296.27	544.61	309.11	564.57	322.08	597.76
297.25	545.49	310.11	566.25	323.08	602.36
298.22	546.66	311.10	567.49	324.07	607.41

T, K	$C_{p,m}$, $J \cdot K^{-1} \cdot mol^{-1}$	T, K	$C_{p,m}$, $J \cdot K^{-1} \cdot mol^{-1}$	T, K	$C_{p,m}$, $J \cdot K^{-1} \cdot mol^{-1}$
299.21	547.76	312.10	569.83	325.08	613.33
300.19	549.00	313.09	572.03	326.08	620.57
301.18	550.46	314.09	574.15	327.08	628.10
302.17	551.85	315.09	576.78	328.09	637.16
303.16	553.24	316.08	579.26	329.08	646.15
304.15	554.77	317.08	582.11	330.08	656.68
305.14	556.53	318.08	585.04	331.08	667.64
306.13	558.43	319.08	587.82		

Table A23. The experimental values of the heat capacity of the solid phase of (*R,S*)-ketoprofen averaged over 3 runs.

T, K	$C_{p,m}$, $J \cdot K^{-1} \cdot mol^{-1}$	T, K	$C_{p,m}$, $J \cdot K^{-1} \cdot mol^{-1}$	T, K	$C_{p,m}$, $J \cdot K^{-1} \cdot mol^{-1}$
294.11	312.57	317.20	328.97	334.21	343.98
295.08	312.96	318.20	329.67	335.87	344.68
296.05	313.34	319.20	330.69	336.21	346.52
297.03	313.91	320.20	331.64	337.21	346.90
298.01	314.29	321.20	332.41	338.21	347.98
299.32	315.24	322.19	333.30	339.21	348.94
300.30	315.75	323.19	334.06	340.21	349.95
301.29	316.45	324.19	334.95	341.22	351.03
302.28	316.90	325.20	335.84	342.22	352.30
303.27	317.66	326.20	336.60	343.22	353.00
304.26	318.17	327.21	337.81	344.22	353.70
305.25	318.87	328.21	338.70	345.23	354.59
306.25	319.63	329.21	339.53	346.22	355.61
307.24	320.27	329.54	339.85	347.23	356.50
308.23	320.96	329.87	340.10	348.23	357.33
309.23	321.66	330.20	340.48	349.23	358.85
310.22	322.49	330.54	340.67	350.23	360.89
311.22	323.51	330.87	340.99	351.24	361.08
312.22	324.40	331.20	341.31	352.24	361.90
313.21	325.35	331.54	341.69	353.24	363.56
314.21	326.24	331.87	342.07	354.24	365.65
315.21	327.13	332.20	342.71	355.25	368.32
316.20	328.21	333.20	343.28		

Table A24. The experimental values of the heat capacity of the solid phase of [MetOiPr][KETO] averaged over 3 runs.

T, K	$C_{p,m}$, $J \cdot K^{-1} \cdot mol^{-1}$	T, K	$C_{p,m}$, $J \cdot K^{-1} \cdot mol^{-1}$	T, K	$C_{p,m}$, $J \cdot K^{-1} \cdot mol^{-1}$
294.03	642.66	300.22	665.54	306.16	697.02
295.00	645.19	301.21	670.44	307.15	702.96
296.29	648.90	302.19	675.49	308.15	709.20
297.27	652.47	303.18	680.83	309.14	715.74
298.25	656.33	304.17	686.33	310.13	723.01
299.24	660.78	305.17	691.38	311.13	730.74

Table A25. The experimental values of the heat capacity of the solid phase of [ThrOiPr][KETO] averaged over 3 runs.

T, K	$C_{p,m}$, $J \cdot K^{-1} \cdot mol^{-1}$	T, K	$C_{p,m}$, $J \cdot K^{-1} \cdot mol^{-1}$	T, K	$C_{p,m}$, $J \cdot K^{-1} \cdot mol^{-1}$
294.02	816.55	307.15	848.69	320.11	879.43
295.32	818.77	308.14	851.45	321.01	881.78
296.29	820.71	309.14	854.22	322.21	884.69
297.27	822.93	310.13	856.58	323.17	886.77
298.25	825.14	311.13	859.07	324.20	888.85
299.23	827.77	312.13	861.56	325.11	890.65

T, K	$C_{p,m}$, $J \cdot K^{-1} \cdot mol^{-1}$	T, K	$C_{p,m}$, $J \cdot K^{-1} \cdot mol^{-1}$	T, K	$C_{p,m}$, $J \cdot K^{-1} \cdot mol^{-1}$
300.21	830.68	313.12	864.47	326.15	892.59
301.20	833.45	314.12	867.24	327.11	894.25
302.19	835.94	315.11	869.87	328.11	895.91
303.18	838.16	316.21	871.95	329.11	897.30
304.17	840.79	317.11	873.20	330.11	898.68
305.16	843.42	318.11	875.00	331.11	900.48
306.16	846.05	319.11	877.08		

Table A26. The experimental values of the heat capacity of the solid phase of [IleOiPr][KETO] averaged over 3 runs.

T, K	$C_{p,m}$, $J \cdot K^{-1} \cdot mol^{-1}$	T, K	$C_{p,m}$, $J \cdot K^{-1} \cdot mol^{-1}$	T, K	$C_{p,m}$, $J \cdot K^{-1} \cdot mol^{-1}$
294.13	632.89	305.28	671.94	316.22	721.82
295.10	635.74	306.27	677.21	317.22	726.81
296.08	638.59	307.26	681.77	318.22	732.22
297.06	641.87	308.25	686.48	319.22	738.06
298.03	645.15	309.25	690.89	320.22	744.62
299.02	648.43	310.25	695.31	321.22	751.18
300.00	652.13	311.24	699.87	322.22	758.59
301.32	657.26	312.24	704.00	323.22	766.57
302.30	660.97	313.23	708.28	324.21	775.69
303.30	664.10	314.23	712.98	325.23	785.66
304.28	666.10	315.23	717.54	326.23	797.35

Table A27. The experimental values of the heat capacity of the solid phase of [ValOiPr][KETO] averaged over 3 runs.

T, K	$C_{p,m}$, $J \cdot K^{-1} \cdot mol^{-1}$	T, K	$C_{p,m}$, $J \cdot K^{-1} \cdot mol^{-1}$	T, K	$C_{p,m}$, $J \cdot K^{-1} \cdot mol^{-1}$
294.06	654.79	300.25	683.64	306.18	725.92
295.03	657.69	301.23	690.15	307.18	734.08
296.00	661.20	302.22	696.87	308.17	743.08
297.30	666.47	303.21	703.59	309.16	752.79
298.28	671.64	304.20	710.20	310.16	763.55
299.26	677.33	305.19	717.65	311.16	775.12

Table A28. The experimental values of the heat capacity of the solid phase of *S*-(+)-naproxen averaged over 3 runs.

T, K	$C_{p,m}$, $J \cdot K^{-1} \cdot mol^{-1}$	T, K	$C_{p,m}$, $J \cdot K^{-1} \cdot mol^{-1}$	T, K	$C_{p,m}$, $J \cdot K^{-1} \cdot mol^{-1}$
294.02	286.40	330.30	316.32	370.05	353.85
296.04	288.30	332.30	318.10	372.40	355.06
298.15	290.29	334.30	319.89	374.07	357.54
300.01	292.04	336.30	321.9	376.08	359.38
302.23	293.24	338.30	323.75	378.09	359.95
304.16	293.87	340.31	325.82	380.1	362.31
306.11	294.96	342.31	327.66	382.12	363.81
308.07	296.29	344.31	329.67	384.13	367.09
310.04	297.84	346.32	331.40	386.14	368.59
312.02	299.40	348.32	333.01	388.16	370.72
312.35	299.63	350.33	334.57	390.18	371.12
312.68	299.97	352.00	336.70	392.19	373.77
314.00	301.01	354.00	337.68	394.21	376.99
316.32	303.02	356.00	339.86	396.22	379.58
318.31	304.69	358.01	341.59	398.24	380.56
320.30	306.88	360.01	343.14	400.25	384.07
322.30	309.12	362.02	346.25	402.27	385.11
324.30	310.85	364.36	347.87	404.28	386.72
326.30	312.64	366.03	349.59	406.30	391.56

T, K	$C_{p,m}$, $J \cdot K^{-1} \cdot mol^{-1}$	T, K	$C_{p,m}$, $J \cdot K^{-1} \cdot mol^{-1}$	T, K	$C_{p,m}$, $J \cdot K^{-1} \cdot mol^{-1}$
328.30	314.48	368.04	350.92		

Table A29. The experimental values of the heat capacity of the solid phase of [MetOiPr][NAP] averaged over 3 runs.

T, K	$C_{p,m}$, $J \cdot K^{-1} \cdot mol^{-1}$	T, K	$C_{p,m}$, $J \cdot K^{-1} \cdot mol^{-1}$	T, K	$C_{p,m}$, $J \cdot K^{-1} \cdot mol^{-1}$
294.14	581.04	316.23	628.8	338.24	663.89
296.09	583.99	318.23	632.51	340.24	667.80
298.04	587.78	320.23	636.91	340.57	668.32
300.01	591.72	322.22	641.83	342.25	670.3
302.31	596.91	324.22	644.11	344.25	675.54
304.29	600.71	326.23	646.27	346.25	681.23
306.27	605.06	328.23	648.00	348.26	687.20
308.26	609.42	330.23	651.02	350.26	691.48
310.25	614.06	332.23	654.35	352.27	696.96
312.24	618.69	334.23	656.43	354.27	706.94
314.24	623.61	336.23	660.62	356.27	723.94

Table A30. The experimental values of the heat capacity of the solid phase of [ThrOiPr][NAP] averaged over 3 runs.

T, K	$C_{p,m}$, $J \cdot K^{-1} \cdot mol^{-1}$	T, K	$C_{p,m}$, $J \cdot K^{-1} \cdot mol^{-1}$	T, K	$C_{p,m}$, $J \cdot K^{-1} \cdot mol^{-1}$
294.27	513.59	310.2	539.82	330.20	597.36
296.26	517.12	312.2	543.74	332.20	604.02
298.24	519.86	316.19	553.91	334.20	611.07
298.58	520.64	318.19	559.78	336.20	619.68
300.23	523.38	320.19	566.83	338.20	629.46
302.23	526.12	322.19	573.49	340.21	642.77
304.22	529.25	324.19	579.36	342.21	660.78
306.21	532.77	326.20	585.23	344.21	685.05
308.21	536.30	328.20	591.10	345.22	698.75

Table A31. The experimental values of the heat capacity of the solid phase of [IleOiPr][NAP] averaged over 3 runs.

T, K	$C_{p,m}$, $J \cdot K^{-1} \cdot mol^{-1}$	T, K	$C_{p,m}$, $J \cdot K^{-1} \cdot mol^{-1}$	T, K	$C_{p,m}$, $J \cdot K^{-1} \cdot mol^{-1}$
294.06	563.71	318.14	589.23	338.15	620.30
296.00	564.61	320.13	591.45	340.15	625.14
298.28	566.33	322.13	593.77	342.15	630.79
300.24	568.45	324.13	596.39	344.16	636.64
302.22	570.36	326.14	599.42	346.16	643.80
304.20	572.58	328.14	602.34	346.50	645.01
308.17	577.63	330.14	606.08	346.83	646.43
310.16	579.85	332.14	609.2	348.16	653.08
312.15	581.97	332.48	609.71	350.17	665.29
314.15	584.18	334.15	612.53		
316.14	586.71	336.15	616.16		

Table A32. The experimental values of the heat capacity of the solid phase of [ValOiPr][NAP] averaged over 3 runs.

T, K	$C_{p,m}$, $J \cdot K^{-1} \cdot mol^{-1}$	T, K	$C_{p,m}$, $J \cdot K^{-1} \cdot mol^{-1}$	T, K	$C_{p,m}$, $J \cdot K^{-1} \cdot mol^{-1}$
294.04	519.00	326.13	525.42	360.18	546.07
296.30	518.22	328.46	525.42	362.18	548.40
298.26	518.02	330.13	525.42	364.19	550.94
300.23	518.22	332.12	525.42	366.20	555.22

T, K	$C_{p,m}$, $J \cdot K^{-1} \cdot mol^{-1}$	T, K	$C_{p,m}$, $J \cdot K^{-1} \cdot mol^{-1}$	T, K	$C_{p,m}$, $J \cdot K^{-1} \cdot mol^{-1}$
302.2	517.83	334.13	525.81	368.21	560.09
304.18	518.22	336.13	525.81	370.21	566.51
306.17	518.8	338.13	526.40	372.22	573.53
308.15	519.19	340.13	527.57	374.23	581.7
308.48	519.39	342.14	529.12	376.25	591.44
310.15	520.17	344.14	530.88	378.26	602.35
312.14	520.94	346.14	532.24	380.27	615.59
314.13	521.53	348.15	533.80	382.28	631.17
316.12	522.5	350.15	535.36	384.29	649.28
318.12	523.48	352.16	536.72	386.30	671.29
320.12	524.25	354.16	538.67	388.32	697.77
322.12	524.84	356.16	540.61	390.01	731.66
324.11	525.23	358.17	543.15	390.34	768.66

Table A33. The experimental values of the heat capacity of the solid phase of salicylic acid averaged over 3 runs.

T, K	$C_{p,m}$, $J \cdot K^{-1} \cdot mol^{-1}$	T, K	$C_{p,m}$, $J \cdot K^{-1} \cdot mol^{-1}$	T, K	$C_{p,m}$, $J \cdot K^{-1} \cdot mol^{-1}$
294.31	161.46	322.06	172.51	352.10	184.60
296.25	162.29	324.05	173.34	354.10	185.01
298.21	163.12	326.07	174.03	356.10	185.84
300.17	163.81	328.07	174.86	358.11	186.74
302.15	164.64	330.07	175.48	360.11	187.71
304.13	165.40	332.06	176.10	362.12	188.53
306.11	166.09	334.07	176.79	364.13	189.36
308.10	166.99	336.07	177.48	366.13	190.19
310.09	167.75	338.07	178.24	368.14	191.71
312.08	168.58	340.07	179.07	370.15	193.37
314.08	169.34	342.07	179.63	372.16	194.33
316.07	170.16	344.08	180.52	374.17	193.92
318.06	170.85	346.08	181.21	376.18	195.99
320.06	171.75	348.08	182.25	378.19	196.89
320.73	172.17	350.09	183.63	380.21	199.10

Table A34. The experimental values of the heat capacity of the solid phase of [MetOiPr][SA] averaged over 3 runs.

T, K	$C_{p,m}$, $J \cdot K^{-1} \cdot mol^{-1}$	T, K	$C_{p,m}$, $J \cdot K^{-1} \cdot mol^{-1}$	T, K	$C_{p,m}$, $J \cdot K^{-1} \cdot mol^{-1}$
294.63	458.86	314.07	473.31	334.07	504.59
295.28	459.19	315.07	474.38	335.07	507.06
296.25	459.77	316.07	475.69	336.07	509.60
297.23	460.26	317.06	477.25	337.07	513.13
298.21	460.92	318.06	478.24	338.07	516.74
299.19	461.82	319.06	479.55	339.07	520.36
300.17	462.47	320.06	480.62	340.07	524.13
301.16	462.97	321.06	482.18	341.07	529.31
302.15	463.54	322.06	483.00	342.08	532.59
303.14	465.51	323.06	484.97	343.08	535.46
304.13	465.51	324.06	486.04	344.08	541.78
305.12	465.51	325.07	487.84	345.08	548.19
306.11	467.65	326.07	489.4	346.08	555.33
307.10	467.81	327.07	491.05	347.09	563.46
308.10	468.55	328.07	492.77	348.09	573.06
309.09	469.37	329.07	494.82	349.09	584.31
310.09	470.19	330.07	497.37	350.09	597.61
311.08	470.52	331.07	498.76	351.10	613.46
312.08	471.59	332.07	500.41		
313.08	472.66	333.07	501.80		

Table A35. The experimental values of the heat capacity of the solid phase of [ThrOiPr][SA] averaged over 3 runs.

T, K	$C_{p,m}$, $J \cdot K^{-1} \cdot mol^{-1}$	T, K	$C_{p,m}$, $J \cdot K^{-1} \cdot mol^{-1}$	T, K	$C_{p,m}$, $J \cdot K^{-1} \cdot mol^{-1}$
294.04	541.73	317.12	585.29	340.80	632.72
295.00	543.82	318.12	587.38	341.80	634.81
296.30	546.81	319.12	589.46	342.80	637.79
297.28	548.89	320.12	591.25	343.80	640.48
298.26	551.28	321.12	593.34	344.80	643.16
299.24	553.37	322.12	595.13	345.80	646.14
300.23	555.46	323.11	597.22	346.80	647.93
301.21	557.25	324.11	598.41	347.81	650.32
302.20	558.74	325.12	600.50	349.14	653.90
303.19	560.83	326.13	601.70	350.15	655.99
304.18	562.62	327.13	603.78	351.15	657.48
305.17	564.41	328.12	605.87	352.15	658.08
306.17	565.9	329.12	607.66	353.16	659.27
307.16	567.69	330.12	609.75	354.16	661.36
308.15	569.48	331.12	611.54	355.16	662.55
309.15	571.27	332.12	613.63	356.16	664.04
310.14	573.06	333.12	615.42	357.16	665.83
311.14	574.85	334.12	617.21	357.83	666.13
312.14	576.34	335.12	619.30	358.16	666.43
313.13	578.13	336.13	621.38	358.83	667.03
314.13	579.62	337.13	623.47	359.16	667.32
315.13	581.71	338.13	625.26	360.17	668.82
316.12	583.50	339.80	630.63		

Table A36. The experimental values of the heat capacity of the solid phase of [IleOiPr][SA] averaged over 3 runs.

T, K	$C_{p,m}$, $J \cdot K^{-1} \cdot mol^{-1}$	T, K	$C_{p,m}$, $J \cdot K^{-1} \cdot mol^{-1}$	T, K	$C_{p,m}$, $J \cdot K^{-1} \cdot mol^{-1}$
294.25	469.48	309.03	493.79	324.33	522.14
295.22	471.14	310.03	495.34	325.01	523.90
296.19	472.48	311.02	497.10	326.01	526.48
297.17	474.03	312.02	498.76	327.01	529.28
298.15	475.48	313.02	500.31	328.01	532.28
299.13	477.24	314.01	502.07	329.01	535.59
300.11	478.79	315.01	503.72	330.01	539.11
301.10	480.45	316.01	505.28	331.01	542.83
302.09	482.10	317.00	506.83	332.00	546.66
303.08	483.86	318.00	508.48	333.00	551.11
304.07	485.41	319.33	511.07	334.01	555.66
305.06	487.07	320.00	512.52	335.01	560.73
306.05	488.62	321.00	514.69	336.01	566.00
307.04	490.38	322.00	516.86		
308.04	492.03	323.00	519.04		

Table A37. The experimental values of the heat capacity of the solid phase of [ValOiPr][SA] averaged over 3 runs.

T, K	$C_{p,m}$, $J \cdot K^{-1} \cdot mol^{-1}$	T, K	$C_{p,m}$, $J \cdot K^{-1} \cdot mol^{-1}$	T, K	$C_{p,m}$, $J \cdot K^{-1} \cdot mol^{-1}$
294.06	453.40	318.14	479.34	342.15	526.01
295.03	454.74	319.14	480.37	343.16	529.69
296.00	455.00	320.13	481.29	344.16	532.33
297.3	457.09	321.13	482.73	345.16	536.64
298.28	458.79	322.13	483.84	346.16	541.25
299.26	459.81	323.13	484.17	347.16	545.93
300.25	460.30	324.13	485.46	348.16	551.06

T, K	$C_{p,m}$, $J \cdot K^{-1} \cdot mol^{-1}$	T, K	$C_{p,m}$, $J \cdot K^{-1} \cdot mol^{-1}$	T, K	$C_{p,m}$, $J \cdot K^{-1} \cdot mol^{-1}$
301.23	461.19	325.14	486.54	349.17	557.01
302.22	462.27	326.14	487.06	350.17	563.48
303.21	463.24	327.14	487.8	351.17	570.54
304.20	464.74	328.14	488.84	351.51	573.07
305.19	465.97	329.14	490.26	351.84	575.67
306.18	466.92	330.14	491.52	352.18	578.49
307.18	467.95	331.14	493.45	353.18	587.27
308.17	468.44	332.14	496.91	354.18	597.08
309.17	469.48	333.14	499.03	355.18	608.38
310.16	470.75	334.14	502.26	356.18	621.68
311.16	471.63	335.15	505.44	357.18	637.15
312.15	472.91	336.15	508.06	358.19	655.43
313.15	473.54	337.15	511.9	359.19	676.92
314.14	474.39	338.15	514.77	360.19	703.01
315.14	475.34	339.15	517.52	361.19	735.27
316.14	476.97	340.15	520.89		
317.14	478.66	341.15	523.64		

Stability test results

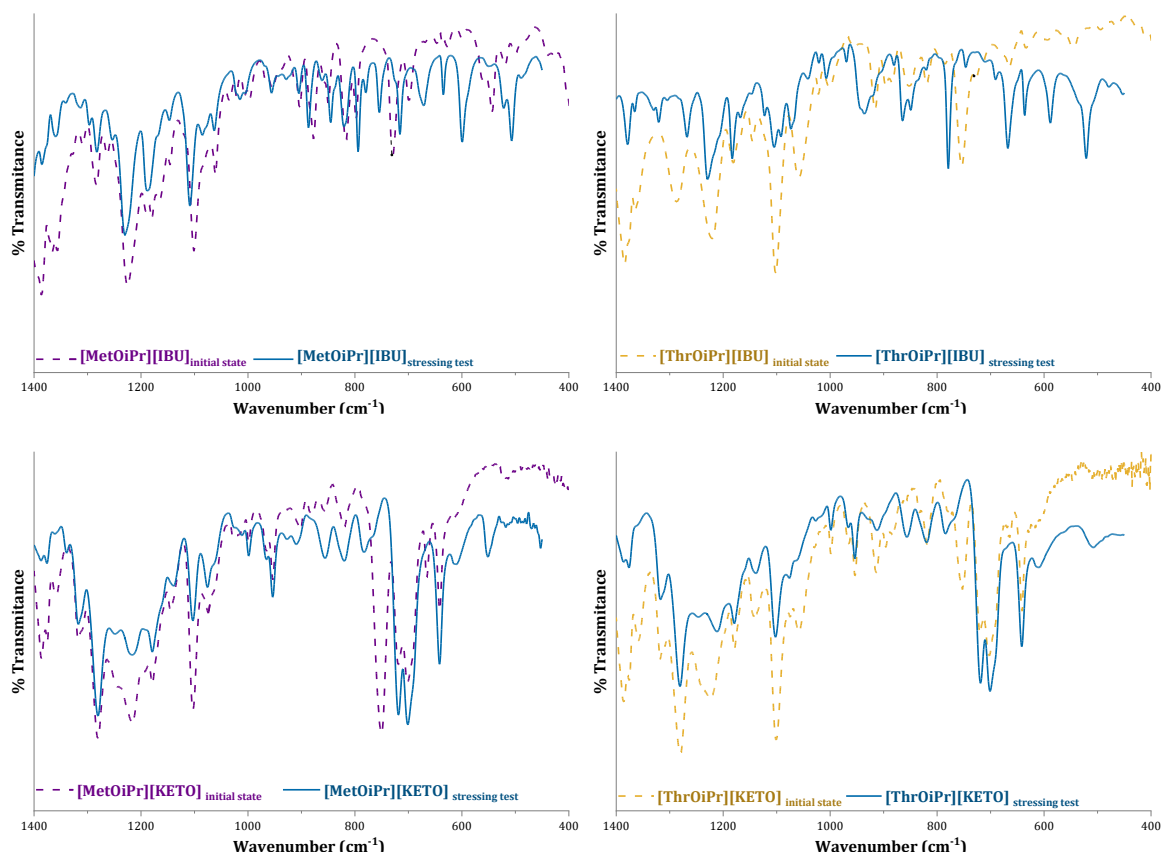


Fig A1. Comparison of ATR-FTIR spectra (finger-print region) for L-methioninium (left) and L-threoninium (right) isopropyl salts of ketoprofen and ibuprofen before and after the stress testing step.

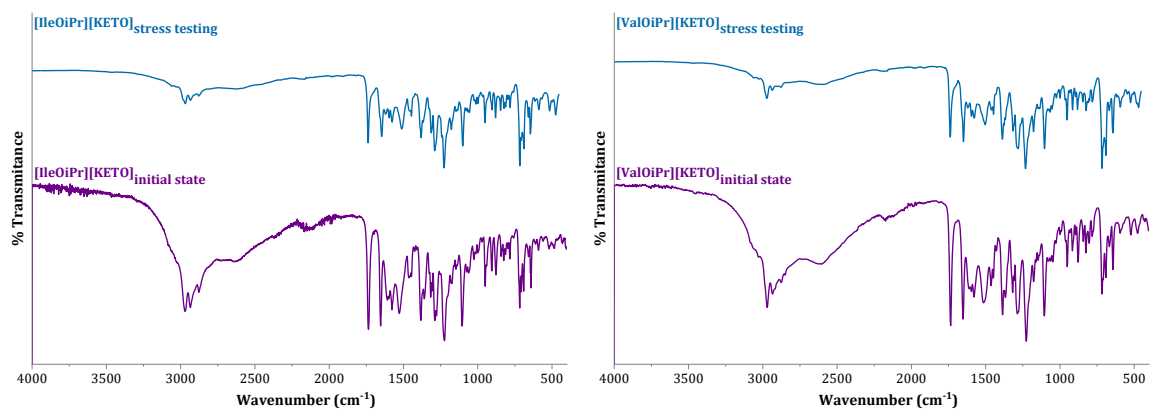


Fig A2. Comparison of ATR-FTIR spectra for L-isoleucinium (left) and L-valinium (right) isopropyl salts of ketoprofen before and after the stress testing step.

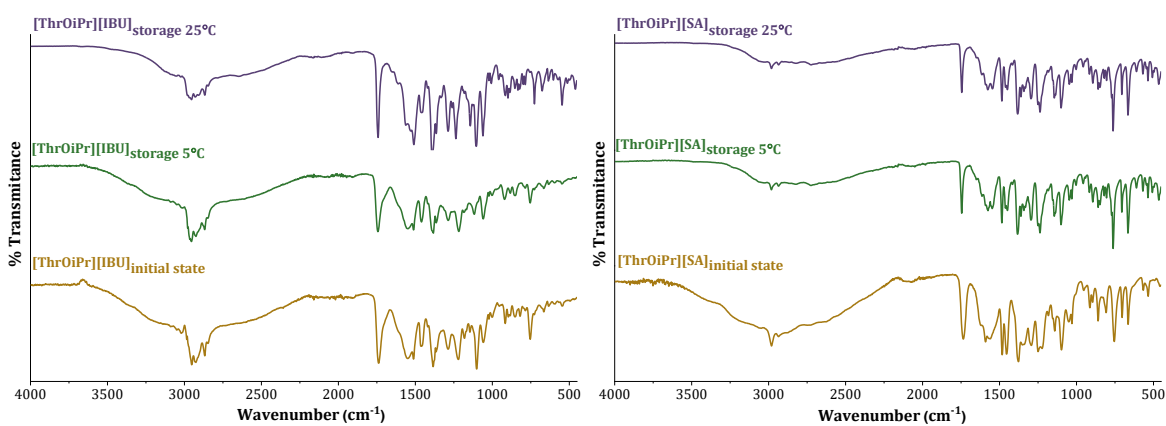


Fig A3. Comparison of ATR-FTIR spectra for [ThrOipr][IBU] (left) and [ThrOipr][SA] (right) before and after the storage for 12 months.

Table A38. Thermal stability specification evaluated by DSC analysis for NSAIDs and their L-amino acid isopropyl salts.

Compound	Initial state			Storage at 5°C±2°C			Storage at 25°C±2°C			Stress testing ^a		
	T _{DSC} Conset (°C)	T _{DSC} Cmax (°C)	T _{Conset} (°C)	T _{DSC} Conset (°C)	T _{DSC} Cmax (°C)	T _{Conset} (°C)	T _{DSC} Conset (°C)	T _{DSC} Cmax (°C)	T _{Conset} (°C)	T _{DSC} Conset (°C)	T _{DSC} Cmax (°C)	T _{Conset} (°C)
IBU	76.23	78.58	–	72.57	75.01	–	72.36	75.06	–	71.87	74.51	–
[MetOiPr][IBU]	63.79	65.72	52.16	64.13	66.22	51.24	61.65	64.76	48.32	65.21	74.25	–
[ThrOiPr][IBU]	40.70	48.52	–	41.16	50.15	–	–	–	–	59.87	70.74	–
[IleOiPr][IBU]	72.70/78.90	76.07/80.07	52.10	70.93/78.41	74.75/79.58	50.70	66.85/75.91	72.92/78.58	48.19	61.84/73.36	65.25/76.05	50.59
[ValOiPr][IBU] ^b	68.18/78.06	72.91/89.87	63.93	67.73/77.97	73.10/89.06	63.90	75.11/82.74	79.24/86.39	52.48	69.55/75.88	73.39/78.54	59.36
KETO	95.14	97.03	–	91.57	93.67	–	91.70	94.66	–	90.38	92.85	–
[MetOiPr][KETO]	50.06	59.60	–	55.98	61.43	–	43.46	57.29	–	–	–	–
[ThrOiPr][KETO]	–	–	–	–	–	–	–	–	–	–	–	–
[IleOiPr][KETO]	62.25/72.57	67.58/78.22	–	65.28/75.07	70.75/80.39	–	63.68/74.55	70.40/79.87	–	55.76/72.10	68.78/77.09	–
[ValOiPr][KETO]	45.53/ 63.32	56.28/ 75.70	–	51.33/64.18	58.78/ 76.56	–	57.32/67.42	64.10/76.56	–	48.04/67.61	67.44/74.92	–
NAP	155.98	158.41	80.12	153.61	155.69	82.81	153.91	155.84	85.96	152.95	154.87	86.03
[MetOiPr][NAP]	94.51	95.97	71.44	94.73	96.54	70.44	94.15	96.03	70.43	94.50	96.81	71.00
[ThrOiPr][NAP]	86.0	89.86	–	84.90	89.20	–	87.37	90.70	–	79.44/90.18	88.35/91.51	–
[IleOiPr][NAP]	89.82 /103.19	93.53 /107.38	64.84	89.30 /102.97	93.38 /108.22	65.14	87.18 /101.68	91.20 /107.88	64.13	87.00/104.32	91.01/108.85	63.11
[ValOiPr][NAP]	124.04 /130.15	127.13 /132.66	86.69	124.02 /130.32	127.13 /132.49	81.86	124.79 /130.59	127.91 /132.94	82.42	123.15/129.99	125.70/133.73	84.45

Compound	Initial state			Storage at 5°C±2°C			Storage at 25°C±2°C			Stress testing ^a		
	T _{DSConset} (°C)	T _{DSCmax} (°C)	T _{Conset} (°C)	T _{DSConset} (°C)	T _{DSCmax} (°C)	T _{Conset} (°C)	T _{DSConset} (°C)	T _{DSCmax} (°C)	T _{Conset} (°C)	T _{DSConset} (°C)	T _{DSCmax} (°C)	T _{Conset} (°C)
SA	158.05	160.04	107.61	156.73	159.13	100.98	156.05	158.37	106.18	156.28	158.65	105.25
[MetOiPr][SA]	87.47	88.83	65.03	85.16	88.36	65.47	87.21	88.69	65.30	87.26	88.83	62.81
[ThrOiPr][SA]	—	—	—	78.36	83.04	—	80.86	84.20	—	—	—	—
[IleOiPr][SA]	84.19	87.53	67.25	84.03	86.38	66.50	85.56	87.53	66.02	85.26	87.33	65.06
[ValOiPr][SA]	96.89	98.85	84.46	93.33	97.19	80.67	93.30	97.02	81.58	97.54	99.32	84.32

T_{DSConset}: the peak onset temperature in DSC, T_{DSCmax}: the peak maximum temperature in DSC, T_C: crystallization maximum peak temperature

^astorage at 40°C±2°C for 6 months

^bcooling rate at 30°C/min

DSC curves for the stability study evaluation for NSAIDs and their L-amino acid isopropyl ester salts

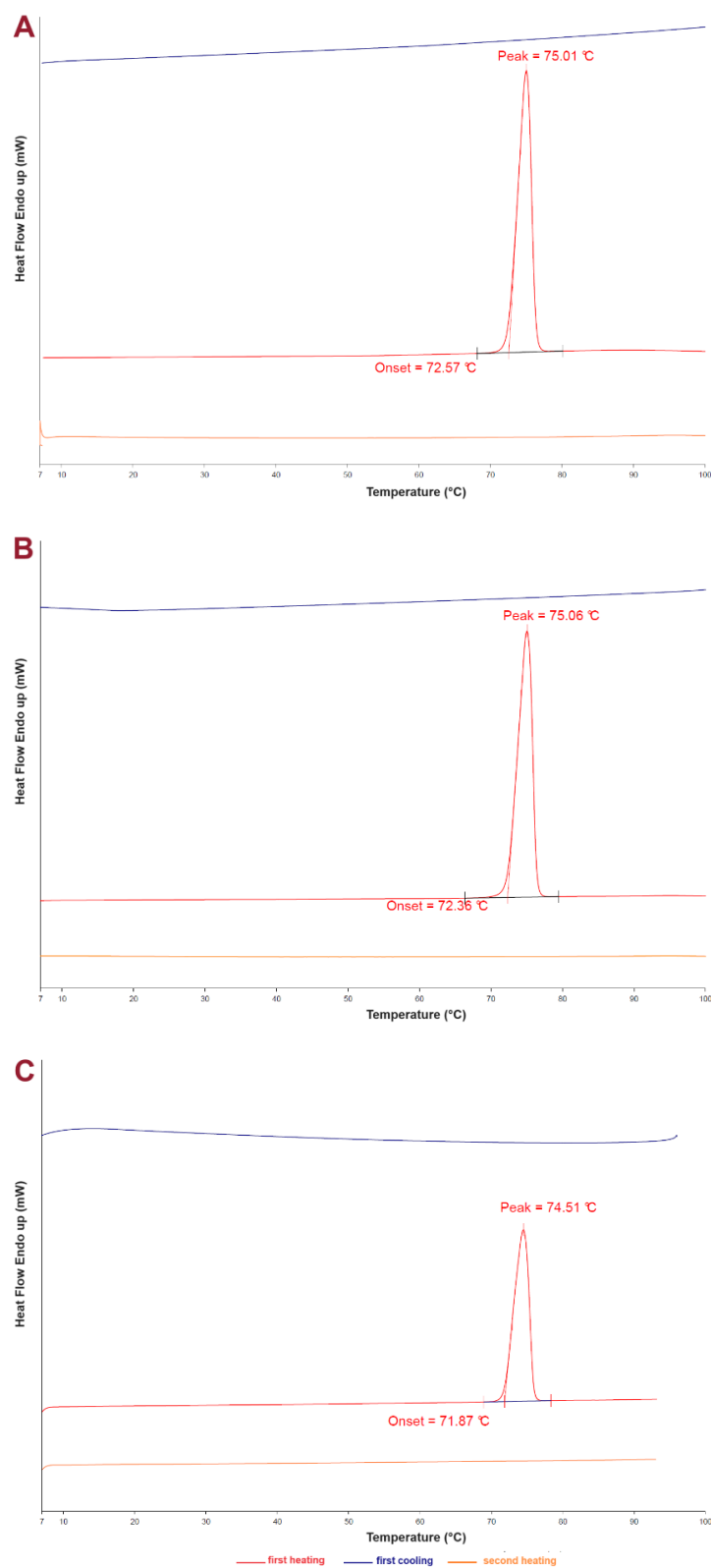


Fig A4. The thermal stability specification evaluated for ibuprofen stored at A: 5°C (for 12 months), B: 25°C (for 12 months), and C: 40°C (for 6 months).

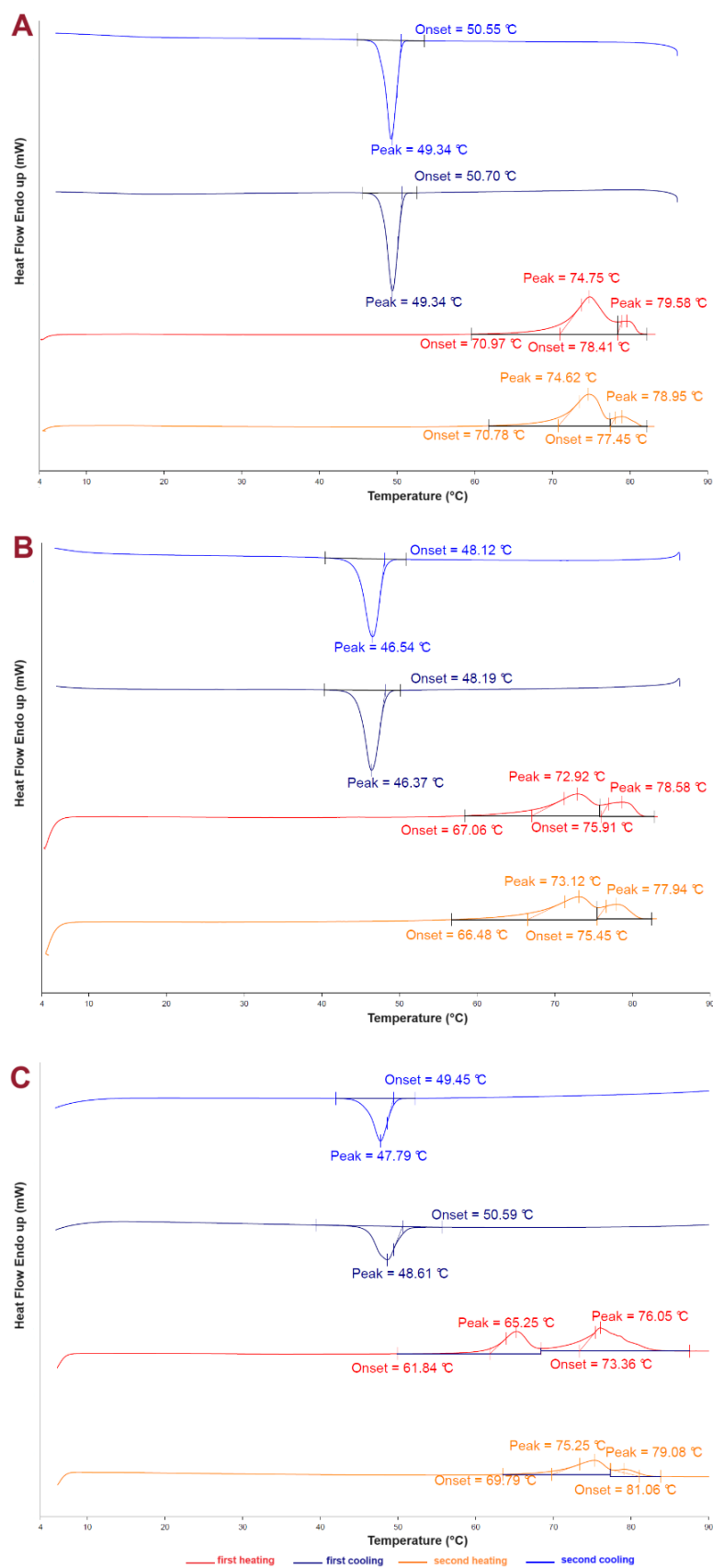


Fig A5. The thermal stability specification evaluated for [IlcOiPr][IBU] stored at A: 5°C (for 12 months), B: 25°C (for 12 months), and C: 40°C (for 6 months).

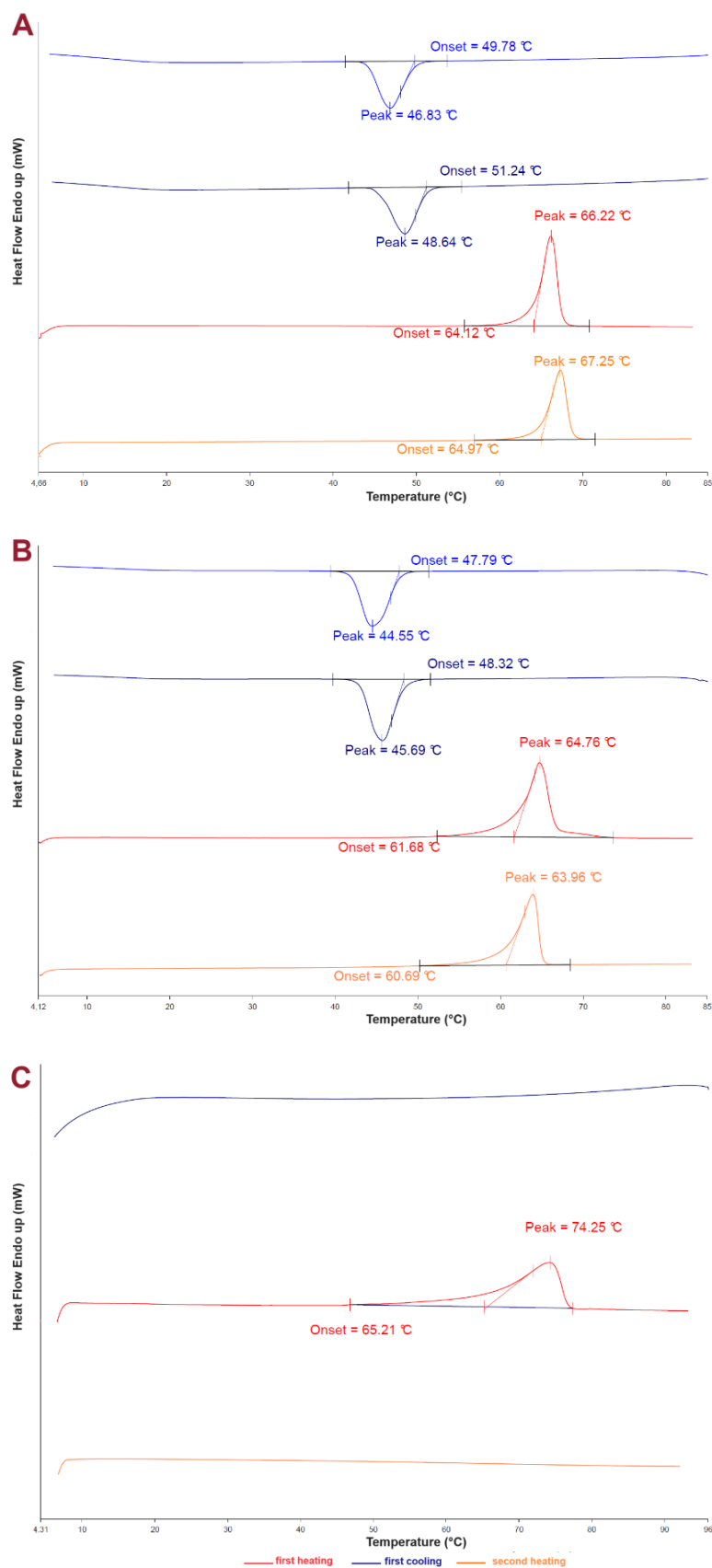


Fig A6. The thermal stability specification evaluated for [MetOiPr][IBU] stored at A: 5°C (for 12 months), B: 25°C (for 12 months), and C: 40°C (for 6 months).

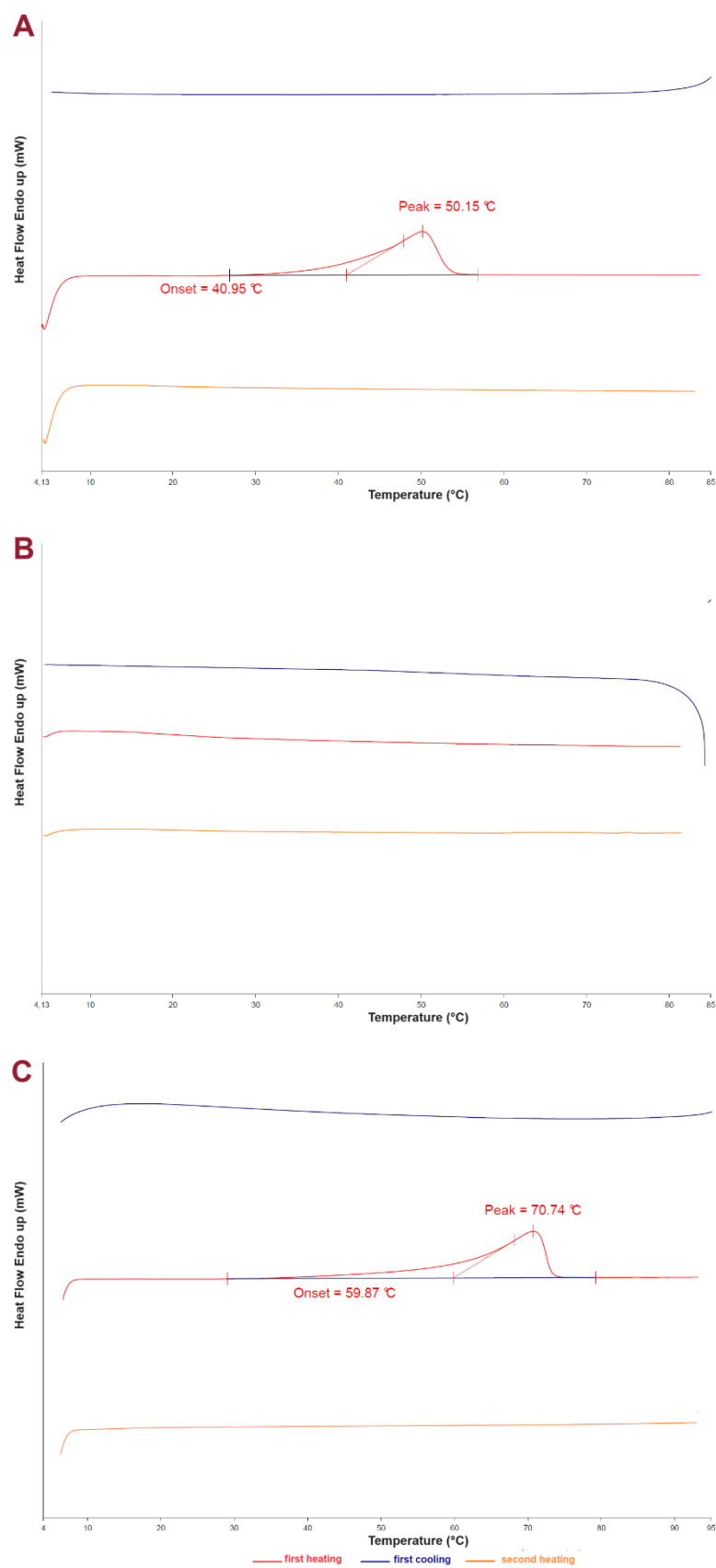


Fig A7. The thermal stability specification evaluated for [ThrOiPr][IBU] stored at A: 5°C (for 12 months), B: 25°C (for 12 months), and C: 40°C (for 6 months).

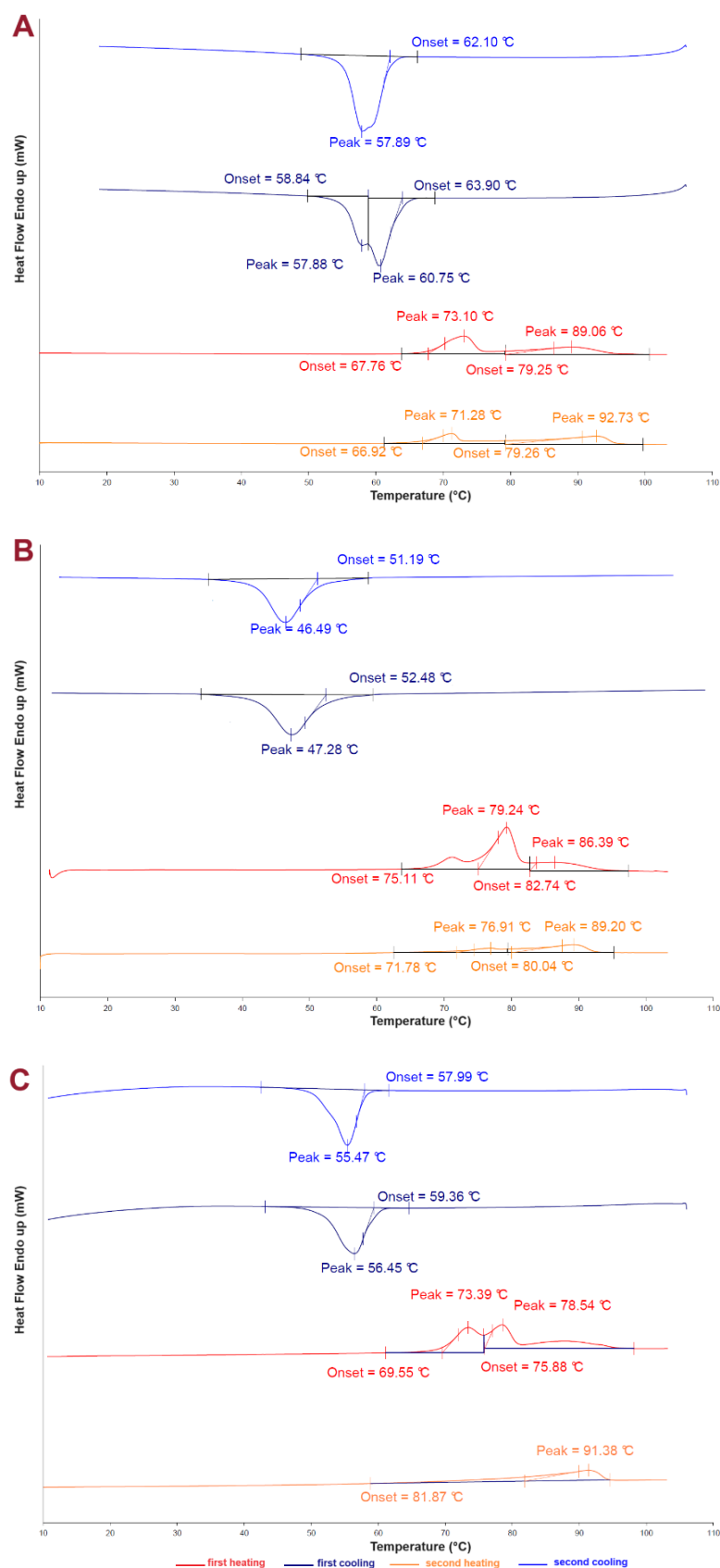


Fig A8. The thermal stability specification evaluated for [ValOipr][IBU] stored at A: 5°C (for 12 months), B: 25°C (for 12 months), and C: 40°C (for 6 months).

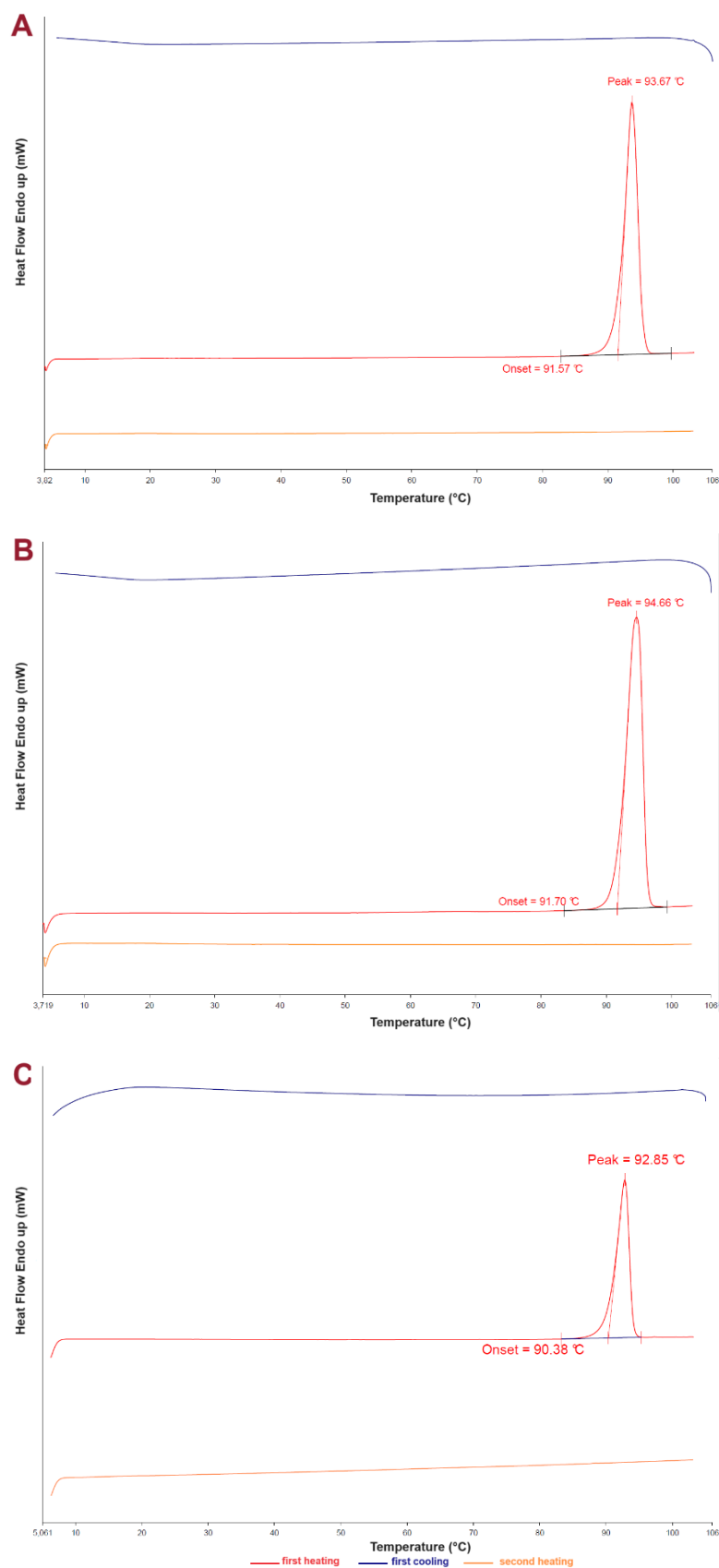


Fig A9. The thermal stability specification evaluated for KETO stored at A: 5°C (for 12 months), B: 25°C (for 12 months), and C: 40°C (for 6 months).

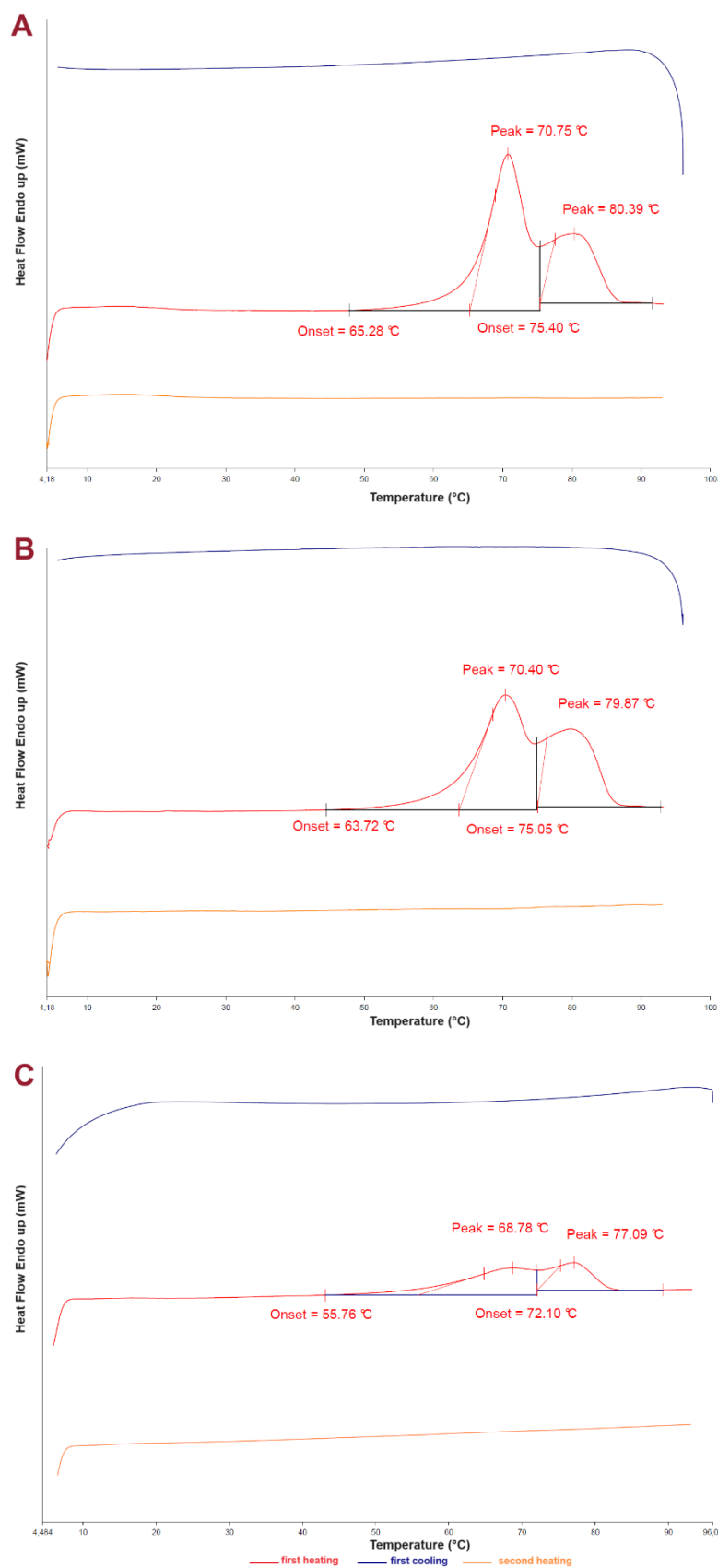


Fig A10. The thermal stability specification evaluated for [IleOiPr][KETO] stored at A: 5°C (for 12 months), B: 25°C (for 12 months), and C: 40°C (for 6 months).

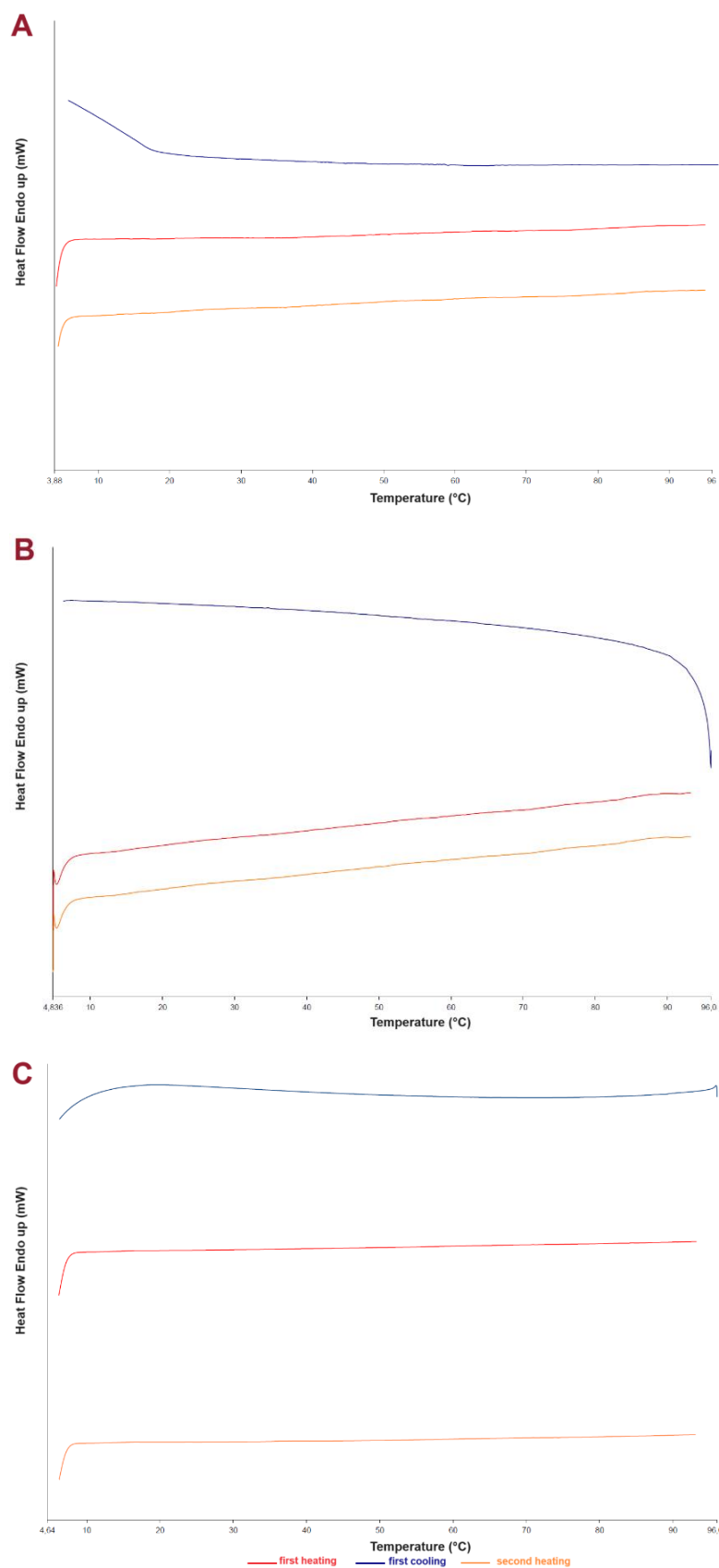


Fig A11. The thermal stability specification evaluated for [ThrOiPr][KETO] stored at A: 5°C (for 12 months), B: 25°C (for 12 months), and C: 40°C (for 6 months).

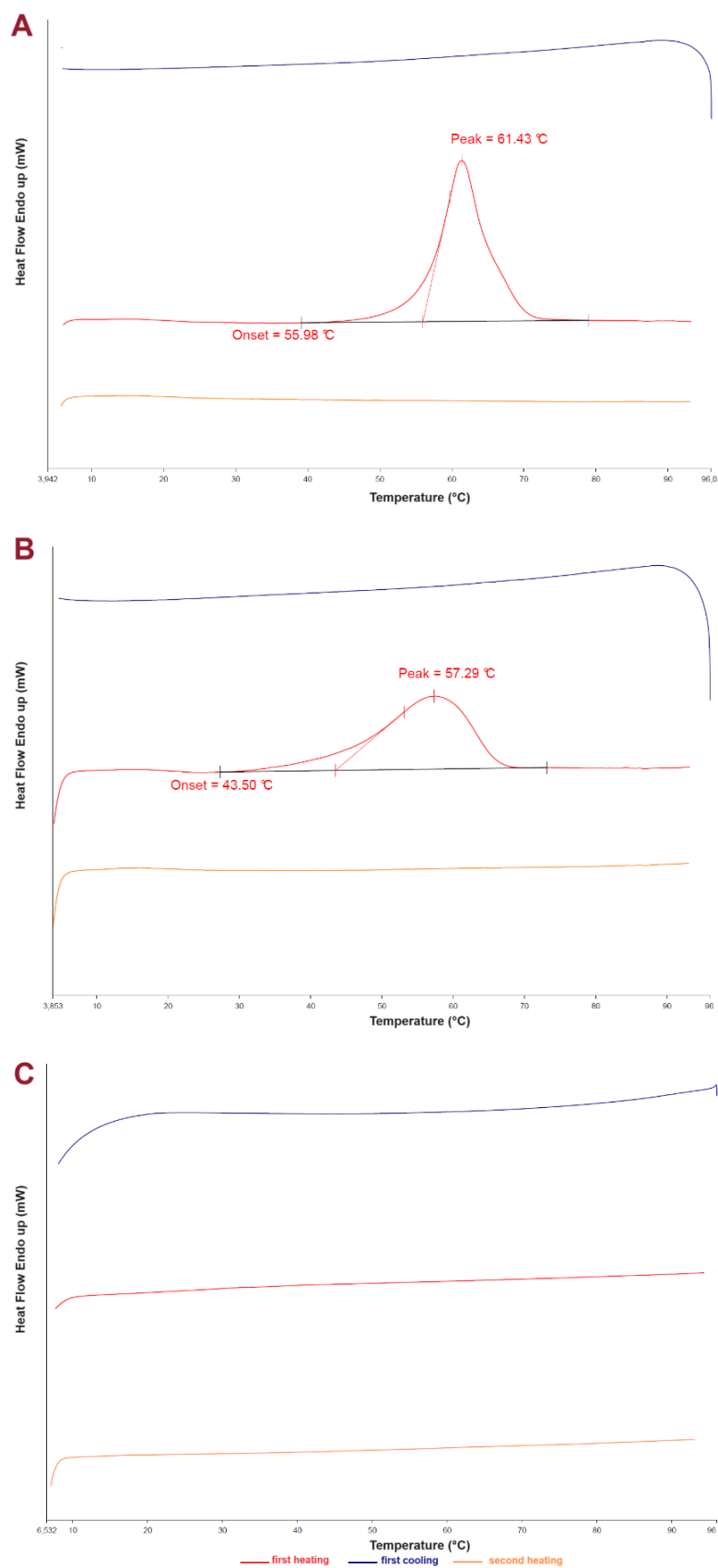


Fig A12. The thermal stability specification evaluated for [MetOiPr][KETO] stored at A: 5°C (for 12 months), B: 25°C (for 12 months), and C: 40°C (for 6 months).

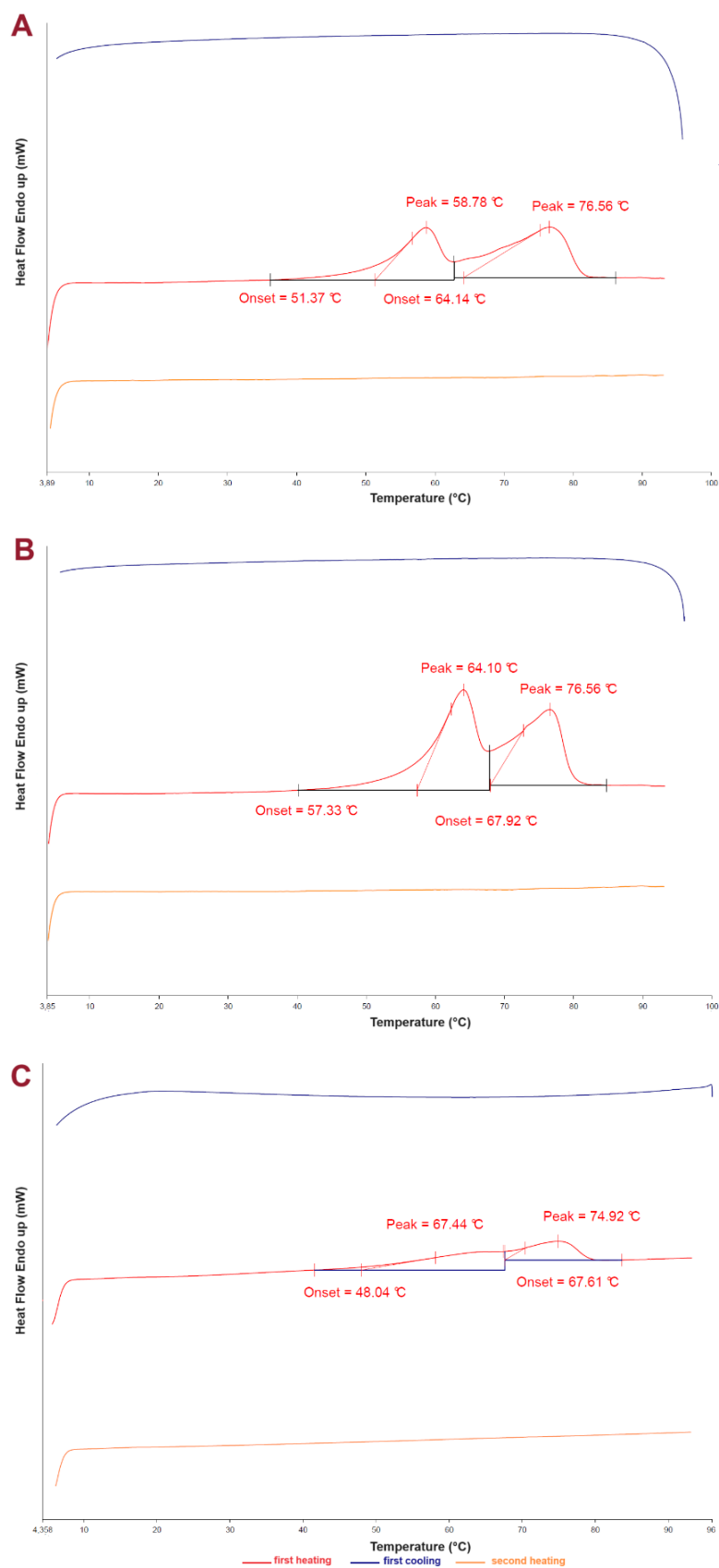


Fig A13. The thermal stability specification evaluated for [ValOipr][KETO] stored at A: 5°C (for 12 months), B: 25°C (for 12 months), and C: 40°C (for 6 months).

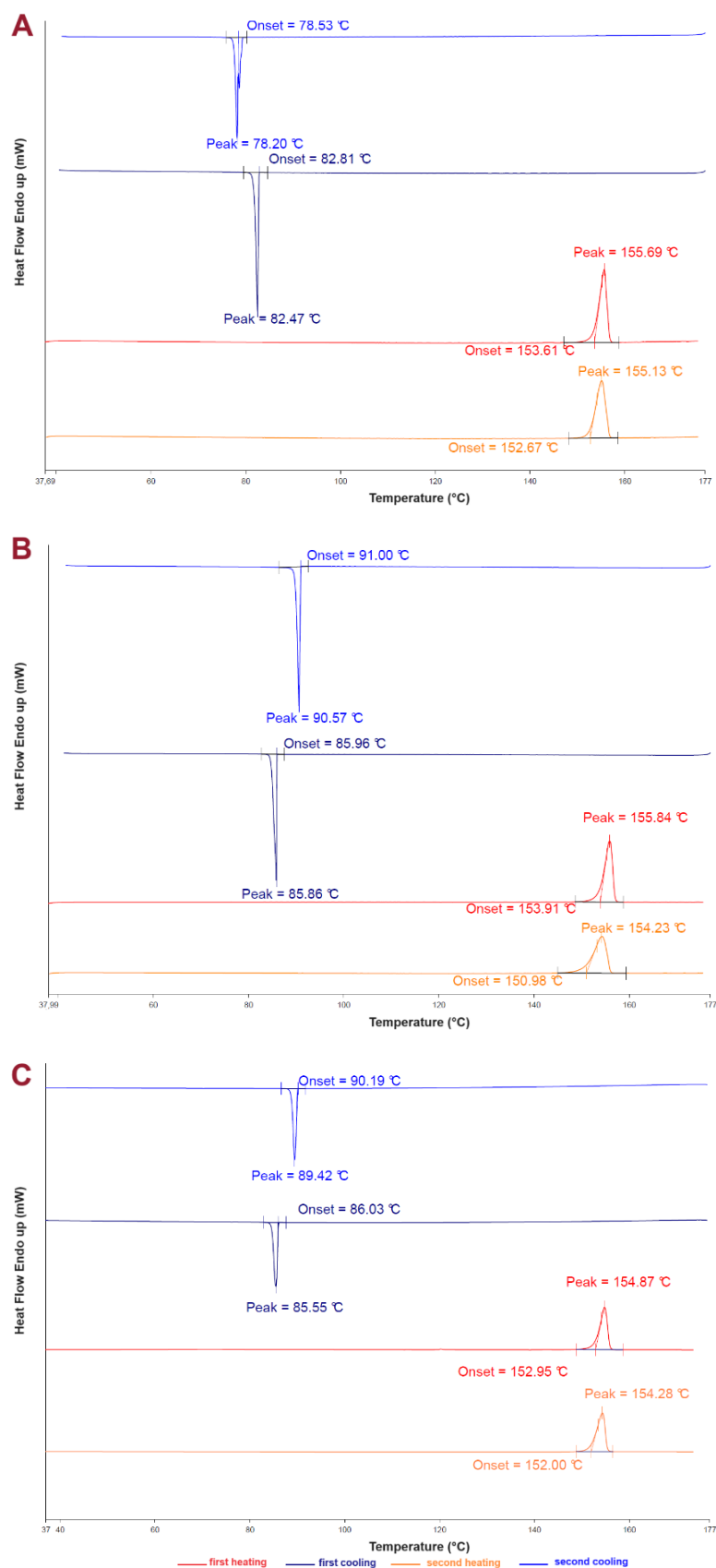


Fig A14. The thermal stability specification evaluated for naproxen stored at A: 5°C (for 12 months), B: 25°C (for 12 months), and C: 40°C (for 6 months).

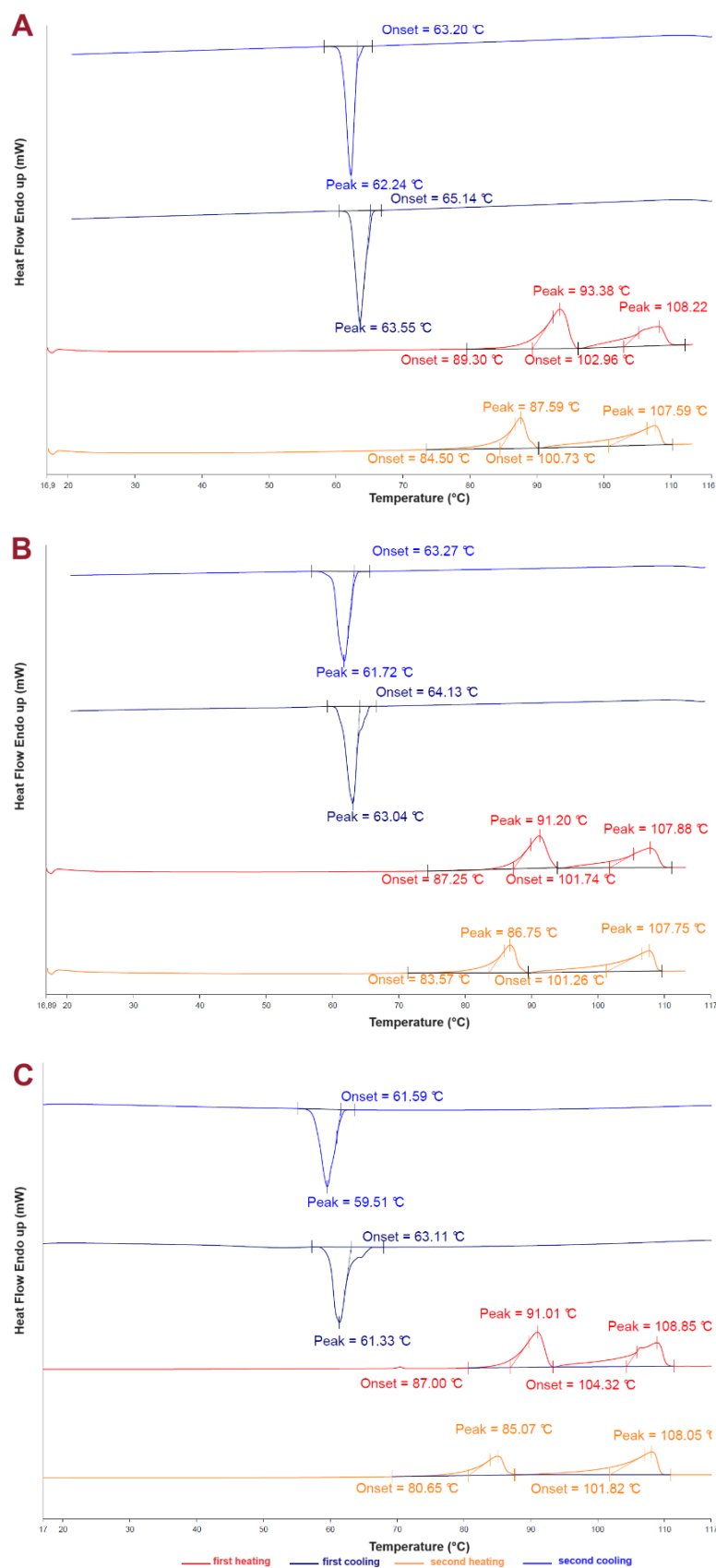


Fig A15. The thermal stability specification evaluated for [IleOiPr][NAP] stored at A: 5°C (for 12 months), B: 25°C (for 12 months), and C: 40°C (for 6 months).

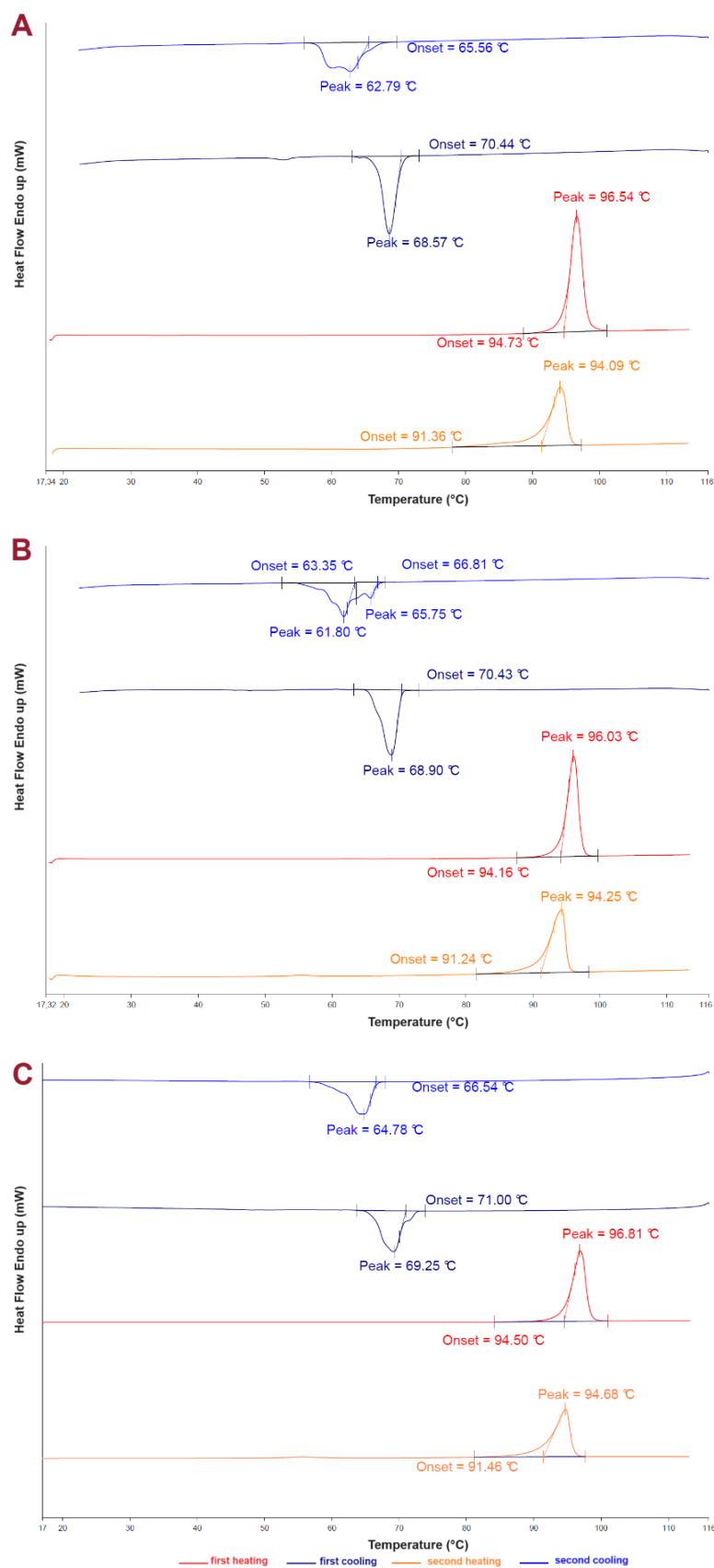


Fig A16. The thermal stability specification evaluated for [MetOiPr][NAP] stored at A: 5°C (for 12 months), B: 25°C (for 12 months), and C: 40°C (for 6 months).

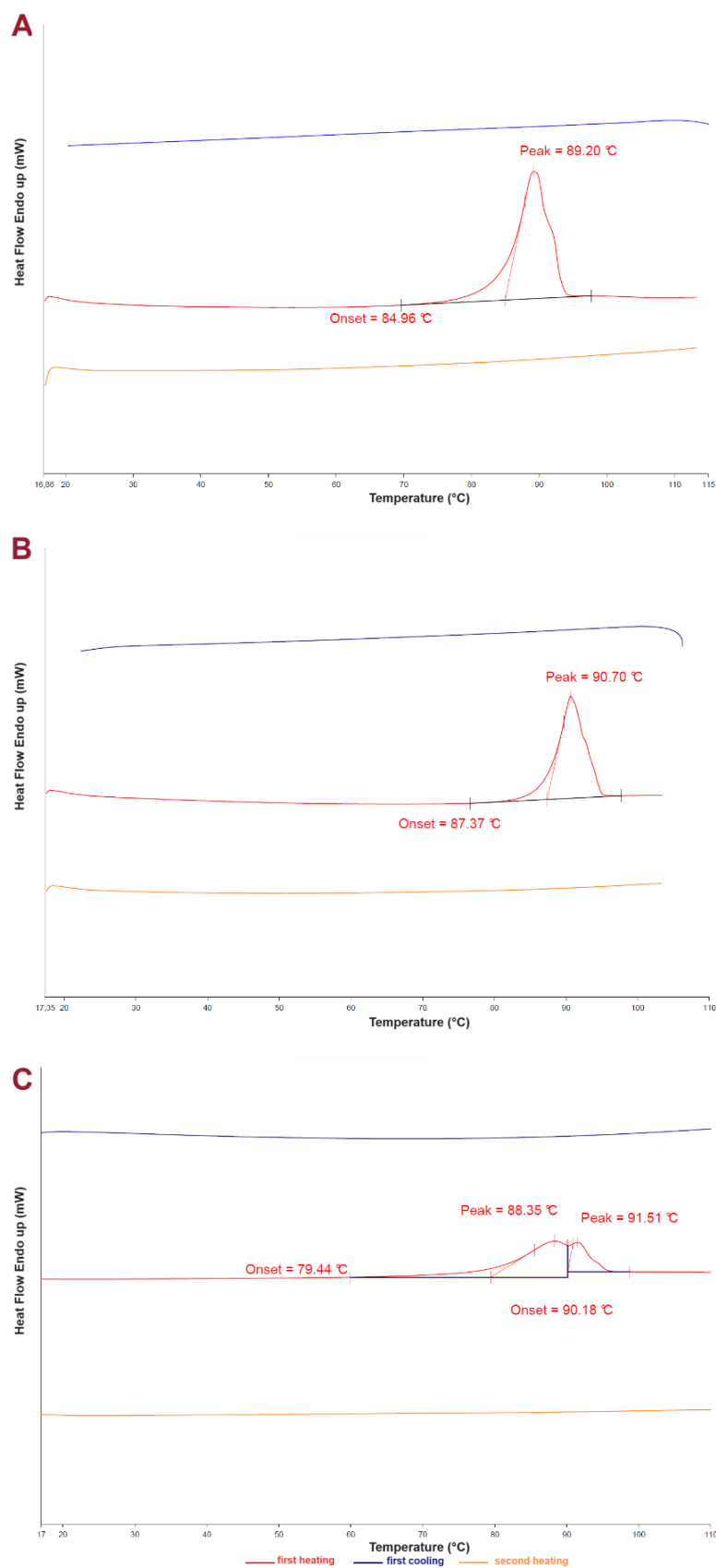


Fig A17. The thermal stability specification evaluated for [ThrOiPr][NAP] stored at A: 5°C (for 12 months), B: 25°C (for 12 months), and C: 40°C (for 6 months).

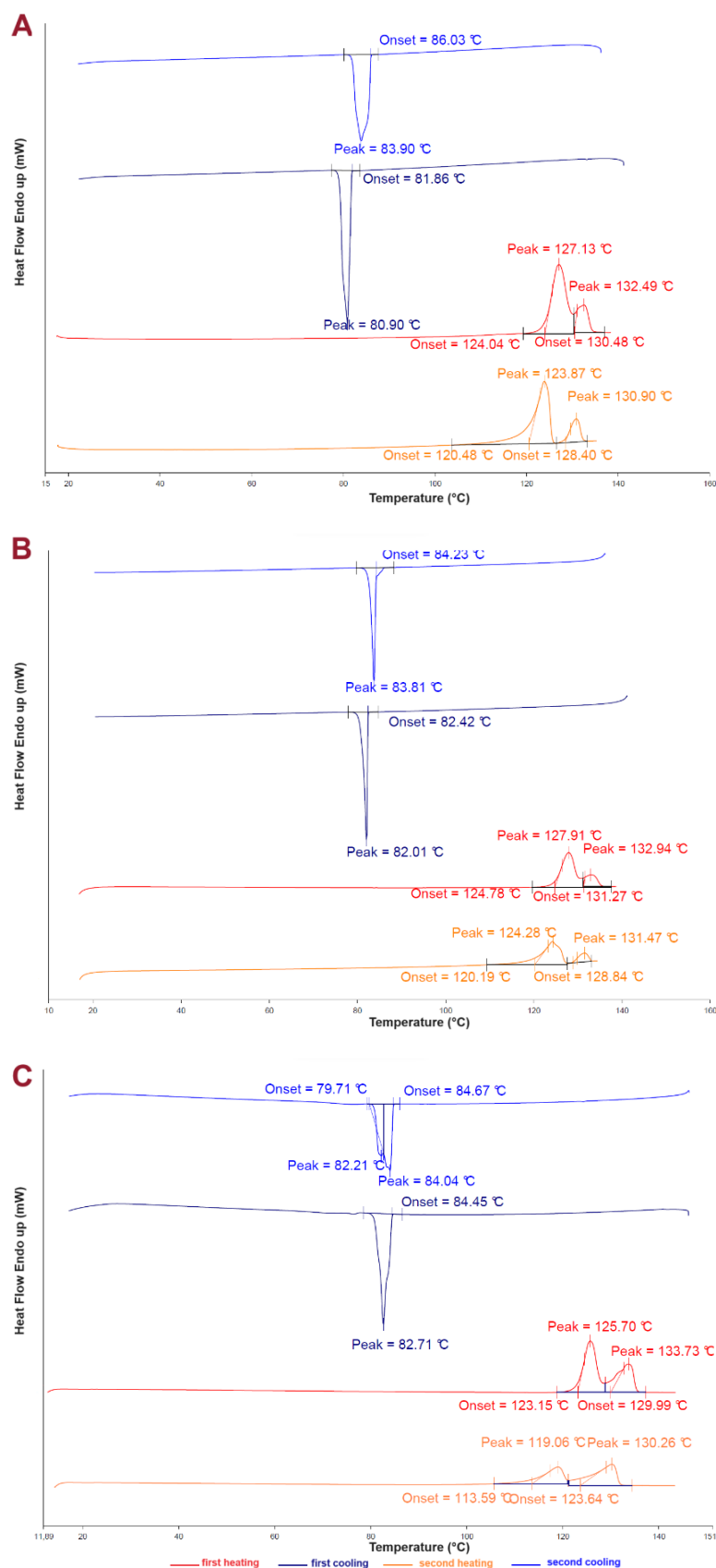


Fig A18. The thermal stability specification evaluated for [ValOipr][NAP] stored at A: 5°C (for 12 months), B: 25°C (for 12 months), and C: 40°C (for 6 months).

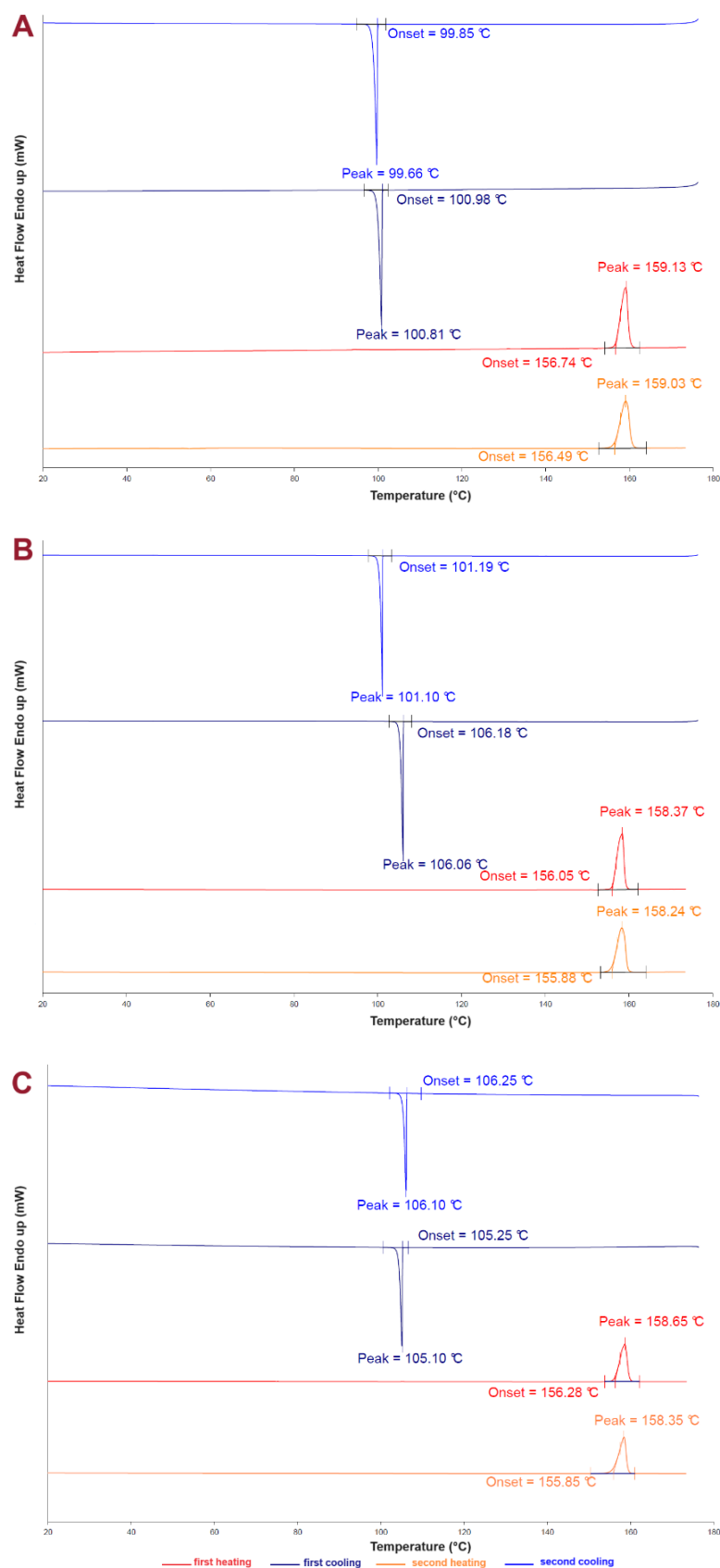


Fig A19. The thermal stability specification evaluated for salicylic acid stored at A: 5°C (for 12 months), B: 25°C (for 12 months), and C: 40°C (for 6 months).

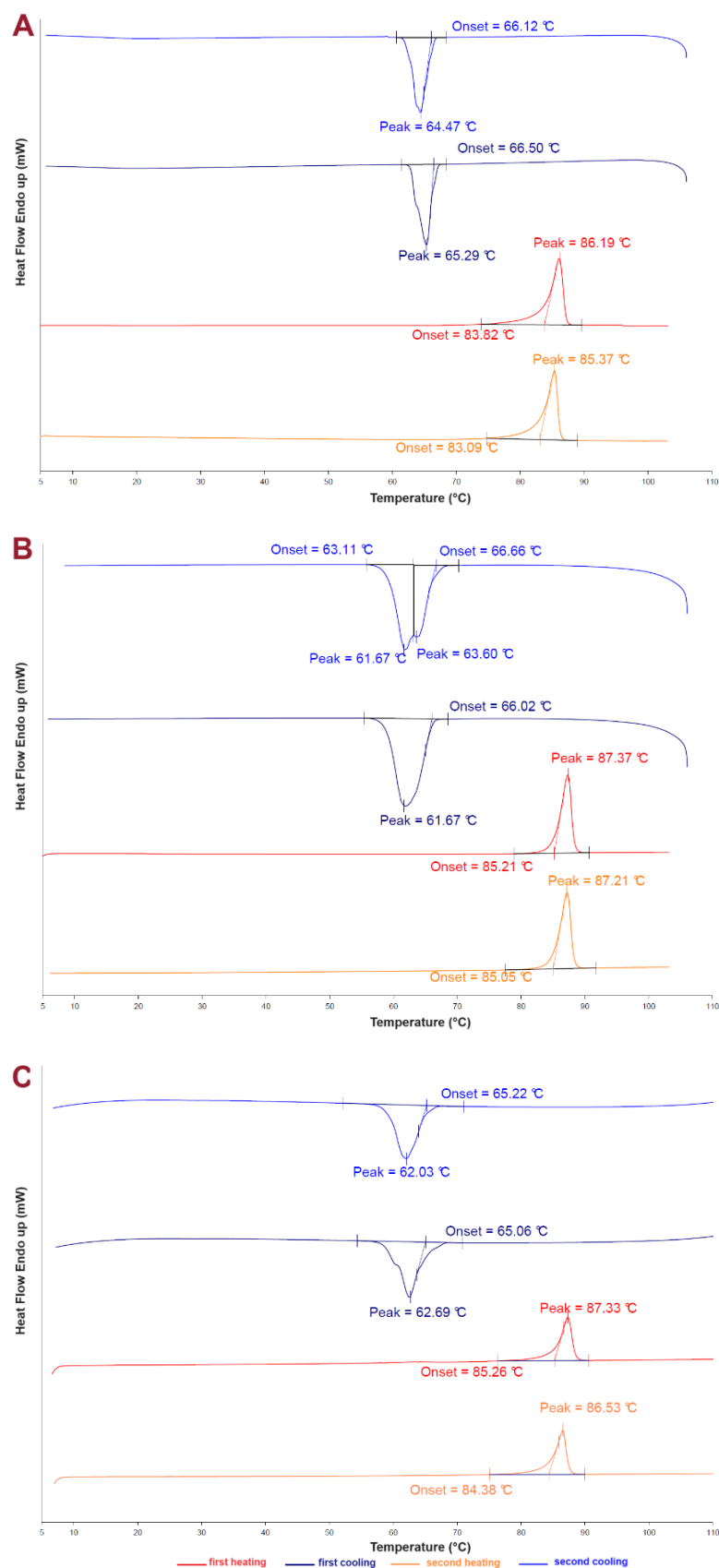


Fig A20. The thermal stability specification evaluated for [IleOiPr][SA] stored at A: 5°C (for 12 months), B: 25°C (for 12 months), and C: 40°C (for 6 months).

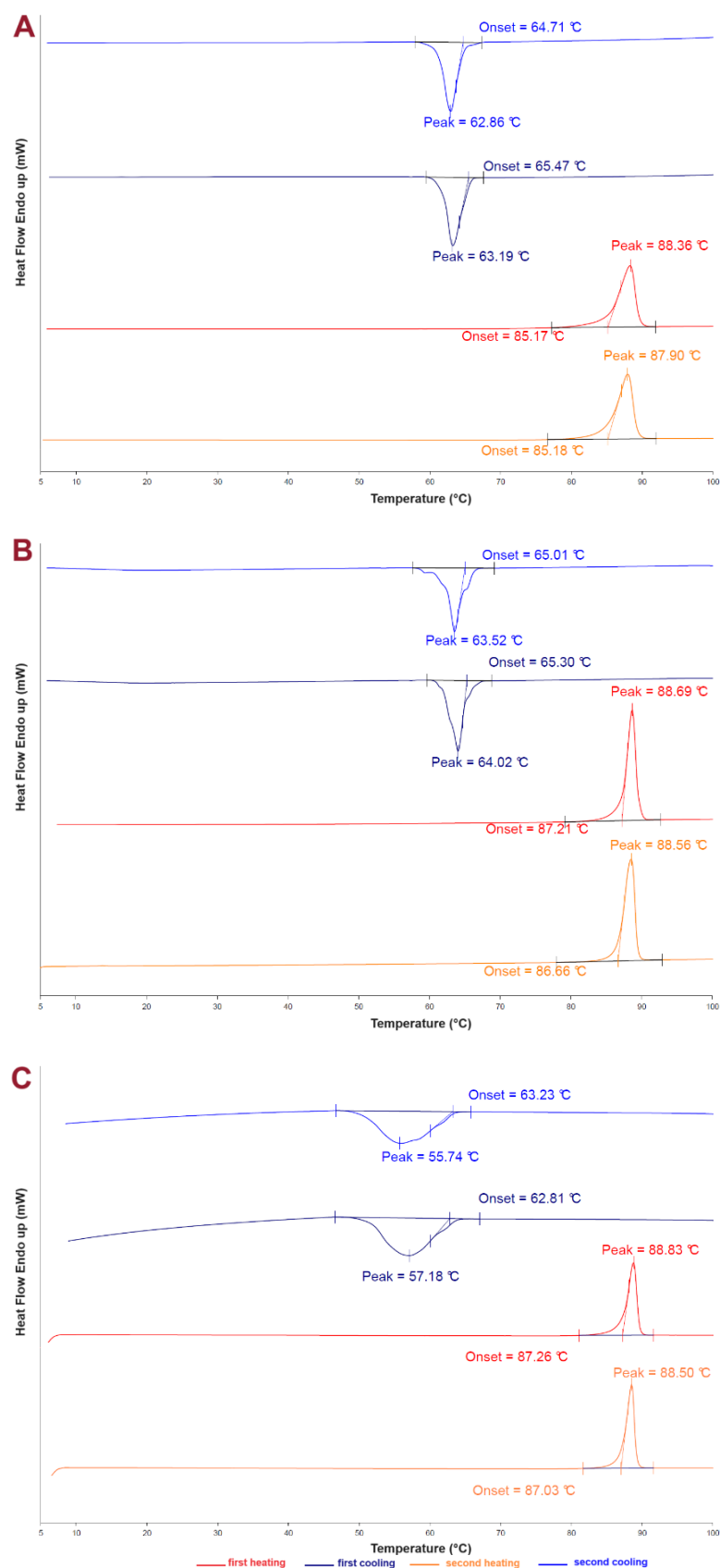


Fig A21. The thermal stability specification evaluated for [MetOiPr][SA] stored at A: 5°C (for 12 months), B: 25°C (for 12 months), and C: 40°C (for 6 months).

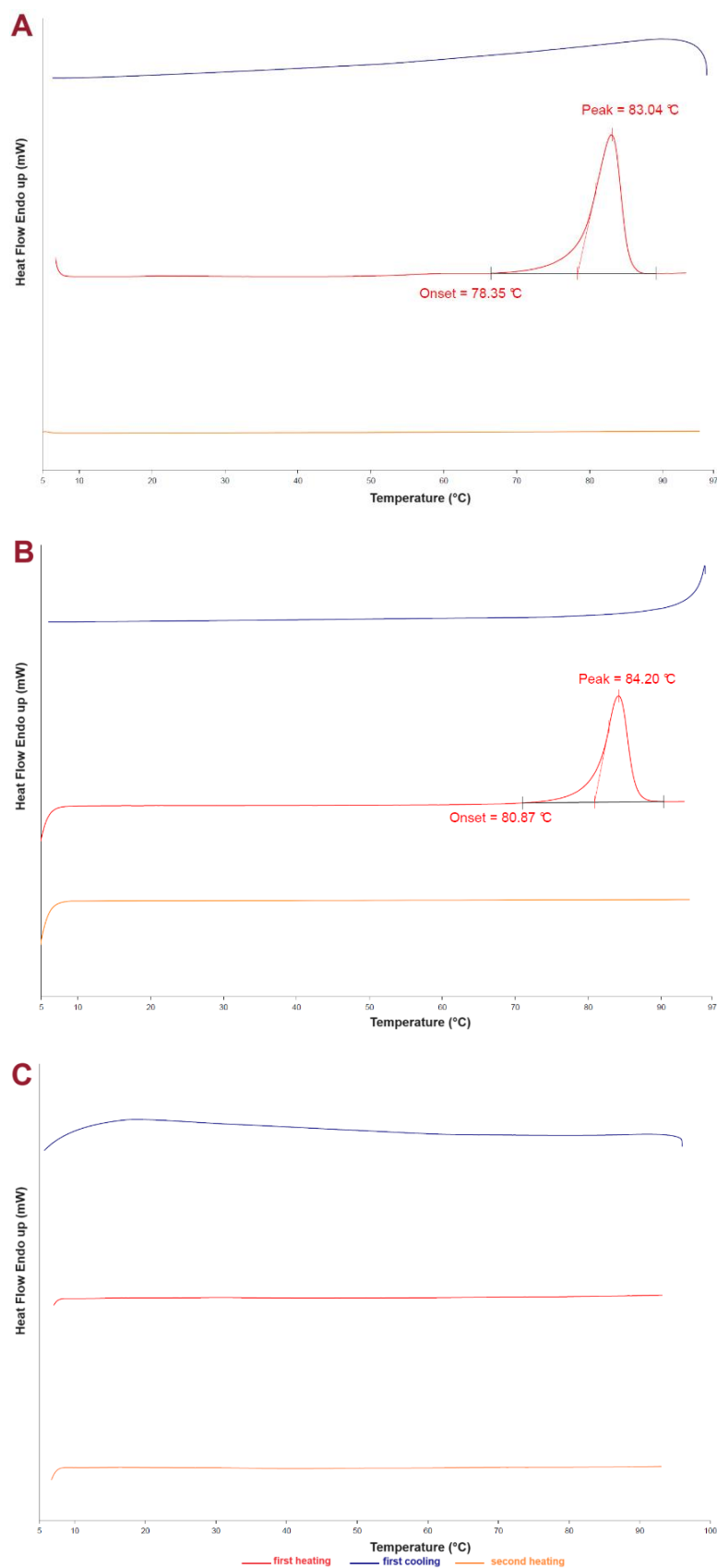


Fig A22. The thermal stability specification evaluated for [ThrOiPr][SA] stored at A: 5°C (for 12 months), B: 25°C (for 12 months), and C: 40°C (for 6 months).

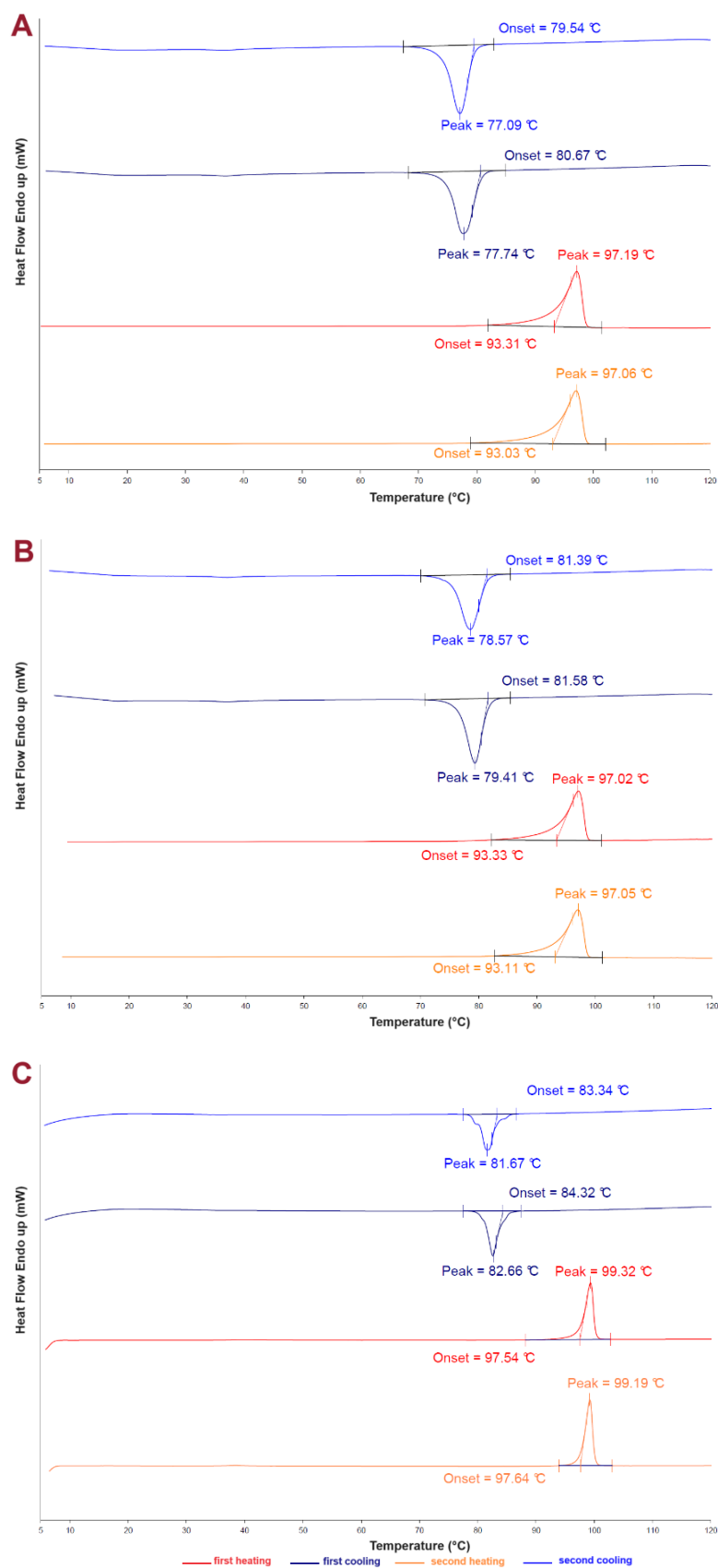


Fig A23. The thermal stability specification evaluated for [ValOiPr][SA] stored at A: 5°C (for 12 months), B: 25°C (for 12 months), and C: 40°C (for 6 months).

SKIN PERMEATION RESULTS

Skin permeation profiles

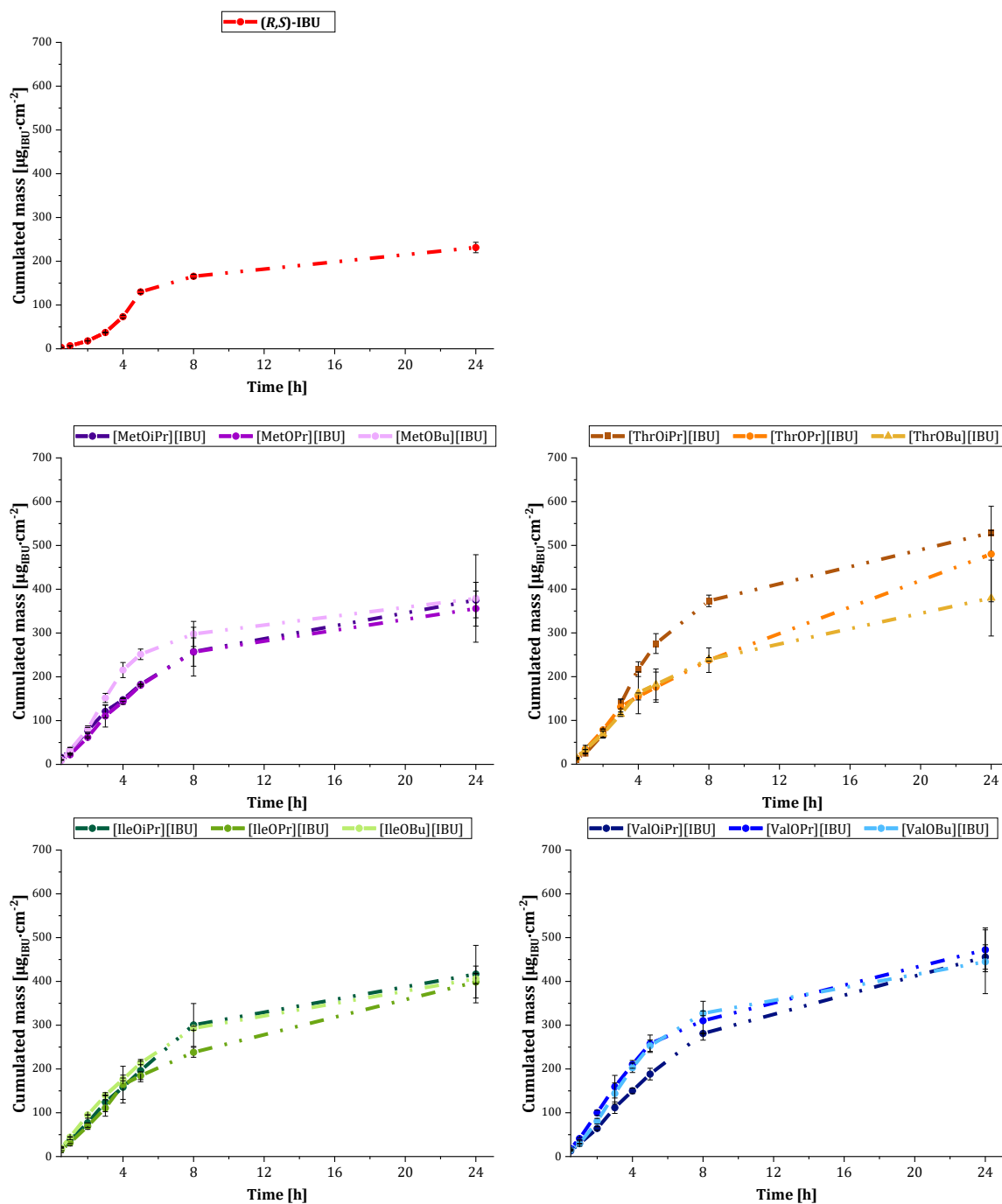


Fig A24. Permeation profiles for (R,S) -ibuprofen and its L-amino alkyl ester salts through human skin from ethanolic solution to acceptor phase with pH 7.40. Values are the means with standard deviation; n=3 (data presented in: [182]).

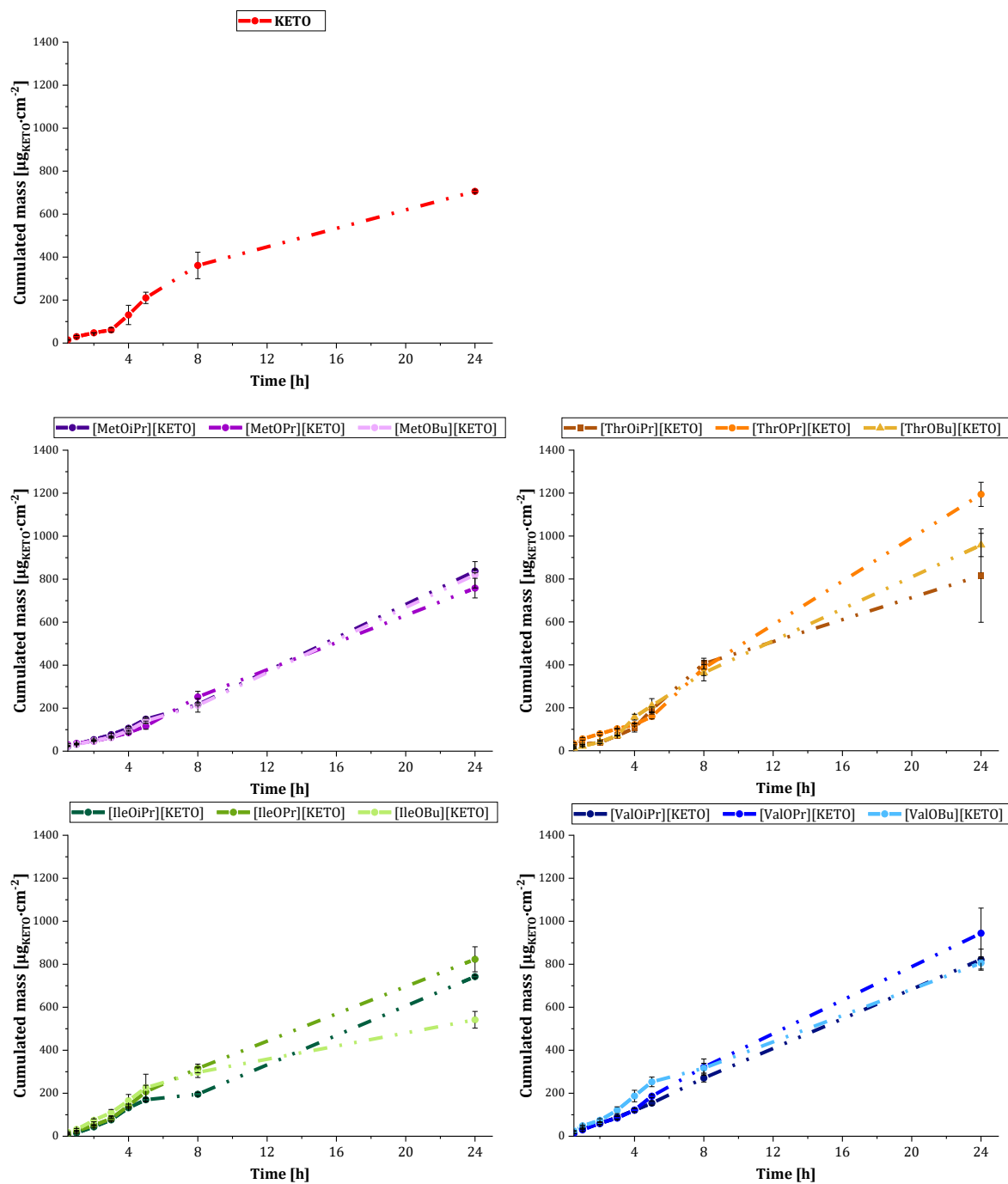


Fig A25. Permeation profiles for ketoprofen and its L-amino alkyl ester salts through human skin from ethanolic solution to acceptor phase with pH 7.40. Values are the means with standard deviation; n=3 (data presented in: [182]).

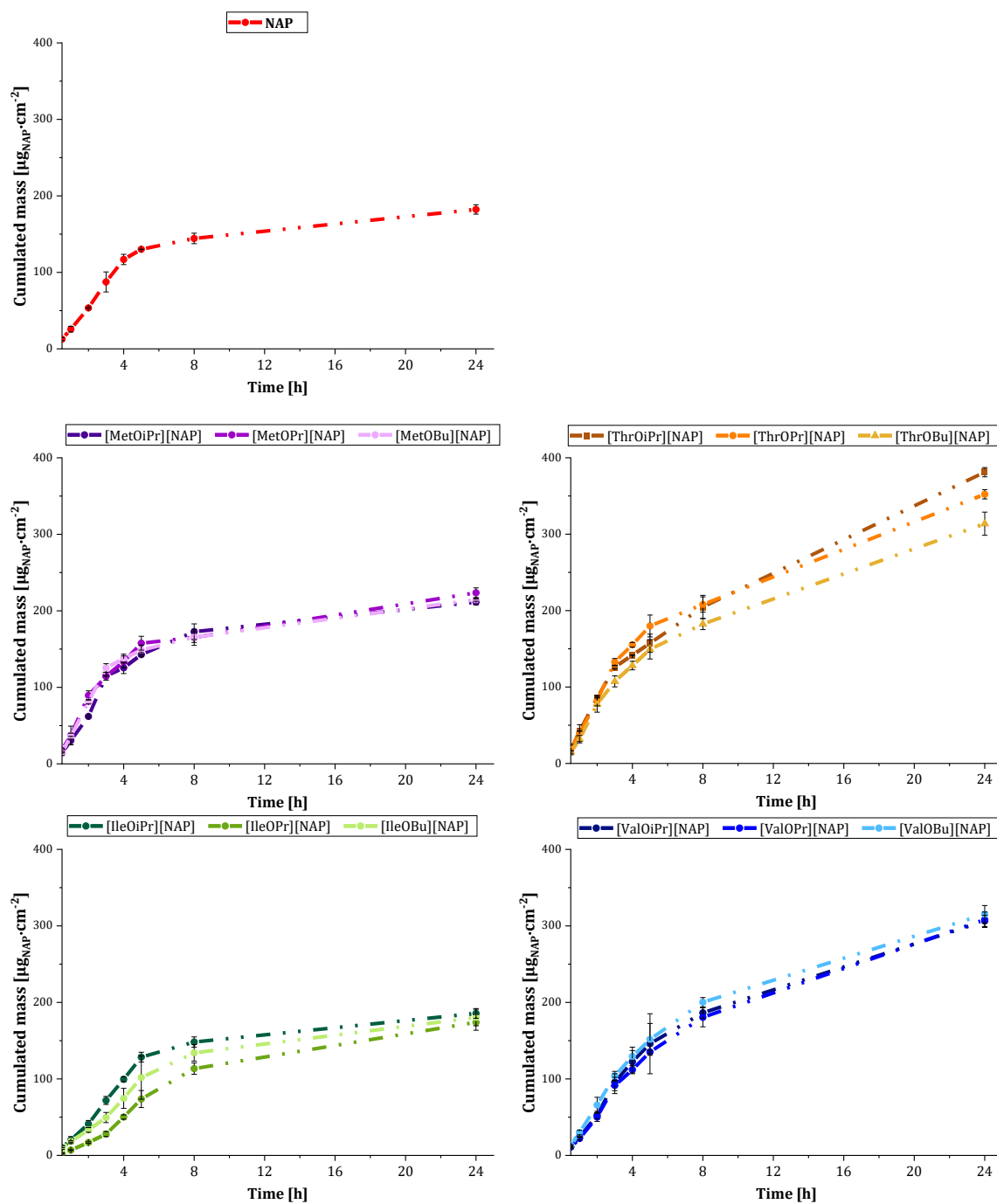


Fig A26. Permeation profiles for naproxen and its L-amino alkyl ester salts through human skin from ethanolic solution to acceptor phase with pH 7.40. Values are the means with standard deviation; n=3 (data presented in: [182]).

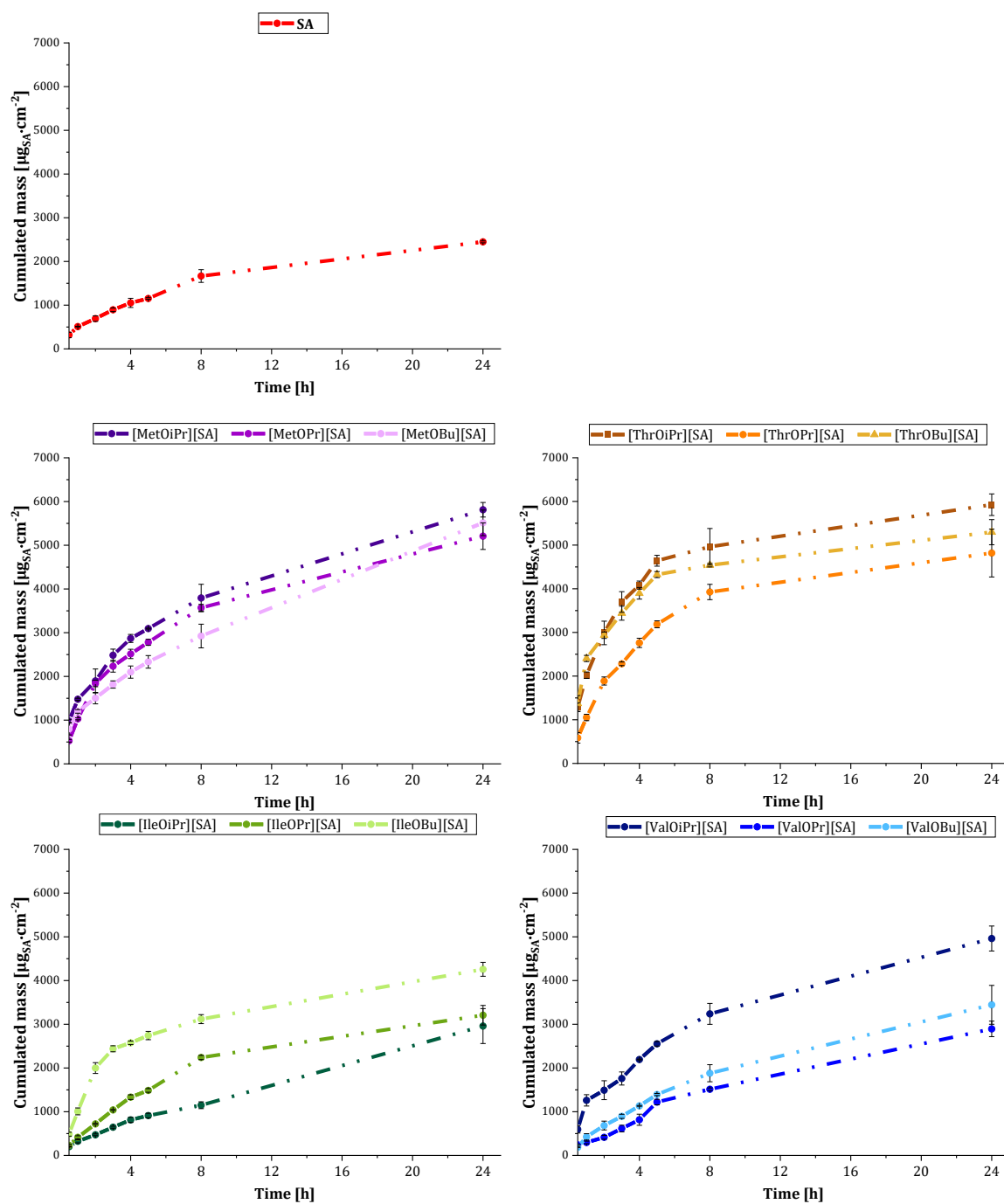


Fig A27. Permeation profiles for salicylic acid and its L-amino alkyl ester salts through human skin from ethanolic solution to acceptor phase with pH 7.40. Values are the means with standard deviation; n=3 (data presented in: [182]).

SKIN PERMEATION PARAMETERS

Table A39. Skin permeation parameters for ibuprofen and its L-amino acid alkyl ester salts across abdominal porcine skin *in vitro* (data partly presented in: [182]).

Compound	Cumulated mass, $\mu\text{g IBU}/\text{cm}^2$	J_{ss} , $\mu\text{g IBU}/(\text{cm}^2\text{h})$	$K_P \cdot 10^3$, cm/h	L_T , h	$D \cdot 10^4$, cm^2/h	K_m	$Q\%_{24h}$
IBU	231.392±11.924	46.407±1.665	4.453±0.159	2.273±0.037	1.834±0.030	1.215±0.063	2.221±0.103
(S+)-IBU	317.111±30.659	25.000±0.016	2.394±0.153	1.293±0.270	3.223±1.016	0.372±0.078	3.038±0.299
[MetOiPr][IBU]	378.991±99.899*	62.009±4.010	5.707±0.369	0.563±0.124	7.389±1.907	0.386±0.104	3.488±0.919
[MetOPr][IBU]	355.828±40.085	39.934±2.104	3.670±0.193	0.238±0.154	17.518±4.545	0.105±0.075	3.270±0.261
[MetOBu][IBU]	375.327±40.497*	44.692±2.567	4.345±0.250	0.287±0.130	14.494±8.984	0.150±0.063	3.649±0.308
[ThrOiPr][IBU]	529.048±5.168	62.193±2.069	5.959±0.189	0.709±0.069	5.902±0.581	0.485±0.063	4.842±0.644
[ThrOPr][IBU]	480.287±109.089*	46.839±9.328	4.333±0.863	0.252±0.098	16.562±6.331	0.131±0.079	4.443±0.741
[ThrOBu][IBU]	379.663±86.710	42.124±7.960	3.338±0.631	0.225±0.048	14.239±6.329	0.146±0.072	5.008±1.112
[IleOiPr][IBU]	416.684±65.633*	39.897±4.883	3.667±0.654	0.337±0.050	12.509±1.857	0.134±0.019	3.830±0.603
[IleOPr][IBU]	398.537±36.453*	40.117±3.907	3.467±0.338	0.204±0.098	20.345±14.279	0.085±0.122	3.445±0.315
[IleOBu][IBU]	406.191±11.924*	45.254±0.944	4.159±0.089	0.102±0.012	40.997±4.968	0.050±0.022	3.733±0.636
[ValOiPr][IBU]	455.665±27.885*	40.300±3.342	3.722±0.308	0.300±0.139	13.866±8.393	0.134±0.073	4.208±0.258
[ValOPr][IBU]	472.102±50.035*	54.379±5.104	5.381±0.505	0.173±0.198	24.053±9.858	0.112±0.075	4.672±0.495
[ValOBu][IBU]	444.884±72.864*	56.960±2.790	5.630±0.276	0.507±0.076	8.212±1.144	0.343±0.051	4.397±0.720
[ValOiPr][(S+)]IBU]	561.830±25.716	44.881±3.102	4.090±0.283	0.286±0.078	14.582±1.128	0.140±0.045	5.120±0.430
[ValOPr][(S+)]IBU]	617.240±47.149	66.747±2.859	6.621±0.284	0.315±0.125	13.221±2.0429	0.250±0.019	6.123±0.255
[ValOBu][(S+)]IBU]	557.550±39.358	50.330±3.949	5.067±0.398	0.346±0.043	12.034±1.304	0.211±0.042	5.614±0.308

*- significant differences of the derivatives compared to the control (unmodified acid) $p < 0.001$, $\alpha = 0.05$, mean \pm SD, $n = 3$; the statistically significant difference was estimated by ANOVA using the Tuckey's test; J_{ss} : steady-state flux; K_P : permeability coefficient; L_T : lag time; D : diffusion coefficient; K_m : skin partition coefficient; Q : the percentage of the applied dose

Table A40. Skin permeation parameters for ketoprofen and its L-amino acid alkyl ester salts across abdominal porcine skin *in vitro* (data presented in: [182]).

Compound	Cumulated mass, $\mu\text{g KETO}/\text{cm}^2$	J_{ss} , $\mu\text{g KETO}/(\text{cm}^2\text{h})$	$K_P \cdot 10^3$, cm/h	L_T , h	$D \cdot 10^4$, cm^2/h	K_m	$Q\%_{24h}$
KETO	705.858±6.370	74.611±8.188	7.138±0.784	2.204±0.190	1.891±0.167	1.888±0.291	6.750±0.291
[MetOiPr][KETO]	837.557±7.662*	36.118±6.931	3.355±0.815	0.934±0.498	4.461±0.908	0.376±0.241	7.780±0.411
[MetOPr][KETO]	758.329±45.558*	42.340±3.445	4.359±0.747	2.087±0.719	1.996±0.645	1.092±0.515	7.808±0.398
[MetOBu][KETO]	820.463±61.393	37.942±4.191	3.891±0.429	1.351±0.336	3.083±1.334	0.631±0.199	8.413±0.484
[ThrOiPr][KETO]	815.963±217.725	74.006±6.838	7.365±0.681	2.500±0.144	1.669±0.100	2.206±0.291	8.121±1.841
[ThrOPr][KETO]	1194.219±56.275*	67.922±9.394	6.916±0.957	2.398±0.270	1.737±0.194	1.990±0.504	12.160±0.573

Compound	Cumulated mass, $\mu\text{g}_{\text{KETO}}/\text{cm}^2$	J_{ss} , $\mu\text{g}_{\text{KETO}}/(\text{cm}^2\text{h})$	$K_p \cdot 10^3$, cm/h	L_T , h	$D \cdot 10^4$, cm^2/h	K_m	$Q\%_{24\text{h}}$
[ThrOBu][KETO]	958.306 \pm 54.243*	69.458 \pm 0.380	6.424 \pm 1.230	1.902 \pm 0.168	2.190 \pm 0.177	1.467 \pm 0.435	8.863 \pm 1.839
[IleOiPr][KETO]	742.448 \pm 6.023	46.829 \pm 3.776	4.693 \pm 0.378	1.306 \pm 0.267	3.190 \pm 1.009	0.735 \pm 0.188	7.441 \pm 0.060
[IleOPr][KETO]	823.165 \pm 58.130*	62.548 \pm 0.639	5.625 \pm 0.575	1.704 \pm 0.314	2.445 \pm 0.832	1.150 \pm 0.165	7.403 \pm 0.668
[IleOBu][KETO]	541.753 \pm 38.895	62.964 \pm 0.100	5.914 \pm 0.937	0.978 \pm 0.091	4.258 \pm 0.568	0.694 \pm 0.053	5.090 \pm 0.032
[ValOiPr][KETO]	821.448 \pm 49.123*	36.721 \pm 2.138	3.845 \pm 0.224	0.684 \pm 0.107	6.090 \pm 0.298	0.316 \pm 0.088	8.600 \pm 0.327
[ValOPr][KETO]	944.496 \pm 116.759*	48.113 \pm 6.792	4.685 \pm 0.661	1.295 \pm 0.268	3.226 \pm 0.762	0.726 \pm 0.244	9.198 \pm 1.137
[ValOBu][KETO]	806.129 \pm 28.380*	60.287 \pm 3.941	5.782 \pm 0.378	0.866 \pm 0.241	4.810 \pm 0.227	0.601 \pm 0.185	7.731 \pm 0.185

*- significant differences of the derivatives compared to the control (unmodified acid) $p < 0.001$, $\alpha = 0.05$, mean \pm SD, $n = 3$; the statistically significant difference was estimated by ANOVA using the Tuckey's test; J_{ss} : steady-state flux; K_p : permeability coefficient; L_T : lag time; D : diffusion coefficient; K_m : skin partition coefficient; Q : the percentage of the applied dose

Table A41. Skin permeation parameters for naproxen and its L-amino acid alkyl ester salts across abdominal porcine skin *in vitro* (data presented in: [182]).

Compound	Cumulated mass, $\mu\text{g}_{\text{NAP}}/\text{cm}^2$	J_{ss} , $\mu\text{g}_{\text{NAP}}/(\text{cm}^2\text{h})$	$K_p \cdot 10^3$, cm/h	L_T , h	$D \cdot 10^4$, cm^2/h	K_m	$Q\%_{24\text{h}}$
NAP	182.268 \pm 6.158	29.813 \pm 4.914	2.832 \pm 0.467	0.119 \pm 0.111	34.893 \pm 13.674	0.041 \pm 0.005	1.731 \pm 0.053
[MetOiPr][NAP]	211.465 \pm 3.742*	31.560 \pm 2.667	3.186 \pm 0.269	0.034 \pm 0.063	121.288 \pm 21.073	0.013 \pm 0.024	2.135 \pm 0.037
[MetOPr][NAP]	223.604 \pm 6.420*	48.174 \pm 7.020	4.503 \pm 0.656	0.166 \pm 0.189	25.162 \pm 12.835	0.089 \pm 0.012	2.091 \pm 0.073
[MetOBu][NAP]	214.681 \pm 2.153*	44.310 \pm 2.791	4.155 \pm 0.262	0.171 \pm 0.061	24.300 \pm 7.993	0.085 \pm 0.037	2.013 \pm 0.020
[ThrOiPr][NAP]	381.113 \pm 6.070	43.290 \pm 3.729	3.644 \pm 0.314	0.056 \pm 0.016	73.806 \pm 11.321	0.025 \pm 0.009	3.208 \pm 0.072
[ThrOPr][NAP]	352.171 \pm 6.073*	45.592 \pm 5.457	4.146 \pm 0.496	0.129 \pm 0.254	32.314 \pm 2.483	0.064 \pm 0.016	3.203 \pm 0.055
[ThrOBu][NAP]	313.677 \pm 15.154*	38.080 \pm 6.441	3.482 \pm 0.589	0.107 \pm 0.062	38.882 \pm 6.491	0.045 \pm 0.041	2.868 \pm 0.631
[IleOiPr][NAP]	185.623 \pm 6.388*	28.984 \pm 1.115	2.735 \pm 0.105	0.559 \pm 0.168	7.458 \pm 4.729	0.183 \pm 0.053	1.752 \pm 0.060
[IleOPr][NAP]	174.000 \pm 10.341	22.874 \pm 7.131	1.906 \pm 0.594	1.786 \pm 0.380	2.333 \pm 0.619	0.408 \pm 0.177	1.450 \pm 0.086
[IleOBu][NAP]	180.282 \pm 10.805	26.132 \pm 3.102	2.335 \pm 0.277	1.118 \pm 0.364	3.276 \pm 0.314	0.313 \pm 0.087	1.611 \pm 0.012
[ValOiPr][NAP]	306.438 \pm 7.373*	35.960 \pm 4.656	3.618 \pm 0.468	0.402 \pm 0.168	10.358 \pm 7.302	0.174 \pm 0.041	3.083 \pm 0.074
[ValOPr][NAP]	308.096 \pm 10.047*	34.644 \pm 4.393	3.047 \pm 0.386	0.424 \pm 0.089	9.834 \pm 2.515	0.155 \pm 0.048	2.710 \pm 0.088
[ValOBu][NAP]	315.214 \pm 11.446*	36.525 \pm 1.369	3.389 \pm 0.127	0.169 \pm 0.084	24.569 \pm 1.444	0.068 \pm 0.036	2.949 \pm 0.106

*- significant differences of the derivatives compared to the control (unmodified acid) $p < 0.001$, $\alpha = 0.05$, mean \pm SD, $n = 3$; the statistically significant difference was estimated by ANOVA using the Tuckey's test; J_{ss} : steady-state flux; K_p : permeability coefficient; L_T : lag time; D : diffusion coefficient; K_m : skin partition coefficient; Q : the percentage of the applied dose

Table A42. Skin permeation parameters for salicylic acid and its L-amino acid alkyl ester salts across abdominal porcine skin *in vitro* (data presented in: [182]).

Compound	Cumulated mass, $\mu\text{g SA}/\text{cm}^2$	J_{ss} , $\mu\text{g SA}/(\text{cm}^2\text{h})$	$K_p \cdot 10^3$, cm/h	L_T , h	$D \cdot 10^4$, cm^2/h	K_m	$Q\%_{24h}$
SA	2447.850±21.729	192.570±30.440	18.017±2.848	1.627±0.688	2.560±1.047	3.519±0.825	22.902±0.543
[MetOiPr][SA]	5811.842±166.614*	231.560±46.320	22.769±4.555	8.363±1.721	0.498±0.025	19.633±3.155	57.147±3.054
[MetOPr][SA]	5208.204±303.942*	176.110±1.308	16.173±0.663	5.520±0.512	0.755±0.066	10.714±0.749	31.887±1.454
[MetOBu][SA]	5512.883±292.161*	301.174±31.198	27.723±3.120	2.992±0.696	1.393±0.246	9.952±0.245	50.746±1.915
[ThrOiPr][SA]	5924.986±247.467*	1122.600±119.560	100.640±10.718	0.697±0.106	5.979±0.967	8.416±0.544	53.117±1.665
[ThrOPr][SA]	4818.309±547.936*	863.710±8.197	82.740±0.785	0.193±0.062	21.502±8.606	1.924±0.631	46.157±5.249
[ThrOBu][SA]	5295.787±288.079*	480.250±13.329	47.107±0.934	4.079±0.161	1.021±0.041	23.060±0.875	51.946±2.826
[IleOiPr][SA]	2959.264±399.319*	170.530±25.078	16.459±2.420	0.775±0.471	5.380±2.906	1.530±0.642	28.562±3.854
[IleOPr][SA]	3207.085±224.157*	313.710±16.844	30.101±1.616	0.284±0.141	14.685±1.149	1.025±0.463	30.772±2.150
[IleOBu][SA]	4257.321±159.240*	1006.200±120.698	100.716±12.081	0.010±0.007	428.296±14.415	0.118±0.090	42.614±1.594
[ValOiPr][SA]	4961.426±285.725*	396.540±59.363	35.749±5.352	1.470±0.098	2.834±1.278	6.307±1.164	44.729±2.575
[ValOPr][SA]	2894.337±177.308*	200.870±34.691	16.897±2.918	0.064±0.029	65.270±8.038	0.129±0.035	24.347±1.492
[ValOBu][SA]	3445.336±444.431*	238.710±5.522	21.760±0.503	0.800±0.105	5.237±0.676	2.078±0.227	31.406±4.051

*- significant differences of the derivatives compared to the control (unmodified acid) $p < 0.001$, $\alpha = 0.05$, mean \pm SD, $n = 3$; the statistically significant difference was estimated by ANOVA using the Tuckey's test; J_{ss} : steady-state flux; K_p : permeability coefficient; L_T : lag time; D : diffusion coefficient; K_m : skin partition coefficient; Q : the percentage of the applied dose

Skin accumulation results

Table A43. Skin accumulation of acids from NSAIDs group and its L-amino acid alkyl ester salts, after 24 h abdominal porcine skin permeation into acceptor phase PBS (data partly presented in: [182]).

[Cation] \ [Anion]	Skin accumulation, $\mu\text{g API}/\text{g}$				
	[(S+)-IBU]	[IBU]	[KETO]	[NAP]	[SA]
Unmodified acid	972.568±103.990	896.652±126.579	1799.932±100.629	1108.243±101.031	1145.136±35.179
[MetOiPr]	—	620.588±40.312*	1563.653±154.519	614.665±150.796*	668.548±20.146
[MetOPr]	—	732.565±52.574	1554.474±166.957	634.922±141.974*	733.990±109.997
[MetOBu]	—	524.231±33.680*	1048.082±12.335*	872.359±103.045*	716.335±169.135*
[ThrOiPr]	—	508.048±57.282*	1076.330±201.563*	1360.970±215.527	470.668±63.074
[ThrOPr]	—	645.021±115.665	1291.916±205.055*	1134.149±141.093	609.593±88.895*
[ThrOBu]	—	592.0325±75.584*	1207.247±54.059*	936.253±230.808*	611.209±126.257*
[IleOiPr]	—	820.727±14.801	1735.675±353.141	1466.536±393.383	829.560±149.219*
[IleOPr]	—	717.356±68.292	1922.724±68.837	1744.563±275.166	938.187±80.993*

	Skin accumulation, $\mu\text{g API/g}$				
	[(S+)-IBU]	[IBU]	[KETO]	[NAP]	[SA]
[IleOBu]	—	848.935 \pm 73.864	1689.502 \pm 160.838	1771.402 \pm 334.348	660.959 \pm 36.071*
[ValOiPr]	727.045 \pm 27.375	725.788 \pm 76.063	1107.356 \pm 120.024*	841.733 \pm 84.734*	723.586 \pm 73.542*
[ValOPr]	823.521 \pm 52.372	622.152 \pm 73.835*	1317.001 \pm 163.791*	1297.198 \pm 204.582	1028.609 \pm 38.506
[ValOBu]	569.106 \pm 75.474	621.944 \pm 99.838*	1012.513 \pm 415.770*	1604.658 \pm 314.882	844.405 \pm 105.749

*- significant differences of the derivatives compared to the control (unmodified acid) $p < 0.001$, $\alpha = 0.05$, mean \pm SD, $n = 3$ (the statistically significant difference was estimated by ANOVA using the Tuckey's test)

ANTIOXIDANT STUDY RESULTS

Table A44. The antioxidant activity of acids from NSAIDs group and its L-amino acid alkyl ester salts expressed as DPPH radical scavenging activity (%) (data partly presented in: [182]).

[Cation]	[Anion]	DPPH radical scavenging activity, %				
		[(S+)-IBU]	[IBU]	[KETO]	[NAP]	[SA]
Unmodified acid		9.339 \pm 0.305	9.607 \pm 0.554	13.772 \pm 0.691	13.522 \pm 1.334	14.215 \pm 0.867
[MetOiPr]		—	9.185 \pm 0.737	15.624 \pm 0.607	9.214 \pm 0.507	13.859 \pm 0.057
[MetOPr]		—	11.263 \pm 1.032	14.995 \pm 0.716	8.687 \pm 1.121	11.298 \pm 1.171
[MetOBu]		—	10.451 \pm 0.731	11.299 \pm 1.259	10.224 \pm 0.097	11.790 \pm 1.436
[ThrOiPr]		—	11.847 \pm 1.656	15.359 \pm 0.152	9.510 \pm 0.057	13.043 \pm 1.885
[ThrOPr]		—	12.723 \pm 0.691	11.619 \pm 0.860	9.049 \pm 0.399	12.516 \pm 1.681
[ThrOBu]		—	10.646 \pm 0.828	15.624 \pm 0.448	9.872 \pm 0.616	10.408 \pm 0.507
[IleOiPr]		—	19.182 \pm 0.446	13.240 \pm 0.959	16.129 \pm 0.339	11.989 \pm 0.579
[IleOPr]		—	17.916 \pm 0.639	12.043 \pm 1.515	16.846 \pm 0.694	13.453 \pm 0.349
[IleOBu]		—	15.644 \pm 1.799	12.744 \pm 1.019	7.601 \pm 0.171	11.298 \pm 1.440
[ValOiPr]		10.302 \pm 0.251	9.899 \pm 1.297	13.506 \pm 1.447	14.370 \pm 0.339	14.480 \pm 0.940
[ValOPr]		9.804 \pm 0.549	9.380 \pm 1.013	12.109 \pm 1.698	15.314 \pm 0.903	13.751 \pm 0.402
[ValOBu]		10.435 \pm 0.208	9.770 \pm 0.851	12.409 \pm 1.604	14.239 \pm 0.651	14.148 \pm 0.547

BIODEGRADATION STUDY RESULTS

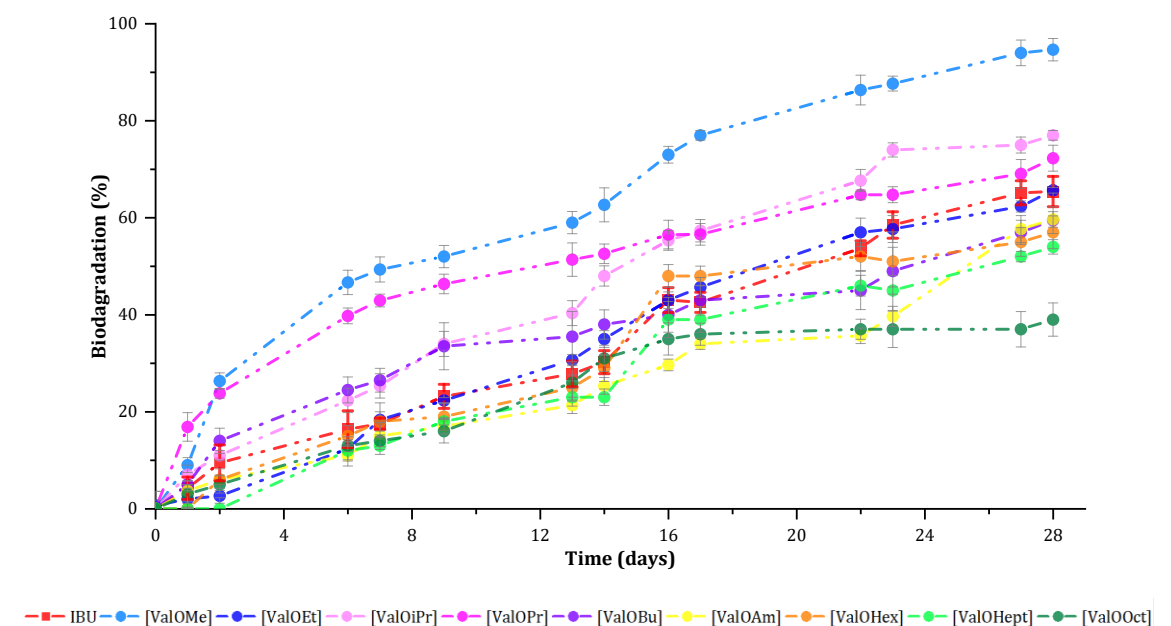


Fig A28. Biodegradation profiles for ibuprofen and its L-valinium alkyl ester salts (data presented in: [260]).

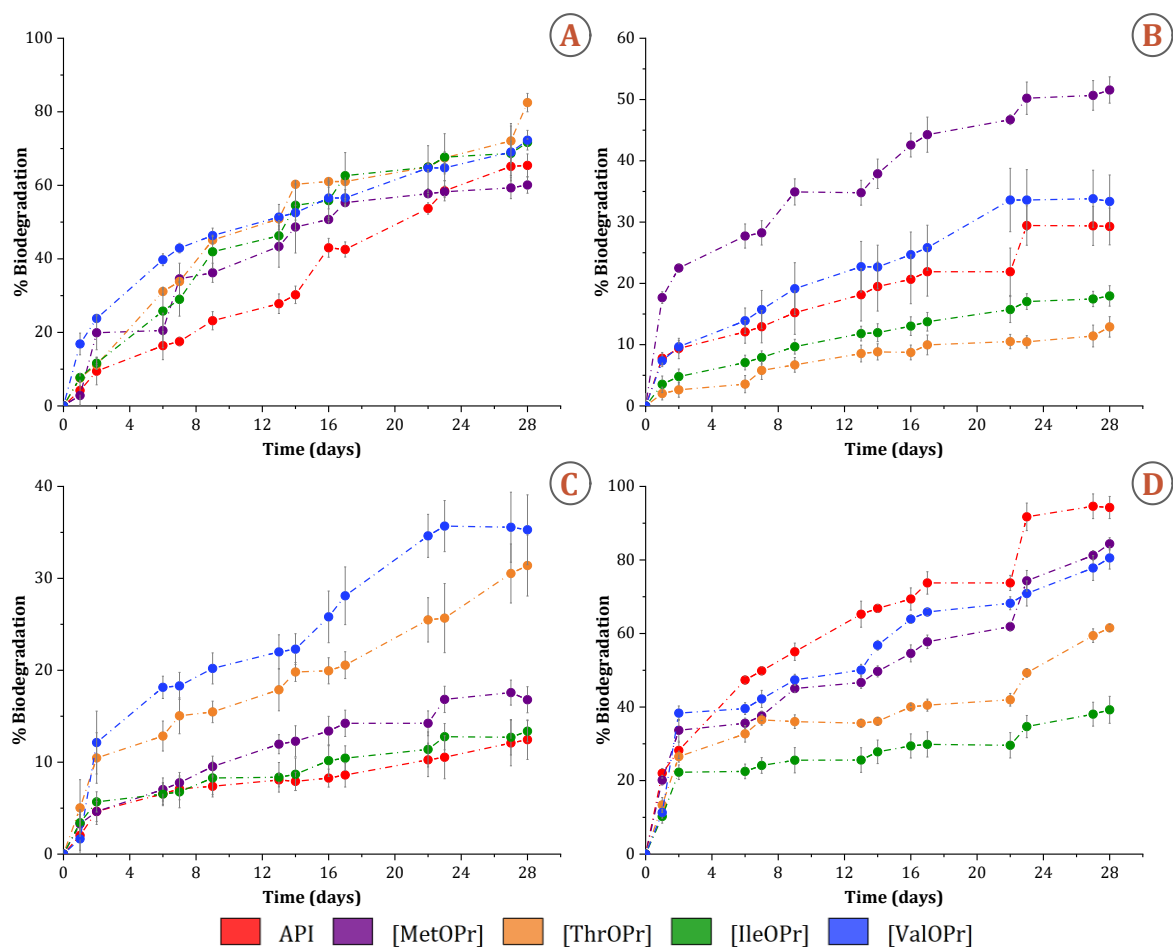


Fig A29. Biodegradation profiles for acids from NSAIDs group (A: ibuprofen B: ketoprofen C: naproxen, and D: salicylic acid) and their L-amino acid propyl ester salts (data presented in: [182]).

Table A45. Assessment of biodegradability of ibuprofen and its L-amino acid alkyl ester salts by bacterial cultures (data partly presented in: [182] and [260]).

Compound	Biodegradation (after 28 days), %	Half-life, h (days)	Phase of Degradation, %/h		
			Lag Phase	Degradation Phase	Plateau Phase
IBU	65.42±3.12	491.6 (20.5)	0-7/0-33	7-59/33-556	59-65/556-672
(S+)-IBU	75.68±3.47	373.1 (15.5)	0-8/0-13	8-68/13-527	68-76/527-672
[MetOPr][IBU]	60.10±2.24	457.4 (19.1)	0-6/0-14	6-54/14-513	54-60/513-672
[ThrOPr][IBU]	82.50±2.50	403.1 (16.8)	0-8/0-34	8-73/34-584	73-83/584-672
[IleOPr][IBU]	71.67±0.92	406.5 (16.9)	0-7/0-30	7-64/30-526	64-71/526-672
[ValOMe][IBU]	94.67±2.31	305.8 (12.7)	0-9/0-17	9-85/17-536	85-95/536-672
[ValOEt][IBU]	64.78±0.58	463.2 (19.3)	0-7/0-118	7-59/118-556	59-65/566-672
[ValOiPr][IBU]	69.50±5.61	347.0 (14.5)	0-8/0-34	8-69/34-517	63-77/517-672
[ValOPr][IBU]	72.28±0.58	308.9 (12.9)	0-7/0-15	7-63/15-539	63-70/539-672
[ValOBu][IBU]	59.89±9.76	568.4 (24.4)	0-6/0-20	6-54/20-603	54-60/603-672
[ValOAm][IBU]	59.66±10.61	740.2 (30.8)	0-6/0-48	6-54/48-603	54-60/603-672
[ValOHex][IBU]	57.00±3.39	507.7 (21.2)	0-6/0-46	6-51/46-555	51-57/555-672
[ValOHept][IBU]	54.32±1.49	623.1 (26.0)	0-5/0-65	5-49/65-596	49-54/596-672
[ValOOct][IBU]	39.17±5.43	861.5 (35.9)	0-4/0-37	4-35/37-524	35-39/524-672
[ValOiPr][(S+)-IBU]	67.43±3.26	425.9 (17.7)	0-7/0-12	7-61/12-517	6-67/517-672
[ValOPr][(S+)-IBU]	80.00±1.31	380.4 (15.8)	0-8/0-13	8-72/13-557	72-80/557-672
[ValOBu][(S+)-IBU]	60.95±5.18	461.3 (19.2)	0-6/0-11	6-55/11-524	55-61/524-672

Table A46. Assessment of biodegradability of ketoprofen and its L-amino acid propyl ester salts by bacterial cultures (data presented in: [182]).

Compound	Biodegradation (after 28 days), %	Half-life, h (days)	Phase of Degradation, %/h		
			Lag Phase	Degradation Phase	Plateau Phase
KETO	29.28±6.19	1205.5 (50.2)	0-3/0-15	3-26/15-494	26-29/494-672
[MetOPr][KETO]	51.56±2.15	565.2 (23.6)	0-5/0-11	5-46/11-510	46-51/510-672
[ThrOPr][KETO]	12.90±1.78	2512.7 (104.7)	0-1/0-24	1-12/24-613	12-13/613-672
[IleOPr][KETO]	17.95±1.67	1678.2 (69.9)	0-2/0-18	2-16/18-524	16-18/524-672
[ValOPr][KETO]	33.36±4.33	1061.3 (44.2)	0-3/0-17	3-30/17-493	30-33/493-672

Table A47. Assessment of biodegradability of naproxen and its L-amino acid propyl ester salts by bacterial cultures (data presented in: [182]).

Compound	Biodegradation (after 28 days), %	Half-life, h (days)	Phase of Degradation, %/h		
			Lag Phase	Degradation Phase	Plateau Phase
NAP	12.45±2.48	2680.5 (111.7)	0-1/0-27	1-11/27-587	11-12/587-672
[MetOPr][NAP]	16.79±0.42	1855.3 (77.3)	0-2/0-17	2-15/17-496	15-17/496-672
[ThrOPr][NAP]	31.40±3.32	1035.9 (43.2)	0-3/0-14	3-28/14-608	28-31/608-672
[IleOPr][NAP]	13.37±1.93	2318.8 (96.6)	0-1/0-11	1-12/11-520	12-13/520-672
[ValOPr][NAP]	35.29±3.80	762.5 (31.8)	0-4/0-14	4-32/14-491	32-35/491-672

Table A48. Assessment of biodegradability of salicylic acid and its L-amino acid propyl ester salts by bacterial cultures (data presented in: [182]).

Compound	Biodegradation (after 28 days), %	The half-life, h (days)	Phase of Degradation, %/h		
			Lag Phase	Degradation Phase	Plateau Phase
SA	94.61±6.36	357.9 (14.9)	0-9/0-16	9-86/16-510	86-95/510-672
[MetOPr][SA]	84.40±0.66	426.7 (17.8)	0-8/0-12	8-76/12-564	76-84/564-672
[ThrOPr][SA]	61.54±0.94	628.9 (26.2)	0-6/0-11	6-55/11-620	55-62/620-672
[IleOPr][SA]	39.24±3.67	892.0 (37.2)	0-4/0-8	4-35/8-526	35-39/526-672
[ValOPr][SA]	80.55±3.02	386.9 (16.1)	0-8/0-10	8-72/10-564	72-81/562-672

ANTIMICROBIAL ACTIVITY RESULTS

Table A49. Antimicrobial activity against *Escherichia coli* of acids from NSAIDs group and their L-amino acid isopropyl ester salts – Inhibition diameter (mm). Data presented in: [181].

Compound	Concentration of Solution Transferred to Disc, mg/mL							
	25	50	100	200	400	600	800	1000
IBU	–	–	–	–	–	–	–	–
[MetOiPr][IBU]	–	–	6.1±0.1	6.2±0.1	6.5±0.2	7.1±0.3	7.6±0.2	8.1±0.1
[ThrOiPr][IBU]	–	–	–	–	–	–	–	–
[IleOiPr][IBU]	–	–	–	–	6.3±0.1	6.4±0.3	7.1±0.2	7.8±0.3
[ValOiPr][IBU]	–	–	–	–	6.2±0.1	6.3±0.2	6.8±0.5	7.1±0.3
KETO	–	–	–	–	–	–	–	–
[MetOiPr][KETO]	–	–	–	7.3±0.5	8.0±0.6	8.9±0.5	10.6±0.7	12.9±0.4
[ThrOiPr][KETO]	–	–	–	–	–	–	–	–
[IleOiPr][KETO]	–	–	–	–	–	–	–	–
[ValOiPr][KETO]	–	–	–	–	6.7±0.3	7.0±0.2	7.6±0.3	8.3±0.4
NAP	–	–	–	–	–	–	–	–
[MetOiPr][NAP]	–	–	–	–	6.4±0.3	7.1±0.1	7.3±0.2	7.7±0.2
[ThrOiPr][NAP]	–	–	–	–	–	–	–	–
[IleOiPr][NAP]	–	–	–	–	–	–	–	–
[ValOiPr][NAP]	–	–	–	–	–	–	–	–
SA	–	–	–	–	6.1±0.1	6.4±0.1	11.0±0.8	13.1±1.2
[MetOiPr][SA]	–	–	–	7.8±0.2	14.4±0.8	16.4±0.3	18.8±0.4	21.8±0.7
[ThrOiPr][SA]	–	–	–	–	–	7.3±0.2	9.3±0.4	13.2±0.8
[IleOiPr][SA]	–	–	–	–	6.2±0.1	7.3±0.3	13.7±0.7	14.8±0.7
[ValOiPr][SA]	–	–	6.2±0.1	6.3±0.2	7.5±0.1	8.9±0.4	12.6±0.3	16.5±1.0

(–): no zone of inhibition

Table A50. Antimicrobial activity against *Staphylococcus epidermidis* of acids from NSAIDs group and their L-amino acid isopropyl ester salts – Inhibition diameter (mm). Data presented in: [181].

Compound	Concentration of Solution Transferred to Disc, mg/mL							
	25	50	100	200	400	600	800	1000
IBU	10.8±0.3	11.5±0.3	14.9±0.3	15.3±0.3	16.4±0.2	17.6±0.2	18.6±0.2	20.6±0.2
[MetOiPr][IBU]	–	–	8.3±0.1	13.6±0.2	14.7±0.2	15.4±0.2	17.0±0.2	17.7±0.3
[ThrOiPr][IBU]	7.5±0.2	10.5±0.2	15.4±0.1	16.9±0.2	17.5±0.2	18.3±0.2	19.8±1.4	23.2±0.1
[IleOiPr][IBU]	7.5±0.2	9.5±0.4	14.4±0.2	15.4±0.4	17.0±0.2	17.5±0.1	18.0±0.1	19.3±0.1
[ValOiPr][IBU]	10.8±0.3	11.5±0.3	14.9±0.3	15.3±0.3	16.4±0.2	17.6±0.2	18.6±0.2	20.6±0.2
KETO	–	–	–	–	–	–	–	–
[MetOiPr][KETO]	–	–	–	–	–	–	–	7.4±0.2
[ThrOiPr][KETO]	–	–	–	–	–	–	–	–
[IleOiPr][KETO]	–	–	–	–	6.2±0.1	7.3±0.2	8.3±0.1	10.4±0.2
[ValOiPr][KETO]	–	–	–	–	6.2±0.1	6.3±0.1	6.3±0.2	6.9±0.2
NAP	–	–	–	–	–	–	–	–
[MetOiPr][NAP]	–	–	–	–	–	–	–	7.5±0.3
[ThrOiPr][NAP]	–	–	–	–	–	–	–	–
[IleOiPr][NAP]	–	–	–	–	–	12.0±0.3	12.4±0.2	13.5±0.3
[ValOiPr][NAP]	–	–	–	–	–	–	6.6±0.3	7.4±0.1

Compound	Concentration of Solution Transferred to Disc, mg/mL							
	25	50	100	200	400	600	800	1000
SA	–	–	–	–	6.2±0.1	7.0±0.2	8.6±0.3	12.6±0.7
[MetOiPr][SA]	–	–	–	6.6±0.2	7.1±0.1	7.5±0.2	9.2±0.5	10.7±0.6
[ThrOiPr][SA]	–	–	–	–	–	–	–	–
[IleOiPr][SA]	–	–	–	–	–	7.3±0.4	10.5±0.3	16.6±0.5
[ValOiPr][SA]	–	–	–	–	6.6±0.2	7.1±0.1	9.2±0.5	10.7±0.6

(–): no zone of inhibition

Table A51. Antimicrobial activity against *Micrococcus Luteus* of acids from NSAIDs group and their L-amino acid isopropyl ester salts – Inhibition diameter (mm). Data presented in: [181].

Compound	Concentration of Solution Transferred to Disc, mg/mL							
	25	50	100	200	400	600	800	1000
IBU	8.6±0.3	9.4±0.2	9.7±0.2	10.2±0.1	10.6±0.1	11.5±0.2	12.7±0.2	13.4±0.1
[MetOiPr][IBU]	–	7.3±0.2	8.5±0.2	10.4±0.1	12.6±0.1	14.1±0.1	14.3±0.1	14.6±0.3
[ThrOiPr][IBU]	7.3±0.2	10.4±0.2	15.5±0.2	16.3±0.1	17.0±0.2	17.5±0.1	18.2±0.2	19.3±0.2
[IleOiPr][IBU]	7.2±0.2	7.6±0.1	8.6±0.1	9.4±0.2	10.7±0.1	11.2±0.1	11.6±0.1	12.3±0.2
[ValOiPr][IBU]	8.4±0.3	9.4±0.2	9.6±0.1	10.5±0.2	11.2±0.2	11.7±0.2	12.6±0.3	13.2±0.2
KETO	8.3±0.3	9.6±0.2	10.2±0.2	11.1±0.4	12.5±0.2	13.3±0.2	14.2±0.2	17.3±0.2
[MetOiPr][KETO]	–	7.2±0.3	8.2±0.2	8.5±0.3	9.2±0.1	9.6±0.2	12.4±0.2	14.3±0.2
[ThrOiPr][KETO]	–	–	–	7.4±0.3	9.6±0.1	14.3±0.2	15.4±0.2	17.4±0.1
[IleOiPr][KETO]	–	6.3±0.2	6.6±0.3	7.1±0.2	7.3±0.1	8.3±0.2	8.4±0.3	9.4±0.2
[ValOiPr][KETO]	6.3±0.2	7.4±0.1	8.5±0.3	9.1±0.3	10.3±0.2	11.7±0.1	14.5±0.2	15.1±0.2
NAP	6.2±0.1	6.4±0.1	6.7±0.1	6.8±0.1	7.3±0.2	7.6±0.2	8.5±0.2	8.7±0.1
[MetOiPr][NAP]	–	–	–	–	6.4±0.1	7.1±0.2	7.5±0.1	7.8±0.2
[ThrOiPr][NAP]	6.2±0.1	6.6±0.1	6.9±0.1	7.6±0.1	8.5±0.1	8.8±0.2	9.6±0.1	10.8±0.5
[IleOiPr][NAP]	6.4±0.1	6.7±0.1	7.0±0.1	7.3±0.1	7.5±0.2	8.1±0.6	8.7±0.1	9.5±0.1
[ValOiPr][NAP]	6.2±0.1	6.3±0.1	6.4±0.1	7.2±0.1	7.3±0.1	7.2±0.2	8.2±0.2	8.6±0.2
SA	–	–	–	–	7.4±0.4	8.7±0.8	9.4±0.8	13.1±1.9
[MetOiPr][SA]	–	–	6.1±0.1	6.3±0.1	7.3±0.4	8.1±0.9	10.5±1.0	11.1±0.9
[ThrOiPr][SA]	6.3±0.1	6.6±0.2	7.0±0.1	7.6±0.2	8.1±0.1	8.7±0.5	10.2±0.7	12.7±1.0
[IleOiPr][SA]	–	–	–	–	–	10.8±0.5	12.4±0.4	23.5±2.2
[ValOiPr][SA]	–	–	–	–	–	8.6±0.3	15.9±1.2	17.4±1.4

(–): no zone of inhibition

Scientific achievements

PUBLICATIONS

1. P. Ossowicz, J. Klebeko, B. Roman, E. Janus, Z. Rozwadowski, The Relationship the Structure and Properties of Amino Acid Ionic Liquids, *Molecules*, 2019, 24, 3252-3277.
2. P. Ossowicz, P. Kardaleva, M. Guncheva, J. Klebeko, E., Świątek, E. Janus, D. Yancheva, I. Angelov, Ketoprofen-Based Ionic Liquids: Synthesis and Interactions with Bovine Serum Albumin, *Molecules*, 2020, 25, 1, 90.
3. E. Janus, P. Ossowicz, J. Klebeko, A. Nowak, W. Duchnik, Ł. Kucharski, A. Klimkiewicz, Enhancement of ibuprofen solubility and skin permeation by conjugation with L-valine alkyl esters, *RSC Adv.*, 2020, 10, 7570-7584.
4. P. Ossowicz, E. Janus, J. Klebeko, E. Świątek, P. Kardaleva, S. Taneva, E. Krachmarova, M. Rangelov, N. Todorova, M. Guncheva, Modulation of the binding affinity of naproxen to bovine serum albumin by conversion of the drug into amino acid ester salts, *Journal of Molecular Liquids*, 2020, 391, 1, 114283.
5. P. Ossowicz, J. Klebeko, E. Janus, A. Nowak, W. Duchnik, Ł. Kucharski, A. Klimowicz, The effect of alcohols as vehicles on the percutaneous absorption and skin retention of ibuprofen modified with L-valine alkyl esters, *RCS Advances*, 2020, 68.
6. M. Gano, J. Klebeko, R. Pełech, Efficient esterification of curcumin in bis(trifluoromethylsulfonyl)imide-based ionic liquids, *Journal of Molecular Liquids*, 2021, 337, 1, 116420.
7. E. Makuch, P. Ossowicz-Rupniewska, J. Klebeko, E. Janus, Biodegradation of L-Valine Alkyl Ester Ibuprofenates by Bacterial Cultures, *Materials*, 2021, 14, 3180.
8. P. Ossowicz-Rupniewska, R. Rakoczy, A. Nowak, M. Konopacki, J. Klebeko, E. Świątek, E. Janus, W. Duchnik, K. Wenelska, Ł. Kucharski, A. Klimowicz, Transdermal Delivery Systems for Ibuprofen and Ibuprofen Modified with Amino Acids Alkyl Esters Based on Bacterial Cellulose, *Int. J. Mol. Sci.*, 2021, 22, 12, 6252.
9. J. Klebeko, P. Ossowicz-Rupniewska, A. Nowak, E. Janus, W. Duchnik, U. Adamiak-Giera, Ł. Kucharski, P. Prowans, J. Petriczko, N. Czapla, P. Bargiel, M. Markowska, A. Klimowicz, Permeability of Ibuprofen in the Form of Free Acid and Salts of L-Valine Alkyl Esters from a Hydrogel Formulation through Strat-M™ Membrane and Human Skin, *Materials*, 2021, 14, 6678.
10. P. Ossowicz-Rupniewska, A. Nowak, J. Klebeko, E. Janus, W. Duchnik, U. Adamiak-Giera, Ł. Kucharski, P. Prowans, J. Petriczko, N. Czapla, P. Bargiel, M. Markowska, A. Klimowicz, Assessment of the Effect of Structural Modification of Ibuprofen on the Penetration of Ibuprofen from Pentravan® (Semisolid)

Formulation Using Human Skin and a Transdermal Diffusion Test Model, *Materials*, 2021, 14, 6808.

11. J. Klebko, P. Ossowicz-Rupniewska, E. Świątek, J. Szachnowska, E. Janus, S.G. Taneva, E. Krachmarova, M. Guncheva, Salicylic Acid as Ionic Liquid Formulation May Have Enhanced Potency to Treat Some Chronic Skin Diseases, *Molecules*, 2022, 27, 216.
12. P. Ossowicz-Rupniewska, J. Klebko, E. Świątek, K. Bilaska, A. Nowak, W. Duchnik, Ł. Kucharski, Ł. Struk, K. Wenelska, A. Klimowicz, E. Janus, Influence of the Type of Amino Acid on the Permeability and Properties of Ibuprofenates of Isopropyl Amino Acid Esters, *Int. J. Mol. Sci.* 2022, 23, 4158.
13. P. Ossowicz-Rupniewska, J. Klebko, E. Świątek, J. Szachnowska, E. Janus, M. Rangelov, N. Stefka, E. Krachmarova, M. Guncheva, Binding behavior of ibuprofen-based ionic liquids with bovine serum albumin: Thermodynamic and molecular modeling studies, *Journal of Molecular Liquids*, 2022, 360, 119367.
14. P. Ossowicz-Rupniewska, P. Bednarczyk, M. Nowak, A. Nowak, W. Duchnik, Ł. Kucharski, J. Klebko, E. Świątek, K. Bilaska, J. Rokicka, E. Janus, A. Klimowicz, Z. Czech, Evaluation of the Structural Modification of Ibuprofen on the Penetration Release of Ibuprofen from a Drug-In-Adhesive Matrix Type Transdermal Patch, *Int. J. Mol. Sci.*, 2022, 23, 7752.
15. J. Klebko, O. Krüger, M. Dubicki, P. Ossowicz-Rupniewska, E. Janus, Isopropyl amino acid esters ionic liquids as vehicles for non-steroidal anti-inflammatory drugs in potential topical drug delivery systems with antimicrobial activity, *Int. J. Mol. Sci.*, 2022, 23, 13863.
16. P. Bednarczyk, K. Mozelewska, J. Klebko, J. Rokicka, P. Ossowicz-Rupniewska, Impact of the Chemical Structure of Photoreactive Urethane (Meth)Acrylates with Various (Meth)Acrylate Groups and Built-In Diels–Alder Reaction Adducts on the UV-Curing Process and Self-Healing Properties, *Polymers*, 2023, 15(4):924.
17. P. Ossowicz-Rupniewska, A. Nowak, M. Konopacki, M. Kordas, Ł. Kucharski, J. Klebko, E. Świątek, R. Rakoczy, Increase of ibuprofen penetration through the skin by forming ion pairs with amino acid alkyl esters and exposure to the electromagnetic field, *European Journal of Pharmaceutics and Biopharmaceutics*, May 2023.
18. J. Klebko, P. Ossowicz-Rupniewska, A. Nowak, E. Kucharska, Ł. Kucharski, W. Duchnik, Ł. Struk, A. Klimowicz, E. Janus, Cations of amino acid alkyl esters conjugated with an anion from the group of NSAIDs - as tunable pharmaceutical active ionic liquids, *Journal of Molecular Liquids*, 2023, 122200.
19. P. Bednarczyk, K. Mozelewska, M. Nowak, J. Klebko, J. Rokicka, P. Ossowicz-Rupniewska, Effect of hard segment chemistry and structure on the self-healing

properties of UV -curable coatings based on the urethane acrylates with built-in Diels–Alder adduct, *J. of Applied Polymer Sci*, 2023.

20. P. Bednarczyk, P. Ossowicz-Rupniewska, J. Klebko, J. Rokicka, Y. Bai, Z. Czech, Self-Healing UV-Curable Urethane (Meth)acrylates with Various Soft Segment Chemistry, *Coatings*, 2023.
21. P. Ossowicz-Rupniewska, E. Kucharska, J. Klebko, E. Kopciuch, K. Bilka, E. Janus, Effect of the type of amino acid on the biodegradation of ibuprofen derivatives, *Archives of Environmental Protection*, 2023, 49, p. 46–69.
22. P. Ossowicz-Rupniewska, J. Klebko, I. Georgieva, S. Apostolova, Ł. Struk, S. Todinova, R. Tzoneva, M. Guncheva, Tuning of the Anti-Breast Cancer Activity of Betulinic Acid via Its Conversion to Ionic Liquids, *Pharmaceutics*, 2024.

ABSTRACTS AND SUMMARIES IN THE CONFERENCE PROCEEDINGS

1. J. Klebko, P. Ossowicz, Zastosowanie aminokwasowych cieczy jonowych w syntezie organicznej, Conference proceedings: II Ogólnopolskie Seminarium Chemii Bioorganicznej, Organicznej i Biomateriałów, Wydział Technologii Chemicznej Politechniki Poznańskiej, Poznań 2017, ISBN 978-83-916087-5-3, p. 335-337.
2. J. Klebko, P. Ossowicz, Reakcje wieloskładnikowe MCR w środowisku aminokwasowych cieczy jonowych, III Szczecińskie Sympozjum Młodych Chemików, Conference proceedings: *Postępy w technologii i inżynierii chemicznej 2018*, Wydawnictwo Uczelniane Zachodniopomorskiego Uniwersytetu Technologicznego w Szczecinie, Szczecin 2018, ISBN 978-83-7663-256-8, p. 104-107.
3. B. Roman, M. Gano, J. Klebko, M. Retajczyk, J. Tołpa, Ł. Sałaciński, Znaczenie chiralności na aktywność enancjomerów, Conference proceedings: IV Szczecińskie Sympozjum Młodych Chemików, *Postępy w technologii i inżynierii chemicznej 2019*, Wydawnictwo Uczelniane Zachodniopomorskiego Uniwersytetu Technologicznego w Szczecinie, Szczecin 2019, ISBN 978-83-7663-291-9, p. 158-162.
4. J. Klebko, P. Ossowicz, Badanie lipofilowości ibuprofenu, IV Szczecińskie Sympozjum Młodych Chemików, Conference proceedings: *Postępy w technologii i inżynierii chemicznej 2019*, Wydawnictwo Uczelniane Zachodniopomorskiego Uniwersytetu Technologicznego w Szczecinie, Szczecin 2019, ISBN 978-83-7663-291-9, p. 20-22.
5. S. Kugler, P. Ossowicz, J. Klebko, K. Malarczyk-Matusiak, E. Wierzbicka, Technologia wytwarzania użytecznej pochodnej kalafonii, Conference proceedings: *11th Conference Wasteless Technologies and Waste Management in Industry and Agriculture*, Wydawnictwo Uczelniane Zachodniopomorskiego Uniwersytetu

Technologicznego w Szczecinie, Szczecin 2019, ISBN 978-83-7663-281-0, p. 243-246.

6. P. Ossowicz, J. Klebeko, S. Kugler, K. Malarczyk-Matusiak, E. Wierzbicka, Składniki polimerowych farb proszkowych z surowców naturalnych, XXIV Konferencja Naukowa Modyfikacja Polimerów, Conference proceedings: *Modyfikacja polimerów, stan i perspektywy w roku 2019*, ISBN 978-83-86520-24-4, p. 133-136.
7. S. Kugler, P. Ossowicz, K. Malarczyk-Matusiak, E. Wierzbicka, J. Klebeko, J. Łopiński, Ekologiczne powłoki ochronne modyfikowane nanonapełniaczami pochodzenia naturalnego, XXIV Konferencja Naukowa Modyfikacja Polimerów, Conference proceedings: *Modyfikacja polimerów, stan i perspektywy w roku 2019*, ISBN 978-83-86520-24-4, p. 236-240.
8. J. Klebeko, Wpływ budowy cieczy jonowej na wydajność procesu estryfikacji kurkuminy, Conference proceedings: 49 Międzynarodowe Seminarium Kół Naukowych w Olsztynie; Koła Naukowe Szkoła Twórczego Działania, Olsztyn 2020, ISBN 978-83-66264-52-6, p. 91.
9. E. Świątek, P. Ossowicz-Rupniewska, J. Klebeko, Aminokwasowe pochodne ketoprofenu i naproksenu – synteza, właściwości i potencjał aplikacyjny, Conference proceedings: *VI Szczecińskie Sympozjum Młodych Chemików - streszczenia*, Wydawnictwo Uczelniane Zachodniopomorskiego Uniwersytetu Technologicznego w Szczecinie, Szczecin 2021, ISBN 978-83-7663-320-6, p. 75.
10. J. Klebeko, P. Ossowicz-Rupniewska, E. Świątek, Modyfikacje strukturalne ibuprofenu jako potencjalne leki do podawania na skórę, Conference proceedings: *VI Szczecińskie Sympozjum Młodych Chemików - streszczenia*, Wydawnictwo Uczelniane Zachodniopomorskiego Uniwersytetu Technologicznego w Szczecinie, Szczecin 2021, ISBN 978-83-7663-320-6, p. 28.
11. J. Klebeko, Wpływ rodzaju aminokwasu na właściwości fizykochemiczne soli estrów alkilowych aminokwasów, Conference proceedings: *Materiały X Kongresu Technologii Chemicznej we Wrocławiu*, Wrocław 2022, ISBN 978-83-7493-200-4, p. 351.
12. J. Klebeko, O. Krüger, M. Dubicki, Influence of type Amino Acid on Thermochemical and Antimicrobial Properties of Active Pharmaceutical Ionic Liquids, *Book of Abstracts, Modeling and Design of Molecular Materials 2022*, University of Gdańsk, ISBN 978-83-941194-6-1, p. 109.
13. P. Bednarczyk, K. Mozelewska, J. Klebeko, J. Rokicka, M. Nowak, P. Ossowicz-Rupniewska, Photoreactive urethane (meth)acrylate oligomers with built-in Diels-Alder reaction adduct – synthesis and thermally reversible mechanism, *Book of Abstracts, 24th Polish Conference of Chemical and Process Engineering 2023*, The West Pomeranian University of Technology in Szczecin, ISBN 978-83-7663-359-6, p. 172.

14. J. Klebeko, P. Ossowicz-Rupniewska, E. Janus, M. Guncheva, Binding behavior of converted drugs into amino acid-based ionic liquids with bovine serum albumin, *Book of Abstracts, 24th Polish Conference of Chemical and Process Engineering 2023*, The West Pomeranian University of Technology in Szczecin, ISBN 978-83-7663-359-6, p. 326.
15. P. Ossowicz-Rupniewska, J. Klebeko, I. Georgieva, S. Apostolova, R. Tzoneva, M. Guncheva, Triterpenoid-based ionic liquids with enhanced antitumor potency, *Book of contributions, 12TM International Conference structure and stability of Biomacromolecules SSB 2023*, 5-7 September, Košice, Slovakia, ISBN 978-89656-26-4, p. 89.
16. S. Apostolova, I. Georgieva, P. Ossowicz-Rupniewska, J. Klebeko, M. Guncheva, R. Tzoneva, Conversion of betulinic acid into organic salts improves its anticancer potency in a hormonedependent vs. hormone-independent breast cancer cell line, *Book of abstract: Satellite Scientific Symposium "Medicinal and Aromatic plants for Innovative Bioactive Products"*, International Conference "Kliment's Days 2023 - 60 Years Faculty of Biology", Sofia, Bulgaria, November 9-11, 2023, ISSN: 1314–4960.

MONOGRAPH CHAPTERS

1. J. Klebeko, P. Ossowicz, Reakcje wieloskładnikowe w cieczach jonowych, *Postępy w technologii i inżynierii chemicznej 2018*, Wydawnictwo Uczelniane Zachodniopomorskiego Uniwersytetu Technologicznego w Szczecinie, ISBN 978-83-7663-266-7, p. 85-94.
2. J. Klebeko, P. Ossowicz, Lipofilowość ibuprofenu, *Postępy w technologii i inżynierii chemicznej 2019*, Wydawnictwo Uczelniane Zachodniopomorskiego Uniwersytetu Technologicznego w Szczecinie, ISBN 978-83-7663-296-4, p. 82-91.
3. B. Roman, M. Gano, J. Klebeko, M. Retajczyk, J. Tołpa, Ł. Sałaciński, Znaczenie chiralności w aktywności enancjomerów, *Postępy w technologii i inżynierii chemicznej 2019*, Wydawnictwo Uczelniane Zachodniopomorskiego Uniwersytetu Technologicznego w Szczecinie, ISBN 978-83-7663-296-4, p. 171-188.
4. J. Klebeko, Wpływ budowy cieczy jonowej na wydajność procesu estryfikacji kurkuminy, *Nowoczesne rozwiązania proekologiczne w naukach zootechnicznych, weterynaryjnych, rolniczych i technicznych*, Wydawnictwo Naukowe FNCE, Poznań 2020, ISBN 978-83-66264-56-4, p. 435-445.
5. J. Klebeko, P. Ossowicz-Rupniewska, E. Świątek, Modyfikacje strukturalne ibuprofenu, jako metoda zwiększania przenikalności przez skórę, *Postępy w technologii i inżynierii chemicznej 2021*, Wydawnictwo Uczelniane Zachodniopomorskiego Uniwersytetu Technologicznego w Szczecinie, ISBN 978-83-7663-326-8, p. 26-34.

6. E. Świątek, P. Ossowicz-Rupniewska, J. Klebeko, Aminokwasowe pochodne naproksenu i ketoprofenu, jako alternatywa dla dotychczas stosowanych leków z grupy NLPZ, Postępy w technologii i inżynierii chemicznej 2021, Wydawnictwo Uczelniane Zachodniopomorskiego Uniwersytetu Technologicznego w Szczecinie, ISBN 978-83-7663-326-8, p. 121-132.

NATIONAL CONFERENCES

ORAL SPEECHES

1. J. Klebeko, P. Ossowicz, Badanie lipofilowości ibuprofenu, IV Szczecińskie Sympozjum Młodych Chemików, Szczecin, May 14, 2019.
2. J. Klebeko, P. Ossowicz-Rupniewska, E. Świątek, Modyfikacje strukturalne ibuprofenu jako potencjalne leki do podawania na skórę, VI Szczecińskie Sympozjum Młodych Chemików, Szczecin, May 10-14, 2021.

POSTERS

1. J. Klebeko, P. Ossowicz, Zastosowanie aminokwasowych cieczy jonowych w syntezie organicznej, II Ogólnopolskie Seminarium Chemii Bioorganicznej, Organicznej i Biomateriałów, Poznań, December 2, 2017.
2. J. Klebeko, P. Ossowicz, Reakcje wieloskładnikowe MCR w środowisku aminokwasowych cieczy jonowych, III Szczecińskie Sympozjum Młodych Chemików, Szczecin, May 8, 2018.
3. B. Roman, M. Gano, J. Klebeko, M. Retajczyk, J. Tolpa, Ł. Salaciński, Znaczenie chiralności na aktywność enancjomerów, IV Szczecińskie Sympozjum Młodych Chemików, Szczecin, May 14, 2019.
4. S. Kugler, P. Ossowicz, J. Klebeko, K. Malarczyk-Matusiak, E. Wierzbicka, The production technology of useful rosin derivative, XI Konferencja Technologie bezodpadowe i Zagospodarowanie Odpadów w Przemśle i Rolnictwie, Międzyzdroje, June 11-14, 2019.
5. J. Klebeko, P. Ossowicz, E. Janus, Wpływ rodzaju aminokwasu na właściwości fizykochemiczne soli estrów alkilowych aminokwasów, X Kongres Technologiczny, Wrocław, May 11-14, 2022.
6. J. Klebeko, O. Krüger, M. Dubicki, Influence of type Amino Acid on Thermochemical and Antimicrobial Properties of Active Pharmaceutical Ionic Liquids, Modeling and Design of Molecular Materials 2022, Gdańsk, September 19-22, 2022.
7. P. Bednarczyk, K. Mozelewska, J. Klebeko, J. Rokicka, M. Nowak, P. Ossowicz-Rupniewska, Photoreactive urethane (meth)acrylate oligomers with built-in Diels-Alder reaction adduct - synthesis and thermally reversible mechanism, 24th Polish Conference of Chemical and Process Engineering 2023, Szczecin, June 13-16, 2023.

8. J. Klebko, P. Ossowicz-Rupniewska, E. Janus, M. Guncheva, Binding behavior of converted drugs into amino acid-based ionic liquids with bovine serum albumin, 24th Polish Conference of Chemical and Process Engineering 2023, Szczecin, June 13-16, 2023.
9. P. Ossowicz-Rupniewska, J. Klebko, I. Georgieva, S. Apostolova, R. Tzoneva, M. Guncheva, Triterpenoid-based ionic liquids with enhanced antitumor potency, 12TM International Conference structure and stability of Biomacromolecules SSB2023, September 5-7, Košice, Slovakia.

PATENTS GRANTED:

1. P. Ossowicz, J. Klebko, E. Janus, Organiczna sól kwasu salicylowego i sposób wytwarzania organicznej soli kwasu salicylowego, Patent no. PL236161, 14.12.2020.
2. P. Ossowicz, J. Klebko, E. Janus, Aminokwasowa pochodna ibuprofenu i sposób wytwarzania aminokwasowej pochodnej ibuprofenu, Patent no. PL237699, 17.05.2021.
3. P. Ossowicz-Rupniewska, J. Klebko, E. Janus, Organiczna pochodna ketoprofenu i sposób wytwarzania organicznej pochodnej ketoprofenu, Patent no. PL237698, 17.05.2021.
4. P. Ossowicz, J. Klebko, E. Janus, Pochodna naproksenu i sposób wytwarzania pochodnej naproksenu, Patent no. PL237318, 06.04.2021.
5. P. Ossowicz, E. Janus, J. Klebko, Sposób wytwarzania chlorowodorku estru alkilowego aminokwasu, Patent no. PL238790, 04.10.2021.
6. P. Ossowicz, J. Klebko, E. Janus, Sposób wytwarzania chlorowodorku estru alkilowego L-waliny, Patent No. PL239320, 22.11.2021.
7. E. Wierzbicka, P. Ossowicz-Rupniewska, S. Kugler, J. Klebko, Sposób modyfikacji kwasu maleopimarowego, Patent No. PL241883, 22.09.2022.
8. S. Kugler, P. Ossowicz, J. Klebko, K. Malarczyk-Matusiak, E. Wierzbicka, Sposób wytwarzania diestru kwasu maleopimarowego, Patent No. PL242183, 02.11.2022.
9. P. Bednarczyk, P. Ossowicz-Rupniewska, J. Klebko, Sposób wytwarzania żywicy uretanometakrylanowej i kompozycja do wytwarzania powłoki, Patent No. PL 244108, 12.09.2023.
10. P. Bednarczyk, P. Ossowicz-Rupniewska, J. Klebko, Sposób wytwarzania spoiwa na bazie żywicy uretano(met)akrylanowej i kompozycja do wytwarzania powłoki zawierająca spoiwo na bazie żywicy uretano(met)akrylanowej, Patent No. PL244309, 17.10.2023.

11. E. Janus, P. Ossowicz-Rupniewska, J. Klebeko, E. Świątek, Naproksenian estru alkilowego aminokwasu oraz sposób otrzymywania naproksenianu estru alkilowego aminokwasu, Patent No. PL 244292, 03.01.2024.
12. E. Janus, P. Ossowicz-Rupniewska, J. Klebeko, E. Świątek, Sposób wytwarzania naproksenianu estru alkilowego L-leucyny, Patent No. PL245375, 08.07.2024.

PATENT APPLICATIONS

1. P. Ossowicz-Rupniewska, J. Klebeko, E. Świątek, E. Janus, Aminokwasowa pochodna ibuprofenu i sposób wytwarzania aminokwasowej pochodnej ibuprofenu, Application no. PL.438193, 18.06.2021.
2. P. Ossowicz-Rupniewska, P. Bednarczyk, M. Nowak, J. Klebeko, E. Świątek, A. Nowak, W. Duchnik, Ł. Kucharski, Plaster transdermalny i sposób wytwarzania plastra transdermalnego, Application no. P.441307, 30.05.2022.
3. P. Ossowicz-Rupniewska, J. Klebeko, M. Guncheva, Aminokwasowa pochodna kwasu betulinowego i sposób wytwarzania aminokwasowej pochodnej kwasu betulinowego, Application no. P.445638, 20.07.2023.

PARTICIPATION IN RESEARCH PROJECTS

1. Contractor in the period 10/2018–04/2020 of the project: *Ochronne farby proszkowe z konkurencyjnych cenowo surowców pochodzenia biologicznego: synteza składników, komponowanie i ocena właściwości powłok na podłożu stalowym*, LIDER-VIII, research grant funded by: The National Centre for Research and Development (Narodowe Centrum Badań i Rozwoju). Project No. LIDER/7/0045/L-8/16/NCBR/2017 (01.01.2018-30.04.2021).
2. Contractor in the period 02/2020–12/2022 of the project: *Inteligentne powłoki lakierowe sieciowane technikami UV/LED*, LIDER-X, research grant funded by: The National Centre for Research and Development (Narodowe Centrum Badań i Rozwoju). Project No. LIDER/16/0102/L10/18/NCBiR/2019 (01.01.2020-31.12.2022).
3. Contractor in the period 01/2021–12/2023 of the project: *Opracowanie technologii otrzymywania nowych modyfikacji leków o zwiększonej przenikalności przez skórę*, LIDER-XI, research grant funded by: The National Centre for Research and Development (Narodowe Centrum Badań i Rozwoju). Project No. LIDER/53/0225/L-11/19/NCBR/2020 (02.01.2021 – 02.01.2024).
4. Contractor in the period 12/2022–09/2023 of the project: *Potency of series of betulinic acid-based ionic liquids as modulators of Toll-like receptors in normal blood mononuclear cells and breast cancer cell lines*, research grant funded by: Bulgarian National Science Fund (BSFN), Project No. BG-175467353-2022-04-0019 (15.12.2022-15.12.2025).

OBTAINED GRANTS

Project: *Targeted delivery of non-steroidal anti-inflammatory drugs in the form of amino acid ionic liquids*. The research Grant of the Rector of the West Pomeranian University of Technology in Szczecin for PhD students of the Doctoral School, grant number: ZUT/7/2022 (13.06.2022–15.12.2022).

INTERNSHIPS

1. Internship within the Erasmus+ Programme at the Berlin University of Technology (BHT) (Berlin, Germany), Faculty of Physical Chemistry of Drugs (FB II Mathematics - Physics - Chemistry) 1.06.2022 – 31.08.2022 and 1.10.2023 – 30.05.2024. Academic supervisor: Prof. Oliver Krüger, PhD.
2. Internship within the Erasmus+ Programme at the Bulgarian Academy of Sciences, Institute of Organic Chemistry (Sofia, Bulgaria) 1.06.2023–30.06.2023. Academic supervisor: Maya Guncheva, PhD, Assoc. Prof.